



Universidad del País Vasco  
Euskal Herriko Unibertsitatea  
The University of the Basque Country

*Novel Studies on Enamine and Acid  
Organocatalysis in Carbon-Carbon  
Bond Forming Reactions*

Andrea Ruiz-Olalla Fernández  
Donostia-San Sebastián, 2015



The following Thesis Dissertation has been carried at the Organic Chemistry Department I of the Chemistry Faculty at the University of the Basque Country, in San Sebastián under the supervision of Prof. Fernando P. Cossío Mora and Dr. M<sup>a</sup> de Gracia Retamosa Hernández.

Financial support has been provided by the Ministerio de Ciencia e Innovación “Ayudas PFI, Convocatoria 2011” and “Ayuda a la Movilidad Predoctoral para la Realización de Estancias Breves en Centros de I+D, Convocatoria 2013”.

The numbering of the tables, figures, schemes and references of this dissertation are independent for each chapter. Additionally, molecule numbering in the introductory sections (these are: chapter 1 and sections 2.1, 3.1, 4.1 and 5.1) is written independently in Roman numerals. On the contrary, molecule numbering within the content of each chapter is written consecutively in Arabic numerals.



# TABLE OF CONTENTS

Spanish summary	1
List of abbreviations	7
<b>1. Introduction</b>	<b>11</b>
Note	13
1.1. Introduction	15
1.2. Methods for the acquisition of enantiopure compounds	16
1.2.1. Chiral auxiliaries	17
1.2.2. Asymmetric catalysis	17
1.3. Asymmetric organocatalysis	20
1.3.1. Types of organocatalysis	23
1.3.1.1. Acid/base classification	23
1.3.1.2. Covalent/non-covalent classification	25
<b>2. Densely Substituted 4-Amino Pyrrolidines. Design and Organocatalysis</b>	<b>29</b>
2.1. Introduction. Organocatalysts in enamine-activated type reactions	31
2.1.1. Intermolecular aldol reaction	31
2.1.2. Intermolecular Michael reaction	39
2.2. Objectives	47
2.3. Synthesis of densely substituted 3,5-diphenyl-4-amino proline parent compounds	48
2.4. Scope as organocatalysts in addition reactions based on enamine intermediates	50
2.4.1. Aldol reaction between cyclohexanone and pentafluorobenzaldehyde	50
2.4.2. Conjugate reaction with cyclohexanone as nucleophile	52
2.4.2.1. Nitroalkenes and 1,2-bis(phenylsulfonyl)ethene as electrophiles	52
2.4.2.2. Detection via NMR experiments of enamine-iminium intermediate species	57
2.4.2.3. Computational study of the proposed reaction mechanism	61
2.5. Reactivity of densely 3,5-disubstituted-4-amino and 4-amido prolines	65
2.5.1. Synthesis of organocatalytic derivatives	65
2.5.2. Scope of the conjugate addition between cyclohexanone and <i>trans</i> - $\beta$ -nitrostyrene	67
2.6. Follow up chemistry: Chemoselective aldol/conjugate addition	68
2.7. Conclusions	73
2.8. Experimental section	74
<b>3. <math>\gamma</math>-Dipeptides Based on Units of Densely Substituted Pyrrolidines. Design and Organocatalysis</b>	<b>101</b>
3.1. Introduction	103
3.1.1. Background. Peptides in organocatalysis in enamine-activated type reactions	104
3.1.2. Aldol reaction	104
3.1.3. Michael reaction	107
3.1.4. Objectives	110
3.2. Synthesis of dimers	110
3.3. Aldol reaction between cyclohexanone and pentafluorobenzaldehyde	115
3.3.1. Optimization screening	115

3.3.2. Detection of intermediates	117
3.3.3. Kinetic studies	120
3.4. Michael reaction between cyclohexanone and <i>trans</i> - $\beta$ -nitrostyrene	123
3.5. Synthesis of <i>N</i> -methylated and hybrid dimers. Effects on the reactivity in aldol and Michael reactions	126
3.5.1. Synthesis	126
3.5.2. Effect on the aldol reaction between cyclohexanone and pentafluorobenzaldehyde	130
3.5.3. Effect of <i>N</i> -methylated and functionalized catalysts on the Michael reaction between cyclohexanone and <i>trans</i> - $\beta$ -nitrostyrene	131
3.5.3.1. Hybrid dimers	131
3.5.3.2. <i>N</i> -methylated dimers	132
3.5.3.3. Exploring the scope of the reaction: 1,1-bis(phenylsulphonyl)ethene as electrophile and acetone as nucleophile	135
3.6. Follow up chemistry: Synthesis of 7a-hydroxy-2-oxo-3-aryloctahydro-1 <i>H</i> -indol-1-yl benzoate	137
3.7. Conclusions	138
3.8. Experimental section	139
<b>4. Stereoselective Synthesis of 7a-Hydroxy-2-oxo-3-aryloctahydro-1<i>H</i>-indol-1-yl Carboxylates. A Concise Formal Synthesis of (+)-Pancracine</b>	<b>155</b>
4.1. Introduction	157
4.1.1. Organocatalysis in total synthesis of alkaloids and secondary metabolites	157
4.1.2. Objectives	163
4.2. The discovery of an unprecedented cyclization reaction	164
4.2.1. Optimization studies	164
4.2.2. Scope	167
4.3. Searching for the reaction mechanism	172
4.3.1. Mechanistic proposal based on a stepwise radical lactamization reaction	173
4.3.2. Mechanistic proposal based on sigmatropic rearrangements	175
4.4. Follow up chemistry. Hydrogenation	178
4.5. Total and formal syntheses of pancracine alkaloid	179
4.6. Formal synthesis of (+)-pancracine via organocatalyzed lactamization reaction	183
4.7. Conclusions	188
4.8. Experimental section	189
<b>5. Organocatalyzed Pictet-Spengler Reaction for the Synthesis of 1-Benzyl-1,2,3,4-tetrahydroisoquinolines and Total Synthesis of (<i>R</i>)-Trimetoquinol Hydrochloride</b>	<b>211</b>
5.1. Introduction	213
5.1.1. Asymmetric synthesis of 1-substituted-1,2,3,4-tetrahydroisoquinolines	213
5.1.2. Pictet-Spengler reaction	216
5.1.3. Organocatalyzed Pictet-Spengler reaction towards 1-substituted THIQs	220
5.1.4. Objectives	221
5.2. Synthesis of ( <i>R</i> )-TRIP <b>80</b> catalyst and analogues	223
5.3. Synthesis of the precursors for the Pictet-Spengler reaction	226
5.3.1. <i>N</i> -protected dopamine analogue	226
5.3.2. Phenylacetaldehydes	227

5.4. Optimization screenings: Additives, concentration/temperature dependence and catalysts screening	228
5.5. Proposed reaction mechanism. Influence of the protecting group	232
5.6. Total synthesis of (+)-trimetoquinol hydrochloride	233
5.7. Follow up chemistry	234
5.8. Conclusions	235
5.9. Experimental section	236

## **Annexes**

<b>I. NMR spectra</b>	
a. NMR spectra selection for Chapter 2	245
b. NMR spectra selection for Chapter 3	283
c. NMR spectra selection for Chapter 4	319
d. NMR spectra selection for Chapter 5	357
<b>II. X ray structures for Chapters 2, 3 and 4</b>	<b>365</b>
<b>III. Pseudo-first order linear plots, standard deviations and error calculation</b>	<b>375</b>





Entre las diversas biomoléculas presentes en la naturaleza cabe destacar las enzimas, macromoléculas capaces de catalizar de manera eficiente procesos bioquímicos en sistemas vivos. A su vez, también se encuentran moléculas más pequeñas, como aminoácidos y alcaloides, que pueden emplearse como organocatalizadores en diferentes reacciones químicas.

La organocatálisis, junto con las enzimas y los complejos metálicos, está emergiendo como una de las herramientas más útiles en síntesis de compuestos ópticamente activos. En los últimos años se ha prestado mucha atención al desarrollo de ésta en su forma asimétrica con importantes avances en química orgánica. El empleo de pequeñas moléculas naturales presenta importantes ventajas como su bajo coste, disponibilidad a partir de fuentes naturales, estabilidad frente a condiciones atmosféricas y respeto al medio ambiente. Esta tesis se ha dividido en cuatro capítulos recogiendo el primero, de forma introductoria, las diferentes formas en que las reacciones son activadas de manera enantioselectiva.

En nuestro grupo de investigación se han diseñado los ligandos híbridos de tipo ferrocenil pirrolidinas **NH-D-EhuPhos-1** y **NMe-L-EhuPhos-2**. Estos se han empleado en reacciones de cicloadición (3+2) entre iminoésteres y nitroalquenos para dar lugar a los cicloaductos **NO<sub>2</sub>-X<sub>L</sub>-OMe-5aa** y **NO<sub>2</sub>-N<sub>L</sub>-OMe-5aa** con elevados excesos enantioméricos. Estos productos poseen un gran interés en los campos de la química y biología ya que pueden complementar a los aminoácidos naturales. Es por ello, que se está empleando un gran esfuerzo en conocer la relación configuración/reactividad de estas moléculas y sus derivados al emplearlos como organocatalizadores en diferentes procesos químicos.

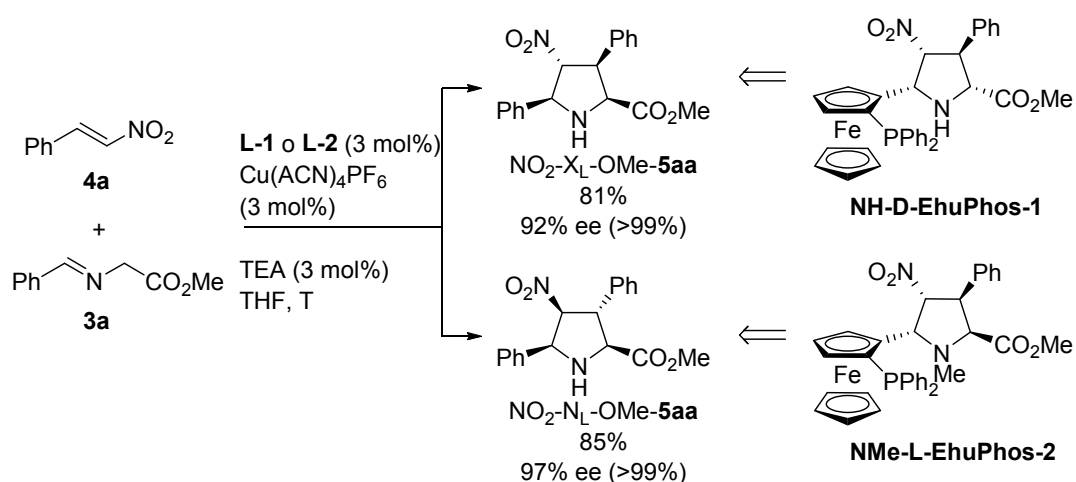


**Figura 1.** Síntesis de las prolina densamente sustituidas **NO<sub>2</sub>-X<sub>L</sub>-OMe-5aa** y **NO<sub>2</sub>-N<sub>L</sub>-OMe-5aa** establecido en el grupo de investigación (también conocidas como organocatalizadores de primera generación).

El segundo capítulo inicia los estudios de la presente tesis doctoral y comienza describiendo el empleo de aminas quirales como organocatalizadores en reacciones de formación de enlace carbono-carbono. Por ello, se decidió evaluar los catalizadores de segunda generación **10aa** en reacciones de activación via enamina como la reacción aldólica y de Michael. Estas moléculas fueron obtenidas con altos rendimientos mediante la hidrogenación catalítica de los precursores **5aa** empleando Ni/Ra como catalizador (Figura 2A).

Iniciamente se evaluó la reacción aldólica empleando los catalizadores  $\text{NH}_2\text{-X}_L\text{-OMe-10aa}$  y  $\text{NH}_2\text{-N}_L\text{-OMe-10aa}$ , observándose resultados similares a los de sus predecesores  $\text{NO}_2\text{-X}_L\text{-OMe-5aa}$  y  $\text{NO}_2\text{-N}_L\text{-OMe-5aa}$ . Además, nuestros catalizadores de segunda generación fueron capaces de catalizar la reacción Michael entre cetonas cíclicas como ciclohexanona **11a** y nitroalquenos aromáticos **4**. Esta reacción proporcionó los productos Michael con elevados rendimientos y excesos enantioméricos al contrario que lo observado con los catalizadores de primera generación (Figura 2B).

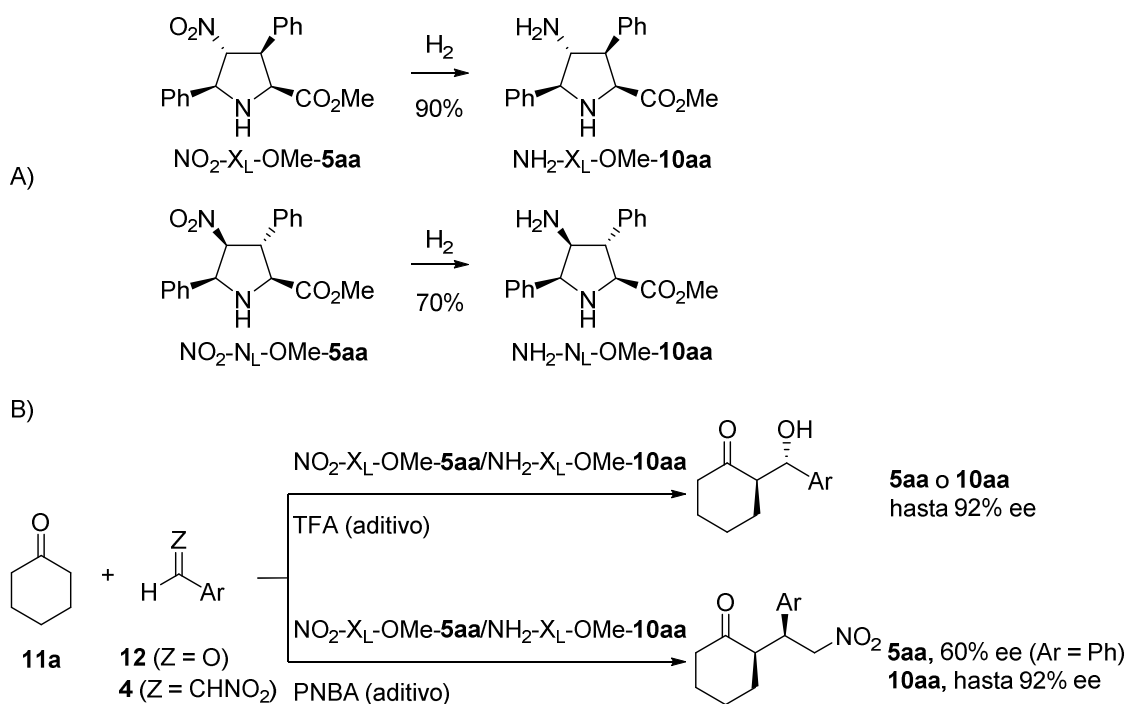


**Figura 2.** A) Síntesis de los catalizadores de segunda generación  $\text{NH}_2\text{-N}_L\text{-OMe-10aa}$  y  $\text{NH}_2\text{-X}_L\text{-OMe-10aa}$ . B) Reactividad e inducción de los catalizadores  $\text{NO}_2\text{-X}_L\text{-OMe-5aa}$  y  $\text{NH}_2\text{-X}_L\text{-OMe-10aa}$  en la reacción aldólica y de Michael con ciclohexanona **11a** como nucleófilo.

Al igual que ocurría en la reacción aldólica, los resultados obtenidos en la reacción de Michael han puesto de manifiesto que la inducción quiral depende de la configuración del catalizador. Así, mientras el catalizador *endo*-,  $\text{NH}_2\text{-N}_L\text{-OMe-10aa}$ , proporcionó los

productos con la misma configuración que aquellos obtenidos bajo la influencia de los catalizadores tipo L-Prolina, el catalizador *exo*-, NH<sub>2</sub>-X<sub>L</sub>-OMe-**10aa**, produjo el enantiómero opuesto. Tras estos resultados se evaluó un aceptor dielectrofílico, con la presencia simultánea de un grupo cetónico y alqueno electrodeficiente, para obtener una síntesis enantiodivergente dependiente del catalizador empleado. Sin embargo, los resultados obtenidos no fueron los deseados. Adicionalmente mediante métodos experimentales y computacionales se explicó tanto la reactividad de estas moléculas como el origen de la diferente inducción enantiomérica dependiendo del tipo de catalizador empleado.

El tercer capítulo se centra en la síntesis y análisis de las propiedades organocatalíticas de la tercera generación de organocatalizadores o dímeros basados en prolina densamente sustituidas. Para la obtención de estos dímeros se sintetizaron previamente los precursores ácidos 4-nitropirrolidin-2-carboxílicos y 4-aminopirrolidin-2-carboxilatos mediante hidrólisis de los grupos éster y la hidrogenación catalítica del grupo nitro de los sustratos correspondientes, respectivamente. Una vez sintetizados los precursores necesarios se llevó a cabo el acoplamiento empleando PyBOP o HATU en función de sustrato ácido utilizado (pirrolidina no *N*-metilada vs. *N*-metilada). Estas transformaciones proporcionaron una larga familia de  $\gamma$ -dipeptidos basados en unidades de prolina no naturales densamente funcionalizadas (Figura 3A). Posteriormente, estos catalizadores fueron analizados en las mismas reacciones de activación via enamina, aldólica y Michael, descritas en el capítulo previo. Se observó que la inducción enantiomérica dependía de las dos unidades de pirrolidinas constituyentes de los catalizadores, actuando ambas como centros catalíticos independientes.

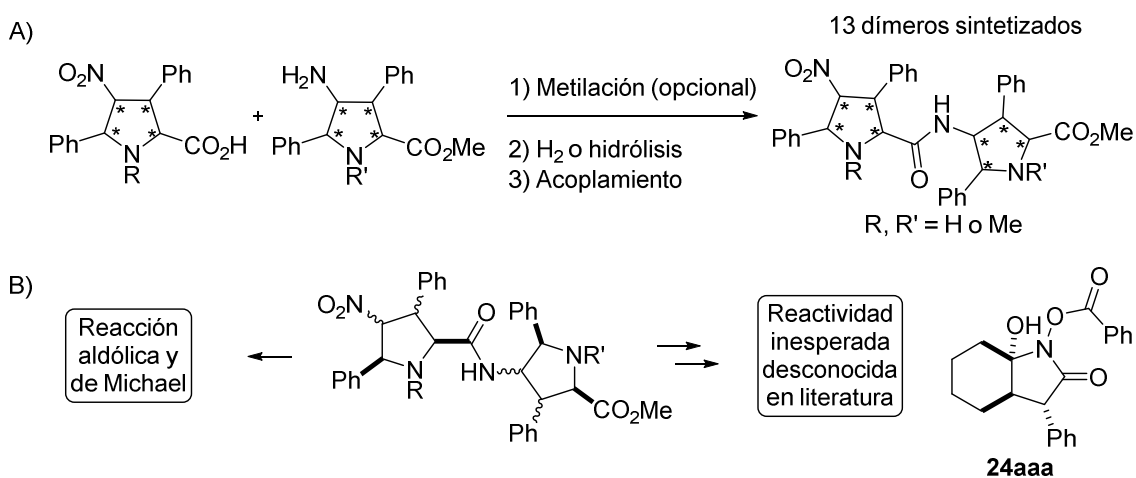


**Figura 3.** Péptidos diméricos basados en unidades de pirrolidina densamente funcionalizadas.

Por otro lado, la relación estructura/reactividad de estos catalizadores oligoméricos también fue estudiada mediante análisis cinético en la reacción aldólica entre ciclohexanona y un aldehído aromático fluorado activo en resonancia magnética nuclear de  $^{19}\text{F}$ . Cabe mencionar, que al llevar a cabo la reacción Michael entre ciclohexanona y nitroestireno catalizada por los dímeros con ácido benzoico como aditivo, se observó la formación de la especie carboxilato de 7a-hidroxi-2-oxo-3-feniloctahidro-1*H*-indoilo **24aaa**. Esta pudo ser aislada y caracterizada como producto secundario dando lugar así, a una nueva reactividad no descrita previamente en la literatura (Figura 3B). La aparición de esta nueva entidad dio lugar al desarrollo del siguiente capítulo.

En el cuarto capítulo se estudió la versatilidad de los diferentes organocatalizadores  $\text{NO}_2\text{-X}_L\text{-OMe-5aa}$  y  $\text{NO}_2\text{-N}_L\text{-OMe-5aa}$ ,  $\text{NH}_2\text{-X}_L\text{-OMe-10aa}$  y  $\text{NH}_2\text{-N}_L\text{-OMe-10aa}$  y los dímeros en este proceso de formación del compuesto **24aaa** (Figura 4). Los resultados mostraron que el monómero  $\text{NO}_2\text{-X}_L\text{-OMe-5aa}$  proporcionaba el producto deseado de forma exclusiva (>99:1 con respecto al producto de adición Michael) y con un elevado exceso enantiomérico. A su vez, los dímeros  $\text{NO}_2\text{-X}_L\text{X}_L\text{-OMe-25a}$  y  $\text{NO}_2\text{-X}_D\text{X}_L\text{-OMe-25a}$  dieron lugar con total enantiocontrol (ee >99% ee) el producto correspondiente de ciclación, con relaciones altas con respecto al producto Michael.

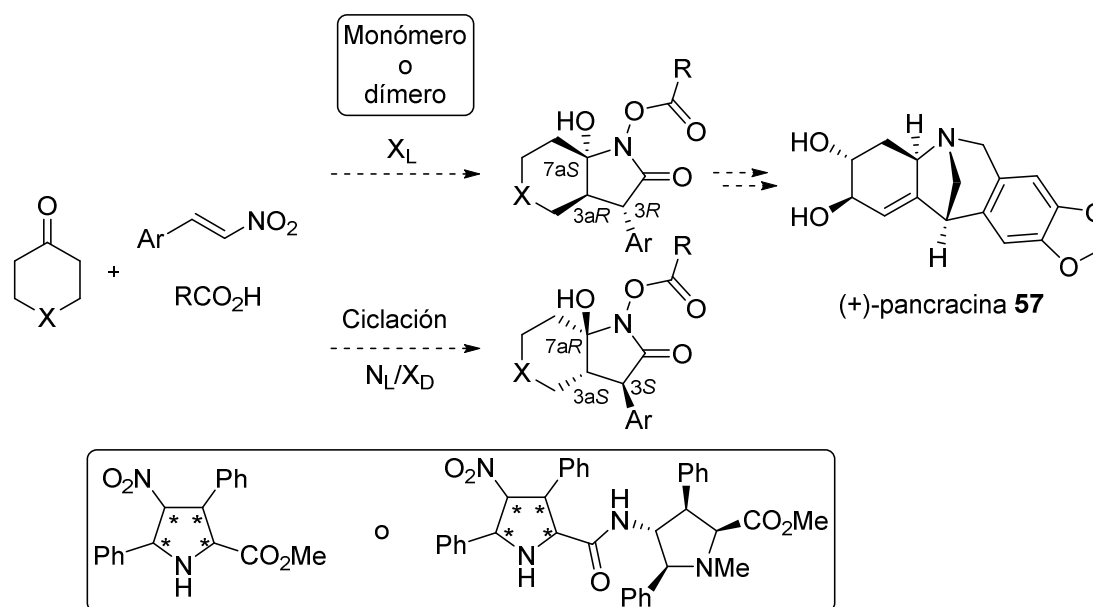


**Figura 4.** Reacción multicomponente de ciclación entre cetonas cíclicas de seis miembros, nitroalquenos aromáticos y ácidos carboxílicos catalizada por los catalizadores de primera y tercera generación, y síntesis hacia el alcaloide (+)-pancracina **57**.

También se llevó a cabo una posterior reacción de derivatización como la hidrogenación catalítica sobre el sustrato **24aaa** proporcionando un rápido acceso a

*cis*- ariloctahidroindoles aromáticos. Por lo tanto, empleando los reactivos de partida adecuados se pudo acceder a una nueva y reducida ruta sintética formal organocatalítica para la formación del alcaloide (+)-pancracina **57**. Además, se muestran los numerosos esfuerzos experimentales realizados para poder determinar el posible mecanismo de reacción.

Para concluir, el quinto capítulo aborda el trabajo que se realizó durante la estancia doctoral de cinco meses de duración en el grupo dirigido por el Profesor H. Hiemstra, Synthetic Organic Chemistry group, de la Universidad de Ámsterdam. El trabajo consistió en la síntesis organocatalítica enantioselectiva del compuesto 1,2,3,4-tetrahidroisoquinolina (THIQ)-1-sustituido **109a** (Figura 5). A pesar de la existencia de una gran variedad de métodos sintéticos para la construcción de estas estructuras, dependientes de la presencia de compuestos metálicos, la versión organocatalítica a partir de la reacción de Pictet-Spengler no está tan expandida.

La reacción original de Pictet-Spengler implica la ciclación entre compuestos  $\beta$ -ariletilamínicos (como triptamina) con aldehídos o cetonas. También se conoce la existencia de la enzima norcoclaurina sintasa, también identificada como Pictet-Spenglerasa, que produce la condensación entre dopamina y 4-hidroxifenilacetaldehído produciendo la 1,2,3,4-THIQ-1-sustituida correspondiente. Como consecuencia, se visualizó un método sintético organocatalítico con feniletilaminas como nucleófilos, las cuales son menos electrofílicas que la triptamina. Trabajos previos del grupo demostraron la eficacia de la reacción organocatalítica de Pictet-Spengler empleando (*R*)-TRIP como organocatalizador entre feniletilaminas protegidas con aldehídos aromáticos y alifáticos.

El nuevo trabajo desarrollado presenta un nuevo sustrato feniletilamínico **101a** convenientemente protegido. Este fue preparado para su empleo en la reacción Pictet-Spengler organocatalítica con arilacetaldehídos. Tras un intenso trabajo de optimización de las condiciones de la reacción se obtuvo el producto **109a** con alto exceso enantiométrico. Más tarde, se pudo completar la síntesis total hacia el compuesto hidrocloreuro de (*R*)-trimetoquinol **LXIII** enantiopuro. Por último, se pudo confirmar la versatilidad del método a través del cual se lograron sintetizar otros 9 alcaloides tetrahidroisoquinolínicos 1-sustituidos de relevancia farmacológica.

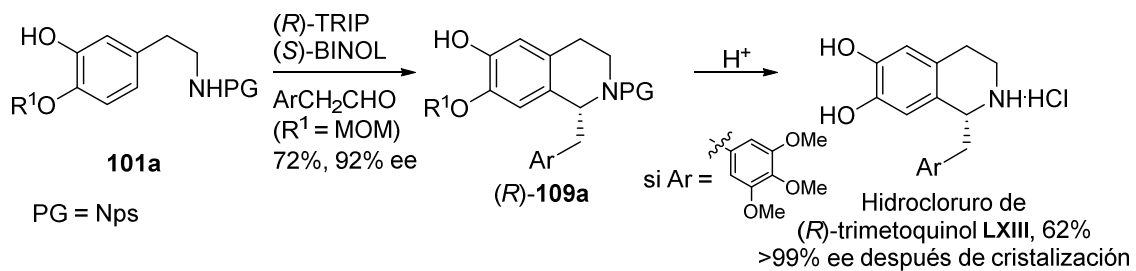


**Figura 5.** Reacción de Pictet-Spengler entre la feniletilamina protegida **101a** y el arilacetaldehído correspondiente catalizada por (*R*)-TRIP y síntesis total del alcaloide hidrocloreuro de (*R*)-trimetoquinol LXIII en su forma enantiopura.

## LIST OF ABBREVIATIONS

Ac	acetyl	DDQ	2,3-dichloro-5,6-dicyano-1,4-benzoquinone
ACN	acetonitrile	de	diastereomeric excess
APT	attached proton test	deg	degrees
aq.	aqueous	DEPC	diethyl cyanophosphonate
Ar	aryl	DET	diethyl tartrate
Atm	atmosphere	DFT	density functional theory
av	average	DHAP	dihydroxyacetone phosphate
B	base	DIPEA	<i>N,N</i> -diisopropylethyl amine
BINAP	(2,2'-bis(diphenylphosphino)-1,1'-binaphthyl)	DMAP	<i>para</i> -dimethylaminopyridine
BINOL	1,1'-bi-2-naphthol	DMEAD	di-2-methoxyethyl azodicarboxylate
Bn	benzyl	DMF	<i>N,N</i> -dimethyl formamide
Boc	<i>tert</i> -butoxycarbonyl	DMSO	dimethyl sulfoxide
br	broad	dr	diastereomeric excess
<sup>t</sup> Bu	<i>tert</i> -butyl	E	electrophile
Bz	benzoyl	EDC	1-ethyl-3-(3-dimethylaminopropyl)carbodiimide
cat.	catalyst	EDG	electron-donating group
Cbz	benzyloxycarbonyl	ee	enantiomeric excess
cont	continuation	EI (ESI)	electrospray ionization
conv	conversion	ent	enantiomer
COSY	correlation spectroscopy	eq	equivalent(s)
CSA	camphorsulfonic acid	Et	ethyl
d	day(s)	EWG	electron-withdrawing group
d	doublet (in NMR)	FD+	field desorption
DCC	<i>N,N</i> -dicyclohexylcarbodiimide	g	gram(s)
DCE	dichloroethane	Gly	glycine
DCM	dichloromethane	h	hour(s)
dd	double doublet (in NMR)		

List of abbreviations

---

HATU	1-[bis(dimethylamino)methylene]-1 <i>H</i> -1,2,3-triazolo[4,5- <i>b</i> ]pyridinium 3-oxid hexafluorophosphate	MS	molecular sieves
hep	heptane	N	<i>endo</i>
hex	hexane	NCS	norcoclaurine synthase
HOBt	hydroxybenzotriazole	nd	not determined
HOMO	highest occupied molecular orbital	NMM	<i>N</i> -Methylmorpholine
HPLC	high pressure/performance liquid chromatography	NMMO	<i>N</i> -methylmorpholine <i>N</i> -oxide
HRMS	high resolution mass spectrometry	NMP	<i>N</i> -methylpyrrolidone
Hz	Hertz	NMR	nuclear magnetic resonance
IBCF	isobutyl chloroformate	Nps	<i>ortho</i> -nitrophenylsulfenyl
INT	intermediate	Nu	nucleophile
FTIR	Fourier transform infrared spectroscopy	obs	observed
<i>J</i>	coupling constants	OPLS	optimized potentials for liquid simulations
LAH	lithium aluminium hydride	P	product
Ln	Naperian logarithm	PE	petroleum ether
LUMO	lowest unoccupied molecular orbital	PG	protecting group
Lys	lysine	Ph	phenyl
M	multiplet (in NMR)	P <sub>i</sub>	inorganic phosphate
M	molar	PNBA	<i>para</i> -nitro benzoic acid
MD	molecular dynamics	ppm	parts per million
Me	methyl	Pr	propyl
MEM	2-methoxyethoxymethyl	<sup>i</sup> Pr	<i>iso</i> -propyl
mg	milligram(s)	Pro	proline
min	minute(s)	ps	picosecond
mL	millilitre(s)	PS	Pictet-Spengler
MOM	methyloxymethyl	PTSA	<i>para</i> -toluenesulphonic acid
m <sub>p</sub>	melting point	Py	pyridine
Ms	methanesulfonyl	PyBOP	(benzotriazol-1-yl-oxy)tripyrrolidinophosphonium hexafluorophosphate
MS	mass spectrum	R	arbitrary substituent



---

rt	room temperature	TES	triethylsilyl ether
s	singlet (in NMR)	Tf	trifluoromethane sulfonyl
Ser	serine	TFA	trifluoroacetic acid
solv	solvent	THBQ	tetrahydro- $\beta$ -carbonile
SPINOL	1,1'-spirobiindane-7-7'-diol	THF	tetrahydrofuran
STRIP	12-hydroxy-1,10-bis(2,4,6-triisopropylphenyl)-4,5,6,7-tetrahydroindeno[7,1- <i>de</i> :1',7'- <i>fg</i> ][1,3,2]dioxaphosphocine 12-oxide	THIQ	tetrahydroisoquinoline
t	time	TLC	thin layer chromatography
t	triplet (in NMR)	TMDA	tetramethylethylenediamine
T	temperature	tol	toluene
TBBP	3,3',5,5'-tetrabromobiphenol	TRIP	3,3'-bis(2,4,6-triisopropylphenyl)-1,1'-binaphthyl-2,2'-diyl hydrogen phosphate
TBS	<i>tert</i> -butyldimethylsilyl	Ts	tosyl
TBTU	2-(1H-benzotriazol-1-yl)-1,1,3,3-tetramethyluronium tetrafluoroborate	T3P	propylphosphonic anhydride
TEA	triethyl amine	vs.	<i>versus</i>
		X	<i>exo</i>



# Chapter 1. Introduction

## **Abstract**

The science of catalysis has been dominated for decades by organometallic chemistry and biocatalysis. However, due to the deeper understanding of organic molecules' reactivity, currently this is being put into practice in order to promote catalysis. As a consequence, the organocatalysis field was born. This chapter briefly introduces the origins of the organocatalysis and modes of classification.



## Note

The field of organocatalysis has rocketed when comparing the number of publications that are published every year. Out of a sudden, a plethora of works appeared in the scientific community and leader authors, overwhelmed by these works, made enormous efforts in order to organize, describe and decode such an impressive mode of action. A great number of small molecules are able to perform organocatalysis, and each of them, depending on the reaction, are able to create interaction on numerous manners. Amines, aminoacids, oligopeptides, alkaloids, carbohydrates, imidazolidinones, metallocenes, biaryl derivatives, sulfoxides... these are an intuitive manner to classify them according to the chiral inductor classes within their structures. Additionally, every now and then, novel species appear in the field which need to be characterized.

This is the reason why almost every year different reviews and books are written in order to gather together the new discoveries, putting great effort on the mode of activation. Due to all these reasons, the present introduction section is brief, presenting as fast as possible the importance of organocatalysis, and then followed by some milestones that need to be mentioned.

### Selected books:

- Berkessel, A.; Gröger, H. *Asymmetric Organocatalysis: from Biomimetic Concepts to Applications in Asymmetric Synthesis*, **2005**, Wiley-VCH.
- Kocovsky, P.; Malkov, A. V. *Organocatalysis in Organic Synthesis*, **2006**, Elsevier.
- Edited Dalko, P. I. *Enantioselective Organocatalysis: Reactions and Experimental Procedures*, **2007**, Wiley-VCH.
- Reetz, M. T.; List, B.; Jaroch, S.; Weinmann, H. *Ernst Schering Foundation Symposium Proceedings: Organocatalysis*, **2008**, Springer.
- List, B. *Topics in Current Chemistry: Asymmetric Organocatalysis*, **2009**, Springer.
- Edited by Song, C. E. *Cinchona Alkaloids in Synthesis and Catalysis: Ligands, Immobilization and Organocatalysis*, **2009**, Wiley-VCH.
- Vicario, J. L.; Badía, D.; Carrillo, L.; Reyes, E. *Organocatalytic Enantioselective Conjugate Addition: a Powerful Tool for the Stereocontrolled Synthesis of Complex Molecules*, **2010**, RSC Publishing.

- Pellissier, H. *Recent Developments in Asymmetric Organocatalysis*, **2010**, Royal Society of Chemistry.
- Edited by Maruoka, K. *Asymmetric Organocatalysis. Volume 1: Lewis Base and Acid Catalysts*. Edited by List, B. *Volume 2: Brønsted Base and Acid Catalysts, and Additional Topics*, **2012**, Thieme.
- Waser, M. *Asymmetric Organocatalysis in Natural Product Syntheses*, **2012**, Springer.
- Ríos, R. *Stereoselective Organocatalysis: Bond Formation Methodologies and Activation Modes*, **2013**, Wiley.
- Edited by Dalko, P. I. *Comprehensive Enantioselective Organocatalysis: Catalysts, Reactions and Applications*, **2013**, Wiley-VCH.

## 1.1. Introduction

Nature is chiral. Chirality refers to the differing behaviour of two entities which are not superimposable mirror images. At molecule scale, each entity receives the name of enantiomer. For instance, the *R*- and *S*- enantiomers (*R* and *S* refer to Latin words *rectus* and *sinister* meaning right and left, respectively) of asparagine I produces sweet or bitter taste when consumed and those of  $\alpha$ -terpene alcohol II gives the smell of lilac or cold pipe, respectively (Figure 1).

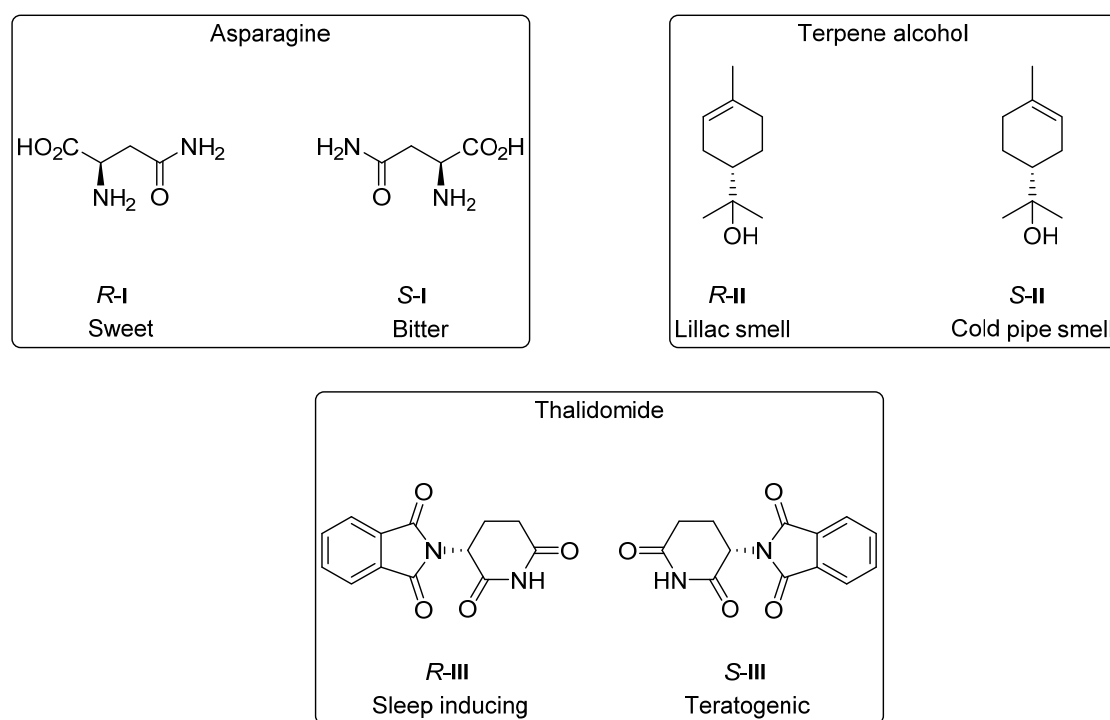


**Figure 1.** Biological effect of different enantiomers.

The property of chirality was independently recognized in 1874 by J. Van't Hoff<sup>1</sup> and J. Le Bel<sup>2</sup>. They proposed that a molecule bearing a carbon atom with four different groups namely asymmetric carbon and having then a tetrahedral structure, two arrangements can be made around this center, which turns out the molecules to be mirror images of one another.

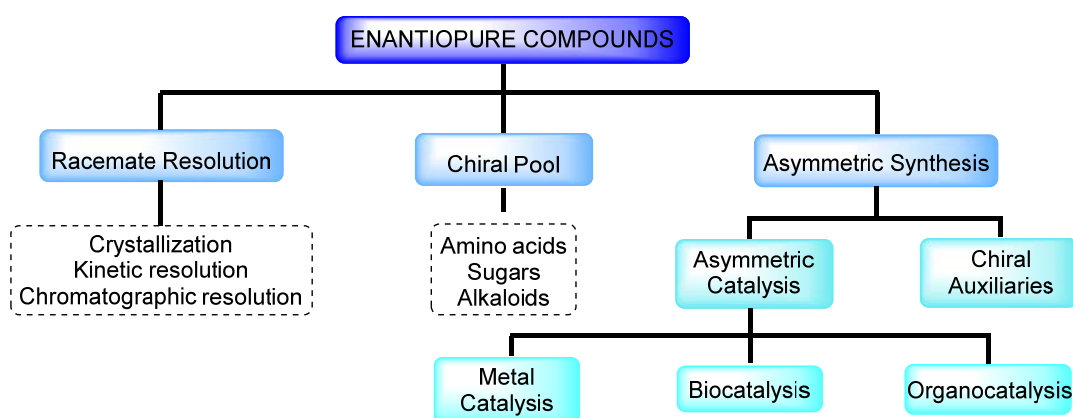
The active ingredients of a great amount of medicines are formed by chiral molecules and the proper interaction of these with the chiral center of biomolecules is essential for life. Well-known example is the case of Thalidomide III (Figure 1). This drug was marketed due to its sleeping inducing<sup>3</sup> effect and as a treatment of vomiting in early pregnancy in the late 50s. It was also advertised as a "completely safe" for everyone. Nevertheless, the thalidomide molecule is a racemic glutamic analog consisting in both *S*- and *R*- forms with the additional capacity to interconvert chirality under physiological

conditions.<sup>4</sup> While the *R*- isomer generated the desired effect, the *S*- isomer produced teratogenic effects on the fetus of pregnant patients. Due to this tragedy and since that moment on, deeper care has been put on the stereochemistry of molecules and a strong push has been given to the chiral or asymmetric synthesis which focuses on the synthesis of compounds favouring the formation of one specific isomer.

## 1.2. Methods for the acquisition of enantiopure compounds

Also known as stereoselective synthesis, asymmetric synthesis is the synthetic process in which onto achiral substrates one or more elements of chirality are formed producing stereomeric products in unequal amounts. Other methods for the obtention of enantiomerically pure forms comprise the resolution of racemates where crystallization, kinetic and chromatographic resolution are frequently used techniques. On the other hand, the employment of the Chiral Pool allows enantiomerically pure forms by modification of already available chiral natural starting material as aminoacids, sugars or alkaloids (Scheme 1).

By employing achiral compounds and reagents in asymmetric processes in absence of any chirality inducing agent, the products are obtained in a 50:50 ratio of enantiomers. In order to unbalance this ratio one of the two following methods are required: the use of chiral auxiliaries that transfer the chiral information or the use of asymmetric catalytic processes.



**Scheme 1.** Strategies to obtain enantiopure substrates.



### 1.2.1. Chiral auxiliaries

These are chiral small molecules that are temporarily and covalently attached to the substrates and transfer chiral information during the synthetic process. After the reaction, the removal of the entity allows enantioenriched final products. Desiderable properties of these units are that they should be cheap and readily available, chemically inert and easily attached and removed. Good examples are Evan's oxazolidinone **IV**, Oppolzer's chiral sultam **V** or Myers' pseudoephedrine **VI** which are employed in diverse reactions such as the aldol (**IV** and **V**), Diels-Alder (**V**) and alkylation (**V** and **VI**) reactions, among others (Figure 2).

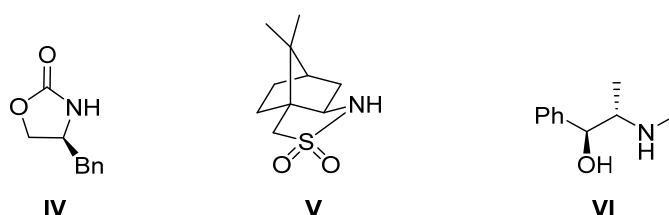


**Figure 2.** Representative chiral auxiliaries.

As said, this method adds two extra steps in the process: attachment to the initial substrate and cleavage of the chiral auxiliary from the final product. Since stoichiometric amounts of it are needed, more desirable methods are of choice for asymmetric synthesis.

### 1.2.2. Asymmetric catalysis

As a consequence, asymmetric catalysis has emerged as The Method to achieve enantioinduced reactions. It consists of the use of a chiral catalyst which acts as a template for the stereoselective synthesis, providing predominantly the desired enantiomeric product (Figure 3). As Nicolau reported in *Classics in Total Synthesis*<sup>5</sup> in the middle 90s "In a catalytic asymmetric reaction, a small amount of an enantiomerically pure catalysts, either an enzyme or a synthetic, soluble transition metal complex, is used to produce large quantities of an optically active compound from a precursor that may chiral or achiral".

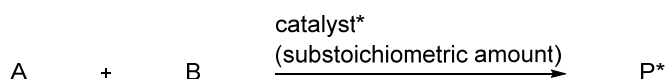


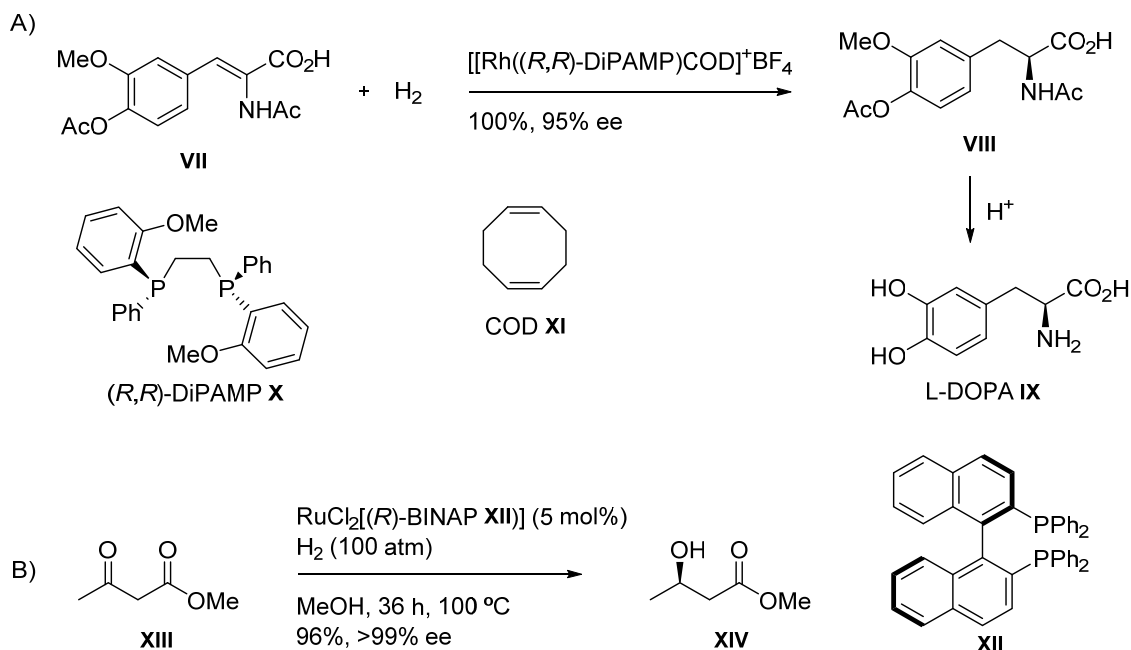
**Figure 3.** General scheme for asymmetric catalyzed reaction.

Nevertheless nowadays, three main streams can be considered within asymmetric catalysis: biocatalysis, organometallic catalysis and organocatalysis. Biocatalysis uses protein enzymes (or few catalytic RNA molecules) in order to get the mentioned goal. These macromolecules fold producing tridimensional structures. They contain both binding and active sites, where the substrates are binded (the “lock and key” model<sup>6</sup> and more refined “induced fit” model<sup>7</sup> have been suggested) and properly oriented. Then, the catalyst’s site, which is able to decrease the chemical activation energy, allows the reaction process to occur. Although this methodology provides high enantioselectivities and regioselectivities under mild conditions or even in water solvent, the enzyme instability at extreme temperatures or pH values and its high specific reactivity makes this methodology only useful for selected reactions.

On the other side, both organometallic catalysis and organocatalysis rely in the same principle in which a substoichiometric amount of chiral catalyst is able to induce chirality in the reaction process by producing interactions with the substrates. Due to the reversibility of the interaction, once the process has occurred, the product splits from the complex releasing the catalyst and allowing it to participate in a new catalytic cycle.

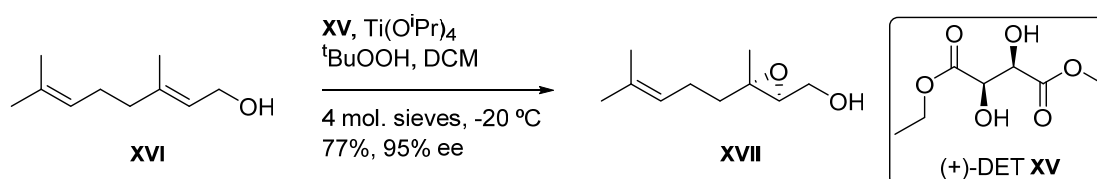
Organometallic catalysis makes use of the reactivity of molecular compounds with metallic centers containing at least one (even temporary) metal-carbon bond. These catalysts are widely employed in homogeneous catalysis. In general, the mechanistic pathway involves first the replacement of ligands by the substrates. Then, due to the close proximity of the reagents the chiral information flows from the chiral environment around the metallic centre and the C-C bond forming step takes place in an enantioselective manner. Release of the product recovers the catalyst which can be introduced in another cycle. This chemistry has been the tool of choice for the last decades<sup>8</sup> and awarded Professors W. S. Knowles, R. Noyori and K. B. Sharpless the Nobel Prize of Chemistry in 2001<sup>9</sup> for the chirally catalyzed hydrogenation (Knowles, Noyori) and oxidation (Sharpless) reactions. Knowles and co-workers at Monsanto developed the first industrial asymmetric synthesis of the rare aminoacid L-DOPA **IX** via olefin hydrogenation reaction of **VII**, which is proven to be a successful drug against Parkinson disease (Scheme 2A). In this case a cationic rhodium complex was employed containing (*R,R*)-DiPAMP **X** as chiral ligand.<sup>10</sup> Noyori, on the other hand, proposed a similar hydrogenation method, this time involving the reduction of ketones to provide optically active secondary alcohols such as **XIV**.<sup>11</sup> Ruthenium-BINAP **XII**

complexes are usually employed as source of enantioinduction in this kind of reactions (Scheme 2B).



**Scheme 2.** A) The Monsanto synthesis of L-DOPA IX aminoacid using catalytic asymmetric hydrogenation developed by Knowles. B) Catalytic asymmetric hydrogenation of ketones developed by Noyori.

Sharpless on the contrary, promoted the oxidation reaction of the allylic alcohol XVI to prepare enantioselectively the epoxyalcohol XVII by employing a titanium complex and diethyl tartrate XV (Scheme 3).<sup>12</sup> In this reaction, the stereochemistry is determined by the chiral environment created by the titanium/chiral tartrate diester complex. These epoxyalcohols can be later functionalized as diols, aminoalcohols or ethers, becoming a common methodology found in the synthesis of valuable products.



**Scheme 3.** Sharpless asymmetric epoxidation reaction.

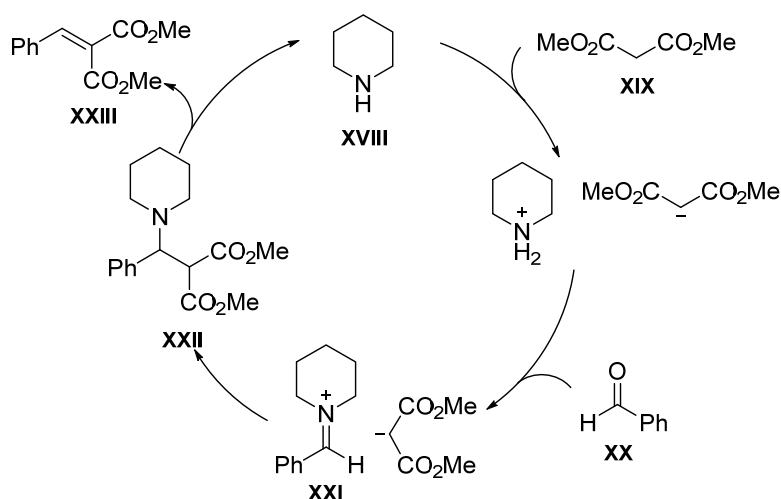
This field has been greatly explored and developed and it is employed in a vast array of reactions as reductions, oxidations, insertion in  $\sigma$  bonds or activations of  $\pi$  bonds. Nevertheless, the high cost of some toxic complexes, the high demanding reaction conditions and the easy contamination of the final products make this methodology difficult to apply to the synthesis of commercially available drugs.

Due to the necessity to remove highly contaminating additives from the chemical processes and in order to get a closer mimicry to Nature, which rarely uses metals in the biocatalytical processes, the field of organocatalysis is becoming the target field to be exploited due to its favourable reaction conditions. The following section focuses more deeply into this field.

### 1.3. Asymmetric organocatalysis

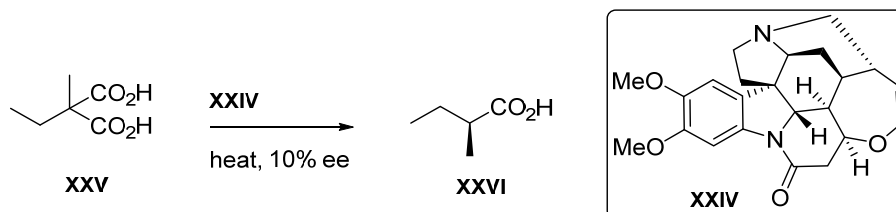
The third main stream is organocatalysis<sup>13</sup> which uses substoichiometric quantities of small organic molecules to induce chirality in chemical processes. Main advantages and characteristics of this field is the absence of any metal element in the catalyst providing in general lower toxic compounds. Other attributes are their stability towards oxygen or moisture and straightforward synthesis, as a vast majority of organocatalysts are derived from the chiral pool and can be obtained in large quantities. Thus, Nicolau's definition became outdated when List in 2007 claimed organocatalysis at the same level as catalysis with transition metal complexes and biocatalysis.<sup>14</sup>

Although organocatalysis has been recognized lately, the use of small organic molecules in order to accelerate or catalyze reactions has already been known for years giving as an example the Knoevenagel condensation<sup>15</sup> which uses piperidine **XVIII** in catalytic quantities to accelerate the condensation between diethyl malonate **XIX** and benzaldehyde **XX** (Scheme 4). The reaction mechanism is believed to go through the iminium intermediate **XXI** formed upon condensation with **XX**. This way, the electrophilicity of the electrophile **XX** is increased and nucleophilic attack and later detachment provides the condensation product **XXIII** recovering piperidine **XVIII**.



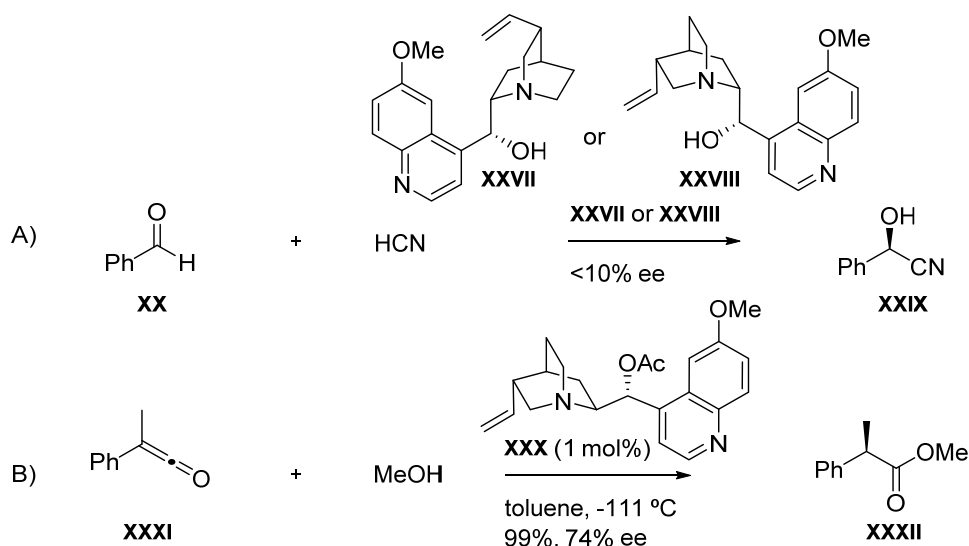
**Scheme 4.** Knoevenagel condensation catalyzed by piperidine **XVIII**.

Nevertheless, it was not until 1904 when Marckwald carried out the decarboxylation reaction of malonate derivative **XXV** in the presence of brucine **XXIV** allowing the product **XXVI** with 10% of enantiomeric excess (Scheme 5).<sup>16</sup> As brucine was appointed as the enantioselectivity inductor, this reaction is considered the very first organocatalytic reaction.



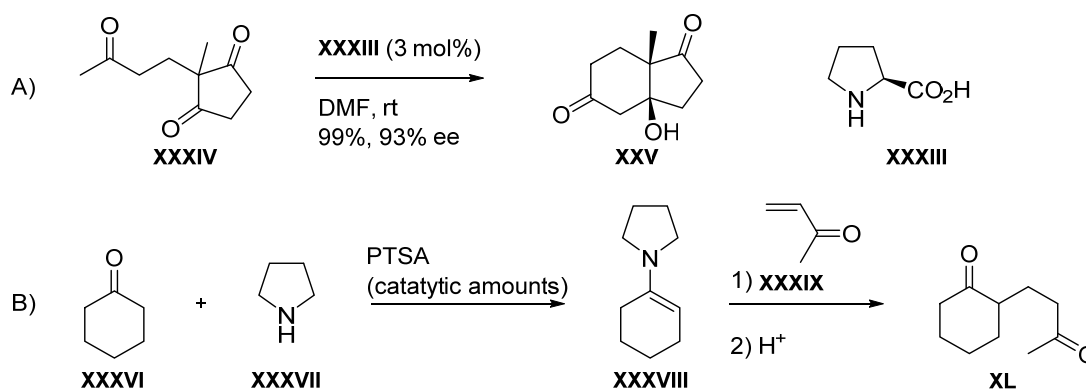
**Scheme 5.** First organocatalytic reaction performed by Marckwald.

Other isolated organocatalyzed reactions occurred years later. For instance, the addition of hydrogen cyanide to benzaldehydes in the presence of quinine **XXVII** or quinidine **XXVIII** with low ee's was carried out by Bredig and Fiske in 1912 (Scheme 6A).<sup>17</sup> Then, the addition of methanol to phenylmethyl ketene **XXXI** employing O-benzoylquinine **XXX**, as described by Pracejus<sup>18</sup> in 1960, provided higher enantiomeric excesses. This latter transformation has been highlighted as the first organocatalytic asymmetric reaction (Scheme 6B). This reaction is also considered as the starting point of organocatalysis based on cinchona alkaloid units.<sup>19</sup>



**Scheme 6.** Other organocatalytic reactions performed by A) Bredig and Fiske, and B) Pracejus.

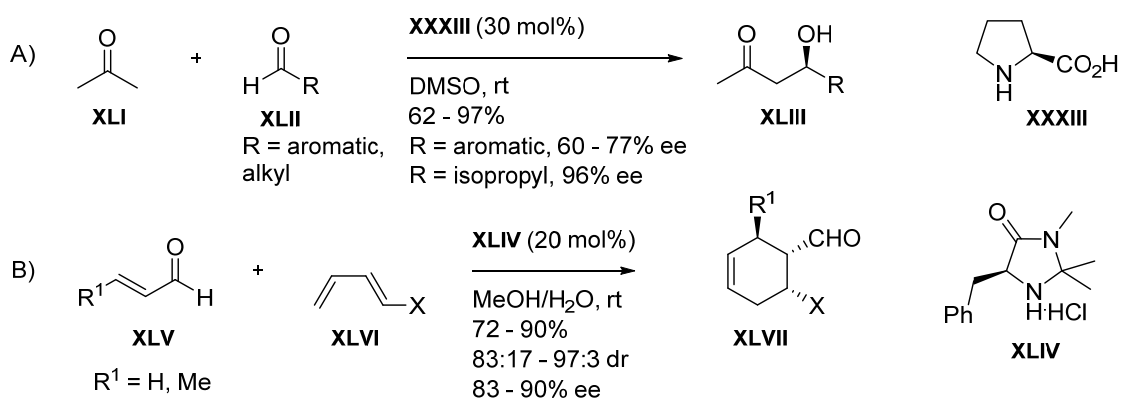
However, it was in 1971 when two independent industrial research groups at Hoffmann-La Roche<sup>20</sup> and Schering<sup>21</sup> described the intramolecular aldol reaction catalyzed by L-Proline **XXXIII** to provide the bicyclic ketol **XXV**, also known as the Hajos-Parrish-Eder-Wiechert-Sauer reaction (Scheme 7A). This reaction was based on the Stork enamine reaction<sup>22</sup> as substoichiometric amount of the secondary amine pyrrolidine **XXXVII** could provide a reversible formation of a nucleophilic enamine **XXXVIII** (Scheme 7B).



**Scheme 7.** A) Intramolecular aldol reaction catalyzed by L-Proline **XXXIII** inspired in the B) Stork enamine reaction.

From that date, some other works were published but no less important as the alkylation of enolates using cinchona alkaloids based ammonium salts<sup>23</sup>, Julia's epoxidation aided by polyaminoacids<sup>24</sup> or Denmark's phosphoramidate-catalyzed aldol reaction<sup>25</sup>. However, it was not until the year 2000 that the field experienced an explosive growth. That year, two groups published simultaneously landmarks for the enamine and iminium activated based organocatalysis. While the group of Barbas III

introduced the intermolecular variant of the aldol reaction<sup>26</sup> between unmodified ketones as **XLI** and aldehydes (Scheme 8A), MacMillan introduced for the first time the term “organocatalysis” by displaying the enantioselective organocatalyzed Diels-Alder reaction (Scheme 8B) promoted by imidazolidinone salt **XLIV**<sup>27</sup>.



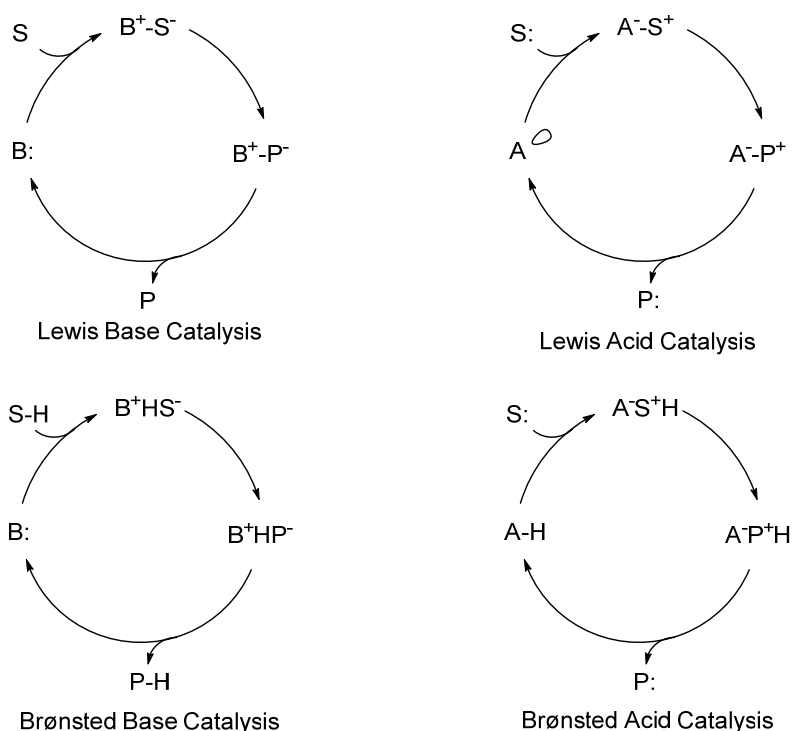
**Scheme 8.** A) Intermolecular aldol reaction catalyzed by L-Proline **XXXIII** and B) Diels-Alder reaction catalyzed by imidazolidinone salt **XLIV**, respectively.

### 1.3.1. Types of organocatalysis

Organocatalysts can be classified according to different criteria such as their structure, interactions they perform, mechanistic pathway in which they are involved and/or even regarding the reactions that are capable to activate. The most common approach to classify these molecules is, according to their structure: they can be distinguished as Lewis acids or bases, or Brønsted acids or bases. Nevertheless, they are mainly categorized due to the mechanistic pathways they generate, via covalent or non-covalent interactions.

#### 1.3.1.1. Acid/base classification

List started this task by reporting four manners in which most of the organocatalysts could be defined. This way, the catalysts could be accordingly catalogued to the two complementary definitions of acids and bases: using the Lewis definition for their electron donor-acceptor nature<sup>28</sup>, or Brønsted definition involving the ability to donate or accept a proton<sup>29</sup>. The simplified catalytic cycles associated with this classification are depicted in Scheme 9.



**Scheme 9.** Organocatalysts classified according to their basicity/acidity reactivity.

Catalytic cycles that are under the influence of Lewis base (B:) organocatalysts usually commence by a nucleophilic attack to one of the substrates (S). The corresponding intermediate  $B^+S^-$  reacts to give the product (P) and also recovers the catalysts. Catalytic cycles under the influence of Lewis acid (A) organocatalysts start in a similar manner via an electrophilic addition to the substrate to give rise to intermediates  $A^+S^-$  (Scheme 9). Examples of Lewis bases are those derived from amines, phosphines or *N*-heterocyclic carbenes. Phase-transfer catalysts, Denmark's phosphoramides<sup>30</sup> or chiral *N*-oxides<sup>31</sup> are considered as Lewis acid catalysts.

On the other side, Brønsted bases and acids involve cycles proceeding via protonation or deprotonation.<sup>32</sup> While Brønsted bases activate the pro-nucleophilic substrate via the removal of a proton transforming it into more reactive specie ( $B^+HS^-$ ), Brønsted acids are able to activate the substrate by donating or providing H bonding interactions. Typical models of Brønsted bases are guanidines<sup>33</sup> or chiral amines<sup>34</sup> that by deprotonation activate the pro-nucleophiles, and examples of Brønsted acids, as phosphoric acids<sup>35</sup>, *N*-triflyl phosphamides<sup>36</sup> or chiral carboxylic acids<sup>37</sup>, are those which interact via hydrogen bonding with the substrates.



### 1.3.1.2. Covalent/non-covalent classification

A different type of classification is based on the kind of interactions that occur between the organocatalyst and the substrates. These interactions can be weak and non-covalent such as hydrogen bonds<sup>38</sup> or ionic pairs<sup>39</sup>. The alternative interaction is stronger and involves formation and cleavage of covalent bonds (Figure 4). This classification was proposed by Langenbeck in 1949<sup>40</sup>, but is still applicable to the current organocatalytic reactions.

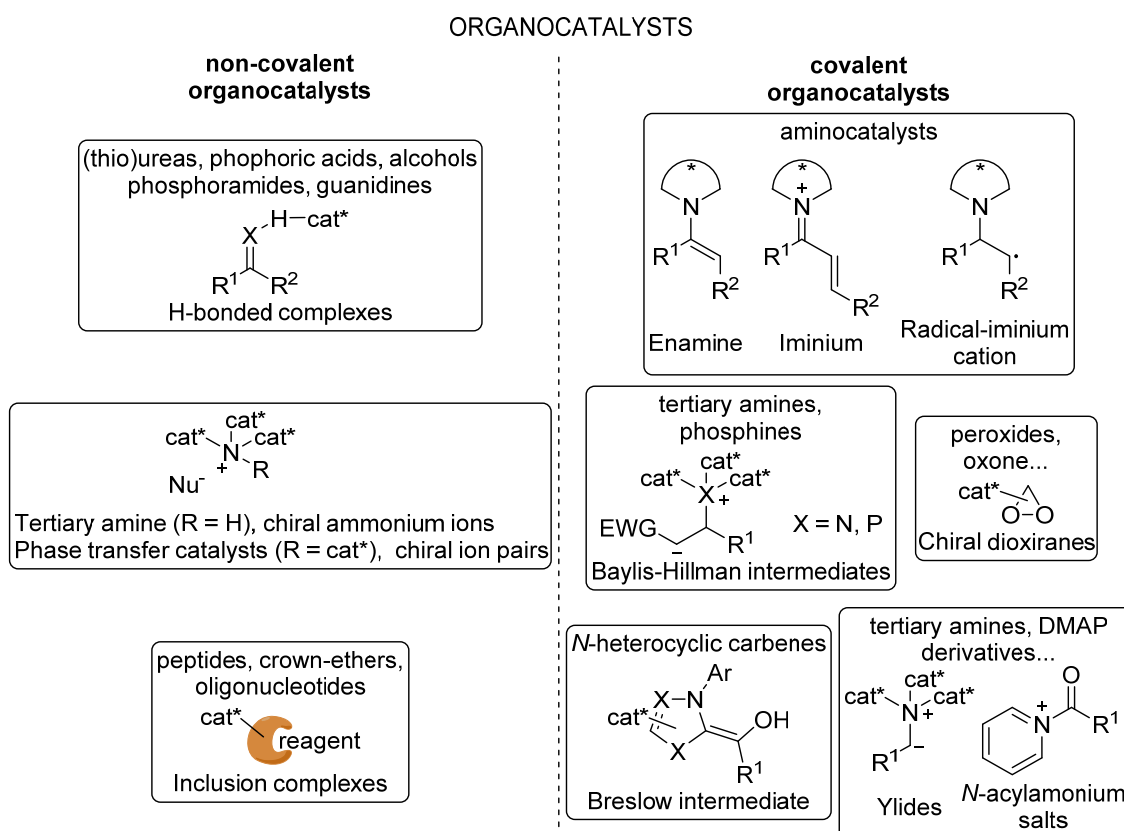


**Figure 4.** Organocatalysts classified according to non-covalent/covalent terms.

Non-covalent organocatalysis refers to the catalysis including the acid-base ion pairing or catalyst-substrate complexation. The first one can be accomplished by the formation of a hydrogen bond array provided by, for instance, Brønsted acids as phosphoric acids, thioureas or guanidines. Additionally, ion pairing can be formed in enantiomeric manner by chiral quaternary ammonium ions.

Covalent activation, on the contrary, involves to the activation of a substrate via covalent bond formation. It directly implies reversible procedures of attaching to create the active substrate, followed by the chemical reaction *per se*, and lastly, detaching to allow the product and release the catalyst. Since this type of interaction is in strong

nature, covalent organocatalysis usually requires higher catalytic loading in order to aid full conversions and to ease the catalytic cycle to completion. Aminocatalysts belong to this group. These chiral amines are able to form enamine<sup>41</sup>, iminium<sup>42</sup> or iminium-radical<sup>43</sup> intermediates depending on the substrate they are activating. In addition, other tertiary amines (acting as Lewis bases) activate substrates by forming the corresponding ylides as well as trialkylphosphines and trialkylamines for, for instance, the Morita-Baylis-Hillman reaction. *N*-heterocyclic carbenes also lay in this group and are known for providing Breslow intermediates.<sup>44</sup> Lastly, chiral oxiranes find their place in organocatalysis for being able to catalyze oxidation reactions.<sup>45</sup>

<sup>1</sup> Van't Hoff, J. H. *Bull. Soc. Chim. France* **1875**, 23, 295-301.

<sup>2</sup> Le Bel, J. A. *Bull. Soc. Chim. France* **1874**, 22, 337-347.

<sup>3</sup> Lasagna, L. *J. Chronic. Dis.* **1960**, 11, 627-631.

<sup>4</sup> Franks, M. E.; Macpherson, G. R.; Figg, W. D. *The Lancet* **2004**, 363, 1802-1811.

<sup>5</sup> Nicolau, K. C.; Sorensen, E. J. *Classics in Total Synthesis*, **1996**, Wiley-VCH.

<sup>6</sup> Fischer, E. *Einfluss der Configuration auf die Wirkung der Enzyme. Ber Dtsch Chem Ges.* **1894**, 27, 2985-2993.

<sup>7</sup> Koshland, D. E. *Proc. Natl. Acad. Sci.* **1958**, 44, 98-104.

<sup>8</sup> (a) Jacobsen, E. N.; Pfaltz, A.; Yamamoto, H. *Comprehensive Asymmetric Catalysis I-III*, **1999**, Springer: Heidelberg. (b) Steinborn, D. *Fundamentals of Organometallic Catalysis*, **2011**, Wiley-VCH.

<sup>9</sup> [http://www.nobelprize.org/nobel\\_prizes/chemistry/laureates/2001/](http://www.nobelprize.org/nobel_prizes/chemistry/laureates/2001/).

<sup>10</sup> (a) Vineyard, B. D.; Knowles, W. S.; Sabacky, M. J.; Bachman, G. L.; Weinkauff, D. J. *J. Am. Chem. Soc.* **1977**, 99, 5946-5952. (b) Knowles, W. S. *Acc. Chem. Res.* **1983**, 16, 106-112.

<sup>11</sup> Noyori, R.; Ohkuma, T.; Kitamura, M.; Takaya, H.; Sayo, N.; Kumobayashi, H.; Akutagawa, S. *J. Am. Chem. Soc.* **1987**, 109, 5856-5858.

<sup>12</sup> Katsuki, T.; Sharpless, K. B. *J. Am. Chem. Soc.* **1980**, 102, 5974-5976.

<sup>13</sup> (a) *Acc. Chem. Res.* **2004**, 37, 487-631. (b) Bertelsen, S.; Jørgensen, K. A. *Chem. Soc. Rev.* **2009**, 38, 2178-2189.

<sup>14</sup> List, B. *Chem. Rev.* **2007**, 107, 5413-5415.

<sup>15</sup> Knoevenagel, E. *Ber. Dtsch. Chem. Ges.* **1896**, 29, 172-174.

<sup>16</sup> Marckwald, W. *Ber. Dtsch. Chem. Ges.* **1904**, 37, 349-354.

<sup>17</sup> Bredig, G.; Fiske, W. S. *Biochem. Z.* **1912**, 46, 7-23.

<sup>18</sup> (a) Pracejus, H. *Justus Liebigs Ann. Chem.* **1960**, 634, 9-22. (b) Pracejus, H.; Mätje, H. *J. Prakt. Chem.* **1964**, 24, 195-205.

<sup>19</sup> (a) Langström, B.; Berson, G. *Acta Chem. Scand.* **1973**, 27, 3118-3119. (b) Wynberg, H.; Helder, R. *Tetrahedron Lett.* **1975**, 16, 4057-4060. (c) Hiemstra, H.; Wynberg, H. *J. Am. Chem. Soc.* **1981**, 103, 417-430.

<sup>20</sup> (a) Hajos Z. G.; Parrish, D. R. *Ger. Pat.* July 29<sup>th</sup> **1971**, DE 2102623. (b) Hajos Z. G.; Parrish, D. R. *J. Org. Chem.* **1974**, 39, 1615-1621.

<sup>21</sup> (a) Eder, U.; Sauer, G.; Wiechert, R. *Ger. Pat.* October 7<sup>th</sup> **1971**, DE 2014757. (b) Eder, U.; Sauer, G.; Wiechert, R. *Angew. Chem. Int. Ed.* **1971**, 10, 496-497.

<sup>22</sup> Stork, G.; Terrell, R.; Szmuszkovicz, J. *J. Am. Chem. Soc.* **1954**, 76, 2029-2030.

<sup>23</sup> Dolling, U.-H.; Davis, P.; Grabowski, E. J. *J. Am. Chem. Soc.* **1984**, 106, 446-447.

<sup>24</sup> Julià, S.; Masana, J.; Vega, J. C. *Angew. Chem. Int. Ed.* **1980**, 19, 929-931.

<sup>25</sup> Denmark, S. E.; Winter, S. B. D.; Su, X.; Wong, K.-T. *J. Am. Chem. Soc.* **1996**, 118, 7404-7405.

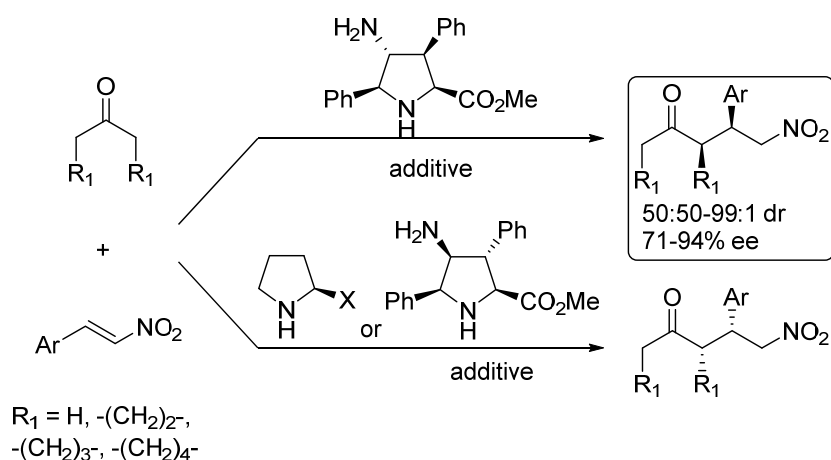
<sup>26</sup> List, B.; Lerner, R. A.; Barbas III, C. F. *J. Am. Chem. Soc.* **2000**, 122, 2395-2396.

<sup>27</sup> Ahrendt, K. A.; Borths, C. J.; MacMillan, D. W. C. *J. Am. Chem. Soc.* **2000**, 122, 4243-4244.

- <sup>28</sup> Ratjen, L.; van Gemmeren, M.; Pesciaioli, F.; List, B. *Angew. Chem. Int. Ed.* **2014**, *53*, 8765-8769.
- <sup>29</sup> Parmar, D.; Sugiono, E.; Raja, S.; Rueping, M. *Chem. Rev.* **2014**, *114*, 9047-9153.
- <sup>30</sup> Denmark, S. E. *Chimia*, **2008**, *62*, 37-40.
- <sup>31</sup> (a) Malkov, A.; Kocovsky, P. *Eur. J. Org. Chem.* **2007**, 29-36. (b) Chen, J.; Takenaka, N. *Chem. Eur. J.* **2009**, *15*, 7268-7276.
- <sup>32</sup> Palomo, C.; Oiarbide, M.; López, R. *Chem. Soc. Rev.* **2009**, 632-653.
- <sup>33</sup> Ye, W.; Jiang, Z.; Zhao, Y.; Goh, S. L. M.; Leow, D.; Soh, Y.-T.; Tan, C.-H. *Adv. Synth. Catal.* **2007**, *349*, 2454-2458.
- <sup>34</sup> Wu, F.; Li, H.; Hong, R.; Deng, L. *Angew. Chem. Int. Ed.* **2006**, *45*, 947-950.
- <sup>35</sup> Akiyama, T.; Itoh, J.; Yokota, K.; Fuchibe, K. *Angew. Chem. Int. Ed.* **2004**, *43*, 1566-1568.
- <sup>36</sup> Nakashima, D.; Yamamoto, H. *J. Am. Chem. Soc.* **2006**, *128*, 9626-9627.
- <sup>37</sup> Momiyama, N.; Yamamoto, H. *J. Am. Chem. Soc.* **2005**, *127*, 1080-1081.
- <sup>38</sup> Doyle, A. G.; Jacobsen, E. N. *Chem. Rev.* **2007**, *107*, 5713-5743.
- <sup>39</sup> Brière, J.-F.; Oudeyer, S.; Dalla, V.; Levacher, V. *Chem. Soc. Rev.* **2012**, *41*, 1696-1707.
- <sup>40</sup> Langenbeck, W. *Die organischen Katalysatoren und ihre Beziehungen zu den Fermenten*, **1949**, Springer.
- <sup>41</sup> Kano, T.; Maruoka, K. *Chem. Commun.* **2008**, 5465-5473.
- <sup>42</sup> Erkkilä, A.; Majander, I.; Pihko, P. M. *Chem. Rev.* **2007**, *107*, 5416-5470.
- <sup>43</sup> Melchiorre, P. *Angew. Chem. Int. Ed.* **2009**, *48*, 1360-1363.
- <sup>44</sup> Enders, D.; Niemeier, O.; Henseler, A. *Chem. Rev.* **2007**, *107*, 5606-5655.
- <sup>45</sup> Denmark, S. E.; Wu, Z. *Synlett.* **1999**, 847-859.



# Chapter 2. Densely Substituted 4-Amino Pyrrolidines. Design and Organocatalysis



## Abstract

*Exo*- and *endo*- densely substituted 4-aminoprolinate esters can easily be synthesized via (3+2) cycloaddition between nitroalkenes and azomethine ylides followed by catalytic hydrogenation. Encouraged by the efficiency of L-Proline based organocatalysts in several C-C bond transformations, these new entities were analyzed in the aldol and Michael reaction. It has been found out that the enantiomeric outcome depends on the configuration of each substituent in the catalysts. While *endo*- catalysts provide the same enantioinduction that L-Proline, *exo*- catalysts provide the opposite enantiomer, belonging both catalysts to the same L-aminocid series.

Part of this chapter has been published as: Ruiz-Olalla, A.; Retamosa, M. G.; Cossío, F. P. *J. Org. Chem.* **2015**, *80*, 5588-5599.

Article also selected by the ACS Catalysis Journal: Ooi, T. Virtual Issue Posts on Organocatalysis: Design, Applications, and Diversity. *ACS Catal.* **2015**, *5*, 6980-6988.

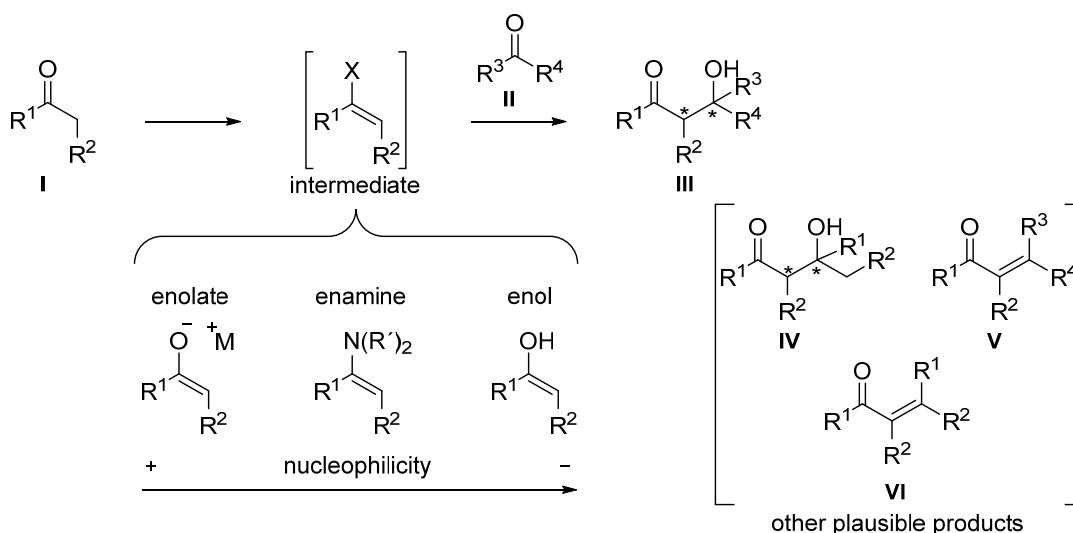


## 2.1. Introduction. Organocatalysts in enamine-activated type reactions

Primary and secondary amines can react in a reversible manner with enolizable ketones and aldehydes affording nucleophilic enamines. If chiral amines are employed as organocatalysts, the nucleophilic attack can occur in an enantioselective manner. This introduction will focus on two well-described organocatalytic processes such as the aldol and the Michael reactions. Both are typically activated by means of chiral pyrrolidine-based secondary amines to produce enantioenriched products.

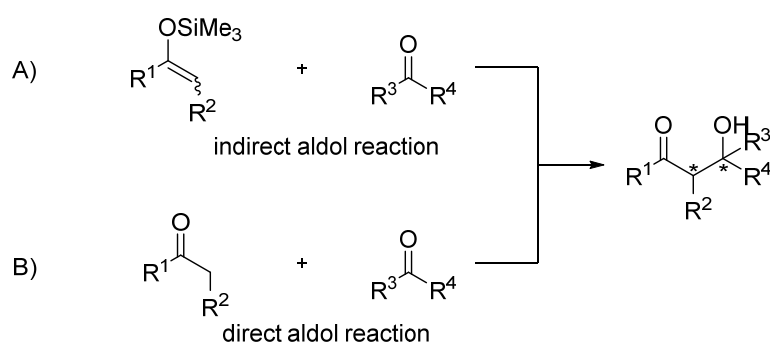
### 2.1.1. Intermolecular aldol reaction

The aldol reaction was discovered by Kane in 1838<sup>1</sup> and Wurtz in 1872<sup>2</sup>. It involves the condensation between an enolizable carbonyl compound and a second carbonyl compound, usually an aldehyde. Ketones can also be used as electrophiles but due to their lower electrophilicity, activated ketones are employed instead, for instance phenylglyoxylates.<sup>3</sup> There are different methods according to the nucleophilic attack to the electrophile in this reaction (Scheme 1). If **I** is treated with a base, then the enolate is the nucleophilic species. When an addition reaction occurs between this enolizable ketone and a primary or secondary amine, then the enamine is the nucleophilic species. Finally, enols can act as nucleophiles. Nevertheless, if the reaction conditions are not well designed, side reactions can easily occur yielding self and cross aldol products **IV** and **V**, or aldol condensation product **VI**.



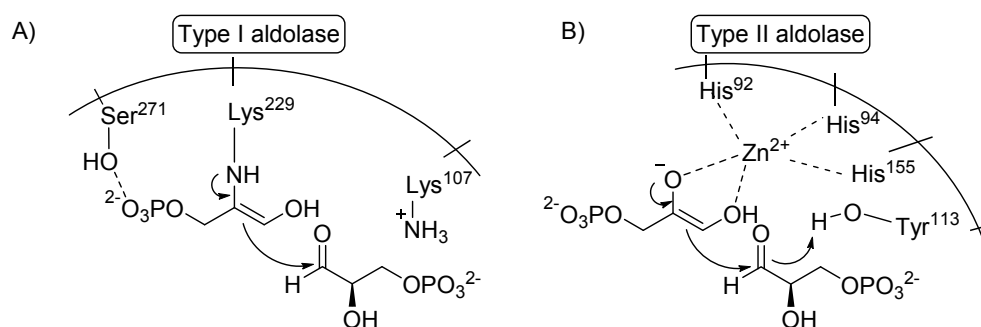
**Scheme 1.** Aldol reaction between carbonyl compounds.

This  $\beta$ -hydroxycarbonyl moiety **IV** is largely found in nature and drugs. As a consequence, this transformation has gathered considerable attention among the synthetic community. One of the most outstanding reactions for aldol C-C bond formation is the Mukaiyama “indirect” aldol reaction (Scheme 2A). However, it implies the preactivation of the carbonyl group as nucleophilic silyl enol ether and additionally, the reaction is assisted with metallic Lewis acids.<sup>4</sup> Additionally, the set up of this method brings intrinsically toxic wastes derived from the stoichiometric needs of silylating agent and base. Thus, the organocatalyzed reaction (Scheme 2B), in which the reaction occurs “directly” providing atom economy, seems a better approach.



**Scheme 2.** Indirect and direct aldol reactions.

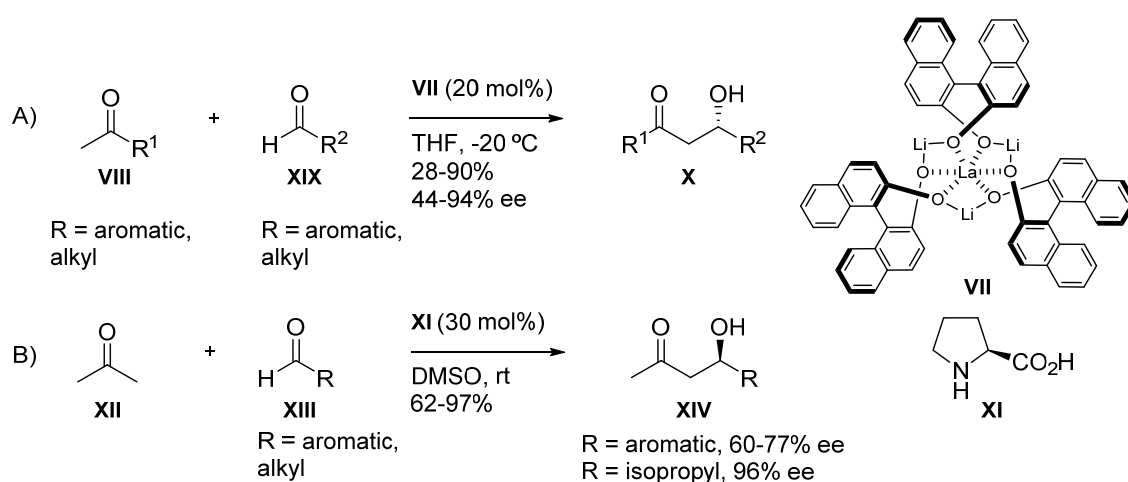
Aldolases<sup>5</sup> are a subgroup of lyase enzymes that catalyze in vivo the addition of a ketone donor to an aldehyde in enantioselective manner. Around 30 different aldolases have been identified, which can be classified according to the mechanism they perform. Type I aldolases, which are mainly found in higher plants and animals, activate the donor by creating a temporary Schiff base helped by the Lysine 229 residue followed by enamine formation which adds stereoselectively to the aldehyde (Scheme 3A). On the other hand, type II aldolases, located in fungi and bacteria, possess a  $Zn^{2+}$  cofactor in the active site, which interacts with the donor ketone as a Lewis acid creating a metallic enolate (Scheme 3B).



**Scheme 3.** Aldol reaction catalyzed by aldolases A) types I and B) type II.

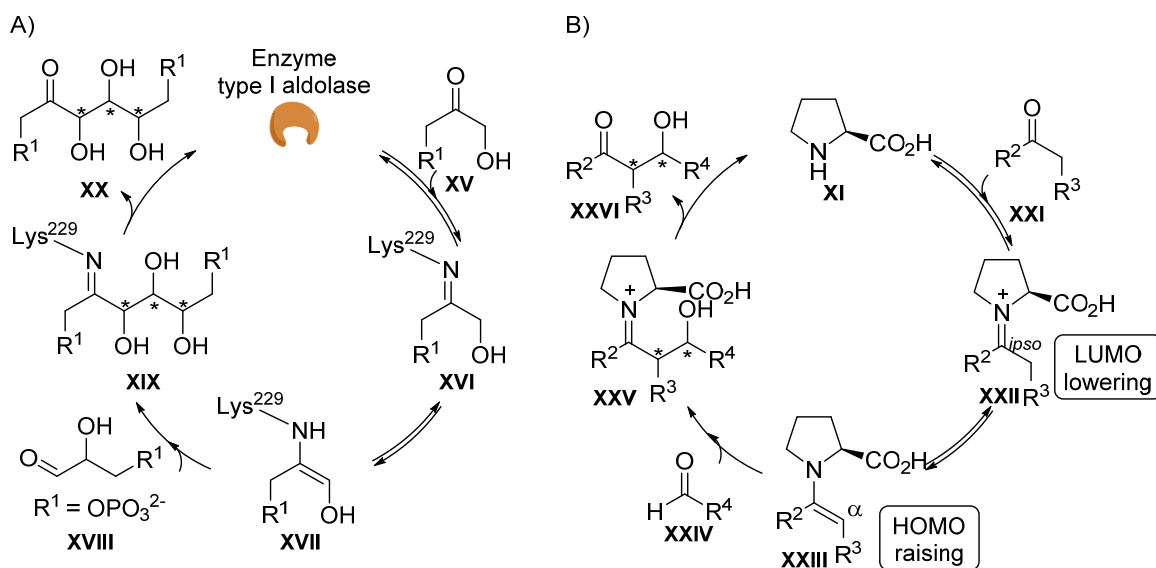


As shown in Scheme 7A of the previous chapter, in 1971 the L-Proline organocatalyzed intramolecular direct aldol reaction of triketone **XXXIV** was reported by Hajos and Parrish, and Eder, Wiechert and Sauer. Years later in 1997, Shibasaki showed that bifunctional metal complex **VII**, thus mimicking type II aldolases<sup>6</sup>, could also perform the reaction. This catalyst provided the aldol addition products in moderate yields and enantioselectivities with either aromatic or aliphatic ketones and aldehydes (Scheme 4A).<sup>7</sup> This work was soon followed by the other studies of Barbas III in which the intermolecular variant of the aldol reaction catalyzed by L-Proline **XI**, simulating type I aldolases<sup>8</sup> was reported (Scheme 4B).



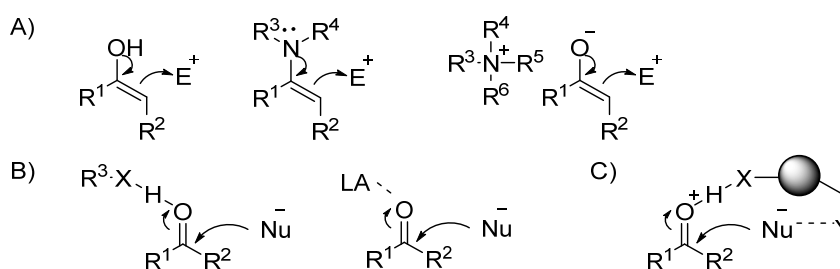
**Scheme 4.** Intermolecular aldol reaction catalyzed by A) bifunctional metal complex by Shibasaki and B) L-Proline performed by the group of Barbas III.

The accepted reaction mechanism for type I aldolases involves activation of the donor substrate **XV** via Lysine 229 residue (Scheme 5A) forming first the imine **XVI** which yields enamine **XVII** after tautomerization. This latter intermediate has a higher HOMO energy (comparing to **XV**). This enamine attacks now the proper face of the aldehyde electrophile **XVIII**, and lastly, the enzyme-bound imine **XIX** is hydrolyzed providing the addition product **XX** and recovering the aldolase. Similarly, an enamine mechanism is considered for the L-Proline catalyzed aldol reaction (Scheme 5B). L-Proline activates the donor **XXI**, which in first instance is transformed into the iminium intermediate **XXII**. This generates a decrease on the electron density on the *ipso*- carbon (LUMO decrease), activating it towards a possible electrophilic attack. Tautomerization towards the enamine **XXIII**, generates an increase in electron density in the  $\alpha$ - carbon (HOMO rising), which is now a suitable nucleophile, able to attack the electrophilic aldehyde **XXIV**. Lastly, the imine intermediate **XXV** is hydrolyzed recovering the organocatalyst and releasing the aldol product **XXVI**.



**Scheme 5.** Enamine mechanism of A) type I aldolase and B) L-Proline.

There are three modes of organocatalytic activation for the aldol reaction: activation of the donor, activation of the acceptor or bifunctional activation (Scheme 6). Donor activation involves the modification of the pronucleophilic ketone into a more powerful donor. In the presence of acid, a ketone is able to provide an enol intermediate which can react with the activated carbonyl electrophile through a Brønsted acid mechanism. Carbonyl groups in the presence of primary or secondary amines react to provide enamines, which becomes the nucleophilic counterpart. Lastly, an enolate species can be formed by  $\alpha$ -deprotonation by a Brønsted base.

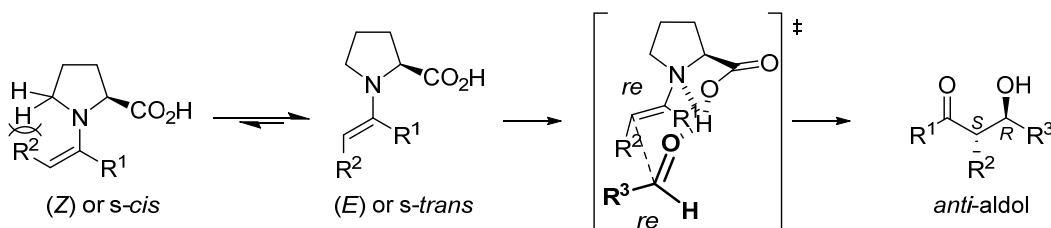


**Scheme 6.** Activation modes and reactive intermediates in organocatalyzed aldol reaction: A) donor activation, B) acceptor activation, C) bifunctional activation.

Acceptor activation can also occur by hydrogen bonding or Brønsted acid effect (Scheme 6B), which is, in the end, the same effect induced by Lewis acids activation. Lastly, the simultaneous activation of both counterparts by the same catalyst leads to the named bifunctional activation, which can shuffle between the activation modes previously described (Scheme 6C).

### Intermolecular ketone-aldehyde aldol reaction

The possible products that can arise in an aldol reaction employing enolizable compounds are gathered in Scheme 1. In the case of using a ketone as nucleophile and aiming a single aldol product, a highly chemoselective and enantioselective catalyst is desirable. In 2000, Barbas III and List reported that L-Proline could provide the aldol products with (*R*)- absolute configuration between acetone **XII** and aromatic and saturated aldehydes with high enantioselectivity (Scheme 4B).<sup>9</sup> In this work, they recognized the carboxylic group as a cocatalyst acting as a Brønsted acid, and thus, L-Proline acting as a “minimalistic-aldolase”. The enantioinduction was explained making use of the Zimmerman-Traxler type transition state (Scheme 7).<sup>10</sup> Although this is the most accepted transition state, other authors have proposed different transition structures.<sup>11</sup>



**Scheme 7.** Zimmerman-Traxler transition state model for the aldol reaction catalyzed by L-Proline.

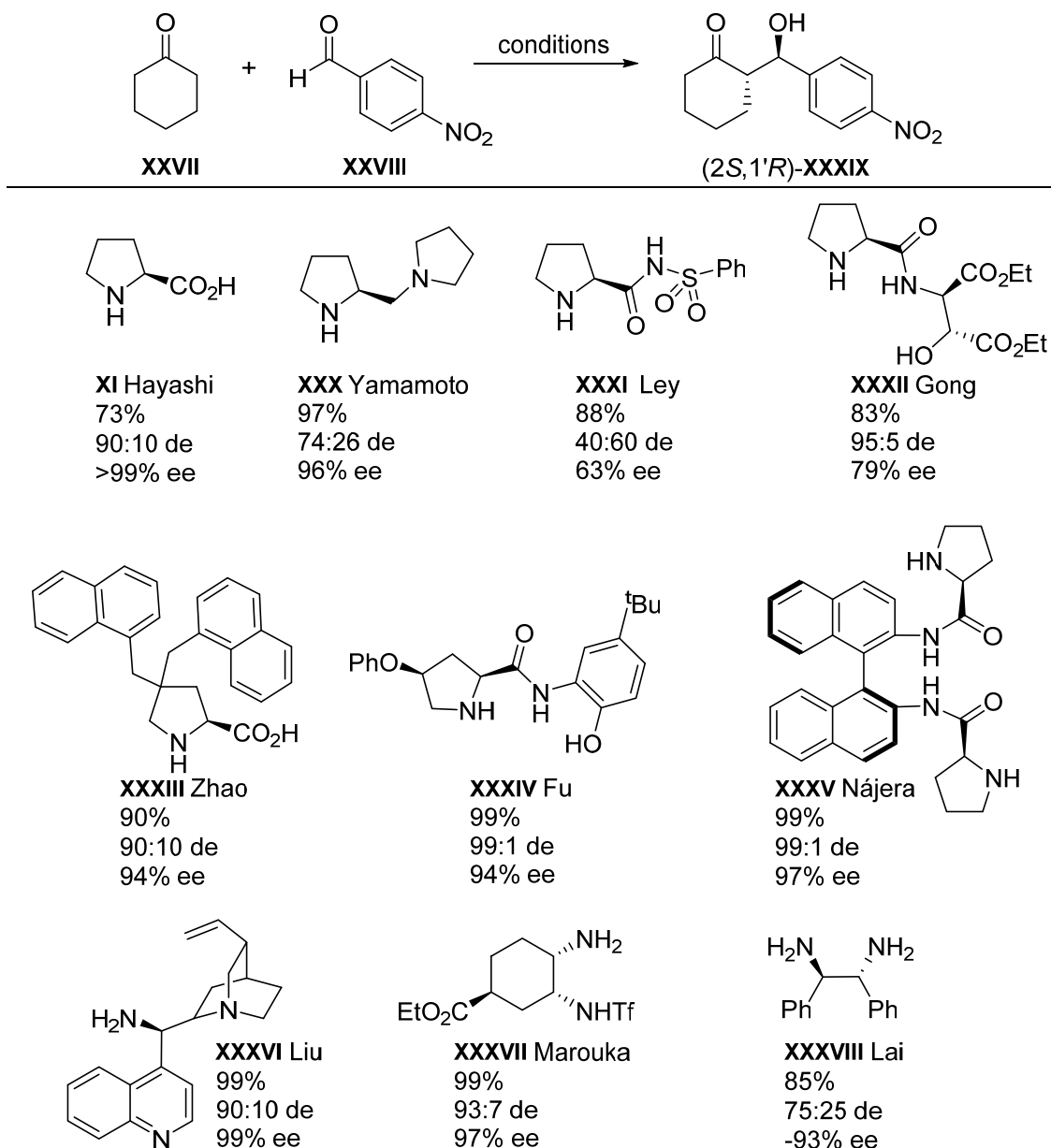
If L-Proline is used as catalyst, the predominant intermediate is the (*E*)-enamine (or *s-trans*) due to the steric interactions the (*Z*)-enamine (or *s-cis*) suffers. Since the *re* face of the enamine reacts preferentially with the *re* face of the aldehyde, *anti*-stereochemistry is expected to occur thus providing the (2*S*,1'*R*)-enantiomer.

Large efforts have been made in order to advance the utility of the enamine-activated aldol reaction providing more efficient variants of L-Proline.<sup>12</sup> Other aminoacids owing primary amino groups<sup>13</sup> were found out to catalyze the reaction, as well as primary and secondary amines<sup>14</sup>, imidazolidinones<sup>15</sup> or even cinchona alkaloid-derived amines<sup>16</sup> (other examples such as peptides will be shown in chapter 3). In pyrrolidine-based aldol reactions the enantioselectivities are usually high but depend on multiple factors. For instance, among different nucleophiles, cyclohexanone usually provides the highest enantioinductions. As far as the electrophile is concerned, aromatic aldehydes usually give better results. However, the obtained enantiocontrol depends on a delicate balance of all these aspects.

Focusing in L-Proline scaffold, main derivatizations deal with changes at the C-2 position with different groups, which can also promote hydrogen bonding interactions as carboxylic

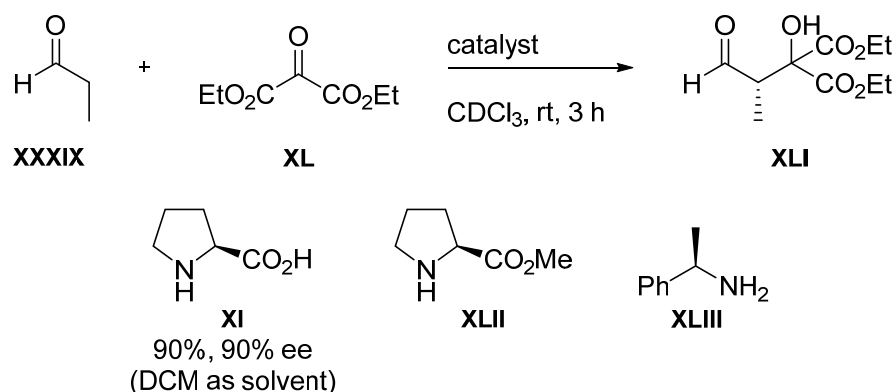
acid does. For instance, prolinamides are easily synthesized from L-Proline and the internal amide bond can act as a proper hydrogen bonding moiety. Different derivatizations consist of the introduction of bulky substituents in order to act as shielding groups. Scheme 8 shows a concise selection of organocatalysts that can be found in the literature for the aldol reaction between cyclohexanone **XXVII** and *p*-nitrobenzaldehyde **XXVIII**. More examples can be found in the excellent review published by Trost and Brindle in 2010.<sup>17</sup>

L-Proline **XI** can catalyze nicely the aldol reaction between cyclohexanone **XXVII**, usually used as solvent, and *p*-nitrobenzaldehyde **XXVIII** providing with total enantiocontrol the desired diastereoisomer.<sup>18</sup> Many other catalysts have also been tested as 4-disubstituted proline **XXXIII**<sup>19</sup>, prolinamine **XXXIV**<sup>20</sup> or binaphthyl catalyst **XXXV**<sup>21</sup> gave also good results. However, other designs as secondary-tertiary amine **XXX**<sup>22</sup>, sulphonamide **XXXI**<sup>23</sup> or prolinamide derived from  $\beta$ -aminoalcohol **XXXII**<sup>24</sup> provided lower enantio- or diastereocontrol. As primary amines can also promote the enamine condensation, some groups decided to test catalysts as the cinchona derivative **XXXVI**<sup>25</sup>, cyclohexyl catalyst **XXXVII**<sup>26</sup> or stilbene catalyst **XXXVIII**<sup>27</sup> providing also high performance.



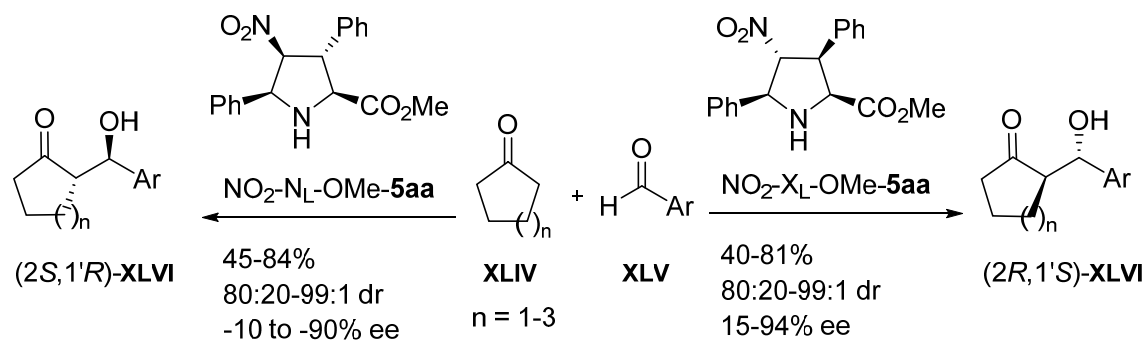
**Scheme 8.** Reported pyrrolidine derivatives providing the enantioselective aldol addition between cyclohexanone **XXVII** and *p*-nitrobenzaldehyde **XXVIII**.

An interesting work presented by Jørgensen in 2002 reported the direct catalytic aldol reaction between aldehydes and diethyl ketomalonate as the activated carbonyl compound (Scheme 9).<sup>28</sup> The first catalyst screening of different chiral amines in the reaction between propanal **XXXIX** and diethylketomalonate **XL** revealed L-Proline **XI** as the most promising organocatalyst which provided the product in 90% of enantiomeric excess. Surprisingly, primary amine phenylethylamine **XLIII** and the protected L-Proline methyl ester **XLII** catalyzed the reaction towards **XLI** but with no control in the enantioselectivity of the process.



**Scheme 9.** Representative results of the catalyst screening in the aldol reaction between propanal **XXXIX** and diethyl ketomalonate **XL**.

Due to these precedents, previous work of our group focused on the structure-reactivity relationship study of unnatural densely substituted 4-nitroproline ester derivatives  $\text{NO}_2\text{-N}_L\text{-OMe-5aa}$  and  $\text{NO}_2\text{-X}_L\text{-OMe-5aa}$  with *endo*- and *exo*- configuration, respectively, in the aldol reaction depicted in Scheme 10. Catalyst  $\text{NO}_2\text{-N}_L\text{-OMe-5aa}$ , bearing the methyl ester and the nitro moiety in relative *cis* configuration, promoted the reaction between cyclohexanone and aromatic aldehydes providing the  $(2S,1'R)\text{-XLVI}$  product. On the contrary,  $\text{NO}_2\text{-X}_L\text{-OMe-5aa}$ , with the named groups in relative *trans* configuration, provided the opposite chiral induction to that obtained under L-Proline catalyst and its derivatives with good enantiomeric excesses.<sup>29</sup> In a subsequent study, unexpected organocatalytic properties were described, as remote effects derived from the conformational preference of the pyrrolidinic ring explaining. These studies could explain the opposite sense of the induction in the studied aldol reaction, which is absent in any kind of L-Proline derived catalyst described to date.<sup>30</sup>



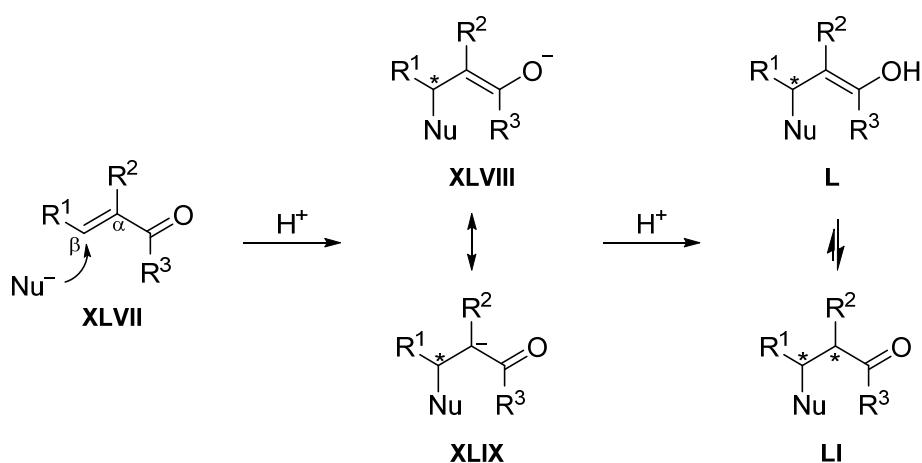
**Scheme 10.** Ketone-aldehyde aldol process catalyzed by densely substituted 4-nitroprolines **XLVI**.

Higher enantiocontrol was observed when cyclohexanone **XLIV** ( $n = 2$ ) was employed as nucleophile as the use of cyclopentanone **XLIV** ( $n = 1$ ) and cycloheptanone **XLIV** ( $n = 3$ ) gave in both cases poorer results. Moreover, the structure-activity relationship was deeply

studied as well as the reaction mechanism and kinetic constants which were analyzed through  $^{19}\text{F}$  NMR and kinetic isotope effect experiments.

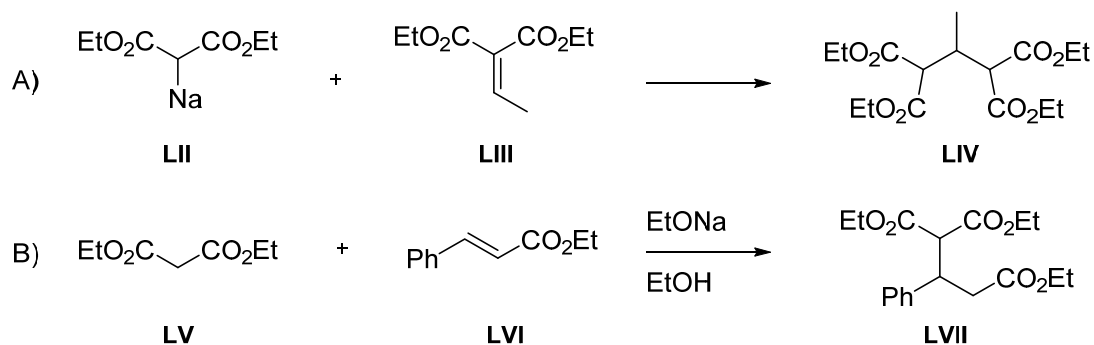
### 2.1.2. Intermolecular Michael reaction

The Michael addition is a powerful method that generates new C-C bonds by means of the nucleophile addition to the  $\beta$  position of  $\alpha,\beta$ -unsaturated carbonyl compound (Scheme 11). A nucleophile approaches to the electrophilic site of **XLVII**, the  $\beta$  carbon. The protonation of intermediate enolate **XLVIII-XLIX** gives carbonyl compound **LI**, which is thermodynamically more stable than **L**.



**Scheme 11.** Nucleophilic conjugate addition.

The first conjugate reaction was described by Komnenos at the end of the 19<sup>th</sup> century reporting the addition of diethyl sodium malonate **LII** to diethyl ethylidene malonate **LIII** (Scheme 12A).<sup>31</sup> Nevertheless, it was not until the work of Michael few years later, in which the addition of diethylmalonate **LV** to ethyl cinnamate **LVI** was described (Scheme 12B), that this type of reaction started to be broadly used.<sup>32</sup>

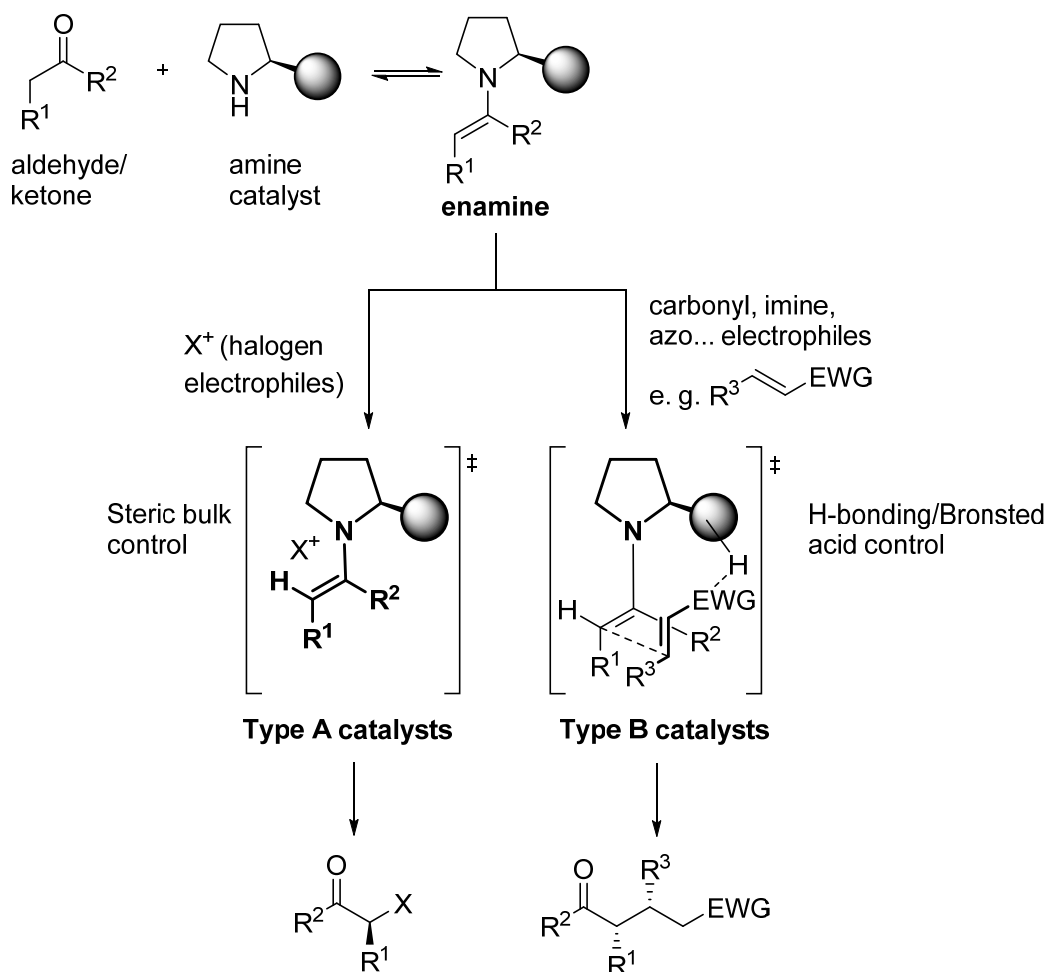


**Scheme 12.** First examples of conjugate additions described by Komnenos and Michael in 1883 and 1887, respectively.

Since then, wide variations of this reaction have been pursued. Not only malonates are used as nucleophiles, also other  $\pi$ -stabilized carbanions as  $\beta$ -keto-<sup>33</sup> or  $\beta$ -cyano<sup>34</sup> esters, nitroalkanes<sup>35</sup> or even organometallic compounds<sup>36</sup> be also used. According to the acceptors, electronwithdrawing groups as the carbonyl<sup>37</sup>, nitro<sup>38</sup>, nitrile<sup>39</sup> or sulphones<sup>40</sup> conjugated to (at least) one double bond are usually employed.

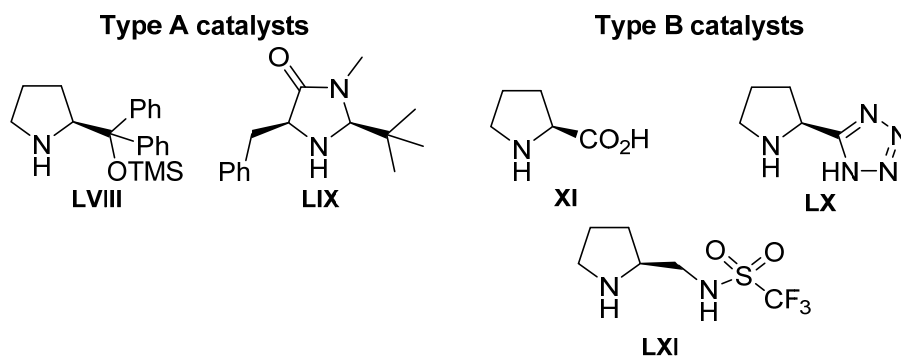
The conjugate addition reaction between ketones and nitroalkenes is a useful and versatile reaction since it permits the synthesis of nitroalkanes, that in turn can be further converted into a large extend of other functional groups as amines, ketones, carboxylic acids or nitrile oxides.<sup>41</sup> In this case, primary and secondary amines can be employed to temporarily activate these ketones. Due to the success of L-Proline as organocatalyst, its pyrrolidinic framework has been largely used in organocatalytic studies on conjugate additions. Thus, it has been postulated that the stereocontrol in the reactions which are catalyzed by pyrrolidine-based organocatalysts can occur by two opposite bias (Scheme 13). It depends whether the stereodirecting element interacts with the electrophile or not by means of hydrogen donor motifs (usually at the  $\alpha$ -position of the pyrrolidine ring) or bulky groups. Type A catalysts include nonacidic groups which preorganize the enamine moiety and block one prochiral face. This model has been postulated in some conjugate additions<sup>42</sup>, generally with aldehydes as nucleophiles. Characteristic catalysts are those developed by Jørgensen and Hayashi, such as the diarylprolinol ether **LVIII**, or the imidazolidinone **LIX** created by McMillan<sup>43</sup> (Scheme 14).





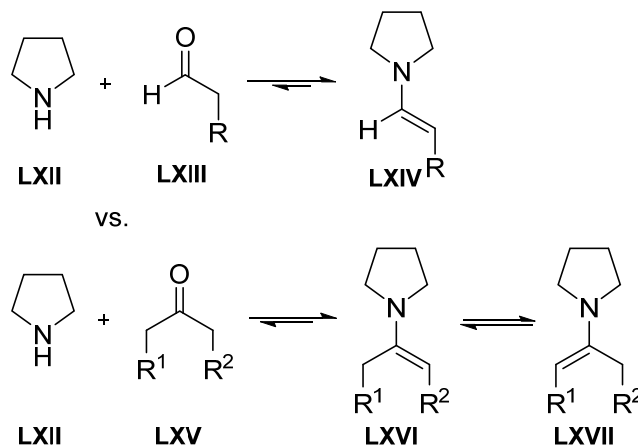
**Scheme 13.** Modes of stereochemical induction with enamine catalysis.

Type B catalysts possess an inherent H bond donor that orientates the approach of the electrophile. A synclinal transition state, generated by the formed electrostatic interaction between the partial positive nitrogen in the enamine and the negatively charged oxygen beared by the EWG of the electrophile, has been described by Seebach and Golinski (Scheme 13).<sup>44</sup> For instance, L-proline **XI** or other amino acids belong to this group, in the same manner as tetrazole **LX** or sulfonamide **LXI** (Scheme 14).<sup>45</sup>



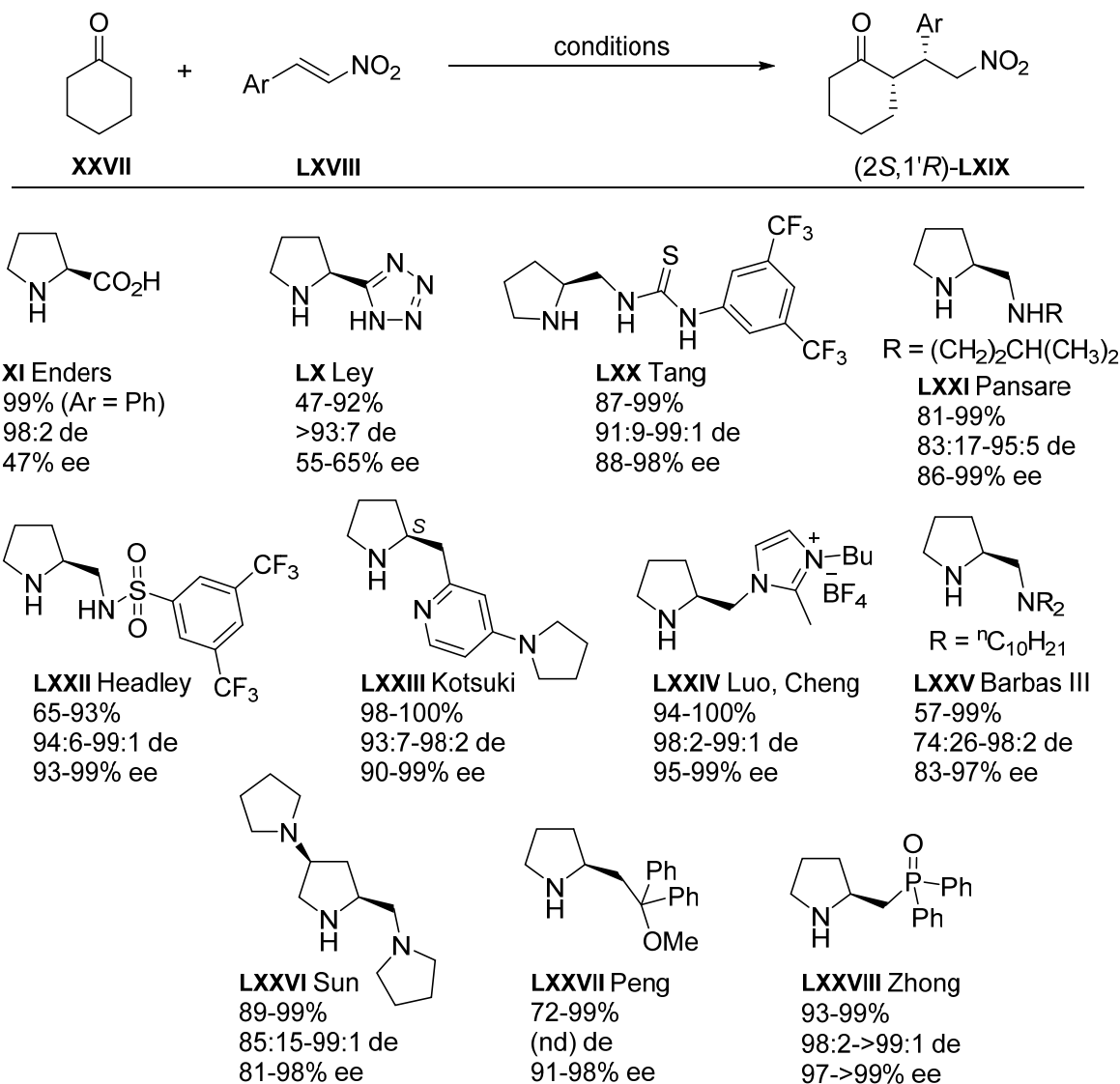
**Scheme 14.** Model catalysts for the Michael reaction.

It is known that aldehydes provide better results than ketones as the former condense much faster with secondary amines. This is also supported by the fact that when ketones are used with secondary amines, the formed enamines are sterically congested. In addition, regioselectivity issues can be encountered when unsymmetrical ketones are used. Symmetric ketones as cyclohexanone do not pose these problems as both regioisomers **LXVI** and **LXVII** are regiochemically equivalent (Scheme 15).



**Scheme 15.** Reactivity and regioselectivity of ketones vs. aldehydes.

Taking the model Michael reaction between cyclohexanone **XXVII** and nitrostyrene **LXVIII**, a small selection of different organocatalyst will be shown in the following schemes. The group of Enders modified the reaction conditions proposed by List, and found that L-Proline **XI** could provide a better outcome in the model reaction by just modifying the reaction conditions<sup>46</sup> (Scheme 16 and Scheme 17 **TS I** for the proposed transition state). Other authors designed different pyrrolidines with proton donating groups at the alpha position. For instance, Ley *et al.* reported the pyrrolidine-tetrazole catalyst **LX** which improved solubility in the reaction medium but did not increase the enantioselectivity.<sup>47</sup> Tang's group envisaged that thiourea<sup>48</sup> functional group in **LXX** would interact additionally with the electrophilic nitroalkene **LXVIII**, by hydrogen bond interactions (see Scheme 17 **TS II**) giving higher enantiomeric inductions. Other characteristic examples are diamine **LXXI**<sup>49</sup> and pyrrolidine-sulphonamide **LXXII**<sup>50</sup>. The first performed well in the model reaction but gave poorer results when using other ketones rather than cyclohexanone (see Scheme 17 **TS III**) and the second provided high enantiomeric excesses even with tetrahydro-4*H*-(thio)pyranone.

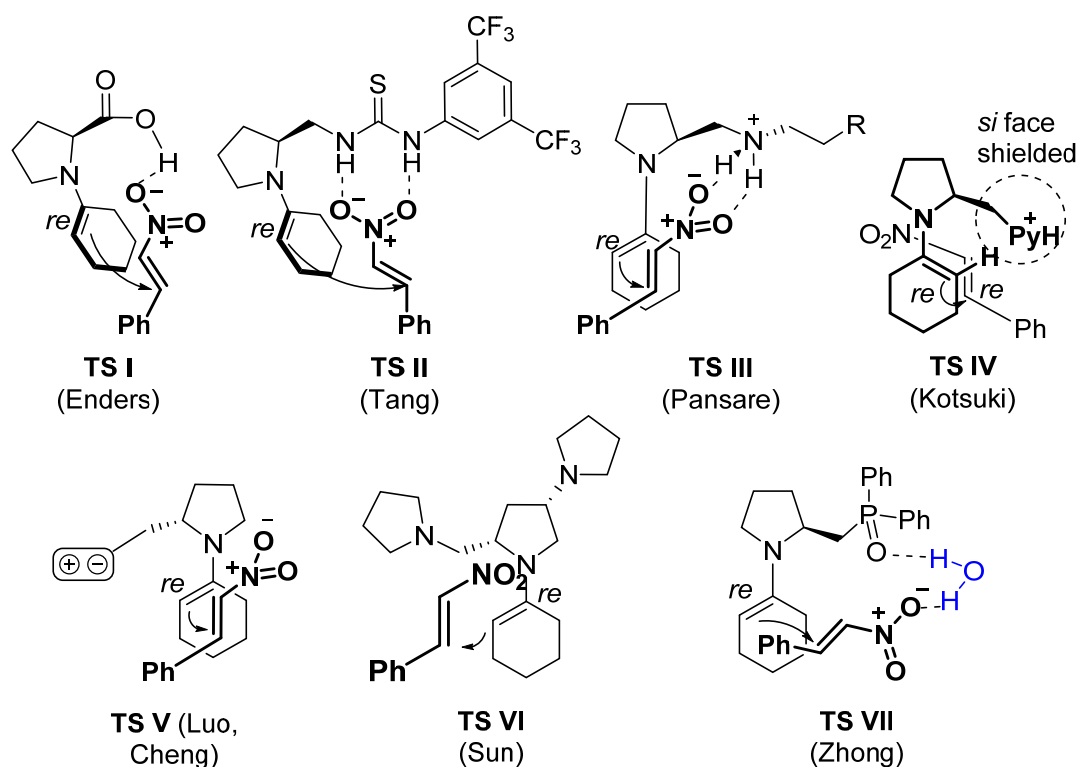


**Scheme 16.** Reported pyrrolidine derivatives providing enantioselective Michael addition between cyclohexanone **XXVII** and aromatic nitroalkenes **LXVIII**.

Catalysts **XI**, **LXX** and **LXXI** induced the stereocontrol by means of the hydrogen bonding with the donating group (neutral or amine salts). While some catalysts were intended to activate the nitroalkene by one point (**TS I** in Scheme 17), others activated it through a bidentated model, as depicted in transition states **TS II** and **TS III**.

Other catalysts have been reported that include functional groups lacking H-donors. Kotsuki's bifunctional catalyst **LXXIII**<sup>51</sup> provided the (2S,1'R)-Michael adducts **LXIX** with high enantioinduction by means of *si* face shielding due to steric and/or electronic repulsions but again by promoting the enamine in *s-cis* orientation which is the responsible to promote the *re-re* attack. (Scheme 17 **TS IV** shows the proposed transition state). The ionic liquid **LXXIV** developed by Luo and Cheng, promoted the same enantioinduction.<sup>52</sup> Although the  $\alpha$  group orientates the electrophilic attack by steric

hindrance (see Scheme 17 **TS V**), the formed enamine adopted a *s-cis* conformation and, therefore, the attacking *re* enamine face provided again the (2*S*,1'*R*)- configuration in the Michael product. Barbas' secondary-tertiary amine **LXXV**<sup>53</sup>, Sun's triamine **LXXVI**<sup>54</sup> or Peng's homodiphenylprolinol methyl ether **LXXVII**<sup>55</sup> catalysts provided the (2*S*,1'*R*)-Michael adducts **LXIX** with high enantioinduction by means of *si* face shielding due to steric and/or electronic repulsions. Also in this case, the promoted enamine adopted the *s-cis* orientation, which is the responsible for promoting the *re-re* attack (Scheme 17 **TS VI** for **LXXVI** catalyst). A last representative example is Zhong's pyrrolidine-phosphine oxide derivative **LXXVIII**, which promoted the electrophilic orientation through the formation of a hydrogen bond due to the participation of a molecule of water (see Scheme 17 **TS VII**).<sup>56</sup>

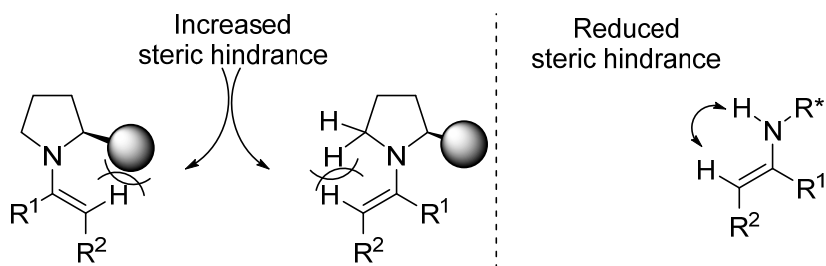


**Scheme 17.** Proposed transition states by the authors for the described organocatalysts in Scheme 16.

In the reported transition states (**TS I**, **II** and **III**) enantiocontrol occurs through face shielding, and the enamine adopts the *s-trans* rotamer orientation, whereas the proposed transition states for catalysts bearing bulky groups (**TS IV**, **V** and **VI**), assume that the enamine adopt a *s-cis* conformation. In addition, while in the former transition state the nitroalkene is oriented in a manner that the *si* face is attacked, in the latter transition state, the orientation of the electrophile is reversed, allowing the *re* face to be attacked. The final

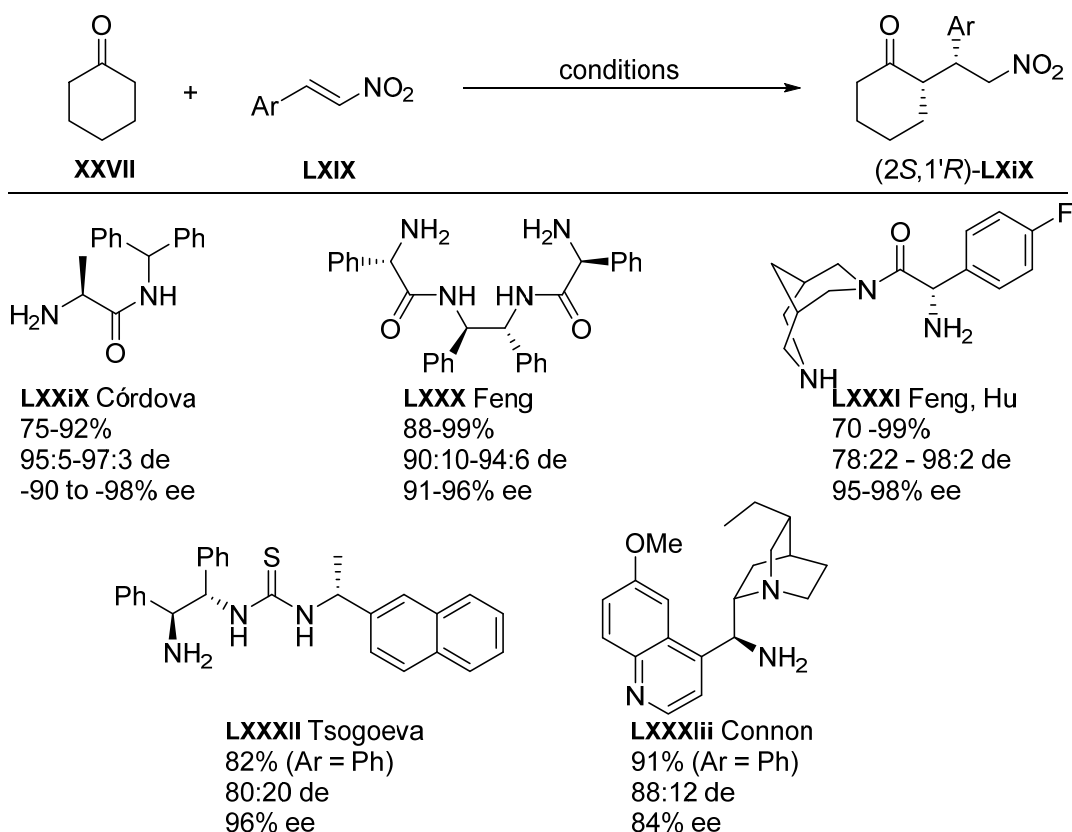
outcome is that both types of organocatalysts generate the same (2*S*,1'*R*)-stereochemistry in the corresponding Michael adducts.

On the other hand, the discovery that primary amines can also act as organocatalysts via enamine activation has solved some inconvenients, as its condensation with ketones is more feasible, and the enamine intermediate generates a preferential geometry control due to the higher difference between the *s-cis* and *s-trans* conformers (Scheme 18).



**Scheme 18.** Secondary vs. primary amine catalysts in ketone activation via enamine intermediate.

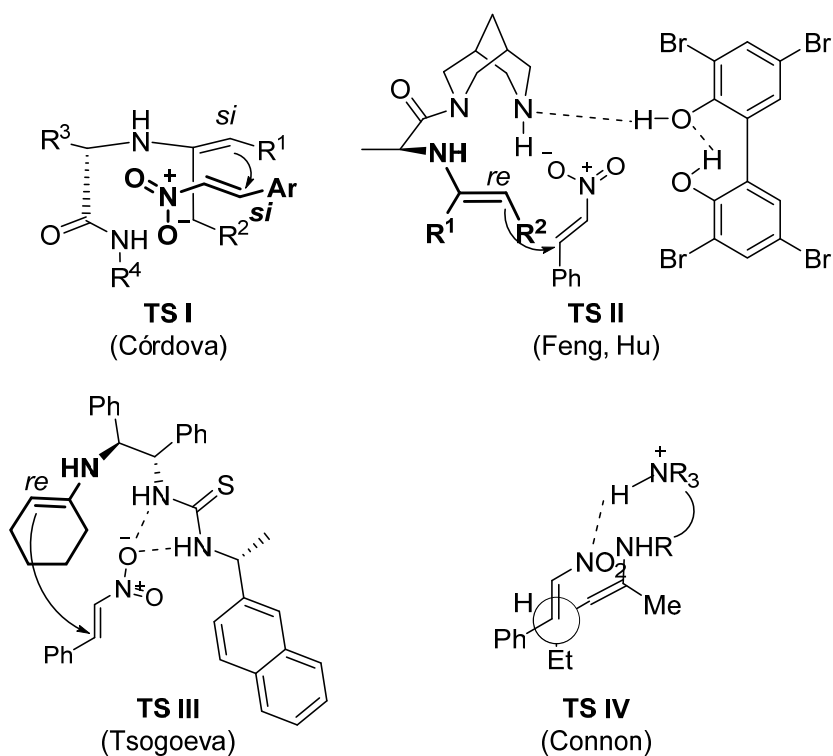
Several examples of organocatalysts bearing primary amines as the key scaffold have been found in literature. Some representative examples are illustrated in Scheme 19. Córdova reported the first example in this field when showed that simple chiral primary amines as (*S*)-alanine amide **LXXIX** derived from acyclic aminoacids could furnish cyclic nitroketones in high yield and enantioselectivities in the presence of water or Brønsted acids as co-catalysts.<sup>57</sup> However, acyclic ketones provided good regioselectivity but low enantiocontrol. However, it was found that the obtained product was released with the (2*R*,1'*S*) absolute configuration, according to the proposed transition state in which the *si* face of the enamine approached the *si* face of the nitro olefin (Scheme 20, **TS I**). Moreover, these authors suggested that the primary amide was a key feature of the catalyst due to the fact that its NH group could interact *via* hydrogen bonding with the nitro moiety of the nitroalkene. Following this pattern, other catalysts have been designed as diamide **LXXX**<sup>58</sup> and bispidine-derived catalyst **LXXXI**<sup>59</sup>.



**Scheme 19.** Enantioselective Michael reactions of ketones with nitrostyrene catalyzed by primary amines.

Feng and Hu's bispidine-derived catalysts **LXXXI** in combination with TBBP turned out to be an excellent catalyst for the model Michael addition not only with cyclohexanone **XXVII** but also with acyclic ketones (90 to 99% ee). In this case, the mechanism was investigated by theoretical calculations. The proposed transition state is shown in Scheme 20, **TS II**. It revealed the enamine formation at the primary amine while the secondary amine participated in hydrogen bonding with TPPB thus activating and approaching the electrophile. The nucleophilic attack occurred from the *re* face of the enamine to give the (2*S*,1'*R*)-**LXIX** enantiomer.

Several groups<sup>60</sup> found in the thiourea moiety an effective fitting mode in order to approach and activate the nitroalkene via double hydrogen bonding from the NH to the nitro moiety. Tsogoeva<sup>61</sup> reported the catalyst **LXXXII** for the addition of acetone or acyclic ketones with higher enantiocontrol when compared to pyrrolidine-based organocatalysts. Tsogoeva's group was able to determine an enamine intermediate through ESI-MS experiments. As a consequence, they proposed the transition state **TS III** (in Scheme 20) in which the nucleophilic attack occurred from the *re* face of the active enamine towards the nitroalkene activated by the thiourea moiety.



**Scheme 20.** Proposed transition states by the authors for the described organocatalysts in Scheme 19.

Cinchona alkaloids, which are another pillar type of organocatalysis<sup>62</sup>, have also found its place in the organocatalytic conjugate addition. For instance, primary amine cinchona alkaloid derivative **LXXXIII** described by the group of Connon was also employed for the reaction of acyclic and cyclic ketones as well as aldehydes to nitrostyrenes in the presence of benzoic acid.<sup>63</sup> They obtained a successful catalyst for the *syn*-selective addition reaction of a broad scope of enolizable carbonyl compounds and straight-chain and aldehydes. The proposed transition structure postulated that the quinuclidine's tertiary amine is protonated activating the nitroalkene via hydrogen bonding (**TS IV** in Scheme 20).

## 2.2. Objectives

Despite the large variety of organocatalysts based on proline scaffolds, all of them are based on simple derivatives of the natural amino acid. We intended to study the behaviour of densely substituted unnatural proline derivatives possessing one primary amino group and different stereochemistry at the C4 Position of the pyrrolidine ring. The points that are pursued in the present chapter are first, the synthesis of the named catalysts  $\text{NH}_2\text{-X}_L\text{-CO}_2\text{Me-10}$  and  $\text{NH}_2\text{-N}_L\text{-CO}_2\text{Me-10}$  and, second, the subsequent enamine type

catalysis performed by these novel compounds in aldol and Michael reactions. Also, in order to get experimental insight into the reaction mechanism of the studied enamine based reactions, catalysts with modifications in the core structure will be designed and further organocatalytic reactions will be pursued. To conclude, further experiments will be carried out to validate the performed computational studies and follow up chemistry with a double electrophilic acceptor will be tested.

### 2.3. Synthesis of densely substituted 3,5-diphenyl-4-amino proline parent compounds

Previous studies of our group showed that ligands based on hybrid ferrocenyl pyrrolidine units **NH-D-EhuPhos-1** and **NMe-L-EhuPhos-2** (Figure 1), when assisted by copper salts successfully promote (3+2) cycloaddition reactions between imines **3** and  $\pi$ -deficient alkenes **4** to give densely substituted unnatural proline esters  $\text{NO}_2\text{-X}_L\text{-CO}_2\text{R}^1\text{-5}$  and  $\text{NO}_2\text{-N}_L\text{-CO}_2\text{R}^1\text{-5}$  in high yields and enantioselectivities.<sup>29</sup>

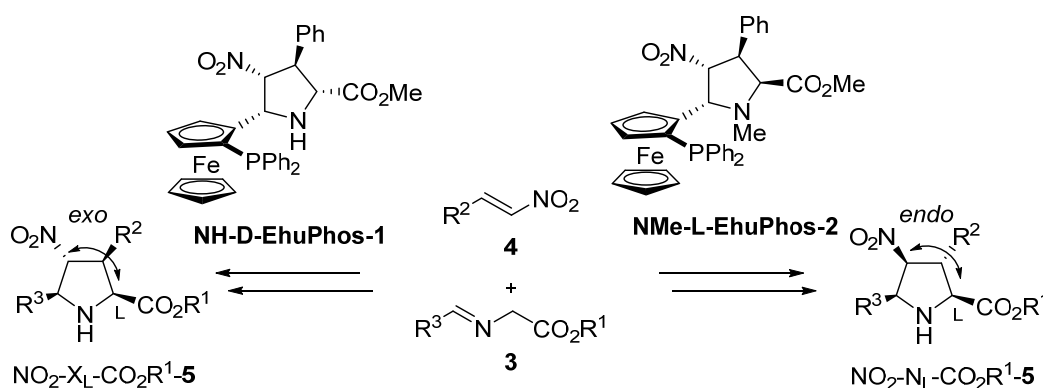


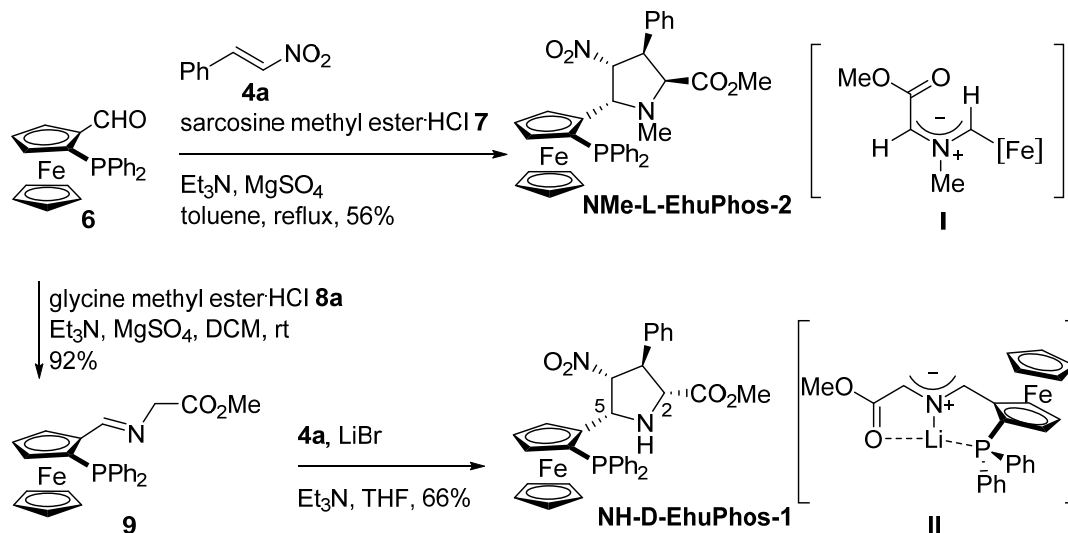
**Figure 1.** Hybrid ferrocenyl-pyrrolidine ligands **NH-D-EhuPhos-1** and **NMe-L-EhuPhos-2**. The *exo* and *endo* diastereoselectivities and the L- configuration of the proline derivatives are highlighted.

Depending on the ligand used two different diastereoisomers of the pyrrolidine, *exo*-L,  $\text{NO}_2\text{-X}_L\text{-CO}_2\text{R}^1\text{-5}$ , or *endo*-L,  $\text{NO}_2\text{-N}_L\text{-CO}_2\text{R}^1\text{-5}$ , cycloadducts can be obtained, respectively. This outcome is determined by the interaction pattern between the Cu (I) centre and the used ligand. **NMe-L-EhuPhos-2** acts as a monodentate ligand whereas **NH-D-EhuPhos-1** behaves as a bidentate one, providing the  $\text{NO}_2\text{-N}_L\text{-CO}_2\text{R}^1\text{-5}$  and  $\text{NO}_2\text{-X}_L\text{-CO}_2\text{R}^1\text{-5}$  pyrrolidines, respectively.<sup>29</sup>

Thus, this methodology was employed in order to obtain the nitro- derivatives, which are suitable precursors for the synthesis of the desired amino-pyrrolidines  $\text{NH}_2\text{-X}_L\text{-CO}_2\text{Me-10}$



and  $\text{NH}_2\text{-N}_\text{L}\text{-CO}_2\text{Me}$ -**10**. The synthesis of these ligands was carried out as described in Scheme 21. Enantiopure ferrocenyl carbaldehyde **6** was synthesized according to the procedure described by Kagan *et al.*<sup>64</sup>

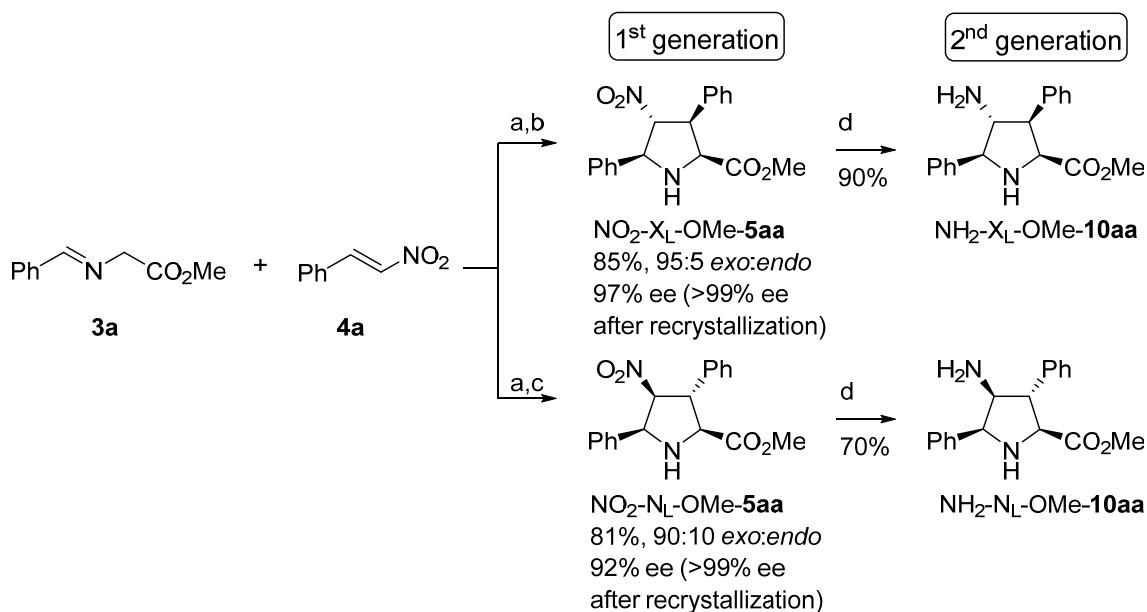


**Scheme 21.** Synthesis of ligands **NMe-L-EhuPhos-2** and **NH-D-EhuPhos-1**.

**NMe-L-EhuPhos-2** was the result of the multicomponent reaction between **6**, sarcosine methyl ester hydrochloride **7** and *trans*- $\beta$ -nitrostyrene **4a**. The *trans* orientation of the ferrocenyl and methylcarboxylate groups arises from the presence of the methyl group attached to the nitrogen atom avoiding steric repulsions between the carboxylic oxygen and the methyl group and additionally stabilized by a hydrogen bond (shown as **I** in Scheme 21). On the contrary, the synthesis of **NH-D-EhuPhos-1** required a stepwise procedure where imine **9** was first isolated before performing a (3+2) cycloaddition with *trans*- $\beta$ -nitrostyrene **4a** in the presence of LiBr. The *cis* disposition of the substituents at the 2<sup>nd</sup> and the 5<sup>th</sup> position of **NH-D-EhuPhos-1** is due to the most stable geometry **II** of the lithiated azomethine ylide due to the coordination array resulting among the lithium cation with the phosphine atom and one carboxylic oxygen.<sup>29</sup>

By using this diastereodivergent method, pyrrolidines  $\text{NO}_2\text{-X}_\text{L}\text{-OMe}$ -**5aa** and  $\text{NO}_2\text{-N}_\text{L}\text{-OMe}$ -**5aa** were obtained by employing **NH-D-EhuPhos-1** and **NMe-L-EhuPhos-2** as ligands, respectively, (Scheme 22).<sup>29</sup> These pyrrolidines (1<sup>st</sup> generation catalysts) were obtained in high diastereomeric ratios and yields. The obtained enantiomeric excesses, 97% ee for  $\text{NO}_2\text{-X}_\text{L}\text{-OMe}$ -**5aa** and 92% ee for  $\text{NO}_2\text{-N}_\text{L}\text{-OMe}$ -**5aa**, were increased to >99% ee in both cases by a simple recrystallization of the products. Later, a catalytic hydrogenation was performed in a hydrogenator flow reactor at 65 °C with Raney-Ni as

catalyst in methanol to produce amines (2<sup>nd</sup> generation catalysts) NH<sub>2</sub>-X<sub>L</sub>-OMe-**10aa** and NH<sub>2</sub>-N<sub>L</sub>-OMe-**10aa** in 90% and 70% yield, respectively.



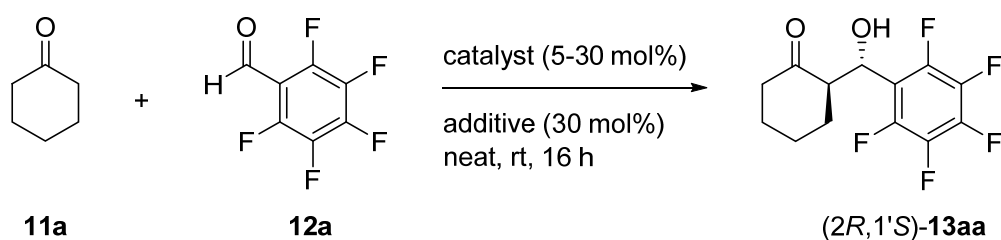
**Scheme 22.** Synthesis of organocatalysts NO<sub>2</sub>-X<sub>L</sub>/N<sub>L</sub>-OMe-**5aa** and NH<sub>2</sub>-X<sub>L</sub>/N<sub>L</sub>-OMe-**10aa**. Reagents and conditions: a) Cu(CH<sub>3</sub>CN)<sub>4</sub>PF<sub>6</sub> (3 mol%), Et<sub>3</sub>N (5 mol%), THF; b) **NH-D-EhuPhos-1** (3 mol %), -20 °C; c) **NMe-L-EhuPhos-2** (3 mol%), -60 °C; d) H<sub>2</sub> (20 bar), Ra-Ni, MeOH, 65 °C, 1mL/min.

## 2.4. Scope as organocatalysts in addition reactions based on enamine intermediates

### 2.4.1. Aldol reaction between cyclohexanone and pentafluorobenzaldehyde

The second generation of organocatalysts, NH<sub>2</sub>-X<sub>L</sub>-OMe-**10aa** and NH<sub>2</sub>-N<sub>L</sub>-OMe-**10aa**, was tested and compared with the previously described organocatalysts<sup>30</sup>, NO<sub>2</sub>-X<sub>L</sub>-OMe-**5aa** and NO<sub>2</sub>-N<sub>L</sub>-OMe-**5aa**, in the aldol reaction between cyclohexanone **11a** and pentafluorobenzaldehyde **12a** (Table 1).

**Table 1.** Aldol reaction between cyclohexanone **11a** and 2,3,4,5,6-pentafluorobenzaldehyde **12a** catalyzed by cycloadducts **5aa** and **10aa**.<sup>a</sup>



entry	catalyst	mol %	additive	<i>anti:syn</i> <sup>b</sup>	yield <sup>c</sup> (%)	ee <sup>d</sup> (%)
1 <sup>30</sup>	NO <sub>2</sub> -X <sub>L</sub> -OMe- <b>5aa</b>	30	TFA	95:5	73	89
2 <sup>30</sup>	NO <sub>2</sub> -X <sub>L</sub> -OMe- <b>5aa</b>	5	TFA	95:5	81	89
3 <sup>30</sup>	NO <sub>2</sub> -N <sub>L</sub> -OMe- <b>5aa</b>	30	TFA	96:4	83	-81
4	NH <sub>2</sub> -X <sub>L</sub> -OMe- <b>10aa</b>	30	none	95:5	75	66
5	NH <sub>2</sub> -N <sub>L</sub> -OMe- <b>10aa</b>	30	none	95:5	60	-10
6	NH <sub>2</sub> -X <sub>L</sub> -OMe- <b>10aa</b>	30	PhCO <sub>2</sub> H	92:8	61	45
7	NH <sub>2</sub> -N <sub>L</sub> -OMe- <b>10aa</b>	30	PhCO <sub>2</sub> H	77:23	65	-12
8	NH <sub>2</sub> -X <sub>L</sub> -OMe- <b>10aa</b>	30	TFA	85:15	63	80
9	NH <sub>2</sub> -N <sub>L</sub> -OMe- <b>10aa</b>	30	TFA	81:19	62	-70
10	NH <sub>2</sub> -X <sub>L</sub> -OMe- <b>10aa</b>	10	TFA	91:9	67	82
11	NH <sub>2</sub> -X <sub>L</sub> -OMe- <b>10aa</b>	5	TFA	90:10	68	82
12 <sup>e</sup>	NH <sub>2</sub> -X <sub>L</sub> -OMe- <b>10aa</b>	5	TFA	92:8	65	88

<sup>a</sup>Reactions were monitored by TLC and stirred for 1 to 16 hours at room temperature until consumption of the starting material. <sup>b</sup>*Anti:syn* ratios were measured by <sup>19</sup>F NMR of crude reaction mixtures. <sup>c</sup>Yields refer to isolated pure aldol adducts. <sup>d</sup>Enantiomeric excesses measured by HPLC correspond to the major *anti*-diastereomers **13aa**. <sup>e</sup>Performed at 0 °C for 48 h.

Entries 1-3 show the results obtained in previous studies employing 4-nitroprolines NO<sub>2</sub>-X<sub>L</sub>-OMe-**5aa** and NO<sub>2</sub>-N<sub>L</sub>-OMe-**5aa** as organocatalysts, with different catalytic loading (from 30 to 5 mol% for the case of NO<sub>2</sub>-X<sub>L</sub>-OMe-**1aa**). They provided the *anti* aldol products in good yields and high *anti:syn* ratio and enantiomeric excesses. Then, we studied the influence of the 2<sup>nd</sup> generation organocatalyst NH<sub>2</sub>-X<sub>L</sub>-OMe-**10aa** and NH<sub>2</sub>-N<sub>L</sub>-OMe-**10aa** in the same reaction (entries 4 and 5). It was observed that the same enantioinduction as under NO<sub>2</sub>-X<sub>L</sub>-OMe-**5aa** and NO<sub>2</sub>-N<sub>L</sub>-OMe-**5aa** was achieved. One enantiomer (*anti*-proline-like aldol or (2*S*,1'*R*)-**13aa**) or the opposite (*proline*-like aldol or (2*S*,1'*R*)-, not shown in Table 1) were obtained depending on the catalyst used NH<sub>2</sub>-X<sub>L</sub>-OMe-**10aa** and NH<sub>2</sub>-N<sub>L</sub>-OMe-**10aa**, respectively. Nevertheless, these values were far from those obtained with the 1<sup>st</sup> generation catalysts, obtaining almost a racemic mixture for the NH<sub>2</sub>-N<sub>L</sub>-OMe-**10aa** case (entry 5). Then, the additive influence was tested and, meanwhile a detrimental effect was observed for the case of benzoic acid mainly for the *exo*- catalyst (entries 6 and 7), the employment of TFA (therefore, under same reaction conditions as the original example) increased the enantiomeric excesses (entries 8 and 9). As the catalyst loading and temperature were reduced, not only the diastereomeric ratio slightly improved but also the enantiomeric excesses slowly increased to finally equalize the results with the 1<sup>st</sup> generation catalysts (entries 12 vs. 1).

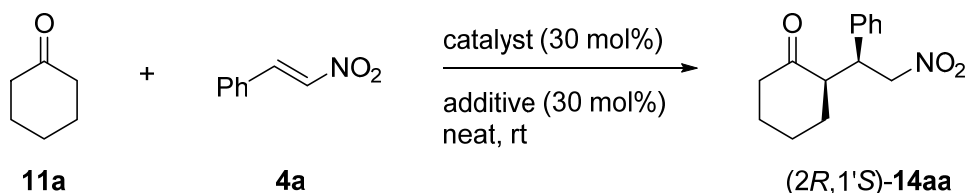
From these studies, we concluded that second generation catalysts  $\text{NH}_2\text{-X}_\text{L}\text{-OMe-10aa}$ , into a slightly better extent, and  $\text{NH}_2\text{-N}_\text{L}\text{-OMe-10aa}$  behave similarly to their first generation analogues in the aldol reaction between cyclohexanone **11a** and 2,3,4,5,6-pentafluorobenzaldehyde **12a**. Therefore, no new catalytic properties were observed on passing from the nitro to the amino series in this aldol reaction.

## 2.4.2. Conjugate reaction with cyclohexanone as nucleophile

### 2.4.2.1. Nitroalkenes and 1,2-bis(phenylsulfonyl)ethene as electrophiles

Firstly, the performance of the nitro derivatives  $\text{NO}_2\text{-X}_\text{L}\text{-OMe-5aa}$  and  $\text{NO}_2\text{-N}_\text{L}\text{-OMe-5aa}$  was studied in the model reaction of cyclohexanone **11a** with *trans*- $\beta$ -nitrostyrene **4a** (Table 2). Catalyst  $\text{NO}_2\text{-X}_\text{L}\text{-OMe-5aa}$  in the presence of benzoic acid or alone did not produce any trace of the Michael product (entries 1 and 2). In addition, low conversion and moderate diastereo- and enantio- induction was observed when TFA was used as additive (entry 3 and 4).

**Table 2.** Reaction conditions screening for the conjugate addition between cyclohexanone **11a** and *trans*- $\beta$ -nitrostyrene **4a** catalyzed by cycloadducts **5aa** and **10aa**.



entry	catalyst	additive	conv. <sup>a</sup> (%)	time (h)	<i>syn:anti</i> <sup>b</sup>	yield <sup>c</sup> (%)	ee <sup>d</sup> (%)
1	$\text{NO}_2\text{-X}_\text{L}\text{-OMe-5aa}$	-	0	72	nd	nd	nd
2	$\text{NO}_2\text{-X}_\text{L}\text{-OMe-5aa}$	$\text{PhCO}_2\text{H}$	0	168	nd	nd	nd
3	$\text{NO}_2\text{-X}_\text{L}\text{-OMe-5aa}$	TFA	50	144	66:33	nd	60
4	$\text{NO}_2\text{-N}_\text{L}\text{-OMe-5aa}$	TFA	20	24	nd	nd	nd
5	$\text{NH}_2\text{-X}_\text{L}\text{-OMe-10aa}$	-	>99	48	93:7	65	77
6	$\text{NH}_2\text{-N}_\text{L}\text{-OMe-10aa}$	-	>99	16	94:4	72	-44
7	$\text{NH}_2\text{-X}_\text{L}\text{-OMe-10aa}$	$\text{TsOH}\cdot\text{H}_2\text{O}$	21	168	nd	nd	66 <sup>e</sup>
8	$\text{NH}_2\text{-X}_\text{L}\text{-OMe-10aa}$	4-nitrophenol	>99	64	98:2	61	78

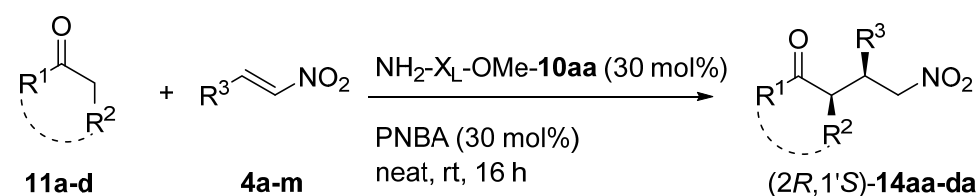
9	NH <sub>2</sub> -X <sub>L</sub> -OMe- <b>10aa</b>	butyric acid	>99	96	88:12	63	86
10	NH <sub>2</sub> -X <sub>L</sub> -OMe- <b>10aa</b>	salicylic acid	>99	16	94:6	70	90
11	NH <sub>2</sub> -X <sub>L</sub> -OMe- <b>10aa</b>	AcOH	>99	40	90:10	60	84
12	NH <sub>2</sub> -X <sub>L</sub> -OMe- <b>10aa</b>	TFA	>99	24	93:7	75	91
13	NH <sub>2</sub> -N <sub>L</sub> -OMe- <b>10aa</b>	TFA	>99	72	95:5	65	-78
14 <sup>f</sup>	NH <sub>2</sub> -X <sub>L</sub> -OMe- <b>10aa</b>	TFA	>99	36	87:13	85	91
15 <sup>g</sup>	NH <sub>2</sub> -X <sub>L</sub> -OMe- <b>10aa</b>	TFA	44	96	nd	nd	nd
16	NH <sub>2</sub> -X <sub>L</sub> -OMe- <b>10aa</b>	PhCO <sub>2</sub> H	>99	36	99:1	65	88
17	NH <sub>2</sub> -N <sub>L</sub> -OMe- <b>10aa</b>	PhCO <sub>2</sub> H	>99	24	90:10	58	-64
18	NH <sub>2</sub> -X <sub>L</sub> -OMe- <b>10aa</b>	PNBA <sup>h</sup>	>99	16	93:7	81	92
19	NH <sub>2</sub> -N <sub>L</sub> -OMe- <b>10aa</b>	PNBA	>99	16	89:11	79	-42
20 <sup>f</sup>	NH <sub>2</sub> -X <sub>L</sub> -OMe- <b>10aa</b>	PNBA	>99	36	95:5	70	87
21 <sup>g</sup>	NH <sub>2</sub> -X <sub>L</sub> -OMe- <b>10aa</b>	PNBA	>99	60	86:14	83	89

<sup>a</sup>Conversions to Michael adducts were measured by <sup>1</sup>H NMR of crude reaction mixtures. <sup>b</sup>*Syn:anti* ratio was measured by <sup>1</sup>H NMR of crude reaction mixtures. <sup>c</sup>Yields refer to isolated pure Michael adducts. <sup>d</sup>Enantiomeric excesses were measured by HPLC correspond to the major *syn*-diastereomers **14aa**. <sup>e</sup>Enantiomeric excess measured by HPLC correspond to the major *syn*-diastereomers **14aa** of the crude reaction mixture. <sup>f</sup>20 mol % catalyst. <sup>g</sup>Reaction performed at 0 °C. <sup>h</sup>PNBA: 4-nitrobenzoic acid.

In contrast, second generation catalysts NH<sub>2</sub>-X<sub>L</sub>-OMe-**10aa** and NH<sub>2</sub>-N<sub>L</sub>-OMe-**10aa** were found to be more efficient in this process. Thus, formation of Michael adduct **14aa** was observed in almost quantitative conversions in most cases. In addition, different *syn:anti* relationships or enantiomeric excesses were obtained depending on the additive used. It is noteworthy that, as it happened in the aldol reaction, catalyst NH<sub>2</sub>-X<sub>L</sub>-OMe-**10aa** provided the “anti-proline-like Michael adduct” (*2R,1'S*)-enantiomer whereas NH<sub>2</sub>-N<sub>L</sub>-OMe-**10aa** induced the “proline-like Michael product” (*2S,1'R*)-enantiomer (entries 5 to 21). Proper choice of the acidic additive proved to be crucial for both organocatalysts (entries 5,6 vs. 7 to 21). The organocatalyst NH<sub>2</sub>-X<sub>L</sub>-OMe-**10aa** provided a better result when carboxylic acids were employed. Benzoic acid (entry 16) provided higher *syn:anti* relationship, whereas salicylic acid, trifluoroacetic acid and 4-nitrobenzoic acid gave higher enantiomeric excesses (entries 10, 12 and 18, respectively). The use of butyric acid did not improve the enantiocontrol (entry 9). Other additives such as 4-toluenesulfonic acid (entry 7), 4-nitrophenol (entry 8) or acetic acid (entry 11) were found to be inefficient or did not improve the enantiocontrol of the process. Also, lower catalytic load and temperature were tested but did not improve the values of enantio- or diastereoselectivities obtained under 30 mol% catalytic load at room temperature (entry

12 vs. 14 and 15, and entry 18 vs. 20 and 21). On the other hand,  $\text{NH}_2\text{-N}_L\text{-OMe-10aa}$  provided the corresponding product (2*S*,1'*R*)-**14aa** in lower enantiomeric excess no matter which additive was used (entries 13, 17 and 19). In this process, TFA provided the Michael adduct with the highest enantiomeric excess albeit lower enantiocontrol (entry 13) to the desired enantiomer.

From the data gathered in Table 2, the best reaction conditions were established. Therefore, 4-nitrobenzoic acid and  $\text{NH}_2\text{-X}_L\text{-OMe-10aa}$  catalyst in 30% ratio provided the desired Michael product **14aa** in 81% yield, 93:7 *syn:anti* diastereomeric ratio and 92% of enantiomeric excess. These conditions were chosen in order to evaluate the catalytic activity in the presence of other ketones **11a-d**, and different nitroalkenes **4a-k** (Scheme 23). These results are gathered in Table 3 and Table 4.



- |   |   |   |
|---|---|---|
| <b>11a:</b> $\text{R}^1, \text{R}^2 = -(\text{CH}_2)_4-$      | <b>4a:</b> $\text{R}^3 = \text{Ph}$                         | <b>14aa:</b> $\text{R}^1, \text{R}^2 = -(\text{CH}_2)_4-, \text{R}^3 = \text{Ph}$                         |
| <b>11b:</b> $\text{R}^1, \text{R}^2 = -(\text{CH}_2)_3-$      | <b>4b:</b> $\text{R}^3 = 4\text{-MeC}_6\text{H}_4$          | <b>14ab:</b> $\text{R}^1, \text{R}^2 = -(\text{CH}_2)_4-, \text{R}^3 = 4\text{-MeC}_6\text{H}_4$          |
| <b>11c:</b> $\text{R}^1, \text{R}^2 = -(\text{CH}_2)_5-$      | <b>4c:</b> $\text{R}^3 = 4\text{-MeOC}_6\text{H}_4$         | <b>14ac:</b> $\text{R}^1, \text{R}^2 = -(\text{CH}_2)_4-, \text{R}^3 = 4\text{-MeOC}_6\text{H}_4$         |
| <b>11d:</b> $\text{R}^1 = \text{CH}_3, \text{R}^2 = \text{H}$ | <b>4d:</b> $\text{R}^3 = 4\text{-CF}_3\text{C}_6\text{H}_4$ | <b>14ad:</b> $\text{R}^1, \text{R}^2 = -(\text{CH}_2)_4-, \text{R}^3 = 4\text{-CF}_3\text{C}_6\text{H}_4$ |
|   | <b>4e:</b> $\text{R}^3 = 4\text{-NO}_2\text{C}_6\text{H}_4$ | <b>14ae:</b> $\text{R}^1, \text{R}^2 = -(\text{CH}_2)_4-, \text{R}^3 = 4\text{-NO}_2\text{C}_6\text{H}_4$ |
|   | <b>4f:</b> $\text{R}^3 = 3\text{-BrC}_6\text{H}_4$          | <b>14af:</b> $\text{R}^1, \text{R}^2 = -(\text{CH}_2)_4-, \text{R}^3 = 3\text{-BrC}_6\text{H}_4$          |
|   | <b>4g:</b> $\text{R}^3 = 3\text{-MeOC}_6\text{H}_4$         | <b>14ag:</b> $\text{R}^1, \text{R}^2 = -(\text{CH}_2)_4-, \text{R}^3 = 3\text{-MeOC}_6\text{H}_4$         |
|   | <b>4h:</b> $\text{R}^3 = 2\text{-FC}_6\text{H}_4$           | <b>14ah:</b> $\text{R}^1, \text{R}^2 = -(\text{CH}_2)_4-, \text{R}^3 = 2\text{-FC}_6\text{H}_4$           |
|   | <b>4i:</b> $\text{R}^3 = 2\text{-MeOC}_6\text{H}_4$         | <b>14ai:</b> $\text{R}^1, \text{R}^2 = -(\text{CH}_2)_4-, \text{R}^3 = 2\text{-MeOC}_6\text{H}_4$         |
|   | <b>4j:</b> $\text{R}^3 = 2\text{-furyl}$                    | <b>14aj:</b> $\text{R}^1, \text{R}^2 = -(\text{CH}_2)_4-, \text{R}^3 = 2\text{-furyl}$                    |
|   | <b>4k:</b> $\text{R}^3 = 2\text{-naphthyl}$                 | <b>14ak:</b> $\text{R}^1, \text{R}^2 = -(\text{CH}_2)_4-, \text{R}^3 = 2\text{-naphthyl}$                 |
|   | <b>4l:</b> $\text{R}^3 = \text{tBu}$                        | <b>14ba:</b> $\text{R}^1, \text{R}^2 = -(\text{CH}_2)_3-, \text{R}^3 = \text{Ph}$                         |
|   | <b>4m:</b> $\text{Ph-CH=CH-NO}_2$                           | <b>14ca:</b> $\text{R}^1, \text{R}^2 = -(\text{CH}_2)_5-, \text{R}^3 = \text{Ph}$                         |
|   |   | <b>14da:</b> $\text{R}^1 = \text{CH}_3, \text{R}^2 = \text{H}, \text{R}^3 = \text{Ph}$                    |

**Scheme 23.** Michael reaction between ketones **11a-d** and nitrostyrenes **4a-m** catalyzed by  $\text{NH}_2\text{-X}_L\text{-OMe-10aa}$ .

The catalyst behaved in a similar manner in the reaction between cyclohexanone **11a** and diverse nitrostyrenes **4** assisted by  $\text{NH}_2\text{-X}_L\text{-OMe-10aa}$  cycloadduct and PNBA as additive, providing the desired addition products with high diastereoselectivity and enantiomeric excesses. According to our results, both the position and the nature of the substituents in the aromatic ring did not provoke significant variations in the enantiocontrol. Nevertheless, the nature of the substituent at the aromatic ring influenced the diastereomeric ratio as less electrophilic 4-Me-nitrostyrene **4b** gave the highest diastereocontrol (entry 2 vs. 4, 6

and 8). While not significant differences were found in the nature of the substituent at the *meta*- position (entries 9 and 10), substituent at *ortho*-position had great weight in both the diastereo- or enantiocontrol (entries 11 vs. 13). This reaction was also tested with success with nitroalkenes bearing the 2-thienyl heterocycle group **4j** and bulky 2-naphthyl group **4k** providing high enantiomeric excesses and good diastereomeric ratios, albeit the yields were moderate (entries 14 and 15). The use of TFA, which in the model reaction provided comparable results as with PNBA (Table 2, entries 12 vs. 18) did not improve the observed diastereo- and enantiocontrol (Table 3, entries 3, 5, 7 and 12).

**Table 3.** **11a+4a-k**  $\rightarrow$  **14aa-ak** reaction scope catalyzed by NH<sub>2</sub>-X<sub>L</sub>-OMe-**10aa** cycloadduct.<sup>a</sup>

entry	Ar	product (2 <i>R</i> ,1' <i>S</i> )- <b>14</b>	<i>syn:anti</i> <sup>b</sup>	yield <sup>c</sup> (%)	ee <sup>d</sup> (%)
1	Ph	<b>14aa</b>	93:7	81	92
2	4-MeC <sub>6</sub> H <sub>4</sub>	<b>14ab</b>	93:7	58	87
3 <sup>e</sup>	4-MeC <sub>6</sub> H <sub>4</sub>	<b>14ab</b>	92:8	60	76
4	4-MeOC <sub>6</sub> H <sub>4</sub>	<b>14ac</b>	89:11	75	88
5 <sup>e</sup>	4-MeOC <sub>6</sub> H <sub>4</sub>	<b>14ac</b>	84:16	70	69
6	4-CF <sub>3</sub> C <sub>6</sub> H <sub>4</sub>	<b>14ad</b>	73:27	90	88
7 <sup>e</sup>	4-CF <sub>3</sub> C <sub>6</sub> H <sub>4</sub>	<b>14ad</b>	69:31	53	76
8	4-NO <sub>2</sub> C <sub>6</sub> H <sub>4</sub>	<b>14ae</b>	78:22	89	86
9	3-BrC <sub>6</sub> H <sub>4</sub>	<b>14af</b>	95:5	93	88
10	3-MeOC <sub>6</sub> H <sub>4</sub>	<b>14ag</b>	99:1	72	88
11	2-FC <sub>6</sub> H <sub>4</sub>	<b>14ah</b>	84:16	90	92
12 <sup>e</sup>	2-FC <sub>6</sub> H <sub>4</sub>	<b>14ah</b>	83:17	80	85
13	2-MeOC <sub>6</sub> H <sub>4</sub>	<b>14ai</b>	97:3	83	74
14	2-furyl	<b>14aj</b>	90:10	59	84
15	2-naphthyl	<b>14ak</b>	77:23	23	82

<sup>a</sup>Reactions were monitored by TLC or <sup>1</sup>H NMR and stirred at room temperature until consumption of the starting material. <sup>b</sup>*Syn:anti* ratios were measured by <sup>1</sup>H NMR or HPLC of crude reaction mixtures. <sup>c</sup>Yields refer to isolated pure Michael adducts. <sup>d</sup>Enantiomeric excesses were measured by HPLC correspond to the major *syn*-diastereomers **14**. <sup>e</sup>TFA was used instead of PNBA. The reaction time fluctuated between 3 and 6 days.

When other cyclic ketones were used as nucleophiles such as cyclopentanone **11b** or cycloheptanone **11c** a severe decrease in both the diastereo- and enantiocontrol ratio was

observed (Table 4, entries 1 and 3). However, these values were improved in both cases by the addition of TFA instead of 4-nitrobenzoic acid (entries 2 and 4). In the case of acetone **11d**, the enantiomeric ratio was lowered albeit the yield was acceptable (entry 5). Aliphatic nitroalkenes such as (*E*)-1-*tert*-butyl-2-nitropropene **4l** and 1-phenyl-2-nitropropene **4m** were also tested but the former provided complex reaction mixtures difficult to analyze and the later did not react under these reaction conditions.

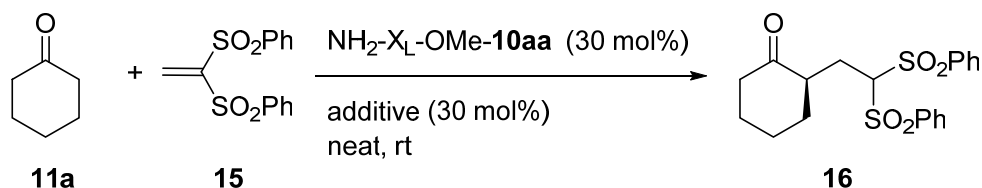
**Table 4.** **11b-d+4a** → **14ba-da** reaction scope catalyzed by NH<sub>2</sub>-X<sub>L</sub>-OMe-**10aa** cycloadduct.<sup>a</sup>

entry	R <sup>1</sup> , R <sup>2</sup>	product (2 <i>R</i> ,1' <i>S</i> )- <b>14</b>	<i>syn:anti</i> <sup>b</sup>	yield <sup>c</sup> (%)	ee <sup>d</sup> (%)
1	-(CH <sub>2</sub> ) <sub>3</sub> -	<b>14ba</b>	47:53	88	64
2 <sup>e</sup>	-(CH <sub>2</sub> ) <sub>3</sub> -	<b>14ba</b>	50:50	75	72
3	-(CH <sub>2</sub> ) <sub>5</sub> -	<b>14ca</b>	78:22	20	71
4 <sup>e</sup>	-(CH <sub>2</sub> ) <sub>5</sub> -	<b>14ca</b>	93:7	84	80
5 <sup>f</sup>	CH <sub>3</sub> , H	<b>14da</b>	-	79	-41

<sup>a</sup>Reactions were monitored by TLC or <sup>1</sup>H NMR and stirred at room temperature until consumption of the starting material. <sup>b</sup>*Syn:anti* ratios were measured by <sup>1</sup>H NMR or HPLC of crude reaction mixtures. <sup>c</sup>Yields refer to isolated pure Michael adducts. <sup>d</sup>Enantiomeric excesses were measured by HPLC correspond to the major *syn*-diastereomers **14**. <sup>e</sup>TFA was used instead of PNBA. <sup>f</sup>The reaction was carried out in the presence of 16 eq of acetone **11d** and NH<sub>2</sub>-X<sub>D</sub>-OMe-**10aa** as catalyst to give (*R*)-**14da**.

Other Michael acceptors were tested such as *N*-substituted maleimides, aromatic chalcones and phenyl 2-phenylvinyl sulfone but they did not provide addition reaction of any kind. Among these electrophiles, only 1,2-bis(phenylsulfonyl)ethene<sup>65</sup> **15** provided the Michael reaction in low enantiocontrol in the presence of TFA or benzoic acid (Table 5, entries 2 and 3). It was surprising to find that in this case the standard reaction conditions with PNBA as additive did not allow the reaction to occur (entry 1).

**Table 5.** Screening of acidic additives in the reaction between cyclohexanone **11a** and vinyl disulfone **15** catalyzed by NH<sub>2</sub>-X<sub>L</sub>-OMe-**10aa** cycloadduct.<sup>a</sup>





entry	additive	time (h)	ee <sup>b</sup> (%)
1 <sup>c</sup>	PNBA	72	-
2	TFA	16	26
3	PhCO <sub>2</sub> H	16	24
4 <sup>d</sup>	PhCO <sub>2</sub> H	16	28

<sup>a</sup>Reactions stirred at room temperature were monitored by TLC or <sup>1</sup>H NMR. <sup>b</sup>Enantiomeric excesses were measured by HPLC correspond to the major isomer **16** of crude reaction mixtures <sup>c</sup>No consumption was observed. <sup>d</sup>CHCl<sub>3</sub> was employed as solvent.

#### 2.4.2.2. Detection via NMR experiments of enamine-iminium intermediate species

In order to get a better understanding of the reaction mechanism, first of all, the active amine group (primary or secondary) had to be identified. Taking into account the reported p*K*<sub>a</sub> values for the protonated pyrrolidine and benzylamine in acetonitrile<sup>66</sup> (19.58 and 16.76, respectively) and water<sup>67</sup> (11.27 and 9.30, respectively) it can be estimated that the ratio **10H**<sup>+</sup>:**10'H**<sup>+</sup> is approximately 99:1.

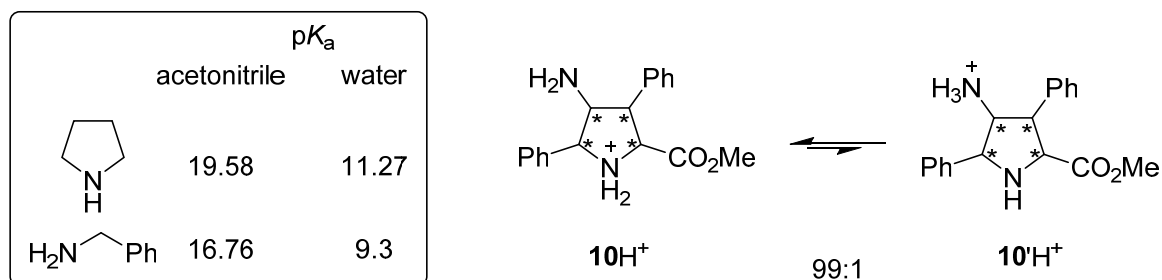


**Figure 2.** p*K*<sub>a</sub> values for pyrrolidine and benzylamine in different solvents and **10H**<sup>+</sup>:**10'H**<sup>+</sup> ratio estimation of the protonated 4-amino pyrrolidine specie in the reaction mixture in the presence of acidic additives.

In order to verify this hypothesis, experimental studies were performed in order to capture by NMR experiments intermediates of the reaction. As a control experiment, the behaviour of NO<sub>2</sub>-X<sub>L</sub>-OMe-**5aa** was analyzed by <sup>1</sup>H NMR. When a mixture of NO<sub>2</sub>-X<sub>L</sub>-OMe-**5aa** (1 eq) and cyclohexanone **11a** (8 eq) was stirred for two hours at 70 °C, the proton NMR spectrum of this reaction mixture (Figure 3B) showed the formation of enamine **5-INT2** in the presence of unreacted NO<sub>2</sub>-X<sub>L</sub>-OMe-**5aa**. Figure 4 shows the corresponding COSY experiment, in which the distinction of free NO<sub>2</sub>-X<sub>L</sub>-OMe-**5aa** and the enamine **5-INT2** is

readily appreciated. Thus, in **5-INT2** the vinyl proton correlates with other protons of the cyclohexene ring (highlighted in a circle).

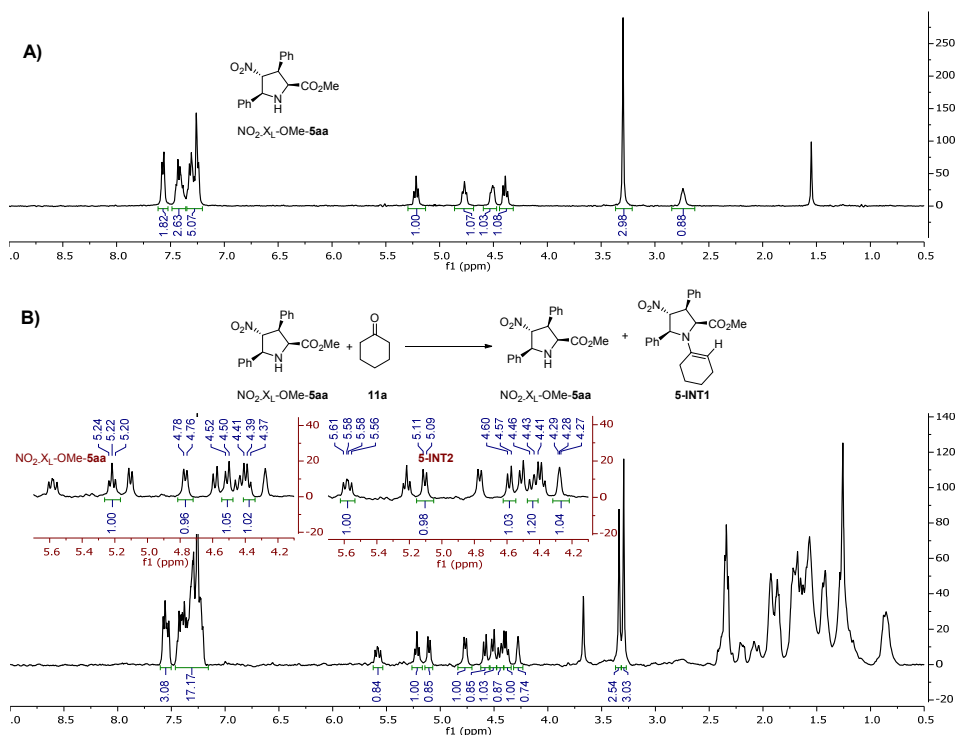


**Figure 3.** A) <sup>1</sup>H NMR spectrum of catalyst **NO<sub>2</sub>-X<sub>L</sub>-OMe-5aa**. B) <sup>1</sup>H NMR spectrum of the reaction mixture between **NO<sub>2</sub>-X<sub>L</sub>-OMe-5aa** (1 eq) and cyclohexanone **11a** as solvent after stirring at 70 °C for 2 hours.

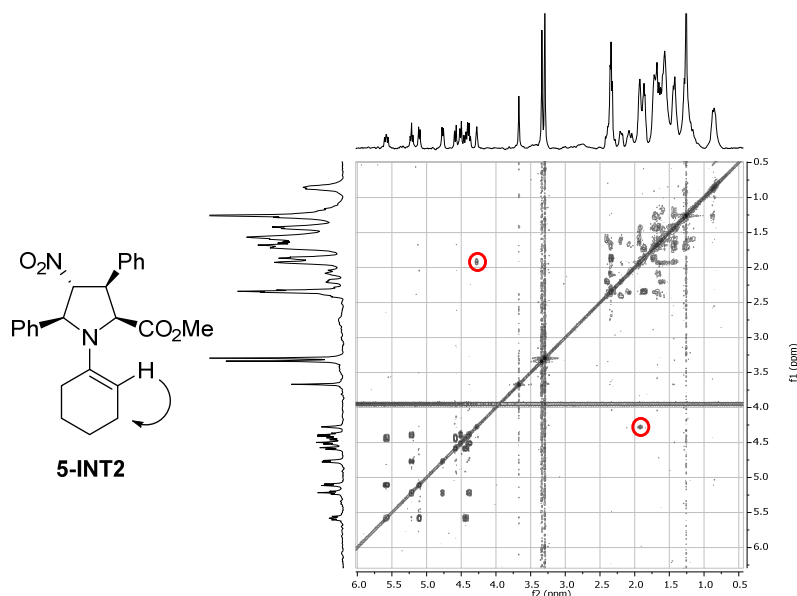


**Figure 4.** COSY experiment related to <sup>1</sup>H NMR in Figure 3B. The correlation between the vinylic proton of **5-INT2** and the rest of the cyclohexene moiety is highlighted by a circle.

In a similar manner, **NH<sub>2</sub>-X<sub>L</sub>-OMe-10aa** (1 eq), cyclohexanone **11a** (8 eq) and PNBA (1 eq) were stirred for five minutes at room temperature and the NMR spectrum (Figure 5)

of this reaction mixture revealed the imine **10-INT1** together with protonated  $\text{NH}_2\text{-X}_\text{L}\text{-OMe-10aaH}^+$ . The mixture components were confirmed by COSY analysis (Figure 6). In this case, **10-INT1** does not show correlation with any aliphatic proton of the cyclohexyl group of **11a**.

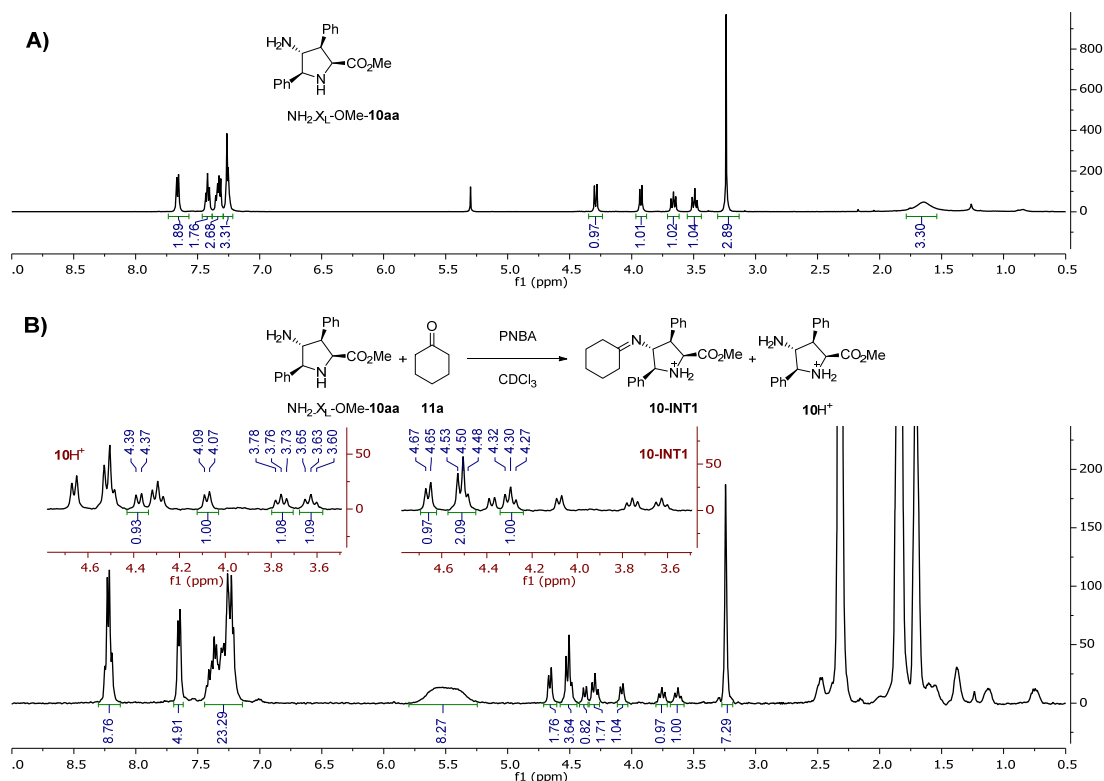


**Figure 5.** A) <sup>1</sup>H NMR spectrum of catalyst **NH<sub>2</sub>-X<sub>L</sub>-OMe-10aa**. B) <sup>1</sup>H NMR spectrum of the reaction mixture between **NH<sub>2</sub>-X<sub>L</sub>-OMe-10aa** (1 eq), cyclohexanone **11a** (8 eq) and PNBA (1 eq).

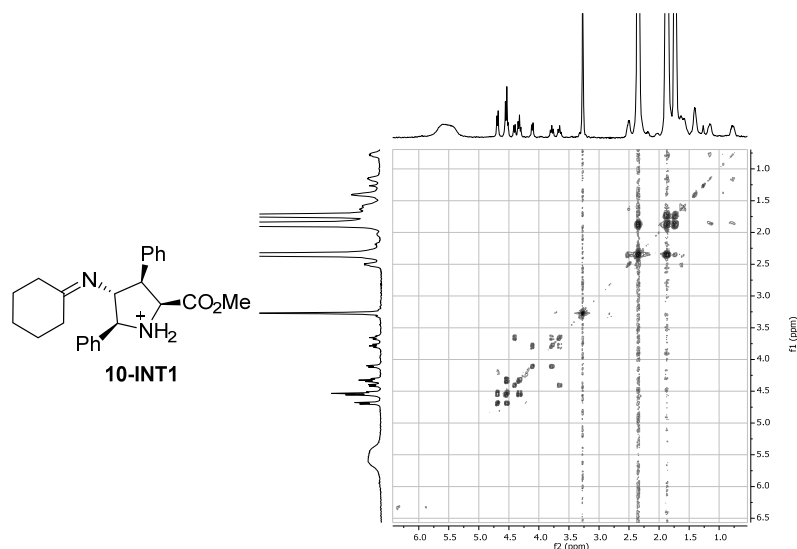
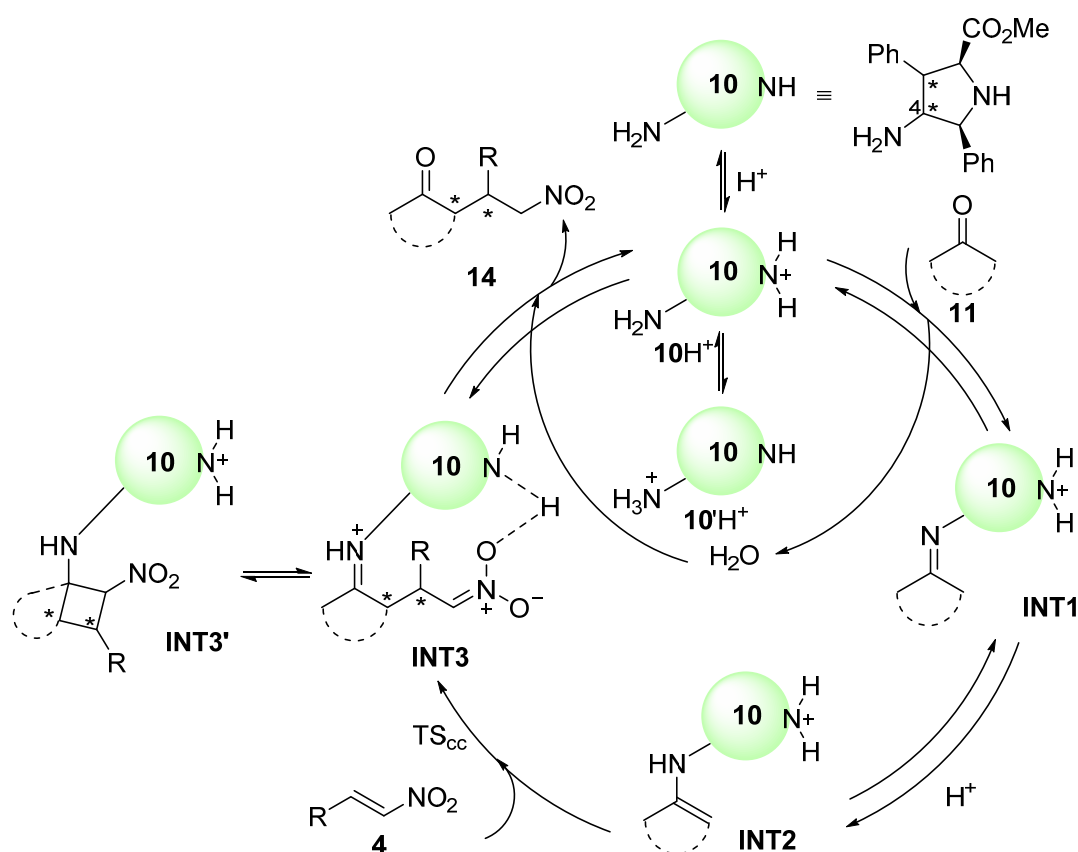


**Figure 6.** COSY of the reaction mixture between **NH<sub>2</sub>-X<sub>L</sub>-OMe-10aa** (1 eq), cyclohexanone **11a** (8 eq) and PNBA (1 eq).

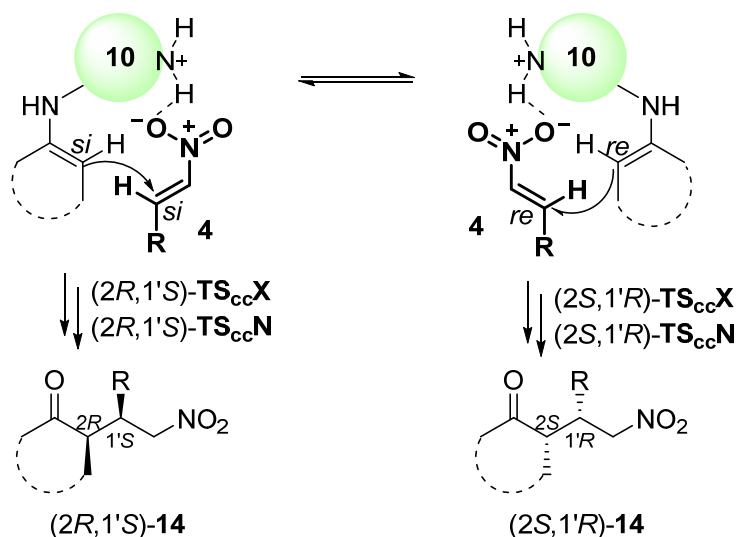
Therefore, the reported values of  $pK_a$ , the above described experimental results and the accepted mechanisms<sup>68</sup> for enamine activated organocatalysis which possess primary amino groups<sup>69</sup>, permitted us to suggest a reaction mechanism for the Michael reaction catalyzed by amine cycloadducts **10aa** (Scheme 24): Our unnatural densely substituted amine  $\text{NH}_2\text{-X}_L\text{-OMe-10aa}$  protonates to **10H+** which then condensates with ketone **11** providing the imine intermediate **INT1**, which in turn tautomerizes at least partially to **INT2**. This latter intermediate produces a nucleophilic addition to the Michael acceptor **4** to give the iminium-nitronate intermediate **INT3** via a carbon-carbon bond formation transition structure ( $\text{TS}_{\text{CC}}$ ). This step determines the stereochemical outcome of the process (vide infra). Progression towards completion of the catalytic cycle can be hindered by the competing Henry-Mannich addition reaction<sup>70</sup> to form the (2+2) cyclobutane intermediate **INT3'**. This dead-end intermediate has been identified in Michael reactions with aldehydes as nucleophiles. Finally, the hydrolysis of **INT3** releases the addition adduct **14** and recovers the catalyst in the protonated active form **10H+**.



**Scheme 24.** Proposed reaction mechanism between ketones **11** and nitroalkenes **4** in presence of  $\text{NH}_2\text{-X}_L\text{-OMe-10aa}$  or  $\text{NH}_2\text{-N}_L\text{-OMe-10aa}$  catalysts.

### 2.4.2.3. Computational study of the proposed reaction mechanism

Due to the protonated nature of the catalyst  $\text{NH}_2\text{-X}_L\text{-OMe-10aa}$  in the reaction medium, it was then expected that not only the ketone was activated by the primary amine (Lewis base) at the 4<sup>th</sup> position by means of HOMO activation *via* enamine. The electrophilic *trans*- $\beta$ -nitrostyrene **4a** could be also activated by means of a LUMO activation induced by the possibly formed hydrogen bond between the protonated secondary amine (Brønsted acid) and the nitro scaffold. Scheme 25 illustrates the plausible activation modes of the reactants and the corresponding origins of stereocontrol. Thus, the stereocontrol of this reaction could stem from the absolute configuration of the employed catalyst, and, additionally, the relative position, *exo*- or *endo*- of the primary amine at the 4<sup>th</sup> position.



**Scheme 25.** Bifunctional simultaneous activation of ketone **11** and nitroalkene **4** in the presence of *exo*- or *endo*- 4-amino-pyrrolidines **10** and subsequent enantioinduction.

In order to investigate the origins of the enantiocontrol, computational calculations were performed by means of density functional theory (DFT), Monte Carlo conformational searches molecular dynamics (MD) simulations. Conformational search calculations revealed structural rigidity in the pyrrolidine ring. The enamine moiety and the phenyl group at C3 are placed in equatorial positions and the methoxycarbonyl group exhibits an isoclinal arrangement, in both *endo*-**INT2** and *exo*-**INT2** fully optimized structures (Figure 7A). The main difference resided in the disposition of the phenyl at the C5 carbon atom. While it takes isoclinal position in *endo*-**INT2**, it has an equatorial conformation in *exo*-**INT2** structure. Additionally, comparison of the molecular dynamics studies on these intermediates showed the distribution of the defined dihedral angles  $\Omega = \text{C8-C7-N6-C4}$  and  $\varphi = \text{C7-N6-C4-C5}$ , and for the case of the *exo*-**INT2**, it is localized in a narrower area of the conformational space (Figure 7B, right) showing less flexibility than *endo*-**INT2**.

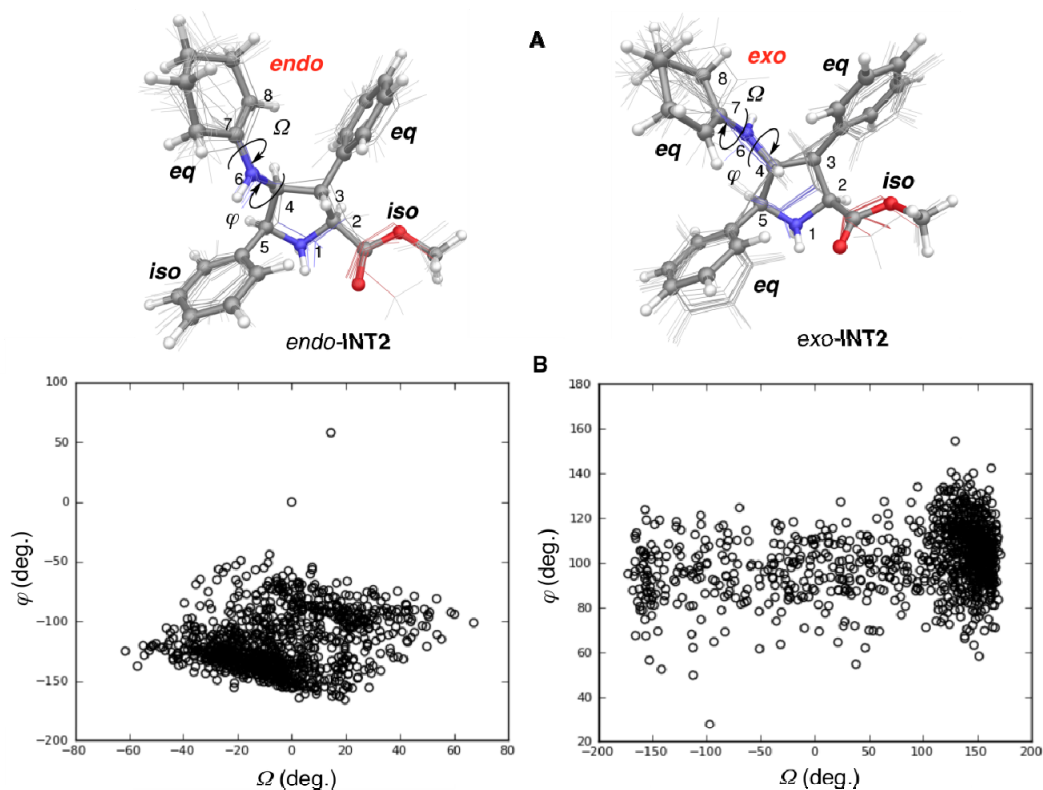


**Figure 7.** A) Fully optimized (OPLS-2005 force field) structures of *endo*-INT2 (left) and *exo*-INT2 (right). The ball-and-stick structures correspond to the minimum energy conformations after Monte Carlo conformational searches and the stick representations correspond to the ten structures of lower energy (ca. 4 kcal/mol).  $\Omega$  and  $\varphi$  dihedral angles are defined as  $\Omega = \text{C8-C7-N6-C4}$  and  $\varphi = \text{C7-N6-C4-C5}$ . Descriptors *ax*, *eq* and *iso* denote axial, equatorial and isoclinal positions, respectively. B) Molecular dynamics simulations (OPLS-2005 force field, 1000 ps) showing the distribution of  $\Omega$  and  $\varphi$  dihedral angles of *endo*-INT2 (left) and *exo*-INT2 (right) along the production time.

Once the conformational rigidity of the catalysts were assessed the mechanism of the C-C bond formation step was explored at DFT level. Initially, all the possible transition states were considered occurring through the enamine at the primary amine for the reaction with  $\text{NH}_2\text{-X}_L\text{-OMe-10aa}$  and  $\text{NH}_2\text{-N}_L\text{-OMe-10aa}$  catalysts. Figure 8 and Figure 9 show fully optimized geometries and relative Gibbs energies at 298K for each catalyst, respectively. As illustrated in Scheme 25 for enamine formation through the primary amine, LUMO activation of the electrophile was identified to occur due to the formation of a hydrogen bond between the pyrrolidinium ion and the nitro moiety of the nitroalkene. Moreover, the same pyrrolidinium cation also interacted through a second hydrogen bond with the methoxycarbonyl group, thus conferring more rigidity to the transition structures. This hydrogen bonding array affects the disposition of the enamine moiety, which cannot adopt the ideal equatorial position respect to the ring placing it in axial or isoclinal conformations for the *exo*- and *endo*- catalysts, respectively. All these transition states provide nucleophilic attack angles  $\theta$  between  $106\text{-}109^\circ$  close to the preferred Bürgi-Dunitz angle.<sup>71</sup>

The least energetic transition structures associated with the catalyst  $\text{NH}_2\text{-X}_L\text{-OMe-10aa}$  towards the formation of the *syn*- Michael adducts ( $2R,1'S$ ) and ( $2S,1'R$ )-**14aa** are shown in Figure 8 left and right, respectively. Both saddle points provide almost antiperiplanar orientation (related to the dihedral  $\omega$  angle) which ensures the nucleophilic attack between the enamine moiety and the phenyl group of *trans*- $\beta$ -nitrostyrene **4a**, with values rounding  $170^\circ$ . However, due to the steric hindrance that is present in the ( $S,1'R$ )- $\text{TS}_{\text{ccX}}$  between the cyclohexyl group and the phenyl group in isoclinal position at C3 provokes the transition structure ( $S,1'R$ )- $\text{TS}_{\text{ccX}}$  to lie 2.3 kcal/mol above ( $R,1'S$ )- $\text{TS}_{\text{ccX}}$ , thus favoring the formation of the ( $2R,1'S$ )-**14aa** enantiomer.

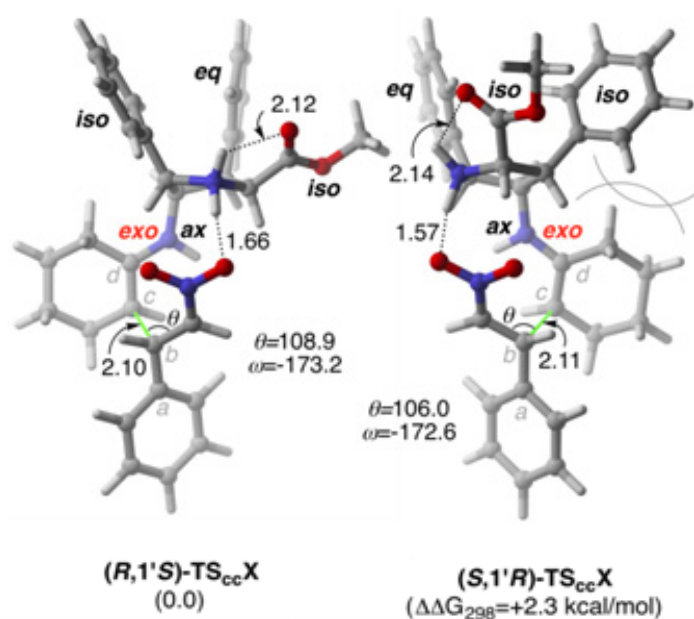


**Figure 8.** Fully optimized geometries and single-point Gibbs energies at 298 K (M06-2X/6-31+G\*\*//B3LYP/6-31G\*+TCGE level of theory) of transition structures ( $R,1'S$ )- $\text{TS}_{\text{ccX}}$  and ( $S,1'R$ )- $\text{TS}_{\text{ccX}}$  corresponding to the C-C bond forming step associated with the Michael reaction between cyclohexanone **11a** and *trans*- $\beta$ -nitrostyrene **4a** in the presence of organocatalysts  $\text{NH}_2\text{-X}_L\text{-OMe-10aa}$ . Dihedral angles  $\omega$  are defined as  $\omega = \text{Ca-Cb-Cc-Cd}$  and distances and angles are given in Å and deg., respectively. For ( $R,1'S$ )- $\text{TS}_{\text{ccX}}$  transition structure, formation of enamines associated with the *NH*-pyrrolidine scaffold has been assumed.  $\Delta\Delta G'_{298}$  values correspond to the relative free energies with respect to ( $R,1'S$ )- $\text{TS}_{\text{ccX}}$ .

On the other hand, the analysis of the least energetic transition structures related to  $\text{NH}_2\text{-N}_L\text{-OMe-10aa}$  (Figure 9A left and right, respectively) leading to the *syn*- Michael adducts showed some similarities to the saddle points examined before. For instance, Bürgi-Dunitz angle  $\theta$  values fall in the same range and the general hydrogen bonding array previously described is also observed. Nevertheless, the distances of the hydrogen bonds formed between the methoxycarbonyl group and the pyrrolidinium cation are longer compared to the previous catalyst, with distances of ca. 2.60 Å in both cases, related to hydrogen bonds with moderate strength.<sup>72</sup> On the contrary, the enamine moiety is forced

to take an isoclinal conformation with respect the pyrrolidine ring in both possibilities. As a consequence, transition state which would lead to the (2*R*,1'*S*) Michael product (Figure 9) suffers from a steric congestion between the cyclohexyl moiety and the phenyl group of nitrostyrene, generating the dihedral  $\omega$  angle to adopt ca. 120°. This fact increases the relative Gibbs energy 2.3 kcal/mol with respect the transition state (*S*,1'*R*)-**TS<sub>cc</sub>N** allowing (2*S*,1'*R*)-**14aa** as the preferential product. However, NH<sub>2</sub>-N<sub>L</sub>-OMe-**10aa** provides lower enantiomeric excesses (Table 2, entries 13, 17 and 19) than NH<sub>2</sub>-X<sub>L</sub>-OMe-**10aa**, and it could be explained due to a larger flexibility of the cyclohexyl moiety (depicted by the  $\Omega$  angle in Figure 7, left) reducing the probability to encounter the analyzed (*S*,1'*R*)-**TS<sub>cc</sub>N** conformation and, as a result, decreasing measured the energetic barrier of 2.3 kcal/mol. In the same manner as calculated before, the ketone condensation with the secondary amine **10**H<sup>+</sup> of the NH<sub>2</sub>-N<sub>L</sub>-OMe-**10aa** catalyst provided the most stable (*R*,1'*S*)-**TS<sub>cc</sub>X'** saddle point. This case provided an energetic value of 5.6 kcal/mol higher than the previously analyzed transition states corroborating thus, the catalytic cycle to occur only through the protonated **10**H<sup>+</sup> specie for both catalysts.

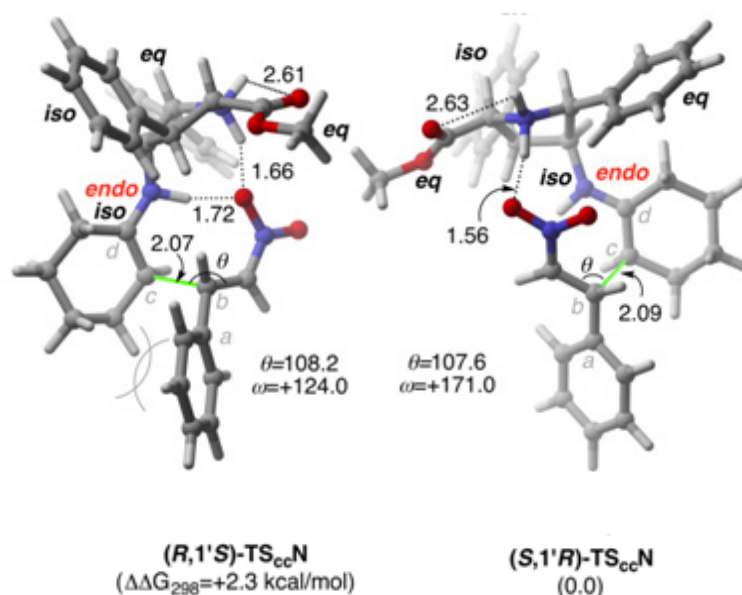


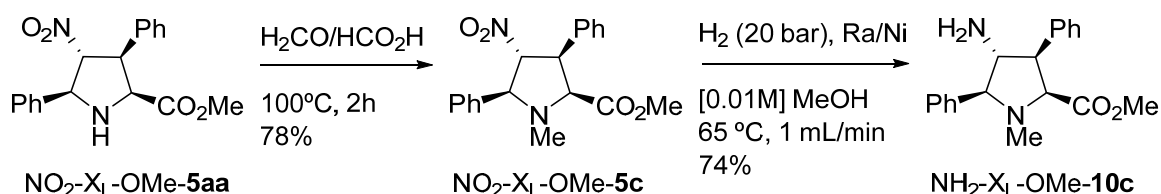
**Figure 9.** Fully optimized geometries and single-point Gibbs energies at 298 K (M06-2X/6-31+G\*\*//B3LYP/6-31G\*+TCGE level of theory) of transition structures (*R*,1'*S*)-**TS<sub>cc</sub>N** and (*S*,1'*R*)-**TS<sub>cc</sub>N** corresponding to the C-C bond forming step associated with the Michael reaction between cyclohexanone **11a** and *trans*- $\beta$ -nitrostyrene **4a** in the presence of organocatalysts NH<sub>2</sub>-X<sub>L</sub>-OMe-**10aa**. Dihedral angles  $\omega$  are defined as  $\omega = \text{Ca-Cb-Cc-Cd}$  and distances and angles are given in Å and deg., respectively. For (*S*,1'*R*)-**TS<sub>cc</sub>N'** transition structure, formation of enamines associated with the *NH*-pyrrolidine scaffold has been assumed.  $\Delta\Delta G'_{298}$  values correspond to the relative free energies with respect to (*S*,1'*R*)-**TS<sub>cc</sub>X**.



## 2.5. Reactivity of densely 3,5-disubstituted-4-amino and 4-amido prolines

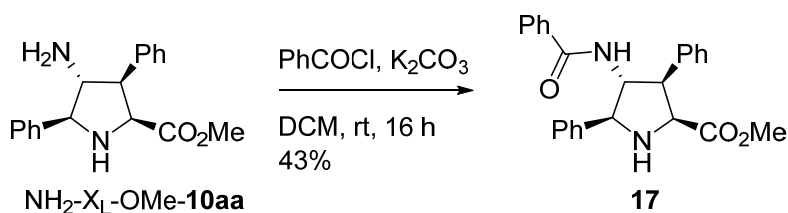
### 2.5.1. Synthesis of organocatalytic derivatives

In order to confirm the reaction model previously calculated, modified pyrrolidines were synthesized in which the primary or secondary amino groups were derivatized. To cancel the possible catalytic activity of the secondary amino group of the pyrrolidinic ring, several attempts based on borohydride reductive amination or *N*-methylation with methyl iodide were tested, but these experiments were not reproducible. Moreover, these attempts provided the desired tertiary amine with low conversions, not good enough for synthetic purposes. Reductive amination with formaldehyde in the presence of formic acid became an efficient reaction that provided the desired product **NO<sub>2</sub>-X<sub>L</sub>-OMe-5c** in good yield.<sup>73</sup> Then, **NO<sub>2</sub>-X<sub>L</sub>-OMe-5c** was hydrogenated in the presence of Raney nickel catalyst to provide **NH<sub>2</sub>-X<sub>L</sub>-OMe-10c**.



**Scheme 26.** Synthesis of primary-tertiary amine **NH<sub>2</sub>-X<sub>L</sub>-OMe-10c**.

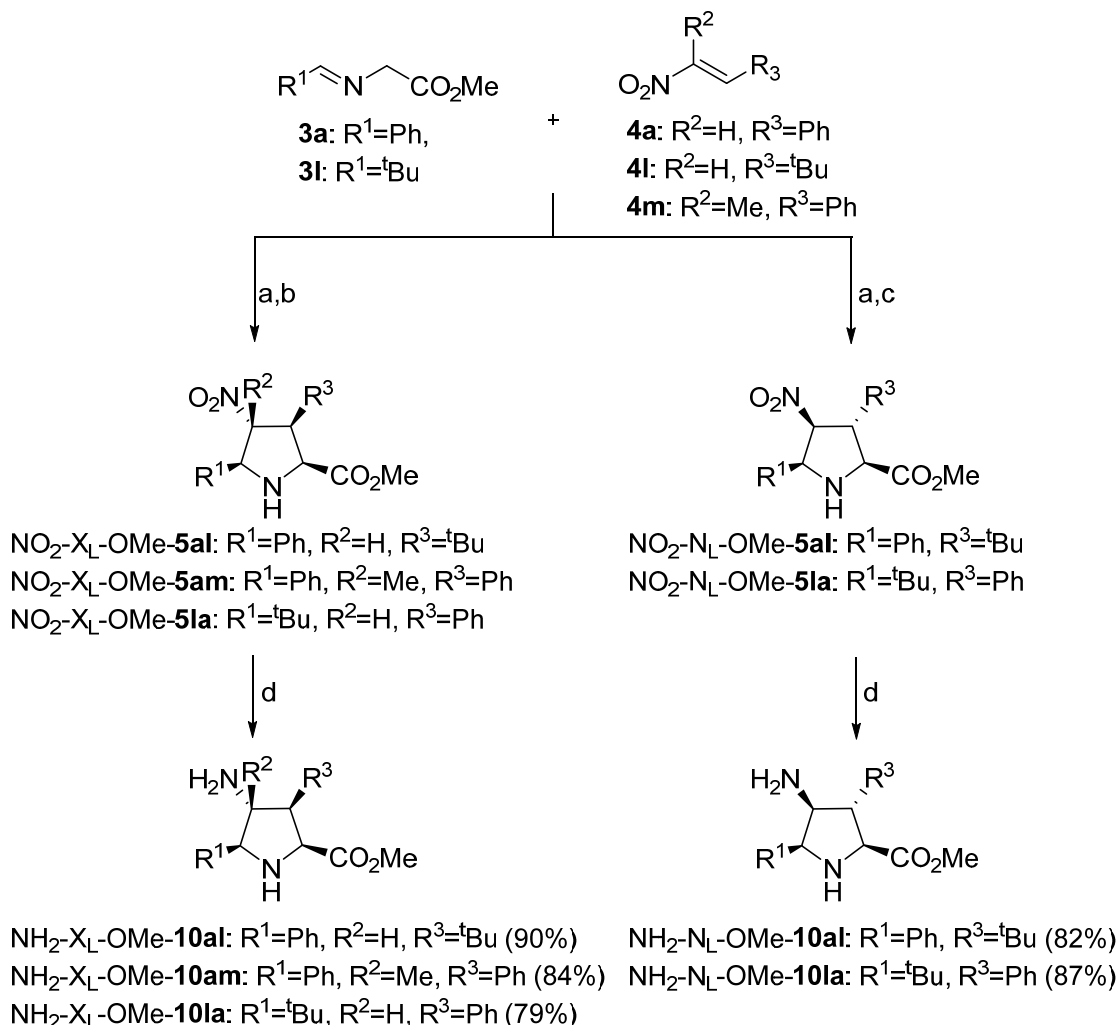
In addition, a modification at the primary amine moiety was performed. In this case, it was envisioned that a derivatization towards an amide scaffold could also disrupt its reactivity. Therefore, benzamide derivative **17** was prepared by *N*-acylation with benzoyl chloride in moderate yield (Scheme 27).



**Scheme 27.** Preparation of compound **17**.

Additionally, to study the steric influence of the groups at the C3 and C5 position of the pyrrolidine ring, it was decided to replace the phenyl groups with bulkier groups. Attempts to promote (3+2) cycloaddition with imines or nitroalkenes obtained from 3,5-di-*tert*-butylbenzaldehyde turned out to be sterically too hindered providing low diastereoselectivity and enantioselectivity. Nevertheless, *tert*-butyl analogues **10aI** and

**10la** of the amino-pyrrolidines were successfully synthesized (Scheme 28). They were achieved employing **NH-D-EhuPhos-1** and **NMe-L-EhuPhos-2** catalysts under reaction conditions similar to those used for the chemical synthesis of their phenyl congeners (Table 6).



**Scheme 28.** Synthesis of organocatalysts NH<sub>2</sub>-X<sub>L</sub>-OMe and NH<sub>2</sub>-N<sub>L</sub>-OMe-**10al** and **la**.  
 Reagents and conditions: a) Cu(CH<sub>3</sub>CN)<sub>4</sub>PF<sub>6</sub> (3 mol%), Et<sub>3</sub>N (5 mol%), THF; b) **NH-D-EhuPhos-1** (3 mol%), -20 °C; c) **NMe-L-EhuPhos-2** (3 mol%), -60 °C; d) H<sub>2</sub> (20 bar), Ra-Ni, MeOH, 65 °C, 1 mL/min. (Reaction for NO<sub>2</sub>-X<sub>L</sub>-OMe-**5am** was carried out at room temperature).

All *exo* cycloadducts obtained under **NH-D-EhuPhos-1** catalytic ligand were obtained in good yields and excellent enantiomeric excesses from 94 to >99% (Table 6, entries 1 to 3). Although the ligand **NMe-L-EhuPhos-2** provided high diastereomeric ratios to get the *endo* adducts (entries 4 and 5), NO<sub>2</sub>-N<sub>L</sub>-OMe-**5la** was obtained with moderate ee (entry 5) and was purified by semipreparative chiral HPLC column. Other additional purifications involved the recrystallization of NO<sub>2</sub>-X<sub>L</sub>-OMe-**5am** to get an enantiopure catalyst. Cycloadducts NO<sub>2</sub>-X<sub>L</sub>-OMe-**5al** and NO<sub>2</sub>-N<sub>L</sub>-OMe-**5al** were taken to the next step without

further purifications. Catalytic hydrogenation with Raney nickel under standard conditions gave all the amine products straightforwardly in high yields (Scheme 28).

**Table 6.** Synthesis of *exo*- and *endo*- prolines esters **5al** and **la** catalyzed by **NH-D-EhuPhos-1** and **NMe-L-EhuPhos-2** (Scheme 28).<sup>a</sup>

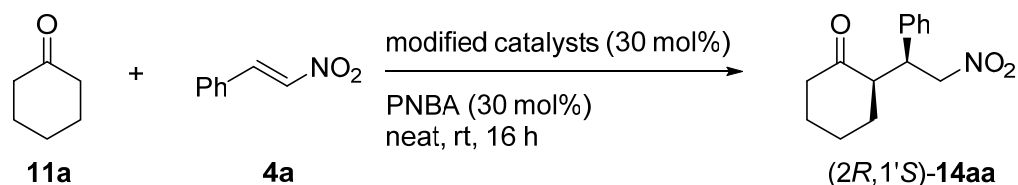
entry	product	<i>endo:exo</i> <sup>b</sup>	yield <sup>c</sup> (%)	ee <sup>d</sup> (%)
1	NO <sub>2</sub> -X <sub>L</sub> -OMe- <b>5al</b>	13:87	72 (83)	98
2	NO <sub>2</sub> -X <sub>L</sub> -OMe- <b>5am</b>	26:74	66	94(99)
3 <sup>30</sup>	NO <sub>2</sub> -X <sub>L</sub> -OMe- <b>5la</b>	1:99	90	>99
4	NO <sub>2</sub> -N <sub>L</sub> -OMe- <b>5al</b>	99:1	84	95
5	NO <sub>2</sub> -N <sub>L</sub> -OMe- <b>5la</b>	82:18	68 (91)	77(99)

<sup>a</sup>Reactions were monitored by TLC or <sup>1</sup>H NMR and stirred until consumption of the starting material. <sup>b</sup>*Endo:exo* ratios were measured by <sup>1</sup>H NMR or HPLC of crude reaction mixtures. <sup>c</sup>Yields refer to isolated major pure cycloadducts. Yields in parentheses refer to isolated mixtures of cycloadducts. <sup>d</sup>Enantiomeric excesses were measured by HPLC correspond to the major enantiomers. Enantiomeric excesses in parentheses were obtained after recrystallization.

## 2.5.2. Scope of the conjugate addition between cyclohexanone and *trans*-β-nitrostyrene

All these newly synthesized pyrrolidines were tested as catalyst in the Michael reaction between cyclohexanone **11a** and nitrostyrene **4a** with 30 mol% of catalyst load in the presence of PNBA (Table 7).

**Table 7.** Conjugate addition reaction between cyclohexanone **11a** and nitrostyrene **4a** catalyzed by the modified organocatalysts.



entry	catalyst	time (d)	conv <sup>a</sup> (%)	<i>syn:anti</i> <sup>b</sup>	yield <sup>c</sup> (%)	ee <sup>d</sup> (%)
1	NH <sub>2</sub> -X <sub>L</sub> -OMe- <b>10aa</b>	16 h	>99	93:7	81	92
2	NH <sub>2</sub> -N <sub>L</sub> -OMe- <b>10aa</b>	16 h	>99	89:11	79	42
3	NH <sub>2</sub> -X <sub>L</sub> -OMe- <b>10al</b>	16 h	>99	93:7	77	94
4	NH <sub>2</sub> -X <sub>L</sub> -OMe- <b>10am</b>	16 h	85	89:11	69	73

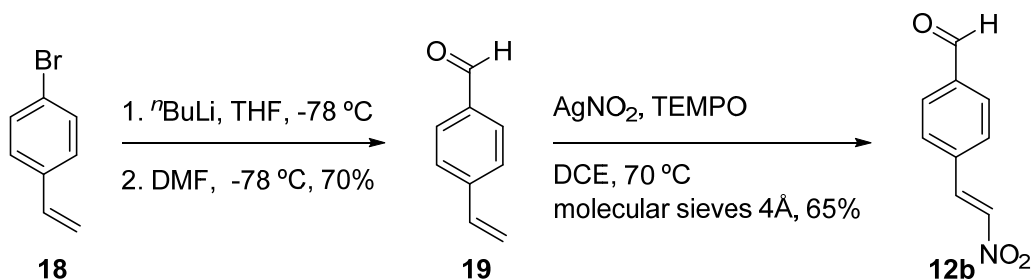
5 <sup>e</sup>	NH <sub>2</sub> -X <sub>L</sub> -OMe- <b>10am</b>	16 h	35	75:25	28	48
6	NH <sub>2</sub> -X <sub>L</sub> -OMe- <b>10la</b>	2	<1	-	-	-
7 <sup>f</sup>	NH <sub>2</sub> -N <sub>L</sub> -OMe- <b>10al</b>	16 h	>99	52:48	61	-16
8	NH <sub>2</sub> -N <sub>L</sub> -OMe- <b>10la</b>	6	87	44:56	45	-11
9	NH <sub>2</sub> -X <sub>L</sub> -OMe- <b>10c</b>	4	<1	-	-	-
10	<b>17</b>	4	<1	-	-	-

<sup>a</sup>Conversions were monitored by <sup>1</sup>H NMR. <sup>b</sup>*Syn:anti* ratio was measured by <sup>1</sup>H NMR or HPLC of crude reaction mixtures. <sup>c</sup>Yields refer to isolated pure Michael adducts. <sup>d</sup>Enantiomeric excesses were measured by HPLC correspond to the major *syn*-diastereomers **14aa**. <sup>e</sup>TFA was employed as additive. <sup>f</sup>Catalyst employed with 95% ee.

The best result was obtained with NH<sub>2</sub>-X<sub>L</sub>-OMe-**10al** catalyst (Table 7, entry 3) providing the Michael adduct with the same diastereocontrol and slightly higher enantiocontrol than the product obtained under NH<sub>2</sub>-X<sub>L</sub>-OMe-**10aa** catalyst (entry 1). It stated that the substitution pattern at C3 of the *exo*- cycloadducts would be of relevance to promote the preferential formation of (2*R*,1'*S*) enantiomer. Substitution at the C5 position of the *exo*-catalyst disrupted totally the catalytic activity (entry 6), and the catalyst NH<sub>2</sub>-X<sub>L</sub>-OMe-**10am** with a methyl group at C4 reduced the activity of the catalyst, but did not influence into a large extent the stereocontrol (entries 4 and 5). On the other hand, substitution of the phenyl groups with *tert*-butyl groups on the *endo*-catalysts decreased the catalytic activity of NH<sub>2</sub>-N<sub>L</sub>-OMe-**10la** and the stereocontrol was affected in both cases (entries 7 and 8). Finally, derivatives NH<sub>2</sub>-X<sub>L</sub>-OMe-**10c** and **17** were unable to perform the catalytic process (entries 9 and 10), implying that both amino groups need to be present simultaneously. All these results are in good agreement with the substituent effects predicted by the previously described DFT-based computational model.

## 2.6. Follow up chemistry: Chemoselective aldol/conjugate addition

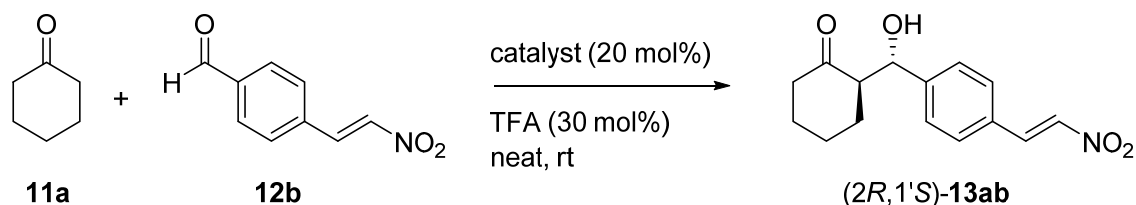
To conclude this study, we aimed to find some applications of these reactions in synthetic chemistry. A chemoselective aldol/conjugate addition onto a double electrophile was envisioned. For that purpose, (*E*)-4-(2-nitrovinyl)benzaldehyde **12b** play a crucial role in this sequential reaction, as it includes an aldol and a Michael acceptor. This substrate was smoothly achieved by lithiation/formylation<sup>74</sup> of **18** with DMF, followed by a nitration<sup>75</sup> step to give **12b** in good yield.



**Scheme 29.** Synthesis of (*E*)-4-(2-nitrovinyl)benzaldehyde **12b**.

Firstly, the aldol reaction between cyclohexanone **11a** and **12b** was carried out (Table 8) with L-Proline-**20**, NO<sub>2</sub>-X<sub>L</sub>-OMe-**5aa** and NO<sub>2</sub>-X<sub>D</sub>-OMe-**5aa** organocatalysts. While aminoacid L-Proline **20** gave the (2*S*,1'*R*)-**13ab** aldol product with moderate enantiocontrol (entry 1), it provided similar *anti:syn* relationship as NO<sub>2</sub>-X<sub>L</sub>-OMe-**5aa** and NO<sub>2</sub>-X<sub>D</sub>-OMe-**5aa** catalysts did. Nevertheless, higher enantiomeric excesses were achieved when employing the first generation catalysts NO<sub>2</sub>-X<sub>D</sub>-OMe-**5aa** and NO<sub>2</sub>-X<sub>L</sub>-OMe-**5aa** at lower temperature (entries 2 and 4). This high chemoselectivity was expected from our previous results, since we found out that organocatalysts NO<sub>2</sub>-X<sub>D</sub>-OMe-**5aa** and NO<sub>2</sub>-N<sub>L</sub>-OMe-**5aa** are efficient aldol catalysts, but do not promote Michael additions on substituted nitrostyrenes (*vide supra*).

**Table 8.** Catalytic aldol reaction of cyclohexanone **11a** and (*E*)-4-(2-nitrovinyl)benzaldehyde **12b**.<sup>a</sup>

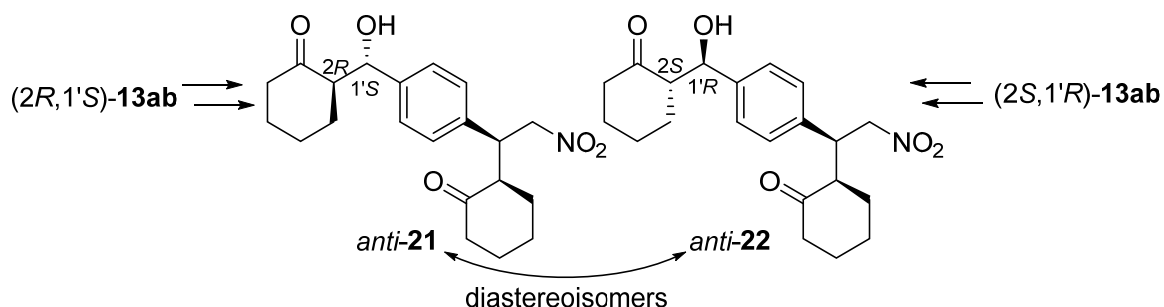


entry	catalyst	<i>anti:syn</i> <sup>b</sup>	yield <sup>c</sup> (%)	ee <sup>d</sup> (%)
1	Pro <sub>L</sub> -OH- <b>20</b>	83:17	75	-64
2	NO <sub>2</sub> -X <sub>D</sub> -OMe- <b>5aa</b>	78:22	73	-86
3	NO <sub>2</sub> -X <sub>L</sub> -OMe- <b>5aa</b>	80:20	60	84
4 <sup>e</sup>	NO <sub>2</sub> -X <sub>L</sub> -OMe- <b>5aa</b>	88:12	70	86

<sup>a</sup>Reactions were monitored by TLC until consumption of the starting material. <sup>b</sup>*Anti:syn* were measured by <sup>1</sup>H NMR of crude reaction mixtures. <sup>c</sup>Yields refer to isolated pure aldol adducts. <sup>d</sup>Enantiomeric excesses measured by HPLC correspond to the major *anti*-diastereomers **13ab**. <sup>e</sup>Performed at 0 °C for 48 hours.

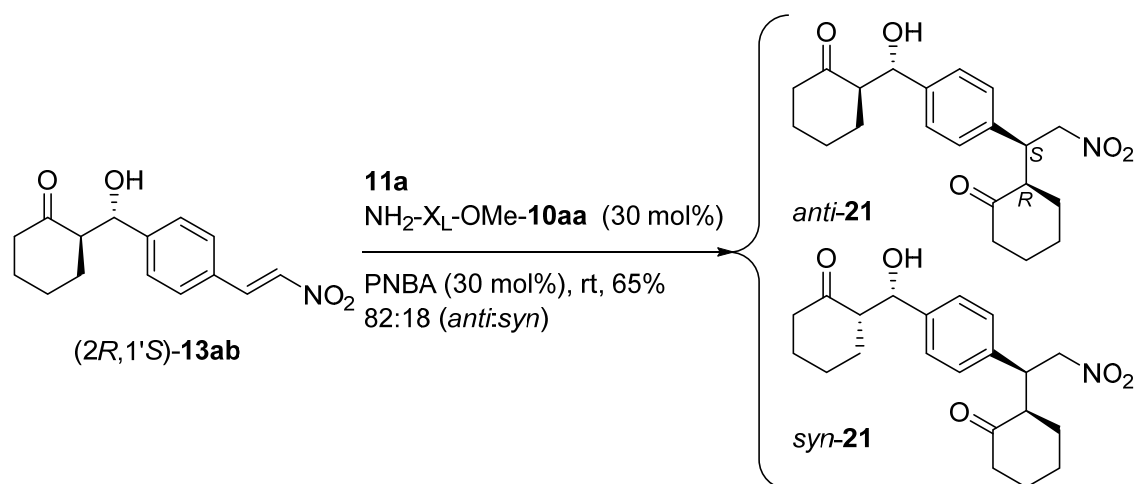
Next, we proceeded with the Michael addition with the second generation catalyst NH<sub>2</sub>-X<sub>L</sub>-OMe-**10aa**. According to our previous results with this organocatalyst, we

expected to obtain diastereoisomers *anti-21* and *anti-22* (Scheme 30) from aldol adducts (*2R,1'S*)-**13ab** and (*2S,1'R*)-**13ab**, respectively.

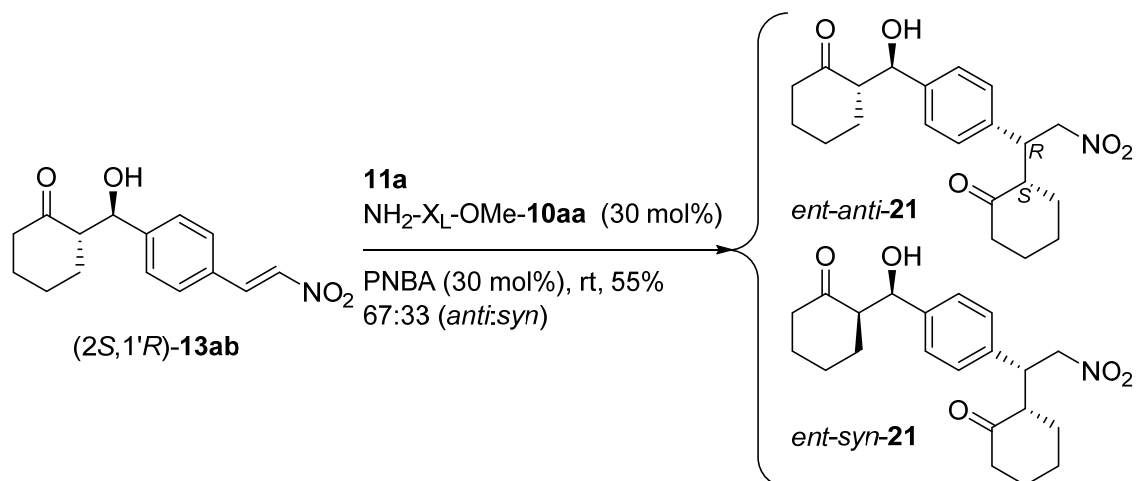


**Scheme 30.** Expected Michael addition adducts *anti-21* and *anti-22* under  $\text{NH}_2\text{-X}_L\text{-OMe-10aa}$  organocatalyst.

Surprisingly, when  $\text{NH}_2\text{-X}_L\text{-OMe-10aa}$  catalyzed the Michael reactions of (*2R,1'S*)-**13ab** and (*2S,1'R*)-**13ab** with cyclohexanone **11a**, it did not provide the expected diastereomeric couple *anti-21* and *anti-22* depicted in Scheme 30. Instead, adducts **21** were obtained as *anti:syn* diastereomeric mixtures. Thus, when the reaction was carried out on (*2R,1'S*)-**13ab** adduct **21** was obtained in 82:18 *anti:syn* ratio (Scheme 31). Similarly, aldol adduct (*2S,1'R*)-**13ab** yielded the enantiomeric forms of **21** adducts in a diastereomeric *anti:syn* ratio of 67:33 (Scheme 32).



**Scheme 31.** Synthesis of compounds **21** from (*2R,1'S*)-**13ab**.



**Scheme 32.** Synthesis of compounds **21** from (2*S*,1'*R*)-**13ab**.

These diastereoisomers in Scheme 32 were isolated for discussion purposes and their  $^1\text{H}$  NMR spectra are included in Figure 10. The upper A spectrum shows the  $^1\text{H}$  NMR of the aldol (2*S*,1'*R*)-**13ab** in which the proton geminal to the hydroxyl group is *cis* with respect to the cyclohexyl chain, thus providing a doublet signal around 4.80 ppm. Below in the B spectrum, the compound *ent-anti-21* shows a doublet at 4.80 ppm in the same manner as its parental (2*S*,1'*R*)-**13ab**. Lastly at the C spectrum, provides a singlet signal downfield at 4.40 ppm for the proton which is *anti* with respect to the cyclohexyl chain corresponding to the compound *ent-syn-21*.

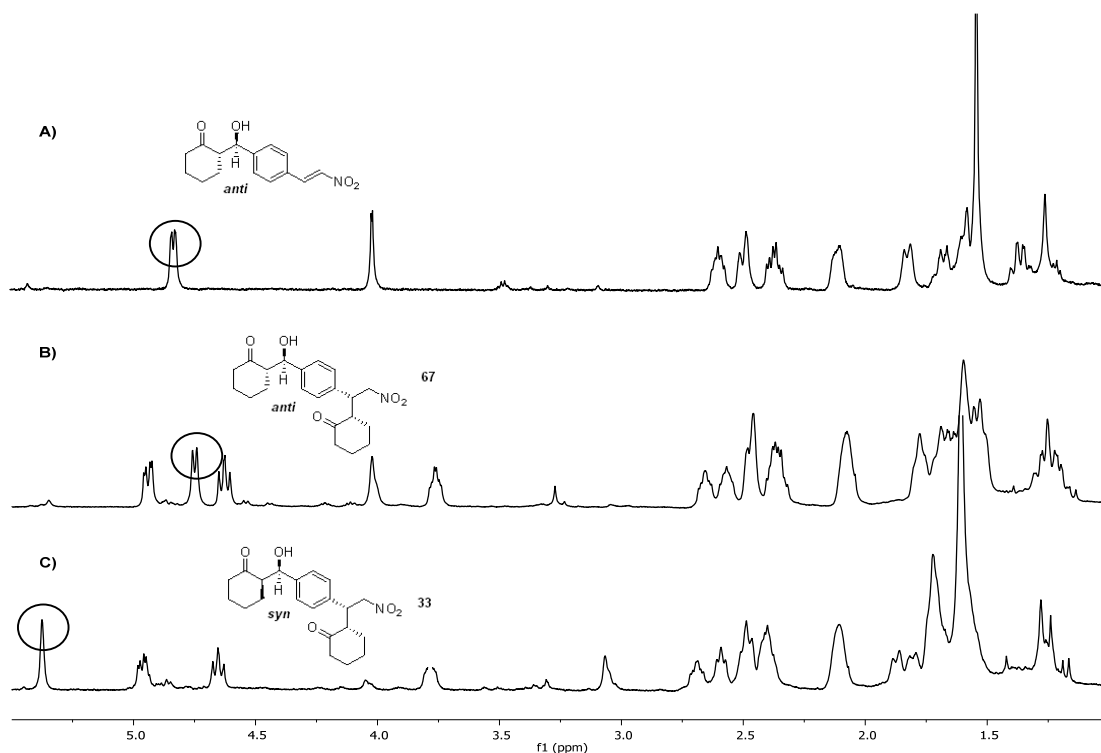


**Figure 10.**  $^1\text{H}$  NMR details and comparison of A) aldol product (2*S*,1'*R*)-**13ab**, and further Michael addition onto it forming diastereoisomers B) *ent-anti-21* and C) *ent-syn-21*.

Crystallization efforts were made and an X-ray analysis of *syn-21* confirmed the proposed structure (Figure 11). It clearly could be seen that both proton atoms of the aldol site are facing the same side of the molecule confirming thus, that some epimerization occurred during the reaction time.

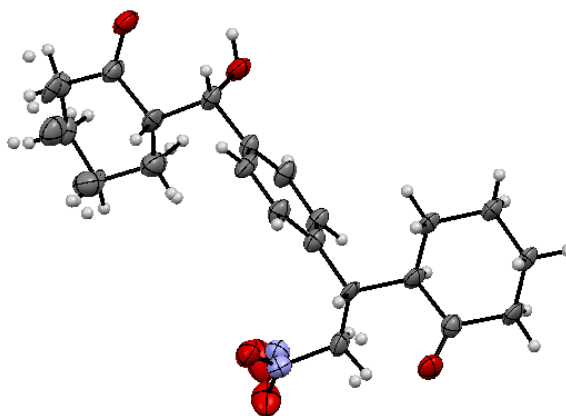
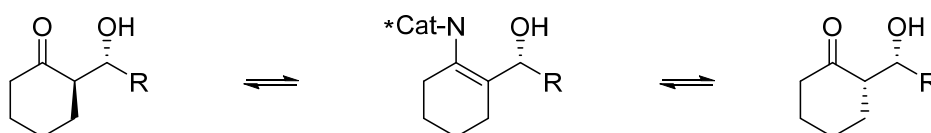


**Figure 11.** ORTEP drawing of *syn-21*.

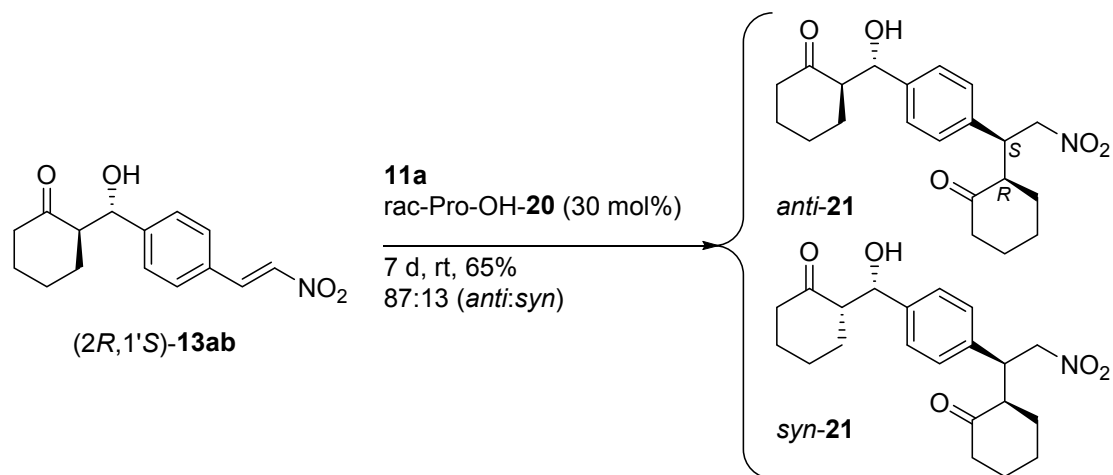
The origin of *syn*- adducts was envisioned as an epimerization reaction at the  $\alpha$ -centre of the aldol ketone scaffold which could occur through an enamine intermediate formed by condensation with the catalyst (Scheme 33). This fact was further confirmed due to a partial epimerization of *anti-21* to *syn-21* when isolated *anti-21* was stirred for 24 hours at room temperature under the standard reaction conditions.



**Scheme 33.** Origins of *syn-23* compound.

The stereocontrol in the Michael addition step also needed to be explained as each reaction (Scheme 31) provided opposite enantiomers [(2*R*,1'*S*) and (2*S*,1'*R*)] of the Michael scaffold regardless of the employed catalyst. It was then concluded that the preformed aldol site could act as a chiral auxiliary in the following process. To validate this hypothesis the Michael addition reaction was carried out in the presence of racemic proline (Scheme 34). It could be observed the formation of both diastereoisomers *anti*- and *syn-21*, this time even with a larger diastereomeric ratio probably due to a less steric hindrance from the aldol site towards the Michael electrophilic site.





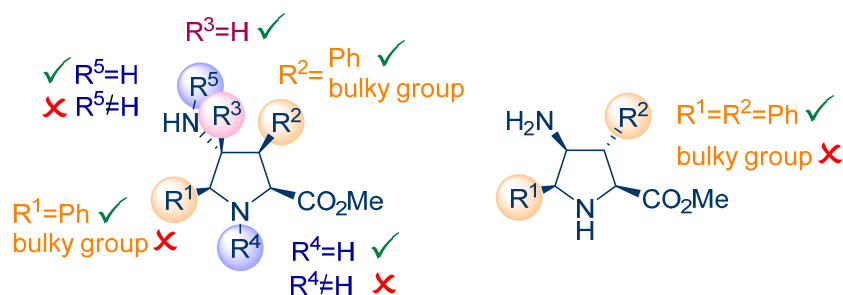
**Scheme 34.** Michael addition between cyclohexanone **11a** and **(2R,1'S)-13ab** catalyzed by racemic proline **20**.

## 2.7. Conclusions

From the experimental and computational studies which have been exposed along this chapter, the following conclusions can be drawn. Some of them are summarised in a graphical form in Scheme 35):

- (3+2) cycloadditions employing **NH-D-EhuPhos-1** and **NMe-L-EhuPhos-2** ligands assisted by copper salts and followed by a hydrogenation step constitutes a robust method to provide 4-aminopyrrolidine methyl ester carboxylates.
- These 4-aminopyrrolidine methyl ester carboxylates are efficient organocatalysts for enamine activated reactions such as aldol and Michael addition with cyclohexanone as nucleophile.
- As occurred with the previous studies with 4-nitropyrrolidine methyl ester carboxylates, *exo*- cycloadducts of the L series, lead to the opposite stereochemistry obtained under L-proline conditions.
- *Endo*- analogues of the L series lead to the same stereochemistry obtained under L-proline conditions. Nevertheless, these catalysts are less efficient in terms of stereocontrol and reactivity.
- Both amine units are simultaneously needed as whichever substitution at any center destroys the catalytic activity.
- Bulkier groups at C3 position of the *exo*- cycloadduct can improve the catalytic outcome in the conjugate addition with respect its aromatic analogue.

- DFT-based computational models are in agreement with the experimental results. These in addition to a hydrogen bond net involving a pyrrolidinium cation providing quite rigid transition structures.
- It is possible to promote sequential aldol and Michael reactions in compounds bearing two different electrophiles. By employing organocatalysts belonging to different series it is possible to obtain enantiodivergent aldol products. Nevertheless, the following Michael addition depends on the preformed aldol as it behaves as a chiral auxiliary.



**Scheme 35.** Design of *exo*- and *endo*- 4-aminopyrrolidine organocatalysts for the Michael addition with cyclohexanone as nucleophile.

## 2.8. Experimental section

**General Remarks.** Unless otherwise stated, reagents and substrates were purchased from commercial suppliers. Cyclohexanone **11a** was freshly distilled on thermally activated 4 Å molecular sieves before use. Ligands **NH-D-EhuPhos-1** and **NMe-L-EhuPhos-2** were prepared following our previously described procedure.<sup>29</sup>

TLC was performed on silica gel 60 F254, using aluminum plates and visualized with UV lamps or potassium permanganate stain. Flash chromatography was carried out on columns of silica gel 60 (230–400 mesh).

Hydrogenation reactions were performed with a flow reactor equipped with a Raney-Nickel cartridge. Hydrogen gas was generated electrochemically.

Optical rotations were measured using a polarimeter with a thermally jacketed 5 cm cell at approximately 20 °C, and concentrations (c) are given in g/100 mL.

FT-IR spectra were recorded with a spectrophotometer equipped with a single-reflection ATR module; wavenumbers are given in cm<sup>-1</sup>.

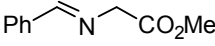
HRMS analyses were carried out using the electron impact (EI) mode at 70 eV or by Q-TOF using electrospray ionization (ESI) mode.

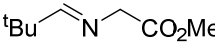
$^1\text{H}$  NMR spectra were recorded at 400 or 500 MHz for  $^1\text{H}$  NMR and 75 or 100 MHz for  $^{13}\text{C}$  NMR, using  $\text{CDCl}_3$  as the solvent and TMS as an internal standard (0.00 ppm). The data are reported as s = singlet, d = doublet, t = triplet, m = multiplet or unresolved, bs = broad signal, coupling constant(s) in Hz, integration.  $^{13}\text{C}$  NMR spectra were recorded with  $^1\text{H}$ -decoupling at 100 MHz and referenced to  $\text{CDCl}_3$  at 77.16 ppm.

Enantioselectivities were measured by HPLC using chiral stationary phases. In these experiments the racemic mixtures were analyzed in order to establish the enantiomeric parameters for each enantiomer.

### General procedure for the synthesis of imines **3**

Glycine methyl ester hydrochloride **8a** (3.0 mmol, 376.6 mg), triethylamine (3.0 mmol, 420  $\mu\text{L}$ ) and  $\text{MgSO}_4$  were dissolved in 5 mL of dry DCM. The suspension was stirred for one hour at room temperature and then, 2.3 mmol of the corresponding aldehyde **12** were added. This mixture was then allowed to stir for 16 hours. Later, the reaction mixture was filtered, washed three times with  $\text{H}_2\text{O}$ , dried on  $\text{Na}_2\text{SO}_4$  and dried over reduced pressure. The resulting products were employed without further purification.

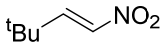
 *Methyl (E)-2-(benzylideneamino)acetate (3a)*. Yield: 446 mg, 84%, colorless oil.  $^1\text{H}$  NMR (500 MHz,  $\text{CDCl}_3$ )  $\delta$  8.29 (s, 1H, CH), 7.80 – 7.75 (m, 2H, ArH), 7.47 – 7.38 (m, 3H, ArH), 4.42 (s, 2H,  $\text{CH}_2$ ), 3.78 (s, 3H, OMe).

 *Methyl (E)-2-((2,2-dimethylpropylidene)amino)acetate (3l)*. Yield: 339 mg, 72%, yellowish oil.  $^1\text{H}$  NMR (500 MHz,  $\text{CDCl}_3$ )  $\delta$  7.59 – 7.53 (m, 1H, CH), 4.17 (s, 2H,  $\text{CH}_2$ ), 3.74 (s, 3H, OMe), 1.11 (s, 9H,  $(\text{CH}_3)_3$ ).

### Synthesis of nitroalkene **4l**

Pivalaldehyde **12l** (5.5 mmol, 600  $\mu\text{L}$ ), nitromethane (22.0 mmol, 1.20 ml), sodium acetate (5.5 mmol, 427 mg) and methylamine hydrochloride (5.5 mmol, 371 mg) were dissolved in 30 mL of methanol. The resulting mixture was stirred for 16 hours at room temperature. Then, the reaction mixture was concentrated to half volume, and washed with brine and dried onto  $\text{Na}_2\text{SO}_4$  and

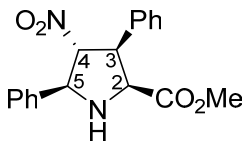
concentrated under reduced pressure. The residue was purified by flash chromatography on silica gel (EtOAc/Hex 1/10) to yield the corresponding nitroalkene **4I**.

 *(E)*-3,3-Dimethyl-1-nitrobutene (**4I**).<sup>76</sup> Yield: 178 mg, 25%, yellow oil. <sup>1</sup>H NMR (400 MHz, CDCl<sub>3</sub>) δ 7.27 (d, *J* = 13.9 Hz, 1H, CH), 6.90 (d, *J* = 13.5 Hz, 1H, CH), 1.16 (s, 9H, (CH<sub>3</sub>)<sub>3</sub>).

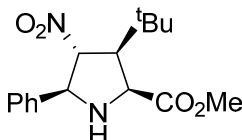
### General Procedure for the Synthesis of *exo*-Cycloadducts **5**

A solution of **NH-D-EhuPhos-1** (0.015 mmol, 9.27 mg) and Cu(CH<sub>3</sub>CN)<sub>4</sub>PF<sub>6</sub> (0.014 mmol, 5.2 mg) in 1.0 mL of dry THF was stirred at -20 °C for 15 min. Then, a solution of imine **3** (0.45 mmol) in 1.0 mL of solvent, triethylamine (0.023 mmol, 3.2 μl) and the corresponding nitroalkene **4** (0.50 mmol) in 1.0 mL of solvent were successively added. The course of the reaction was monitored by TLC and, once the starting material was consumed, the mixture was filtered through a celite pad and the filtrate was concentrated under reduced pressure. The residue was purified by flash chromatography on silica gel (EtOAc/Hex) to yield the corresponding *exo*-cycloadducts **5**. The enantiomeric excess was determined by comparison of the HPLC chromatogram recorded for the racemic mixture with that corresponding to the enantiomerically enriched cycloadduct.

**Nomenclature:** Carbon atoms in densely substituted pyrrolidine rings are numbered as in pyrrolidine, the nitrogen atom numbered 1, and proceeding towards the ester group.<sup>77</sup>

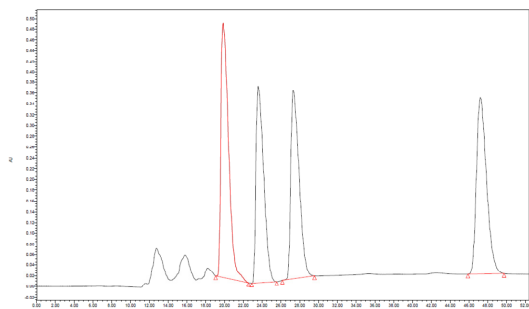
 *Methyl (2S,3S,4R,5S)-4-nitro-3,5-diphenylpyrrolidine-2-carboxylate* (NO<sub>2</sub>-X<sub>L</sub>-OMe-**5aa**).<sup>78</sup> The expected product was obtained from imine **3a** and nitroalkene **4a**. Yield: 125 mg, 85%, white solid. 97% ee after column chromatography and >99% ee after recrystallization in AcOEt/Hexane

mixture. Analytical and spectroscopic data were in good agreement with those reported in the literature. <sup>1</sup>H NMR (500 MHz, CDCl<sub>3</sub>) δ 7.58 – 7.55 (m, 2H, ArH), 7.47 – 7.18 (m, 8H, ArH), 5.22 (t, *J* = 8.1, 1H, C<sup>4</sup>H), 4.77 (d, *J* = 8.2, 1H, C<sup>5</sup>H), 4.51 (d, *J* = 9.1, 1H, C<sup>2</sup>H), 4.39 (t, *J* = 8.5, 1H, C<sup>3</sup>H), 3.29 (s, 3H, OMe), 2.75 (sa, 1H, NH). HPLC (Chiralcel IB, hexane/<sup>i</sup>PrOH = 80/20, flow rate 1.0 mL/min, λ = 254 nm), *t*<sub>R</sub> (major) = 6.92 min, *t*<sub>R</sub> (minor) = 12.49; ee = 97%.

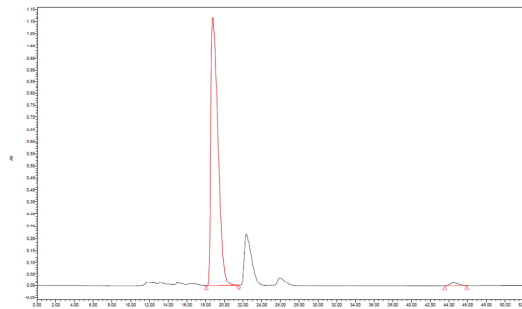
 *Methyl (2S,3S,4R,5S)-(3-tert-butyl)-4-nitro-5-phenylpyrrolidine-2-carboxylate* (NO<sub>2</sub>-X<sub>L</sub>-OMe-**5al**). The expected product was obtained from imine **3a** and nitroalkene **4I**. Yield: 99 mg, 72% (83% yield was obtained as 87:13 diastereomeric ratio *exo:endo*), white syrup. [α]<sub>D</sub><sup>25</sup> = +11.4 (c 1.28,

CHCl<sub>3</sub>), 98% ee. FTIR (neat, cm<sup>-1</sup>) 1735, 1549, 1200, 1174, 730, 699. <sup>1</sup>H NMR (400 MHz, CDCl<sub>3</sub>) δ 7.47 (d, *J* = 7.0 Hz, 2H, ArH), 7.41 – 7.32 (m, 3H, ArH), 5.07 (t, *J* = 8.2 Hz, 1H, C<sup>4</sup>H), 4.67 (d, *J* = 7.9 Hz, 1H, C<sup>5</sup>H), 4.23 (d, *J* = 7.9 Hz, 1H, C<sup>2</sup>H), 3.77 (s, 3H, CO<sub>2</sub>Me), 3.11 (t, *J* = 8.2 Hz, 1H,

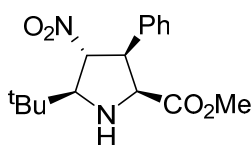
$\text{C}^3\text{H}$ ), 2.42 (bs, 1H, NH), 0.98 (s, 9H,  $(\text{CH}_3)_3$ ).  $^{13}\text{C}$  NMR (101 MHz,  $\text{CDCl}_3$ )  $\delta$  173.8, 138.8, 128.9, 128.6, 126.7, 92.7, 68.1, 61.7, 59.6, 52.0, 32.8, 27.8. HRMS (ESI) for  $\text{C}_{16}\text{H}_{22}\text{N}_2\text{O}_4$ : calculated  $[\text{M} + \text{H}]^+$ : 307.1658. Found  $[\text{M} + \text{H}]^+$ : 307.1676. HPLC (Chiralcel IB, hexane/ $\text{PrOH}$  = 80/20, flow rate 1.0 mL/min,  $\lambda$  = 210 nm),  $t_{\text{R}}$  (major) = 18.76 min,  $t_{\text{R}}$  (minor) = 44.74 min; ee = 98%.



	Time	Area	% Height	% Area
1	19.857	26881869	31.23	28.68
2	23.575	20878555	24.09	22.27
3	27.295	21481940	23.06	22.92
4	47.203	24497140	21.62	26.13



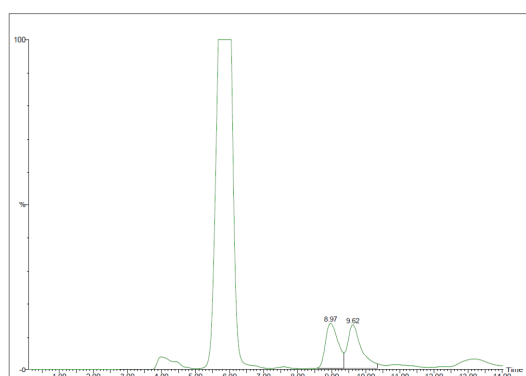
	Time	Area	% Height	% Area
1	18.762	59598375	98.97	98.82
2	44.474	714680	1.03	1.18



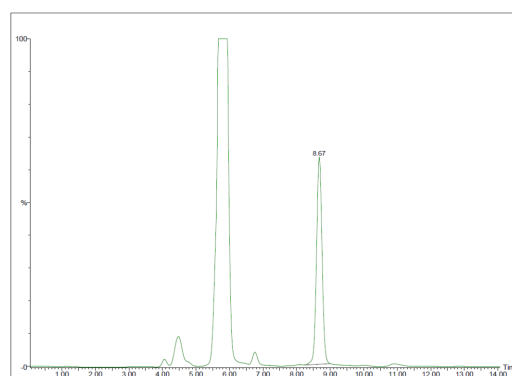
*Methyl (2S,3S,4R,5S)-5-(tert-butyl)-4-nitro-3-phenylpyrrolidine-2-carboxylate* ( $\text{NO}_2\text{-X}_L\text{-OMe-51a}$ ).<sup>30</sup> The expected product was obtained from imine **3** and nitroalkene **4a**. Yield: 124 mg, 90%, white solid. 99% ee after

column chromatography. Analytical and spectroscopic data were in good

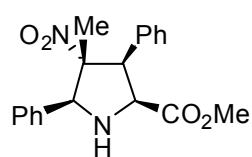
agreement with those reported in the literature.  $^1\text{H}$  NMR (500 MHz,  $\text{CDCl}_3$ )  $\delta$  7.33 – 7.15 (m, 5H, ArH), 4.96 (dd,  $J$  = 7.8, 6.5, 1H,  $\text{C}^4\text{H}$ ), 4.42 (d,  $J$  = 8.6, 1H,  $\text{C}^2\text{H}$ ), 4.06 (dd,  $J$  = 8.4, 6.5, 1H,  $\text{C}^3\text{H}$ ), 3.63 (d,  $J$  = 7.5, 1H,  $\text{C}^5\text{H}$ ), 3.25 (s, 3H), 2.45 (sa, 1H), 1.06 (s, 9H). HPLC (Chiralcel IB, hexane/ $\text{PrOH}$  = 80/20, flow rate 1.0 mL/min,  $\lambda$  = 254 nm),  $t_{\text{R}}$  (major) = 8.67 min; ee = 99%.



	Time	Area	% Height	% Area
1	8.97	86937.52	50.80	48.12
2	9.62	93724.50	49.20	51.88



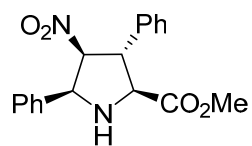
	Time	Area	% Height	% Area
1	8.67	27493.55	100	100.00



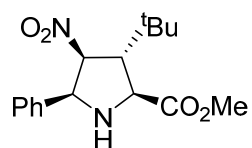
*Methyl* (2*S*,3*S*,4*R*,5*S*)-4-methyl-4-nitro-3,5-diphenylpyrrolidine-2-carboxylate (NO<sub>2</sub>-X<sub>L</sub>-OMe-5am). The expected product was obtained from imine **3a** and nitroalkene **2m**. Yield: 101 mg, 66 %, white solid. *m*<sub>p</sub> = 114 – 115 °C. [α]<sub>D</sub><sup>25</sup> = +84.2 (c 1.00, CHCl<sub>3</sub>), 94% ee. FTIR (neat, cm<sup>-1</sup>) 3339, 1742, 1536, 1381. <sup>1</sup>H NMR (400 MHz, CDCl<sub>3</sub>) δ 7.61 – 7.18 (m, 10H, ArH), 5.04 (s, 1H, C<sup>5</sup>H), 4.67 (d, *J* = 8.2 Hz, 1H, C<sup>3</sup>H), 4.47 (d, *J* = 8.2 Hz, 1H, C<sup>2</sup>H), 3.44 (s, 3H, CO<sub>2</sub>Me), 2.84 (bs, 1H, NH), 0.88 (s, 3H, CH<sub>3</sub>). <sup>13</sup>C NMR (400 MHz, CDCl<sub>3</sub>) δ 171.3, 136.7, 136.5, 129.7, 128.5 (two signals), 128.3, 127.8, 127.8, 98.3, 69.8, 63.0, 56.0, 51.8, 20.8. HRMS (ESI) for C<sub>19</sub>H<sub>20</sub>N<sub>2</sub>O<sub>4</sub>: calculated [M + H]<sup>+</sup>: 341.1501. Found [M + H]<sup>+</sup>: 341.1503. HPLC (Chiralcel IA, hexane/PrOH = 85/15, flow rate 1.0 mL/min, λ = 254 nm), *t*<sub>R</sub> (minor) = 10.9 min, *t*<sub>R</sub> (major) = 13.4 min; ee = 94%.

### General Procedure for the Synthesis of *endo*-Cycloadducts **5**

A solution of **NMe-L-EhuPhos-2** (9.48 mg, 0.015 mmol) and Cu(CH<sub>3</sub>CN)<sub>4</sub>PF<sub>6</sub> (5.2 mg, 0.014 mmol) in 1.0 mL of dry THF was stirred at -60 °C for 15 min. Then, a solution of imine **3** (0.45 mmol) in 1.0 mL of solvent, triethylamine (3.2 μl, 0.023 mmol) and the corresponding nitroalkenes **4** (0.50 mmol) in 1.0 mL of solvent were successively added. The reaction was monitored by TLC and, once the starting material was consumed, the mixture was filtered through a celite pad and the filtrate was concentrated under reduced pressure. The residue was purified by flash chromatography on silica gel (ethyl acetate:hexanes 1:2) to yield the corresponding *endo*-cycloadducts **5**. The enantiomeric excess was determined by comparison of the HPLC chromatogram recorded for the racemic mixture with that corresponding to the enantiomerically enriched cycloadduct.

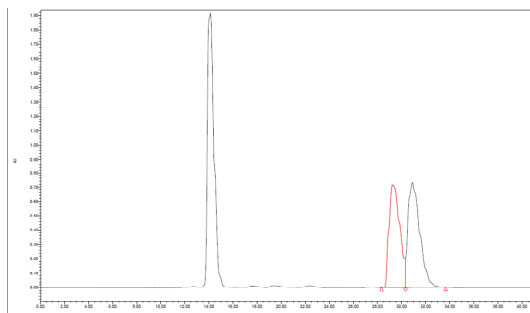


*Methyl* (2*S*,3*R*,4*S*,5*S*)-4-nitro-3,5-diphenylpyrrolidine-2-carboxylate (NO<sub>2</sub>-N<sub>L</sub>-OMe-5aa).<sup>78</sup> The expected product was obtained from imine **3a** and nitroalkene **4a**. Yield: 119 mg, 81%, white solid. 92% ee after column chromatography and >99% ee after recrystallization in AcOEt/Hexane recrystallization mixture. Analytical and spectroscopic data were in good agreement with those reported in the literature. <sup>1</sup>H NMR (500 MHz, CDCl<sub>3</sub>) δ 7.46 – 7.27 (m, 10H, ArH), 5.28 (dd, *J* = 6.4, 3.5, 1H, C<sup>4</sup>H), 4.91 (d, *J* = 6.4, 1H, C<sup>5</sup>H), 4.22 (dd, *J* = 7.2, 3.4, 1H, C<sup>3</sup>H), 4.15 (d, *J* = 7.3, 1H, C<sup>2</sup>H), 3.81 (s, 3H, OMe), 2.90 (sa, 1H, NH). HPLC (Chiralcel IB, hexane/PrOH = 85/15, flow rate 1.0 mL/min, λ = 254 nm), *t*<sub>R</sub> (major) = 14.84 min, *t*<sub>R</sub> (minor) = 21.02; ee = 92%.

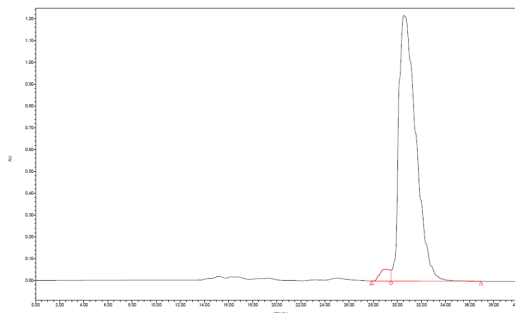


*Methyl* (2*S*,3*R*,4*S*,5*S*)-(3-*tert*-butyl)-4-nitro-5-phenylpyrrolidine-2-carboxylate (NO<sub>2</sub>-N<sub>L</sub>-OMe-5al). The expected product was obtained from imine **3a** and nitroalkene **4l**. Yield: 116 mg, 84%, orange solid. *m*<sub>p</sub> = 113°C. [α]<sub>D</sub><sup>25</sup> = +14.4 (c 0.50, CHCl<sub>3</sub>), 95% ee. FTIR (neat, cm<sup>-1</sup>) 1728, 1545, 1197, 1198, 733, 694. <sup>1</sup>H NMR (400 MHz, CDCl<sub>3</sub>) δ 7.32 (m, 5H, ArH), 5.12 (m, 1H, C<sup>4</sup>H), 4.45 (dd,

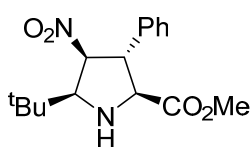
$J = 11.6, 6.1$  Hz, 1H, C<sup>5</sup>H), 3.85 (s, 3H, CO<sub>2</sub>Me), 3.27 (t,  $J = 10.8$  Hz, 1H, C<sup>2</sup>H), 2.97 (d,  $J = 5.3$  Hz, 1H, C<sup>3</sup>H), 1.05 (s, 9H, (CH<sub>3</sub>)<sub>3</sub>). <sup>13</sup>C NMR (101 MHz, CDCl<sub>3</sub>)  $\delta$  172.6, 134.3, 128.4, 128.2, 126.0, 93.2, 67.9, 61.9, 61.1, 52.5, 32.4, 27.4; HRMS (ESI) for C<sub>16</sub>H<sub>22</sub>N<sub>2</sub>O<sub>4</sub>: calculated [M + H]<sup>+</sup>: 307.1658. Found [M + H]<sup>+</sup>: 307.1673. HPLC (Chiralcel IB, hexane/<sup>i</sup>PrOH = 90/10, flow rate 0.5 mL/min,  $\lambda = 210$  nm),  $t_R$  (minor) = 29.05 min,  $t_R$  (major) = 30.53 min; ee = 95%.



	Time	Area	% Height	% Area
1	29.241	44538767	49.51	47.35
2	30.889	49520180	50.49	52.65

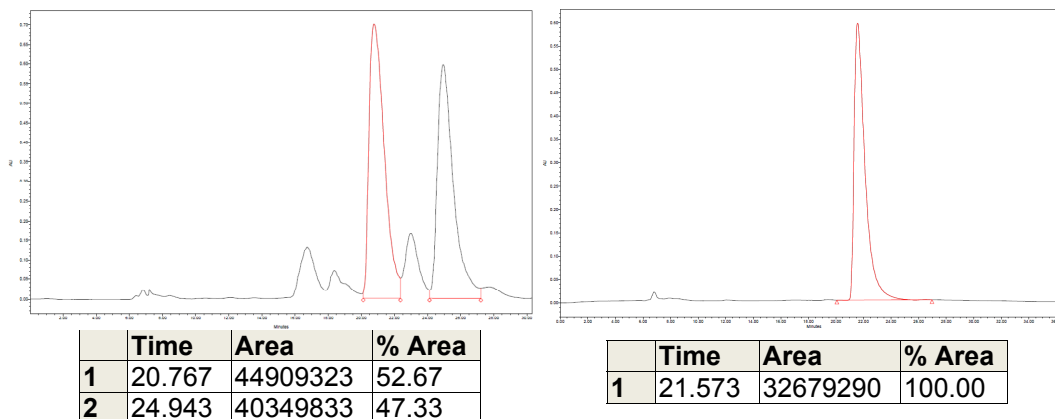


	Time	Area	% Height	% Area
1	29.055	3188195	4.24	2.58
2	30.533	120212188	95.76	97.42



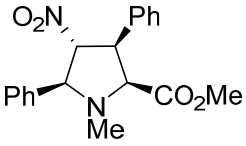
*Methyl* (2*S*,3*R*,4*S*,5*S*)-(5-*tert*-butyl)-4-nitro-3-phenylpyrrolidine-2-carboxylate (NO<sub>2</sub>-N<sub>L</sub>-OMe-5la). The expected product was obtained from imine **3I** and nitroalkene **4a**. Yield: 94 mg, 68%, 77% ee (91% yield was obtained as an 82:18 diastereomeric ratio *exo:endo*), orange syrup.

$[\alpha]_D^{25} = -113.6$  (c 1.08, CHCl<sub>3</sub>), >99% ee after semipreparative HPLC purification (Chiralcel IA, hexane/<sup>i</sup>PrOH = 99:1, flow rate 3 mL/min,  $\lambda = 210$  nm). FTIR (neat, cm<sup>-1</sup>) 1740, 1543, 908, 729, 698. <sup>1</sup>H NMR (400 MHz, CDCl<sub>3</sub>)  $\delta$  7.39 (t,  $J = 7.4$  Hz, 2H, ArH), 7.33 (d,  $J = 7.1$  Hz, 1H, ArH), 7.22 (d,  $J = 7.4$  Hz, 2H, ArH), 4.98 (d,  $J = 4.2$  Hz, 1H, C<sup>4</sup>H), 4.04 (d,  $J = 5.7$  Hz, 1H, C<sup>2</sup>H), 3.97 (d,  $J = 5.7$  Hz, 1H, C<sup>3</sup>H), 3.82 (s, 3H, CO<sub>2</sub>Me), 3.23 (s, 1H, C<sup>5</sup>H), 3.11 (s, 1H, NH), 1.08 (s, 9H, (CH<sub>3</sub>)<sub>3</sub>). <sup>13</sup>C NMR (101 MHz, CDCl<sub>3</sub>)  $\delta$  171.8, 139.5, 129.0, 127.7, 127.1, 92.6, 74.8, 67.4, 56.7, 52.3, 32.5, 26.7. HRMS (ESI) for C<sub>16</sub>H<sub>22</sub>N<sub>2</sub>O<sub>4</sub>: calculated [M + H]<sup>+</sup>: 307.1658. Found [M + H]<sup>+</sup>: 307.1673. HPLC (Chiralcel IA, hexane/<sup>i</sup>PrOH = 99/1, flow rate 1.0 mL/min,  $\lambda = 210$  nm),  $t_R$  (major) = 21.57 min; ee = >99%.



### General Procedure for the methylation of NO<sub>2</sub>-X<sub>L</sub>-OMe-5aa<sup>79</sup>

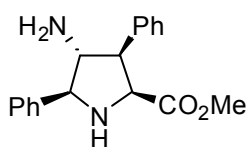
Pyrrolidine NO<sub>2</sub>-X<sub>L</sub>-OMe-5aa (500 mg, 1.53 mmol) was dissolved in 10 mL of 88% aqueous formic acid. 10 mL of 35% aqueous formaldehyde were added and the reaction mixture was heated at 100°C for two hours. After cooling to room temperature, the acidic solution was basified with saturated K<sub>2</sub>CO<sub>3</sub> solution from which a precipitated appeared. Then, this solution was diluted with H<sub>2</sub>O and extracted with CH<sub>2</sub>Cl<sub>2</sub>. The combined organic layers were dried over Na<sub>2</sub>SO<sub>4</sub>, filtered and concentrated under reduced pressure. The crude mixture was filtered through a plug of silica eluting with ethyl acetate affording the pure product.


*Methyl (2S,3S,4R,5S)-1-methyl-4-nitro-3,5-diphenylpyrrolidine-2-carboxylate* (NO<sub>2</sub>-X<sub>L</sub>-OMe-5c). Yield: 406 mg, 78 %, dark yellow solid. *m*<sub>p</sub> = 63 – 64 °C. [α]<sub>D</sub><sup>25</sup> = +31.9 (c 0.75, CHCl<sub>3</sub>). FTIR (neat, cm<sup>-1</sup>) 3061, 3030, 2951, 1739, 1702, 1551, 1448, 1365, 1203, 1175, 751, 696. <sup>1</sup>H NMR (400 MHz, CDCl<sub>3</sub>) δ 7.51 (d, *J* = 7.3 Hz, 2H, ArH), 7.45 – 7.21 (m, 8H, ArH), 5.00 (m, 1H, C<sup>4</sup>H), 4.24 (dd, *J* = 9.3, 5.9 Hz, 1H, C<sup>3</sup>H), 3.97 (d, *J* = 8.0 Hz, 1H, C<sup>5</sup>H), 3.92 (d, *J* = 9.3 Hz, 1H, C<sup>2</sup>H), 3.27 (s, 3H, CO<sub>2</sub>Me), 2.33 (s, 3H, NCH<sub>3</sub>). <sup>13</sup>C NMR (400 MHz, CDCl<sub>3</sub>) δ 169.7, 137.8, 137.2, 129.1, 129.0, 128.6, 128.4, 128.0, 127.6, 97.1, 75.1, 71.8, 51.4, 51.1, 39.3. HRMS (ESI) for C<sub>19</sub>H<sub>20</sub>N<sub>2</sub>O<sub>4</sub>: calculated [M + H]<sup>+</sup>: 341.1501. Found [M + H]<sup>+</sup>: 341.1501.

### General Procedure for the Synthesis of Amino Derivatives 10

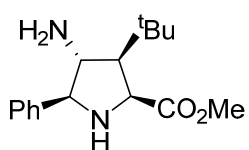
A solution of the corresponding 4-nitro cycloadducts **5** (1 mmol) in 100 mL of methanol was pumped at 1 mL/min through the H-Cube® Hydrogenation Reactor using a Raney/Nickel CatCart® as catalyst. The pressure of the system was set to 20 bars and the temperature to 65°C. After all the reaction mixture had passed through the reactor, the solvent was reduced to dryness. The crude mixture was filtered through a plug of silica eluting with ethyl acetate affording the pure product.





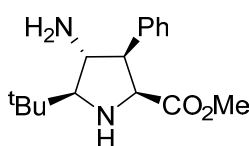
*Methyl (2S,3R,4R,5S)-4-amino-3,5-diphenylpyrrolidine-2-carboxylate* (NH<sub>2</sub>-X<sub>L</sub>-OMe-**10aa**). The expected product was obtained from NO<sub>2</sub>-X<sub>L</sub>-OMe-**5aa**. Yield: 266 mg, 90%, white solid. *m*<sub>p</sub> = 75 – 77 °C. [α]<sub>D</sub><sup>25</sup> = +100.1 (c 0.50, CHCl<sub>3</sub>). FTIR (neat, cm<sup>-1</sup>) 1731, 1173, 1107, 696.

<sup>1</sup>H NMR (500 MHz, CDCl<sub>3</sub>) δ 7.70 - 7.64 (m, 2H, ArH), 7.42 (dd, *J* = 10.3, 4.7 Hz, 2H, ArH), 7.38 – 7.30 (m, 3H, ArH), 7.28 – 7.24 (m, 3H, ArH), 4.29 (d, *J* = 9.8 Hz, 1H, C<sup>5</sup>H), 3.93 (d, *J* = 8.9 Hz, 1H, C<sup>2</sup>H), 3.66 (dd, *J* = 10.3, 9.0 Hz, 1H, C<sup>3</sup>H), 3.49 (t, *J* = 10.1 Hz, 1H, C<sup>4</sup>H), 3.24 (s, 3H, CO<sub>2</sub>Me), 1.65 (bs, 2H, NH<sub>2</sub>). <sup>13</sup>C NMR (126 MHz, CDCl<sub>3</sub>) δ 174.3, 140.8, 137.5, 128.7, 128.4, 128.2, 127.9, 127.3, 127.3, 70.3, 63.8, 62.9, 57.1, 51.3. HRMS (ESI) for C<sub>18</sub>H<sub>20</sub>N<sub>2</sub>O<sub>2</sub>: calculated [M + H]<sup>+</sup>: 297.1603. Found [M + H]<sup>+</sup>: 297.1604.



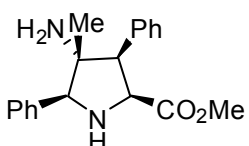
*Methyl (2S,3R,4R,5S)-4-amino-3-(tert-butyl)-5-phenylpyrrolidine-2-carboxylate* (NH<sub>2</sub>-X<sub>L</sub>-OMe-**10al**). The expected product was obtained from NO<sub>2</sub>-X<sub>L</sub>-OMe-**5al**. Yield: 248 mg, 90%, white syrup. [α]<sub>D</sub><sup>25</sup> = +62.7 (c 1.85, CHCl<sub>3</sub>). FTIR (neat, cm<sup>-1</sup>) 2948, 1729, 1196, 1175, 701. <sup>1</sup>H NMR (400 MHz, CDCl<sub>3</sub>) δ 7.58 (d, *J* = 7.3 Hz, 2H, ArH), 7.37 (t, *J* = 7.3 Hz, 2H, ArH), 7.31 (d, *J* = 7.1 Hz, 1H, ArH), 4.05 (d, *J* = 7.9 Hz, 1H, C<sup>5</sup>H), 3.76 (s, 3H, CO<sub>2</sub>Me), 3.71 (d, *J* = 8.1 Hz, 1H, C<sup>2</sup>H), 3.43 (t, *J* = 8.4 Hz, 1H, C<sup>4</sup>H), 2.10 (t, *J* = 8.3 Hz, 1H, C<sup>3</sup>H), 1.49 (bs, 2H, NH<sub>2</sub>), 1.05 (s, 9H, (CH<sub>3</sub>)<sub>3</sub>). <sup>13</sup>C NMR (101 MHz, CDCl<sub>3</sub>) δ 175.6, 142.0, 128.5, 127.6, 127.4, 71.5, 61.4, 61.1, 60.5, 51.6, 32.2, 28.6. HRMS (ESI) for C<sub>16</sub>H<sub>24</sub>N<sub>2</sub>O<sub>2</sub>: calculated [M + H]<sup>+</sup>: 277.1916. Found [M + H]<sup>+</sup>: 277.1921.

<sup>1</sup>H NMR (400 MHz, CDCl<sub>3</sub>) δ 7.58 (d, *J* = 7.3 Hz, 2H, ArH), 7.37 (t, *J* = 7.3 Hz, 2H, ArH), 7.31 (d, *J* = 7.1 Hz, 1H, ArH), 4.05 (d, *J* = 7.9 Hz, 1H, C<sup>5</sup>H), 3.76 (s, 3H, CO<sub>2</sub>Me), 3.71 (d, *J* = 8.1 Hz, 1H, C<sup>2</sup>H), 3.43 (t, *J* = 8.4 Hz, 1H, C<sup>4</sup>H), 2.10 (t, *J* = 8.3 Hz, 1H, C<sup>3</sup>H), 1.49 (bs, 2H, NH<sub>2</sub>), 1.05 (s, 9H, (CH<sub>3</sub>)<sub>3</sub>). <sup>13</sup>C NMR (101 MHz, CDCl<sub>3</sub>) δ 175.6, 142.0, 128.5, 127.6, 127.4, 71.5, 61.4, 61.1, 60.5, 51.6, 32.2, 28.6. HRMS (ESI) for C<sub>16</sub>H<sub>24</sub>N<sub>2</sub>O<sub>2</sub>: calculated [M + H]<sup>+</sup>: 277.1916. Found [M + H]<sup>+</sup>: 277.1921.



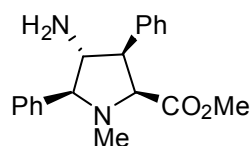
*Methyl (2S,3R,4R,5S)-4-amino-5-(tert-butyl)-3-phenylpyrrolidine-2-carboxylate* (NH<sub>2</sub>-X<sub>L</sub>-OMe-**10la**). The expected product was obtained from NO<sub>2</sub>-X<sub>L</sub>-OMe-**5la**. Yield: 218 mg, 79%, yellow oil. [α]<sub>D</sub><sup>25</sup> = +81.7 (c 0.52, CHCl<sub>3</sub>). FTIR (neat, cm<sup>-1</sup>) 2950, 1734, 1204, 700. <sup>1</sup>H NMR (400 MHz, CDCl<sub>3</sub>) δ 7.31 (d, *J* = 6.7 Hz, 2H), 7.25 (d, *J* = 7.2 Hz, 3H), 4.20 (d, *J* = 9.4 Hz, 1H), 3.43 (t, *J* = 7.8 Hz, 1H), 3.30 (t, *J* = 8.5 Hz, 1H), 3.23 (s, 3H, CO<sub>2</sub>Me), 2.72 (d, *J* = 8.1 Hz, 1H), 1.14 (s, 9H).

<sup>13</sup>C NMR (101 MHz, CDCl<sub>3</sub>) δ 173.5, 139.6, 128.3, 128.3, 127.0, 74.7, 63.1, 59.2, 58.9, 51.2, 33.1, 27.3. HRMS (ESI) for C<sub>16</sub>H<sub>24</sub>N<sub>2</sub>O<sub>2</sub>: calculated [M + H]<sup>+</sup>: 277.1916. Found [M + H]<sup>+</sup>: 277.1923.

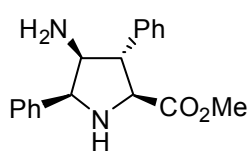


*Methyl (2S,3S,4R,5S)-4-amino-4-methyl-3,5-diphenylpyrrolidine-2-carboxylate* (NH<sub>2</sub>-X<sub>L</sub>-OMe-**10am**). The expected product was obtained from NO<sub>2</sub>-X<sub>L</sub>-OMe-**5am**. Yield: 260 mg, 84%, white solid. *m*<sub>p</sub> = 102 – 103 °C. [α]<sub>D</sub><sup>25</sup> = +61.7 (c 0.40, CHCl<sub>3</sub>). FTIR (neat, cm<sup>-1</sup>) 3347, 1735, 1205, 728, 702. <sup>1</sup>H NMR (400 MHz, CHCl<sub>3</sub>) δ 7.53 (d, *J* = 7.3 Hz, 2H, ArH), 7.37 (d, *J* = 7.5 Hz, 2H, ArH), 7.29 (m, 6H, ArH), 4.41 (d, *J* = 10.2 Hz, 1H, C<sup>2</sup>H), 4.11 (s, 1H, C<sup>5</sup>H), 3.51 (d, *J* = 10.3 Hz, 1H, C<sup>3</sup>H), 3.45 (s, 3H, CO<sub>2</sub>Me), 1.51 (bs, 2H, NH<sub>2</sub>), 0.62 (s, 3H, CH<sub>3</sub>). <sup>13</sup>C NMR (101 MHz, CDCl<sub>3</sub>) δ 173.8, 138.6, 137.3, 129.7, 128.0, 127.8, 127.4, 127.2, 126.9, 72.9, 62.3, 61.7, 61.3, 51.4, 22.3. HRMS (ESI) for C<sub>19</sub>H<sub>22</sub>N<sub>2</sub>O<sub>2</sub>: calculated [M + H]<sup>+</sup>: 311.1760. Found [M + H]<sup>+</sup>: 311.1770.

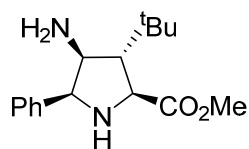
<sup>13</sup>C NMR (101 MHz, CDCl<sub>3</sub>) δ 173.8, 138.6, 137.3, 129.7, 128.0, 127.8, 127.4, 127.2, 126.9, 72.9, 62.3, 61.7, 61.3, 51.4, 22.3. HRMS (ESI) for C<sub>19</sub>H<sub>22</sub>N<sub>2</sub>O<sub>2</sub>: calculated [M + H]<sup>+</sup>: 311.1760. Found [M + H]<sup>+</sup>: 311.1770.



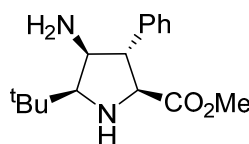
*Methyl (2S,3R,4R,5S)-4-amino-1-methyl-3,5-diphenylpyrrolidine-2-carboxylate* ( $\text{NH}_2\text{-X}_L\text{-OMe-10c}$ ). The expected product was obtained from  $\text{NO}_2\text{-X}_L\text{-OMe-10c}$ . Yield: 242 mg, 78 %, bright yellow solid.  $m_p = 108 - 110$  °C.  $[\alpha]_D^{25} = +93.5$  (c 0.51,  $\text{CHCl}_3$ ). FTIR (neat,  $\text{cm}^{-1}$ ) 3389, 3027, 2950, 2796, 1741, 1453, 1435, 1197, 1177, 1056, 746, 696.  $^1\text{H NMR}$  (400 MHz,  $\text{CDCl}_3$ )  $\delta$  7.57 (d,  $J = 7.5$  Hz, 2H, ArH), 7.40 (t,  $J = 7.5$  Hz, 2H, ArH), 7.37 – 7.19 (m, 6H, ArH), 3.72 (d,  $J = 10.4$  Hz, 1H,  $\text{C}^5\text{H}$ ), 3.52 (t,  $J = 8.4$  Hz, 1H,  $\text{C}^3\text{H}$ ), 3.40 – 3.32 (m, 1H,  $\text{C}^4\text{H}$ ), 3.21 (s, 3H,  $\text{CO}_2\text{Me}$ ), 3.18 (d,  $J = 8.3$  Hz, 1H,  $\text{C}^2\text{H}$ ), 2.25 (s, 3H, NMe), 1.35 (bs, 2H,  $\text{NH}_2$ ).  $^{13}\text{C NMR}$  (101 MHz,  $\text{CDCl}_3$ )  $\delta$  171.9, 140.3, 139.5, 128.7, 128.6, 128.3, 127.9, 127.9, 127.1, 78.9, 72.1, 66.0, 55.4, 51.1, 39.9. HRMS (ESI) for  $\text{C}_{19}\text{H}_{22}\text{N}_2\text{O}_2$ : calculated  $[\text{M} + \text{H}]^+$ : 311.1760. Found  $[\text{M} + \text{H}]^+$ : 311.1773.



*Methyl (2S,3S,4S,5S)-4-amino-3,5-diphenylpyrrolidine-2-carboxylate* ( $\text{NH}_2\text{-N}_L\text{-OMe-10aa}$ ). The expected product was obtained from  $\text{NO}_2\text{-N}_L\text{-OMe-5aa}$ . Yield: 207 mg, 70%, yellow syrup.  $[\alpha]_D^{25} = +24.2$  (c 0.60,  $\text{CHCl}_3$ ). FTIR (neat,  $\text{cm}^{-1}$ ) 3382, 1727, 1219, 700.  $^1\text{H NMR}$  (500 MHz,  $\text{CDCl}_3$ )  $\delta$  7.51 (d,  $J = 7.3$  Hz, 2H, ArH), 7.44 – 7.31 (m, 8H, ArH), 4.63 (d,  $J = 6.1$  Hz, 1H,  $\text{C}^5\text{H}$ ), 4.12 (d,  $J = 7.8$  Hz, 1H,  $\text{C}^2\text{H}$ ), 3.74 (s, 3H,  $\text{CO}_2\text{Me}$ ), 3.64 (t,  $J = 6.2$  Hz, 1H,  $\text{C}^3\text{H}$ ), 3.24 (t,  $J = 6.2$  Hz, 1H,  $\text{C}^4\text{H}$ ), 1.70 (bs, 2H,  $\text{NH}_2$ ).  $^{13}\text{C NMR}$  (126 MHz,  $\text{CDCl}_3$ )  $\delta$  174.3, 140.2, 139.8, 128.6, 128.2, 127.6, 127.5, 127.2, 126.9, 65.4, 64.9, 62.9, 57.0, 52.0. HRMS (ESI) for  $\text{C}_{18}\text{H}_{20}\text{N}_2\text{O}_2$ : calculated  $[\text{M} + \text{H}]^+$ : 297.1603. Found  $[\text{M} + \text{H}]^+$ : 297.1610.



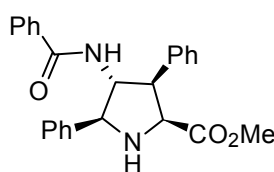
*Methyl (2S,3S,4S,5S)-4-amino-3-(tert-butyl)-5-phenylpyrrolidine-2-carboxylate* ( $\text{NH}_2\text{-N}_L\text{-OMe-10al}$ ). The expected product was obtained from  $\text{NH}_2\text{-N}_L\text{-OMe-5al}$ . Yield: 226 mg, 82%, orange syrup.  $[\alpha]_D^{25} = +37.4$  (c 0.34,  $\text{CHCl}_3$ ) (95% ee). FTIR (neat,  $\text{cm}^{-1}$ ) 2952, 1735, 1199, 1170, 755, 701.  $^1\text{H NMR}$  (400 MHz,  $\text{CDCl}_3$ )  $\delta$  7.35 (s, 5H, ArH), 4.19 (d,  $J = 3.5$  Hz, 1H,  $\text{C}^5\text{H}$ ), 3.78 (s, 3H,  $\text{CO}_2\text{Me}$ ), 3.73 (d,  $J = 6.2$  Hz, 1H,  $\text{C}^2\text{H}$ ), 3.30 (d,  $J = 3.3$  Hz, 1H,  $\text{C}^4\text{H}$ ), 2.05 (d,  $J = 5.6$  Hz, 1H,  $\text{C}^3\text{H}$ ), 1.02 (s, 9H,  $(\text{CH}_3)_3$ ).  $^{13}\text{C NMR}$  (101 MHz,  $\text{CDCl}_3$ )  $\delta$  175.1, 138.5, 128.2, 127.0 (two signals ArC), 67.2, 62.5, 60.4, 57.5, 52.1, 32.3, 27.8. HRMS (ESI) for  $\text{C}_{16}\text{H}_{24}\text{N}_2\text{O}_2$ : calculated  $[\text{M} + \text{H}]^+$ : 277.1916. Found  $[\text{M} + \text{H}]^+$ : 277.1926.



*Methyl (2S,3S,4S,5S)-4-amino-5-(tert-butyl)-3-phenylpyrrolidine-2-carboxylate* ( $\text{NH}_2\text{-N}_L\text{-OMe-10la}$ ). The expected product was obtained from  $\text{NH}_2\text{-N}_L\text{-OMe-5la}$ . Yield: 240 mg, 87%, yellow syrup.  $[\alpha]_D^{25} = +51.3$  (c 0.87,  $\text{CHCl}_3$ ). FTIR (neat,  $\text{cm}^{-1}$ ) 3342, 2951, 1735, 1217, 757, 701.  $^1\text{H NMR}$  (500 MHz,  $\text{CDCl}_3$ )  $\delta$  7.38 – 7.16 (m, 5H, ArH), 3.90 (d,  $J = 4.9$  Hz, 1H,  $\text{C}^2\text{H}$ ), 3.73 (s, 3H,  $\text{CO}_2\text{Me}$ ), 3.46 (s, 1H, NH), 3.44 – 3.40 (m, 1H,  $\text{C}^4\text{H}$ ), 3.20 – 3.19 (m, 1H,  $\text{C}^3\text{H}$ ), 2.90 (d,  $J = 4.4$  Hz, 1H,  $\text{C}^5\text{H}$ ), 2.26 (bs, 2H,  $\text{NH}_2$ ), 1.11 (s, 9H,  $(\text{CH}_3)_3$ ).  $^{13}\text{C NMR}$  (126 MHz,  $\text{CDCl}_3$ )  $\delta$  175.1, 142.1, 128.6, 127.3, 126.8, 70.4, 65.0, 62.2, 60.3, 52.3, 32.6, 28.3. HRMS (ESI) for  $\text{C}_{16}\text{H}_{24}\text{N}_2\text{O}_2$ : calculated  $[\text{M} + \text{H}]^+$ : 277.1916. Found  $[\text{M} + \text{H}]^+$ : 277.1923.

**General Procedure for the Synthesis of amide derivative 17**

Amine  $\text{NH}_2\text{-X}_L\text{-OMe-10aa}$  (0.67 mmol, 200 mg) and  $\text{K}_2\text{CO}_3$  (0.80 mmol, 111 mg) were added to 2.5 mL of DCM. Benzoyl chloride (0.67 mmol, 78  $\mu\text{L}$ ) was added to the reaction mixture and it was stirred until consumption of the starting materials, monitored by TLC. Then, the reaction mixture was washed with  $\text{H}_2\text{O}$  three times, brine and dried onto  $\text{Na}_2\text{SO}_4$ . The solvent was evaporated under reduced pressure to afford **17**.



*Methyl (2S,3R,4R,5S)-4-benzamido-3,5-diphenylpyrrolidine-2-carboxylate*

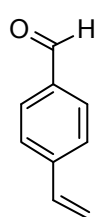
(**17**). Yield: 115 mg, 43%, white solid.  $m_p = 258 - 260$  °C.  $[\alpha]_D^{25} = -54.9$

(c 0.49, DMF). FTIR (neat,  $\text{cm}^{-1}$ ) 1734, 1654, 1383, 1174, 1153, 726.

$^1\text{H NMR}$  (500 MHz,  $\text{DMSO-}d_6$ )  $\delta$  7.50 (s, 2H), 7.43 – 7.06 (m, 13H), 4.67 (d,  $J = 8.5$  Hz, 1H), 3.81 (dd,  $J = 11.8, 8.5$  Hz, 1H), 3.70 (dd,  $J = 11.7, 9.0$  Hz, 1H), 3.26 (s, 1H, signal under water peak), 3.04 (s, 3H), 1.48 (bs, 1H).  $^{13}\text{C NMR}$  (126 MHz,  $\text{DMSO-}d_6$ , 70°C)  $\delta$  171.1, 169.4, 141.2, 136.1, 134.9, 128.9, 128.2, 127.8, 127.4, 127.3, 126.9, 126.8, 126.2, 126.1, 70.1, 64.9, 61.7, 52.3, 50.6. HRMS (ESI) for  $\text{C}_{25}\text{H}_{24}\text{N}_2\text{O}_3$ : calculated  $[\text{M} + \text{H}]^+$ : 401.1865. Found  $[\text{M} + \text{H}]^+$ : 401.1869.

**Synthesis of 12b**

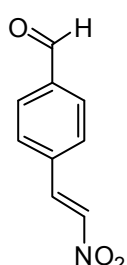
To a solution of compound **18** (2.0 g, 10.9 mmol) in dry THF (30 mL) at  $-78$  °C  $^n\text{BuLi}$  (2.5 M in hexane, 5.2 mL, 13.1 mmol) was added dropwise. Once the mixture was stirred at  $-78$  °C for 30 minutes, anhydrous DMF (1.7 mL, 21.8 mmol) was added dropwise. Then, the mixture was stirred at  $-78$  °C for another 30 min.  $\text{H}_2\text{O}$  (2 mL) was added to quench the reaction and the reaction mixture was allowed to reach room temperature. Additional  $\text{H}_2\text{O}$  (100 mL) was added and the mixture was extracted with DCM three times and the organic phases were dried with anhydrous  $\text{Na}_2\text{SO}_4$ . After removal of the solvent, the residue was purified by silica gel chromatography (hexane/EtOAc, 95:5) to give **19**.



*4-Vinylbenzaldehyde (19)*.<sup>80</sup> Yield: 1.01 g, 70%, pale yellow oil. Analytical and spectroscopic data were in good agreement with those reported in the literature.  $^1\text{H NMR}$  (500 MHz,  $\text{CDCl}_3$ )  $\delta$  9.99 (s, 1H, CHO), 7.85 (d,  $J = 8.1$  Hz, 1H, ArH), 7.56 (d,  $J = 8$  Hz, 1H, ArH), 6.78 (dd,  $J = 17.5, 10.9$  Hz, 1H, ArCH), 5.91 (d,  $J = 17.6$  Hz, 1H,  $\text{CH}_{cis}$ ), 5.44 (d,  $J = 10.9$  Hz, 1H,  $\text{CH}_{trans}$ ).

$\text{AgNO}_2$  (23.4 mmol, 3.6 g), TEMPO (3.12 mmol, 487 mg) and oven-dried molecular sieves 4 Å (2.34 g) were mixed in a flask. Then, olefin **19** (7.8 mmol, 1.012 g), previously dissolved in 32 mL of

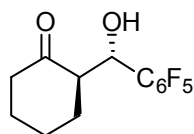
1,2-dichloroethane, was added. The reaction mixture was placed in a preheated oil bath at 70 °C and stirred vigorously for 12 hours. Then the mixture was cooled to room temperature and filtered through a plug of celite and diluted with ethyl acetate. After removal of the solvents, the residue was purified by silica gel chromatography (hexane/EtOAc 80/20) to afford **12b**.



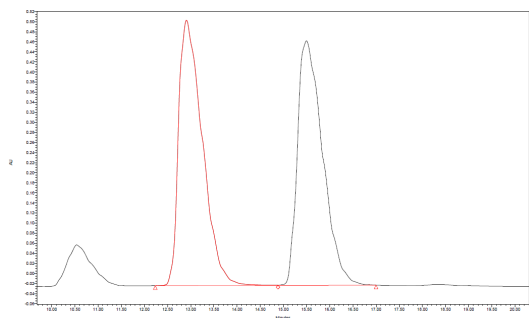
*(E)*-4-(2-Nitrovinyl)benzaldehyde (**12b**). Yield: 898 mg, 65%, yellow solid.  $m_p$  = 113 – 114 °C. FTIR (neat,  $\text{cm}^{-1}$ ) 3112, 2837, 1639, 1538, 966, 810, 730.  $^1\text{H}$  NMR (500 MHz,  $\text{CDCl}_3$ )  $\delta$  10.07 (s, 1H, CHO), 8.03 (d,  $J$  = 13.7 Hz, 1H,  $\text{CHNO}_2$ ), 7.97 (d,  $J$  = 8.1 Hz, 2H, ArH), 7.72 (d,  $J$  = 8 Hz, 2H, ArH), 7.64 (d,  $J$  = 13.7 Hz, 1H, CHAr).  $^{13}\text{C}$  NMR (126 MHz,  $\text{CDCl}_3$ )  $\delta$  191.2, 139.1, 138.5, 137.4, 135.7, 130.5, 129.7, 77.4, 77.2, 76.9. HRMS (ESI) for  $\text{C}_9\text{H}_8\text{NO}_3$ : calculated  $[\text{M} + \text{H}]^+$ : 178.0504. Found  $[\text{M} + \text{H}]^+$ : 178.0504.

### General Procedure for the Synthesis of Aldol Adducts **13** under Different Conditions

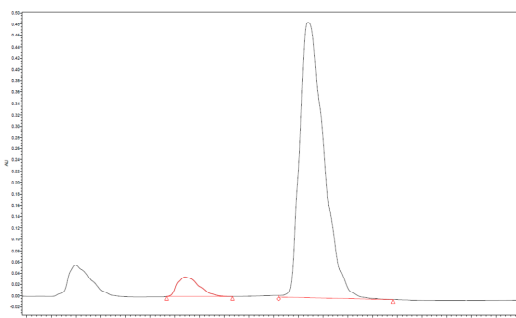
The corresponding aldehyde **12** (0.25 mmol) was dissolved in neat ketone **11a** (1.5 mL, 15.3 mmol, 61.2 equiv). The resulting mixture was cooled to 0 °C and the organocatalyst (0.0125-0.075 mmol, 0.05-0.3 equiv) was added, followed by the selected acid (75.0  $\mu\text{mol}$ , 0.3 equiv). The resulting mixture was stirred at room temperature or at 0 °C, then warmed to room temperature, diluted with ethyl acetate, washed with 0.1 M (pH 7) phosphate buffer solution, dried onto sodium sulfate, filtered and concentrated under reduced pressure. The afforded crude product was purified by flash chromatography over silica gel using ethyl acetate:hexane system as eluent.



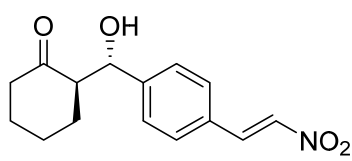
*(R)*-2-((*S*)-Hydroxy(perfluorophenyl)methyl)cyclohexan-1-one (**13aa**).<sup>81</sup> Yield: 47.8 mg, 65%, white solid. Analytical and spectroscopic data were in good agreement with that reported in the literature.  $^1\text{H}$  NMR (500 MHz,  $\text{CDCl}_3$ )  $\delta$  5.39 – 5.30 (m, 1H, CHOH), 3.92 (d,  $J$  = 3.3 Hz, 1H, CH), 3.09 – 2.99 (m, 1H,  $\text{CH}_2$ ), 2.60 – 2.48 (m, 1H,  $\text{CH}_2$ ), 2.43 (td,  $J$  = 12.9, 6.3 Hz, 1H,  $\text{CH}_2$ ), 2.22 – 2.11 (m, 1H,  $\text{CH}_2$ ), 1.95 – 1.85 (m, 1H,  $\text{CH}_2$ ), 1.76 – 1.61 (m, 3H,  $\text{CH}_2$ ), 1.41 – 1.26 (m, 1H,  $\text{CH}_2$ ).  $^{19}\text{F}$  NMR (376 MHz, cyclohexanone)  $\delta$  -143.00 (dd,  $J$  = 22.3, 7.1 Hz, 2Fo), -157.75 (t,  $J$  = 21.0 Hz, 1Fp), -164.31 (td,  $J$  = 22.1, 7.4 Hz, 2Fm). HPLC (Daicel Chiralpak IA, hexane/ $i$ PrOH = 90/10, flow rate 1.0 mL/min,  $\lambda$  = 210 nm),  $t_R$  (minor) = 13.21 min,  $t_R$  (major) = 15.70 min; ee = 88%.



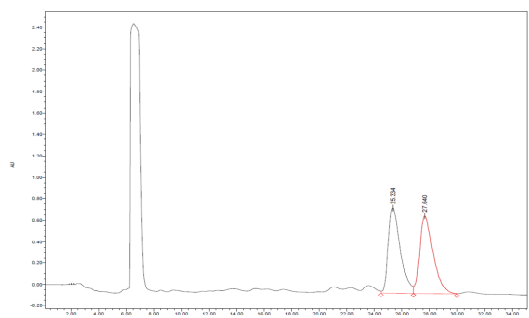
	Time	Area	% Height	% Area
1	12.908	18723559	52.08	50.59
2	15.497	18289342	47.92	49.41



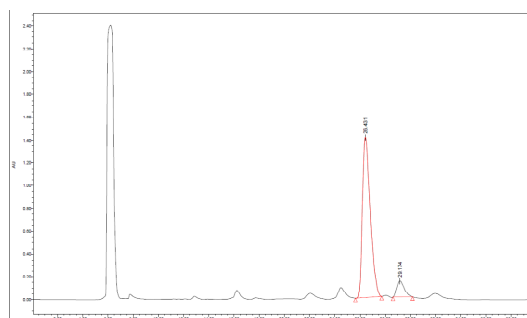
	Time	Area	% Height	% Area
1	13.211	1046507	6.47	5.96
2	15.700	16517888	93.53	94.04



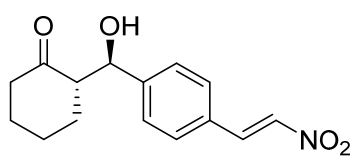
*(R)*-2-[(*S*)-Hydroxy(4-((*E*)-2-nitrovinyl)phenyl)methyl]cyclohexan-1-one (**13ab**). Yield: 48 mg, 70%, yellow solid-  $m_p = 137 - 138$  °C.  $[\alpha]_D^{25} = -12.8$  (c 0.60,  $\text{CHCl}_3$ ), 86% ee. FTIR (neat,  $\text{cm}^{-1}$ ) 3498, 2944, 2858, 1678, 1337, 827.  $^1\text{H}$  NMR (500 MHz,  $\text{CDCl}_3$ )  $\delta$  8.00 (d,  $J = 13.7$  Hz, 1H,  $\text{CHNO}_2$ ), 7.58 (d,  $J = 13.6$  Hz, 1H,  $\text{CHAr}$ ), 7.54 (d,  $J = 8.4$  Hz, 2H, ArH), 7.42 (d,  $J = 7.9$  Hz, 2H, ArH), 4.83 (dd,  $J = 8.6, 3.1$  Hz, 1H,  $\text{CHOH}$ ), 4.02 (d,  $J = 2.8$  Hz, 1H, OH), 2.60 (m, 1H,  $\text{COCHCOH}$ ), 2.49 (m, 1H,  $\text{CH}_2$ ), 2.36 (m, 1H,  $\text{CH}_2$ ), 2.15 – 2.07 (m, 1H,  $\text{CH}_2$ ), 1.82 (d,  $J = 13.1$  Hz, 1H,  $\text{CH}_2$ ), 1.68 (m, 1H,  $\text{CH}_2$ ), 1.62 – 1.56 (m, 2H,  $\text{CH}_2$ ), 1.36 (m, 1H,  $\text{CH}_2$ ).  $^{13}\text{C}$  NMR (101 MHz,  $\text{CDCl}_3$ )  $\delta$  215.0, 145.5, 138.6, 137.0, 129.1, 129.0, 128.0, 74.3, 57.2, 42.6, 30.7, 27.6, 24.7. HRMS (ESI) for  $\text{C}_{15}\text{H}_{17}\text{NO}_4\text{Na}$ : calculated  $[\text{M} + \text{Na}]^+$ : 298.1055. Found  $[\text{M} + \text{Na}]^+$ : 298.1056. HPLC (Chiralcel AD-H, hexane/ $\text{PrOH} = 80/20$ , flow rate 1.0 mL/min,  $\lambda = 210$  nm),  $t_R$  (major) = 26.43 min,  $t_R$  (minor) = 29.17 min; ee = 86%.



	Time	Area	% Height	% Area
1	25.334	48931472	52.22	49.63
2	27.640	49657775	47.78	50.37

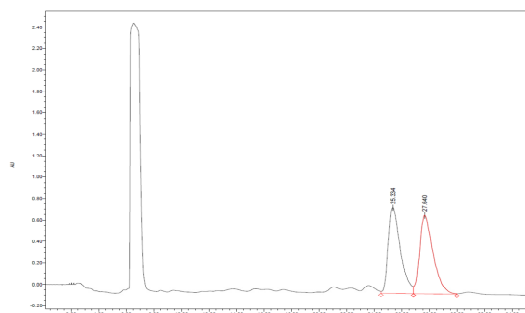


	Time	Area	% Height	% Area
1	26.431	63800170	91.82	92.75
2	29.174	4990765	8.18	7.25

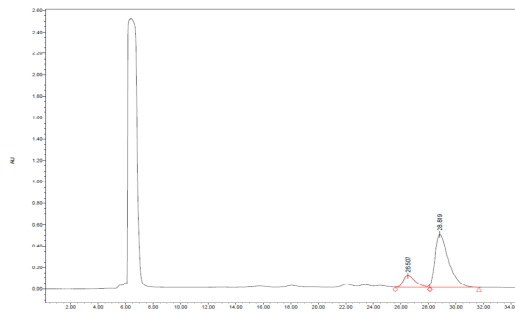


*(S)*-2-[(*R*)-Hydroxy(4-((*E*)-2-nitrovinyl)phenyl)methyl]cyclohexan-1-one (*ent*-**13ab**). Yield: 51 mg, 75%, yellow solid.  $[\alpha]_D^{25} = 8.00$  (c 0.90,  $\text{CHCl}_3$ ), -64% ee.  $^1\text{H}$  NMR (500 MHz,  $\text{CDCl}_3$ )  $\delta$  8.00 (d,  $J = 13.6$  Hz, 1H,  $\text{CHNO}_2$ ), 7.58 (d,  $J = 13.6$  Hz, 1H,  $\text{CHAr}$ ), 7.54 (d,  $J = 7.9$  Hz, 2H, ArH), 7.42 (d,  $J = 7.9$  Hz, 2H, ArH), 4.83 (dd,  $J = 8.1, 2.9$  Hz, 1H,  $\text{CHOH}$ ), 4.02 (d,

$J = 3.0$  Hz, 1H, OH), 2.61 (m, 1H, COCHCOH), 2.49 (m, 1H, CH<sub>2</sub>), 2.36 (td,  $J = 13.4, 6.2$  Hz, 1H, CH<sub>2</sub>), 2.11 (m, 1H, CH<sub>2</sub>), 1.82 (d,  $J = 12.7$  Hz, 1H, CH<sub>2</sub>), 1.74 – 1.49 (m, 3H, CH<sub>2</sub>), 1.37 (m, 1H, CH<sub>2</sub>). HPLC (Chiralcel AD-H, hexane/<sup>i</sup>PrOH = 80/20, flow rate 1.0 mL/min,  $\lambda = 210$  nm),  $t_R$  (minor) = 26.51 min,  $t_R$  (major) = 28.82 min; ee = -64%.



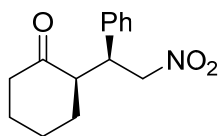
	Time	Area	% Height	% Area
1	25.334	48931472	52.22	49.63
2	27.640	49657775	47.78	50.37



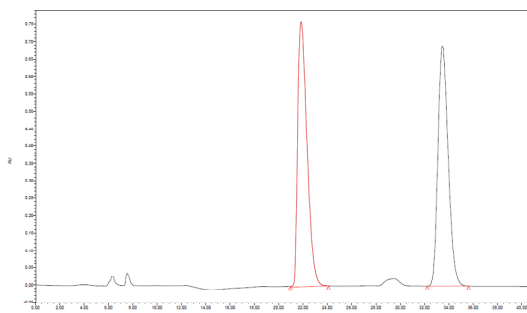
	Time	Area	% Height	% Area
1	26.507	7231256	17.68	17.66
2	28.819	33715832	82.32	82.34

### General Procedure for the Synthesis of Michael Adducts 14

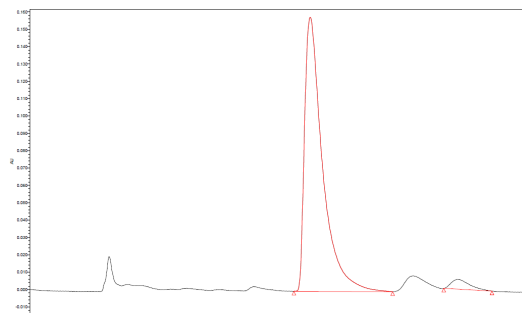
A reaction mixture of amine catalyst **10** (0.03 mmol), acid (0.03 mmol), ketone **11** (0.8 mmol) and nitroalkene **4** (0.1 mmol) was stirred at room temperature. The progress of the reaction was monitored by TLC (1/3 of EtOAc/Hex). After consumption of the nitroalkene, unreacted ketone was evaporated under reduced pressure. The afforded crude product was purified by flash chromatography over silica gel using ethyl acetate:hexane system as eluent.



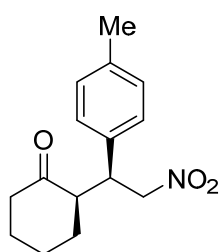
(*R*)-2-((*S*)-2-Nitro-1-phenylethyl)cyclohexanone (**14aa**).<sup>82</sup> Yield: 19 mg, 77%, white solid. Analytical and spectroscopic data were in good agreement with those reported in the literature. <sup>1</sup>H NMR (500 MHz, CDCl<sub>3</sub>)  $\delta$  7.37 – 7.30 (m, 3H, ArH), 7.17 (d,  $J = 7.1$  Hz, 2H, ArH), 4.94 (dd,  $J = 12.4, 4.4$  Hz, 1H, CHNO<sub>2</sub>), 4.69 – 4.57 (m, 1H, CHNO<sub>2</sub>), 3.81 – 3.68 (m, 1H, CHAr), 2.76 – 2.62 (m, 1H, CH), 2.48 (d,  $J = 13.3$  Hz, 1H, CH<sub>2</sub>), 2.40 (dd,  $J = 12.4, 6.2$  Hz, 1H, CH<sub>2</sub>), 2.07 (m, 1H, CH<sub>2</sub>), 1.85 – 1.58 (m, 4H, CH<sub>2</sub>), 1.24 (m, 1H, CH<sub>2</sub>). HPLC (Daicel Chiralpak AS-H, hexane/<sup>i</sup>PrOH = 90/10, flow rate 1.0 mL/min,  $\lambda = 210$  nm),  $t_R$  (major) = 22.24 min,  $t_R$  (minor) = 33.90 min; ee = 94%.



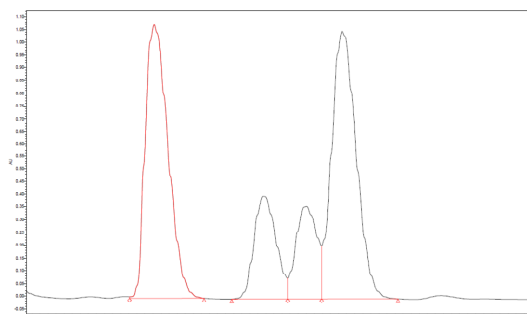
	Time	Area	% Height	% Area
1	21.839	40695306	52.43	50.10
2	33.471	40532099	47.57	49.90



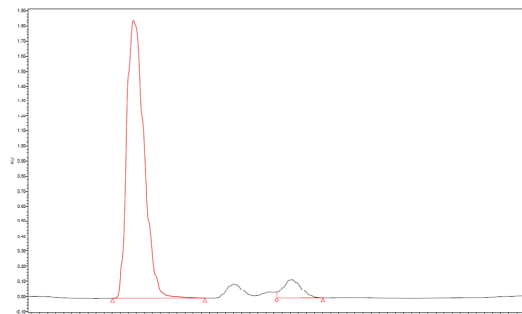
	Time	Area	% Height	% Area
1	22.244	15611841	96.58	96.48
2	33.905	569851	3.42	3.52



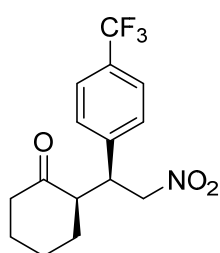
*(R)*-2-((*S*)-2-Nitro-1-(*p*-tolyl)ethyl)cyclohexanone (**14ab**).<sup>83</sup> Yield: 15.1 mg, 58%, white solid. Analytical and spectroscopic data were in good agreement with those reported in the literature. <sup>1</sup>H NMR (500 MHz, CDCl<sub>3</sub>) δ 7.12 (d, *J* = 6.8 Hz, 2H, ArH), 7.04 (d, *J* = 7.8 Hz, 2H, ArH), 4.91 (dd, *J* = 12.3, 4.4 Hz, 1H, CHNO<sub>2</sub>), 4.61 (dd, *J* = 12.1, 10.0 Hz, 1H, CHNO<sub>2</sub>), 3.72 (td, *J* = 9.7, 4.3 Hz, 1H, CHAR), 2.65 (m, 1H, CH), 2.46 (m, 1H, CH<sub>2</sub>), 2.39 (m, 1H, CH<sub>2</sub>), 2.33 (s, 3H, Me), 2.13 – 2.03 (m, 1H, CH<sub>2</sub>), 1.80 – 1.49 (m, 4H, CH<sub>2</sub>), 1.23 (m, 1H, CH<sub>2</sub>). HPLC (Daicel Chiralpak AD-H, hexane/*i*PrOH = 95/5, flow rate 0.5 mL/min, λ = 210 nm), *t*<sub>R</sub> (major) = 37.30 min, *t*<sub>R</sub> (minor) = 47.11 min; ee = 87%.



	Time	Area	% Height	% Area
1	40.079	105636239	37.20	36.67
2	46.828	38234130	13.90	13.27
3	49.504	32721997	12.51	11.36
4	51.718	111495941	36.38	38.70

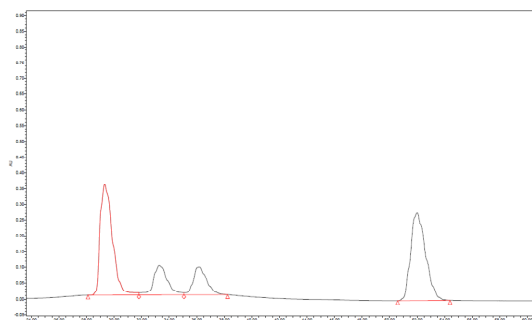


	Time	Area	% Height	% Area
1	37.304	136674075	94.02	93.52
2	47.109	9463967	5.98	6.48

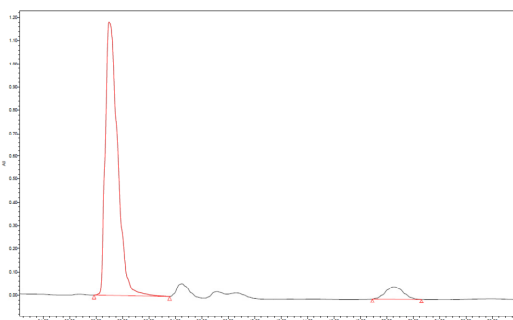


*(R)*-2-((*S*)-2-Nitro-1-(4-(trifluoromethyl)phenyl)ethyl)cyclohexanone (**14ac**).<sup>84</sup> Yield: 28.3 mg, 90%, white solid. Analytical and spectroscopic data were in good agreement with those reported in the literature. <sup>1</sup>H NMR (500 MHz, CDCl<sub>3</sub>) δ 7.61 (d, *J* = 7.8 Hz, 2H, ArH), 7.34 (d, *J* = 7.7 Hz, 2H, ArH), 4.99 (dd, *J* = 12.8, 4.4 Hz, 1H, CHNO<sub>2</sub>), 4.69 (dd, *J* = 12.7, 10.1 Hz, 1H, CHNO<sub>2</sub>), 3.89 (m, 1H, CHAR), 2.83 – 2.66 (m, 1H, CH), 2.51 (d, *J* = 12.8 Hz, 1H, CH<sub>2</sub>), 2.47 – 2.37 (m, 1H, CH<sub>2</sub>), 2.18 – 2.06 (m, 1H, CH<sub>2</sub>), 1.90 – 1.52 (m, 4H, CH<sub>2</sub>), 1.27 (d, *J* = 11.1 Hz,

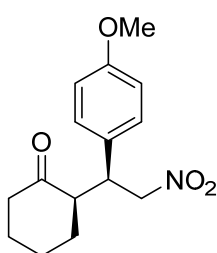
1H, CH<sub>2</sub>). HPLC (Daicel Chiralpak AD-H, hexane/*i*PrOH = 95/5, flow rate 0.5 mL/min, λ = 210 nm), *t*<sub>R</sub> (major) = 28.99 min, *t*<sub>R</sub> (minor) = 50.56 min; ee = 88%.



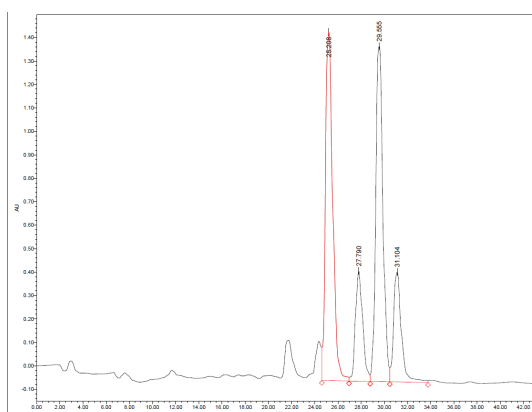
	Time	Area	% Height	% Area
1	29.314	21727359	43.68	39.49
2	33.277	6558133	11.42	11.92
3	36.179	5932904	10.78	10.78
4	52.000	20803541	34.13	37.81



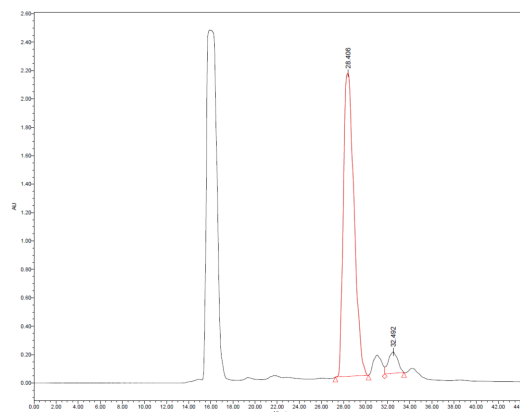
	Time	Area	% Height	% Area
1	28.988	75946728	95.72	93.94
2	50.562	4902881	4.28	6.06



(*R*)-2-((*S*)-1-(4-Methoxyphenyl)-2-nitroethyl)cyclohexanone (**14ad**).<sup>82</sup> Yield: 20.8 mg, 75%, white solid. Analytical and spectroscopic data were in good agreement with those reported in the literature. <sup>1</sup>H NMR (500 MHz, CDCl<sub>3</sub>) δ 7.08 (d, *J* = 8.5 Hz, 2H, ArH), 6.85 (d, *J* = 8.5 Hz, 2H, ArH), 4.90 (dd, *J* = 12.3, 4.5 Hz, 1H, CHNO<sub>2</sub>), 4.58 (dd, *J* = 12.1, 10.2 Hz, 1H, CHNO<sub>2</sub>), 3.78 (s, 3H, OMe), 3.71 (m, 1H, CHAR), 2.73 – 2.61 (m, 1H, CH), 2.47 (d, *J* = 12.8 Hz, 1H, CH<sub>2</sub>), 2.38 (td, *J* = 12.5, 5.6 Hz, 1H, CH<sub>2</sub>), 2.07 (d, *J* = 2.6 Hz, 1H, CH<sub>2</sub>), 1.89 – 1.51 (m, 4H, CH<sub>2</sub>), 1.23 (dd, *J* = 22.8, 10.7 Hz, 1H, CH<sub>2</sub>). HPLC (Daicel Chiralpak AD-H, hexane/*i*PrOH = 80/20, flow rate 0.5 mL/min, λ = 210 nm), *t*<sub>R</sub> (major) = 28.41 min, *t*<sub>R</sub> (minor) = 32.49 min; ee = 88%.

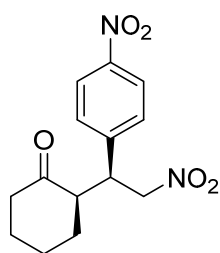


	Time	Area	% Height	% Area
1	25.208	64994971	38.56	38.48
2	27.790	20491354	12.18	12.13
3	29.555	61422712	37.09	36.37
4	31.104	21987842	12.16	13.02

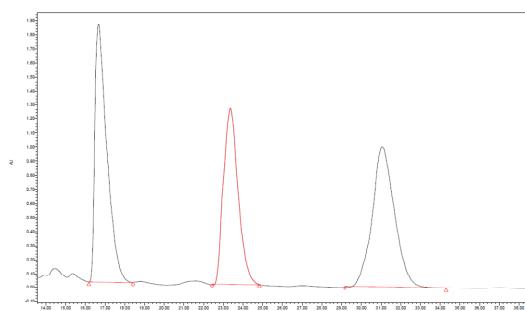


	Time	Area	% Height	% Area
1	28.406	143074864	93.46	94.14
2	32.492	8900039	6.54	5.86

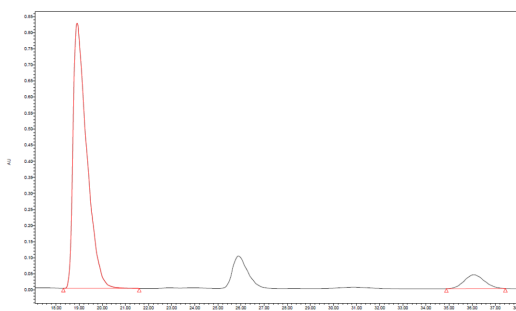




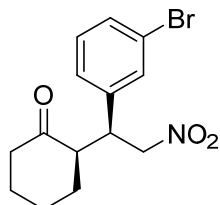
(*R*)-2-((*S*)-2-Nitro-1-(4-nitrophenyl)ethyl)cyclohexanone (**14ae**).<sup>85</sup> Yield: 26.0 mg, 89%, white solid. Analytical and spectroscopic data were in good agreement with those reported in the literature. <sup>1</sup>H NMR (500 MHz, CDCl<sub>3</sub>) δ 8.20 (d, *J* = 8.7 Hz, 2H, ArH), 7.39 (d, *J* = 8.6 Hz, 2H, ArH), 4.99 (dd, *J* = 13.0, 4.4 Hz, 1H, CHNO<sub>2</sub>), 4.70 (dd, *J* = 12.9, 10.1 Hz, 1H, CHNO<sub>2</sub>), 3.93 (dd, *J* = 9.3, 5.3 Hz, 1H, CHAr), 2.70 (d, *J* = 13.2 Hz, 1H, CH), 2.50 (d, *J* = 13.2 Hz, 1H, CH<sub>2</sub>), 2.45 – 2.37 (m, 1H, CH<sub>2</sub>), 2.10 (m, 1H, CH<sub>2</sub>), 1.83 (d, *J* = 12.0 Hz, 1H, CH<sub>2</sub>), 1.75 – 1.60 (m, 3H, CH<sub>2</sub>), 1.27 (m, 1H, CH<sub>2</sub>). HPLC (Daicel Chiralpak AD-H, hexane/*i*PrOH = 80/20, flow rate 1.0 mL/min, λ = 254 nm), *t*<sub>R</sub> (major) = 18.91 min, *t*<sub>R</sub> (minor) = 36.08 min; ee = 86%.



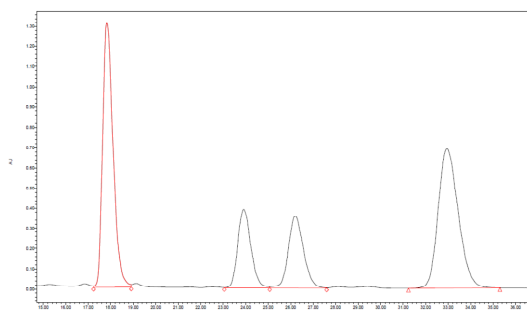
	Time	Area	% Height	% Area
<b>1</b>	16.671	77607269	44.97	35.15
<b>2</b>	23.360	64820755	30.58	29.36
<b>3</b>	31.051	78351233	24.45	35.49



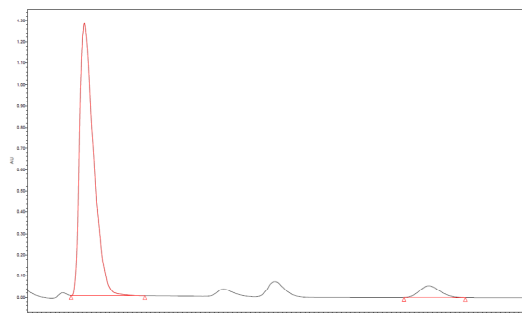
	Time	Area	% Height	% Area
<b>1</b>	18.912	33957647	95.05	92.85
<b>2</b>	36.076	2614035	4.95	7.15



(*R*)-2-((*S*)-1-(3-Bromophenyl)-2-nitroethyl)cyclohexanone (**14af**).<sup>86</sup> Yield: 30.2 mg, 93%, white solid. Analytical and spectroscopic data were in good agreement with those reported in the literature. <sup>1</sup>H NMR (500 MHz, CDCl<sub>3</sub>) δ 7.41 (d, *J* = 7.2 Hz, 1H, ArH), 7.33 (s, 1H, ArH), 7.20 (t, *J* = 7.8 Hz, 1H, ArH), 7.12 (d, *J* = 7.5 Hz, 1H, ArH), 4.93 (dd, *J* = 12.8, 4.3 Hz, 1H, CHNO<sub>2</sub>), 4.69 – 4.53 (m, 1H, CHNO<sub>2</sub>), 3.74 (td, *J* = 9.9, 4.4 Hz, 1H, CHAr), 2.71 – 2.60 (m, 1H, CH), 2.48 (m, 1H, CH<sub>2</sub>), 2.39 (m, 1H, CH<sub>2</sub>), 2.08 (m, 1H, CH<sub>2</sub>), 1.81 – 1.58 (m, 4H, CH<sub>2</sub>), 1.26 (m, 1H, CH<sub>2</sub>). HPLC (Daicel Chiralpak AS-H, hexane/*i*PrOH = 80/20, flow rate 1.0 mL/min, λ = 210 nm), *t*<sub>R</sub> (major) = 16.86 min, *t*<sub>R</sub> (minor) = 32.05 min; ee = 88%.

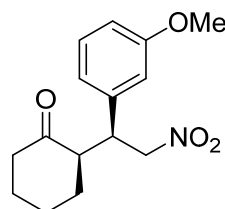


	Time	Area	% Height	% Area
1	17.828	42299734	47.77	36.06
2	23.910	15618984	14.17	13.32
3	26.199	16545240	12.88	14.11
4	32.948	42827951	25.18	36.51



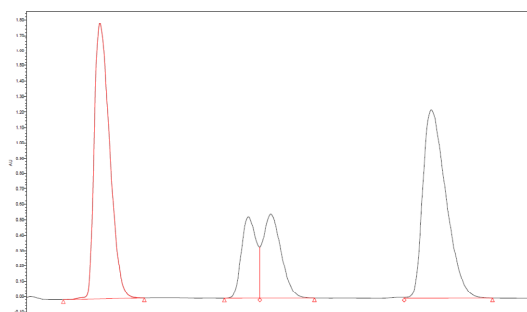
	Time	Area	% Height	% Area
1	16.855	54174586	95.89	93.96
2	32.047	3482505	4.11	6.04

*(R)*-2-((*S*)-1-(3-Methoxyphenyl)-2-nitroethyl)cyclohexanone (**14ag**).<sup>86</sup> Yield:

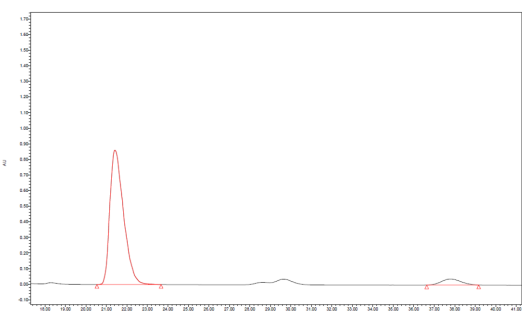


20.0 mg, 72%, white solid. Analytical and spectroscopic data were in good agreement with those reported in the literature. <sup>1</sup>H NMR (500 MHz, CDCl<sub>3</sub>) δ 7.15 (m, 1H, ArH), 6.79 – 6.70 (m, 3H, ArH), 4.91 (d, *J* = 12.4 Hz, 1H, CHNO<sub>2</sub>), 4.63 (d, *J* = 10.1 Hz, 1H, CHNO<sub>2</sub>), 3.79 (s, 3H, OMe), 3.72 (m, 1H, CHAr), 2.66 (m, 1H, CH), 2.46 (m, 1H, CH<sub>2</sub>), 2.38 (m, 1H, CH<sub>2</sub>), 2.06 (m, 1H, CH<sub>2</sub>), 1.72 – 1.61 (m, 4H, CH<sub>2</sub>), 1.26 (m, 1H, CH<sub>2</sub>).

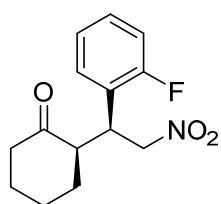
HPLC (Daicel Chiralpak AS-H, hexane/*i*PrOH = 80/20, flow rate 1.0 mL/min, λ = 210 nm), *t*<sub>R</sub> (major) = 21.42 min, *t*<sub>R</sub> (minor) = 37.79 min; ee = 88%.



	Time	Area	% Height	% Area
1	20.986	88730287	43.81	37.44
2	27.827	25312094	12.91	10.68
3	28.855	31961423	13.31	13.49
4	36.246	90998114	29.97	38.40



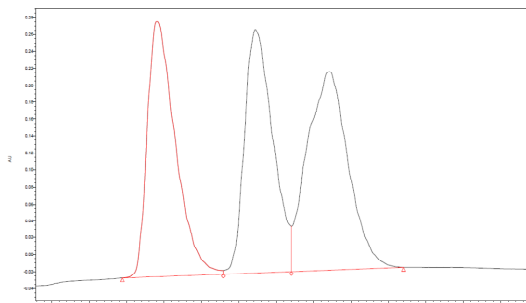
	Time	Area	% Height	% Area
1	21.416	4010338	95.69	93.98
2	37.795	2570459	4.31	6.02



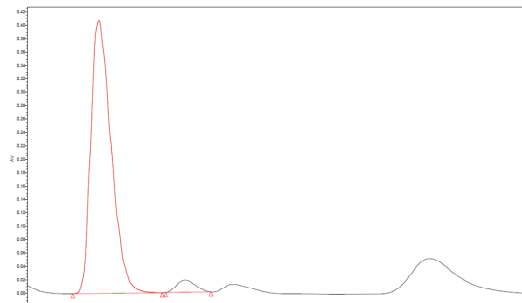
*(R)*-2-((*S*)-1-(2-Fluorophenyl)-2-nitroethyl)cyclohexanone (**14ah**).<sup>87</sup> Yield:

23.8 mg, 90%, white solid. Analytical and spectroscopic data were in good agreement with those reported in the literature. <sup>1</sup>H NMR (500 MHz, CDCl<sub>3</sub>) δ 7.32 – 7.21 (m, 1H, ArH), 7.20 – 7.16 (m, 1H, ArH), 7.14 – 7.03 (m, 2H, ArH), 4.92 (dd, *J* = 12.6, 4.3 Hz, 1H, CHNO<sub>2</sub>), 4.73 (d, *J* = 12.5, 10.2 Hz, 1H, CHNO<sub>2</sub>), 4.02 (m, 1H, CHAr), 2.87 – 2.82 (m, 1H, CH), 2.52 – 2.35 (m, 2H, CH<sub>2</sub>), 2.12 – 2.05

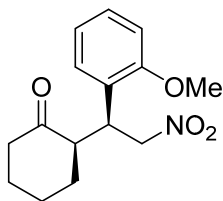
(m, 1H, CH<sub>2</sub>), 1.80 – 1.55 (m, 4H, CH<sub>2</sub>), 1.32 – 1.20 (m, 1H, CH<sub>2</sub>). HPLC (Daicel Chiralcel OD-H, hexane/<sup>i</sup>PrOH = 95/5, flow rate 1.0 mL/min, λ = 210 nm), *t*<sub>R</sub> (major) = 22.07 min, *t*<sub>R</sub> (minor) = 24.62 min; ee = 92%.



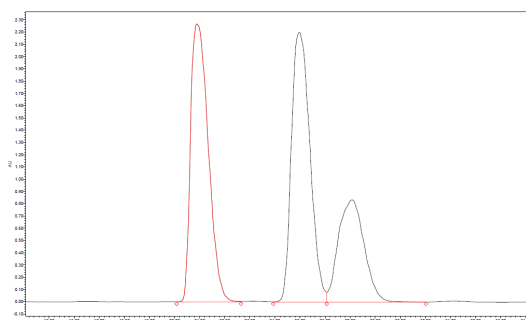
	Time	Area	% Height	% Area
1	20.813	15684976	36.56	32.24
2	23.440	15123744	34.96	31.09
3	25.418	17836871	28.48	36.67



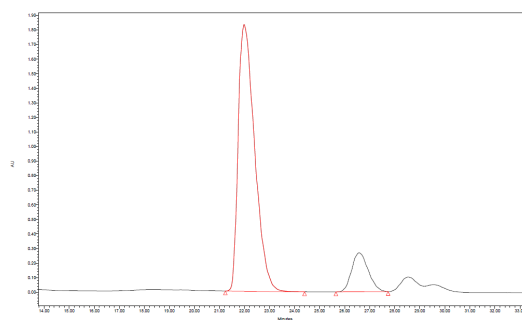
	Time	Area	% Height	% Area
1	22.070	17094779	95.67	96.01
2	24.624	709553	4.33	3.99



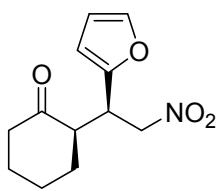
(*R*)-2-((*S*)-1-(2-Methoxyphenyl)-2-nitroethyl)cyclohexanone (**14ai**).<sup>86</sup> Yield: 23.0 mg, 83%, white solid. Analytical and spectroscopic data were in good agreement with those reported in the literature. <sup>1</sup>H NMR (500 MHz, CDCl<sub>3</sub>) 7.24 (dd, 1H, *J* = 1.6, 8.0 Hz, ArH), 7.09 (dd, 1H, *J* = 1.6, 7.6 Hz, ArH), 7.86 – 6.91 (m, 2H, ArH), 4.82 – 4.85 (m, 2H, CHNO<sub>2</sub>), 3.96 (td, 1H, *J* = 4.0, 9.2 Hz, CHAr), 3.85 (s, 3H, OMe), 2.94 – 3.02 (m, 1H, CH), 2.36 – 2.50 (m, 2H, CH<sub>2</sub>), 2.04 – 2.08 (m, 1H, CH<sub>2</sub>), 1.76 – 1.80 (m, 1H, CH<sub>2</sub>), 1.55 – 1.69 (m, 3H, CH<sub>2</sub>), 1.19 – 1.26 (m, 1H, CH<sub>2</sub>). HPLC (Daicel Chiralpak AS-H, hexane/<sup>i</sup>PrOH = 90/10, flow rate 1.0 mL/min, λ = 210 nm), *t*<sub>R</sub> (major) = 21.99 min, *t*<sub>R</sub> (minor) = 26.58 min; ee = 74%.



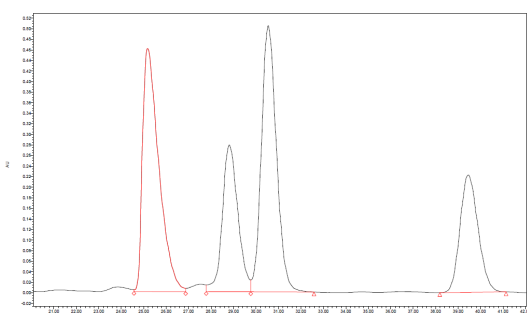
	Time	Area	% Height	% Area
1	20.888	111264360	42.79	39.23
2	24.972	112817421	41.49	39.78
3	27.076	59514769	15.72	20.99



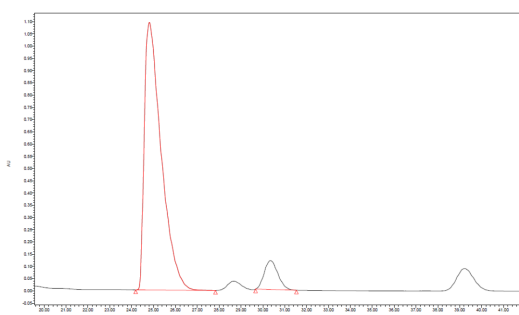
	Time	Area	% Height	% Area
1	21.986	83536700	87.24	87.15
2	26.577	12316696	12.76	12.85



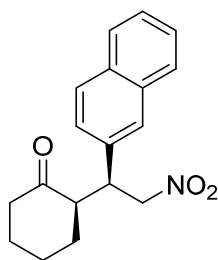
(*R*)-2-((*R*)-1-(Furan-2-yl)-2-nitroethyl)cyclohexanone (**14aj**).<sup>86</sup> Yield: 14.0 mg, 59%, white solid. Analytical and spectroscopic data were in good agreement with those reported in the literature. <sup>1</sup>H NMR (500 MHz, CDCl<sub>3</sub>) δ 7.34 (d, *J* = 0.6 Hz, 1H, ArH), 6.29 (dd, *J* = 2.8, 1.6 Hz, 1H, ArH), 6.18 (d, *J* = 2.6 Hz, 1H, ArH), 4.79 (dd, *J* = 12.4, 4.7 Hz, 1H, CHNO<sub>2</sub>), 4.67 (dd, *J* = 12.4, 9.4 Hz, 1H, CHNO<sub>2</sub>), 3.97 (m, 1H, CHAr), 2.82 – 2.68 (m, 1H, CH), 2.47 – 2.45 (d, *J* = 11.8 Hz, 1H, CH<sub>2</sub>), 2.41 – 2.31 (m, 1H, CH<sub>2</sub>), 2.18 – 2.05 (m, 1H, CH<sub>2</sub>), 1.85 – 1.83 (m, 1H, CH<sub>2</sub>), 1.77 – 1.74 (m, 1H, CH<sub>2</sub>), 1.69 – 1.62 (m, 2H, CH<sub>2</sub>), 1.30 – 1.25 (m, 1H, CH<sub>2</sub>). HPLC (Daicel Chiralpak AS-H, hexane/<sup>i</sup>PrOH = 90/10, flow rate 1.0 mL/min, λ = 210 nm), *t*<sub>R</sub> (major) = 24.81 min, *t*<sub>R</sub> (minor) = 30.34 min; ee = 84%.



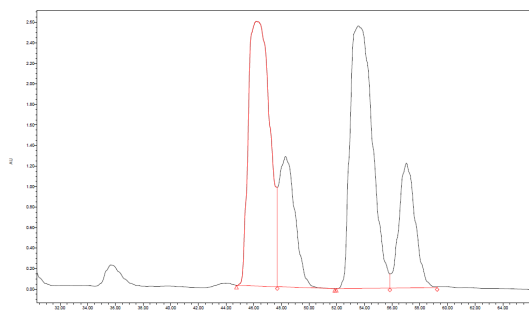
	Time	Area	% Height	% Area
1	25.174	23233036	31.42	32.02
2	28.809	13421733	18.98	18.50
3	30.544	23468755	34.43	32.35
4	39.456	12433897	15.16	17.14



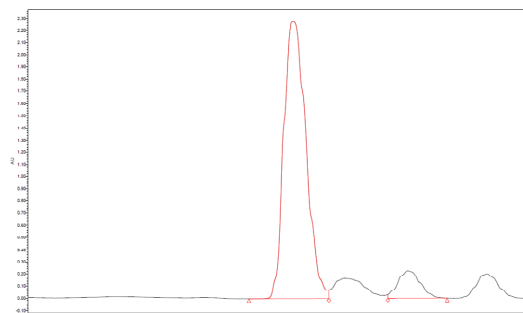
	Time	Area	% Height	% Area
1	24.810	58563814	90.26	91.96
2	30.340	5117731	9.74	8.04



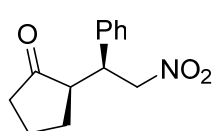
(*R*)-2-((*S*)-1-(Naphthalen-2-yl)-2-nitroethyl)cyclohexanone (**14ak**).<sup>87</sup> Yield: 6.83 mg, 23%, white solid. Analytical and spectroscopic data were in good agreement with those reported in the literature. <sup>1</sup>H NMR (500 MHz, CDCl<sub>3</sub>) δ 7.81 (dd, *J* = 14.3, 8.2 Hz, 3H, ArH), 7.63 (s, 1H, ArH), 7.52 – 7.41 (m, 2H, ArH), 7.35 – 7.23 (m, 1H, ArH), 5.02 (dd, *J* = 12.5, 4.4 Hz, 1H, CHNO<sub>2</sub>), 4.74 (dd, *J* = 12.2, 10.2 Hz, 1H, CHNO<sub>2</sub>), 3.95 (td, *J* = 9.8, 4.4 Hz, 1H, CHAr), 2.78 (td, *J* = 11.2, 4.8 Hz, 1H, CH), 2.68 – 2.46 (m, 1H, CH<sub>2</sub>), 2.41 (td, *J* = 12.5, 5.7 Hz, 1H, CH<sub>2</sub>), 2.13 – 2.03 (m, 1H, CH<sub>2</sub>), 1.85 – 1.53 (m, 4H, CH<sub>2</sub>), 1.39 – 1.15 (m, 1H, CH<sub>2</sub>). HPLC (Daicel Chiralpak AD-H, hexane/<sup>i</sup>PrOH = 90/10, flow rate 0.5 mL/min, λ = 210 nm), *t*<sub>R</sub> (major) = 40.88 min, *t*<sub>R</sub> (minor) = 46.43 min; ee = 82%.



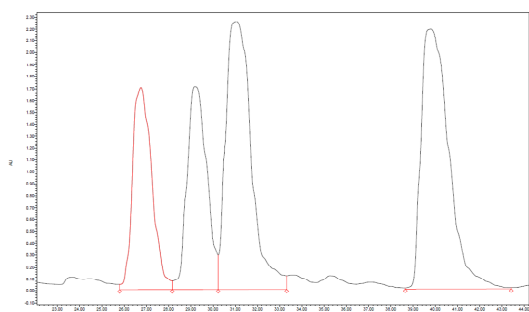
	Time	Area	% Height	% Area
1	46.176	275654227	33.84	36.14
2	48.292	102040501	16.69	13.38
3	53.551	285831775	33.53	37.47
4	57.029	99247094	15.95	13.01



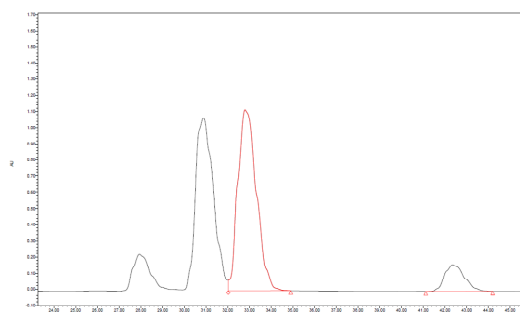
	Time	Area	% Height	% Area
1	40.879	169367330	91.02	90.90
2	46.453	16946862	8.98	9.10



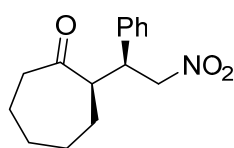
*(R)*-2-((*S*)-2-Nitro-1-phenylethyl)cyclopentan-1-one (**14ba**).<sup>83</sup> Yield: 17.5 mg, 75%, white solid. Analytical and spectroscopic data were in good agreement with those reported in the literature. <sup>1</sup>H NMR (500 MHz, CDCl<sub>3</sub>) δ 7.32 – 7.26 (m, 3H, ArH), 7.20 – 7.16 (m, 2H, ArH), 5.35 (dd, 1H, *J* = 4.2, 12.8 Hz, CHNO<sub>2</sub>), 4.72 (dd, 1H, *J* = 10, 12.8 Hz, CHNO<sub>2</sub>), 3.66 – 3.74 (m, 1H, CHAr), 2.23 – 2.40 (m, 2H, CH<sub>2</sub>), 2.08 – 2.18 (m, 1H, CH), 1.94 – 1.85 (m, 2H, CH<sub>2</sub>), 1.78 – 1.66 (m, 1H, CH<sub>2</sub>), 1.53 – 1.39 (m, 1H, CH<sub>2</sub>). HPLC (Daicel Chiralpak AD-H, hexane/*i*PrOH = 90/10, flow rate 0.5 mL/min, λ = 210 nm, *t*<sub>R</sub> (major) = 32.79 min, *t*<sub>R</sub> (minor) = 42.36 min; ee = 72%.



	Time	Area	% Height	% Area
1	26.760	103350454	21.67	17.81
2	29.194	106230855	21.75	18.31
3	31.062	180733982	28.73	31.15
4	39.789	189959688	27.86	32.74

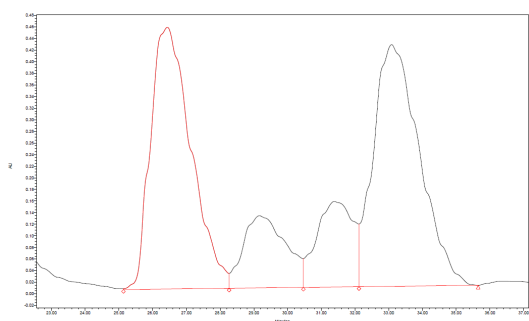


	Time	Area	% Height	% Area
1	32.794	67216811	86.90	86.19
2	42.360	10766547	13.10	13.81

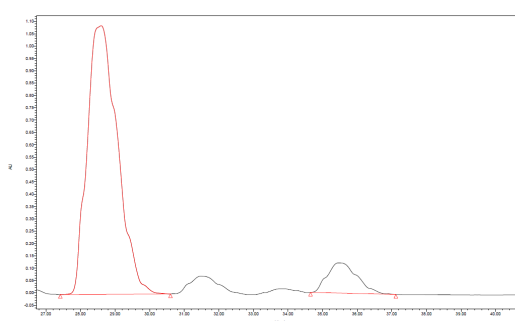


*(R)*-2-((*S*)-2-Nitro-1-phenylethyl)cycloheptanone (**14ca**).<sup>88</sup> Yield: 21.9 mg, 84%, white solid. Analytical and spectroscopic data were in good agreement with those reported in the literature. <sup>1</sup>H NMR (500 MHz, CDCl<sub>3</sub>) δ 7.38 – 7.25 (m, 3H, ArH), 7.21 – 7.16 (m, 2H, ArH), 4.65 – 4.50 (m, 2H, CHNO<sub>2</sub>), 3.69 (m, 1H, CHAr), 2.98 (td, 1H, *J* = 10.3, 3.3 Hz, CH), 2.56 – 2.45 (m, 2H, CH<sub>2</sub>), 1.98 – 1.84 (m, 2H, CH<sub>2</sub>), 1.78 – 1.41 (m, 3H, CH<sub>2</sub>), 1.27 – 1.13 (m, 3H, CH<sub>2</sub>). HPLC (Daicel Chiralpak AD-H,

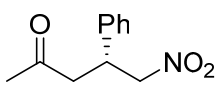
hexane/<sup>i</sup>PrOH = 90/10, flow rate 0.5 mL/min,  $\lambda$  = 210 nm),  $t_R$  (major) = 28.59 min,  $t_R$  (minor) = 35.47 min; ee = 80%.

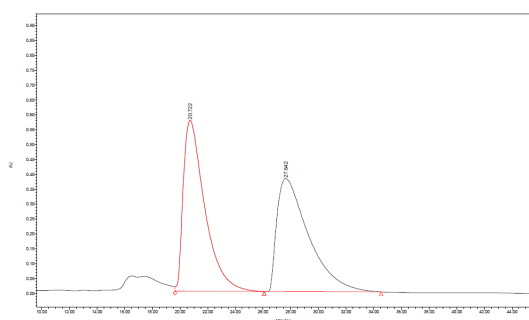


	Time	Area	% Height	% Area
1	26.433	37534022	39.58	37.58
2	29.167	10921633	10.92	11.02
3	31.385	11102239	12.94	11.20
4	33.086	39526398	36.55	39.89

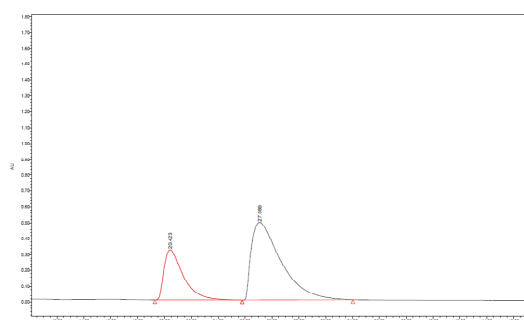


	Time	Area	% Height	% Area
1	28.594	66254554	89.92	89.98
2	35.469	7380896	10.08	10.02

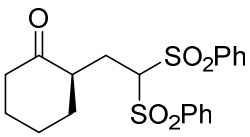

 (*R*)-5-Nitro-4-phenylpentan-2-one (**14da**).<sup>89</sup> NH<sub>2</sub>-X<sub>D</sub>-OMe-**10aa** was employed as catalyst. Yield: 16.4 mg, 79%, white solid. Analytical and spectroscopic data were in good agreement with those reported in the literature. <sup>1</sup>H NMR (500 MHz, CDCl<sub>3</sub>)  $\delta$  7.28 – 7.35 (m, 3H, ArH), 7.21 – 7.23 (m, 2H, ArH), 4.71 (dd, 1H,  $J$  = 6.8, 12.4 Hz, CHNO<sub>2</sub>), 4.61 (dd, 1H,  $J$  = 8.0,  $J_2$  = 12.4 Hz, CHNO<sub>2</sub>), 4.01 (t, 1H,  $J$  = 7.2 Hz, CHAr), 2.92 (d, 2H,  $J$  = 7.2 Hz, CH<sub>2</sub>), 2.12 (s, 3H, CH<sub>3</sub>). HPLC (Daicel Chiralpak AS-H, hexane/<sup>i</sup>PrOH = 80/20, flow rate 1.0 mL/min,  $\lambda$  = 210 nm),  $t_R$  (minor) = 20.42 min,  $t_R$  (major) = 27.09 min; ee = -41%.



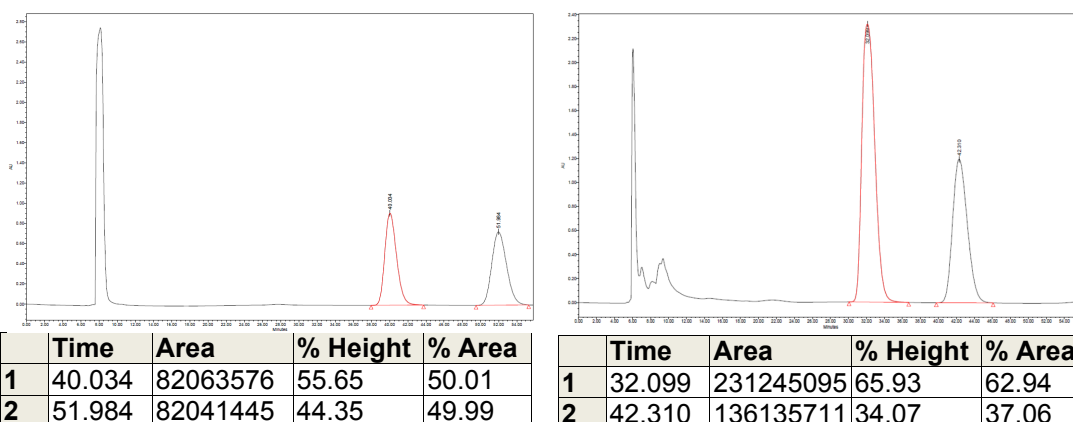
	Time	Area	% Height	% Area
1	20.722	62009854	60.19	50.54
2	27.642	60676252	39.81	49.46



	Time	Area	% Height	% Area
1	20.423	31826687	39.34	29.52
2	27.089	75996921	60.66	70.48

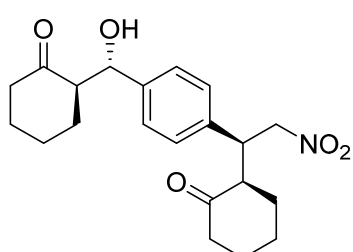

 (*R*)-2-(2,2-bis(Phenylsulfonyl)ethyl)cyclohexan-1-one (**16**).<sup>65</sup> Yield: not determined, white solid. Analytical and spectroscopic data were in good agreement with that reported in the literature. <sup>1</sup>H NMR (500 MHz, CDCl<sub>3</sub>)  $\delta$  7.92 (dd,  $J$  = 24.2, 7.8 Hz, 4H), 7.68 (q,  $J$  = 8.2 Hz, 2H), 7.56 (q,  $J$  = 7.0 Hz, 4H), 4.98 (dd,  $J$  = 9.2, 3.8 Hz, 1H), 3.07 (dt,  $J$  = 8.2, 4.7 Hz, 1H), 2.52 (ddd,  $J$  = 13.8, 9.3, 3.7 Hz, 1H), 2.38 – 2.24 (m, 2H), 2.23 – 2.03 (m, 1H), 1.95 (td,  $J$  = 9.5, 9.0, 4.6 Hz, 2H), 1.86 (p,

$J = 6.1$  Hz, 2H), 1.29 (qd,  $J = 12.4, 3.4$  Hz, 2H); HPLC (Daicel Chiralpak AS-H, hexane/ $i$ PrOH = 70/30, flow rate 1.0 mL/min,  $\lambda = 220$  nm),  $t_R$  (major) = 32.10 min,  $t_R$  (minor) = 42.31 min; ee = 26%.



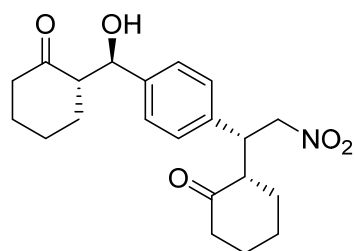
### Synthesis of Adducts 21

Adduct **21** was synthesized according to the procedure described above using alkene **13ab** and amine  $\text{NH}_2\text{-X-L-OMe-10aa}$  (30 mol%) as catalyst. The reaction mixture was stirred at room temperature until consumption of the starting material.



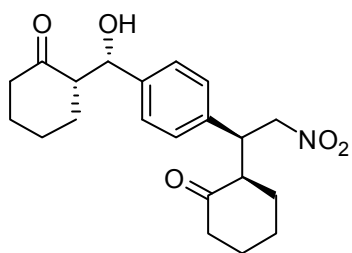
*(R)*-2-[(*S*)-1-(4-((*S*)-Hydroxy(*R*)-2-oxocyclohexyl)methyl)phenyl)-2-nitroethyl]cyclohexan-1-one (*anti*-**21**). Yield: 20 mg, 53%, white solid.  $m_p = 82 - 83$  °C.  $[\alpha]_D^{25} = 6.8$  ( $c$  0.31,  $\text{CHCl}_3$ ). FTIR (neat,  $\text{cm}^{-1}$ ) 3517, 2925, 2856, 1700, 1550.  $^1\text{H NMR}$  (500 MHz  $\text{CDCl}_3$ )  $\delta$  7.27 (d,  $J = 8.9$  Hz, 2H, ArH), 7.15 (d,  $J = 7.6$  Hz, 2H, ArH), 4.94 (dd,  $J = 12.8, 4.4$  Hz, 1H,  $\text{CHNO}_2$ ), 4.75 (d,  $J = 8.9$  Hz, 1H,  $\text{CHOH}$ ), 4.63

(dd,  $J = 12.6, 9.8$  Hz, 1H,  $\text{CHNO}_2$ ), 4.02 (s, 1H, OH), 3.76 (q,  $J = 5.3$  Hz, 1H,  $\text{CHAr}$ ), 2.66 (d,  $J = 3.2$  Hz, 1H, CH), 2.57 (t,  $J = 13.7$  Hz, 1H, CH), 2.47 (d,  $J = 9.6$  Hz, 2H,  $\text{CH}_2$ ), 2.36 (d,  $J = 11.8$  Hz, 2H,  $\text{CH}_2$ ), 2.07 (m, 2H,  $\text{CH}_2$ ), 1.87 – 1.45 (m, 8H,  $\text{CH}_2$ ), 1.24 (m, 2H,  $\text{CH}_2$ ).  $^{13}\text{C NMR}$  (101 MHz,  $\text{CDCl}_3$ )  $\delta$  215.6, 211.9, 140.5, 137.4, 128.2, 127.6, 78.8, 74.5, 57.2, 52.6, 43.6, 42.8, 42.7, 33.2, 30.8, 28.5, 27.8, 25.0, 24.7. HRMS (ESI) for  $\text{C}_{21}\text{H}_{27}\text{NO}_5\text{Na}$ : calculated  $[\text{M} + \text{Na}]^+$ : 396.1787. Found  $[\text{M} + \text{Na}]^+$ : 396.1793.

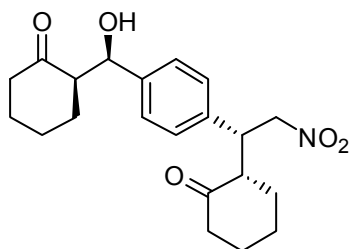


*(S)*-2-[(*R*)-1-(4-((*R*)-Hydroxy(*S*)-2-oxocyclohexyl)methyl)phenyl)-2-nitroethyl]cyclohexan-1-one (*ent-anti*-**21**). Yield: 14 mg, 37%, white solid.  $[\alpha]_D^{25} = -4.7$  ( $c$  0.41,  $\text{CHCl}_3$ ).  $^1\text{H NMR}$  (400 MHz,  $\text{CDCl}_3$ )  $\delta$  7.27 (d,  $J = 8.9$  Hz, 2H, ArH), 7.15 (d,  $J = 7.5$  Hz, 2H, ArH), 4.94 (d,  $J = 12.7$  Hz, 1H,  $\text{CHNO}_2$ ), 4.75 (d,  $J = 8.7$  Hz, 1H,  $\text{CHOH}$ ), 4.63 (t,  $J = 11.4$  Hz, 1H,  $\text{CHNO}_2$ ), 4.02 (s, 1H, OH), 3.75

(d,  $J = 11.1$  Hz, 1H,  $\text{CHAr}$ ), 2.65 (s, 1H, CH), 2.56 (s, 1H, CH), 2.52 – 2.32 (m, 4H,  $\text{CH}_2$ ), 2.07 (m, 2H,  $\text{CH}_2$ ), 1.84 – 1.48 (m, 8H,  $\text{CH}_2$ ), 1.23 (m, 2H,  $\text{CH}_2$ ).



(*R*)-2-[(*S*)-1-(4-((*S*)-Hydroxy(*S*)-2-oxocyclohexyl)methyl)phenyl)-2-nitroethyl]cyclohexan-1-one (*syn*-**21**). Yield: 4 mg, 11%, pale yellow solid.  $m_p = 110$ -112 °C.  $[\alpha]_D^{25} = 7.9$  (c 0.31 CHCl<sub>3</sub>). FTIR (neat, cm<sup>-1</sup>) 3498, 2935, 2860, 1700, 1549. <sup>1</sup>H NMR (500 MHz, CDCl<sub>3</sub>)  $\delta$  7.28 (d,  $J = 8.4$  Hz, 2H, ArH), 7.16 (d,  $J = 7.9$  Hz, 2H, ArH), 5.37 (s, 1H, CHOH), 4.97 (dd,  $J = 12.5, 4.5$  Hz, 1H, CHNO<sub>2</sub>), 4.65 (dd,  $J = 12.7, 9.9$  Hz, 1H, CHNO<sub>2</sub>), 3.78 (m, 1H, CHAr), 3.07 (bs, 1H, OH), 2.69 (m, 1H, CH), 2.58 (d,  $J = 8.5$  Hz, 1H, CH), 2.48 (m, 2H, CH<sub>2</sub>), 2.40 (m, 2H, CH<sub>2</sub>), 2.11 (m, 2H, CH<sub>2</sub>), 1.89 – 1.54 (m, 8H, -CH<sub>2</sub>), 1.26 (m, 2H, CH<sub>2</sub>). <sup>13</sup>C NMR (101 MHz, CDCl<sub>3</sub>)  $\delta$  214.9, 211.9, 141.0, 136.4, 128.0, 126.4, 78.8, 70.4, 56.9, 52.6, 43.6, 42.7, 42.7, 33.2, 28.5, 28.0, 26.0, 25.0, 24.8. HRMS (ESI) for C<sub>21</sub>H<sub>27</sub>NO<sub>5</sub>Na: calculated  $[M + Na]^+$ : 396.1787. Found  $[M + Na]^+$ : 396.1789.



(*S*)-2-[(*R*)-1-(4-((*R*)-Hydroxy(*R*)-2-oxocyclohexyl)methyl)phenyl)-2-nitroethyl]cyclohexan-1-one (*ent-syn*-**21**). Yield: 7 mg, 19%, pale yellow solid.  $[\alpha]_D^{25} = -5.4$  (c 0.34, CHCl<sub>3</sub>). <sup>1</sup>H NMR (400 MHz, CDCl<sub>3</sub>)  $\delta$  7.25 (d,  $J = 8.4$  Hz, 2H, ArH), 7.13 (d,  $J = 7.9$  Hz, 2H, ArH), 5.35 (s, 1H, CHOH), 4.94 (dd,  $J = 12.3, 4.9$  Hz, 1H, CHNO<sub>2</sub>), 4.62 (t,  $J = 11.2$  Hz, 1H, CHNO<sub>2</sub>), 3.76 (m, 1H, CHAr), 3.04 (bs, 1H, OH), 2.66 (td,  $J = 11.2, 5.0$  Hz, 1H, CH), 2.56 (t,  $J = 9.2$  Hz, 1H, CH), 2.50 – 2.33 (m, 4H, CH<sub>2</sub>), 2.07 (s, 2H, CH<sub>2</sub>), 1.89 – 1.49 (m, 8H, CH<sub>2</sub>), 1.23 (m, 2H, CH<sub>2</sub>).

<sup>1</sup> (a) Kane, R. *J. Prakt. Chem.* **1838**, 15, 129-155. (b) Kane, R. *Ann. Phys. Chem. Ser.* **1838**, 44, 475.

<sup>2</sup> Wurtz, C. A. *Bull. Soc. Chim. Fr.* **1872**, 17, 436-442. (b) Wurtz, C. A. *J. Prakt. Chem.* **1872**, 5, 457-464.

<sup>3</sup> Use of glyoxylates: Tokuda, O.; Kano, T.; Gao, W.-G.; Ikemoto, T.; Maruoka, K. *Org. Lett.* **2005**, 7, 5103-5105. Other examples: (b) Samanta, S.; Zhao, C.-G. *Tetrahedron Lett.* **2006**, 47, 3383-3386. (c) Samanta, S.; Zhao, C.-G. *J. Am. Chem. Soc.* **2006**, 128, 7442-7443.

<sup>4</sup> (a) Mukaiyama, T.; Narasaka, K.; Banno, K. *Chem. Lett.* **1973**, 1011-1014. (b) Mukaiyama, T.; Banno, K.; Narasaka, K. *J. Am. Chem. Soc.* **1974**, 96, 7503-7509. (c) Palomo, C.; Oiarbide, M.; García, J. M. *Chem. Eur. J.* **2002**, 8, 36-44.

<sup>5</sup> Machajewski, T. D.; Wong, C.-H. *Angew. Chem. Int. Ed.* **2000**, 39, 1352-1375.

<sup>6</sup> Fessner, W.-D.; Schneider, A.; Held, H.; Sinerius, G.; Walter, C.; Hixon, M.; Schloss, J. V. *Angew. Chem. Int. Ed. Engl.* **1996**, 35, 2219-2221.

<sup>7</sup> Yamada, Y. M. A.; Yoshika, N.; Sasai, H. M.; Shibasaki, M. *Angew. Chem. Int. Ed. Engl.* **1997**, 36, 1871-1872.

<sup>8</sup> Wagner, J.; Lerner, R.; Barbas III, C. F. *Science* **1995**, 270, 1797-1800.

<sup>9</sup> List, B.; Lerner, R. A.; Barbas III, C. F. *J. Am. Chem. Soc.* **2000**, 122, 2395-2396.

<sup>10</sup> Zimmerman, H. E.; Traxler, M. D. *J. Am. Chem. Soc.* **1957**, 79, 1920-1923.

<sup>11</sup> (a) Bahmanyar, S.; Houk, K. N. *J. Am. Chem. Soc.* **2001**, 123, 12911-12912. (b) Hoang, L.; Bahmanyar, S.; Houk, K. N.; List, B. *J. Am. Chem. Soc.* **2003**, 125, 16-17. (c) Cheong, P. H.-Y.; Legault, C. Y.; Um, J. M.; Celebi-Ölçüm, N.; Houk, K. N. *Chem. Rev.* **2011**, 111, 5042-5137. (d) Allemann, C.; Gordillo, R.; Clemente, F. R.; Cheong, P. H.; Houk, K. N. *Acc. Chem. Res.* **2004**, 37, 558-569. (e) Puchot, C.; Samuel, O.; Dunach, E.; Zhao, S.; Agami, C.; Kagan, H. B. *J. Am. Chem. Soc.* **1986**, 108, 2353-2357.

<sup>12</sup> (a) Notz, W.; Tanaka, F.; Barbas III, C. F. *Acc. Chem. Res.* **2004**, 37, 580-591. (b) Dalko, P. I.; Moisan, L. *Angew. Chem. Int. Ed.* **2004**, 43, 5138-5175. (c) Gryko, D.; Lipinski, R. *Adv. Synth. Catal.* **2005**, 347, 1948-1952. (d) Enders, D.; Grondal, C. *Angew. Chem. Int. Ed.* **2005**, 44,



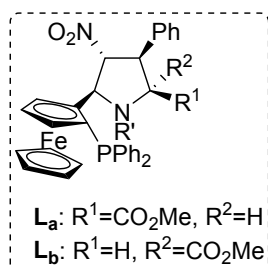
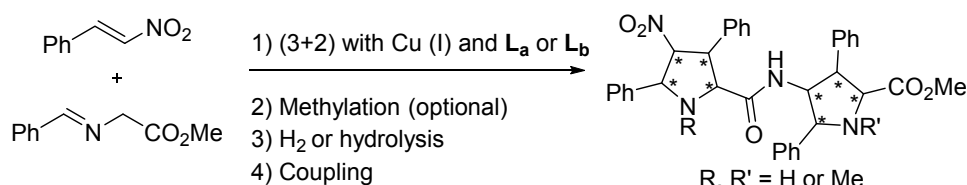
- 1210-1212. (e) Hayashi, Y.; Sumiya, T.; Takahashi, J.; Gotoh, H.; Urushima, T.; Shoji, M. *Angew. Chem. Int. Ed.* **2006**, *45*, 958-961.
- <sup>13</sup> (a) Córdova, A.; Zou, W.; Ibrahim, I.; Reyes, E.; Engqvist, M.; Liao, W.-W. *Chem. Commun.* **2005**, 3596-3588. (b) Wu, X.; Jiang, Z.; Shen, H.-M.; Lu, Y. *Adv. Synth. Catal.* **2007**, *349*, 812-816.
- <sup>14</sup> (a) Kano, T.; Takai, J.; Tokuda, O.; Maruoka, K. *Angew. Chem. Int. Ed.* **2005**, *44*, 3055-3057. (b) Nugent, T. C.; Bibi, A.; Sadiq, A.; Shoaib, M.; Umar, N.; Tehrani, F. N. *Org. Biomol. Chem.* **2012**, *10*, 9287-9294.
- <sup>15</sup> Mangion, I. K.; Northrup, A. B.; MacMillan, D. W. C. *Angew. Chem. Int. Ed.* **2004**, *43*, 6722-6724.
- <sup>16</sup> Zheng, B.-L.; Liu, Q.-Z.; Guo, C.-S.; Wang, X.-L.; He, L. *Org. Biomol. Chem.* **2007**, *5*, 2913-2915.
- <sup>17</sup> Trost, B. M.; Brindle, C. S. *Chem. Soc. Rev.* **2010**, *39*, 1600-1632.
- <sup>18</sup> Hayashi, Y.; Aratake, S.; Itoh, T.; Okano, T.; Sumiya, T.; Shoji, M. *Chem. Commun.* **2007**, 957-959.
- <sup>19</sup> Gu, L. Q.; Yu, M. L.; Wu, X. Y.; Zhang, Y. Z.; Zhao, G. *Adv. Synth. Catal.* **2006**, *348*, 2223-2228.
- <sup>20</sup> Zhang, S.-P.; Fu, X.-K.; Fu, S.-D. *Tetrahedron Lett.* **2009**, *50*, 1173-1176.
- <sup>21</sup> Guillena, G.; Hita, M. C.; C. Nájera, C. *Tetrahedron: Asymmetry*, **2006**, *17*, 1493-1497.
- <sup>22</sup> Nakadai, M.; Saito, S.; Yamamoto, H. *Tetrahedron*, **2002**, *58*, 8167-8177.
- <sup>23</sup> Cobb, A. J. A.; Shaw, D. M.; Longbottom, D. A.; Gold, J. B.; Ley, S. V. *Org. Biomol. Chem.* **2005**, *3*, 84-96.
- <sup>24</sup> Tang, Z.; Yang, Z. H.; Chen, X. H.; Cun, L. F.; Mi, A. Q.; Jiang, Y. Z.; Gong, L. Z. *J. Am. Chem. Soc.* **2005**, *127*, 9285-9289.
- <sup>25</sup> Zheng, B. L.; Liu, Q. Z.; Guo, C. S.; Wang, X. L.; He, L. *Org. Biomol. Chem.* **2007**, *5*, 2913-2915.
- <sup>26</sup> Nakayama, K.; Maruoka, K. *J. Am. Chem. Soc.* **2008**, *130*, 17666-17667.
- <sup>27</sup> Li, L.; Xu, L.-W.; Ju, Y.-D.; Lai, G.-Q. *Synth. Commun.* **2009**, *39*, 764-774.
- <sup>28</sup> Bøgevig, A.; Kumaragurubaran, N.; Jørgensen, K. A. *Chem. Commun.* **2002**, 620-621.
- <sup>29</sup> Conde, E.; Bello, D.; de Cózar, A.; Sánchez, M.; Vázquez, M. A.; Cossío, F. P. *Chem. Sci.* **2012**, *3*, 1486-1491.
- <sup>30</sup> Retamosa, M. G.; de Cózar, A.; Sánchez, M.; Miranda, J. I.; Sansano, J. M.; Castelló, L. M.; Nájera, C.; Jiménez, A. I.; Sayago, F. J.; Cativiela, C.; Cossío, F. P. *Eur. J. Org. Chem.* **2015**, 2503-2516.
- <sup>31</sup> Komnenos, T. *Liebigs. Ann. Chem.* **1883**, *218*, 145-167.
- <sup>32</sup> Michael, A. *Prakt. Chem.* **1887**, *36*, 349-356.
- <sup>33</sup> (a) Elsner, P.; Bernardi, L.; Dela Salla, G.; Overgaard, J.; Jørgensen, K. A. *J. Am. Chem. Soc.* **2008**, *130*, 4897-4905. (b) Wu, F.; Li, H.; Hong, R.; Deng, L. *Angew. Chem. Int. Ed.* **2006**, *45*, 947-950.
- <sup>34</sup> Li, Y.; Wang, C.; Jia, G.; Lu, S.; Li, C. *Tetrahedron* **2013**, *69*, 6585-6590.
- <sup>35</sup> (a) Rabalakos, C.; Wulff, W. D. *J. Am. Chem. Soc.* **2008**, *130*, 13524-13525. (b) Jensen, K. L.; Poulsen, P. H.; Donslund, B. S.; Morana, F.; Jørgensen, K. A. *Org. Lett.* **2012**, *14*, 1516-1519. (c) Li, L.; Zhang, S.; Hu, Y.; Li, Y.; Li, C.; Zha, Z.; Wang, Z. *Chem. Eur. J.* **2015**, *21*, 12885-12888.
- <sup>36</sup> (a) Thaler, T.; Knochel, P. *Angew. Chem. Int. Ed.* **2009**, *48*, 645-648. (b) Gremaud, L.; Alexakis, A. *Angew. Chem. Int. Ed.* **2012**, *51*, 794-797.
- <sup>37</sup> Li, B.-J.; Lin, J.; Liu, M.; Chen, Y.-C.; Ding, L.-S.; Wu, Y. *Synlett* **2005**, *4*, 603-606.
- <sup>38</sup> (a) Ganesh, M.; Seidel, D. *J. Am. Chem. Soc.* **2008**, *130*, 16464-16465. (b) Almaşi, D.; Alonso, D. A.; Gómez-Bengoa, E.; Nájera, C. *J. Org. Chem.* **2009**, *74*, 6163-6168. (c) Saha, P.; Biswas, A.; Molleti, N.; Singh, V. K. *J. Org. Chem.* **2015**, *80*, 11115-11122.
- <sup>39</sup> (a) Penon, O.; Carlone, A.; Mazzanti, A.; Locatelli, M.; Sambri, L.; Bartoli, G.; Melchiorre, P. *Chem. Eur. J.* **2008**, *14*, 4788-4791. (b) Kang, J. Y.; Carter, R. G. *Org. Lett.* **2012**, *14*, 3178-3181. (c) Fu, N.; Zhang, L.; Luo, S. *Org. Lett.* **2015**, *17*, 382-385.
- <sup>40</sup> (a) Li, H.; Song, J.; Deng, L. *J. Am. Chem. Soc.* **2005**, *127*, 8948-8949. (b) Sulzer-Mossé, S.; Alexakis, A. *Chem. Commun.* **2007**, 3123-3135.
- <sup>41</sup> (a) Berner, O. M.; Tedeschi, L.; Enders, D. *Eur. J. Org. Chem.* **2002**, 1877-1894. (b) Ono, E. *The Nitro Group in Organic Synthesis*, **2001**, Wiley-VCH.
- <sup>42</sup> (a) Franzén, J.; Marigo, M.; Fielenbach, D.; Wabnitz, T. C.; Kjærsgaard, A.; Jørgensen, K. A. *J. Am. Chem. Soc.* **2005**, *127*, 18296-18304. (b) Hayashi, Y.; Gotoh, H.; Hayashi, T.; Shoji, M. *Angew. Chem. Int. Ed.* **2005**, *44*, 4212-4213.
- <sup>43</sup> Austin, J. F.; MacMillan, D. W. C. *J. Am. Chem. Soc.* **2002**, *124*, 1172-1173.
- <sup>44</sup> Seebach, D.; Golinski, J. *Helv. Chim. Acta* **1981**, *64*, 1413-1423.
- <sup>45</sup> (a) Mukherjee, S.; Yang, J. W.; Hoffmann, S.; List, B. *Chem. Rev.* **2007**, *107*, 5471-5569. (b) List, B. *Synlett.* **2004**, 1675-1686.

- <sup>46</sup> Enders, D.; Seki, A. *Synlett* **2002**, 28, 26-28.
- <sup>47</sup> Cobb, A. J. A.; Longbottom, D. A.; Shaw, D. M.; Ley, S. V. *Chem. Commun.* **2004**, 1808-1809.
- <sup>48</sup> Cao, C.-L.; Ye, M.-C.; Sun, X.-L.; Tang, Y. *Org. Lett.* **2006**, 8, 2901-2904.
- <sup>49</sup> Pansare, S. V.; Pandya, K. *J. Am. Chem. Soc.* **2006**, 128, 9624-9625.
- <sup>50</sup> Ni, B.; Zhang, Q.; Headley, A. D. *Tetrahedron: Asymm.* **2007**, 18, 1443-1447.
- <sup>51</sup> Ishii, T.; Fujioka, S.; Sekiguchi, Y.; Kotsuki, H. *J. Am. Chem. Soc.* **2004**, 126, 9558-9559.
- <sup>52</sup> Luo, S.; Mi, X.; Zhang, L.; Liu, S.; Xu, H.; Cheng, J.-P. *Angew. Chem. Int. Ed.* **2006**, 45, 3093-3097.
- <sup>53</sup> Mase, N.; Watanabe, K.; Yoda, H.; Takabe, K.; Tanaka, F.; Barbas III, C. F. *J. Am. Chem. Soc.* **2006**, 128, 4966-4967.
- <sup>54</sup> Chen, H.; Wang, Y.; Wei, S.; Sun, J. *Tetrahedron: Asymm.* **2007**, 18, 1308-1312.
- <sup>55</sup> Wang, S.-W.; Chen, J.; Chen, G.-H.; Peng, Y.-G. *Synlett*, **2009**, 1457-1462.
- <sup>56</sup> Tan, B.; Zeng, X.; Lu, Y.; Chua, P. J.; Zhong, G. *Org. Lett.* **2009**, 11, 1927-1930.
- <sup>57</sup> Xu, Y.; Córdova, A. *Chem. Commun.* **2006**, 460-462.
- <sup>58</sup> Xiong, Y.; Wen, Y.; Wang, F.; Gao, B.; Liu, X.; Huang, X.; Feng, X. *Adv. Synth. Catal.* **2007**, 349, 2156-2166.
- <sup>59</sup> Yang, Z.; Liu, J.; Liu, X.; Wang, Z.; Feng, X.; Su, Z.; Hu, C. *Adv. Synth. Catal.* **2008**, 350, 2001-2006.
- <sup>60</sup> (a) Liu, K.; Cui, H.-F.; Nie, J.; Dong, K.-Y.; Li, X.-J.; Ma, J.-A. *Org. Lett.* **2007**, 9, 923-925. (b) Jiang, X.; Zhang, Y.; Chan, A. S. C.; Wang, R. *Org. Lett.* **2009**, 11, 153-156. (c) Huang, H.; Jacobsen, E. N. *J. Am. Chem. Soc.* **2006**, 128, 7170-7171.
- <sup>61</sup> (a) Tsogoeva, S. B.; Wei, S. *Chem. Commun.* **2006**, 1451-1453. (b) Yalalov, D. A.; Tsogoeva, S. B.; Schmatz, S. *Adv. Synth. Catal.* **2006**, 348, 826-832.
- <sup>62</sup> (a) Marcelli, T.; van Maarseveen, J. H.; Hiemstra, H. *Angew. Chem. Int. Ed.* **2006**, 45, 7496-7504. (b) Connon, S. J. *Chem. Commun.* **2008**, 2499-2510.
- <sup>63</sup> McCooney, S. H.; Connon, S. J. *Org. Lett.* **2007**, 9, 599-602.
- <sup>64</sup> Riant, O.; Samuel, O.; Flessner, T.; Taudien, S.; Kagan, H. B. *J. Org. Chem.* **1997**, 62, 6733-6745.
- <sup>65</sup> Zhu, Q.; Cheng, L.; Lu, Y. *Chem. Commun.* **2008**, 6315-6317.
- <sup>66</sup> Coetzee, J. F.; Padmanabhan, G. R. *J. Am. Chem. Soc.* **1965**, 87, 5005-5010.
- <sup>67</sup> (a) Kaljurand, I.; Kütt, A.; Sooväli, L.; Rodima, T.; Mäemets, V.; Leito, I.; Koppel, I. A. *J. Org. Chem.* **2005**, 70, 1019-1028. (b) Searles, S.; Tamres, M.; Block, F.; Quarterman, L. A. *J. Am. Chem. Soc.* **1956**, 78, 4917-4920.
- <sup>68</sup> (a) Moberg, C. *Angew. Chem. Int. Ed.* **2013**, 52, 2160-2162. (b) Sahoo, G.; Rahman, H.; Madarász, A.; Pápai, I.; Melarto, M.; Valkonen, A.; Pihko, P. *Angew. Chem. Int. Ed.* **2012**, 51, 13144-13148. (c) Buré, J.; Armstrong, A.; Blackmond, D. G. *J. Am. Chem. Soc.* **2012**, 134, 6741-6750. (d) Buré, J.; Armstrong, A.; Blackmond, D. G. *J. Am. Chem. Soc.* **2011**, 133, 8822-8825. (e) Yang, H.; Wong, M. W. *Org. Biomol. Chem.* **2012**, 10, 3229-3235. (f) Arnó, M.; Zaragozá, R. J.; Domingo, L. R. *Tetrahedron: Asymmetry* **2007**, 18, 157-164.
- <sup>69</sup> (a) McCooney, S. H.; Connon, S. J. *Org. Lett.* **2007**, 9, 599-602. (b) Rasappan, R.; Reiser, O. *Eur. J. Org. Chem.* **2009**, 1305-1308.
- <sup>70</sup> (a) Patora-Komisarska, K.; Benhoud M.; Ishikawa, H.; Seebach, D.; hayashi, Y. *Helv. Chim. Acta* **2011**, 94, 719-745. (b) Parra, A.; Reboredo, S.; Alemán, J. *Angew. Chem. Int. Ed.* **2012**, 51, 9734-9736.
- <sup>71</sup> Bürgi, H. B.; Dunitz, J. D. *J. Am. Chem. Soc.* **1973**, 95, 5065-5067.
- <sup>72</sup> Jeffrey, G. A. *An Introduction to Hydrogen Bonding*, **1997**, Oxford University Press.
- <sup>73</sup> (a) Denmark, S. E.; Matsushashi, H. *J. Org. Chem.* **2002**, 67, 3479-3486. (b) Kudryavtsev, K. V.; Tsentlovich, M. Y.; Yegorov, A. S.; Kolychev, E. L. *J. Het. Chem.* **2006**, 43, 1461-1466.
- <sup>74</sup> Song, D.; Cho, S.; Han, Y.; You, Y.; Nam, W. *Org. Lett.* **2013**, 15, 3582-3585.
- <sup>75</sup> Maity, S.; Manna, S.; Rana, S.; Naveen, T.; Mallick, A.; Maiti, D. *J. Am. Chem. Soc.* **2013**, 135, 3355-3358.
- <sup>76</sup> Denmark, S. E.; Marcin, L. R. *J. Org. Chem.* **1995**, 60, 3221-3235.
- <sup>77</sup> Nomenclature and Symbolism for Amino Acids and Peptides. *Eur. J. Biochem.* **1984**, 138, 9-37.
- <sup>78</sup> Yan, X.-X.; Peng, Q.; Zhang, Y.; Zhang, K.; Hong, W.; Hou, X.-L.; Wu, Y.-D. *Angew. Chem. Int. Ed.* **2006**, 45, 1979-1983.
- <sup>79</sup> (a) Denmark, S. E.; Matsushashi, H.; *J. Org. Chem.* **2002**, 67, 3479-3486. (b) Kudryavtsev, K. V.; Tsentlovich, M. Y.; Yegorov, A. S.; Kolychev, E. L. *J. Het. Chem.* **2006**, 43, 1461-1466.

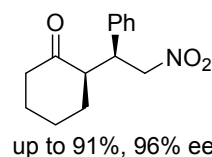
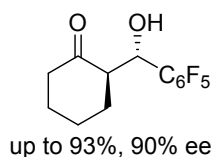
- 
- <sup>80</sup> (a) Echavarren, A. M.; Stille, J. K. *J. Am. Chem. Soc.* **1987**, 109, 5478-5486. (b) Song, D.; Cho, S.; Han, Y.; You, Y.; Nam, W. *Org. Lett.* **2013**, 15, 3582-3585.
- <sup>81</sup> Gruttadauria, M.; Giacalone, F.; Marculescu, A. M.; Lo Meo, P.; Riela, S.; Noto, R. *Eur. J. Org. Chem.* **2007**, 4688-4698.
- <sup>82</sup> Mase, N.; Watanabe, K.; Yoda, H.; Takabe, K.; Tanaka, F.; Barbas, C. F., III. *J. Am. Chem. Soc.* **2006**, 128, 4966-4967.
- <sup>83</sup> Vishnumaya, Singh, V. K. *Org. Lett.* **2007**, 9, 1117-1119.
- <sup>84</sup> Cobb, A. J. A.; Shaw, D. M.; Longbottom, D. A.; Gold, J. B.; Ley, S. V. *Org. Biomol. Chem.* **2005**, 3, 84-96.
- <sup>85</sup> Sanzhong, L.; Jiuyuan, L.; Long, Z.; Hui, X.; Jin-Pei, C. *Chem. Eur. J.* **2008**, 14, 1273-1281.
- <sup>86</sup> Xu, D.-Q.; Wang, B.-T.; Luo, S.-P.; Yue, H.-D.; Wang, L.-P.; Xu, Z.-Y. *Tetrahedron: Asymm.* **2007**, 18, 1788-1794.
- <sup>87</sup> Syu, S.-e.; Kao, T.-T.; Lin, W. *Tetrahedron*, **2010**, 66, 891-897.
- <sup>88</sup> Gu, L.; Wu, Y.; Zhang, Y.; Zhao, G. *Journal of Molecular Catalysis A: Chemical* **2007**, 263, 186-194.
- <sup>89</sup> Wang, C.; Yu, C.; Liu, C.; Peng, Y. *Tetrahedron Lett.* **2009**, 50, 2363-2366.



# Chapter 3. $\gamma$ -Dipeptides Based on Units of Densely Substituted Pyrrolidines. Design and Organocatalysis



Aldol or Michael reactions towards the following products



## Abstract.

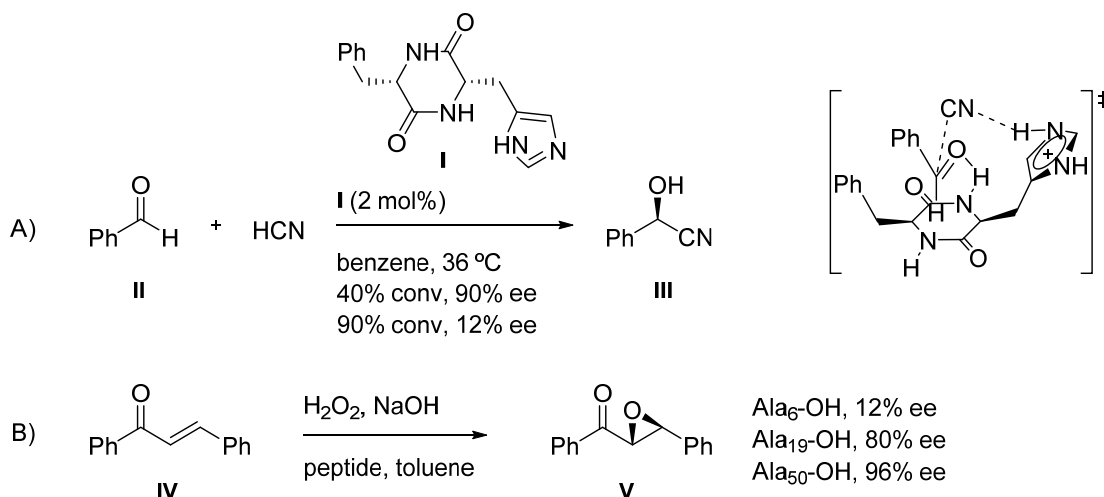
This chapter shows the follow up chemistry of the densely substituted pyrrolidines  $NO_2-X_L-OMe$ -**5aa** and  $NO_2-N_L-OMe$ -**5aa**, such as hydrogenation onto the nitro scaffold and hydrolysis of the ester moiety (in addition to an optional methylation step) and further peptide coupling. These transformations are able to provide a large family of  $\gamma$ -dipeptides which are based on unnatural densely substituted proline units. Subsequently, we have studied the organocatalytic activity of these  $\gamma$ -dipeptides in enamine-activated based reactions, such as Michael and aldol reactions. Additionally, structure-reactivity relationships of these novel catalysts have been studied in the named reactions.



### 3.1. Introduction

Peptides, either natural or synthetic, are found to have a wide range of applications in biology, medicinal chemistry or biotechnology as they are part of neurotransmitters, hormones or active compounds in drugs.<sup>1</sup> Their different behaviour is a consequence of the achieved large structural diversity, as each component bearing different functional groups can generate enormous changes in their activity. Also, due to the chance of hydrogen bonds formation properly selected residues can produce conformational stability and well-defined three-dimensional conformations such as helices, turns or sheets.<sup>2</sup> But it has not been until the last decade that their organocatalytic properties came to light.<sup>3</sup> In effect, it was shown that oligopeptides are able to perform enantioselective transformations such as, for instance, C-C bond formation, bromination or oxidation reactions.<sup>4</sup>

Despite the consciousness that enzymes are proper devices to perform catalytic transformations, peptides have only scarcely been used as catalysts until the advent of organocatalysis. Early examples are the work of Inoue and Oka<sup>5</sup> who developed the application of a histidine-derived diketopiperazine **I** (cyclo-Phe-His) to an enantioselective hydrocyanation of benzaldehyde **II** to give the corresponding cyanohydrin **III** (Scheme 1A). In this case the histidine residue was the catalytic active base. The highest enantiomeric induction was obtained at lower conversions (90% ee at 40% conversion) as the ee value diminished with longer reaction times (12% ee at 90% conversion). In the same years Juliá and Colonna<sup>6</sup> described the asymmetric epoxidation of chalcone **IV** by using polypeptides such as poly-alanines and poly-leucines. These polypeptides folded in a  $\alpha$ -helical structure which was determinant for the asymmetric induction.<sup>7</sup> It was found that the increase in the number of alanine residues produced a rise in the enantiomeric induction up to 96% ee (Scheme 1B).



**Scheme 1.** First examples of peptide catalysis.

Surprisingly, these two catalysts have conceptually different structures as one is a rigid cyclic peptide and the poly-Ala linear peptides, that can fold in three-dimensional structures in solution. Since these pioneering studies, several different peptidic organocatalysts have been synthesized and analyzed which range between these two contrary structures.

### 3.1.1. Background. Peptides in organocatalysis in enamine-activated type reaction

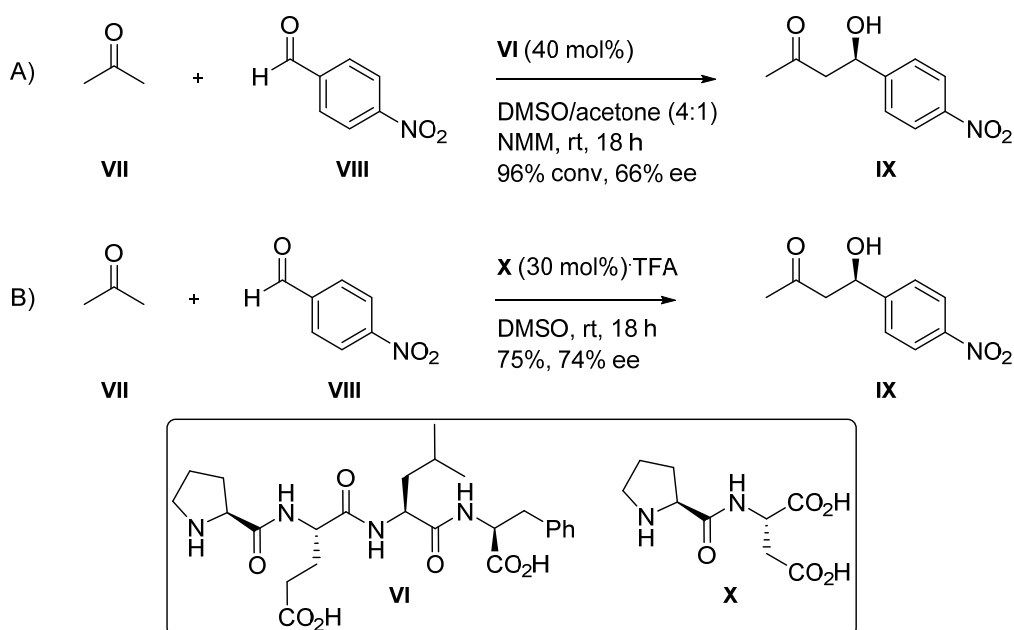
Due to the challenge of promoting enantioselective organocatalyzed C-C bond formation reactions, several catalytic units derived from proline, cinchona alkaloids, phosphoric acids, chiral imidazolidinones have been developed. Oligopeptides or synthetic peptides, on the other side, can possess greater reactivity than simple organocatalysts, which could be translated in a lower catalytic load or reaction times. Following sections will show some examples of oligopeptides employed as organocatalysts in the studied reactions during this thesis: the aldol and Michael reaction.

### 3.1.2. Aldol reaction

Chapter 2 showed the similarities between the aldol reactions carried out by type I aldoses and the enamine-activated aldol reaction. As shown, several catalysts can promote this reaction via enamine pathway, being the proline derivatives the most



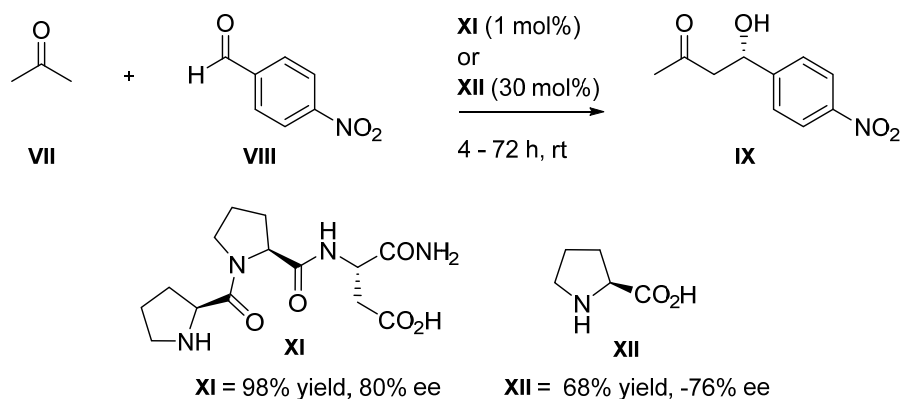
developed ones for this task. First examples of peptide employment in aldol reactions were the works described by the group of Reymond<sup>8</sup> and List<sup>9</sup>, both in 2003 (Scheme 2A and Scheme 2B, respectively). Using *N*-terminal proline derived catalysts in the aldol reaction between acetone **VII** and *p*-nitrobenzaldehyde **VIII**, Reymond used for the first time tetrapeptide Pro-Glu-Leu-Phe **VI** as catalyst. It incorporated one residue of L-Proline as starting secondary amine and at least one carboxylic group, reaching a moderate selectivity of 66% ee of the aldol product (Scheme 2A). List, similarly, used shorter dipeptide Pro-Asp **X** which improved the enantiocontrol (Scheme 2B). Both groups reached the conclusion that a simultaneous presence of one prolyl residue and a carboxy group, acting as co-catalyst, was required in order to observe good conversions.



**Scheme 2.** Aldol reaction catalyzed by A) H-Pro-Glu-Leu-Phe-OH **VI** and B) **X** dipeptide.

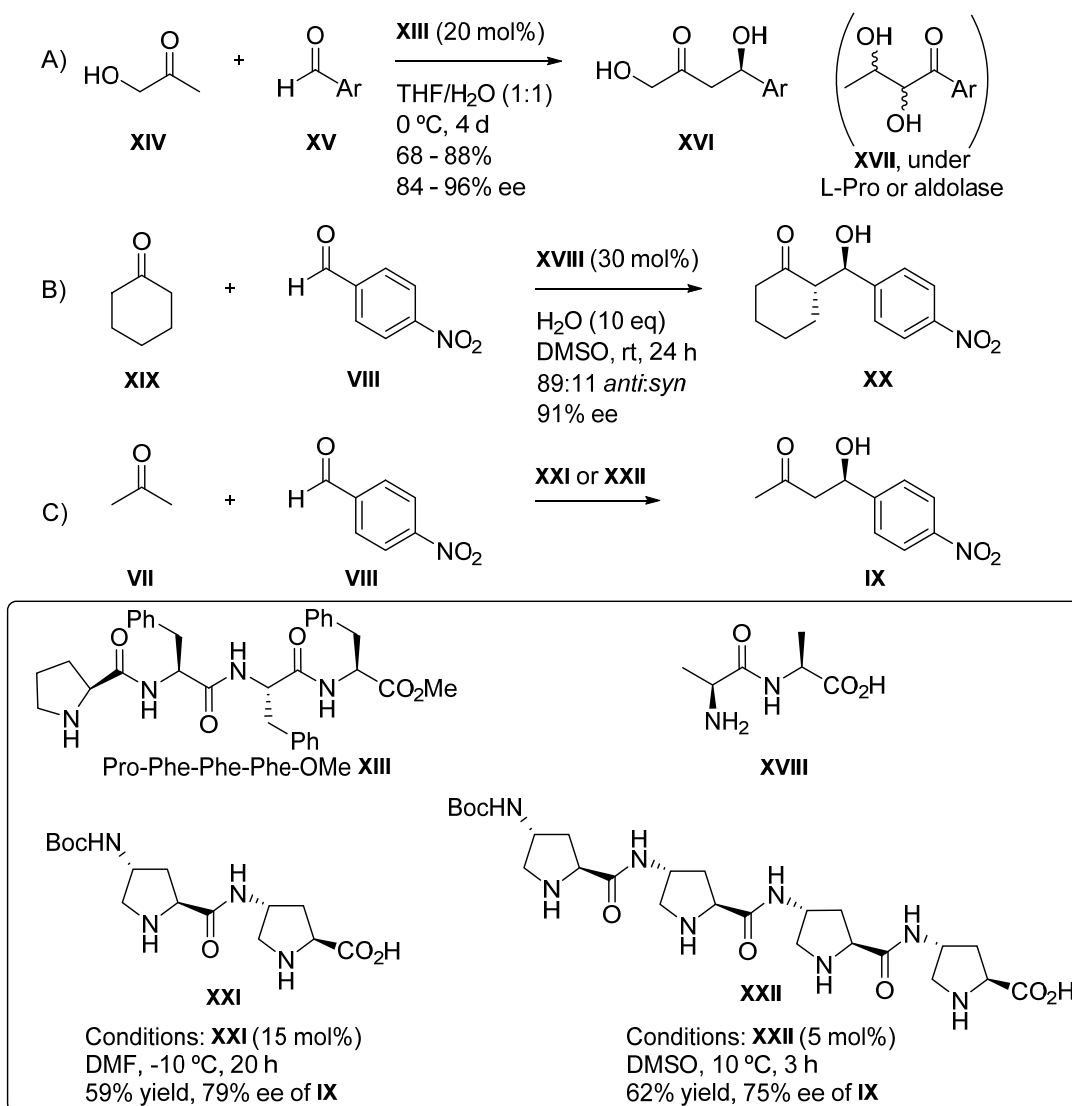
Some years later, the group of Wennemers reported an important screening study related to the organocatalyzed aldol reaction. Employing a “catalyst-substrate co-immobilization” technique, they were able to identify a highly enantioselective tripeptide catalyst out of a combinatorial library of 3375 tripeptides which were generated on a solid support.<sup>10</sup> Soon after, solution phase experiments revealed Pro-Pro-Asp-NH<sub>2</sub> **XI** as the active catalyst, which was able to promote the aldol product **IX** in 98% yield and 80% ee in only four hours with only 1 mol% of catalysts load.<sup>11</sup> In contrast, a catalytic load of 30 mol% of L-Proline was required **XII** to promote the same reaction (Scheme 3). The opposite enantiomeric outcome was rationalized by conformational studies which showed the turn shape the tripeptide was adopting,

allowing the secondary amine and the carboxylic acid in close proximity to perform the efficient catalysis.<sup>12</sup>



**Scheme 3.** Aldol reaction catalyzed by H-Pro-Pro-Asp-NH<sub>2</sub> **XI** and L-Proline **XII**.

Afterwards, other groups also showed the effectiveness of different peptides. Proline-based oligopeptides such as Pro-Phe-Phe-Phe-OMe **XIII** were tested by Gong to catalyze the direct aldol reaction between hydroxyacetone **XIV** with aldehydes to obtain chiral 1,4-diols **XVI** in high yields and enantioselectivities (Scheme 4A).<sup>13</sup> These obtained products were actually the disfavoured products when the reaction was carried out in the presence of L-Proline or aldolases. Córdova, for instance, also presented the dimer based on L-alanine unit **XVIII**, in which the aldol product obtained between cyclohexanone **XIX** and *p*-nitrobenzaldehyde **VIII** reached 91% ee in the presence of water (Scheme 4B).<sup>14</sup> Tsogoeva, on the other side, applied  $\gamma$ -di- and  $\gamma$ -tetra-peptides derived from 4-*trans*-amino-prolines, **XXI** and **XXII**, as chiral organocatalysts in the direct aldol reaction between acetone **VII** and *p*-nitrobenzaldehyde **VIII** showing a performance per active site similar to that observed with L-Proline, which required 30 mol% catalytic load as in Scheme 3. In the case of catalyst **XXII**, which possesses four potential active sites, it was possible to reduce the catalytic load to 5 mol% (Scheme 4C).<sup>15</sup>



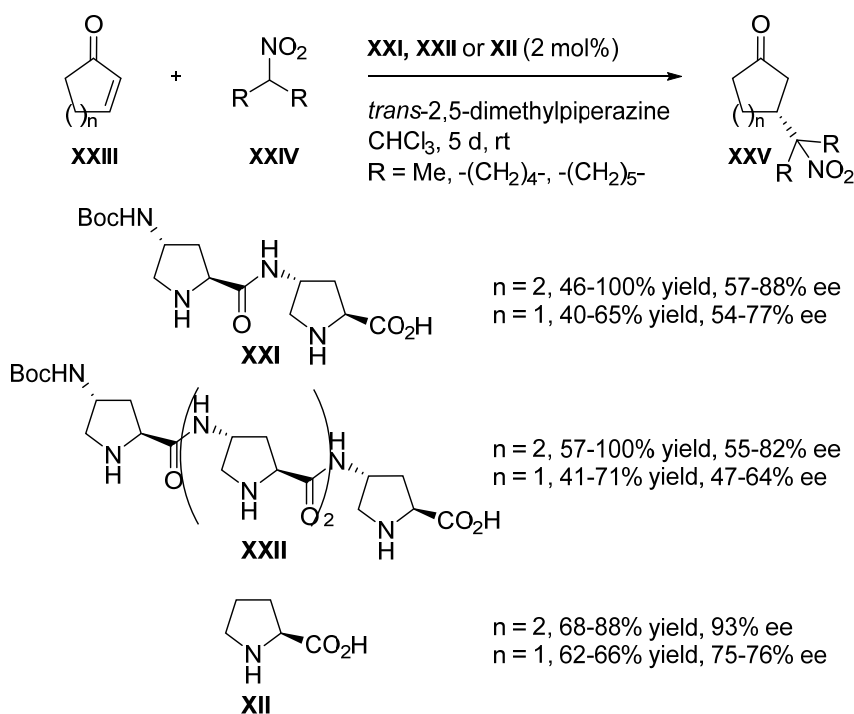
**Scheme 4.** Aldol reaction catalyzed by different oligopeptides.

### 3.1.3. Michael reaction

Similarly to the aldol reaction, Michael reaction has also been a suitable target for organocatalytic peptides. Short peptides have been studied in the conjugate addition of enamines (when the nucleophilic ketone is pre-activated by an amino group of the catalyst) to nitroolefins as well as in the addition of nitroalkanes to  $\alpha,\beta$ -unsaturated ketones.

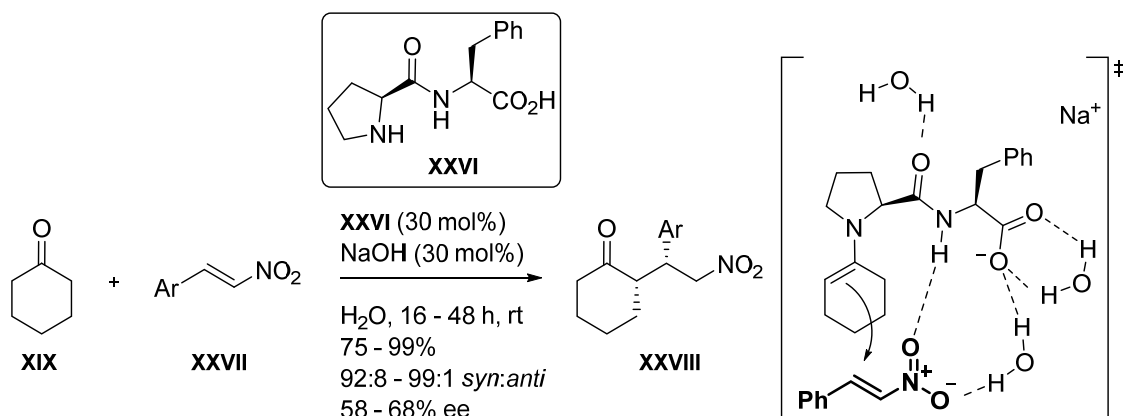
Tsogoeva in the previously discussed work of 2006 (in Scheme 4B) in which the organocatalyzed reaction was described,<sup>15</sup> also reported the use of 4-*trans*-amino-prolines **XXI** and **XXII** in the conjugate addition of nitroalkanes **XXIV** to cyclic enones **XXIII** (Scheme 5). Enones were activated via iminium ion formation with

up to 88% ee's and 100% yield. These authors investigated the reaction outcome while increasing the number of catalytic centres, in the form of pyrrolidine units, and it was revealed that in the case of the studied reaction there was no significant increase in the catalytic activity or selectivity by the chain length of the catalyst. Although their catalytic activity was demonstrated, these catalysts could not improve the outcome observed when L-Proline was used as organocatalyst.<sup>16</sup>



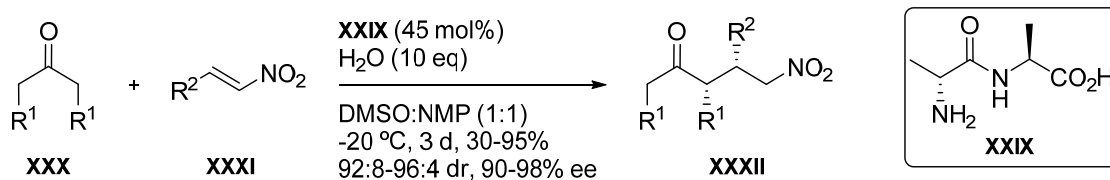
**Scheme 5.** Oligopeptides derived from 4-*trans*-amino-prolines in the conjugate addition between nitroalkanes and cyclic enones.

Some years later, these authors also reported the asymmetric Michael reaction of ketones **XIX** to nitroolefins **XXVII** using *N*-terminal L-proline based dipeptide **XXVI** in combination with NaOH in water.<sup>17</sup>  $\gamma$ -Nitroketones **XXVIII** were furnished with values up to 99% yield, 99:1 of diastereomeric ratio and 68% ee (Scheme 6). The possible role of water was rationalized by means of the proposed transition state, in which a water molecule interacts with the amide moiety to increase the acidity of the NH group, thus strengthening the related hydrogen bond with the nitro group of the olefin. Moreover, they claimed an additional positive effect created by a second water molecule of  $\text{H}_2\text{O}$  which would interact simultaneously with the nitro group and the carboxyl group of the catalyst stabilizing the transition state.



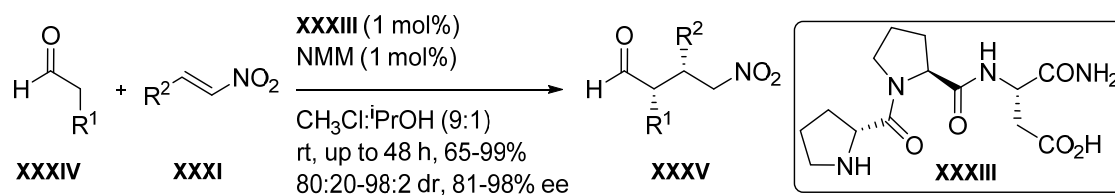
**Scheme 6.** H-Pro-Phe-OH **XXVI** dimer catalyzing the catalyzed nitro-Michael addition and proposed transition state.

Córdova *et al.* tested a similar alanine based dimeric catalyst D-Ala-L-Ala **XXIX** in the Michael reaction between cyclic ketones **XXX** and nitroalkenes **XXXI** to obtain the corresponding adducts in high yields, enantio- and diastereoselectivities (Scheme 7).<sup>14,18</sup> This dipeptide improved the results obtained using alanine monomer and the best results were obtained with symmetrical cyclic ketones as nucleophiles. It was described that both, the acid and amine moieties, were of importance in the stabilization of the transition state, and reported that the addition of water improved the hydrogen bonding array enhancing the enantioselectivities.



**Scheme 7.** Conjugate addition of cyclic ketones to nitroolefins catalyzed by D-Ala-L-Ala **XXIX**.

Catalyst H-Pro-Pro-Asp-NH<sub>2</sub> **XI** reported by Wennemers (in Scheme 3) was very efficient not only for the aldol reaction (*vide supra*), but also for the Michael reaction between aldehydes and nitroolefins.<sup>19</sup> However, further investigation showed that the isomer D-Pro-Pro-Asp-NH<sub>2</sub> **XXXIII** could give better results (Scheme 8). The bifunctional nature of this latter catalyst was responsible for its reactivity as the secondary amine formed the enamine and the carboxylate moiety, acting as a Brønsted base, could activate the nitrostyrene substrate. Only 1 mol% of catalyst was necessary to promote the reaction of a range of aldehydes to both aromatic and aliphatic olefins giving nitroaldehydes **XXXV** in excellent yields and stereoselectivities after 48 hours at room temperature.



**Scheme 8.** Conjugate addition of aldehydes to nitroolefins catalyzed by H-D-Pro-Pro-Asp-NH<sub>2</sub> **XXXIII**.

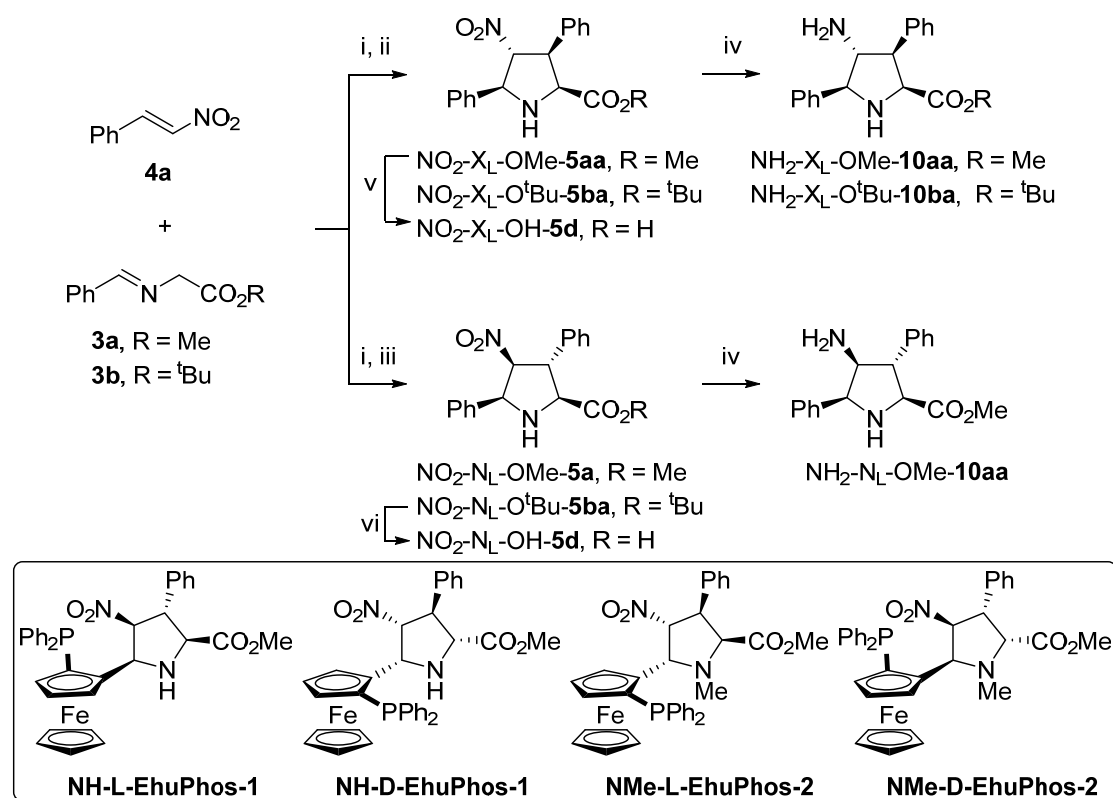
### 3.1.4. Objectives

The previously presented examples of organocatalytic oligopeptides are based on natural or post transcriptional amino acids. Since we have developed a robust methodology to synthesize unnatural densely substituted prolines, in both *exo/endo* and D/L configurations, we decided to study the emergent properties eventually observed on passing from monomeric to dimeric  $\gamma$ -dipeptides. Additionally, dimeric compounds would be of great value in organocatalysis as very few examples are found in literature.<sup>20</sup> For that reason, the points that are pursued in the present chapter are, first, the synthesis of the named dimers by means of derivatization reactions onto the starting building blocks. Then, different studies on the catalytic properties of these compounds are discussed. The aldol and Michael reaction were selected as relevant cases. Finally, further experiments are carried out in order to validate the possible mechanism pathways.

## 3.2. Synthesis of dimers

In order to obtain this 3<sup>rd</sup> new generation of densely substituted proline dimers, first of all the monomeric units were synthesized by the method already described. Thus, ligands **NH-D-EhuPhos-1** and **NMe-L-EhuPhos-2**, already discussed in Chapter 2, were employed in the (3+2) cycloaddition between imines **3** and *trans*- $\beta$ -nitrostyrene **4a** to produce the densely substituted pyrrolidines NO<sub>2</sub>-X<sub>L</sub>-OR-**5** and NO<sub>2</sub>-N<sub>L</sub>-OR-**5** (where R = Me or <sup>t</sup>Bu) in good yields and high diastereo- and enantioselectivities (Table 1). To achieve all the possible diastereoisomeric dimers, the necessary enantiomeric building blocks, using NO<sub>2</sub>-X<sub>D</sub>-OMe-**5aa** and NO<sub>2</sub>-N<sub>D</sub>-OMe-**5aa** were synthesized too by using the enantiomeric versions of the ligands<sup>21</sup> **NH-L-EhuPhos-1** and **NMe-D-EhuPhos-2**. Those pyrrolidines with enantiomeric excesses lower than 99% were purified to >99% and <-99% ee by recrystallization from ethyl acetate/hexane mixtures.

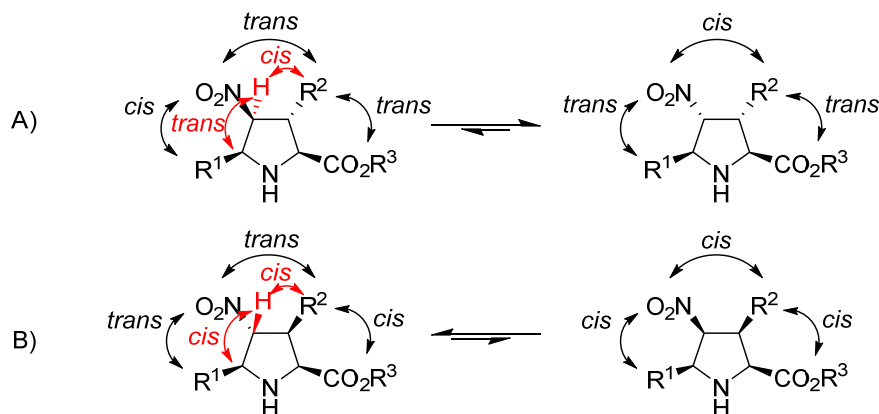
**Table 1.** Synthesis of NO<sub>2</sub>-X<sub>L/D</sub>/N<sub>L/D</sub>-OR-**5**, NO<sub>2</sub>-X<sub>L</sub>/N<sub>L</sub>-OH-**5d** and NH<sub>2</sub>-X<sub>L/D</sub>/N<sub>L/D</sub>-OR-**10** units.



entry	product	conditions <sup>a</sup>	exo:endo <sup>b</sup>	ee <sup>c</sup> (%)	yield <sup>d</sup> (%)
1	NO <sub>2</sub> -X <sub>L</sub> -OMe- <b>5aa</b>	i, ii	95:5	97 (>99)	85
2	NO <sub>2</sub> -X <sub>D</sub> -OMe- <b>5aa</b>	i, ii	95:5	96 (>99)	84
3	NO <sub>2</sub> -X <sub>L</sub> -O <sup>t</sup> Bu- <b>5ba</b>	i, ii	92:8	>99	90
4	NO <sub>2</sub> -N <sub>L</sub> -OMe- <b>5aa</b>	i, iii	10:90	92 (>99)	81
5	NO <sub>2</sub> -N <sub>D</sub> -OMe- <b>5aa</b>	i, iii	7:93	94	83
6	NO <sub>2</sub> -N <sub>L</sub> -O <sup>t</sup> Bu- <b>5ba</b>	i, iii	10:90	94 (>99)	73
7	NH <sub>2</sub> -X <sub>L</sub> -OMe- <b>10aa</b>	iv	-	-	90
8	NH <sub>2</sub> -X <sub>D</sub> -OMe- <b>10aa</b>	iv	-	-	73
9	NH <sub>2</sub> -X <sub>L</sub> -O <sup>t</sup> Bu- <b>10ba</b>	iv	-	-	82
10	NH <sub>2</sub> -N <sub>L</sub> -OMe- <b>10aa</b>	iv	-	-	70
11	NH <sub>2</sub> -N <sub>D</sub> -OMe- <b>10aa</b>	iv	-	-	86
12	NO <sub>2</sub> -X <sub>L</sub> -OH- <b>5d</b>	v	-	-	95
13	NO <sub>2</sub> -N <sub>L</sub> -OH- <b>5d</b>	vi	-	-	77

<sup>a</sup>i) Cu(CH<sub>3</sub>CN)<sub>4</sub>PF<sub>6</sub> (3 mol%), Et<sub>3</sub>N (5 mol%), THF; ii) **NH-D-EhuPhos-1** or **NH-L-EhuPhos-1** (3 mol %), -20 °C; iii) **NMe-L-EhuPhos-2** or **NMe-D-EhuPhos-2** (3 mol%), -60 °C; iv) H<sub>2</sub> (20 bar), Ra-Ni, MeOH, 65 °C, 1.0 mL/min; v) NaOH, acetone/H<sub>2</sub>O, rt, 16 h; vi) TFA, DCM, rt, 16 h. <sup>b</sup>Exo/endo ratio was measured by <sup>1</sup>H NMR of crude reaction mixtures. <sup>c</sup>Enantiomeric excesses were measured by chiral HPLC. <sup>d</sup>Yields refer to isolated pure products.

The required units were later hydrogenated or hydrolyzed to form the corresponding amines or acids, respectively. Hydrogenation of the nitro scaffold occurred uneventfully to provide the desired amines in high yields (entries 7 to 11). In a parallel manner, the methyl ester moiety of the  $\text{NO}_2\text{-X}_L\text{-OMe-5aa}$  cycloadduct was hydrolyzed in basic conditions (entry 12) and the *tert*-butyl ester of the  $\text{NO}_2\text{-N}_L\text{-O}^t\text{Bu-5ba}$  unit was treated with TFA (entry 13) to obtain the desired acids in good yields. Different protecting groups were employed due to the possibility of *endo*-cycloadducts to epimerize at the C4 carbon. This is due to the easiness of the C4 proton abstraction by a base of *endo* cycloadducts as it is placed *cis* and *trans* with respect the substituent at the C3 and C5 position, respectively (in red in Scheme 9A). On the other hand, the proton configuration at *exo* cycloadducts (in red in Scheme 9B) is *cis* to both substituents turning more difficult for a base to approach. As a consequence, C4 epimerization of the *exo* pyrrolidine increases the number of *cis* orientation of vicinal substituents and thus, the new free energy of the epimerized cycloadduct increases (Scheme 9B). On the contrary, this free energy may linger in the case of the *endo* unit as the number of *trans* and *cis* orientation between pairs of adjacent substituents remains the same (Scheme 9A). As a result, treatment under acidic conditions was the best option for the *endo* cycloadduct.



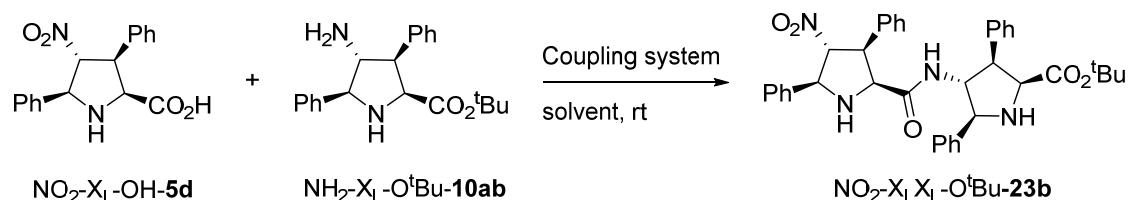
**Scheme 9.** Possible equilibria due to C4 epimerization.

Then, in order to study the best reaction conditions for the dimers synthesis of dimers, different coupling methods were screened in the reaction between  $\text{NO}_2\text{-X}_L\text{-OH-5d}$  and  $\text{NH}_2\text{-X}_L\text{-O}^t\text{Bu-10ba}$  at room temperature (Table 2).<sup>22</sup> Coupling agents such as phosphonic acid derivative DEPC, phosphonic anhydride T3P<sup>23</sup> or  $\text{ZrCl}_4$ <sup>24</sup> did not give any trace of product (entries 1, 3 and 4). Carbodiimide EDC<sup>25</sup> in junction with HOBT provided low yield due to the uncompleted conversion (entry 2). Yields of the  $\gamma$ -peptidic coupling were improved by employing phosphonium salt TBTU<sup>26</sup> and PyBOP<sup>27</sup> coupling agents (entries 5 and 6). When TBTU was used full conversion was achieved



in a moderate yield of 60% (entry 5). This result was improved employing PyBOP instead, for which the yield was raised in a shorter reaction time proving to be the most suitable method for the chemical synthesis of these γ-dipeptides (entry 6).

**Table 2.** Screening of coupling reaction conditions between NO<sub>2</sub>-X<sub>L</sub>-OH-**5d** and NH<sub>2</sub>-X<sub>L</sub>-O<sup>t</sup>Bu-**10ba** to form NO<sub>2</sub>-X<sub>L</sub>X<sub>L</sub>-O<sup>t</sup>Bu-**23b**.

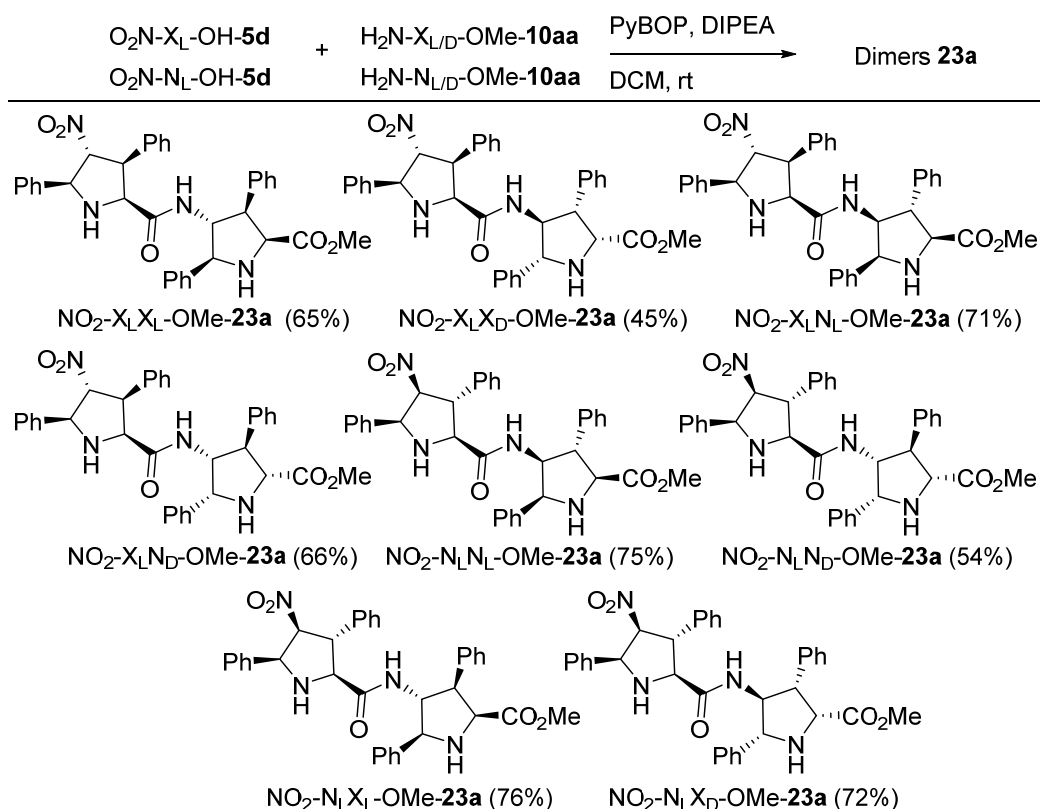


entry	coupling system	solvent	time (h)	conv. <sup>a</sup> (%)	yield <sup>b</sup> (%)
1	DEPC, Et <sub>3</sub> N	DMF	16	0	-
2	EDC, HOBt·2H <sub>2</sub> O, NMM, Et <sub>3</sub> N	DMF	48	80	31
3	T3P (50% H <sub>2</sub> O en DMF)	THF	48	0 <sup>c</sup>	-
4	ZrCl <sub>4</sub> (10%), 4Å MS	THF	24	0	-
5	TBTU, DIPEA	DCM	16	99	60
6	PyBOP, DIPEA	DCM	1	99	74

<sup>a</sup>Reactions were monitored by <sup>1</sup>H NMR. <sup>b</sup>Yields refer to isolated pure NO<sub>2</sub>-X<sub>L</sub>X<sub>L</sub>-O<sup>t</sup>Bu-**23b**.

<sup>c</sup>Starting material NH<sub>2</sub>-X<sub>L</sub>-O<sup>t</sup>Bu-**10ba** was totally consumed according to <sup>1</sup>H NMR.

Once the optimized reaction conditions were achieved, this same methodology was applied in order to get the eight possible dipeptides **25a** from the monomeric units **5d** and the amines belonging to both series L and D **10aa** (Scheme 10). These were obtained in moderate to good yields of 45% for the case of NO<sub>2</sub>-X<sub>L</sub>X<sub>D</sub>-OMe-**23a** and 76% for NO<sub>2</sub>-X<sub>L</sub>N<sub>D</sub>-OMe-**23a** dimer.



**Scheme 10.** Dimers **23a** synthesis using PyBOP as coupling agent (number in parentheses correspond to yields of isolated pure dimers).

The structure and stereochemical integrity of  $\text{NO}_2\text{-X}_L\text{X}_L\text{-O}^t\text{Bu-23b}$  dimer were also secured by X ray diffraction analysis (Figure 1). It can be observed that the pyrrolidinic units in solid state are facing opposite directions which suggests that both possible active sites of the pyrrolidine rings are not equivalent.

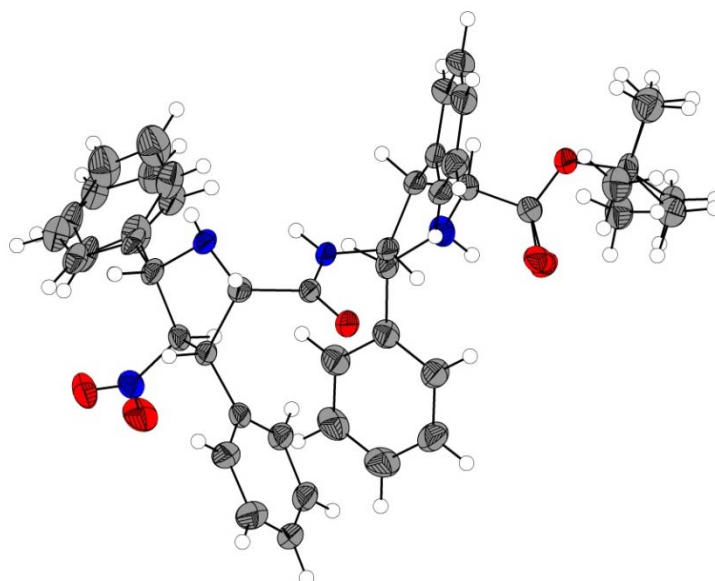


**Figure 1.**  $\text{NO}_2\text{-X}_L\text{X}_L\text{-O}^t\text{Bu-23b}$  X ray structure.

### 3.3. Aldol reaction between cyclohexanone and pentafluorobenzaldehyde

#### 3.3.1. Optimization screening

Once synthesized this new generation of organocatalysts and knowing the efficiency of our 1<sup>st</sup> and 2<sup>nd</sup> generation organocatalysts **5** and **10**, respectively in the aldol reaction (chapter 2), we aimed to evaluate the outcome of these γ-dipeptides in this process. Firstly, the reaction conditions between cyclohexanone **11a** and pentafluorobenzaldehyde **12a** were optimized employing NO<sub>2</sub>-X<sub>L</sub>X<sub>L</sub>-OMe-**23a** as catalyst and TFA as additive under the same conditions studied in the previous chapter (Table 3). The catalytic load could be lowered to 3 mol%, in the presence of 15 mol% of TFA, getting the aldol **13aa** with the configuration (2*R*,1'*S*) in good yield with no apparent loss in the diastereo- and enantioselectivity when compared to the monomer (entry 1,2 vs. 5).

**Table 3.** Catalytic aldol reaction between cyclohexanone **11a** and pentafluorobenzaldehyde **12a** catalyzed by NO<sub>2</sub>-X<sub>L</sub>-OMe-**5aa** and NO<sub>2</sub>-X<sub>L</sub>X<sub>L</sub>-OMe-**23a**.<sup>a</sup>

entry	catalyst/load (mol%)	TFA (mol %)	<i>anti:syn</i> <sup>b</sup>	yield <sup>c</sup> (%)	ee <sup>d</sup> (%)
1 <sup>28</sup>	NO <sub>2</sub> -X <sub>L</sub> -OMe- <b>5aa</b> /30	30	95:5	75	89
2 <sup>28</sup>	NO <sub>2</sub> -X <sub>L</sub> -OMe- <b>5aa</b> /5	30	95:5	81	89
3	NO <sub>2</sub> -X <sub>L</sub> X <sub>L</sub> -OMe- <b>23a</b> /30	30	89:11	66	85
4	NO <sub>2</sub> -X <sub>L</sub> X <sub>L</sub> -OMe- <b>23a</b> /15	15	94:6	66	83
5	NO <sub>2</sub> -X <sub>L</sub> X <sub>L</sub> -OMe- <b>23a</b> /3	15	93:7	86	85

<sup>a</sup>Reactions were monitored by <sup>19</sup>F NMR and were stirred at room temperature until total consumption of aldehyde **12a**. <sup>b</sup>*Anti:syn* ratio was measured by <sup>19</sup>F NMR of crude reaction mixtures. <sup>c</sup>Yields refer to pure aldol adducts. <sup>d</sup>Enantiomeric excesses measured by HPLC correspond to the major *anti*-diastereomers (2*R*,1'*S*)-**13aa**.

Once found the proper reaction conditions, we followed to evaluate the catalytic performance of all the dimers **23a**. The obtained results are gathered in Table 4. When the catalytic aldol reaction between cyclohexanone **11a** and pentafluorobenzaldehyde **12a** was carried out in the presence of the different dimers, all obtained *anti:syn* relationship were excellent providing good to high yields. On the other hand, the enantioselectivity of the process was affected by the configuration of the monomeric units that form the dipeptide. High enantiomeric excesses were obtained when

employing NO<sub>2</sub>-X<sub>L</sub>X<sub>L</sub>-OMe-**23a**, NO<sub>2</sub>-X<sub>L</sub>N<sub>D</sub>-OMe-**23a** or NO<sub>2</sub>-N<sub>L</sub>X<sub>D</sub>-OMe-**23a** catalysts (entries 3, 6 and 10) to racemic mixtures when NO<sub>2</sub>-X<sub>L</sub>X<sub>D</sub>-OMe-**23a** or NO<sub>2</sub>-N<sub>L</sub>N<sub>D</sub>-OMe-**23a** were used (entries 4 and 8).

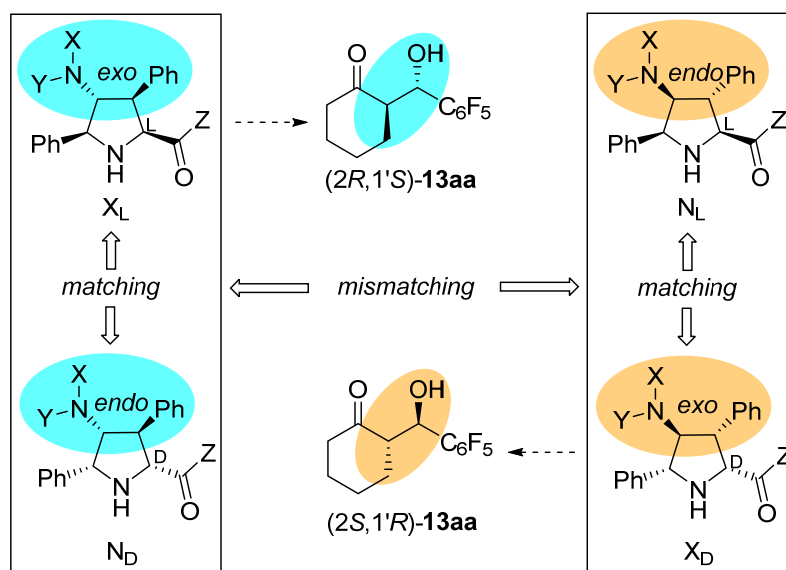
**Table 4.** Catalytic aldol reaction between cyclohexanone **11a** and pentafluorobenzaldehyde **12a** catalyzed by different 3<sup>rd</sup> generation dimers.<sup>a</sup>

Reaction scheme: Cyclohexanone (**11a**) + Pentafluorobenzaldehyde (**12a**)  $\xrightarrow[\text{TFA (15 mol\%), neat, rt}]{\text{catalyst (3 mol\%)}}$  (2*R*,1'*S*)-**13aa** + (2*S*,1'*R*)-**13aa**

entry	catalyst	time (h)	<i>anti:syn</i> <sup>b</sup>	yield <sup>c</sup> (%)	ee <sup>d</sup> (%)	ee <sub>av</sub> <sup>e</sup> (%)
1 <sup>f</sup>	NO <sub>2</sub> -X <sub>L</sub> -OMe- <b>5aa</b>	<1	95:5	75	89	—
2 <sup>f</sup>	NO <sub>2</sub> -N <sub>L</sub> -OMe- <b>5aa</b>	<1	96:4	83	-81	—
3	NO <sub>2</sub> -X <sub>L</sub> X <sub>L</sub> -OMe- <b>23a</b>	8	93:7	86	85	89
4	NO <sub>2</sub> -X <sub>L</sub> X <sub>D</sub> -OMe- <b>23a</b>	16	92:8	84	9	0
5	NO <sub>2</sub> -X <sub>L</sub> N <sub>L</sub> -OMe- <b>23a</b>	8	94:6	84	31	4
6	NO <sub>2</sub> -X <sub>L</sub> N <sub>D</sub> -OMe- <b>23a</b>	36	94:6	72	84	85
7	NO <sub>2</sub> -N <sub>L</sub> N <sub>L</sub> -OMe- <b>23a</b>	24	96:4	91	-65	-81
8	NO <sub>2</sub> -N <sub>L</sub> N <sub>D</sub> -OMe- <b>23a</b>	32	87:13	52	0	0
9	NO <sub>2</sub> -N <sub>L</sub> X <sub>L</sub> -OMe- <b>23a</b>	27	94:6	80	35	4
10	NO <sub>2</sub> -N <sub>L</sub> X <sub>D</sub> -OMe- <b>23a</b>	16	98:2	82	-88	-85

<sup>a</sup>Reactions were monitored by <sup>19</sup>F NMR and were stirred at room temperature until total consumption of aldehyde **12a**. <sup>b</sup>*Anti:syn* ratio was measured by <sup>19</sup>F NMR of crude reaction mixtures. <sup>c</sup>Yields refer to pure aldol adducts. <sup>d</sup>Enantiomeric excesses measured by HPLC correspond to the major *anti*-diastereomer **13aa**. <sup>e</sup>Average enantiomeric excess from the data obtained for the corresponding monomers (entries 1 and 2). <sup>f</sup>Reaction carried out in 30 mol% of monomeric catalyst and TFA.

Comparing the achieved enantiomeric excesses with those obtained under 1<sup>st</sup> generation monomeric organocatalysts (entries 1 and 2), it can be deduced that there are 4 different families of dimeric organocatalysts which differ in the serie (L or D) and configuration (*exo* or *endo*) of the monomer units they bear (which accordingly, follow the pattern shown in Scheme 11).



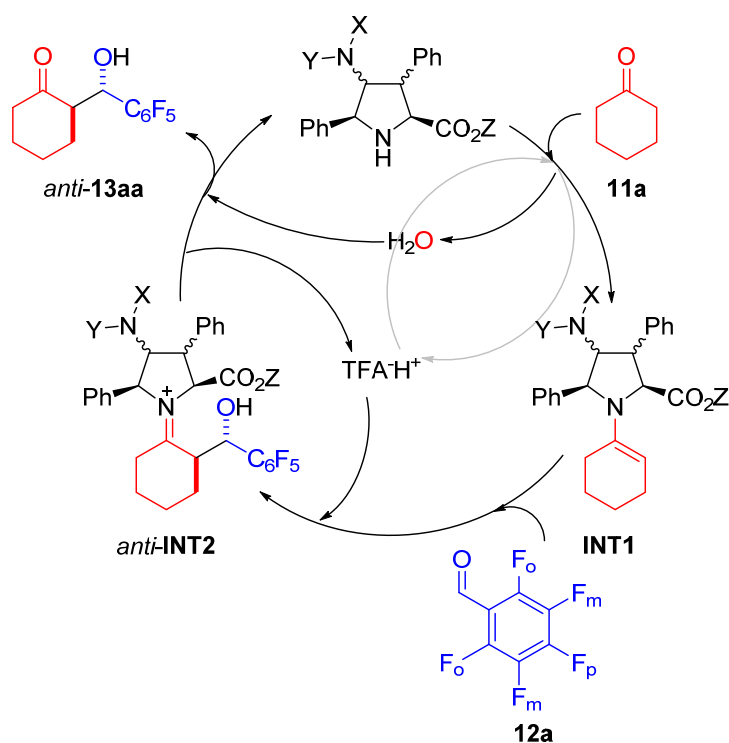
**Scheme 11.** Enantiomeric induction of the monomeric units in the aldol reaction between cyclohexanone and aromatic aldehydes.

According to the data reported in Table 4 and the correlation shown in Scheme 11,  $X_L$  and  $N_D$  units promote formation of (2*R*,1'*S*) aldol adducts, whereas  $N_L$  and  $X_D$  organocatalytic units lead to the corresponding (2*S*,1'*R*) enantiomers. Therefore,  $\gamma$ -dipeptides including matching units reinforce the stereochemical outcome (Table 4, entries 3, 6, 7 and 10), whereas combining mismatching units results in low or negligible enantiomeric excesses (Table 4, entries 4, 5, 8 and 9). These results indicate that both active sites do participate in the aldol reaction catalyzed by these  $\gamma$ -dipeptides, although in some cases the first unit is more active than the second. This proposal is supported by the similarities between the observed enantiomeric excesses for the dimeric units and those expected from the average values resulting from the combination of each active site (see  $ee_{av}$  column in Table 4). Finally, it is interesting to note that the observed stereocontrol is determined by the chiral centres of the distal parts of the organocatalytic units (see Scheme 11) instead of the chiral environment proximal to the catalytic sites.

### 3.3.2. Detection of intermediates

According to the results obtained (Table 4) and previous observations (Scheme 11), it was proposed that each monomeric unit of the catalyst in the aldol reaction process promotes the catalytic activity in independent manner and the total stereocontrol could be determined by a combination of both individual contributions. This conclusion was supported by  $^{19}\text{F}$  NMR analyses based on the accepted pyrrolidine-based

organocatalyzed aldol reaction mechanism (Scheme 12).<sup>29</sup> This catalytic cycle begins with the formation of a first enamine-type intermediate (**INT1**) which reacts with pentafluorobenzaldehyde **12a** evolving to a second iminium-type intermediate (*anti*-**INT2**) which can be observed by <sup>19</sup>F NMR.



**Scheme 12.** Proposed reaction mechanism. F<sub>o</sub>, F<sub>m</sub> and F<sub>p</sub> denote fluorine atoms at *ortho*-, *meta*- or *para*- positions with respect to the carbonyl group.

Figure 2 shows different <sup>19</sup>F NMR spectra of the model reaction between cyclohexanone **11a** and pentafluorobenzaldehyde **12a** catalyzed by NO<sub>2</sub>-N<sub>L</sub>-OMe-**5aa** (Figure 2A), NO<sub>2</sub>-X<sub>L</sub>-OMe-**5aa** (Figure 2B) and NO<sub>2</sub>-N<sub>L</sub>X<sub>L</sub>-OMe-**23a** (Figure 2C) at an instant time of the reaction process. In the first two spectra the fluorine signals (for a better understanding of each species see Figure 3) belonging to the starting material pentafluorobenzaldehyde **12a** (these are **12a**-F<sub>o</sub>, **12a**-F<sub>m</sub> and **12a**-F<sub>p</sub>), the major *anti*-**13a** aldol product (*anti*-**13a**-F<sub>o</sub>, *anti*-**13a**-F<sub>m</sub> and *anti*-**13a**-F<sub>p</sub>) and the minor adduct *syn*-**13a** can be observed, together with the signals provided by the active intermediate belonging to the major intermediate *anti*-**INT2** (F<sub>o</sub>, F<sub>m</sub> and F<sub>p</sub>) and *anti*'-**INT2** (F<sub>o</sub>, F<sub>m</sub> and F<sub>p</sub>), respectively for each catalysts. These latter signals are highlighted in circles in Figure 2A and B. The third <sup>19</sup>F NMR spectrum, which is obtained when the reaction is catalyzed by dimer NO<sub>2</sub>-N<sub>L</sub>X<sub>L</sub>-OMe-**23a** (Figure 2C), shows, aside the signals corresponding to the starting aldehyde and final products (*anti*-**13aa** and *syn*-**13aa**) a different set of signals belonging to *anti*''-**INT2** (F<sub>o</sub>, F<sub>m</sub> and F<sub>p</sub>) which would rise to the

*anti*-**13aa** aldol product. There is only one signal for the *anti'*-INT2-F<sub>m</sub> as the second could be hindered by the surrounding signals.

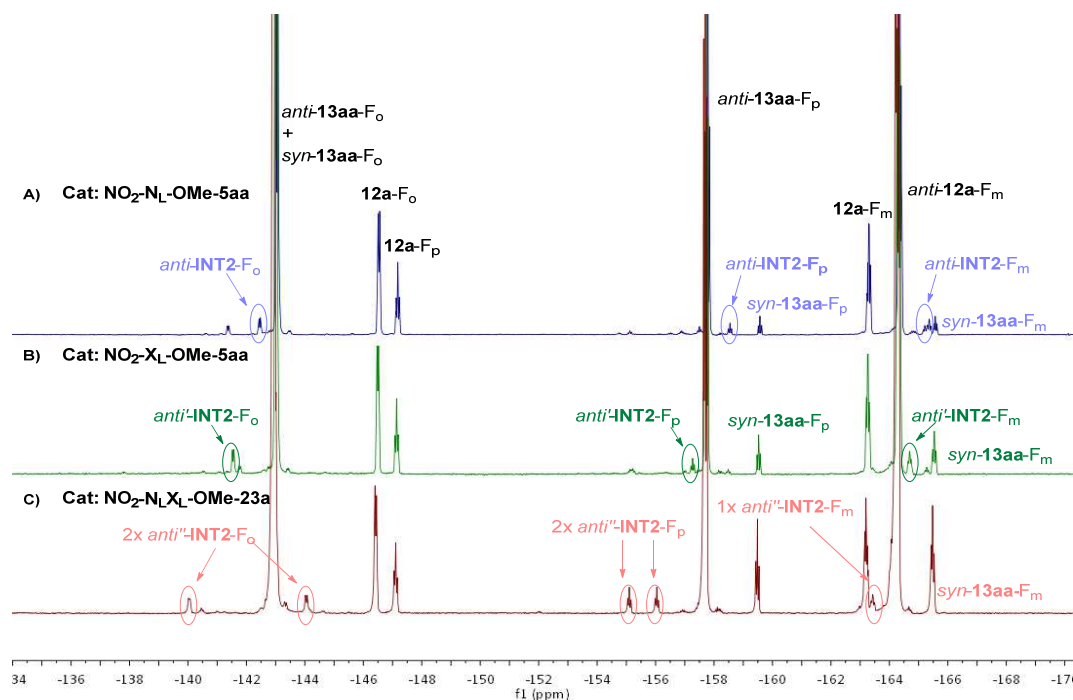


**Figure 2.**  $^{19}\text{F}$  NMR spectra for the aldol reaction between cyclohexanone **11a** and pentafluorobenzaldehyde **12a**. A) catalyzed by  $\text{NO}_2\text{-N}_\text{L}\text{-OMe-5aa}$ ; B) catalyzed by  $\text{NO}_2\text{-X}_\text{L}\text{-OMe-5aa}$ ; C) catalyzed by  $\text{NO}_2\text{-N}_\text{L}\text{X}_\text{L}\text{-OMe-23a}$ .

All these results demonstrate that both monomeric units in the dimers act as independent catalytic centres in the aldol reaction. Thus, it explains why when both catalytic sites provide the same configuration aldols (matching effect) high enantiomeric excesses are achieved (entries 3, 6, 7 and 10), whereas when the active sites provide opposite configuration aldol products (mismatching effect) the enantiomeric excesses are lowered even to racemic values (entries 4, 5, 8 and 9).

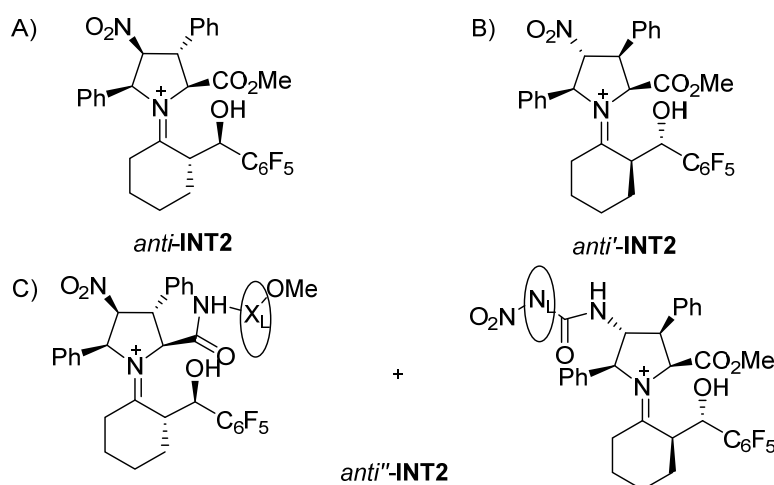
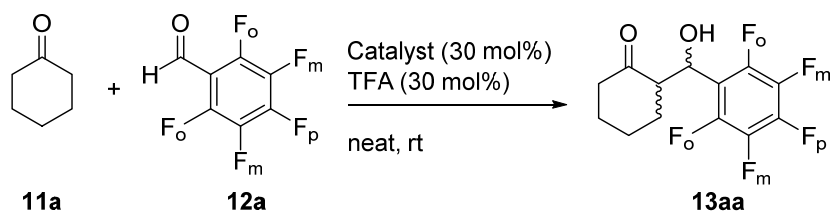


**Figure 3.** Intermediates **2** (INT2) formed out of catalysts A)  $\text{NO}_2\text{-N}_\text{L}\text{-OMe-5aa}$ , B)  $\text{NO}_2\text{-X}_\text{L}\text{-OMe-5aa}$  and C)  $\text{NO}_2\text{-N}_\text{L}\text{X}_\text{L}\text{-OMe-23a}$  to provide *anti* aldol products.

### 3.3.3. Kinetic studies

Once investigated the general effect of both monomeric units with respect the enantioinduction, kinetic studies were performed in order to quantify such effects and to be compared with their monomeric predecessors  $\text{NO}_2\text{-X}_\text{L}\text{-OMe-5aa}$  and  $\text{NO}_2\text{-N}_\text{L}\text{-OMe-5aa}$ . For these studies dimers with both monomeric units belonging to the L series were selected to perform kinetic studies under the reaction conditions shown in Scheme 13. These dimeric organocatalysts are  $\text{NO}_2\text{-X}_\text{L}\text{X}_\text{L}\text{-OMe-23a}$ ,  $\text{NO}_2\text{-N}_\text{L}\text{N}_\text{L}\text{-OMe-23a}$ ,  $\text{NO}_2\text{-X}_\text{L}\text{N}_\text{L}\text{-OMe-23a}$  and  $\text{NO}_2\text{-N}_\text{L}\text{X}_\text{L}\text{-OMe-23a}$ .



**Scheme 13.** Model aldol reaction for kinetic studies.

Due to the high electrophilic nature of **12a**, the progress of the reaction could be analyzed in the presence of different dimeric organocatalysts in quite short reaction times. Additionally, the signals belonging to the three different types of fluorine atoms for each species allow us to quantify the evolution of the reaction mixture in time by  $^{19}\text{F}$  NMR spectroscopy.

The different signals were assigned by the fluorine coupling constants  $^3J_{\text{F},\text{F}}$  and  $^4J_{\text{F},\text{F}}$  in addition to their integral values. Figure 4 shows the evolution in time of the reaction between dry cyclohexanone **11a** and aldehyde **12a** in the presence of 30 mol% of  $\text{NO}_2\text{-X}_\text{L}\text{X}_\text{L}\text{-OMe-23a}$  at 25 °C. The disappearance of starting aldehyde **12a** and its conversion into the major *anti*-**13aa** product and its minor *syn*-congener was readily monitored and appreciated.



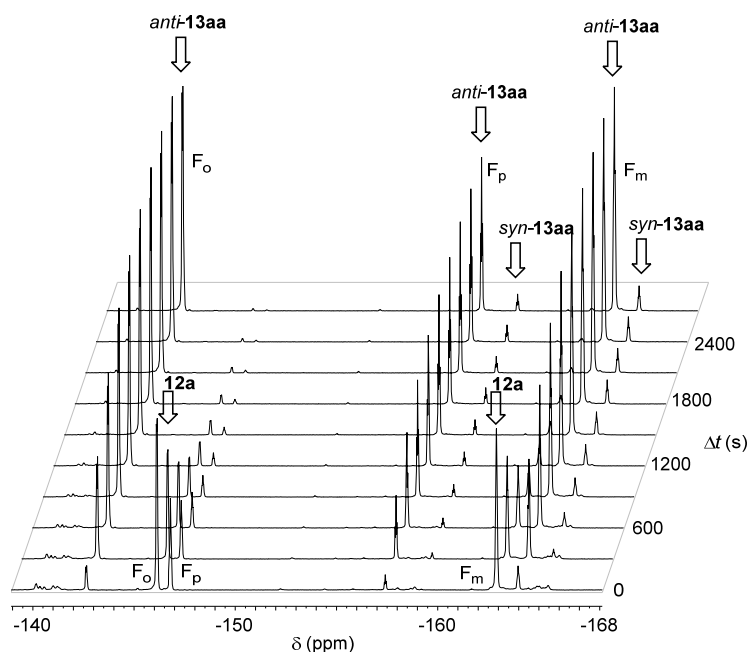


**Figure 4.** Evolution in time of  $^{19}\text{F}$  NMR spectra of the aldol reaction between **11a** and **12a** to give **10a** adducts catalyzed by  $\text{NO}_2\text{-X}_L\text{X}_L\text{-OMe-25a}$ . (Arrows demote the decay of **12a** and the appearance of the desired product.)

Kinetic constants associated with the reaction  $\mathbf{11a} + \mathbf{12a} \rightarrow \mathbf{13aa}$  catalyzed by several organocatalysts were measured under pseudo-first order conditions due to the large ratio  $\mathbf{11a}:\mathbf{12a}$  of 60:1. Under this large excess of cyclohexanone **11a**, the observed reaction rate depends on the concentration of **12a**, according to equation 1:

$$\text{rate} = -\frac{d[\mathbf{12a}]}{dt} \approx k_{\text{obs}}[\mathbf{12a}] \quad (1)$$

The integrated pseudo-first order equation should depend linearly on the logarithms of the aldehyde concentration  $\ln[\mathbf{12a}] - \ln[\mathbf{12a}]_0 = -k_{\text{obs}}t$ . Nevertheless, this expression can also be integrated in terms of the fluorine integral signals on  $^{19}\text{F}$  NMR. As internal reference, the signal provided by the additive TFA was used. For each fluorine atom signal (*ortho*, *meta* and *para*) in the pentafluorophenyl moiety the progress of the reaction was monitored by means of equation 2, from which the observed kinetic constant was obtained (Figure 5).

$$\ln\left(\frac{I_t^i}{I_t^{\text{TFA}}}\right) - \ln\left(\frac{I_0^i}{I_0^{\text{TFA}}}\right) = -k_{\text{obs}}t \quad (2)$$

In equation 2,  $I_0^i$  and  $I_t^i$  refer to the integrals of the different fluorine atoms in **12a** (where  $i = \textit{ortho}$ , *meta* or *para*) at initial and instant times,  $t_0$  and  $t$ , respectively. The experimental measurements were averaged for the three signal systems associated to *ortho*, *meta* and *para* positions of fluorine atoms in the pentafluorophenyl groups

(standard deviations and error calculations are reported in the experimental section). Figure 5 shows the corresponding linear plots obtained by means of equation 2. The obtained correlations are excellent in all cases showing pseudo-first order behaviour under the studied conditions.

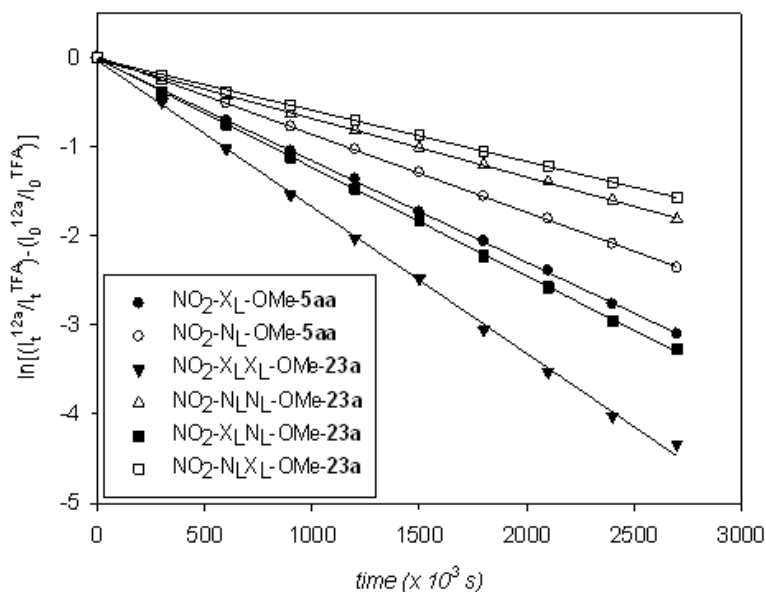


**Figure 5.** Pseudo-first order linear plots of the organocatalyzed reaction showed in Scheme 13.

The observed kinetic constants for the four different organocatalysts are collected in Table 5. These results point out that for the analyzed dimers the catalytic activity order is:  $\text{NO}_2\text{-X}_L\text{X}_L\text{-OMe-23a} > \text{NO}_2\text{-X}_L\text{N}_L\text{-OMe-23a} > \text{NO}_2\text{-N}_L\text{N}_L\text{-OMe-23a} > \text{NO}_2\text{-N}_L\text{X}_L\text{-OMe-23a}$  (entries 3-6). By comparison of these obtained kinetic constants with the ones observed when using first generation catalysts  $\text{NO}_2\text{-X}_L\text{-OMe-5aa}$  and  $\text{NO}_2\text{-N}_L\text{-OMe-5aa}$  (entries 1 and 2), it is possible to estimate the influence of each monomeric scaffold within the dipeptides. It was found that the kinetic value of  $\text{NO}_2\text{-X}_L\text{X}_L\text{-OMe-23a}$  is higher than  $\text{NO}_2\text{-X}_L\text{-OMe-5aa}$  but did not double the value of its monomeric counterpart (entries 1 vs. 3). Additionally, the kinetic value of  $\text{NO}_2\text{-X}_L\text{N}_L\text{-OMe-23a}$  catalyst also exceeded the value of  $\text{NO}_2\text{-X}_L\text{-OMe-5aa}$  (entries 1 vs. 4).

In contrast, it was found that the kinetic constants of the dimers bearing the *endo* 4-nitroprolinamide unit,  $\text{NO}_2\text{-N}_L\text{X}_L\text{-OMe-23a}$  and  $\text{NO}_2\text{-N}_L\text{N}_L\text{-OMe-23a}$ , were slightly lower than their analogous monomer  $\text{NO}_2\text{-N}_L\text{-OMe-5aa}$  (entry 5 and 6 vs. 2). Comparing this two dimers, the dimer with both *endo* units,  $\text{NO}_2\text{-N}_L\text{N}_L\text{-OMe-23a}$ , provides higher kinetic constant than  $\text{NO}_2\text{-N}_L\text{X}_L\text{-OMe-23a}$  (entries 5 vs. 6), an unexpected result considering the expected values provided by the corresponding monomers (entries 1 and 2).

**Table 5.** Measured kinetic constants ( $k_{\text{obs}}$ ) for  $\text{NO}_2\text{-X}_L\text{X}_L\text{-OMe-23a}$ ,  $\text{NO}_2\text{-X}_L\text{N}_L\text{-OMe-23a}$ ,  $\text{NO}_2\text{-N}_L\text{X}_L\text{-OMe-23a}$  and  $\text{NO}_2\text{-N}_L\text{N}_L\text{-OMe-23a}$  dimers in the reaction  $\mathbf{11a+12a} \rightarrow \mathbf{13aa}$ .<sup>a,b,c</sup>

entry	catalyst	$k_{\text{obs}}$ ( $10^{-4} \text{ s}^{-1}$ )
1	$\text{NO}_2\text{-X}_L\text{-OMe-5aa}$	$11.29 \pm 0.30$
2	$\text{NO}_2\text{-N}_L\text{-OMe-5aa}$	$8.83 \pm 0.16$
3	$\text{NO}_2\text{-X}_L\text{X}_L\text{-OMe-23a}$	$16.68 \pm 0.58$
4	$\text{NO}_2\text{-X}_L\text{N}_L\text{-OMe-23a}$	$13.36 \pm 0.54$
5	$\text{NO}_2\text{-N}_L\text{X}_L\text{-OMe-23a}$	$5.72 \pm 0.06$
6	$\text{NO}_2\text{-N}_L\text{N}_L\text{-OMe-23a}$	$6.65 \pm 0.24$

<sup>a</sup>Pseudo-first order constants calculated by means of eq. 2 with a  $\mathbf{11a:12a}$  ratio of 60:1. <sup>b</sup>All reactions were monitored by  $^{19}\text{F}$  NMR at 25 °C. <sup>c</sup>Errors were calculated from the standard deviations of the kinetic constants according to reference 30.

In summary, these dimers in which both pyrrolidine units belong to the L series showed the following trend: those dimers bearing the *exo* 4-nitroprolinamide provide higher kinetic values than their monomeric equivalent ( $\text{NO}_2\text{-X}_L\text{X}_L\text{-OMe-23a} > \text{NO}_2\text{-X}_L\text{N}_L\text{-OMe-23a} > \text{NO}_2\text{-X}_L\text{-OMe-5aa}$ ) and those dimers with the *endo* 4-nitroprolinamide provide lower kinetic values than those observed for their monomeric analogues:  $\text{NO}_2\text{-N}_L\text{X}_L\text{-OMe-23a} < \text{NO}_2\text{-N}_L\text{N}_L\text{-OMe-23a} < \text{NO}_2\text{-N}_L\text{-OMe-5aa}$ . From these kinetic results it can be concluded that not only the configuration of each monomeric units is important but also other parameters should be taken under consideration such as the spatial conformation of the dimers or the existence and influence of the peptidic bond.

### 3.4. Michael reaction between cyclohexanone and *trans*-β-nitrostyrene

After studying the outcome of these dimeric organocatalysts in the aldol reaction, we also aimed to test these dipeptide catalysts in another enamine activated organocatalyzed reaction such as the Michael reaction. The reaction between cyclohexanone **11a** and nitrostyrene **4a** was chosen and carried out in the presence of 20 mol% of catalyst and benzoic acid as additive to evaluate the catalytic behaviour of dimers **23a** (Table 6, entries 1 and 4 to 10). It can be seen that the trend the γ-dipeptides follow is not as easily recognizable as in the aldol reaction. First, in this case the nitro monomeric units did not catalyze the reaction significantly. Therefore, we

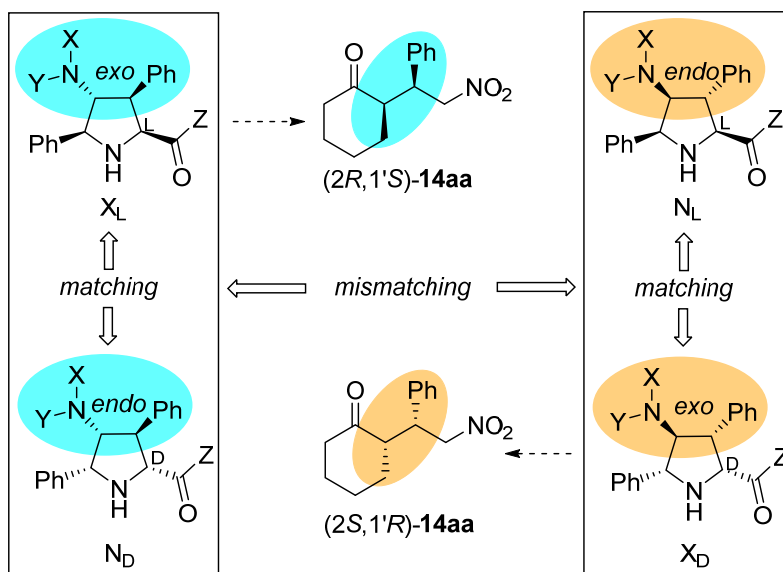
cannot use the outcome provided by the monomeric series as a reference. The enantiomeric excesses can range from even racemic mixtures, for the catalysts  $\text{NO}_2\text{-N}_\text{L}\text{N}_\text{L}\text{-OMe-23a}$  and  $\text{NO}_2\text{-N}_\text{L}\text{N}_\text{D}\text{-OMe-23a}$  (entries 7 and 8), to the high values provided by  $\text{NO}_2\text{-X}_\text{L}\text{X}_\text{L}\text{-OMe-23a}$  and  $\text{NO}_2\text{-N}_\text{L}\text{X}_\text{D}\text{-OMe-23a}$  (entries 1 and 10). The diastereomeric ratios were high in all cases, meanwhile the reaction times, conversions and yields varied considerably depending on the dimer used. For instance, reaction times values of two weeks were found with moderate yield for the case of  $\text{NO}_2\text{-X}_\text{L}\text{N}_\text{D}\text{-OMe-23a}$  (entry 6) and, on the other side, a reaction time of two days with full conversion and good yield was found for the  $\text{NO}_2\text{-X}_\text{L}\text{X}_\text{L}\text{-OMe-23a}$  catalyst (entry 1). To our surprise, a minor formation of lactam **2aaa** was observed in all cases. Further details on this unexpected result will be discussed in depth in chapter 4.

**Table 6.** Direct Michael reaction between cyclohexanone **11a** and *trans*- $\beta$ -nitrostyrene **4a** catalyzed by different dimers.<sup>a</sup>

entry	catalyst	time (d)	conv <sup>a</sup> (%)	<i>syn:anti</i> <sup>b</sup>	yield <sup>c</sup> (%)	ee <sup>d</sup> (%)
1	$\text{NO}_2\text{-X}_\text{L}\text{X}_\text{L}\text{-OMe-23a}$	2	>99	85:15	79	65
2 <sup>e</sup>	$\text{NO}_2\text{-X}_\text{L}\text{X}_\text{L}\text{-OMe-23a}$	1	>99	89:11	82	78
3 <sup>f</sup>	$\text{NO}_2\text{-X}_\text{L}\text{X}_\text{L}\text{-OMe-23a}$	4 h	>99	91:9	75	82
4	$\text{NO}_2\text{-X}_\text{L}\text{X}_\text{D}\text{-OMe-23a}$	4	>99	94:6	71	-46
5	$\text{NO}_2\text{-X}_\text{L}\text{N}_\text{L}\text{-OMe-23a}$	6	84	90:10	78	55
6	$\text{NO}_2\text{-X}_\text{L}\text{N}_\text{D}\text{-OMe-23a}$	13	72	82:18	57	24
7	$\text{NO}_2\text{-N}_\text{L}\text{N}_\text{L}\text{-OMe-23a}$	7	76	93:7	59	-17
8	$\text{NO}_2\text{-N}_\text{L}\text{N}_\text{D}\text{-OMe-23a}$	7	71	95:5	56	6
9	$\text{NO}_2\text{-N}_\text{L}\text{X}_\text{L}\text{-OMe-23a}$	3	>99	84:16	89	46
10	$\text{NO}_2\text{-N}_\text{L}\text{X}_\text{D}\text{-OMe-23a}$	3	86	90:10	78	-70
11 <sup>e</sup>	$\text{NO}_2\text{-N}_\text{L}\text{X}_\text{D}\text{-OMe-23a}$	19 h	>99	94:6	71	-75
12 <sup>f</sup>	$\text{NO}_2\text{-N}_\text{L}\text{X}_\text{D}\text{-OMe-23a}$	16 h	>99	97:3	76	-81

<sup>a</sup>Conversions were measured by  $^1\text{H}$  NMR of crude reaction mixtures. Conversions to **24aaa** product were <20% in all cases. <sup>b</sup>*Syn:anti* ratio was measured by  $^1\text{H}$  NMR of crude reaction mixtures. <sup>c</sup>Yields refer to isolated pure Michael adducts. <sup>d</sup>Enantiomeric excesses measured by HPLC correspond to the major *syn*-diastereomers **14aa**. <sup>e</sup>30 mol% of catalyst and 30 mol%  $\text{PhCO}_2\text{H}$ . <sup>f</sup>40 mol% of catalyst and 40 mol% of  $\text{PhCO}_2\text{H}$ .

The postulated reaction mechanism is the same one as occurred for the aldol reaction between cyclohexanone **11a** and 2,3,4,5-pentafluorobenzaldehyde **12a** (see Table 4 and Scheme 12). Similarly in this Michael reaction, both monomeric units of the dimeric organocatalyst were promoting the catalysis and each was directing towards the corresponding enantiomer as depicted in Scheme 14. Nevertheless, some of the low enantiomeric inductions could be explained according to less enantiocontrol of the units.



**Scheme 14.** Enantiomeric induction of the monomeric units in the Michael reaction between cyclohexanone **11a** and *trans*- $\beta$ -nitrostyrene **4a**.

For instance, catalysts NO<sub>2</sub>-X<sub>L</sub>X<sub>L</sub>-OMe-**23a** and NO<sub>2</sub>-N<sub>L</sub>N<sub>L</sub>-OMe-**23a** (entries 1 and 7) provide each the corresponding enantiomer, (2*R*,1'*S*)- and (2*S*,1'*R*)-, respectively. However, the lower ee value of the latter could be attributed to a higher conformational flexibility of the *endo*- units thus reducing the enantiocontrol. Catalysts NO<sub>2</sub>-X<sub>L</sub>N<sub>D</sub>-OMe-**23a** and NO<sub>2</sub>-N<sub>L</sub>X<sub>D</sub>-OMe-**23a** (entries 6 and 10) also provide the (2*R*,1'*S*)- and (2*S*,1'*S*)- enantiomers, respectively under the influence of each monomeric unit. Again, the possible conformational flexibility of NO<sub>2</sub>-X<sub>L</sub>N<sub>D</sub>-OMe-**23a**, which also needed the longest reaction time, may be responsible for the lower enantiomeric excess. Then, the enantiomeric excesses of NO<sub>2</sub>-X<sub>L</sub>N<sub>L</sub>-OMe-**23a** and NO<sub>2</sub>-N<sub>L</sub>X<sub>L</sub>-OMe-**23a** (entries 5 and 9) are oriented towards the (2*R*,1'*S*)- compound which, would be in accordance with a higher catalytic activity of the *exo*- unit with respect to the *endo*- active site (see Table 5). Finally, the outcome of catalysts NO<sub>2</sub>-X<sub>L</sub>X<sub>D</sub>-OMe-**23a** and NO<sub>2</sub>-N<sub>L</sub>N<sub>D</sub>-OMe-**23a** (entries 4 and 8) which cannot be explained according to the reasoning interpreted for the previous examples,

coordination or stronger conformational factors could be the responsible for the provided enantiomeric excesses of -46 and 6% ee, respectively.

Due to the fact that  $\text{NO}_2\text{-X}_L\text{X}_L\text{-OMe-23a}$  and  $\text{NO}_2\text{-X}_L\text{X}_D\text{-OMe-23a}$  provided the best results (entries 1 and 10), it was decided to increase their catalytic load with the goal of increasing the enantioselectivity of the process. Consequently, reaction times were reduced and the enantioselectivities increased up to ca. 80% ee when 30 and 40 mol% catalytic loads were employed (entries 2-3 vs. 1 and 11-12 vs. 10).

### 3.5. Synthesis of *N*-methylated and hybrid dimers. Effects on the reactivity in aldol and Michael reactions

#### 3.5.1. Synthesis

In order to evaluate the influence of each monomeric unit of the dimers in catalysis at the aldol and Michael reaction,  $\text{NO}_2\text{-X}_L\text{X}_L\text{-OMe-25a}$ ,  $\text{NO}_2\text{-X}_L\text{X}_D\text{-OMe-25a}$ ,  $\text{NO}_2\text{-X}_L\text{X}_L\text{-OMe-26a}$  and  $\text{NO}_2\text{-X}_L\text{X}_D\text{-OMe-26a}$  were synthesized in which one of the pyrrolidine units was *N*-methylated (Figure 6).

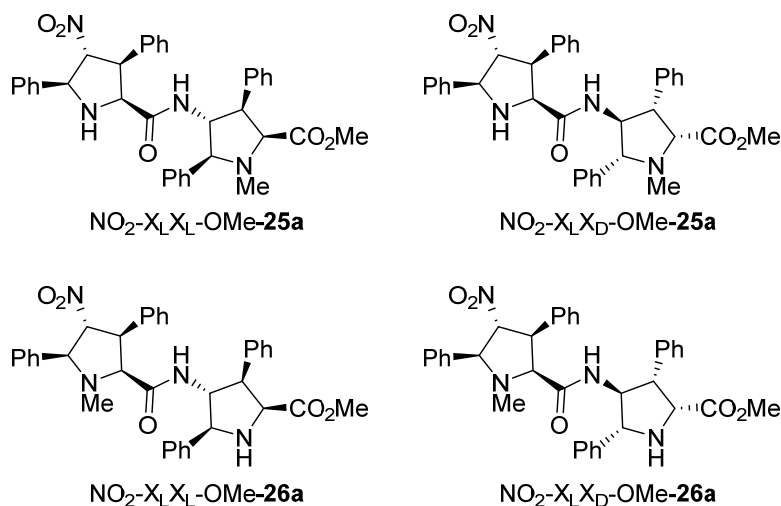
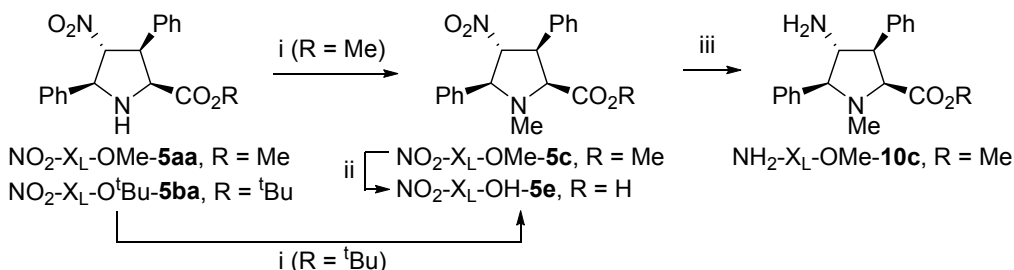


**Figure 6.** *N*-methylated dimers  $\text{NO}_2\text{-X}_L\text{X}_L\text{-OMe-25a}$ ,  $\text{NO}_2\text{-X}_L\text{X}_D\text{-OMe-25a}$ ,  $\text{NO}_2\text{-X}_L\text{X}_L\text{-OMe-26a}$  and  $\text{NO}_2\text{-X}_L\text{X}_D\text{-OMe-26a}$ .

For that purpose,  $\text{NO}_2\text{-X}_L\text{-OMe-4aa}$  and  $\text{NO}_2\text{-X}_D\text{-OMe-4aa}$  were methylated in the first instance to provide the tertiary amines according to the method described in chapter 2 and followed by hydrogenation to give diamines  $\text{NH}_2\text{-X}_L\text{-OMe-10c}$  and  $\text{NH}_2\text{-X}_D\text{-OMe-10c}$ , respectively. When pyrrolidine  $\text{NO}_2\text{-X}_L\text{-O}^t\text{Bu-5ba}$  was subjected to the methylation reaction, simultaneous *N*-methylation and acid formation occurred at the carboxylic moiety as described by literature<sup>31</sup>, in good yields (entry 4). Hydrolysis in

basic medium and hydrogenation occurred uneventfully in good yield (entries 3, 5 and 6).

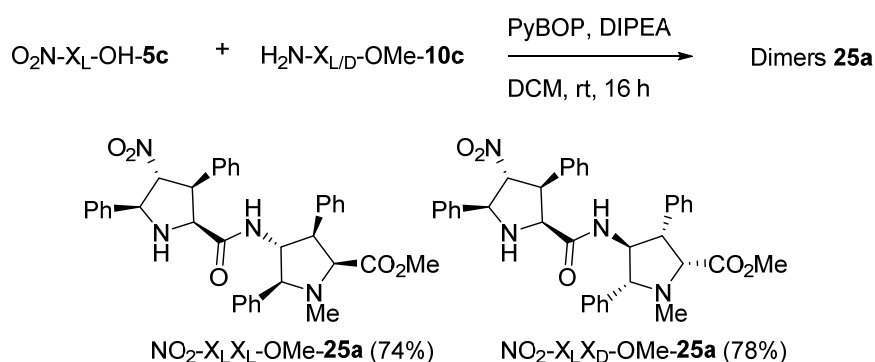
**Table 7.** Synthesis of  $\text{NO}_2\text{-X}_{\text{L/D}}\text{-OMe-5c}$ ,  $\text{NH}_2\text{-X}_{\text{L/D}}\text{-OMe-10c}$  and  $\text{NO}_2\text{-X}_{\text{L}}\text{-OH-5e}$  units (cycloadducts belonging to the L series are only depicted for the sake of simplicity).



entry	product	conditions <sup>a</sup>	yield (%)
1	$\text{NO}_2\text{-X}_{\text{L}}\text{-OMe-5c}$	i	78
2	$\text{NO}_2\text{-X}_{\text{D}}\text{-OMe-5c}$	i	79
3	$\text{NO}_2\text{-X}_{\text{L}}\text{-OH-5e}$	i	90
4	$\text{NO}_2\text{-X}_{\text{L}}\text{-OH-5e}$	ii	63
5	$\text{NH}_2\text{-X}_{\text{L}}\text{-OMe-10c}$	iii	74
6	$\text{NH}_2\text{-X}_{\text{D}}\text{-OMe-10c}$	iii	75

<sup>a</sup>i)  $\text{H}_2\text{CO}/\text{HCO}_2\text{H}$ , 100 °C, 2 h; ii) NaOH, acetone/ $\text{H}_2\text{O}$ , rt, 16 h; iii)  $\text{H}_2$  (20 bar), Ra/Ni, [0.01M], 65 °C, 1 mL/min.

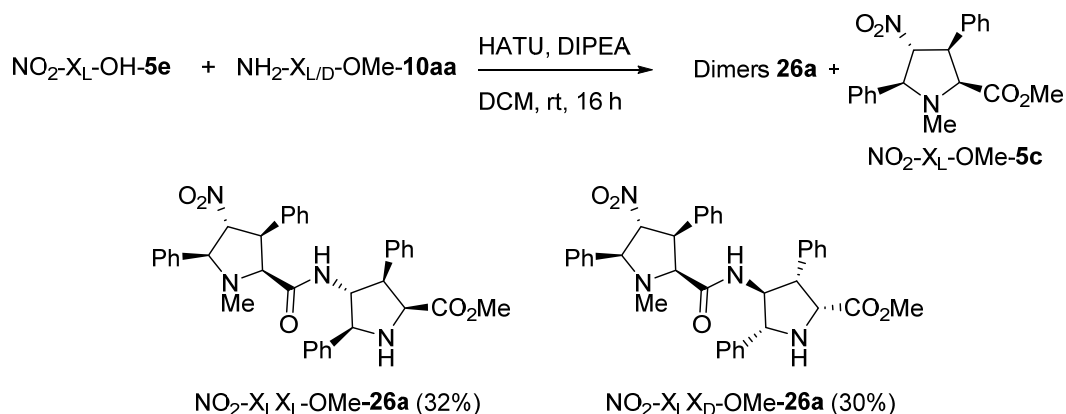
The synthesis of *N*-methylated dimers  $\text{NO}_2\text{-X}_{\text{L}}\text{X}_{\text{L}}\text{-OMe-25a}$  and  $\text{NO}_2\text{-X}_{\text{L}}\text{X}_{\text{D}}\text{-OMe-25a}$  was achieved in good yields employing the procedure already described in Scheme 10 for the obtention of γ-dipeptides. This time,  $\text{NO}_2\text{-X}_{\text{L}}\text{-OH-1c}$  and  $\text{NH}_2\text{-X}_{\text{L/D}}\text{-OMe-2d}$  in both enantiomeric forms were used as starting materials (Scheme 15).



**Scheme 15.** Synthesis of dimers **25a** synthesis using PyBOP as coupling agent. (Numbers in parentheses correspond to yields of isolated pure dimers)

Nevertheless, this methodology failed when applied to the synthesis of  $\text{NO}_2\text{-X}_{\text{L}}\text{X}_{\text{L}}\text{-OMe-26a}$  and  $\text{NO}_2\text{-X}_{\text{L}}\text{X}_{\text{D}}\text{-OMe-26a}$  dimers in which the 4-nitroprolinamide is

*N*-methylated. Thus, reaction conditions screening had to be carried out.<sup>i</sup> The optimized reaction conditions included HATU as a coupling reagent in the presence of DIPEA, which provided the desired dimers together with but also the transesterified monomer  $\text{NO}_2\text{-X}_L\text{-OMe-5c}$  was obtained as byproduct in 1:1 ratio in both cases allowing the coupling products in low yields.



**Scheme 16.** Optimized reaction conditions towards  $\text{NO}_2\text{-X}_L\text{X}_L\text{-OMe-26a}$  and  $\text{NO}_2\text{-X}_L\text{X}_D\text{-OMe-26a}$  dimers.

Out of all these new synthesized dimers,  $\text{NO}_2\text{-X}_L\text{X}_L\text{-OMe-25a}$  could be crystallized and an X ray diffraction analysis could be made showing the spatial disposition in solid state of the two pyrrolidine rings.

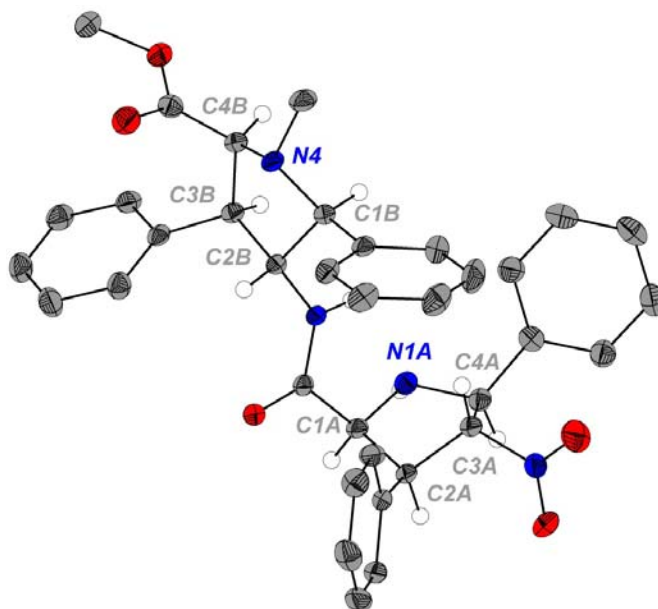


**Figure 7.** ORTEP drawing of  $\text{NO}_2\text{-X}_L\text{X}_L\text{-OMe-25a}$ .

Additionally, in order to understand the activation mode of these densely substituted proline based dimeric organocatalysts in the Michael reaction, other pyrrolidine-based organocatalysts were evaluated (Figure 8). Therefore, dimer  $\text{Pro}_L\text{Gly-OH-27}$  was

<sup>i</sup> This screening of this reaction conditions was performed by the PhD student Maddalen Agirre.



chosen for being the simplest commercially available dimer derived from natural proline. Hybrid thiourea catalyst **28**, benzamido proline **17** and dimer  $\text{NO}_2\text{-X}_L\text{Gly-OMe-29}$ , which were all derived from our highly substituted pyrrolidines, were also targets of choice.

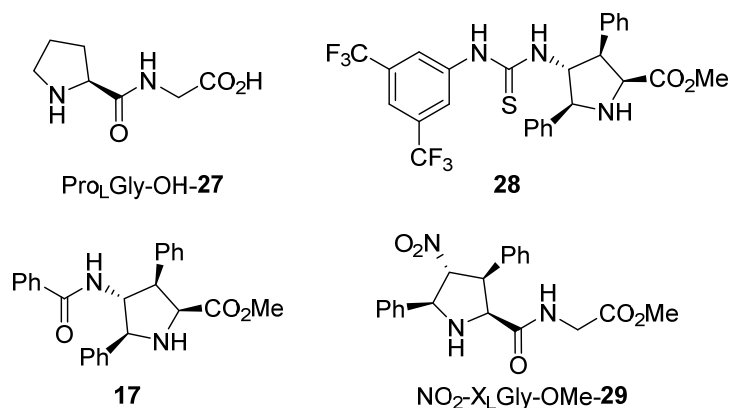
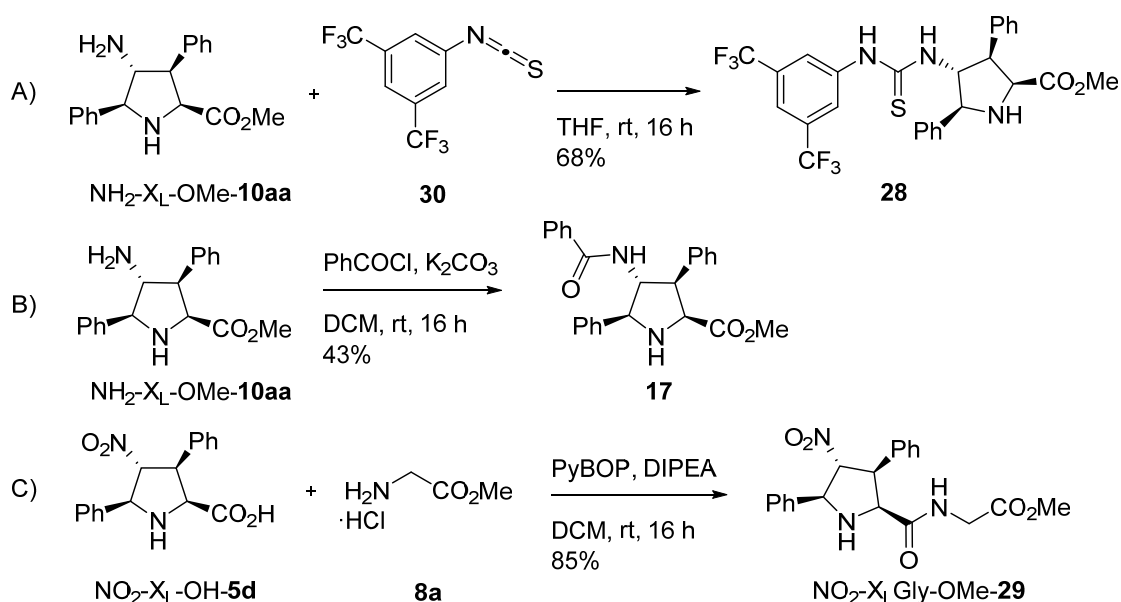


**Figure 8.** Hybrid organocatalysts based in pyrrolidine units.

Firstly, the reaction between  $\text{NH}_2\text{-X}_L\text{-OMe-10aa}$  and bis(trifluoromethyl)phenyl isothiocyanate **30** was carried out to obtain the hydrogen bond donating hybrid catalyst **28** in 68% yield (Scheme 17A). Also, **17** in Scheme 17B and  $\text{NO}_2\text{-X}_L\text{Gly-OMe-29}$  (Scheme 17C), bearing an amide group in the fourth and second position, respectively, were synthesized. Catalyst  $\text{NO}_2\text{-X}_L\text{Gly-OMe-29}$  was obtained in 85% yield from  $\text{NO}_2\text{-X}_L\text{-OH-5d}$ , glycine methyl ester hydrochloride **3a** and PyBOP as coupling agent following the standard procedure for the synthesis of dimers.



**Scheme 17.** **28**, **17** and  $\text{NO}_2\text{-X}_L\text{Gly-OMe-29}$  organocatalysts syntheses.

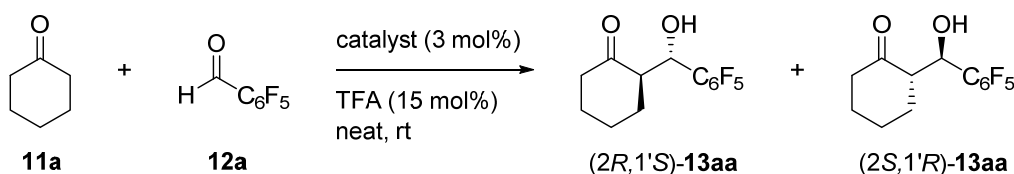
Once these diverse organocatalysts were available, *N*-methylated catalyst  $\text{NO}_2\text{-X}_L\text{X}_D\text{-OMe-25a}$  and  $\text{NO}_2\text{-X}_L\text{X}_D\text{-OMe-26a}$  in Figure 6 were tested in the model aldol

reaction between cyclohexanone **11a** and pentafluorobenzaldehyde **12a**. Concurrently, dimers NO<sub>2</sub>-X<sub>L</sub>X<sub>L</sub>-OMe-**25a** and NO<sub>2</sub>-X<sub>L</sub>X<sub>L</sub>-OMe-**26a** and hybrid catalysts depicted in Scheme 17 were tested in the Michael reaction between cyclohexanone **11a** and nitrostyrene **4a**.

### 3.5.2. Effect on the aldol reaction between cyclohexanone and pentafluorobenzaldehyde

Once the reaction conditions were set up, we followed to evaluate the catalytic performance of dimers NO<sub>2</sub>-X<sub>L</sub>X<sub>D</sub>-OMe-**25a** and NO<sub>2</sub>-X<sub>L</sub>X<sub>D</sub>-OMe-**26a**, in which one of the pyrrolidinic rings is methylated and to compare them to their non-methylated homologous. The results are shown in Table 8.

**Table 8.** Comparison on the aldol reaction between cyclohexanone **11a** and pentafluorobenzaldehyde **12a** catalyzed by different methylated 3<sup>rd</sup> generation dimers.<sup>a</sup>



entry	catalyst	time (h)	<i>anti:syn</i> <sup>b</sup>	yield <sup>c</sup> (%)	ee <sup>d</sup> (%)
1 <sup>e</sup>	NO <sub>2</sub> -X <sub>L</sub> -OMe- <b>5aa</b>	<1	95:5	75	89
2	NO <sub>2</sub> -X <sub>L</sub> X <sub>L</sub> -OMe- <b>23a</b>	8	93:7	86	85
3	NO <sub>2</sub> -X <sub>L</sub> X <sub>D</sub> -OMe- <b>23a</b>	16	92:8	84	9
4	NO <sub>2</sub> -X <sub>L</sub> X <sub>D</sub> -OMe- <b>25a</b>	48	88:12	93	90
5 <sup>f</sup>	NO <sub>2</sub> -X <sub>L</sub> X <sub>D</sub> -OMe- <b>25a</b>	16	92:8	85	88
6	NO <sub>2</sub> -X <sub>L</sub> X <sub>D</sub> -OMe- <b>26a</b>	64	91:9	68 <sup>g</sup>	-82
7 <sup>f</sup>	NO <sub>2</sub> -X <sub>L</sub> X <sub>D</sub> -OMe- <b>26a</b>	24	97:3	84	-85

<sup>a</sup>Reactions were monitored by <sup>19</sup>F NMR and were stirred at room temperature until total consumption of aldehyde **12a**. <sup>b</sup>*Anti:syn* relationships were measured by <sup>19</sup>F NMR of crude reaction mixtures. <sup>c</sup>Yields refer to pure aldol adducts. <sup>d</sup>Enantiomeric excesses measured by HPLC correspond to the major *anti*-diastereomer (2*R*,1'*S*)-**13aa**. <sup>e</sup>Reaction carried out in 30 mol% of catalyst and TFA. <sup>f</sup>6 mol% of catalyst load was employed. <sup>g</sup>98% conversion was achieved.

These further experiments confirmed the model previously discussed in section 3.3. An increase of the enantiocontrol in opposite directions is shown, depending on the nature (L or D series) of the methylated pyrrolidinic ring (Table 8, entries 4 to 7). When one pyrrolidinic ring is methylated, this center loses its catalytic activity, as it is unable to

perform the enamine activation, allowing the unmethylated ring as the sole catalytic active site of the system. Thus, the racemic value obtained by NO<sub>2</sub>-X<sub>L</sub>X<sub>D</sub>-OMe-**23a** catalyst is cancelled, giving 90% ee when employing NO<sub>2</sub>-X<sub>L</sub>X<sub>D</sub>-OMe-**25a** (entries 3 vs. 4). Also, an increase in the catalytic load from 3 to 6 mol% reduced the reaction time providing similar results in terms of enantiocontrol and chemical yield, as well as increasing the diastereocontrol of the process (entries 4 and 5). The same pattern was followed by NO<sub>2</sub>-X<sub>L</sub>X<sub>D</sub>-OMe-**26a** catalyst (entries 6 and 7). In this latter case, **26a** gave the aldol with configuration (2*S*,1'*R*) as expected for the sole active site at the X<sub>D</sub> pyrrolidine unit (see Scheme 11). In this case, by increasing the catalyst load the reaction time decreased, together with an increase in both the enantio- and diastereocontrol as well as with a higher yield (entry 7).

All these results, reinforced our conclusion each pyrrolidine unit in the dimers acts as an independent catalytic center in the aldol reaction. As a consequence, the final stereocontrol is determined by the matching or mismatching combination of each component of the dipeptide.

### 3.5.3. Effect of *N*-methylated and functionalized catalysts on the Michael reaction between cyclohexanone and *trans*-β-nitrostyrene

#### 3.5.3.1. Hybrid dimers

The synthesized hybrid dimers were tested in the Michael reaction between cyclohexanone **11a** and nitrostyrene **4a** in the presence of benzoic acid as additive. The obtained results are shown in Table 9. Reactions were carried out in the presence of 30 mol% of catalyst and additive to be compared to the reaction catalyzed by NO<sub>2</sub>-X<sub>L</sub>X<sub>L</sub>-OMe-**23a** (entry 1).

**Table 9.** Michael reaction between cyclohexanone **11a** and *trans*-β-nitrostyrene **4a** catalyzed by Pro<sub>L</sub>Gly-OH-**27**, **28**, **17** and NO<sub>2</sub>-X<sub>L</sub>Gly-OMe-**29**.

entry	catalyst	time (d)	conv <sup>a</sup> (%)	syn:ant <sup>b</sup>	yield <sup>c</sup> (%)	ee <sup>d</sup> (%)
1 <sup>e</sup>	NO <sub>2</sub> -X <sub>L</sub> X <sub>L</sub> -OMe- <b>23a</b>	1	>99	89:11	80	78
2 <sup>f</sup>	Pro <sub>L</sub> Gly-OH- <b>27</b>	7	22	nd	nd	nd

3	Pro <sub>L</sub> Gly-OH- <b>27</b>	7	72	87:13	45	0
4	<b>28</b>	7	0 <sup>g</sup>	nd	nd	nd
5	<b>17</b>	4	0 <sup>g</sup>	nd	nd	nd
6 <sup>e</sup>	NO <sub>2</sub> -X <sub>L</sub> Gly-OMe- <b>29</b>	7	74	78:22	38	66

<sup>a</sup>Conversions to **14aa** were measured by <sup>1</sup>H NMR of crude reaction mixtures. <sup>b</sup>*Syn:anti* ratio was measured by <sup>1</sup>H NMR of crude reaction mixtures. <sup>c</sup>Yields refer to isolated pure Michael adducts. <sup>d</sup>Enantiomeric excesses measured by HPLC correspond to the major *syn*-diastereomer (2*R*,1'*S*)-**14aa**. <sup>e</sup>Conversion to lactam product was lower than 20%. <sup>f</sup>The reaction was performed in absence of PhCO<sub>2</sub>H. <sup>g</sup>Unreacted **4a** was present in the reaction mixture.

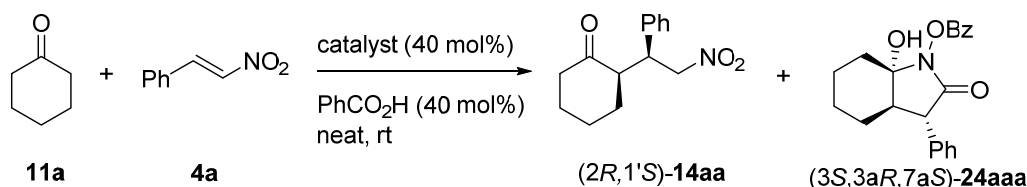
Initially, catalyst Pro<sub>L</sub>Gly-OH-**23** was employed in the absence of additive, as a carboxylic group is already present in the molecule and 22% conversion was observed after one week of reaction time (entry 2). Due to this low conversion, the corresponding amount of benzoic acid was added to the same reaction mixture (entry 3) increasing the conversion to 72% and providing a 87:13 *syn:anti* ratio without any measurable enantiomeric excess after an additional week of reaction time. When hybrid catalysts **28** and **17** were used no reaction of any kind was observed (entries 4 and 5). Finally, when the catalyst NO<sub>2</sub>-X<sub>L</sub>Gly-OMe-**29** was employed (entry 6), the Michael product was obtained in 38% yield (provided by 74% conversion after 7 days) in 78:22 *syn:anti* ratio and 66% of enantiomeric excess. In addition, formation of  $\gamma$ -lactam product **24aaa** was observed (more details in the following chapter 4). As a general remark, none of these hybrid catalysts provided better results than those achieved with NO<sub>2</sub>-X<sub>L</sub>X<sub>L</sub>-OMe-**23a** catalyst (entry 1).

### 3.5.3.2. N-methylated dimers

Organocatalysts in which one of the pyrrolidine units were blocked by *N*-methylation were also employed (Table 10, entries 3-5). It was observed that NO<sub>2</sub>-X<sub>L</sub>X<sub>L</sub>-OMe-**25a** (entry 3) provided the same enantiocontrol as its parental NO<sub>2</sub>-X<sub>L</sub>X<sub>L</sub>-OMe-**23a** catalyst (entry 1). Nevertheless, NO<sub>2</sub>-X<sub>L</sub>X<sub>D</sub>-OMe-**25a** provided lower enantioselectivity when compared with NO<sub>2</sub>-X<sub>L</sub>X<sub>L</sub>-OMe-**25a** even though the free catalytic unit was the same (entry 3 vs. 4) and both provided the opposite enantiomer as its congener NO<sub>2</sub>-X<sub>L</sub>X<sub>D</sub>-OMe-**23a** (entry 2). Finally, it was observed that the methyl blockage of the *exo* 4-nitroprolinamide in NO<sub>2</sub>-X<sub>L</sub>X<sub>L</sub>-OMe-**26a** was detrimental as the enantiocontrol lowered steadily (entry 5). Related to the  $\gamma$ -lactam:Michael product ratio, the values were retained when catalysts NO<sub>2</sub>-X<sub>L</sub>X<sub>L</sub>-OMe-**25a** and NO<sub>2</sub>-X<sub>L</sub>X<sub>L</sub>-OMe-**26a** were

employed, but it increased in the case of the NO<sub>2</sub>-X<sub>L</sub>X<sub>D</sub>-OMe-**25a** catalyst (entries 3 and 5 vs. entry 4).

**Table 10.** Direct Michael reaction between cyclohexanone **11a** and *trans*-β-nitrostyrene **4a** catalyzed by different dimers.



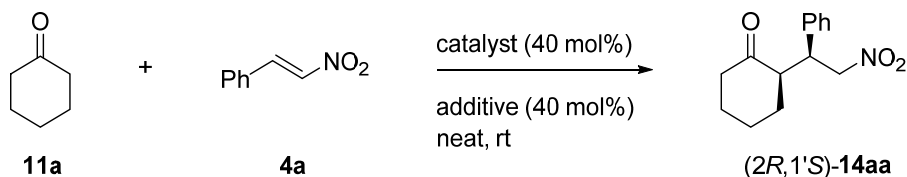
entry	catalyst	time (d)	conv. <sup>a</sup> (%)	<b>14aa</b> <i>syn:anti</i> <sup>b</sup>	<b>14aa:24aaa</b>	yield <sup>c</sup> (%)	ee <sup>d</sup> (%)
1	NO <sub>2</sub> -X <sub>L</sub> X <sub>L</sub> -OMe- <b>23a</b>	4 h	>99	91:9	77:23	75	82
2 <sup>e</sup>	NO <sub>2</sub> -X <sub>L</sub> X <sub>D</sub> -OMe- <b>23a</b>	4	>99	94:6	93:7	71	-46
3	NO <sub>2</sub> -X <sub>L</sub> X <sub>L</sub> -OMe- <b>25a</b>	1	>99	90:10	78:22	60	82
4	NO <sub>2</sub> -X <sub>L</sub> X <sub>D</sub> -OMe- <b>25a</b>	2	>99	89:11	69:31	61	75
5	NO <sub>2</sub> -X <sub>L</sub> X <sub>L</sub> -OMe- <b>26a</b>	16 h	>99	87:13	80:20	91	65

<sup>a</sup>Conversions were measured by <sup>1</sup>H NMR of crude reaction mixtures. <sup>b</sup>*Syn:anti* were measured by <sup>1</sup>H NMR of crude reaction mixtures. <sup>c</sup>Yields refer to isolated pure Michael adducts. <sup>d</sup>Enantiomeric excesses measured by HPLC correspond to the major *syn*-diastereomer (*2R,1'S*)-**14aa**. <sup>e</sup>20 mol% of catalyst and 20 mol% of PhCO<sub>2</sub>H.

With the results mentioned above it can be concluded in contrast with the aldol reaction, our γ-dipeptides exhibit the emergent property of catalyzing this conjugate addition. This reaction is not under the catalytic space of monomeric units. As a consequence, the catalytic behaviour of these dimeric catalysts cannot be reduced to that of the possible active sites. Therefore, other factors such as the dipeptide conformation or the protonation site must be considered. In addition, methylation degree of the pyrrolidine units may be of aid, as in the case of NO<sub>2</sub>-X<sub>L</sub>X<sub>L</sub>-OMe-**25a** the same enantioinduction was achieved compared to NO<sub>2</sub>-X<sub>L</sub>X<sub>L</sub>-OMe-**23a**.

Once studied the dimeric organocatalysts in the Michael reaction and in order to improve the results, screening with different acids was performed in the model reaction between cyclohexanone **11a** and nitrostyrene **4a** with three of the most efficient organocatalysts. The selected dimers were NO<sub>2</sub>-X<sub>L</sub>X<sub>L</sub>-OMe-**23a**, NO<sub>2</sub>-X<sub>L</sub>X<sub>D</sub>-OMe-**23a** and NO<sub>2</sub>-X<sub>L</sub>X<sub>L</sub>-OMe-**25a**. The results obtained by these catalysts are gathered in Table **11**.

**Table 11.** Michael reaction between cyclohexanone **11a** and *trans*- $\beta$ -nitrostyrene **4a** catalyzed by NO<sub>2</sub>-X<sub>L</sub>X<sub>L</sub>-OMe-**23a**, NO<sub>2</sub>-N<sub>L</sub>X<sub>D</sub>-OMe-**23a** and NO<sub>2</sub>-X<sub>L</sub>X<sub>L</sub>-OMe-**25a** in the presence of various acids.



entry	catalyst	additive	time (h)	<i>syn:anti</i> <sup>a</sup>	yield <sup>b</sup> (%)	ee <sup>c</sup> (%)
1 <sup>d</sup>		BA	4	91:9	75	82
2		PNBA	16	94:6	82	89
3	 NO <sub>2</sub> -X <sub>L</sub> X <sub>L</sub> -OMe- <b>23a</b>	Salicylic acid	16	95:5	79	92
4 <sup>e</sup>		Salicylic acid	24	93:7	87	91
5 <sup>f</sup>		Salicylic acid	24	95:5	92	88
6		TFA	16	89:11	75	93
7 <sup>e</sup>		TFA	36	84:16	65	64
8 <sup>g</sup>			BA	16	97:3	76
9	 NO <sub>2</sub> -N <sub>L</sub> X <sub>D</sub> -OMe- <b>23a</b>	PNBA	16	98:2	86	-85
10		Salicylic acid	16	98:2	89	-88
11		TFA	24	86:14	70	-85
12		BA	24	90:10	60	82
13		Salicylic acid	12	98:2	89	95
14 <sup>e</sup>	 NO <sub>2</sub> -X <sub>L</sub> X <sub>L</sub> -OMe- <b>25a</b>	Salicylic acid	16	98:2	91	96
15 <sup>f</sup>		Salicylic acid	24	98:2	83	95
16 <sup>h</sup>		Salicylic acid	7 d	96:4	nd	94
17		TFA	16	98:2	75	96
18 <sup>e</sup>		TFA	60	79:21	76	72

<sup>a</sup>*Syn:anti* relationships were measured by <sup>1</sup>H NMR of crude reaction mixtures. <sup>b</sup>Yields refer to isolated pure Michael adducts. <sup>c</sup>Enantiomeric excesses measured by HPLC correspond to the major *syn*-diastereomer (*2R,1'S*)-**14aa**. <sup>d</sup>This experiment provided a **14:24** ratio of 77:23. <sup>e</sup>Reaction run with 20 mol% of catalyst and 40 mol% of additive. <sup>f</sup>Reaction run with 10 mol% of catalyst and 20 mol % of additive. <sup>g</sup> This experiment provided a **14:24** ratio of 73:27. <sup>h</sup>Reaction run with 5 mol % of catalyst and 20 mol % of additive. Conversion of 88%.

When the reaction was carried out in the presence of 40 mol% of NO<sub>2</sub>-X<sub>L</sub>X<sub>L</sub>-OMe-**23a** or NO<sub>2</sub>-N<sub>L</sub>X<sub>D</sub>-OMe-**23a** and *p*-nitrobenzoic acid a slight increase in all

diastereoselectivity, enantioselectivity and yield was observed (entries 1 vs. 2 and entries 8 vs. 9). Even larger was the increase when salicylic acid was used in these cases (entries 3, 10 and 13). Due to the fact that NO<sub>2</sub>-X<sub>L</sub>X<sub>L</sub>-OMe-**23a** and NO<sub>2</sub>-X<sub>L</sub>X<sub>L</sub>-OMe-**25a** provided better results than their NO<sub>2</sub>-N<sub>L</sub>X<sub>D</sub>-OMe-**23a** analogue, a catalyst load reduction was tested. The catalytic load was reduced to 10 mol% (entries 5 and 15) without considerable loss in the diastereo- and enantioselectivity. Further decrease of the catalytic load to 5 mol% of NO<sub>2</sub>-X<sub>L</sub>X<sub>L</sub>-OMe-**25a** did not allow the reaction to completion (entry 16). Finally, when TFA was used variable results were observed both in diastereo- and enantiocontrol depending on the catalyst used (entries 6, 11 and 17). However, it was not possible to lower the catalytic load in the presence of TFA as when 20 mol% of catalyst was used, the enantiomeric excess dropped drastically (entries 7 and 18). It is noteworthy that using PNBA, salicylic acid and TFA avoided the cyclization reaction towards lactam **24aaa**.

From these results it can be concluded that NO<sub>2</sub>-X<sub>L</sub>X<sub>L</sub>-OMe-**23a** and NO<sub>2</sub>-X<sub>L</sub>X<sub>L</sub>-OMe-**25a** are the most suitable catalysts for the diastereo- and enantioselective Michael reaction between cyclohexanone **11a** and nitrostyrene **4a**. It is interesting to note that only 10 mol% of catalyst load is required for the case of NO<sub>2</sub>-X<sub>L</sub>X<sub>L</sub>-OMe-**25a**.

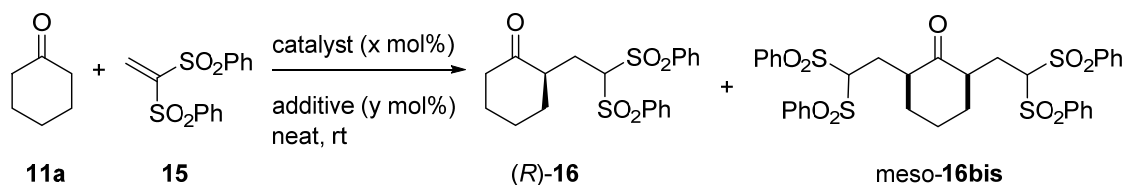
### 3.5.3.3. Exploring the scope of the reaction: 1,1-bis(phenylsulphonyl)ethene as electrophile and acetone as nucleophile

In order to explore the versatility of these catalysts in the Michael reaction, both the nucleophilic and electrophilic scopes were investigated (Table 12 and Table 13). NO<sub>2</sub>-X<sub>L</sub>X<sub>L</sub>-OMe-**23a** and NO<sub>2</sub>-X<sub>L</sub>X<sub>L</sub>-OMe-**25a** were evaluated and compared to the second generation catalyst NH<sub>2</sub>-X<sub>L</sub>-OMe-**10aa**, in the Michael reaction between cyclohexanone **11a** and the Michael acceptor 1,1-bis(phenylsulphonyl)ethylene **15** (Table 12).

When the reaction was carried out employing NO<sub>2</sub>-X<sub>L</sub>X<sub>L</sub>-OMe-**23a** catalyst and TFA in 40 mol% of catalytic load, the desired product was achieved in good yield, high **16:16bis** ratio and enantiomeric excess of 80% (entry 3). This result was improved by employing salicylic acid instead which, additionally, allowed a reduction of the catalytic load as well as higher enantiomeric control and reduction of the **16:16bis** ratio (entries 4 and 5). Nevertheless, when the NO<sub>2</sub>-X<sub>L</sub>X<sub>L</sub>-OMe-**25a**/salicylic acid system was used,

meso- product **16bis** was mainly obtained due to a double Michael addition at the positions 2 and 6 of cyclohexanone **11a** (entry 6).

**Table 12.** NH<sub>2</sub>-X<sub>L</sub>-OMe-**10aa**, NO<sub>2</sub>-X<sub>L</sub>X<sub>L</sub>-OMe-**23a** and NO<sub>2</sub>-X<sub>L</sub>X<sub>L</sub>-OMe-**25a** catalysts evaluation in the Michael reaction between cyclohexanone **11a** and 1,1-bis(phenylsulfonyl)ethylene **15**.



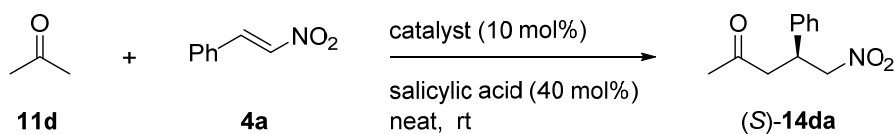
entry	catalyst/load (mol%)	additive/load (mol%)	<b>16:16bis</b> <sup>a</sup>	yield <sup>b</sup> (%)	ee <sup>c</sup> (%)
1 <sup>d</sup>	NH <sub>2</sub> -X <sub>L</sub> -OMe- <b>10aa</b> /30	PNBA/30	-	-	-
2	NH <sub>2</sub> -X <sub>L</sub> -OMe- <b>10aa</b> /30	PhCO <sub>2</sub> H/30	nd	nd	28
3	NO <sub>2</sub> -X <sub>L</sub> X <sub>L</sub> -OMe- <b>23a</b> /40	TFA/40	84:16	70	80
4	NO <sub>2</sub> -X <sub>L</sub> X <sub>L</sub> -OMe- <b>23a</b> /20	salicylic acid/40	78:22	63	93
5	NO <sub>2</sub> -X <sub>L</sub> X <sub>L</sub> -OMe- <b>23a</b> /10	salicylic acid/20	62:38	44 (52 <sup>e</sup> )	95
6	NO <sub>2</sub> -X <sub>L</sub> X <sub>L</sub> -OMe- <b>25a</b> /10	salicylic acid/20	32:68	62 <sup>e</sup>	-

<sup>a</sup>**16:16bis** relationships were measured by <sup>1</sup>H NMR of crude reaction mixtures. <sup>b</sup>Yields refer to isolated pure Michael adduct (R)-**16**. <sup>c</sup>Enantiomeric excesses measured by HPLC correspond to the isomer (R)-**16**. <sup>d</sup>Conversion <5% was measured by <sup>1</sup>H NMR of crude reaction mixture. <sup>e</sup>Yield refers to **16bis**.

The reaction between acetone **11d** and *trans*-β-nitrostyrene **4a** was carried out in the presence of catalysts NO<sub>2</sub>-X<sub>L</sub>X<sub>L</sub>-OMe-**23a** and NO<sub>2</sub>-X<sub>L</sub>X<sub>L</sub>-OMe-**25a** with salicylic acid as additive (Table 13). Both γ-dimers provided the addition product in moderate yield. Although the catalyst NO<sub>2</sub>-X<sub>L</sub>X<sub>L</sub>-OMe-**25a** showed better outcome (entry 3 vs. 2), it could not exceed the full conversion provided by the amine catalyst NH<sub>2</sub>-X<sub>L</sub>-OMe-**10aa** (entry 1).



**Table 13.** NO<sub>2</sub>-X<sub>L</sub>X<sub>L</sub>-OMe-**23a** and NO<sub>2</sub>-X<sub>L</sub>X<sub>L</sub>-OMe-**25a** catalysts evaluation in the Michael reaction between acetone **11d** and *trans*-β-nitrostyrene **4a**<sup>a</sup>.



entry	catalyst	conv <sup>b</sup> (%)	yield <sup>c</sup> (%)	ee <sup>d</sup> (%)
1 <sup>e</sup>	NH <sub>2</sub> -X <sub>D</sub> -OMe- <b>10aa</b>	>99	79	-41
2	NO <sub>2</sub> -X <sub>L</sub> X <sub>L</sub> -OMe- <b>23a</b>	>99	69	20
3	NO <sub>2</sub> -X <sub>L</sub> X <sub>L</sub> -OMe- <b>25a</b>	75	53	41

<sup>a</sup>The reaction was carried out with 16 equivalents of acetone **11d** and stirred for 16 hours. <sup>b</sup>Conversions were measured by <sup>1</sup>H NMR of crude reaction mixtures. <sup>c</sup>Yields refer to isolated pure Michael adduct. <sup>d</sup>Enantiomeric excesses measured by HPLC. <sup>e</sup>Catalysts NH<sub>2</sub>-X<sub>D</sub>-OMe-**10aa** (30 mol%) and PNBA (30 mol%) were employed to provided (*R*)-**11da**.

From these last experimental results it can be concluded that NO<sub>2</sub>-X<sub>L</sub>X<sub>L</sub>-OMe-**23a** and NO<sub>2</sub>-X<sub>L</sub>X<sub>L</sub>-OMe-**25a** are efficient dimeric catalysts to carry out Michael addition reactions. These γ-dimers have been proved to perform with similar reactivity with respect to the amine precursor NH<sub>2</sub>-X<sub>D</sub>-OMe-**10aa** in the presence of acetone **11d**. In addition, both catalysts have provided good results when compound **15** was used as Michael acceptor.

### 3.6. Follow up chemistry: Synthesis of 7a-hydroxy-2-oxo-3-aryloctahydro-1H-indol-1-yl benzoate

As it has been mentioned before, during the course of the investigation a second product was isolated. After X ray analysis experiments this unexpected adduct was identified as lactam (3*S*,3*aR*,7*aS*)-**24aaa** never described before in literature (see figure 1 in chapter 4). This product was obtained in all cases in low conversion. However, due to the difficulties to distinguish it from crude reaction mixtures (as the only remarkable signal is a doublet around 3.5 ppm), it was not until this point that the presence of this novel product was analyzed in detail. Compound (3*S*,3*aR*,7*aS*)-**24aaa** is formed via the multicomponent reaction between cyclohexanone **11a**, nitrostyrene **4a** and benzoic acid **31a** as illustrated in Figure 9. Following chapter 4 focuses on the formation of this novel compound.

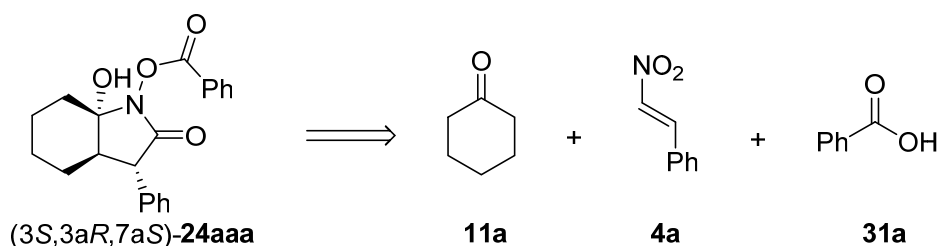


**Figure 9.** Obtained product at the addition reaction between **11a**, **4a** catalyzed by different dimers in the presence of benzoic acid **31a** as additive.

### 3.7. Conclusions

From the experimental studies reported and discussed along this chapter, the following conclusions can be drawn:

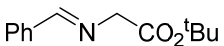
- PyBOP coupling agent is a robust reagent in order to promote the coupling between the corresponding two units of densely substituted pyrrolidines to form dimers **23a** and **25a**.
- Alternatively, HATU was the reagent of choice to synthesize  $\text{NO}_2\text{-X}_L\text{X}_L\text{-OMe-26a}$  and  $\text{NO}_2\text{-X}_L\text{X}_D\text{-OMe-26a}$  catalysts as PyBOP did not succeed.
- These are robust catalysts in order to perform enamine-based organocatalyzed reactions such as the aldol and Michael reaction. These  $\gamma$ -dimeric catalysts are more efficient than their monomeric predecessors  $\text{NO}_2\text{-X}_L\text{-OMe-5aa}$  and  $\text{NO}_2\text{-N}_L\text{-OMe-5aa}$  in the organocatalysis of the Michael reaction.
- In both reactions different effects of each monomeric unit have been identified. As occurred with the previous studies with 4-nitropyrrolidine methyl ester carboxylates, *exo*- units of the L series, lead to the opposite stereochemistry obtained under L-proline catalysis, and *endo*- units of the L series lead to the same stereochemistry obtained with L-proline. The final enantiomeric outcome is a combination of the effect of both units. While in the aldol reaction this trend is identified straightforwardly, it is more difficult to rationalize in the Michael reaction.
- Dimers bearing *exo*-4-nitroprolinate units,  $\text{NO}_2\text{-X}_L\text{X}_L\text{-OMe-23a}$  and  $\text{NO}_2\text{-X}_L\text{N}_L\text{-OMe-23a}$ , have higher kinetic constants than dimers with *endo* nitroprolinate units,  $\text{NO}_2\text{-N}_L\text{X}_L\text{-OMe-23a}$  and  $\text{NO}_2\text{-N}_L\text{N}_L\text{-OMe-23a}$ , in the aldol reaction between cyclohexanone **11a** and pentafluorobenzaldehyde **12a**.
- The use of these dimers has allowed to identify product **24aaa** never described before in literature.

### 3.8. Experimental section

**General remarks.** See section 2.8.

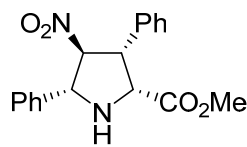
**Determination of pseudo-first order kinetic constants.** 2,3,4,5,6-Pentafluorobenzaldehyde **12a** (0.05 mmol, 10 mg, 1 eq) and the corresponding organocatalyst **23a** (0.015 mmol, 8.85 mg, 0.3 eq) were dissolved in neat, freshly distilled (MS, 3 Å) cyclohexanone **11a** (0.31 mL, 3 mmol, 60 eq) at room temperature. This mixture was transferred to a NMR tube, and then TFA (0.015 mmol, 1.15 μL, 0.3 eq) was added. The resulting mixtures were immediately introduced into the NMR probe. Samples were stabilized at 298 K. The kinetic studies were performed by monitoring the three <sup>19</sup>F NMR signals of free **12a**, together with the other signals also associated with the C<sub>6</sub>F<sub>5</sub> group, obtained with inverse gate <sup>1</sup>H-decoupling. Trifluoroacetic acid (δ = -76 ppm) was used as internal reference. NMR measurements were carried out at 376.40 MHz with a Bruker Advance 400 NMR spectrometer, equipped with a BBOF probe incorporating z-gradients. FID files were obtained with a spectral window of 240 ppm and transformed with 65536 points. All spectra were recorded by accumulating 16 acquisitions, with recycling delays of 1 s. Measurements were performed directly on the reaction mixtures in the NMR tubes every 5 min. Relative concentrations of **12a** at different times were quantified by integration and statistical treatment of the three sets of <sup>19</sup>F signals. Kinetic constants reported in Table 5 were obtained from the NMR experiments and application of equation (2). See Annexe 3 for the pseudo-first linear plots, standard deviation and error calculations.

**General procedure for the synthesis of imines.** See section 2.8.

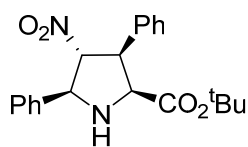
 *tert-Butyl (E)-2-(benzylideneamino)acetate (3b)*.<sup>32</sup> The title product was obtained from **8b** (503 mg, 3.0 mmol) and benzaldehyde (244 mg, 2.3 mmol). Yield: 499 mg, 99%, yellow oil. <sup>1</sup>H NMR (500 MHz, CDCl<sub>3</sub>) δ 8.27 (s, 1H, CH), 7.80 – 7.75 (m, 2H, ArH), 7.46 – 7.36 (m, 3H, ArH), 4.31 (s, 2H, CH<sub>2</sub>), 1.59 (s, 9H, C(CH<sub>3</sub>)<sub>3</sub>).

**General procedure for the synthesis of exo-Cycloadducts 5.** See section 2.8.

**Nomenclature:** For a better assignment of protons on <sup>1</sup>H NMR spectra, the IUPAC carbon order in pyrrolidines-type rings has been used. The following monomeric structures follow the same assignment pattern.

 *Methyl (2R,3R,4S,5R)-4-nitro-3,5-diphenylpyrrolidine-2-carboxylate (NO<sub>2</sub>-X<sub>D</sub>-OMe-5aa)*.<sup>33</sup> The title product was obtained out of 10 parallel reactions from imine **3a** (80 mg, 0.45 mmol). Yield: 1.25 g, 84%, white solid. 94% ee after column chromatography and >99% ee after recrystallization in EtOAc/Hex crystallization mixture. Analytical and spectroscopic data were

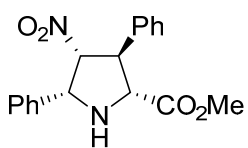
coincident with the previously reported material.  $^1\text{H}$  NMR (500 MHz,  $\text{CDCl}_3$ )  $\delta$  7.57 (d,  $J$  = 7.0 Hz, ArH), 7.45 – 7.36 (m, 3H, ArH), 7.34 – 7.27 (m, 3H, ArH), 7.26 – 7.22 (m, 2H, ArH), 5.22 (t,  $J$  = 8.1 Hz,  $\text{C}^4\text{H}$ ), 4.77 (d,  $J$  = 7.9 Hz,  $\text{C}^5\text{H}$ ), 4.51 (d,  $J$  = 8.9 Hz,  $\text{C}^2\text{H}$ ), 4.39 (t,  $J$  = 8.5 Hz,  $\text{C}^3\text{H}$ ), 3.30 (s, 3H,  $\text{CO}_2\text{Me}$ ), 2.75 (bs, 1H, NH). HPLC (Chiralcel IB, hexane/ $i$ PrOH = 80/20, flow rate 1.0 mL/min,  $\lambda$  = 254 nm),  $t_{\text{R}}$  (minor) = 9.6 min,  $t_{\text{R}}$  (major) = 18.2 min; ee = 94%.



*tert-Butyl* (2*S*,3*S*,4*R*,5*S*)-4-nitro-3,5-diphenylpyrrolidine-2-carboxylate ( $\text{NO}_2\text{-X}_L\text{-O}^t\text{Bu-5ba}$ ).<sup>32</sup> The title product was obtained from imine **3b** (100 mg, 0.45 mmol). Yield: 149 mg, 90%, white solid. >99% ee after column chromatography. Analytical and spectroscopic data were in good

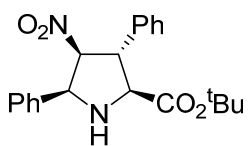
agreement with those reported in the literature.  $^1\text{H}$  NMR (500 MHz,  $\text{CDCl}_3$ )  $\delta$  7.55 (d,  $J$  = 7.2 Hz, 2H, ArH), 7.46 – 7.33 (m, 3H, ArH), 7.33 – 7.23 (m, 5H, ArH), 5.15 (t,  $J$  = 7.7 Hz, 1H,  $\text{C}^4\text{H}$ ), 4.72 (d,  $J$  = 7.5 Hz, 1H,  $\text{C}^5\text{H}$ ), 4.41 (d,  $J$  = 9.0 Hz, 1H,  $\text{C}^2\text{H}$ ), 4.31 (dd,  $J$  = 8.9, 7.4 Hz, 1H,  $\text{C}^3\text{H}$ ), 2.72 (sa, 1H, NH), 1.05 (s, 3H,  $\text{C}(\text{CH}_3)_3$ ). HPLC (Chiralcel IB, hexane/ $i$ PrOH = 90/10, flow rate 1.0 mL/min,  $\lambda$  = 254 nm)  $t_{\text{R}}$  (major) = 9.87 min; ee = >99%.

**General procedure for the synthesis of *endo*-Cycloadducts 5.** See section 2.8.



*Methyl* (2*R*,3*S*,4*R*,5*R*)-4-nitro-3,5-diphenylpyrrolidine-2-carboxylate ( $\text{NO}_2\text{-N}_D\text{-OMe-5aa}$ ).<sup>34</sup> The expected product was obtained from imine **3a** (159.5 mg, 0.9 mmol) and nitroalkene **4a** (134 mg, 0.9 mmol). Yield: 243.8 mg, 83%, yellow oil. 94% ee after column chromatography.

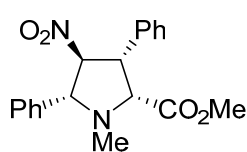
Analytical and spectroscopic data were coincident with the previously reported material.  $^1\text{H}$  NMR (500 MHz,  $\text{CDCl}_3$ )  $\delta$  7.41 – 7.28 (m, 10H, ArH), 5.25 (dd,  $J$  = 6.5, 3.5 Hz, 1H,  $\text{C}^4\text{H}$ ), 4.89 (d,  $J$  = 6.0 Hz, 1H,  $\text{C}^5\text{H}$ ), 4.24 (dd,  $J$  = 7.5, 3.5 Hz, 1H,  $\text{C}^3\text{H}$ ), 4.14 (d,  $J$  = 7.5 Hz, 1H,  $\text{C}^2\text{H}$ ), 3.79 (s, 3H,  $\text{CO}_2\text{Me}$ ). HPLC (Chiralcel IB, hexane/ $i$ PrOH = 85/15, flow rate 1.0 mL/min,  $\lambda$  = 254 nm),  $t_{\text{R}}$  (minor) = 15.05 min,  $t_{\text{R}}$  (major) = 21.56 min; ee = 94%.



*tert-Butyl* (2*S*,3*R*,4*S*,5*S*)-4-nitro-3,5-diphenylpyrrolidine-2-carboxylate ( $\text{NO}_2\text{-N}_L\text{-O}^t\text{Bu-5ba}$ ).<sup>28</sup> The title product was obtained from imine **3b** (197.3 mg, 0.9 mmol) and nitroalkene **4a** (134.2 mg, 0.9 mmol). Yield: 242.0 mg, 73%, white solid. 94% ee after column chromatography and

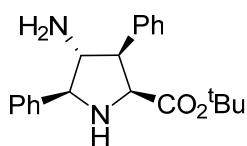
>99% ee after recrystallization in EtOAc/Hex crystallization mixture. Analytical and spectroscopic data were coincident with the previously reported material.  $^1\text{H}$  NMR (500 MHz,  $\text{CDCl}_3$ )  $\delta$  7.42 – 7.23 (m, 10H, ArH), 5.30 (dd,  $J$  = 6.5, 4.0 Hz, 1H,  $\text{C}^4\text{H}$ ), 4.92 (dd,  $J$  = 10.8, 6.7 Hz, 1H,  $\text{C}^3\text{H}$ ), 4.10 (dd,  $J$  = 7.3, 3.9 Hz, 1H,  $\text{C}^5\text{H}$ ), 4.01 (t,  $J$  = 8.2 Hz, 1H, NH), 3.34 (t,  $J$  = 9.6 Hz, 1H,  $\text{C}^2\text{H}$ ), 1.45 (s, 9H,  $\text{C}(\text{CH}_3)_3$ ). HPLC (Chiralcel IB, hexane/ $i$ PrOH = 80/20, flow rate 1.0 mL/min,  $\lambda$  = 254 nm),  $t_{\text{R}}$  (minor) = 7.29 min,  $t_{\text{R}}$  (major) = 9.22 min; ee = 94%.

**General procedure methylation.** See section 2.8.

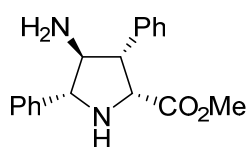


*Methyl (2R,3R,4S,5R)-1-methyl-4-nitro-3,5-diphenylpyrrolidine-2-carboxylate* ( $\text{NO}_2\text{-X}_D\text{-OMe-5c}$ ).<sup>35</sup> The expected product was obtained from  $\text{NO}_2\text{-X}_D\text{-OMe-5aa}$  (100 mg, 0.31 mmol). Yield: 83 g, 79%, white solid. Analytical and spectroscopic data were coincident with the previously reported material.  $^1\text{H}$  NMR (400 MHz,  $\text{CDCl}_3$ )  $\delta$  7.50 (d,  $J = 7.3$  Hz, 2H, ArH), 7.43 – 7.19 (m, 8H, ArH), 5.03 (m, 1H,  $\text{C}^4\text{H}$ ), 4.27 (dd,  $J = 9.3, 5.9$  Hz, 1H,  $\text{C}^3\text{H}$ ), 3.96 (d,  $J = 8.0$  Hz, 1H,  $\text{C}^5\text{H}$ ), 3.90 (d,  $J = 9.3$  Hz, 1H,  $\text{C}^2\text{H}$ ), 3.25 (s, 3H,  $\text{CO}_2\text{Me}$ ), 2.31 (s, 3H,  $\text{NCH}_3$ ).

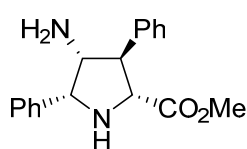
**General procedure for the Synthesis of Amino Derivatives 10.** See section 2.8.



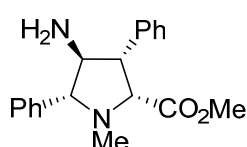
*tert-Butyl (2S,3R,4R,5S)-4-amino-3,5-diphenylpyrrolidine-2-carboxylate* ( $\text{NH}_2\text{-X}_L\text{-O}^t\text{Bu-10ba}$ ). The title product was obtained from  $\text{NO}_2\text{-X}_L\text{-O}^t\text{Bu-5ba}$  (368 mg, 1.0 mmol). Yield: 277 mg, 82%, white solid.  $m_p = 163 - 164$  °C.  $[\alpha]_D^{25} = +67.34$  ( $c$  1.15, acetone). FTIR (neat,  $\text{cm}^{-1}$ ) 1706, 1550, 1157, 697.  $^1\text{H}$  NMR (500 MHz,  $\text{CDCl}_3$ )  $\delta$  7.63 (d,  $J = 7.3$  Hz, 2H, ArH), 7.41 (t,  $J = 7.5$  Hz, 2H, ArH), 7.36 – 7.29 (m, 6H, ArH), 4.18 (d,  $J = 9.9$  Hz, 1H,  $\text{C}^5\text{H}$ ), 3.87 (d,  $J = 8.8$  Hz, 1H,  $\text{C}^2\text{H}$ ), 3.62 (t,  $J = 9.4$  Hz, 1H,  $\text{C}^3\text{H}$ ), 3.45 (t,  $J = 9.9$  Hz, 1H,  $\text{C}^4\text{H}$ ), 1.04 (s, 9H,  $\text{C}(\text{CH}_3)_3$ ).  $^{13}\text{C}$  NMR (126 MHz,  $\text{CDCl}_3$ )  $\delta$  172.6, 141.0, 138.5, 129.0, 128.9, 128.6, 128.0, 127.5, 127.2, 81.1, 70.5, 64.1, 63.7, 56.9, 27.6. HRMS (ESI) for  $\text{C}_{21}\text{H}_{27}\text{N}_2\text{O}_2$ : calculated  $[\text{M}+\text{H}]^+$ : 339.2073. Found: 339.2074.



*Methyl (2R,3S,4S,5R)-4-amino-3,5-diphenylpyrrolidine-2-carboxylate* ( $\text{NH}_2\text{-X}_D\text{-OMe-10aa}$ ).<sup>35</sup> The title product was obtained from  $\text{NO}_2\text{-X}_D\text{-OMe-5aa}$  (1.72 g, 5.29 mmol). Yield: 1.14 g, 73%, white solid. Analytical and spectroscopic data were coincident with the previously reported material.  $^1\text{H}$  NMR (400 MHz,  $\text{CDCl}_3$ )  $\delta$  7.66 (d,  $J = 7.5$  Hz, 2H, ArH), 7.42 (t,  $J = 7.5$  Hz, 2H, ArH), 7.33 (dd,  $J = 11.8, 6.9$  Hz, 3H, ArH), 7.25 (m, 3H, ArH), 4.27 (d,  $J = 9.7$  Hz, 1H,  $\text{C}^5\text{H}$ ), 3.91 (d,  $J = 8.8$  Hz, 1H,  $\text{C}^2\text{H}$ ), 3.64 (t,  $J = 9.7$  Hz, 1H,  $\text{C}^3\text{H}$ ), 3.48 (t,  $J = 10.1$  Hz, 1H,  $\text{C}^4\text{H}$ ), 3.23 (s, 3H,  $\text{CO}_2\text{Me}$ ), 1.76 (s, 2H,  $\text{NH}_2$ ).



*Methyl (2R,3R,4R,5R)-4-amino-3,5-diphenylpyrrolidine-2-carboxylate* ( $\text{NH}_2\text{-N}_D\text{-OMe-10aa}$ ).<sup>35</sup> The title product was obtained from  $\text{NO}_2\text{-N}_D\text{-OMe-5aa}$  (720 mg, 2.20 mmol). Yield: 560 mg, 86%, yellow syrup. Analytical and spectroscopic data were coincident with the previously reported material.  $^1\text{H}$  NMR (500 MHz,  $\text{CDCl}_3$ )  $\delta$  7.46 (d,  $J = 7.3$  Hz, 2H, ArH), 7.42 – 7.24 (m, 8H, ArH), 4.57 (d,  $J = 6.1$  Hz, 1H,  $\text{C}^5\text{H}$ ), 4.07 (d,  $J = 7.8$  Hz, 1H,  $\text{C}^2\text{H}$ ), 3.69 (s, 3H,  $\text{CO}_2\text{Me}$ ), 3.59 (t,  $J = 6.2$  Hz, 1H,  $\text{C}^3\text{H}$ ), 3.19 (t,  $J = 6.9$  Hz, 1H,  $\text{C}^4\text{H}$ ).

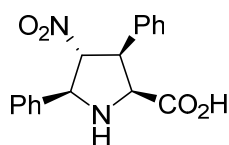


*Methyl (2R,3S,4S,5R)-1-methyl-4-amino-3,5-diphenylpyrrolidine-2-carboxylate* ( $\text{NH}_2\text{-X}_\text{D}\text{-OMe-10c}$ ).<sup>35</sup> The expected product was obtained from  $\text{NO}_2\text{-X}_\text{D}\text{-OMe-5c}$  (143 mg, 0.42 mmol). Yield: 98 mg, 75%, bright yellow solid. Analytical and spectroscopic data were coincident with the

previously reported material.  $^1\text{H NMR}$  (400 MHz,  $\text{CDCl}_3$ )  $\delta$  7.57 (d,  $J = 7.5$  Hz, 2H, ArH), 7.40 (t,  $J = 7.4$  Hz, 2H, ArH), 7.36 – 7.24 (m, 6H, ArH), 3.72 (d,  $J = 10.5$  Hz, 1H,  $\text{C}^5\text{H}$ ), 3.52 (t,  $J = 8.4$  Hz, 1H,  $\text{C}^3\text{H}$ ), 3.35 (t,  $J = 9.4$  Hz, 1H,  $\text{C}^4\text{H}$ ), 3.21 (s, 3H,  $\text{CO}_2\text{Me}$ ), 3.18 (d,  $J = 8.5$  Hz, 1H,  $\text{C}^2\text{H}$ ), 2.25 (s, 3H,  $\text{NCH}_3$ ).

### General procedure for hydrolysis

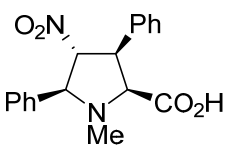
To a solution of  $\text{NO}_2\text{-X}_\text{L}\text{-OMe-5aa}$  (326 mg, 1.0 mmol) in acetone (3 mL) stirred at room temperature, a solution of sodium hydroxide (88 mg, 2.2 mmol) in water (3 mL) was added. The reaction mixture was stirred for 16 hours. Then, the solution was cooled to 0 °C and acidified with 2N HCl to  $\text{pH} \cong 2$ . A solid precipitated from the solution. This solid was filtered, washed with water and dried under vacuum to afford the desired product.



*tert-Butyl (2S,3S,4R,5S)-4-nitro-3,5-diphenylpyrrolidine-2-carboxylic acid* ( $\text{NO}_2\text{-X}_\text{L}\text{-OH-5d}$ ).<sup>28</sup> The expected product was obtained from

$\text{NO}_2\text{-X}_\text{L}\text{-OMe-5aa}$  (326 mg, 1.0 mmol). Yield: 296 mg, 95%, white solid.

Analytical and spectroscopic data were in good agreement with those reported in the literature.  $^1\text{H NMR}$  (500 MHz,  $\text{acetone-}d_6$ )  $\delta$  7.75 (d,  $J = 7.3$  Hz, 2H, ArH), 7.53 (d,  $J = 7.6$  Hz, 2H, ArH), 7.50 – 7.42 (m, 3H, ArH), 7.37 (t,  $J = 7.5$  Hz, 2H, ArH), 7.35 – 7.28 (m, 1H, ArH), 5.72 (t,  $J = 9.2$  Hz, 1H,  $\text{C}^4\text{H}$ ), 5.13 (d,  $J = 9.2$  Hz, 1H,  $\text{C}^5\text{H}$ ), 4.80 (d,  $J = 9.4$  Hz, 1H,  $\text{C}^2\text{H}$ ), 4.66 (t,  $J = 9.4$  Hz, 1H,  $\text{C}^3\text{H}$ ).

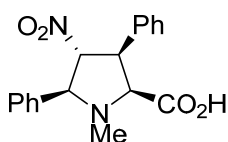


*(2S,3S,4R,5S)-1-Methyl-4-nitro-3,5-diphenylpyrrolidine-2-carboxylic acid* ( $\text{NO}_2\text{-X}_\text{L}\text{-OH-5e}$ ). The title product was obtained from  $\text{NO}_2\text{-X}_\text{L}\text{-OMe-5c}$

(100 mg, 0.29 mmol). Yield: 60 mg, 63%, orange syrup.  $[\alpha]_\text{D}^{25} = +48.58$  (c 0.33,  $\text{CHCl}_3$ ). FTIR (neat,  $\text{cm}^{-1}$ ) 1550, 700.  $^1\text{H NMR}$  (400 MHz,  $\text{CDCl}_3$ )  $\delta$

7.59 – 7.37 (m, 5H, ArH), 7.32 (d,  $J = 4.2$  Hz, 5H, ArH), 5.05 (t,  $J = 7.5$  Hz, 1H,  $\text{C}^4\text{H}$ ), 4.32 (dd,  $J = 9.8, 6.6$  Hz, 1H,  $\text{C}^3\text{H}$ ), 4.09 (d,  $J = 8.2$  Hz, 1H,  $\text{C}^5\text{H}$ ), 3.96 (d,  $J = 9.8$  Hz, 1H,  $\text{C}^2\text{H}$ ), 2.38 (s, 3H, NMe).  $^{13}\text{C NMR}$  (101 MHz,  $\text{CDCl}_3$ )  $\delta$  172.1, 137.2, 136.8, 129.3, 129.1, 128.9, 128.6, 128.4, 127.7, 96.9, 75.0, 71.8, 51.1, 39.6. HRMS (ESI) for  $\text{C}_{18}\text{H}_{19}\text{N}_2\text{O}_4$ : calculated  $[\text{M} + \text{H}]^+$ : 327.1343. Found: 327.1338.

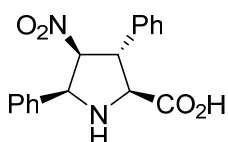
**Simultaneous methylation-hydrolysis of 5ba.** See section 2.8 “General procedure for the methylation of  $\text{NO}_2\text{-X}_\text{L}\text{-OMe-5aa}$ ”.



(2*S*,3*S*,4*R*,5*S*)-1-Methyl-4-nitro-3,5-diphenylpyrrolidine-2-carboxylic acid (NO<sub>2</sub>-X<sub>L</sub>-OH-**5e**). The expected product was obtained from NO<sub>2</sub>-X<sub>L</sub>-O<sup>t</sup>Bu-**5ba** (527 mg, 1.11 mmol). Yield: 327 mg, 90%, orange syrup. Analytical and spectroscopic data were in good agreement with those reported in the literature.

#### General procedure for hydrolysis. Acidic conditions.

To a solution of NO<sub>2</sub>-N<sub>L</sub>-O<sup>t</sup>Bu-**5ba** (326 mg, 1.0 mmol) in dichloromethane (15 mL) stirred at room temperature, trifluoroacetic acid (8 mL) was added. The reaction mixture was stirred for 16 hours. Then, the solvent was evaporated *in vacuo*. The obtained crude product was purified by precipitation to afford the desired compound.

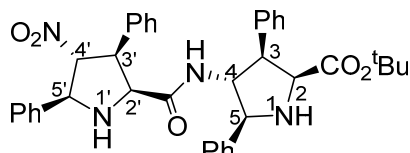


(2*S*,3*R*,4*S*,5*S*)-4-Nitro-3,5-diphenylpyrrolidine-2-carboxylic acid (NO<sub>2</sub>-N<sub>L</sub>-OH-**5d**).<sup>28</sup> The title product was obtained from NO<sub>2</sub>-N<sub>L</sub>-O<sup>t</sup>Bu-**5ba** (368 mg, 1.0 mmol). Yield: 240 mg, 77%, white solid. Analytical and spectroscopic properties were coincident with the previously reported

data. <sup>1</sup>H NMR (500 MHz, acetone-*d*<sub>6</sub>)  $\delta$  7.51 (d, *J* = 7.7 Hz, 4H, ArH), 7.41 (t, *J* = 7.6 Hz, 2H, ArH), 7.38 – 7.29 (m, 4H, ArH), 5.57 (dd, *J* = 6.9, 4.4 Hz, 1H, C<sup>4</sup>H), 5.21 (d, *J* = 6.9 Hz, 1H, C<sup>5</sup>H), 4.28 (dd, *J* = 7.7, 4.3 Hz, 1H, C<sup>3</sup>H), 4.20 (d, *J* = 7.8 Hz, 1H, C<sup>2</sup>H).

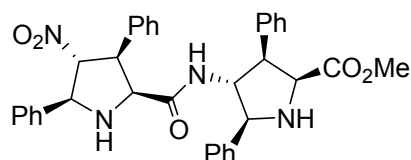
#### General procedure for coupling reactions

To a stirred solution of the corresponding amine (0.8 mmol) in CH<sub>2</sub>Cl<sub>2</sub> (10 mL) was added acid (1.0 mmol), PyBOP (1.0 mmol) and by diisopropyl ethyl amine (1.4 mmol). The resulting mixture was then stirred until completion of the reaction. Then, the reaction mixture was diluted with CH<sub>2</sub>Cl<sub>2</sub>, washed with a 1M HCl solution, saturated aqueous NaHCO<sub>3</sub>, brine and then dried over Na<sub>2</sub>SO<sub>4</sub>. Evaporation of the solvent followed by column chromatography eluting with ethyl acetate/hexanes provided the products described below.



*tert*-Butyl (2*S*,3*R*,4*R*,5*S*)-3,5-dimethyl-4-((2'*S*,3'*S*,4'*R*,5'*S*)-4-nitro-3,5-diphenylpyrrolidine-2-carboxamido)pyrrolidine-2-carboxylate (NO<sub>2</sub>-X<sub>L</sub>X<sub>L</sub>-O<sup>t</sup>Bu-**23b**). The title product was obtained from NH<sub>2</sub>-X<sub>L</sub>-OMe-**10ba**. Yield: 374 mg, 74%, yellow solid. *m*<sub>p</sub> = 135 - 137 °C. [ $\alpha$ ]<sub>D</sub><sup>25</sup> = +106.40 (*c* 0.65, acetone). FTIR (neat, cm<sup>-1</sup>) 1721, 1675, 1553, 1367, 1153, 744, 697. <sup>1</sup>H NMR (500 MHz, CDCl<sub>3</sub>)  $\delta$  7.51 – 7.33 (m, 12H, ArH), 7.28 – 7.18 (m, 3H, ArH), 7.12 (t, *J* = 7.4 Hz, 1H, ArH), 7.01 (m, 2H, ArH and amide NH), 6.80 (d, *J* = 7.5 Hz, 2H, ArH), 4.95 (t, *J* = 8.6 Hz, 1H, C<sup>4</sup>H), 4.77 (d, *J* = 8.4 Hz, 1H, C<sup>5</sup>H), 4.50 (q,

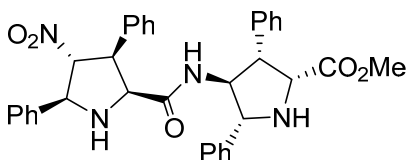
$J = 8.7$  Hz, 1H, C<sup>4</sup>H), 4.26 (t,  $J = 9.2$  Hz, 1H, C<sup>3</sup>H), 4.21 (d,  $J = 9.3$  Hz, 1H, C<sup>2</sup>H), 4.15 – 4.11 (m, 1H, C<sup>2</sup>H), 4.11 – 4.03 (m, 1H, C<sup>5</sup>H), 3.43 (t,  $J = 8.8$  Hz, 1H, C<sup>3</sup>H), 2.47 (broad singlet, 2H, NH), 1.00 (s, 9H, C(CH<sub>3</sub>)<sub>3</sub>). <sup>13</sup>C NMR (126 MHz, CDCl<sub>3</sub>)  $\delta$  171.7, 169.5, 139.9, 138.2, 134.9, 129.6, 129.5, 129.4, 129.3, 129.0, 128.9, 128.8, 128.7, 128.5, 128.4, 127.9, 127.5, 127.0, 94.7, 81.8, 67.2, 66.4, 64.5, 64.0, 60.9, 54.2, 53.7, 27.8. HRMS (ESI) for C<sub>38</sub>H<sub>41</sub>N<sub>4</sub>O<sub>5</sub>: calculated [M + H]<sup>+</sup>: 633.3077. Found: 633.3082.



*Methyl (2S,3R,4R,5S)-4-((2'S,3'S,4'R,5'S)-4-nitro-3,5-diphenylpyrrolidine-2-carboxamido)-3,5-diphenylpyrrolidine-2-carboxylate* (NO<sub>2</sub>-X<sub>L</sub>-OMe-**23a**).

The title product was obtained from NH<sub>2</sub>-X<sub>L</sub>-OMe-**10aa**.

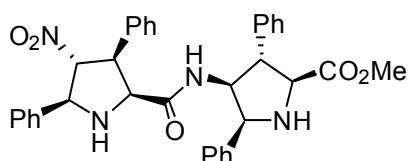
Yield: 307 mg, 65%, white solid.  $m_p = 136 - 137$  °C.  $[\alpha]_D^{25} = +129.88$  (c 0.43, acetone). FTIR (neat, cm<sup>-1</sup>) 1732, 1671, 1546, 790, 696. <sup>1</sup>H NMR (500 MHz, CDCl<sub>3</sub>)  $\delta$  7.56 – 7.33 (m, 10H, ArH), 7.30 – 7.17 (m, 5H, ArH), 7.11 (t,  $J = 7.4$  Hz, 1H, ArH), 7.00 (t,  $J = 7.7$  Hz, 2H, ArH), 6.93 (d,  $J = 8.8$  Hz, 1H, CONH), 6.77 (d,  $J = 7.3$  Hz, 2H, ArH), 4.93 (t,  $J = 8.6$  Hz, 1H, C<sup>4</sup>H), 4.79 (d,  $J = 8.4$  Hz, 1H, C<sup>5</sup>H), 4.59 (q,  $J = 9.0$  Hz, 1H, C<sup>4</sup>H), 4.33 – 4.17 (m, 3H, C<sup>2</sup>H, C<sup>3</sup>H, C<sup>2</sup>H), 4.15 – 4.07 (m, 1H, C<sup>5</sup>H), 3.52 (t,  $J = 9.1$  Hz, 1H, C<sup>3</sup>H), 3.20 (s, 3H, CO<sub>2</sub>Me). <sup>13</sup>C NMR (101 MHz, CDCl<sub>3</sub>)  $\delta$  173.1, 169.3, 137.2, 134.5, 129.4, 129.3, 129.2, 128.7, 128.6, 128.5, 128.4, 128.2 (2 signals), 127.7, 127.5, 126.7, 94.4, 67.08, 66.1, 64.2, 63.7, 60.2, 54.3, 53.5, 51.7. HRMS (ESI) for C<sub>35</sub>H<sub>35</sub>N<sub>4</sub>O<sub>5</sub>: calculated [M + H]<sup>+</sup>: 591.2607. Found: 591.2617.



*Methyl (2R,3S,4S,5R)-4-((2'S,3'S,4'R,5'S)-4-nitro-3,5-diphenylpyrrolidine-2-carboxamido)-3,5-diphenylpyrrolidine-2-carboxylate* (NO<sub>2</sub>-X<sub>L</sub>-OMe-**23a**).

The title product was obtained from NH<sub>2</sub>-X<sub>D</sub>-OMe-**10aa**.

Yield: 217 mg, 46%, white solid.  $m_p = 114 - 115$  °C.  $[\alpha]_D^{25} = +17.07$  (c 0.43, acetone). FTIR (neat, cm<sup>-1</sup>) 1733, 1667, 1603, 697. <sup>1</sup>H NMR (500 MHz, CDCl<sub>3</sub>)  $\delta$  7.47 (m, 6H, ArH), 7.38 – 7.21 (m, 8H, ArH), 7.09 (dt,  $J = 14.9, 7.2$  Hz, 4H, ArH), 6.97 (d,  $J = 7.3$  Hz, 2H, ArH), 6.73 (d,  $J = 8.4$  Hz, 1H, CONH), 5.02 – 4.94 (m, 1H, C<sup>4</sup>H), 4.78 (d,  $J = 8.0$  Hz, 1H, C<sup>5</sup>H), 4.51 (dd,  $J = 16.7, 8.1$  Hz, 1H, C<sup>4</sup>H), 4.23 (dd,  $J = 13.9, 7.2$  Hz, 3H, C<sup>3</sup>H, C<sup>2</sup>H and C<sup>3</sup>H), 4.01 (d,  $J = 8.6$  Hz, 1H, C<sup>5</sup>H), 3.31 – 3.18 (m, 4H, C<sup>2</sup>H and CO<sub>2</sub>Me), 2.56 (bs, 2H, NH). <sup>13</sup>C NMR (126 MHz, CDCl<sub>3</sub>)  $\delta$  172.5, 169.2, 139.4, 138.4, 138.1, 135.5, 129.2, 129.0, 128.8, 128.6, 128.3, 128.3, 128.2, 128.2, 128.1, 127.3, 127.3, 126.7, 95.2, 67.3, 66.2, 64.4, 64.2, 61.2, 54.1, 53.0, 51.6. HRMS (ESI) for C<sub>35</sub>H<sub>35</sub>N<sub>4</sub>O<sub>5</sub>: calculated [M + H]<sup>+</sup>: 591.2607. Found: 591.2609.



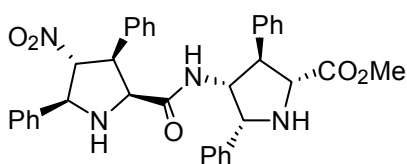
*Methyl (2S,3S,4S,5S)-4-((2'S,3'S,4'R,5'S)-4-nitro-3,5-diphenylpyrrolidine-2-carboxamido)-3,5-diphenylpyrrolidine-2-carboxylate* (NO<sub>2</sub>-X<sub>L</sub>-OMe-**23a**).

The title product was obtained from NH<sub>2</sub>-N<sub>L</sub>-OMe-**10aa**.

Yield: 335 mg, 71%, white solid.  $m_p = 93 - 95$  °C.  $[\alpha]_D^{25} = +74.19$  (c 0.50, acetone). FTIR (neat, cm<sup>-1</sup>) 1733, 1670, 1549, 1494, 697. <sup>1</sup>H NMR (500 MHz, CDCl<sub>3</sub>)  $\delta$  7.47 (d,  $J = 4.3$  Hz, 3H, ArH),



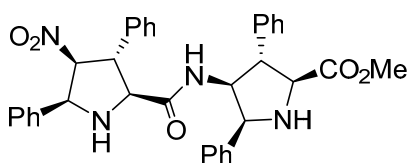
7.41 (dd,  $J = 13.4, 5.9$  Hz, 3H, ArH), 7.35 (t,  $J = 7.3$  Hz, 2H, ArH), 7.31 – 7.23 (m, 5H, ArH), 7.18 (dt,  $J = 16.2, 8.1$  Hz, 3H, ArH and CONH), 7.12 (dd,  $J = 7.3, 5.6$  Hz, 3H, ArH), 6.95 (d,  $J = 7.2$  Hz, 2H, ArH), 4.87 (t,  $J = 7.6$  Hz, 1H, C<sup>4</sup>H), 4.73 (t,  $J = 6.7$  Hz, 1H, C<sup>5</sup>H), 4.71 (t,  $J = 8.4$  Hz, 1H, C<sup>5</sup>H), 4.45 – 4.37 (m, 1H, C<sup>4</sup>H), 4.21 – 4.13 (m, 2H, C<sup>2</sup>H and C<sup>3</sup>H), 4.07 (d,  $J = 9.7$  Hz, 1H, C<sup>2</sup>H), 3.84 (s, 3H, CO<sub>2</sub>Me), 3.04 (t,  $J = 5.7$  Hz, 1H, C<sup>3</sup>H). <sup>13</sup>C NMR (101 MHz, CDCl<sub>3</sub>) δ 168.7, 139.7, 139.7, 138.1, 135.8, 129.2, 129.1, 129.0, 128.6, 128.5, 128.4, 128.1, 127.7, 127.6, 127.5 (2 signals), 126.7, 95.4, 65.8, 64.2, 64.1, 63.5, 59.2, 54.4, 52.7, 52.5. HRMS (ESI) for C<sub>35</sub>H<sub>35</sub>N<sub>4</sub>O<sub>5</sub>: calculated [M + H]<sup>+</sup>: 591.2607. Found: 591.2615.



*Methyl (2R,3R,4R,5R)-4-((2'S,3'S,4'R,5'S)-4-nitro-3,5-diphenylpyrrolidine-2-carboxamido)-3,5-diphenylpyrrolidine-2-carboxylate (NO<sub>2</sub>-X<sub>L</sub>N<sub>D</sub>-OMe-23a).*

The title product was obtained from NH<sub>2</sub>-N<sub>D</sub>-OMe-10aa.

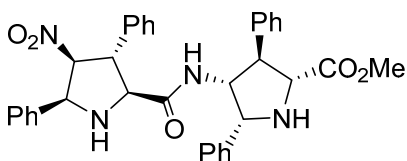
Yield: 312 mg, 66%, white solid.  $m_p = 101 - 102$  °C.  $[\alpha]_D^{25} = +74.29$  ( $c$  0.44, acetone). FTIR (neat, cm<sup>-1</sup>) 1734, 1667, 1548, 1494, 697. <sup>1</sup>H NMR (500 MHz, CDCl<sub>3</sub>) δ 7.53 – 7.22 (m, 16H, ArH and CONH), 7.19 – 7.11 (m, 1H, ArH), 7.07 (t,  $J = 7.0$  Hz, 2H, ArH), 6.67 (d,  $J = 7.2$  Hz, 2H, ArH), 4.75 – 4.71 (m, 2H, C<sup>4</sup>H and C<sup>2</sup> or C<sup>3</sup> or C<sup>5</sup>H), 4.65 (t,  $J = 7.7$  Hz, 1H, C<sup>5</sup>H), 4.22 (m, 3H, C<sup>2</sup>H and C<sup>2</sup> or C<sup>3</sup> or C<sup>5</sup>H), 4.08 (m, 1H, C<sup>4</sup>H), 3.71 (s, 3H CO<sub>2</sub>Me), 3.41 (m, 1H, C<sup>3</sup>H) (C<sup>2</sup>, C<sup>3</sup> and C<sup>5</sup>H cannot be assigned due to signal overlap in <sup>1</sup>H NMR and COSY experiments). <sup>13</sup>C NMR (126 MHz, CDCl<sub>3</sub>) δ 175.3, 169.4, 140.1, 138.6, 137.7, 135.0, 129.0, 129.0, 128.8, 128.7, 128.5, 128.2, 128.1, 127.8, 127.5, 127.4, 127.2, 126.7, 94.6, 66.0, 63.7, 63.0, 62.8, 59.7, 55.7, 52.9, 52.3. HRMS (ESI) for C<sub>35</sub>H<sub>35</sub>N<sub>4</sub>O<sub>5</sub>: calculated [M + H]<sup>+</sup>: 591.2607. Found: 591.2601.



*Methyl (2S,3S,4S,5S)-4-((2'S,3'R,4'S,5'S)-4-nitro-3,5-diphenylpyrrolidine-2-carboxamido)-3,5-diphenylpyrrolidine-2-carboxylate (NO<sub>2</sub>-N<sub>L</sub>N<sub>L</sub>-OMe-23a).*

The title product was obtained from NH<sub>2</sub>-N<sub>L</sub>-OMe-10aa.

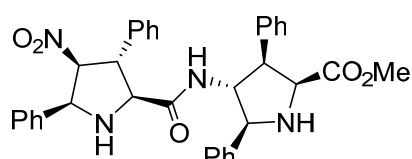
Yield: 354 mg, 75%, light brown solid.  $m_p = 103 - 104$  °C.  $[\alpha]_D^{25} = -9.36$  ( $c$  0.90, acetone). FTIR (neat, cm<sup>-1</sup>) 3358, 1733, 1661, 1551, 739, 698. <sup>1</sup>H NMR (500 MHz, CDCl<sub>3</sub>) δ 7.54 (s, 2H, ArH), 7.46 – 7.26 (m, 14H, ArH), 7.19 – 7.11 (m, 2H, ArH), 6.98 (d,  $J = 9.7$  Hz, 1H, ArH), 6.89 (d,  $J = 6.4$  Hz, 2H, ArH and CONH), 5.03 (dt,  $J = 9.8, 5.0$  Hz, 2H, C<sup>4</sup>H and C<sup>4</sup>H), 4.86 (d,  $J = 7.4$  Hz, 1H, C<sup>5</sup>H or C<sup>5</sup>H), 4.79 (d,  $J = 6.7$  Hz, 1H, C<sup>5</sup>H or C<sup>5</sup>H), 4.28 (d,  $J = 8.2$  Hz, 1H, C<sup>2</sup>H), 3.75 (s, 3H, CO<sub>2</sub>Me), 3.64 (t,  $J = 8.2$  Hz, 1H, C<sup>3</sup>H), 3.62 – 3.58 (m, 2H, C<sup>3</sup>H and C<sup>2</sup>H). <sup>13</sup>C NMR (126 MHz, CDCl<sub>3</sub>) δ 174.2, 170.9, 140.5, 138.7, 138.4, 135.0, 129.0, 128.8, 128.7, 128.4, 128.4, 128.1, 127.7, 127.6, 127.5, 127.4, 127.3, 126.8, 95.8, 67.0, 66.0, 64.2, 62.6, 58.4, 54.0, 53.9, 52.3. HRMS (ESI) for C<sub>35</sub>H<sub>35</sub>N<sub>4</sub>O<sub>5</sub>: calculated [M + H]<sup>+</sup>: 591.2607. Found: 591.2618.



*Methyl (2R,3R,4R,5R)-4-((2'S,3'R,4'S,5'S)-4-nitro-3,5-diphenylpyrrolidine-2-carboxamido)-3,5-diphenylpyrrolidine-2-carboxylate (NO<sub>2</sub>-N<sub>L</sub>N<sub>D</sub>-OMe-23a).*

The title product was obtained from NH<sub>2</sub>-N<sub>D</sub>-OMe-10aa.

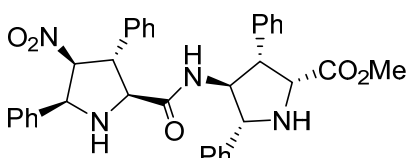
Yield: 255 mg, 54%, light orange solid.  $m_p = 118 - 119$  °C.  $[\alpha]_D^{25} = +45.24$  (c 0.50, acetone). FTIR (neat,  $\text{cm}^{-1}$ ) 1735, 1673, 1550, 1496, 697.  $^1\text{H}$  NMR (500 MHz,  $\text{CDCl}_3$ )  $\delta$  7.55 (d,  $J = 7.3$  Hz, 2H, ArH), 7.42 (t,  $J = 7.5$  Hz, 2H, ArH), 7.38 – 7.23 (m, 12H, ArH), 7.23 – 7.20 (m, 2H, ArH), 7.08 (d,  $J = 7.2$  Hz, 2H, ArH), 6.89 (d,  $J = 7.8$  Hz, 1H, CONH), 5.12 (dd,  $J = 7.3, 4.6$  Hz, 1H,  $\text{C}^4\text{H}$ ), 4.88 (d,  $J = 6.1$  Hz, 1H,  $\text{C}^5\text{H}$ ), 4.86 – 4.80 (m, 1H,  $\text{C}^4\text{H}$ ), 4.78 (d,  $J = 6.8$  Hz, 1H,  $\text{C}^5\text{H}$ ), 4.20 (d,  $J = 6.7$  Hz, 1H,  $\text{C}^2\text{H}$ ), 3.78 – 3.74 (m, 1H,  $\text{C}^2\text{H}$ ), 3.73 (s, 3H,  $\text{CO}_2\text{Me}$ ), 3.65 (dd,  $J = 7.9, 4.5$  Hz, 1H,  $\text{C}^3\text{H}$ ), 3.57 (t,  $J = 6.6$  Hz, 1H,  $\text{C}^3\text{H}$ ).  $^{13}\text{C}$  NMR (101 MHz,  $\text{CDCl}_3$ )  $\delta$  174.5, 170.4, 139.3, 139.1, 138.5, 135.2, 129.2, 128.9, 128.8, 128.6, 127.9, 127.8, 127.7, 127.5, 127.1, 96.4, 67.1, 66.1, 64.4, 63.2, 59.0, 54.3, 53.6, 52.4. HRMS (ESI) for  $\text{C}_{35}\text{H}_{35}\text{N}_4\text{O}_5$ : calculated  $[\text{M} + \text{H}]^+$ : 591.2607. Found: 591.2622.



*Methyl (2S,3R,4R,5S)-4-((2'S,3'R,4'S,5'S)-4-nitro-3,5-diphenylpyrrolidine-2-carboxamide)-3,5-diphenylpyrrolidine-2-carboxylate* ( $\text{NO}_2\text{-N}_L\text{X}_L\text{-OMe-23a}$ ).

The title product was obtained from  $\text{NH}_2\text{-X}_L\text{-OMe-10aa}$ .

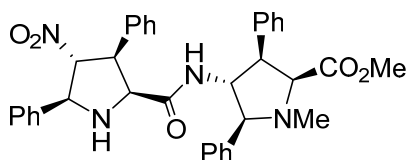
Yield: 359 mg, 76%, yellow solid.  $m_p = 180 - 181$  °C.  $[\alpha]_D^{25} = +29.55$  (c 0.50, acetone). FTIR (neat,  $\text{cm}^{-1}$ ) 1734, 1655, 1554, 1528, 837, 697.  $^1\text{H}$  NMR (500 MHz,  $\text{CDCl}_3$ )  $\delta$  7.74 (d,  $J = 7.2$  Hz, 2H, ArH), 7.42 (t,  $J = 7.3$  Hz, 2H, ArH), 7.33 (m, 10H, ArH), 7.25 – 7.20 (m, 4H, ArH), 6.89 (d,  $J = 9.8$  Hz, 1H, CONH), 6.78 (dd,  $J = 6.4, 2.7$  Hz, 2H, ArH), 5.11 (m, 2H,  $\text{C}^4\text{H}$  and  $\text{C}^4\text{H}$ ), 4.80 (d,  $J = 6.2$  Hz, 1H,  $\text{C}^5\text{H}$ ), 4.41 (d,  $J = 9.5$  Hz, 1H,  $\text{C}^5\text{H}$ ), 4.33 (d,  $J = 9.4$  Hz, 1H,  $\text{C}^2\text{H}$ ), 3.94 (t,  $J = 10.1$  Hz, 1H,  $\text{C}^3\text{H}$ ), 3.66 (d,  $J = 7.5$  Hz, 1H,  $\text{C}^2\text{H}$ ), 3.59 (m, 1H,  $\text{C}^3\text{H}$ ), 3.20 (s, 3H,  $\text{CO}_2\text{Me}$ ).  $^{13}\text{C}$  NMR (126 MHz,  $\text{CDCl}_3$ )  $\delta$  173.6, 171.0, 139.7, 138.3, 136.6, 135.2, 129.2, 129.2, 129.0, 128.8, 128.6, 128.6, 128.5, 128.1, 128.0, 127.7, 127.6, 127.0, 96.2, 67.8, 67.3, 66.7, 63.9, 58.6, 54.8, 53.8, 51.8. HRMS (ESI) for  $\text{C}_{35}\text{H}_{35}\text{N}_4\text{O}_5$ : calculated  $[\text{M} + \text{H}]^+$ : 591.2607. Found: 591.2614.



*Methyl (2R,3S,4S,5R)-4-((2'S,3'R,4'S,5'S)-4-nitro-3,5-diphenylpyrrolidine-2-carboxamide)-3,5-diphenylpyrrolidine-2-carboxylate* ( $\text{NO}_2\text{-N}_L\text{X}_D\text{-OMe-23a}$ ).

The title product was obtained from  $\text{NH}_2\text{-X}_D\text{-OMe-10aa}$ .

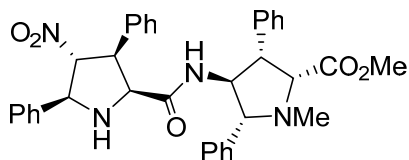
Yield: 340 mg, 72%, white solid.  $m_p = 201 - 202$  °C.  $[\alpha]_D^{25} = -16.08$  (c 0.24, acetone). FTIR (neat,  $\text{cm}^{-1}$ ) 1737, 1654, 1551, 1525, 698.  $^1\text{H}$  NMR (500 MHz,  $\text{CDCl}_3$ )  $\delta$  7.66 (d,  $J = 7.4$  Hz, 2H, ArH), 7.46 – 7.27 (m, 16H, ArH), 6.98 – 6.84 (m, 3H, ArH and CONH), 5.11 (m, 1H,  $\text{C}^4\text{H}$ ), 4.94 (dd,  $J = 19.5, 9.7$  Hz, 1H,  $\text{C}^4\text{H}$ ), 4.87 (d,  $J = 6.9$  Hz, 1H,  $\text{C}^5\text{H}$ ), 4.39 (d,  $J = 9.8$  Hz, 1H,  $\text{C}^2\text{H}$ ), 4.33 (d,  $J = 9.8$  Hz, 1H,  $\text{C}^5\text{H}$ ), 4.00 (t,  $J = 10.0$  Hz, 1H,  $\text{C}^3\text{H}$ ), 3.76 (d,  $J = 6.7$  Hz, 1H,  $\text{C}^2\text{H}$ ), 3.56 (m, 1H,  $\text{C}^3\text{H}$ ), 3.27 (s, 3H,  $\text{CO}_2\text{Me}$ ), 2.66 (broad s, 2H, NH).  $^{13}\text{C}$  NMR (126 MHz,  $\text{CDCl}_3$ )  $\delta$  173.7, 171.2, 139.6, 138.5, 137.1, 135.1, 129.3, 129.21, 129.0, 128.9, 128.7, 128.6, 128.4, 128.1, 127.8, 127.7, 126.9, 96.2, 67.7, 66.7, 66.4, 63.8, 59.5, 54.7, 54.5, 51.8. HRMS (ESI) for  $\text{C}_{35}\text{H}_{35}\text{N}_4\text{O}_5$ : calculated  $[\text{M} + \text{H}]^+$ : 591.2607. Found: 591.2620.



*Methyl (2S,3R,4R,5S)-1-methyl-4-((2'S,3'S,4'R,5'S)-4-nitro-3,5-diphenylpyrrolidine-2-carboxamido)-3,5-diphenylpyrrolidine-2-carboxylate (NO<sub>2</sub>-X<sub>L</sub>-OMe-25a).*

The title product was obtained from NH<sub>2</sub>-X<sub>L</sub>-OMe-10c.

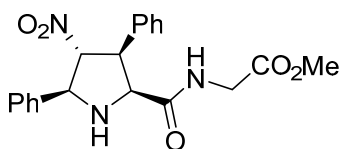
Yield: 358 mg, 74%, white solid.  $m_p = 201 - 204$  °C.  $[\alpha]_D^{25} = +125.30$  (c 0.50, acetone). FTIR (neat,  $\text{cm}^{-1}$ ) 3311, 1745, 1672, 1551, 1194, 1171, 698. <sup>1</sup>H NMR (400 MHz, CDCl<sub>3</sub>)  $\delta$  7.42 (m, 10H, ArH), 7.33 – 7.16 (m, 6H, ArH), 7.10 (t,  $J = 7.4$  Hz, 2H, ArH), 6.90 (d,  $J = 7.4$  Hz, 2H, ArH), 6.83 (d,  $J = 7.8$  Hz, 1H, CONH), 4.98 (d,  $J = 4.9$  Hz, 1H, C<sup>4</sup>H), 4.81 (d,  $J = 7.8$  Hz, 1H, C<sup>5</sup>H), 4.29 (s, 2H, C<sup>2</sup>H and C<sup>3</sup>H), 4.11 (q,  $J = 7.8$  Hz, 1H, C<sup>4</sup>H), 3.68 (d,  $J = 9.5$  Hz, 1H, C<sup>2</sup>H), 3.43 (d,  $J = 8.6$  Hz, 1H, C<sup>5</sup>H), 3.31 (t,  $J = 8.2$  Hz, 1H, C<sup>3</sup>H), 3.19 (s, 3H, CO<sub>2</sub>Me), 2.58 (m, 1H, NH), 2.22 (s, 3H, NMe). <sup>13</sup>C NMR (101 MHz, CDCl<sub>3</sub>)  $\delta$  171.25, 169.5, 139.7, 139.6, 137.9, 135.0, 129.3, 129.3, 129.0, 128.9, 128.9, 128.5, 128.3 (x2), 128.2, 128.0, 127.2, 126.8, 94.8, 74.8, 72.1, 66.3, 64.3, 64.2, 53.4, 51.8, 51.3, 39.9. HRMS (ESI) for C<sub>36</sub>H<sub>37</sub>N<sub>4</sub>O<sub>5</sub>: calculated  $[M + H]^+$ : 605.2764. Found: 605.2778.



*Methyl (2R,3S,4S,5R)-1-methyl-4-((2'S,3'S,4'R,5'S)-4-nitro-3,5-diphenylpyrrolidine-2-carboxamido)-3,5-diphenylpyrrolidine-2-carboxylate (NO<sub>2</sub>-X<sub>D</sub>-OMe-25a).*

The title product was obtained from NH<sub>2</sub>-X<sub>D</sub>-OMe-10c.

Yield: 353 mg, 73%, white solid.  $m_p = 99 - 100$  °C.  $[\alpha]_D^{25} = +18.99$  (c 0.51, acetone). FTIR (neat,  $\text{cm}^{-1}$ ) 1748, 1669, 1547, 698. <sup>1</sup>H NMR (400 MHz, CDCl<sub>3</sub>)  $\delta$  7.59 – 7.11 (m, 20H, ArH), 6.70 (d,  $J = 7.2$  Hz, 1H, CONH), 5.17 – 4.99 (m, 1H, C<sup>4</sup>H), 4.82 (d,  $J = 7.4$  Hz, 1H, C<sup>5</sup>H), 4.28 (m, 2H, C<sup>2</sup>H and C<sup>3</sup>H), 4.04 (dd,  $J = 13.7, 7.2$  Hz, 1H, C<sup>4</sup>H), 3.54 (d,  $J = 9.2$  Hz, 1H, C<sup>2</sup>H), 3.23 (s, 3H, CO<sub>2</sub>Me), 3.16 (d,  $J = 8.1$  Hz, 1H, C<sup>5</sup>H), 2.90 (dd,  $J = 8.7, 6.1$  Hz, 1H, C<sup>3</sup>H), 2.62 (bs, 1H, NH), 2.23 (s, 3H, NMe). <sup>13</sup>C NMR (101 MHz, CDCl<sub>3</sub>)  $\delta$  170.8, 169.0, 140.3, 139.2, 138.0, 136.2, 129.4, 129.2, 128.9, 128.9, 128.7, 128.7, 128.4, 128.4, 128.1, 127.9, 127.1, 126.8, 95.7, 76.4, 72.3, 66.5, 64.9, 64.4, 53.0, 52.2, 51.3, 39.8. HRMS (ESI) for C<sub>36</sub>H<sub>37</sub>N<sub>4</sub>O<sub>5</sub>: calculated  $[M + H]^+$ : 605.2764. Found: 605.2773.

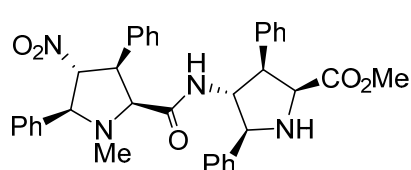


*Methyl 2-((2S,3S,4R,5S)-4-nitro-3,5-diphenylpyrrolidine-2-carboxamido)acetate (NO<sub>2</sub>-X<sub>L</sub>-Gly-OMe-29).* The title product was obtained from glycine methyl ester hydrochloride **8a** (28 mg, 0.22 mmol). Yield: 72 mg, 85%, yellow syrup.  $[\alpha]_D^{25} = +86.07$

(c 1.15, acetone). FTIR (neat,  $\text{cm}^{-1}$ ) 1744, 1666, 1546, 1208, 698. <sup>1</sup>H NMR (500 MHz, CDCl<sub>3</sub>)  $\delta$  7.57 (d,  $J = 7.3$  Hz, 2H, ArH), 7.46 (dd,  $J = 21.7, 14.7$  Hz, 2H, ArH), 7.39 (dd,  $J = 16.2, 9.0$  Hz, 1H, ArH), 7.31 – 7.23 (m, 3H, ArH), 7.23 – 7.18 (m, 2H, ArH), 7.01 (m, 1H, CONH), 5.16 (t,  $J = 7.7$  Hz, 1H, C<sup>4</sup>H), 4.85 (d,  $J = 7.9$  Hz, 1H, C<sup>5</sup>H), 4.44 (d,  $J = 9.5$  Hz, 1H, C<sup>2</sup>H), 4.41 – 4.32 (dd,  $J = 9.4, 7.6$  Hz, 1H, C<sup>3</sup>H), 3.73 (dd,  $J = 18.3, 5.2$  Hz, 1H, CH<sub>2</sub>), 3.72 (s, 3H, CO<sub>2</sub>Me), 3.61 (dd,  $J = 18.5, 5.0$  Hz, 1H, CH<sub>2</sub>). <sup>13</sup>C NMR (101 MHz, CDCl<sub>3</sub>)  $\delta$  170.2, 170.0, 137.7, 135.7, 129.2, 129.1, 128.6, 128.4, 128.2, 126.8, 95.2, 66.6, 64.5, 53.1, 52.4, 40.6. HRMS (ESI) for C<sub>20</sub>H<sub>22</sub>N<sub>3</sub>O<sub>5</sub>: calculated  $[M + H]^+$ : 384.1559. Found: 384.1567.

### Additional procedures for the synthesis of other catalysts

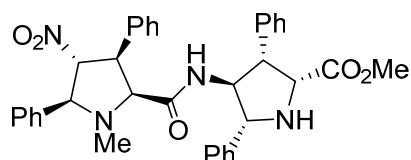
To a stirred solution of the corresponding amine **10aa** (80 mg, 0.27 mmol) in 8 mL of dichloromethane, NO<sub>2</sub>-X<sub>L</sub>-OH-**5e** (104 mg, 0.31 mmol), HATU (104 mg, 0.31 mmol) and diisopropyl ethyl amine (48 μL, 0.31 mmol) were added. The resulting mixture was then stirred until completion of the reaction. Then, the reaction mixture was diluted with CH<sub>2</sub>Cl<sub>2</sub>, washed with a 1M HCl solution, saturated aqueous NaHCO<sub>3</sub>, brine and then dried over Na<sub>2</sub>SO<sub>4</sub>. Filtration and evaporation of the solvent followed by column chromatography eluting with ethyl acetate/hexanes provided the products described below.



*Methyl (2S,3R,4R,5S)-4-((2'S,3'S,4'R,5'S)-1-methyl-4-nitro-3,5-diphenylpyrrolidine-2-carboxamido)-3,5-diphenylpyrrolidine-2-carboxylate* (NO<sub>2</sub>-X<sub>L</sub>-OMe-**26a**).

The title product was obtained from NH<sub>2</sub>-X<sub>L</sub>-OMe-**10aa**.

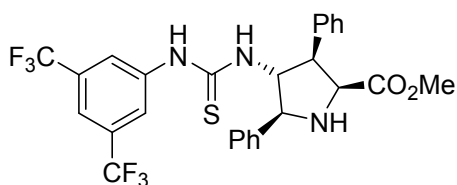
Yield: 52 mg, 32%, light yellow solid.  $m_p = 126 - 130$  °C.  $[\alpha]_D^{25} = +13.87$  (c 1.00, acetone). FTIR (neat, cm<sup>-1</sup>) 1733, 1676, 1549, 1496, 1454, 1210, 727, 696. <sup>1</sup>H NMR (400 MHz, CDCl<sub>3</sub>) δ 7.53 (d,  $J = 7.0$  Hz, 2H, ArH), 7.48 – 7.31 (m, 9H, ArH), 7.22 (t,  $J = 7.8$  Hz, 4H, ArH), 7.06 (d,  $J = 7.6$  Hz, 1H, ArH), 7.01 (d,  $J = 8.7$  Hz, 1H, CONH), 6.93 (t,  $J = 7.6$  Hz, 2H, ArH), 6.84 (d,  $J = 7.7$  Hz, 2H, ArH), 4.89 (t,  $J = 8.6$  Hz, 1H, C<sup>4</sup>H), 4.58 (q,  $J = 9.0$  Hz, 1H, C<sup>4</sup>H), 4.30 (d,  $J = 9.2$  Hz, 1H, C<sup>2</sup>H), 4.27 – 4.15 (m, 2H, C<sup>5</sup>H and C<sup>3</sup>H), 4.03 (d,  $J = 8.4$  Hz, 1H, C<sup>5</sup>H), 3.63 (dd,  $J = 12.4, 9.9$  Hz, 2H, C<sup>3</sup>H and C<sup>2</sup>H), 3.22 (s, 3H, CO<sub>2</sub>Me), 1.99 (s, 3H, NMe). <sup>13</sup>C NMR (101 MHz, CDCl<sub>3</sub>) δ 173.3, 168.4, 139.8, 137.2, 136.4, 135.0, 129.5 (2 signals), 129.1, 128.7, 128.5, 128.5, 128.4, 128.3, 128.2, 127.9, 127.6, 127.3, 95.7, 73.9, 72.5, 66.3, 64.1, 60.3, 54.5, 51.7, 51.3, 39.8. HRMS (ESI) for C<sub>36</sub>H<sub>37</sub>N<sub>4</sub>O<sub>5</sub>: calculated  $[M + H]^+$ : 605.2764. Found: 605.2764.



*Methyl (2R,3S,4S,5R)-4-((2'S,3'S,4'R,5'S)-1-methyl-4-nitro-3,5-diphenylpyrrolidine-2-carboxamido)-3,5-diphenylpyrrolidine-2-carboxylate* (NO<sub>2</sub>-X<sub>D</sub>-OMe-**26a**).

The title product was obtained from NH<sub>2</sub>-X<sub>D</sub>-OMe-**10aa**.

Yield: 49 mg, 30%, light green solid.  $m_p = 96 - 100$  °C.  $[\alpha]_D^{25} = +91.11$  (c 0.65, acetone). FTIR (neat, cm<sup>-1</sup>) 1735, 1677, 1548, 1495, 1369, 1207, 697. <sup>1</sup>H NMR (400 MHz, CDCl<sub>3</sub>) δ 7.45 (dt,  $J = 23.1, 7.6$  Hz, 7H, ArH), 7.37 – 7.20 (m, 6H, ArH), 7.15 (m, 3H, ArH), 7.11 – 6.97 (m, 6H, ArH), 6.86 (d,  $J = 8.5$  Hz, 1H, CONH), 4.99 (t,  $J = 7.9$  Hz, 1H, C<sup>4</sup>H), 4.53 (q,  $J = 8.5$  Hz, 1H, C<sup>4</sup>H), 4.28 – 4.14 (m, 2H, C<sup>3</sup>H and C<sup>2</sup>H), 4.03 (dd,  $J = 8.5, 3.4$  Hz, 2H, C<sup>5</sup>H and C<sup>5</sup>H), 3.63 (d,  $J = 10.2$  Hz, 1H, C<sup>2</sup>H), 3.22 (m, 4H, CO<sub>2</sub>Me and C<sup>3</sup>H), 2.49 (bs, 1H, NH), 2.08 (s, 3H, NMe). <sup>13</sup>C NMR (101 MHz, CDCl<sub>3</sub>) δ 172.7, 168.1, 139.2, 138.1, 136.5, 135.6, 129.4, 129.4, 128.9, 128.6, 128.4, 128.3, 127.5, 127.2, 95.9, 74.1, 72.9, 68.0, 64.5, 60.8, 54.0, 51.7, 51.1, 39.9. HRMS (ESI) for C<sub>36</sub>H<sub>37</sub>N<sub>4</sub>O<sub>5</sub>: calculated  $[M + H]^+$ : 605.2764. Found: 605.2763.



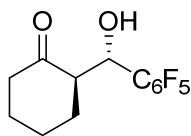
*Methyl (2S,3R,4R,5S)-4-(3-(3,5-bis(trifluoromethyl)phenyl)thioureido)-3,5-diphenylpyrrolidine-2-carboxylate (28)*. Under argon atmosphere to a solution of NH<sub>2</sub>-X<sub>L</sub>-OMe-**10aa** (50 mg, 0.17 mmol) in dry THF (2.5 mL) was added 3,5-bis-(trifluoromethyl)phenyl

isothiocyanate **30** (36 μL, 0.17 mmol) previously dissolved in 2.5 mL of THF.<sup>36</sup> After the reaction mixture was stirred for 16 hours at room temperature, the mixture was concentrated in vacuo. The residue was purified by flash column chromatography with EtOAc:Hex (1:1) to yield the desired thiourea. Yield: 66 mg, 68%, white solid; m<sub>p</sub> = 94 - 95 °C; [α]<sub>D</sub><sup>25</sup> = +72.92 (c 1.60, acetone). FTIR (neat, cm<sup>-1</sup>) 3351, 1739, 1372, 1342, 1277, 1177, 1131. <sup>1</sup>H NMR (500 MHz, CDCl<sub>3</sub>) δ 7.97 (broad s, 2H, thiourea NH), 7.58 (t, *J* = 7.0 Hz, 2H, ArH), 7.53 (d, *J* = 9.0 Hz, 2H, ArH), 7.41 – 7.22 (m, 9H), 5.51 (d, *J* = 9.3 Hz, 1H, C<sup>5</sup>H), 4.58 (d, *J* = 8.5 Hz, 1H, C<sup>2</sup>H), 4.19 (dd, *J* = 11.4, 9.0 Hz, 1H, C<sup>3</sup>H), 3.60 (m, 1H, C<sup>4</sup>H), 3.35 (s, 3H, CO<sub>2</sub>Me); <sup>13</sup>C NMR (126 MHz, CDCl<sub>3</sub>) δ 179.2, 171.1, 140.2, 137.9, 133.7, 131.6 (q, <sup>2</sup>*J*<sub>CF</sub> = 33.6 Hz), 130.4, 130.1, 129.0, 128.4, 127.7, 124.1(2 signals), 123.1 (q, <sup>1</sup>*J*<sub>CF</sub> = 273.4 Hz), 118.9, (m, <sup>3</sup>*J*<sub>CF</sub> = 3.8 Hz), 72.4, 69.9, 63.1, 53.1, 51.9. HRMS (ESI) for C<sub>27</sub>H<sub>24</sub>N<sub>3</sub>O<sub>2</sub>SF<sub>6</sub>: calculated [M + H]<sup>+</sup>: 568.1493. Found: 568.1500.

**General procedure for the synthesis of amide derivative 17.** See section 2.8.

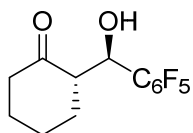
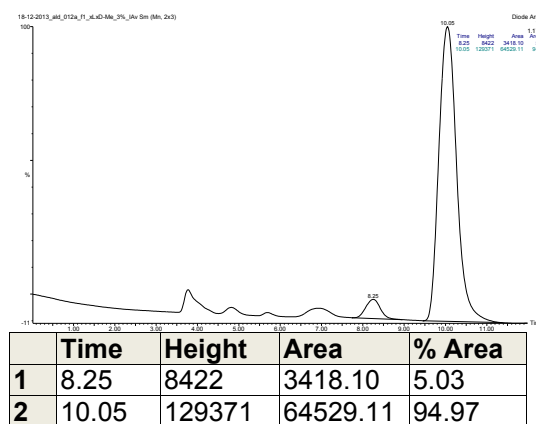
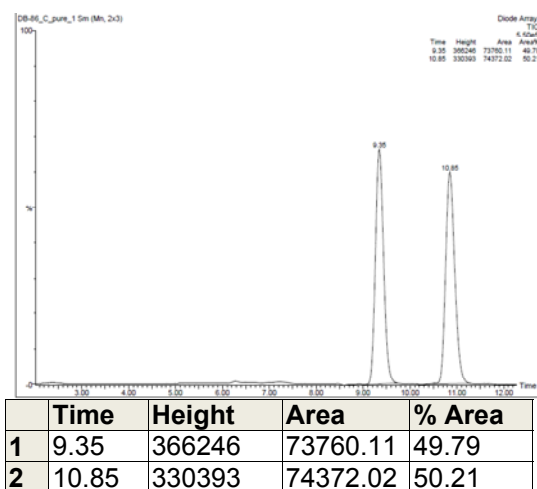
### Procedures for asymmetric transformations

**Organocatalytic asymmetric aldol reaction.** See section 2.8.

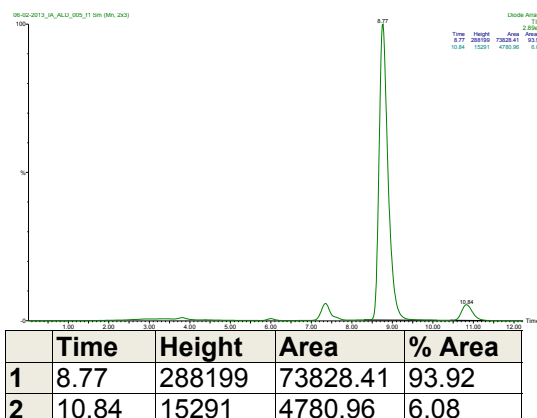


*(R)-2-((S)-Hydroxy(perfluorophenyl)methyl)cyclohexan-1-one (13aa)*.<sup>37</sup> The reaction was carried out under the conditions described in Table 8, entry 4.

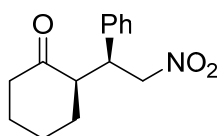
Yield: 68.4 mg, 93%, white solid. Analytical and spectroscopic properties were in good agreement with those reported in the literature. <sup>1</sup>H NMR (500 MHz, CDCl<sub>3</sub>) δ 5.39 – 5.30 (m, 1H, CHOH), 3.92 (d, *J* = 3.3 Hz, 1H, CH), 3.09 – 2.99 (m, 1H, CH<sub>2</sub>), 2.60 – 2.48 (m, 1H, CH<sub>2</sub>), 2.43 (td, *J* = 12.9, 6.3 Hz, 1H, CH<sub>2</sub>), 2.22 – 2.11 (m, 1H, CH<sub>2</sub>), 1.95 – 1.85 (m, 1H, CH<sub>2</sub>), 1.76 – 1.61 (m, 3H, CH<sub>2</sub>), 1.41 – 1.26 (m, 1H, CH<sub>2</sub>). <sup>19</sup>F NMR (376 MHz, cyclohexanone) δ -143.00 (dd, *J* = 22.3, 7.1 Hz, 2F<sub>o</sub>), -157.75 (t, *J* = 21.0 Hz, 1F<sub>p</sub>), -164.31 (td, *J* = 22.1, 7.4 Hz, 2F<sub>m</sub>). HPLC (Daicel Chiralpak IA, hexane/<sup>i</sup>PrOH = 90/10, flow rate 1.0 mL/min, λ = 254 nm), t<sub>R</sub> (minor) = 8.25 min, t<sub>R</sub> (major) = 10.05 min; ee = 90%.



(*S*)-2-((*R*)-Hydroxy(perfluorophenyl)methyl)cyclohexan-1-one (**13aa**).<sup>37</sup> The reaction was carried out under the conditions described in Table 8, entry 5. Yield: 62.5 mg, 85%, white solid. Analytical and spectroscopic properties were in good agreement with those reported in the literature. <sup>1</sup>H NMR (500 MHz, CDCl<sub>3</sub>) δ 5.39 – 5.30 (m, 1H, CHOH), 3.92 (d, *J* = 3.3 Hz, 1H, CH), 3.09 – 2.99 (m, 1H, CH<sub>2</sub>), 2.60 – 2.48 (m, 1H, CH<sub>2</sub>), 2.43 (td, *J* = 12.9, 6.3 Hz, 1H, CH<sub>2</sub>), 2.22 – 2.11 (m, 1H, CH<sub>2</sub>), 1.95 – 1.85 (m, 1H, CH<sub>2</sub>), 1.76 – 1.61 (m, 3H, CH<sub>2</sub>), 1.41 – 1.26 (m, 1H, CH<sub>2</sub>). <sup>19</sup>F NMR (376 MHz, cyclohexanone) δ -143.00 (dd, *J* = 22.3, 7.1 Hz, 2F<sub>o</sub>), -157.75 (t, *J* = 21.0 Hz, 1F<sub>p</sub>), -164.31 (td, *J* = 22.1, 7.4 Hz, 2F<sub>m</sub>). HPLC (Daicel Chiralpak IA, hexane/*i*PrOH = 90/10, flow rate 1.0 mL/min, λ = 254 nm), *t*<sub>R</sub> (minor) = 8.77 min, *t*<sub>R</sub> (major) = 10.84 min; .ee = -88%.

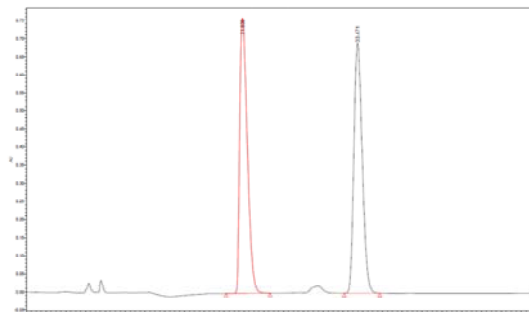


**Organocatalytic asymmetric Michael reaction.** See section 2.8.

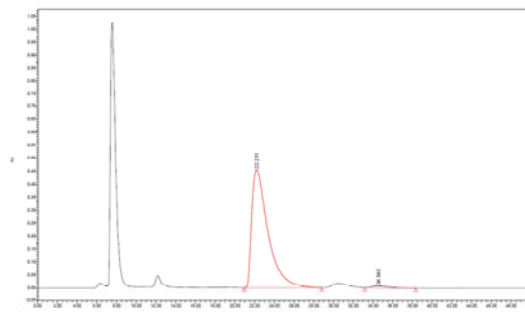


(*R*)-2-((*S*)-2-Nitro-1-phenylethyl)cyclohexanone (**14aa**).<sup>38</sup> The reaction was carried out under the conditions described in Table 11, entry 14. Yield: 22.5 mg, 91%, white solid. Analytical and spectroscopic properties were in good agreement with those reported in the literature. <sup>1</sup>H NMR (500 MHz, CDCl<sub>3</sub>) δ 7.37 – 7.30 (m, 3H, ArH), 7.17 (d, *J* = 7.1 Hz, 2H, ArH), 4.94 (dd, *J* = 12.4, 4.4 Hz, 1H,

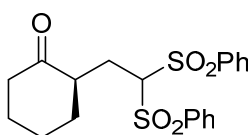
CHNO<sub>2</sub>), 4.69 – 4.57 (m, 1H, CHNO<sub>2</sub>), 3.81 – 3.68 (m, 1H, CHAr), 2.76 – 2.62 (m, 1H, CH), 2.48 (d, *J* = 13.3 Hz, 1H, CH<sub>2</sub>), 2.40 (dd, *J* = 12.4, 6.2 Hz, 1H, CH<sub>2</sub>), 2.07 (m, 1H, CH<sub>2</sub>), 1.85 – 1.58 (m, 4H, CH<sub>2</sub>), 1.24 (m, 1H, CH<sub>2</sub>). HPLC (Daicel Chiralpak AS-H, hexane/PrOH = 90/10, flow rate 1.0 mL/min, λ = 210 nm), *t*<sub>R</sub> (major) = 22.21 min, *t*<sub>R</sub> (minor) = 34.54 min; ee = 96%.



	Time	Area	% Height	% Area
1	21.839	40597597	52.39	50.03
2	33.471	40550593	47.61	49.97

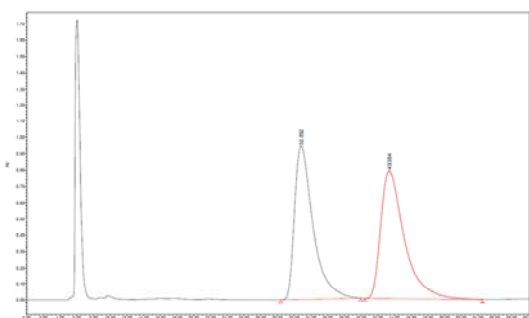


	Time	Area	% Height	% Area
1	22.211	52028937	98.33	98.25
2	34.540	928288	1.67	1.75

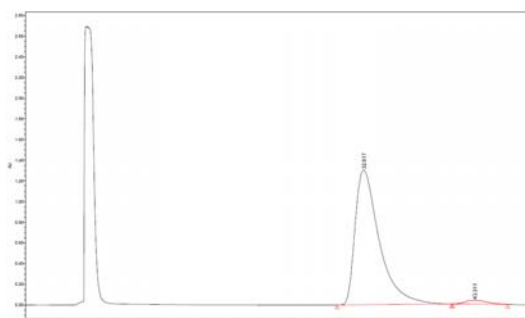


(*R*)-2-(2,2-bis(Phenylsulfonyl)ethyl)cyclohexan-1-one (**16**).<sup>39</sup> The reaction was carried out under the conditions described in Table 12, entry 5. Yield: 17.9 mg, 44%, white solid. Analytical and spectroscopic properties were in good agreement with those reported in the literature.

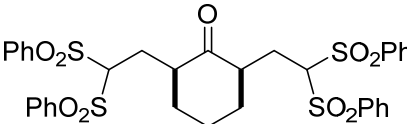
<sup>1</sup>H NMR (500 MHz, CDCl<sub>3</sub>) δ 7.92 (dd, *J* = 24.1, 7.6 Hz, 4H, ArH), 7.68 (q, *J* = 8.2 Hz, 2H, ArH), 7.56 (q, *J* = 7.1 Hz, 4H, ArH), 4.98 (dd, *J* = 9.2, 3.8 Hz, 1H, CH(SO<sub>2</sub>Ph)<sub>2</sub>), 3.07 (dq, *J* = 13.6, 5.2 Hz, 1H, CH<sub>2</sub>), 2.52 (m, 2H, CH<sub>2</sub>), 2.08 (m, 2H, CH<sub>2</sub>), 1.95 (m, 2H, CH<sub>2</sub>), 1.63 – 1.49 (m, 2H, CH<sub>2</sub>), 1.29 (m, 2H, CH<sub>2</sub>). HPLC (Daicel Chiralpak AS-H, hexane/PrOH = 70/30, flow rate 1.0 mL/min, λ = 210 nm), *t*<sub>R</sub> (major) = 32.62 min, *t*<sub>R</sub> (minor) = 43.31 min; ee = 95%.

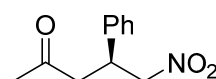


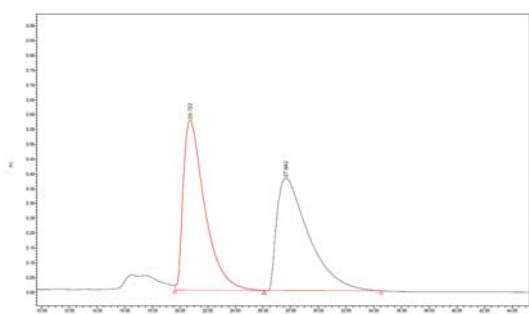
	Time	Area	% Height	% Area
1	32.852	146278858	54.47	48.58
2	43.384	154835276	45.53	51.42



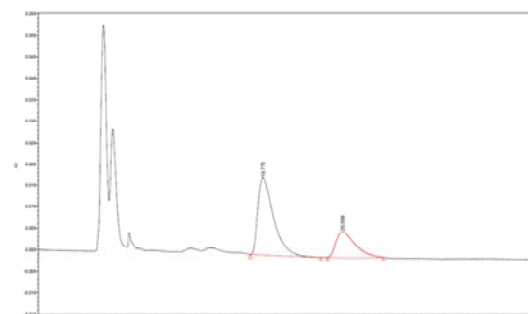
	Time	Area	% Height	% Area
1	32.617	210804474	97.19	97.48
2	43.311	5451911	2.81	2.52


**2,6-bis(2,2-bis(Phenylsulfonyl)ethyl)cyclohexan-1-one (16bis).**<sup>39</sup> The reaction was carried out under the conditions described in Table 12, entry 6. Yield: 11.0 mg, 62%, white solid.  $m_p = 134-135\text{ }^\circ\text{C}$ . FTIR (neat,  $\text{cm}^{-1}$ ) 1704, 1327, 1311, 1147, 730, 686.  $^1\text{H}$  NMR (400 MHz,  $\text{CDCl}_3$ )  $\delta$  7.90 (dd,  $J = 24.4, 7.9$  Hz, 8H, ArH), 7.68 (q,  $J = 7.8$  Hz, 4H, ArH), 7.53 (dt,  $J = 15.8, 7.7$  Hz, 8H, ArH), 4.87 (dd,  $J = 9.4, 4.0$  Hz, 2H,  $\text{CH}(\text{SO}_2\text{Ph})_2$ ), 3.36 – 3.00 (m, 2H,  $\text{CH}_2\text{CH}(\text{SO}_2\text{Ph})_2$ ), 2.48 (ddd,  $J = 14.4, 9.6, 4.2$  Hz, 2H,  $\text{CH}_2\text{CH}(\text{SO}_2\text{Ph})_2$ ), 2.12 (d,  $J = 9.7$  Hz, 2H, COCH), 1.99 (ddd,  $J = 14.5, 9.5, 4.6$  Hz, 2H,  $\text{CH}_2$ ), 1.83 (s, 2H,  $\text{CH}_2$ ), 1.40 – 1.14 (m, 2H,  $\text{CH}_2$ ).  $^{13}\text{C}$  NMR (101 MHz,  $\text{CDCl}_3$ )  $\delta$  212.5, 138.4, 138.0, 134.7, 134.6, 129.8, 129.6, 129.3, 129.2, 80.7, 48.2, 36.1, 26.1, 25.1. HRMS (ESI) for  $\text{C}_{34}\text{H}_{35}\text{O}_9\text{S}_4$ : calculated  $[\text{M} + \text{H}]^+$ : 715.1164. Found: 715.1180.


**(S)-5-Nitro-4-phenylpentan-2-one (14da).**<sup>40</sup> The reaction was carried out under the conditions described in Table 13Table 11, entry 3. Yield: 11.0 mg, 53%, white solid. Analytical and spectroscopic properties were in good agreement with those reported in the literature.  $^1\text{H}$  NMR (400 MHz,  $\text{CDCl}_3$ )  $\delta$  7.45 – 7.13 (m, 5H, ArH), 4.83 – 4.51 (m, 2H,  $\text{CH}_2\text{NO}_2$ ), 4.11 – 3.94 (m, 1H, CH), 2.92 (d,  $J = 7.0$  Hz, 2H,  $\text{CH}_2$ ), 2.12 (s, 3H,  $\text{CH}_3$ ). HPLC (Daicel Chiralpak AS-H, hexane/ $i$ PrOH = 80/20, flow rate 1.0 mL/min,  $\lambda = 210$  nm),  $t_R$  (major) = 19.78 min,  $t_R$  (minor) = 26.67 min; ee = 41%.



	Time	Area	% Height	% Area
1	20.722	62009854	60.19	50.54
2	27.642	60676252	39.81	49.46



	Time	Area	% Height	% Area
1	19.775	1681868	75.12	70.45
2	26.669	705371	24.88	29.55

<sup>1</sup> Sewald, N.; Jakubke, H.-D. *Peptides: Chemistry and Biology*, **2002**, Wiley-VCH.

<sup>2</sup> Venkatraman, J.; Shankaramma, S. C. *Chem. Rev.* **2001**, *101*, 3131-3152.

<sup>3</sup> Colby Davie, E. A.; Mennen, S. M.; Xu, Y.; Miller, S. J. *Chem. Rev.* **2007**, *107*, 5759-5812.

<sup>4</sup> Wennemers, H. *Chem. Commun.* **2011**, *47*, 12036-12041.

<sup>5</sup> (a) Oku, J.-I.; S. Inoue, S. *Makromol. Chem.* **1979**, *180*, 1089-1091. (b) Oku, J.-I.; S. Inoue, S. *J. Chem. Soc. Chem. Commun.* **1981**, 229-230.

<sup>6</sup> (a) Juliá, S.; Masana, J.; Vega, J. C. *Angew. Chem. Int. Ed. Engl.* **1980**, *19*, 929-931. (b) Juliá, S.; Guixer, J.; Masana, J.; Rocas, J.; Colonna, S.; Annuziata, R.; Molinari, H. *J. Chem. Soc. Perkin Trans. 1*, **1982**, 1317-1324.

<sup>7</sup> Kelly, D. R.; Roberts, S. M. *Chem. Commun.* **2004**, 2018-2020.

<sup>8</sup> Kofoed, J.; Nielsen, J.; Reymond, J.-L. *Bioorg. Med. Chem. Lett.* **2003**, *13*, 2445-2447.

<sup>9</sup> Martin, H. J.; List, B. *Synlett*, **2003**, 1901-1902.

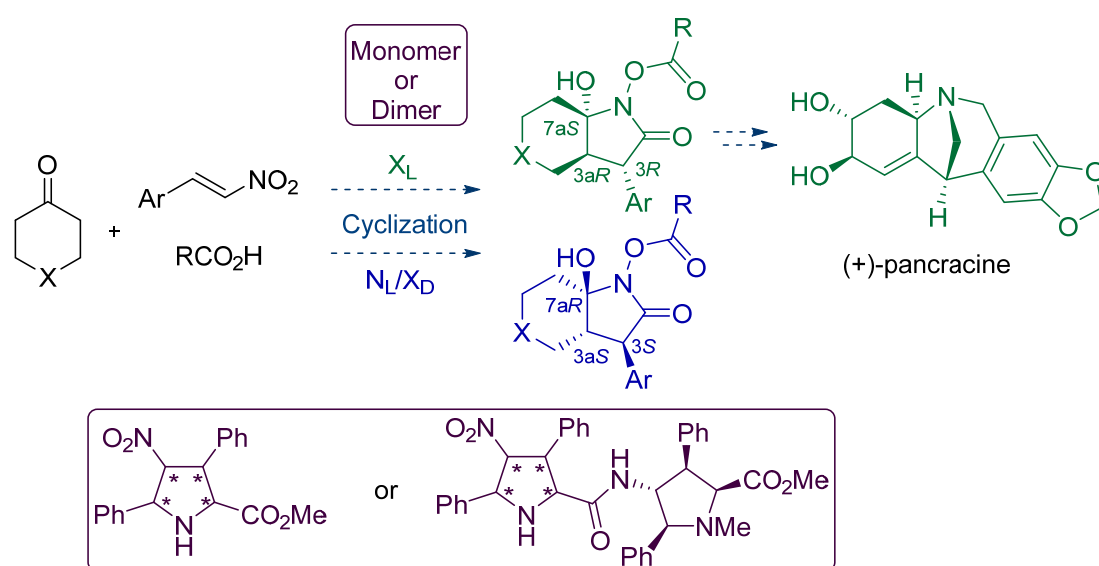
<sup>10</sup> Krattiger, P.; McCarthy, C.; Pfaltz, A.; Wennemers, H. *Angew. Chem. Int. Ed.* **2003**, *42*, 1722-1724.



- <sup>11</sup> Revell, J. D.; Wennemers, H. *Adv. Synth. Catal.* **2008**, *350*, 1046-1052.
- <sup>12</sup> Krattiger, P.; Kovasy, R.; Revell, J. D.; Ivan, S.; Wennemers, H. *Org. Lett.* **2005**, *7*, 1101-1103.
- <sup>13</sup> Tang, Z.; Yang, Z.-H.; Cun, L.-F.; Gong, L.-Z.; Mi, A.-Q.; Jiang, Y.-Z. *Org. Lett.* **2004**, *6*, 2285-2287.
- <sup>14</sup> Córdova, A.; Zou, W.; Dziedzic, P.; Ibrahim, I.; Reyes, E.; Xu, Y. *Chem. Eur. J.* **2006**, *12*, 5383-5397.
- <sup>15</sup> Tsogoeva, S. B.; Jagtap, S. B.; Ardemasova, Z. A. *Tetrahedron Asymm.* **2006**, *17*, 989-992.
- <sup>16</sup> (a) Hanessian, S.; Pham, V. *Org. Lett.* **2000**, *2*, 2975-2978. (b) Hanessian, S.; Govindan, S.; Warrior, J. S. *Chirality*, **2005**, *17*, 540-543.
- <sup>17</sup> Freund, M.; Schenker, S.; Tsogoeva, S. B. *Org. Biomol. Chem.* **2009**, *7*, 4279-4284.
- <sup>18</sup> Xu, Y.; Zou, W.; Sundén, H.; Ibrahim, I.; Córdova, A. *Adv. Synth. Catal.* **2006**, *348*, 418-424.
- <sup>19</sup> (a) Wiesner, M.; Revell, J. D.; Wennemers, H. *Angew. Chem. Int. Ed.* **2008**, *47*, 1871-1874. (b) Wiesner, M.; Revell, J. D.; Tonazzi, S.; Wennemers, H. *J. Am. Chem. Soc.* **2008**, *130*, 5610-5611.
- <sup>20</sup> Wennemers, H. *Chem. Commun.* **2011**, *47*, 12036-12041.
- <sup>21</sup> These ligands are described in the PhD thesis of Amaia Larumbe Gárate: "Utilización de Reacciones de Cicloadición (3+2) en la Síntesis de Nuevas Entidades Químicas con Actividad Inhibitoria del Proteasoma" **2015**, from the University of the Basque Country.
- <sup>22</sup> (a) Montalbetti, C. A. G. N.; Falque, V. *Tetrahedron*, **2005**, *61*, 10827-10852. (b) Valeur, E.; Bradley, M. *Chem. Soc. Rev.* **2009**, *38*, 606-631. (c) Joullié, M. M.; Lassen, K. M. *Arkivoc*, **2010**, *viii*, 189-250.
- <sup>23</sup> Klose, J.; Bienert, M.; Mollenkopf, C.; Wehle, D.; Zhang, C.-W.; Carpino, L. A.; Henklein, P. *Chem. Commun.* **1999**, 1847-1848.
- <sup>24</sup> Lundberg, H.; Tinnis, F.; Adolfsson, H. *Chem. Eur. J.* **2012**, *18*, 3822-3826.
- <sup>25</sup> Wang, B.; Forsyth, C. J. *Org. Lett.* **2006**, *8*, 5223-5226.
- <sup>26</sup> Bastiaans, H. M. M.; van der Baan, J. L.; Ottenheijm, H. C. J. *J. Org. Chem.* **1997**, *62*, 3880-3889.
- <sup>27</sup> Coste, J.; Le-Nguyen, D.; Castro, B. *Tetrahedron Lett.* **1990**, *31*, 205-208.
- <sup>28</sup> Retamosa, M. G.; de Cózar, A.; Sánchez, M.; Miranda, J. I.; Sansano, J. M.; Castelló, L. M.; Nájera, C.; Jiménez, A. I.; Sayago, F. J.; Cativiela, C.; Cossío, F. P. *Eur. J. Org. Chem.* **2015**, 2503-2516.
- <sup>29</sup> (a) Schmid, M. B.; Zeitler, K.; Gschwind, R. M. *Angew. Chem. Int. Ed.* **2010**, *49*, 4997-5003 and *Angew. Chem.* **2010**, *122*, 5117-5123. (b) Zhu, H.; Clemente, F. R.; Houk, K. N.; Meyer, M. P. *J. Am. Chem. Soc.* **2009**, *131*, 1632-1633.
- <sup>30</sup> Harris, D. C. *Quantitative Chemical Analysis*, 8<sup>th</sup> ed., **2010**, W. H. Freeman: New York.
- <sup>31</sup> (a) Denmark, S. E.; Matsubashi, H. *J. Org. Chem.* **2002**, *67*, 3479-3486. (b) Kudryavtsev, K. V.; Tsentralovich, M. Y.; Yegorov, A. S.; Kolychev, E. L. *J. Het. Chem.* **2006**, *43*, 1461-1466.
- <sup>32</sup> Conde, E.; UPV – EHU, **2014**, PhD Thesis: "Síntesis de Pirrolidinas Ferrocenil Sustituidas mediante Cicloadiciones (3+2). Aplicación a las Catálisis de Reacciones Enantioselectivas de Adición y Cicloadición".
- <sup>33</sup> Kim, H. Y.; Li, J. Y.; Kim, S.; Oh, K. *J. Am. Chem. Soc.* **2011**, *133*, 20750-20753.
- <sup>34</sup> Li, J.-Y.; K. H. Y.; Oh, K. *Org. Lett.* **2015**, *17*, 1288-1291.
- <sup>35</sup> Ruiz-Olalla, A.; Retamosa, M. G.; Cossío, F. P. *J. Org. Chem.* **2015**, *80*, 5588-5599.
- <sup>36</sup> Menguy, L.; Couty, F. *Tetrahedron Lett.* **2010**, *21*, 2385-2389.
- <sup>37</sup> Gruttadauria, M.; Giacalone, F.; Marculescu, A. M.; Lo Meo, P.; Riela, S.; Noto, R. *Eur. J. Org. Chem.* **2007**, 4688-4698.
- <sup>38</sup> Mase, N.; Watanabe, K.; Yoda, H.; Takabe, K.; Tanaka, F.; Barbas, C. F., III. *J. Am. Chem. Soc.* **2006**, *128*, 4966-4967.
- <sup>39</sup> Quintard, A.; Alexakis, A. *Chem. Eur. J.* **2009**, *15*, 11109-11113.
- <sup>40</sup> Wang, C.; Yu, C.; Liu, C.; Peng, Y. *Tetrahedron Lett.* **2009**, *50*, 2363-2366.



# Chapter 4. Stereoselective Synthesis of 7a-Hydroxy-2-oxo-3-aryloctahydro-1H-indol-yl Carboxylates. A Concise Formal Synthesis of (+)-Pancracine



## Abstract.

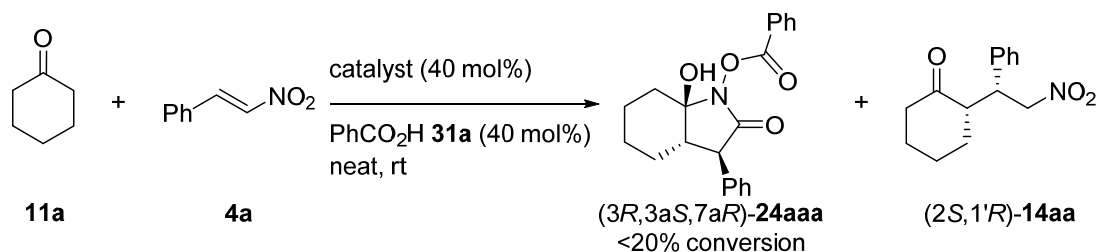
A novel organocatalytic method for the construction of 7a-hydroxy-2-oxo-3-aryloctahydro-1H-indol-yl carboxylates with total enantiocontrol is described. This reaction takes place during the multicomponent reaction among aromatic nitroalkenes, cyclic ketones and carboxylic acids in the presence of densely substituted 4-nitroprolinates in the form of monomers or dimers as catalysts, already described in the previous chapters. This process allows a shorter route towards the organocatalyzed formal synthesis of enantiopure (+)-pancracine.

Retamosa, M. G.; Ruiz-Olalla A.; Cossío, F. P. *Manuscript in preparation*



#### 4.1. Introduction

As it was mentioned in the previous chapter, a secondary product was detected in the reaction between cyclohexanone **11a**, nitrostyrene **4a** and benzoic acid **31a**, acting as an additive. This unexpected adduct was identified as  $\gamma$ -lactam (3*R*,3*aS*,7*aS*)-**24aaa**.



**Scheme 1.** Obtained products when performed the Michael reaction between cyclohexanone **11a**, nitrostyrene **4a** catalyzed by dimeric catalyst in the presence of benzoic acid **31a** as additive.

Thus, it could be expected that by tuning the reaction conditions, e. g. raising the load of the benzoic acid to equimolar amounts or changing the catalyst, the selectivity of the reaction could be shifted towards the exclusive formation of the  $\gamma$ -lactam product.

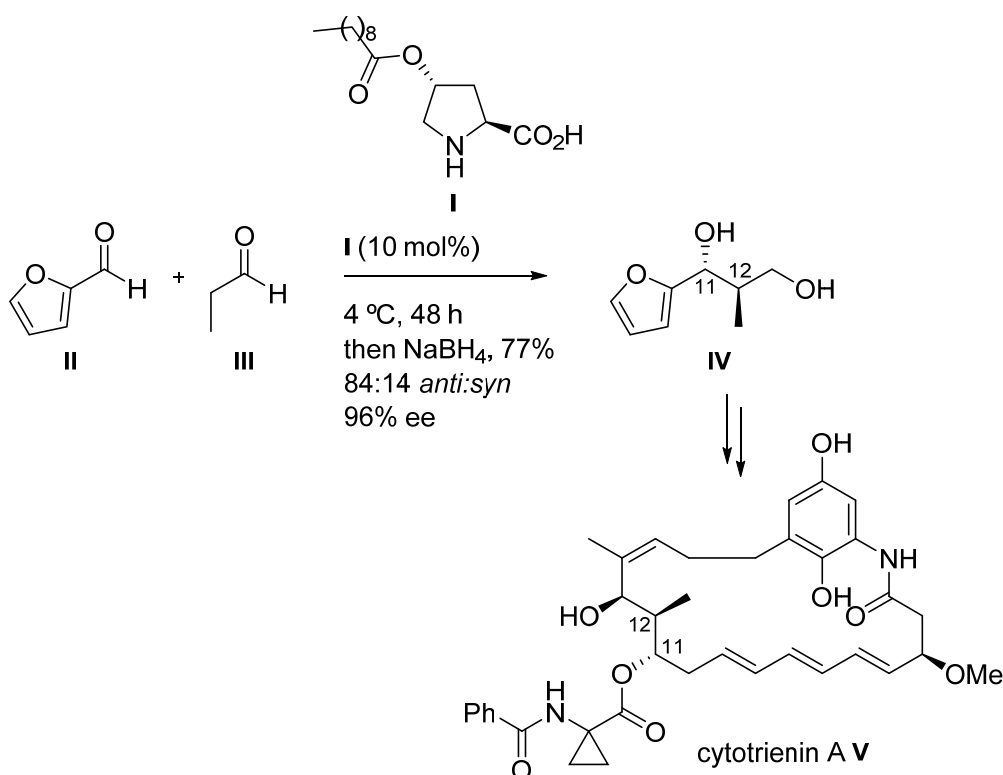
##### 4.1.1. Organocatalysis in total synthesis of alkaloids and secondary metabolites

Asymmetric C-C bond formation reactions are an essential goal in modern organic synthesis. Due to the rapid evolution of organocatalysis, this kind of transformations can be performed efficiently avoiding methods based on transition metal complexes which cause environmental issues or on enzymes, that are less flexible in terms of reaction conditions and scope. This introduction aims to show current applications of organocatalysis in total synthetic processes towards alkaloids and secondary metabolites, focusing on the reactions discussed on previous chapters, namely the aldol and Michael additions.

##### Aldol reaction

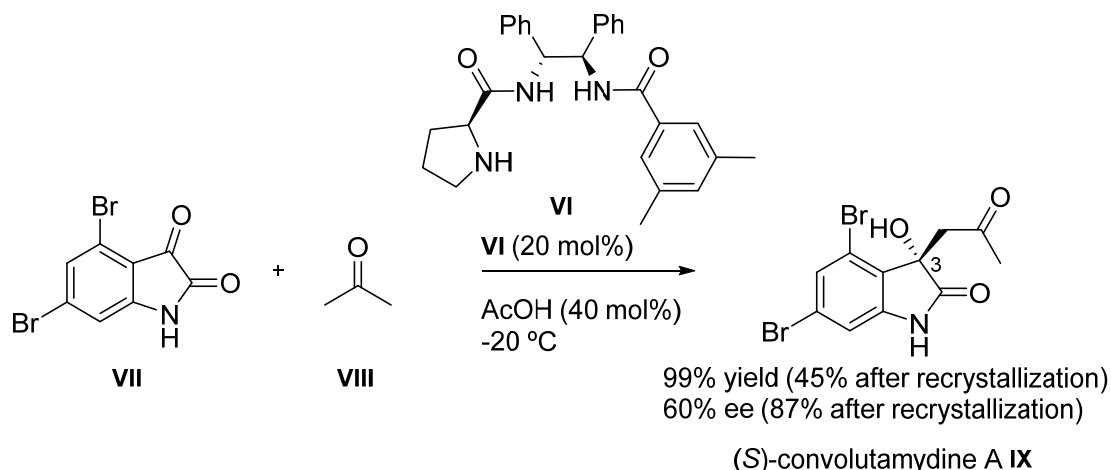
The group of Hayashi used a direct aldol reaction to construct the building block **IV** for the synthesis of (+)-cytotrienin A **V** which is a microbial antitumor secondary metabolite.<sup>1</sup> The diol **IV** was achieved in high enantioselective manner by employing 4-acyloxy-L-Proline organocatalyst **I** in the aldol reaction between furfural **II** and

propanal **III** (Scheme 2).<sup>2</sup> The original procedure, under the influence of L-Proline, was not practical for gram scale purposes as low diastereoselectivities and yields were obtained.<sup>3</sup> The total synthesis towards (+)-cytotrienin A **V** required additional 32 steps from diol **IV**.



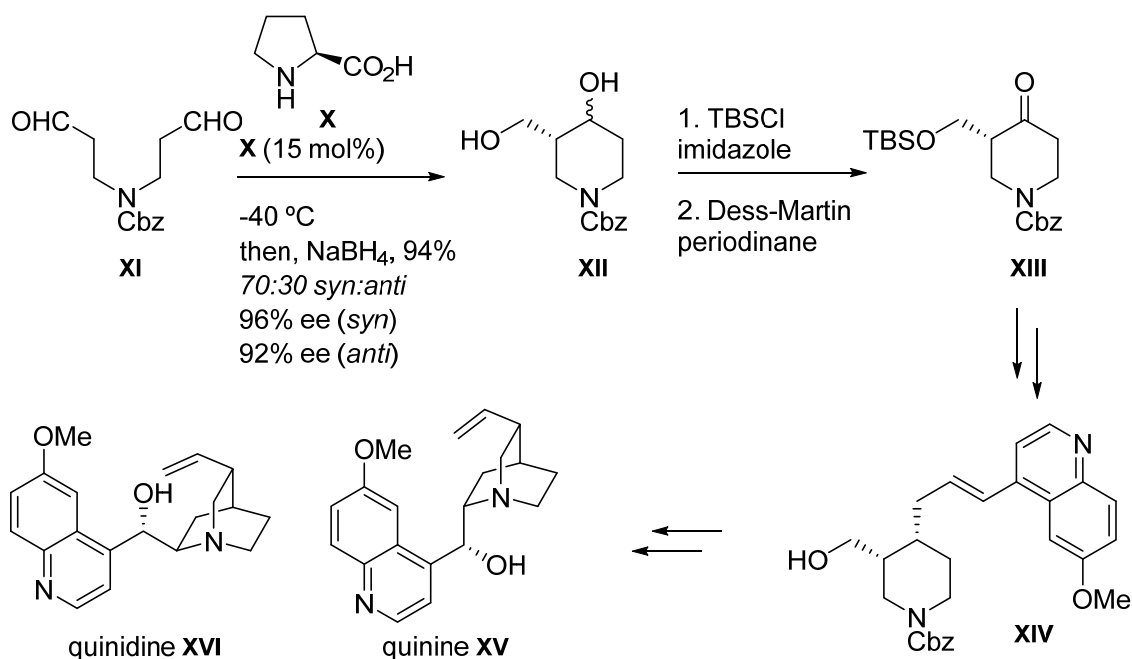
**Scheme 2.** Stereoselective organocatalyzed reaction for the synthesis of secondary metabolite cytotrienin A **V**.

Convolutamydines constitute a family of 3-substituted-3-hydroxyindolin-2-one alkaloids which are isolated from the Floridian *Amathia convolute* marine bryozoans.<sup>4</sup> They have received attention for medicinal purposes because of their biological activities derived from the different substituents (and absolute configuration) at the C-3 position. The challenging formation of the tetrasubstituted carbon from the aldol reaction between isatin **VII** and acetone **VIII** catalyzed by L-Proline-derived bifunctional organocatalyst **VI** was reported by the group of Xiao. This reaction proceeded to give (*S*)-convolutamydine A **IX** in high yield and good enantioselectivity, which was raised after a recrystallization step (Scheme 3).<sup>5</sup>



**Scheme 3.** Synthesis of (*S*)-convolutamydine A IX.

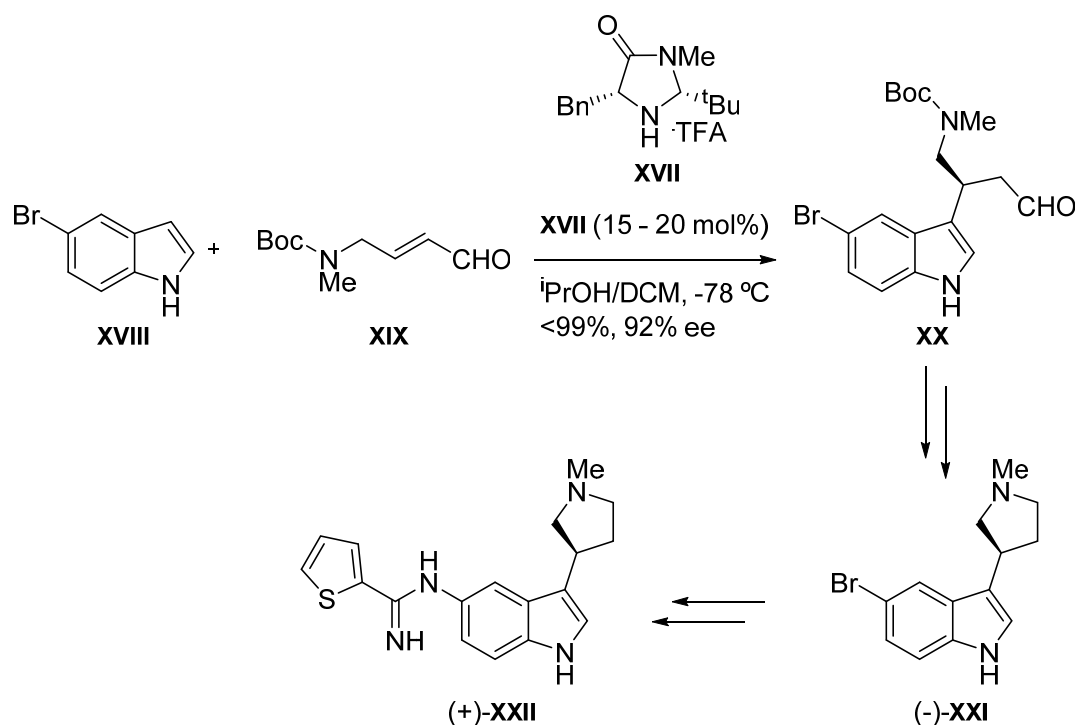
Quinine **XV** and quinidine **XVI** compounds are representative examples of the cinchona alkaloid family, being the former a popular agent used for the treatment of malaria. Also, synthetically modified cinchona alkaloids give rise to a large variety of organocatalysts.<sup>6</sup> The group of Hatakeyama reported the synthesis of key intermediate **XII** via the intermolecular aldol reaction of bis aldehyde **XI** in the presence of L-Proline **X** (Scheme 4).<sup>7</sup> After aldehyde reduction *syn* and *anti*-diols **XII** were obtained in high enantioselectivity. The authors emphasized the reproducibility of the reaction up to ten gram scale. Next, alcohol protection and oxidation of both diastereomers provided the common intermediate **XIII**. Further steps provided precursor **XIV** common for both quinine **XV** and quinidine **XVI** natural products.<sup>8</sup>



**Scheme 4.** Organocatalytic aldol step for the synthesis of quinine **XV** and quinidine **XVI** alkaloids.

## Michael reaction

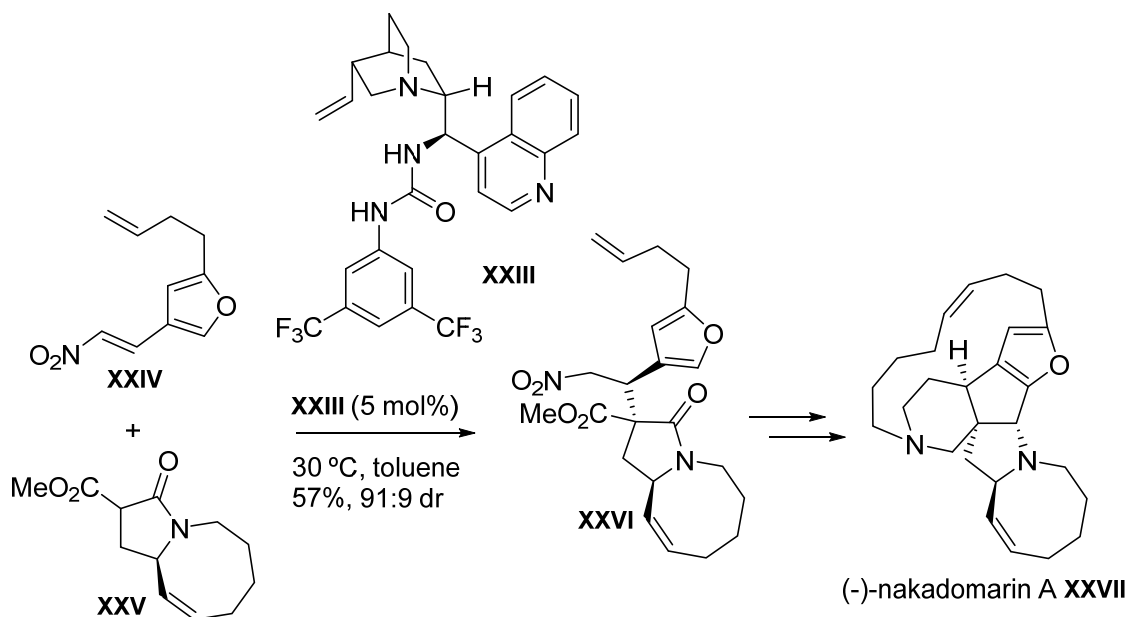
The imidazolidinone MacMillan's catalyst **XVII** is very efficient at forming iminium ions with  $\alpha,\beta$ -unsaturated aldehydes and can catalyze Friedel-Crafts type Michael reactions.<sup>9</sup> The group of Hanessian employed this strategy using (*R,R*)-**XVII** to catalyze the conjugate addition between 5-bromoindole **XVIII** to the electron-rich aldehyde **XIX** to give the addition product **XX** in quantitative yield and high enantiomeric excess (Scheme 5).<sup>10</sup> Intermediate (-)-**XXI** was obtained after 4 steps. This latter compound is the precursor of drug prototype (+)-**XXII**, which possesses great activity against neuronal nitric oxide synthase (nNOS) and is potentially useful for the treatment of migraine headaches.



**Scheme 5.** Organocatalytic step for the synthesis of (-)-**XXII**.

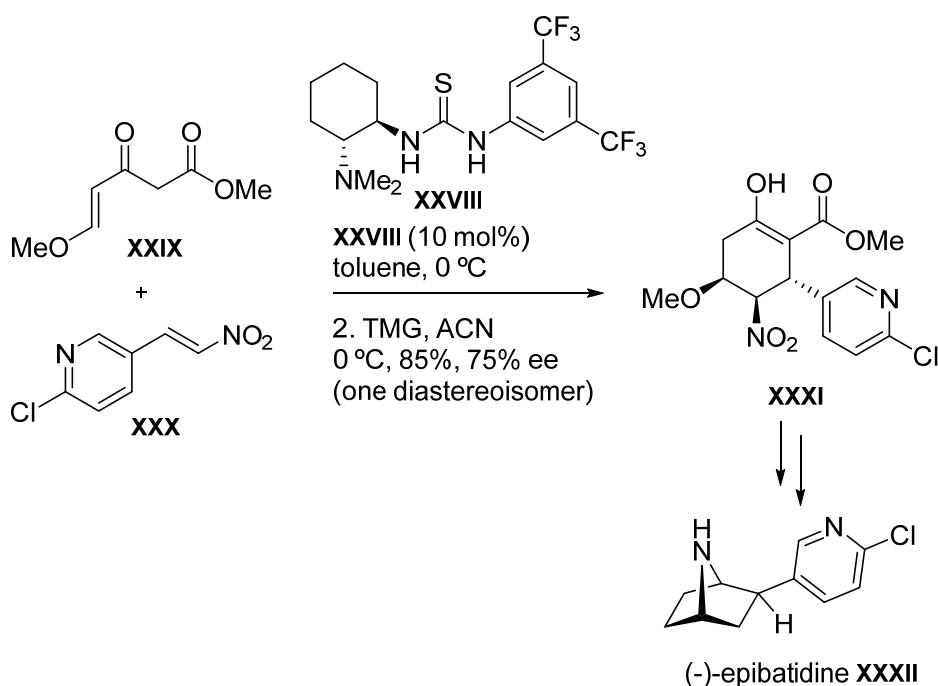
Dixon and co-workers<sup>11</sup> reported the total synthesis of polycyclic (-)-nakadomarin A **XXVII**. This natural product is a marine alkaloid of the manzamine family with potential therapeutic properties such as cytotoxic, antimicrobial and antibacterial activity.<sup>12</sup> Scheme 6 shows the organocatalytic step in which the organocatalyst **XXIII** derived from cinchonidine promoted the effective reaction between nitro olefin **XXIV** and the bicyclic pronucleophile **XXV** in moderate yield and excellent diastereomeric ratio. The total synthesis towards (-)-nakadomarin A **XXVII** was achieved in additional 5 steps.





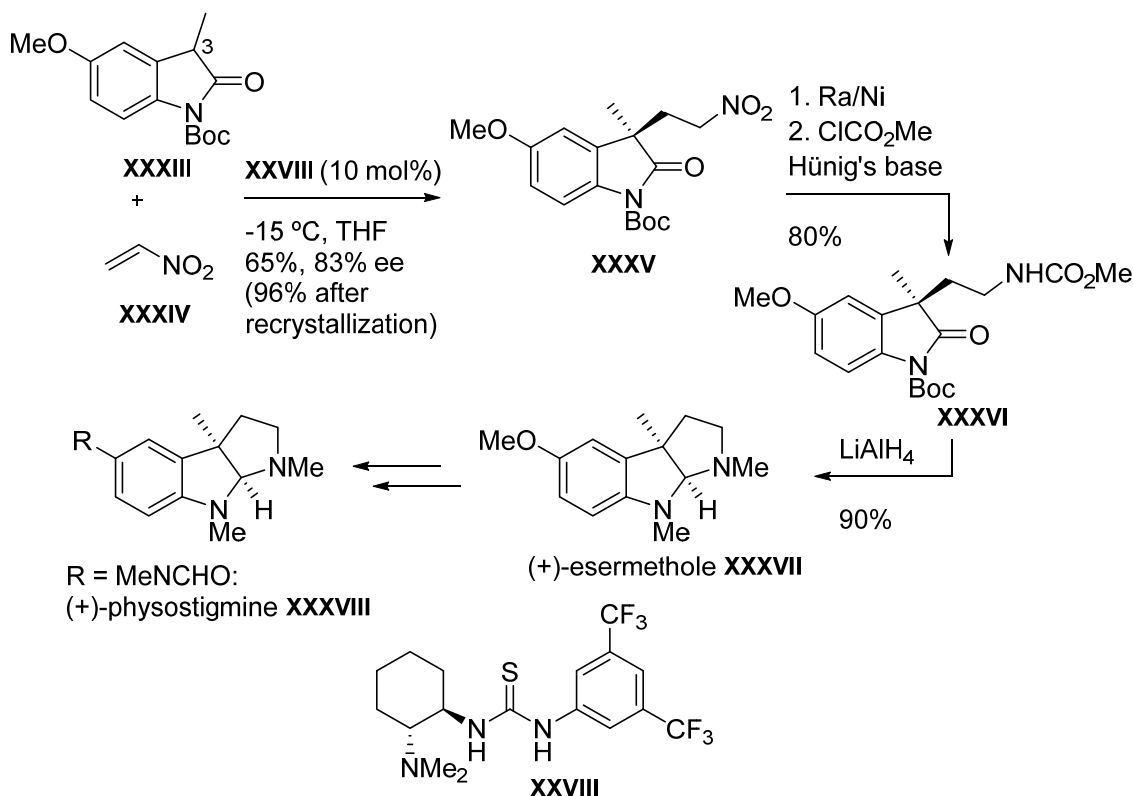
**Scheme 6.** Synthesis of (-)-nakadomarin A **XXVII**.

The versatility of the nitro group has also found its place in the synthetic chemistry of alkaloids. For instance, the group of Takemoto reported the double Michael reaction of  $\gamma,\delta$ -unsaturated- $\beta$ -ketoester **XXIX** to nitroalkene **XXX** to provide cycloadduct **XXXI** bearing three contiguous stereogenic centers in good yield and enantioselectivity (Scheme 7).<sup>13</sup> This intermediate gave the opportunity to afford toxic (-)-epibatidine **XXXII** alkaloid, a strongly toxic natural compound that binds and activates the muscarinic acetylcholine and nicotinic receptors.



**Scheme 7.** Keto-ester addition to nitroolefin towards the synthesis of (-)-epibatidine **XXXII**.

The group of Barbas III reported the enantioselective conjugate addition of oxindole **XXXIII** to olefin **XXXIV** to construct the quaternary stereocenter at C-3.<sup>14</sup> They employed Takemoto's thiourea as catalyst **XXVIII**, which promoted the reaction in 65% yield and good enantioselectivity. Adduct **XXXV** was hydrogenated and transformed into carbamate **XXXVI** in good yield. Subsequent reductive cyclization provided the synthetic precursor (+)-esermethole **XXXVII** which is also an intermediate towards (+)-physostigmine **XXXVIII** alkaloid<sup>15</sup> known by its parasymphathomimetic activity.

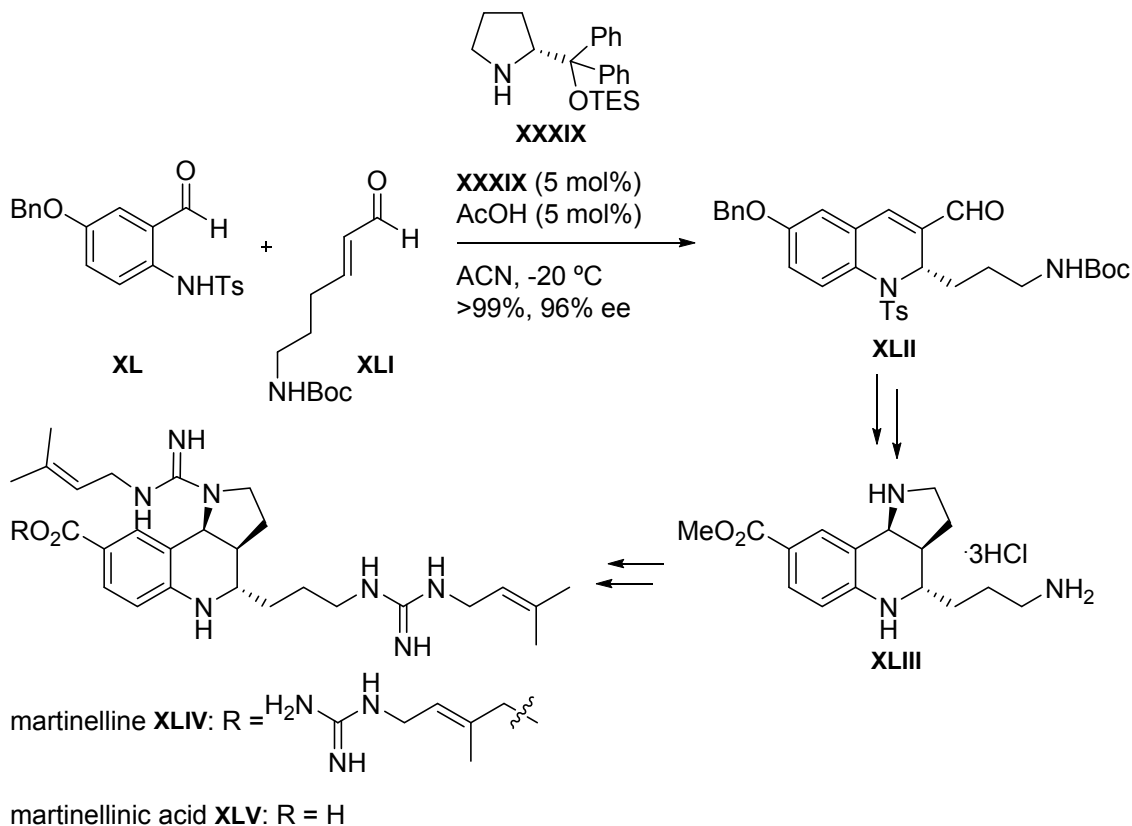


**Scheme 8.** (+)-Esermenthole **XXXVII** synthesis and formal synthesis of (+)-physostigmine **XXXVIII**.

### Michael-aldol cascade reaction

Pyrroloquinoline alkaloids martinelline **XLIV** and martinelic acid **XLV** are isolated from the *Martinella iquitosensis* tropical plant and show bradykinin receptor antagonist activity.<sup>16</sup> The organocatalytic Michael-aldol cascade reaction reported by Hamada and co-workers permitted the synthesis of the chiral martinellin core structure **XLIII**.<sup>17</sup> The tandem reaction took place between anthranilaldehyde **XL** and enal **XLI** under the influence of (*R*)-diphenylprolinol triethylsilyl ether **XXXIX** catalyst to provide dihydroquinoline **XLII** in quantitative yield and enantiocontrol (Scheme 9). The

martinelline chiral core structure **XLIII** was accomplished after 12 steps from **XLII** thus, reporting the formal synthesis of martinelline **XLIV** and martinellinic acid **XLV**.



**Scheme 9.** Formal synthesis of martinelline **XLIV** and martinellinic acid **XLV** via Michael-aldol cascade organocatalyzed reaction.

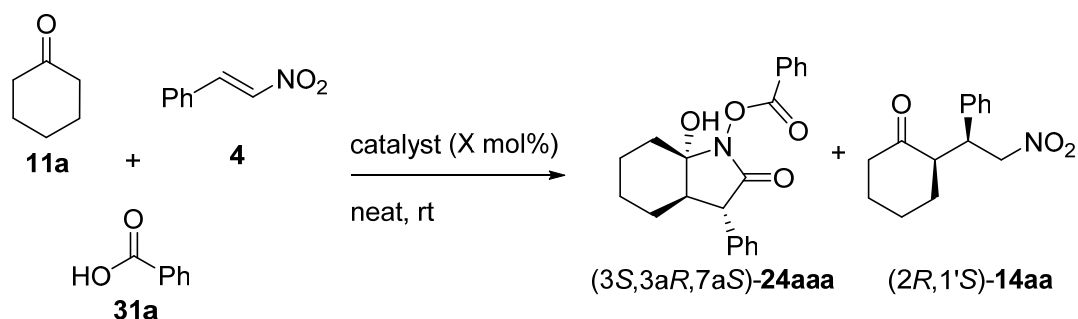
#### 4.1.2. Objectives

Due to the serendipitously isolated secondary 7a-hydroxy-2-oxo-3-phenyloctahydro-1*H*-indol-1-yl benzoate product during the Michael reaction described in the previous chapter, efforts to find the optimized reaction conditions will be pursued. Moreover, different substrates will be analyzed to assess the scope of this reaction. In addition, the reaction mechanism of the process will be tried to be unveiled. Lastly, attempts to derivatize the model lactam will be made in order to perform a total synthesis of the natural product (+)-pancreacine.

## 4.2. The discovery of an unprecedented cyclization reaction

### 4.2.1. Optimization studies

According to table 6 in chapter 3, the lactam product **24aaa** was always formed in diverse proportions under dimers **23a**, but always in conversions lower than 20%. Due to the fact that the employment of methylated dimers **25a** moved the Michael product:lactam **14aa:24aaa** ratio to 69:31, it was thought that the lactam product formation could be favoured by blocking one active site of the dimer or even be removing one catalytic unit. Therefore, the reaction between cyclohexanone **11a**, nitrostyrene **4a** and benzoic acid **31a** was tested under the three different generation catalysts. L-Proline **20** was used as the reference catalyst (Table 1).



**Scheme 10.** Model cyclization reaction.

Firstly, reactions between the cited components were carried at room temperature using 30 mol% of catalytic load. L-Proline did not produce any trace of lactam product and only gave the Michael adduct in 57% conversion after seven days of reaction at room temperature. In contrast, all three generations of densely substituted prolines were able to promote to some extent the cyclization reaction, bringing to light the great importance of the substituents in this kind of catalysts (Table 1, entry 1 vs. entries 2, 6-8, 10, 18).

**Table 1.** Reaction between *trans*- $\beta$ -nitrostyrene **4a**, cyclohexanone **11a** and benzoic acid **31a** catalyzed by different organocatalysts based on densely substituted prolines.<sup>a,b</sup>

entry	catalyst	catalyst (mol %)	time (h)	<b>24aaa:14aa</b> <sup>c</sup>	yield (%) <sup>d</sup>	ee (%) <sup>e</sup>
1	L-Pro <b>20</b>	30	7days	<1:99	- <sup>f</sup>	-
2	NO <sub>2</sub> -X <sub>L</sub> -OMe- <b>5aa</b>	30	72	>99:1	78 <sup>g</sup>	97
3 <sup>h</sup>	NO <sub>2</sub> -X <sub>L</sub> -OMe- <b>5aa</b>	30	16	>99:1	83	97
4 <sup>h</sup>	NO <sub>2</sub> -X <sub>L</sub> -OMe- <b>5aa</b>	20	24	>99:1	91	97
5 <sup>h</sup>	NO <sub>2</sub> -X <sub>L</sub> -OMe- <b>5aa</b>	10	60	>99:1	88	97
6	NO <sub>2</sub> -N <sub>D</sub> -OMe- <b>5aa</b>	30	72	>99:1	- <sup>i</sup>	50
7	NH <sub>2</sub> -X <sub>D</sub> -OMe- <b>10aa</b>	30	16	33:67	20	-90
8	NO <sub>2</sub> -X <sub>L</sub> X <sub>L</sub> -OMe- <b>23a</b>	30	12	29:71	-	-
9 <sup>j</sup>	NO <sub>2</sub> -X <sub>L</sub> X <sub>L</sub> -OMe- <b>23a</b>	30	12	28:72	-	-
10	NO <sub>2</sub> -X <sub>L</sub> X <sub>L</sub> -OMe- <b>25a</b>	30	12	56:44	51	>99
11 <sup>k</sup>	NO <sub>2</sub> -X <sub>L</sub> X <sub>L</sub> -OMe- <b>25a</b>	30	12	54:46	50	>99
12	NO <sub>2</sub> -X <sub>L</sub> X <sub>L</sub> -OMe- <b>25a</b>	20	16	69:31	57	>99
13	NO <sub>2</sub> -X <sub>L</sub> X <sub>L</sub> -OMe- <b>25a</b>	15	24	66:34	62	>99
14	NO <sub>2</sub> -X <sub>L</sub> X <sub>L</sub> -OMe- <b>25a</b>	10	48	70:30	62	>99
15	NO <sub>2</sub> -X <sub>L</sub> X <sub>L</sub> -OMe- <b>25a</b>	5	7days	64:36	- <sup>l</sup>	-
16 <sup>m</sup>	NO <sub>2</sub> -X <sub>L</sub> X <sub>L</sub> -OMe- <b>25a</b>	10	48	69:31	63	>99
17 <sup>n</sup>	NO <sub>2</sub> -X <sub>L</sub> X <sub>L</sub> -OMe- <b>25a</b>	10	48	70:30	61	>99
18	NO <sub>2</sub> -X <sub>D</sub> X <sub>L</sub> -OMe- <b>25a</b>	30	12	78:22	64	<-99
19	NO <sub>2</sub> -X <sub>D</sub> X <sub>L</sub> -OMe- <b>25a</b>	20	16	73:27	65	<-99
20	NO <sub>2</sub> -X <sub>D</sub> X <sub>L</sub> -OMe- <b>25a</b>	15	24	76:24	63	<-99
21	NO <sub>2</sub> -X <sub>D</sub> X <sub>L</sub> -OMe- <b>25a</b>	10	48	79:21	64	<-99
22	NO <sub>2</sub> -X <sub>D</sub> X <sub>L</sub> -OMe- <b>25a</b>	5	7days	71:29	- <sup>o</sup>	-
23 <sup>h</sup>	NO <sub>2</sub> -X <sub>D</sub> X <sub>L</sub> -OMe- <b>25a</b>	5	72	68:32	57	<-99
24 <sup>p</sup>	NO <sub>2</sub> -X <sub>D</sub> X <sub>L</sub> -OMe- <b>25a</b>	10	48	71:29	60	<-99

<sup>a</sup>Reactions were conducted under neat conditions using cyclohexanone (0.8 mmol), *trans*- $\beta$ -nitrostyrene (0.1 mmol) and benzoic acid (0.11 mmol) in the presence of the corresponding amount of catalyst. <sup>b</sup>Reactions were monitored by <sup>1</sup>H NMR and stirred at room temperature until consumption of the starting material. <sup>c</sup>**24aaa:14aa** ratios were measured by <sup>1</sup>H NMR on crude reaction mixtures. <sup>d</sup>Yields refer to isolated pure lactam. <sup>e</sup>Enantiomeric excesses measured by HPLC. <sup>f</sup>57% conversion to **14aa**. <sup>g</sup>92% conv. <sup>h</sup>Performed at 45 °C. <sup>i</sup>35% conv. <sup>j</sup>Performed with 2 eq of benzoic acid (0.2 mmol). <sup>k</sup>Performed with 1.5 eq of benzoic acid (0.15 mmol). <sup>l</sup>85% conv. <sup>m</sup>Performed under an inert atmosphere of argon. <sup>n</sup>Performed in the absence of light. <sup>o</sup>73% conv. <sup>p</sup>CH<sub>2</sub>Cl<sub>2</sub> (150  $\mu$ l) as solvent and 4 eq of cyclohexanone.

The first generation or nitro-prolines **5aa** exclusively produced lactam **24aaa** (entries 2 and 6). Nevertheless, a large influence in the reaction rate and enantioselectivity was observed depending upon the different configuration of the catalysts. Thus, exo-

NO<sub>2</sub>-X<sub>L</sub>-OMe-**5aa** provided higher conversion and almost full enantiocontrol, whilst *endo*-NO<sub>2</sub>-N<sub>D</sub>-OMe-**5aa** only reached 35% conversion with a 50% of enantiomeric excess, both after three days of reaction time. In the case of second generation amino proline NH<sub>2</sub>-X<sub>D</sub>-OMe-**10aa** catalyst, lactam **24aaa** was observed in a much lower **24aaa:14aa** ratio of 33:67 with an enantiomeric excess of 90% (entry 7). Moving to the third generation of *N*-methylated organocatalysts, NO<sub>2</sub>-X<sub>L</sub>X<sub>L</sub>-OMe-**25a** and NO<sub>2</sub>-X<sub>D</sub>X<sub>L</sub>-OMe-**25a** dimers turned out to be more efficient as they promoted chiefly the lactam product whereas non-*N*-methylated NO<sub>2</sub>-X<sub>L</sub>X<sub>L</sub>-OMe-**23a** dimer produced mainly the Michael adduct (entry 8 vs. 10 and 18). These three catalysts provided the lactam **24aaa** with total enantiocontrol. In these reactions, the enantiocontrol was determined by the proline unit bearing the nitro substituent.

With these initial results in hand, a deeper study was focused on NO<sub>2</sub>-X<sub>L</sub>-OMe-**5aa**, NO<sub>2</sub>-X<sub>L</sub>X<sub>L</sub>-OMe-**25a** and NO<sub>2</sub>-X<sub>D</sub>X<sub>L</sub>-OMe-**25a** catalysts as they promoted the best results. Monomeric catalyst NO<sub>2</sub>-X<sub>L</sub>-OMe-**5aa** promoted the desired transformation in acceptable reaction times when the temperature was raised to 45 °C without significant loss in the enantiocontrol (entries 3 to 5). *N*-methylated NO<sub>2</sub>-X<sub>L</sub>X<sub>L</sub>-OMe-**25a** and NO<sub>2</sub>-X<sub>D</sub>X<sub>L</sub>-OMe-**25a** catalysts also were very efficient and furnished the desired lactam in good yield and excellent enantiomeric excesses even with 10 mol% of catalytic load. In all cases, NO<sub>2</sub>-X<sub>D</sub>X<sub>L</sub>-OMe-**25a** catalysts provided higher **24aaa:14aa** ratios (entries 12 to 14 vs. 19 to 21). A catalytic load of 5 mol% did not allow the reaction to reach completion (entries 15 and 22). When the temperature was raised to 45 °C, full conversion was achieved at the cost of a lower **24aaa:14aa** ratio (entry 23).

Increasing the number of benzoic acid up to two equivalents did affect the lactam:Michael adduct ratio when the dimeric catalysts were used (entries 8 vs. 9 and 10 vs. 11). Besides, the presence of solvent, air oxygen or light had no effect in the process outcome as the results were similar to those obtained under standard conditions (entries 16, 17 and 24). Regarding the enantiocontrol given by the dimers, it was found to depend on the configuration of the monomeric unit bearing the nitro group. Thus, NO<sub>2</sub>-X<sub>L</sub>X<sub>L</sub>-OMe-**25a** and NO<sub>2</sub>-X<sub>D</sub>X<sub>L</sub>-OMe-**25a** provided opposite enantiomers with complete stereocontrol (entries 10 vs. 18).

Lactam **24aaa** easily crystallized out of the NMR sample in deuterated chloroform solvent, although ethyl acetate/hexane is also a good solvent mixture for its crystallization. This permitted the study of its absolute configuration by means of X ray diffraction analysis (Figure 1). The lactam obtained under catalysis of NO<sub>2</sub>-X<sub>L</sub>X<sub>L</sub>-OMe-**25a**  $\gamma$ -dipeptide catalysts was determined as (3*S*,3*aR*,7*aS*). It is

remarkable that the absolute configuration of the positions C3 and C3a coincide with the absolute configuration of the positions C2 and C1' of the Michael adduct, under the same catalysts effect (Scheme 11).

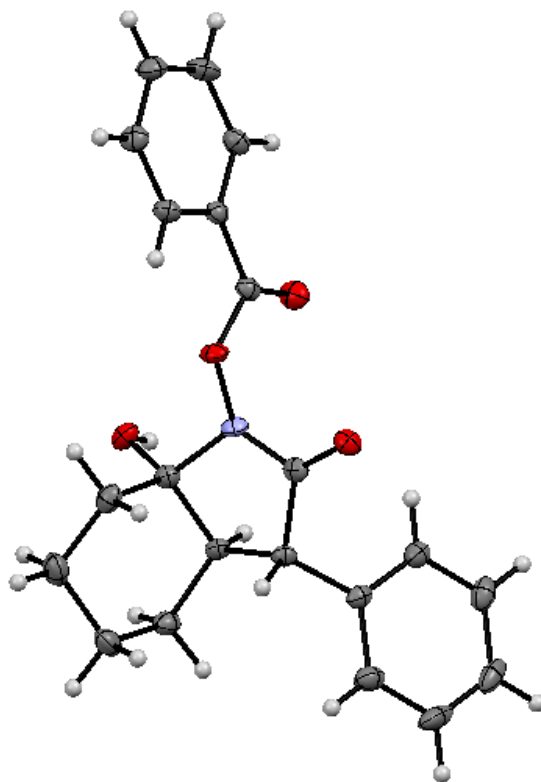
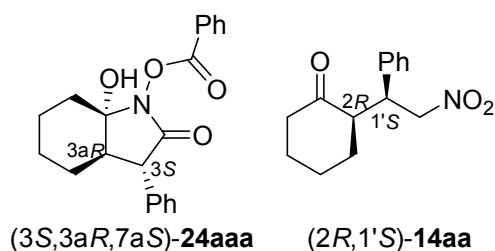


Figure 1. ORTEP drawing of (3*S*,3*aR*,7*aS*)-**9aaa**.

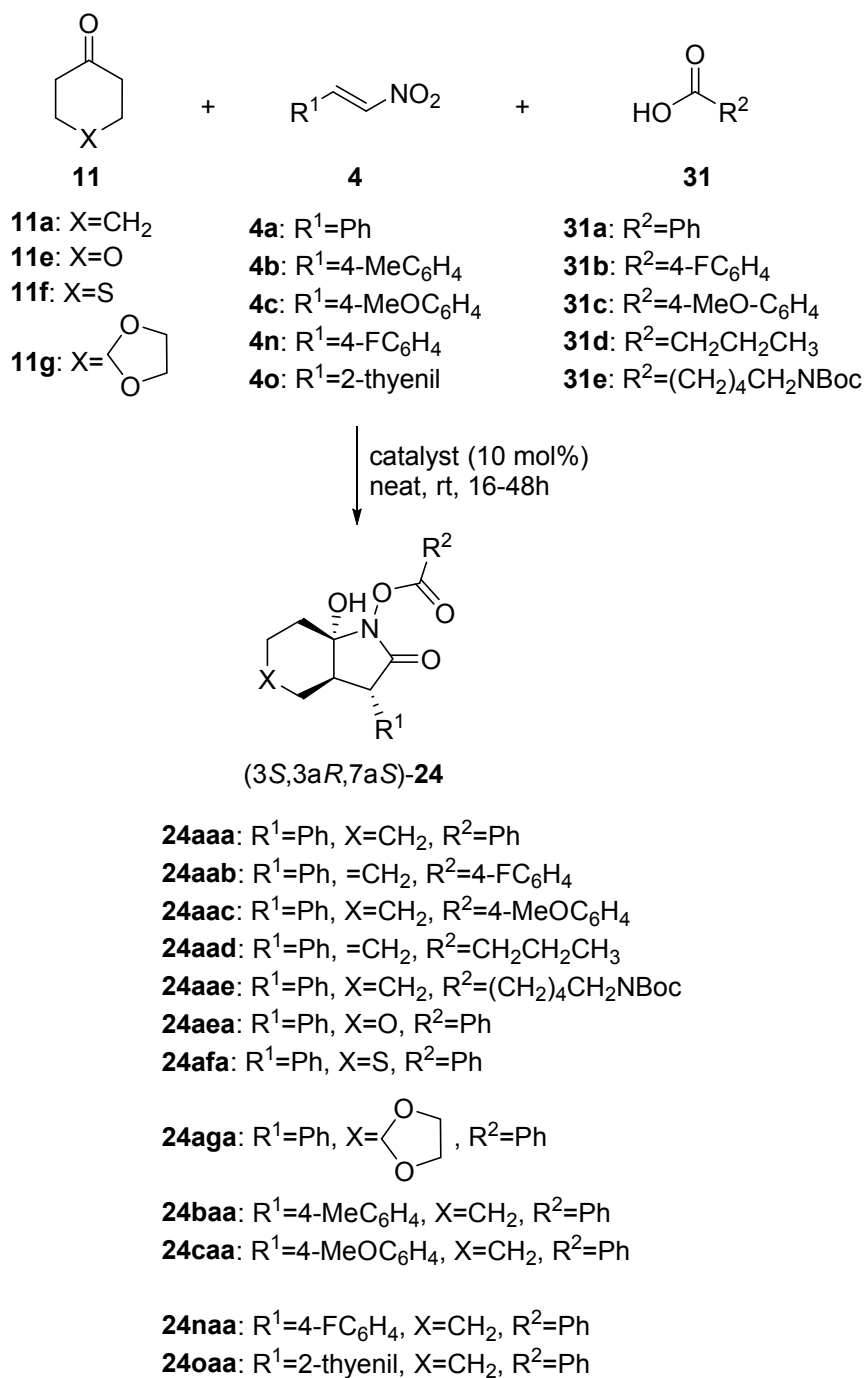


Scheme 11. Comparison of the absolute configuration of the lactam **24aaa** and Michael adduct **14aa** obtained under the influence of NO<sub>2</sub>-X<sub>L</sub>X<sub>L</sub>-OMe-**25a**.

#### 4.2.2. Scope

The three best catalysts NO<sub>2</sub>-X<sub>L</sub>-OMe-**5aa**, NO<sub>2</sub>-X<sub>L</sub>X<sub>L</sub>-OMe-**25a** and NO<sub>2</sub>-X<sub>D</sub>X<sub>L</sub>-OMe-**25a**, were tested in order to analyze the versatility and scope of the reaction. Different

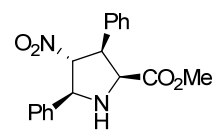
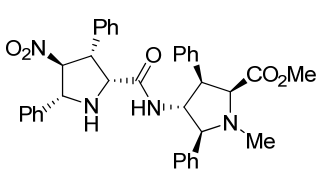
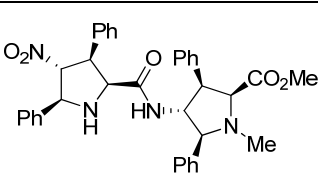
aromatic ketones **11**, nitroalkenes **4**, and acids **31** were used (Scheme 12) and the results obtained are shown in Table 2.



**Scheme 12.** Reaction between different ketones **11**, nitroalkenes **4** and acids **31** catalyzed by NO<sub>2</sub>-X<sub>L</sub>-OMe-**5aa**, NO<sub>2</sub>-X<sub>L</sub>X<sub>L</sub>-OMe-**25a** and NO<sub>2</sub>-X<sub>D</sub>X<sub>L</sub>-OMe-**25a**.



**Table 2.** Stereocontrol and chemical yield observed in the reaction **11+4+31** → **24** catalyzed by NO<sub>2</sub>-X<sub>L</sub>-OMe-**5aa**, NO<sub>2</sub>-X<sub>L</sub>X<sub>L</sub>-OMe-**25a** and NO<sub>2</sub>-X<sub>D</sub>X<sub>L</sub>-OMe-**25a**.<sup>a</sup>

entry	catalyst	lactam <b>24</b>	<b>24:14</b> <sup>b</sup>	yield (%) <sup>c</sup>	ee (%) <sup>d</sup>	
1 <sup>e</sup>		<b>24aab</b>	>99:1	81	97	
2 <sup>e</sup>		<b>24aac</b>	>99:1	86	97	
3 <sup>e,f</sup>		<b>24aad</b>	>99:1 <sup>g</sup>	38	96	
4 <sup>e</sup>		<b>24aae</b>	>99:1	58	96	
5 <sup>e</sup>	 NO <sub>2</sub> -X <sub>L</sub> -OMe- <b>5aa</b>	<b>24aea</b>	>99:1	56 <sup>h</sup>	95	
6 <sup>e,i</sup>		<b>24afa</b>	>99:1	71	97	
7 <sup>e,i</sup>		<b>24aga</b>	>99:1	62	95	
10 <sup>e</sup>		<b>24baa</b>	>99:1	65	95	
9 <sup>e</sup>		<b>24caa</b>	>99:1	66	95	
8 <sup>e</sup>		<b>24naa</b>	>99:1	86	97	
11 <sup>e</sup>		<b>24oaa</b>	>99:1	67	96	
12			<b>24aab</b>	75:25	69	<-99
13			<b>24aac</b>	75:25	66	-99
14			<b>24aad</b>	70:30	62	<-99
15			<b>24aae</b>	70:30	53	<-99
16	 NO <sub>2</sub> -X <sub>D</sub> X <sub>L</sub> -OMe- <b>25a</b>	<b>24aea</b>	80:20	68	<-99	
17 <sup>i</sup>		<b>24afa</b>	83:17	68	<-99	
18 <sup>i</sup>		<b>24aga</b>	98:2	73	-98	
19		<b>24baa</b>	79:21	60	<-99	
20		<b>24caa</b>	84:16	60	<-99	
21		<b>24naa</b>	76:24	54	<-99	
22		<b>24oaa</b>	81:19	67	<-99	
23	 NO <sub>2</sub> -X <sub>L</sub> X <sub>L</sub> -OMe- <b>25a</b>	<b>24aab</b>	62:38	50	>99	
24		<b>24aac</b>	61:39	53	>99	
25		<b>24aae</b>	68:32	48	>99	
26		<b>24caa</b>	66:34	48	>99	
27		<b>24naa</b>	60:40	44	>99	

<sup>a</sup>Reactions were monitored by <sup>1</sup>H NMR and stirred at room temperature until consumption of the starting material. <sup>b</sup>**24:14** ratio was measured by <sup>1</sup>H NMR of crude reaction mixtures. <sup>c</sup>Yields refer to isolated pure lactam. <sup>d</sup>Enantiomeric excesses measured by HPLC correspond to the major lactam (3*S*,3*aR*,7*aS*)-**24**. <sup>e</sup>Performed with 20 mol% of catalysts at 45 °C. <sup>f</sup>Reaction performed with 2 eq of butyric acid **31d**. <sup>g</sup>Other diastereoisomer was observed (75:25 ratio). <sup>h</sup>60% conv. after 4 days. <sup>i</sup>Carried out using 4 eq of ketone **7f** and DCM as solvent.

Results show that when the reaction was carried out in the presence of 20 mol% of monomeric catalyst NO<sub>2</sub>-X<sub>L</sub>-OMe-**5aa** at 45 °C, only lactams **24** were obtained with high enantiomeric excesses (95-97% ee) independently of the nitroalkene, ketone or

acid used (entries 1-11). It is important to mention that such a catalytic load of 20 mol% was necessary because when 10 mol% of catalyst was employed (see Table 1 entry 5) longer reaction time was required. Additionally, this increase on the load was not enough when butyric acid **31d** was employed, as 2 equivalents of the acid were required in order to complete the reaction (entry 3). Also, the use of tetrahydro-4*H*-pyran-4-one **11e** in the reaction only reached 60% conversion after four days (entry 5).

On the other hand, when dimeric NO<sub>2</sub>-X<sub>L</sub>X<sub>L</sub>-OMe-**25a** and NO<sub>2</sub>-X<sub>D</sub>X<sub>L</sub>-OMe-**25a** catalysts were used in 10 mol% of catalytic load, quantitative conversions and total enantioselectivities were achieved in all cases. The only exception was provided by ketone **11g** which gave 98% of ee (entry 18). However, formation of the corresponding Michael adducts was also observed in different ratios depending on the reagents used (entries 12 to 27). When introducing both electron donating or withdrawing groups in the aromatic ring of benzoic acid, no significant effect was observed since good **24:14** ratios and moderate to good yields were obtained (entries 12-13 and 23-24) in all cases. When aliphatic acid **31d** or *N*-protected aminoacid **31e** were used, the lactam:Michael adduct ratios were reduced with NO<sub>2</sub>-X<sub>D</sub>X<sub>L</sub>-OMe-**25a** catalyst (entries 14 and 15). However, this ratio with **31e** increased in combination with NO<sub>2</sub>-X<sub>L</sub>X<sub>L</sub>-OMe-**25a** catalyst (entry 25). The introduction of cyclic ketones bearing heteroatoms as **11e** and **11f** produced a raise in the **24:14** ratio with good yields and complete enantiocontrol (entries 16 and 17). As mentioned, 1,4-cyclohexanedione monoethylene acetal **11e** provided almost complete selectivity towards the lactam product in spite of slightly lower enantiocontrol (entry 18). The use of aryl or heteroaryl substituted nitroalkenes led to the corresponding enantiopure lactams in moderate to good **24:14** ratios and yields (entries 19 to 22, 26 and 27). The introduction of the methoxy electron releasing group in the aromatic ring provided the highest **24:14** ratio obtained for the dimeric catalysts (entry 20). Finally, regardless of the reagent used, the **24:14** ratio was always higher when employing NO<sub>2</sub>-X<sub>D</sub>X<sub>L</sub>-OMe-**25a** catalysts instead of NO<sub>2</sub>-X<sub>L</sub>X<sub>L</sub>-OMe-**25a** (entries 12-22 vs. 23-27).

Once again, the lactam configuration was confirmed by X ray diffraction analysis. Figure 2 shows the (3*S*,3*aR*,7*aS*) absolute configuration of **24aae** lactam that was obtained with NO<sub>2</sub>-X<sub>L</sub>X<sub>L</sub>-OMe-**25a** catalyst (entry 25).

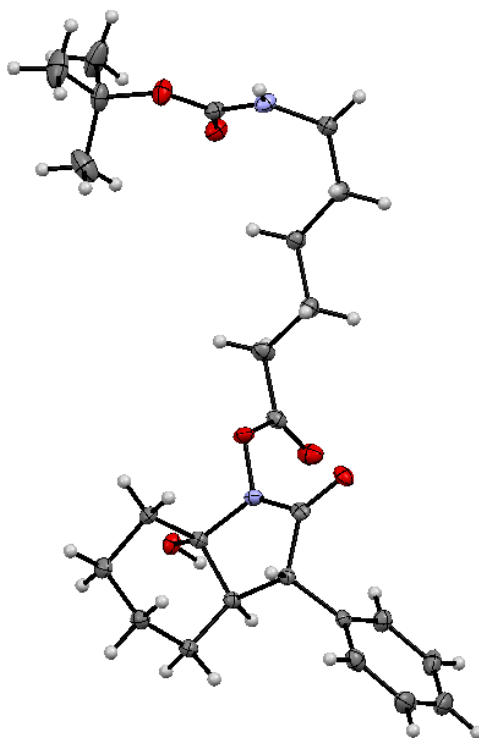


**Figure 2.** ORTEP diagram of (3*S*,3*aR*,7*aS*)-**24aae** lactam.

Apart from different carboxylic acids **31**, thiobenzoic acid **32** was also employed in the process with the purpose to get some experimental information about the reaction mechanism (Figure 3). Neither NO<sub>2</sub>-X<sub>L</sub>-OMe-**5aa** (30 mol%) catalyst at 45 °C nor NO<sub>2</sub>-X<sub>D</sub>X<sub>L</sub>-OMe-**25a** (20 mol%) provided any conclusive result, as the consumption of nitrostyrene did not allow the isolation of any Michael or cyclization product. Monomer NO<sub>2</sub>-X<sub>L</sub>-OMe-**5aa** at 45 °C (20 mol%) in the presence of 4-nitrophenol **33** gave 40% conversion to **14aa** after one day whereas NO<sub>2</sub>-X<sub>D</sub>X<sub>L</sub>-OMe-**25a** in 10 mol% only provided 40% conversion towards the Michael product **14aa**. Lastly, other acids of diverse nature were tested such as diphenylphosphinic acid **34**, methylphosphonic acid **35** or dimethylphosphate **36**. When phosphinic acid **34** was employed in the presence of 10 or 20 mol% of either NO<sub>2</sub>-X<sub>L</sub>-OMe-**5aa**, NO<sub>2</sub>-X<sub>L</sub>X<sub>L</sub>-OMe-**25a** or NO<sub>2</sub>-X<sub>D</sub>X<sub>L</sub>-OMe-**25a**, only Michael product was formed after four days of reaction time. The same outcome was observed when using phosphonic acid **12** together with NO<sub>2</sub>-X<sub>D</sub>X<sub>L</sub>-OMe-**4a**. The case of NO<sub>2</sub>-X<sub>D</sub>X<sub>L</sub>-OMe-**4a**/dimethyl phosphate **13** provided the Michael adduct with other side products after 3 days of reaction time but the conversion did not exceed the 30%.

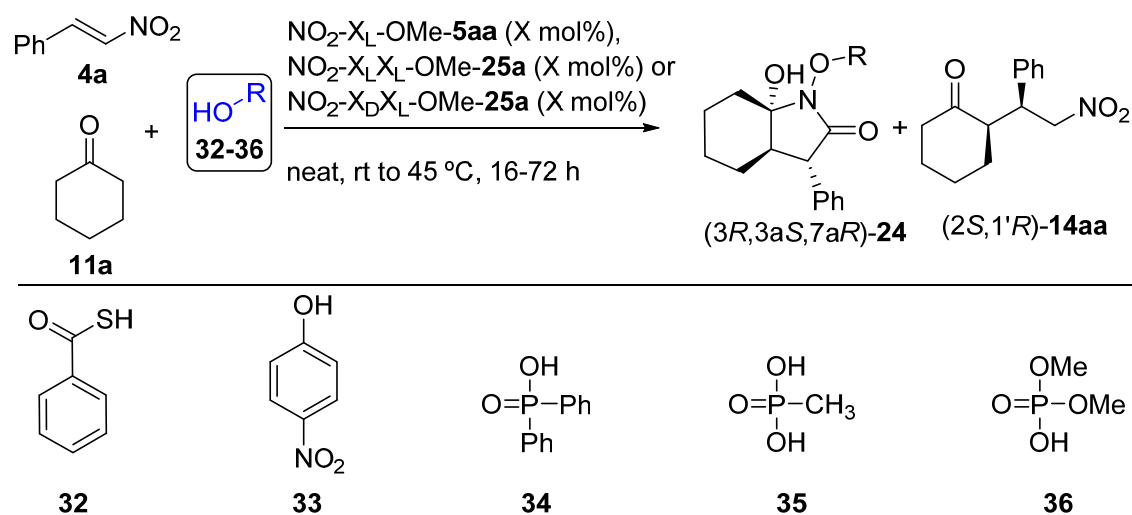


**Figure 3.** Other acids studied in the reaction between cyclohexanone **11a** and nitrostyrene **4a** with catalysts  $\text{NO}_2\text{-X}_L\text{-OMe-5aa}$ ,  $\text{NO}_2\text{-X}_L\text{X}_L\text{-OMe-25a}$  and  $\text{NO}_2\text{-X}_D\text{X}_L\text{-OMe-25a}$ .

Finally, cyclopentanone **11b** and pentanone **11h** were analyzed to study the influence of the chain nature (Figure 4). In the case of using monomer  $\text{NO}_2\text{-X}_L\text{-OMe-5aa}$  (20 mol%) at 45 °C, cyclopentanone **11b** only provided product **14** in conversions lower than 20% while pentanone **11h** did not give traces of Michael or lactam product.

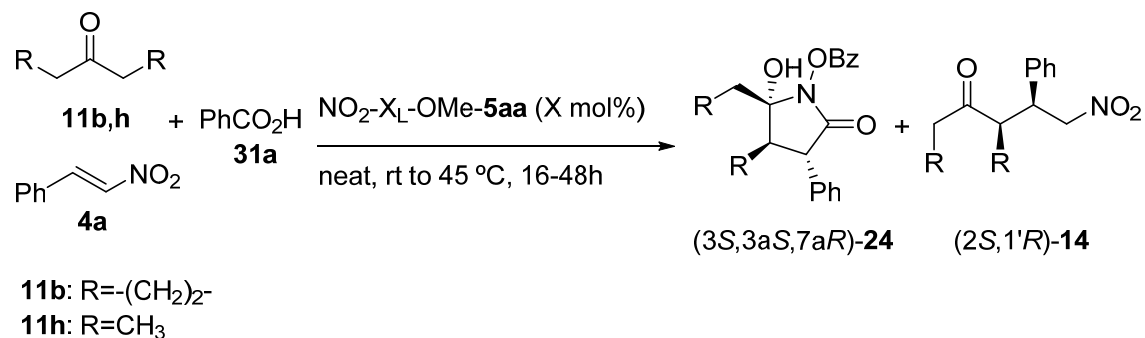
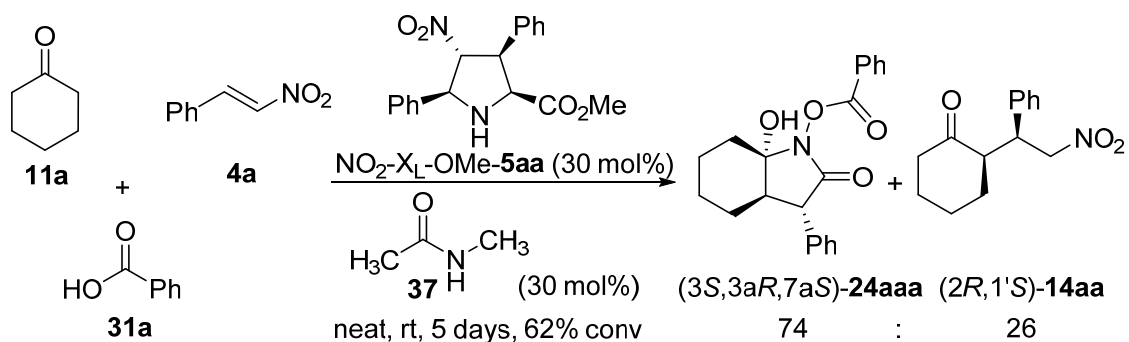


**Figure 4.** Other analyzed ketones in the reaction between nitrostyrene **4a** and benzoic acid **31a** with  $\text{NO}_2\text{-X}_L\text{-OMe-5aa}$  catalyst.

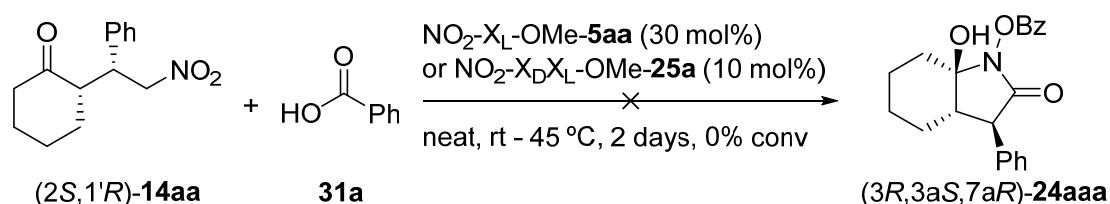
### 4.3. Searching for the reaction mechanism

In order to try to understand the major selectivity towards the lactam formation with  $\text{NO}_2\text{-X}_L\text{-OMe-5aa}$  monomer with respect  $\text{NO}_2\text{-X}_L\text{X}_L\text{-OMe-25a}$  and  $\text{NO}_2\text{-X}_D\text{X}_L\text{-OMe-25a}$  dimers, the reaction was carried out with the former catalyst in the presence of *N*-methylacetamide **37** as additive (Scheme 13). This reaction produced the lactam **24aaa** as well as the Michael addition product in 74:26 ratio. This result could indicate that the absence of the peptidic bond in the catalyst of first generation is responsible for the unique formation of the lactam product **24aaa**.



**Scheme 13.** Reaction between cyclohexanone **11a**, nitrostyrene **4a** and benzoic acid **31a** in the presence of  $\text{NO}_2\text{-X}_\text{L}\text{-OMe-5aa}$  catalyst and *N*-methylacetamide **37**.

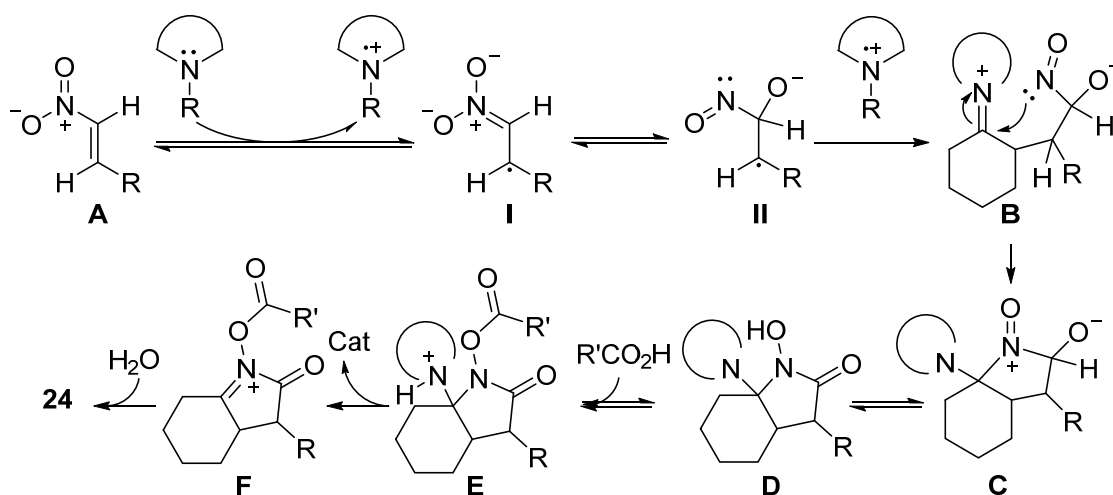
To verify the multicomponent nature of this process, a second reaction involving the Michael addition product was tested under the standard reaction conditions with benzoic acid **31a** employing the catalysts  $\text{NO}_2\text{-X}_\text{L}\text{-OMe-5aa}$  and  $\text{NO}_2\text{-X}_\text{D}\text{X}_\text{L}\text{-OMe-25a}$  (Scheme 14). This process did not show any formation of lactam **24**, thus confirming that the lactam formation is not a stepwise procedure arising from the released Michael adduct.



**Scheme 14.** Reaction between the Michael addition product **14aa** and benzoic acid **31a** in the presence of  $\text{NO}_2\text{-X}_\text{L}\text{-OMe-5aa}$  and  $\text{NO}_2\text{-X}_\text{D}\text{X}_\text{L}\text{-OMe-25a}$  catalysts.

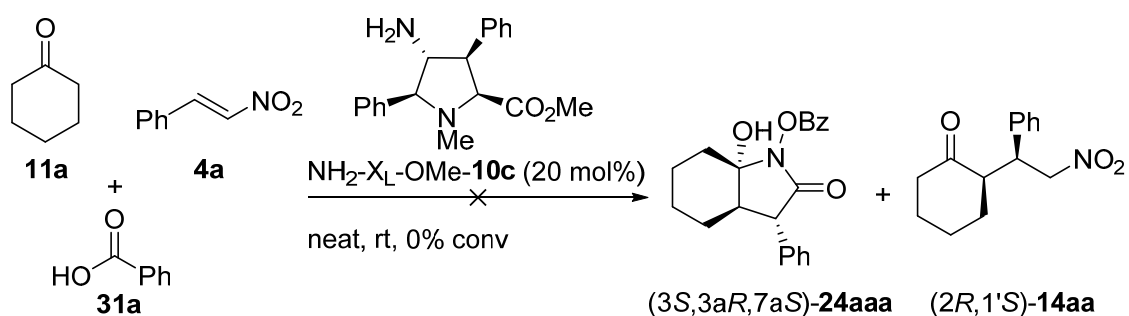
#### 4.3.1. Mechanistic proposal based on a stepwise radical lactamization reaction

On the basis of these results, the search for a plausible mechanism was oriented towards a radical pathway, based on a possible participation of nitroalkene anion radicals<sup>18</sup> (**I** and **II**) generated in the presence of tertiary amines (Scheme 15). Via single electron transfer reduction, the catalyst can add an electron to the nitroalkene to form radical anion **I** which can tautomerize to form the radical cation **II**. The catalyst's radical cation condensates with cyclohexanone which then adds to **II** to give intermediate **B**. The nitroso group then adds to the iminium moiety to provide **C** which tautomerizes giving 1-hydroxypyrrolidinone **D**. Then, the addition of the carboxylic acid **31** gives the protonated intermediate **E**, and catalyst release provides pyrrolium intermediate **F**. Last addition of a molecule of water should lead to the formation of the observed product **24**.



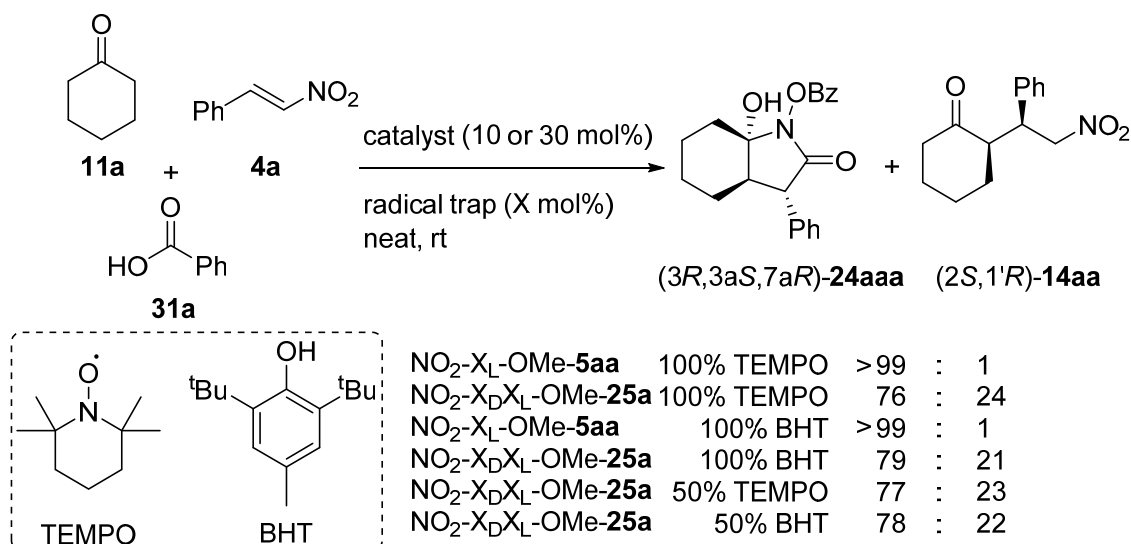
**Scheme 15.** Proposed radical reaction mechanism.

In order to assess the viability of a radical mechanism, the model reaction between **11a**, **4a** and **31a** was carried out catalyzed by  $\text{NH}_2\text{-X}_\text{L}\text{-OMe-10c}$  possessing a tertiary amine in the pyrrolidine scaffold. No product of any kind was observed under these conditions (Scheme 16).



**Scheme 16.** Model reaction between **11a**, **4a** and **31a** in the presence of  $\text{NH}_2\text{-X}_\text{L}\text{-OMe-10c}$ .

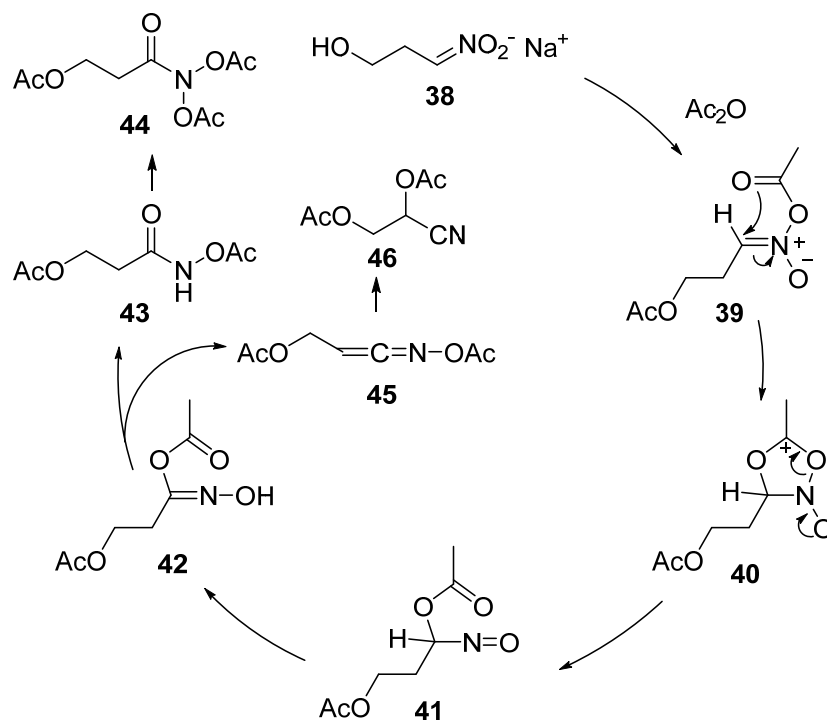
Thus, it was decided to employ radical scavengers in the model reaction (Scheme 17). It was observed that in the presence of different equivalents of either BHT or TEMPO, the cyclization and Michael addition products were obtained in similar ratios to those observed when these reactions were run in the absence of the mentioned agents (see Table 1). On the basis of these experimental results, the proposed radical mechanism was discarded.



**Scheme 17.** Model reaction employing the catalysts NO<sub>2</sub>-X<sub>L</sub>-OMe-**5aa** and NO<sub>2</sub>-X<sub>D</sub>X<sub>L</sub>-OMe-**25a** in the presence of TEMPO or BHT radical scavengers.

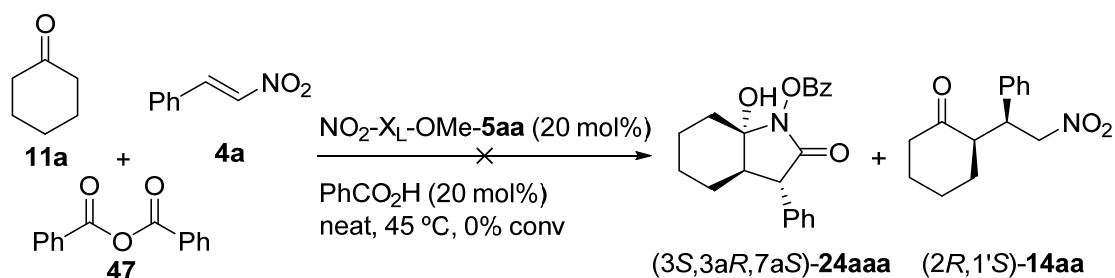
#### 4.3.2. Mechanistic proposal based on sigmatropic rearrangements

The group of Román *et al.* reported the acetylation of nitronates derived from primary or secondary nitroalkanes bearing hydroxy groups.<sup>19</sup> The authors proposed the reaction mechanism gathered in Scheme 18. According to this proposal, sodium nitronate salt **38** would react to form the mixed carboxylic-nitronic anhydride **39** which could be subjected to a N→C acetate migration to produce nitrosoderivative **41**, probably through the cyclic intermediate **40**. This latter intermediate could tautomerize to oxime **42**. Finally, an intramolecular rearrangement would lead to the hydroxamic acid derivative **43** that in turn could be acetylated to yield the final product **44**. A secondary product formed by 1,2-elimination was also proposed by the authors to give O-acyl ketene oxime **45**, precursor of nitrile **46**.



**Scheme 18.** Proposed reaction mechanism by Román *et al.* for the acetylation of nitronates (see reference 19).

In order to assess the possible participation of a related mechanism in the reaction between cyclohexanone **11a**, nitrostyrene **4a** and benzoic anhydride **47**, this process was carried out in the presence of  $\text{NO}_2\text{-X}_\text{L}\text{-OMe-5aa}$  and benzoic acid as additive (Scheme 19). Nevertheless, this reaction did not lead to any kind of cyclization or Michael addition product after 4 days of reaction time.

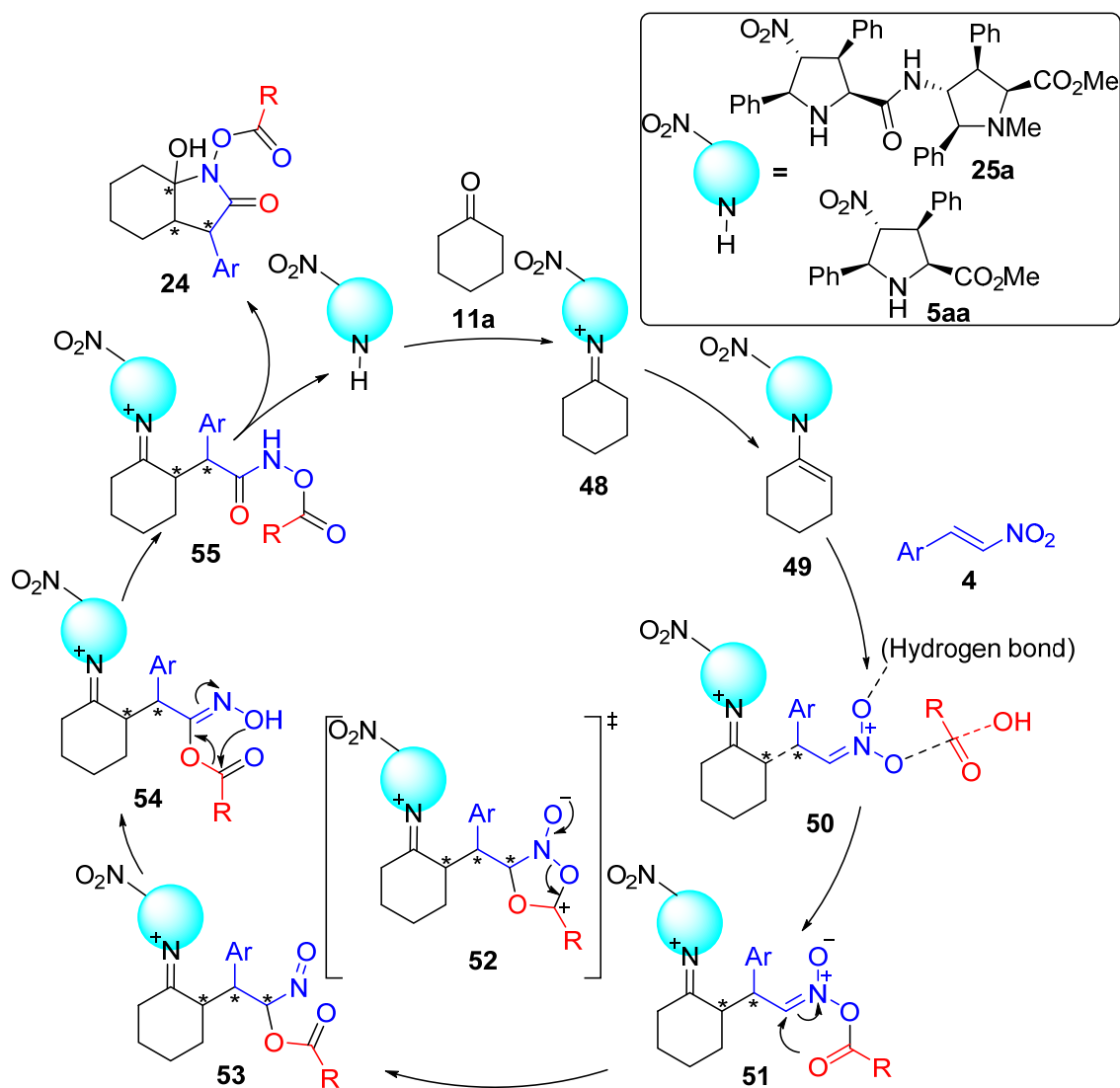


**Scheme 19.** Reaction between cyclohexanone **11a**, nitrostyrene **4a** and benzoic anhydride **47** in the presence of  $\text{NO}_2\text{-X}_\text{L}\text{-OMe-5aa}$  catalyst and benzoic acid as additive.

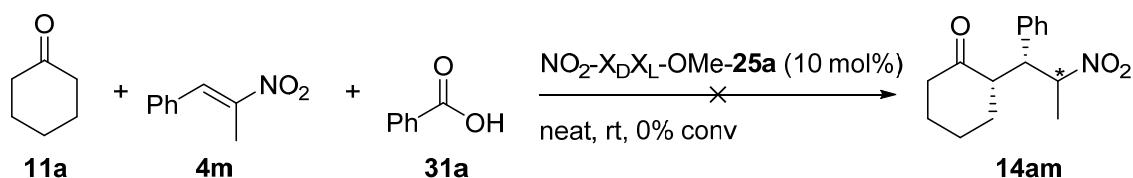
However, based on these mechanistic studies and supported by our experimental results, the mechanism depicted in Scheme 20 was postulated. First of all, the catalyst interacts with ketone **11a** to produce nucleophilic enamine intermediate **49**. Nucleophilic addition to nitroalkene **4**, produces (as proposed before) the carboxylic-nitronic anhydride **51**. This, via carbocationic intermediate **52** would perform the  $\text{N} \rightarrow \text{C}$  benzoate migration to yield the nitrosoderivative **53**. Tautomerization to



oxime **54**, followed by another rearrangement would give hydroxamic acid derivative **55** which could perform the last nucleophilic attack onto the iminium to release the cyclization product **24** and recover the catalyst for a new cycle. Alternatively, the release of catalyst could take place from **55** to yield the ketone form, from which the nucleophilic attack in the carbonyl group could form **24**. The feasibility of this mechanism is under study in our laboratory.



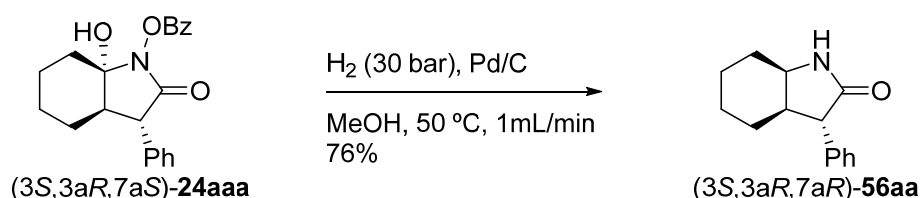
A last experiment was carried out in order to shed some light on the nature of the reaction mechanism. For that purpose nitroalkene **4m** was employed because it would not allow the rearrangement shown in Scheme 20 and maybe, an intermediate type **53** could be isolated. Therefore, cyclohexanone **11a**, nitroalkene **4m** and benzoic acid **31a** were allowed to react in the presence of NO<sub>2</sub>-X<sub>D</sub>X<sub>L</sub>-OMe-**25a** catalyst. Not only the formation of the lactam was impeded but also no Michael product was obtained.



**Scheme 21.** Reaction between cyclohexanone **11a**, nitroalkene **4m** and benzoic acid **31a** in the presence of  $\text{NO}_2\text{-X}_D\text{X}_L\text{-OMe-25a}$  catalyst.

#### 4.4. Follow up chemistry. Hydrogenation

In order to explore to the versatility of these new compounds, a catalytic hydrogenation reaction was of choice. It was performed onto the *N*-benzoyloxylactam (3*S*,3*aR*,7*aS*)-**24aaa** in a flow reactor at 50 °C employing a Pd/C heterogeneous catalyst. This reaction gave lactam **56aa** as the sole product in 76% yield (Scheme 22).



**Scheme 22.** Catalytic hydrogenation onto the *N*-benzoyloxylactam (3*S*,3*aR*,7*aS*)-**24aaa** substrate.

The absolute configuration of bicyclic  $\gamma$ -lactam **56aa** was determined by X ray diffraction analysis. The structure shows that both fused cycles are in *cis*-disposition (Figure 5).

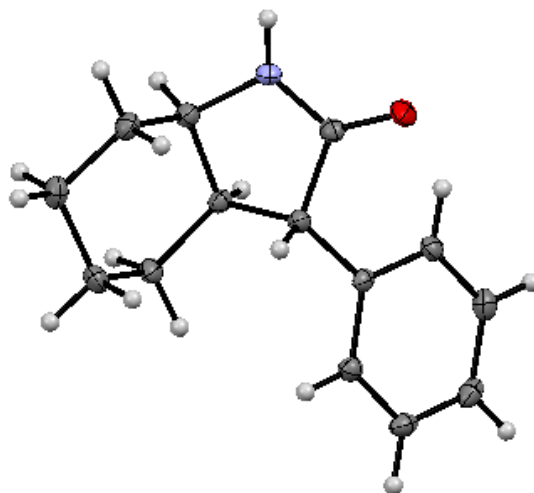


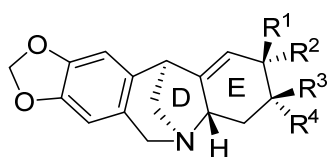
**Figure 5.** ORTEP drawing of  $(3S,3aR,7aR)\text{-56aa}$ .

From these results it can be concluded that the structural diversity of densely substituted proline derivatives confers new catalytic properties on these compounds. Not only the densely substituted pyrrolidines **5aa** have been able to construct lactams **24** in a selective manner, but also  $\gamma$ -dipeptides NO<sub>2</sub>-X<sub>L</sub>X<sub>L</sub>-OMe-**25a** and NO<sub>2</sub>-X<sub>D</sub>X<sub>L</sub>-OMe-**25a** promoted the reaction with a reduced catalytic load and with full enantiocontrol, at the expense of a lower chemoselectivity. If a reduction would be possible on the hydrogenated substrate **56aa**, then, it will open a door to synthesize a large variety of enantiopure 3-aryl octahydroindoles.

#### 4.5. Total and formal syntheses of pancracine alkaloid

(-)-Pancracine **57** belongs to the montanine-type *Amaryllidaceae* alkaloids<sup>20</sup> and incorporates a pentacyclic 5,11-methanomorphanthridine nucleus in its structure. The first members of these alkaloids, such as (-)-pancracine **57**, (-)-montanine **58**, (-)-manthine **59**, (-)-coccinine **60** or (-)-brunsvigine **61**, differing only in the stereochemistry of the C2 and C3 oxygen substituents at the E ring<sup>21</sup>, were isolated by Wildman and co-workers in 1955 from various plant species as *Pancratium amritimum*, *Narcissus poeticus* and *Brunsvigia cooperi* (see Table 3).<sup>22</sup> These polycyclic alkaloids have been reported as biologically important compounds with promising biological activities such as antidepressant, anxiolytic and anticonvulsant-type effects.<sup>23</sup>

**Table 3.** Selected structures of montanine-type *Amaryllidaceae* alkaloids.



**57-61**

entry	R <sup>1</sup>	R <sup>2</sup>	R <sup>3</sup>	R <sup>4</sup>	alkaloid
1	H	OH	OH	H	(-)-pancracine <b>57</b>
2	H	OMe	OH	H	(-)-montanine <b>58</b>
3	H	OMe	OMe	H	(-)-manthine <b>59</b>
4	OMe	H	OH	H	(-)-coccinine <b>60</b>
5	H	OH	H	OH	(-)-brunsvigine <b>61</b>

These natural products interesting possess synthetic challenges due to their distinctive A-E pentacyclic structure. Several groups have achieved several total and formal

syntheses (both in a racemic or enantioselective manner) towards pancracine **57** (Table 4). In this discussion, only those from 2010 are reviewed.<sup>1</sup>

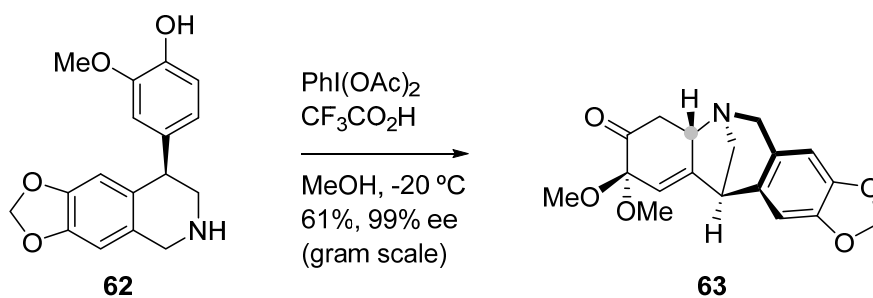
**Table 4.** Compilation of pancracine's total and formal syntheses from 1991 until 2013.

year	authors	alkaloid induction	ref
4 TOTAL SYNTHESSES			
1991	Overman & Shim	racemic	24
1991	Hoshino	racemic	25
1993	Overman & Shim	(-) and racemic	26
1997	Weinreb & Jin	(-)	27
2013	Fan	(-)	28
7 FORMAL SYNTHESSES			
1993	Hoshino	racemic	29
1999	Ikeda	racemic	30
2001	Banwell	racemic	31
2005	Pandey	racemic	32
2005	Chang	(+)	33
2009	Hashimoto	(-)	34
2010	Pansare	(-)	35

#### The total synthesis of (-)-pancracine reported by Fan *et al.*<sup>28</sup>

Fan *et al.* approached the synthesis of (-)-pancracine **57** and four other montanine-type alkaloids through a biologically inspired strategy based on the stable cherylline-type precursor **62**. The key step was the tandem oxidative dearomatization/intramolecular aza-Michael addition shown in Scheme 23. Hypervalent-iodine-mediated phenol dearomatization with  $\text{PhI}(\text{OAc})_2$  as oxidant gave rise to the precursor **62**. A smooth tandem oxidative dearomatization/intramolecular aza-Michael reaction yielded the chiral intermediate **63** with total enantiocontrol and good yield.

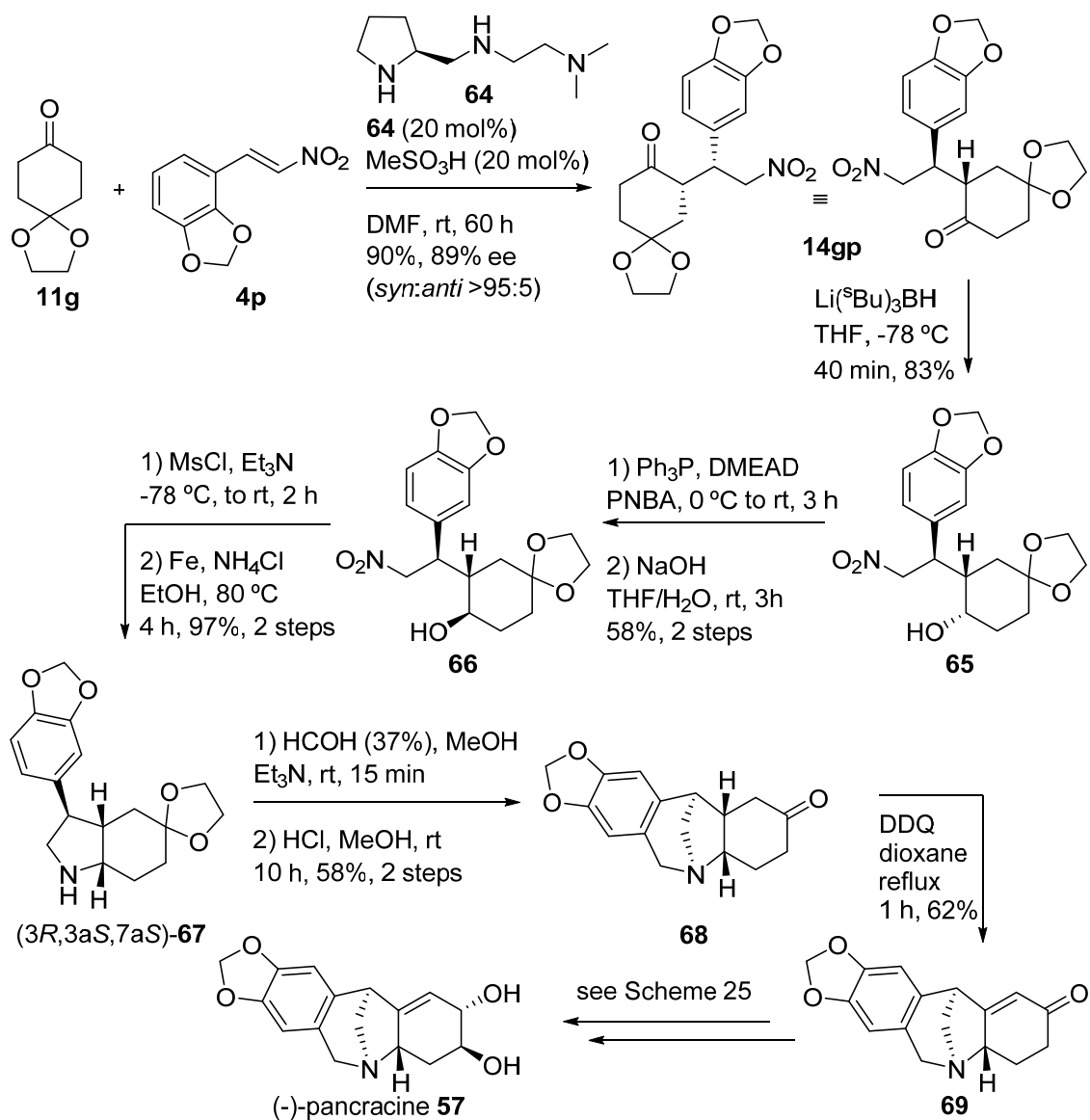
<sup>1</sup> Note: Dr. Rajinikanth Lingampally, from the Memorial University of Newfoundland in Canada, nicely gathered in his PhD thesis "Studies on GuanidinyI Pyrrolidine Catalyzed Conjugate Additions and Synthesis of (-)-Pancracine and (+)-Ipalbidine" disserted in April 2011, all the different synthetic routes (total and formal syntheses) towards pancracine until the year 2009. His dissertation text is available free of charge via the Internet at [http://collections.mun.ca/PDFs/theses/Lingampally\\_Rajinikanth.pdf](http://collections.mun.ca/PDFs/theses/Lingampally_Rajinikanth.pdf)



**Scheme 23.** Bioinspired tandem dearomatization/intramolecular aza-Michael addition.

### The formal synthesis of (-)-pancracine reported by Pansare *et al.*<sup>35</sup>

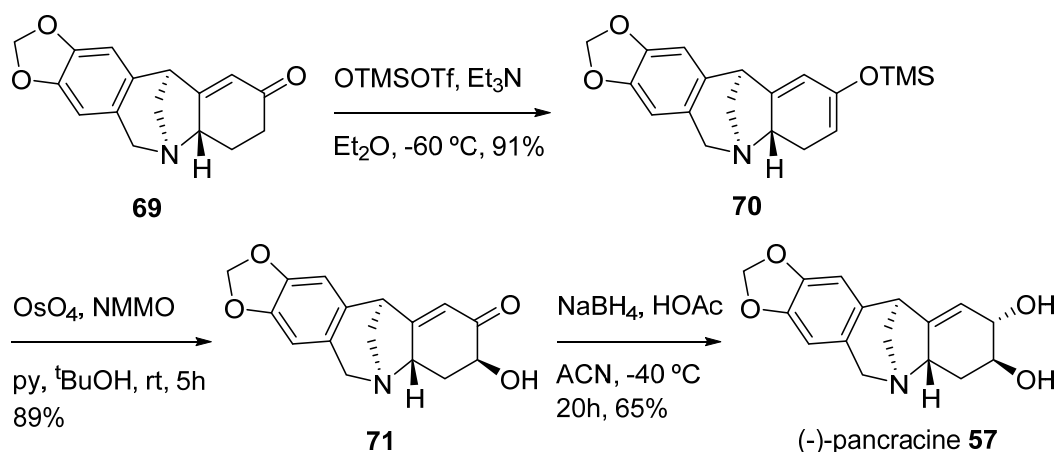
These authors reported the stereoselective synthesis of (-)-pancracine advanced intermediate **69**. The key steps consisted of transformation of  $\gamma$ -nitroketone **14gp** into the *cis*-fused 3-aryloctahydroindole **67** (Scheme 24). **14gp** was obtained via organocatalyzed Michael addition between ketone **11g** and nitrostyrene **4p** aided by the pyrrolidine-based organocatalyst **64** in high yield and enantioselectivity. Then, to promote the C-N assembly, **14gp** was reduced with L-Selectride providing the axial nitro alcohol **65**. A modified Mitsunobu reaction onto **65** followed by hydrolysis of the nitrobenzoate produced the equatorial alcohol **66** as single diastereomer. Mesylation of the hydroxyl group provided the active precursor for the cyclization. Later, reduction of the nitro group gave, via an S<sub>N</sub>2-reaction, the final *cis*-octahydroindole **67** in high yield. A Pictet-Spengler type cyclization occurred when **67** was treated with formaldehyde. Removal of the acetal protecting group furnished the methanomorphanthridine **68** in good yield. Further oxidation with DDQ, as described by Hoshino<sup>29</sup>, resulted in the formation of **69** which is an advanced intermediate in the total synthesis described by Overman (see Scheme 25).



**Scheme 24.** Synthesis of *cis*-octahydroindole **67** and conversion to (-)-pancracine intermediate **69**.

### The total synthesis of (-)-pancracine reported by Overman *et al.*<sup>26</sup>

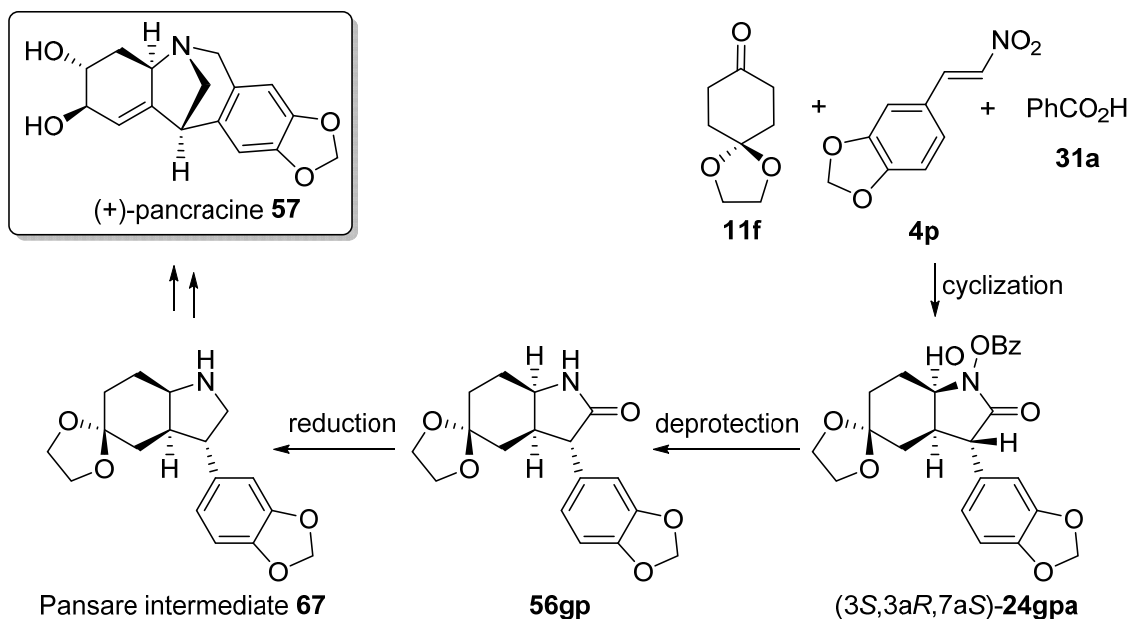
Overman *et al.* reported the total synthesis of (-)-pancracine **57** by means of enolsilylation of **69** with TMSOTf towards dienoxysilane **70** in excellent yield. This intermediate was then treated with catalytic amounts of OsO<sub>4</sub> in the presence of *N*-methylmorpholine *N*-oxide giving  $\alpha$ -hydroxyketone **71** in high yield. Last reduction with sodium triacetoxyborohydride afforded (-)-pancracine **57** in 65% yield.



**Scheme 25.** Total synthesis of (-)-pancracine **57** starting from intermediate **69** according to the procedure described by Overman.

#### 4.6. Formal synthesis of (+)-pancracine via organocatalyzed lactamization reaction

The novel cyclization reaction leading to bicyclic  $\gamma$ -lactams **24** and the successful transformation of (3*S*,3*aR*,7*aS*)-**24aaa** into (3*S*,3*aR*,7*aS*)-**56aa** (Scheme 22) suggested a new synthetic route towards (+)-pancracine **57**. This formal synthesis could be achieved though several modifications performed on lactam (3*S*,3*aR*,7*aS*)-**24gpa** (Scheme 26). Hydrogenation of precursor **24gpa** would simultaneously remove the hydroxy and benzoyloxy groups to give **56gp**. Subsequent reduction of the amide group would provide **67**, which is the enantiomer of the advanced intermediate in the synthesis of (-)-pancracine by Pansare *et al.*

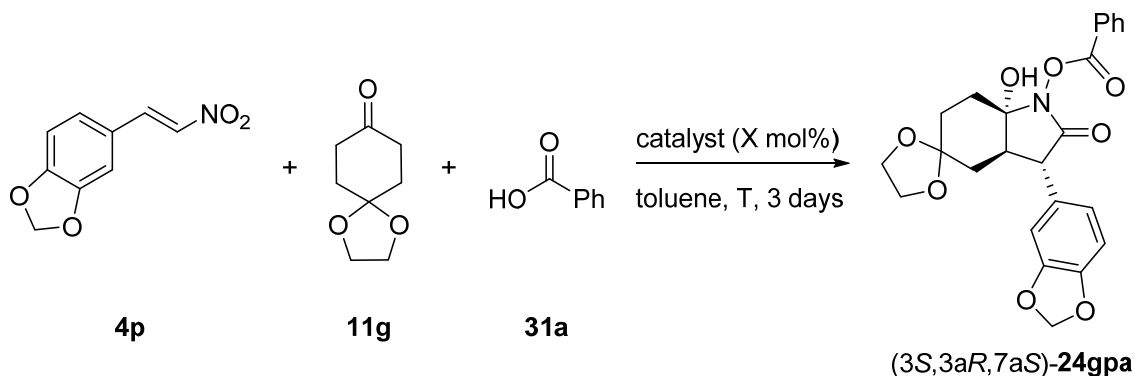


**Scheme 26.** Lactam precursor (3*S*,3*aR*,7*aS*)-**24gpa** towards the formal synthesis of (+)-pancracine **57**.

Ketone **11g**, nitroalkene **4p** and benzoic acid **31a** were employed to carry out the synthesis of lactam **24gpa**. In first instance, a screening was carried out to find the best catalyst for the process.  $\text{NO}_2\text{-X}_\text{L}\text{-OMe-5aa}$ ,  $\text{NO}_2\text{-X}_\text{L}\text{X}_\text{L}\text{-OMe-25a}$  and  $\text{NO}_2\text{-X}_\text{D}\text{X}_\text{L}\text{-OMe-25a}$  were tested with different catalytic loads (10 to 30 mol%) and solvents, such as chloroform, dichloromethane, THF, dioxane or toluene, in temperatures ranging from room temperature to 70 °C (Table 5). In none of the cases any Michael adduct was observed.  $\text{NO}_2\text{-X}_\text{L}\text{-OMe-5aa}$  catalyst was only efficient when 30 mol% of catalytic load was employed at 45 °C, reaching 80% conversion of lactam **24gpa** with total enantiocontrol, after four days of reaction time (entries 1 and 2). The best result was obtained under 20 mol% of  $\text{NO}_2\text{-X}_\text{L}\text{X}_\text{L}\text{-OMe-25a}$  in toluene at 45 °C (entry 3). Under these conditions, lactam (3*S*,3*aR*,7*aS*)-**24gpa** was achieved with total conversion, high yield and full enantiocontrol. On the contrary,  $\text{NO}_2\text{-X}_\text{D}\text{X}_\text{L}\text{-OMe-25a}$  required 70 °C to get 80% conversion and 60% of enantiomeric excess after three days of reaction time (entry 4).



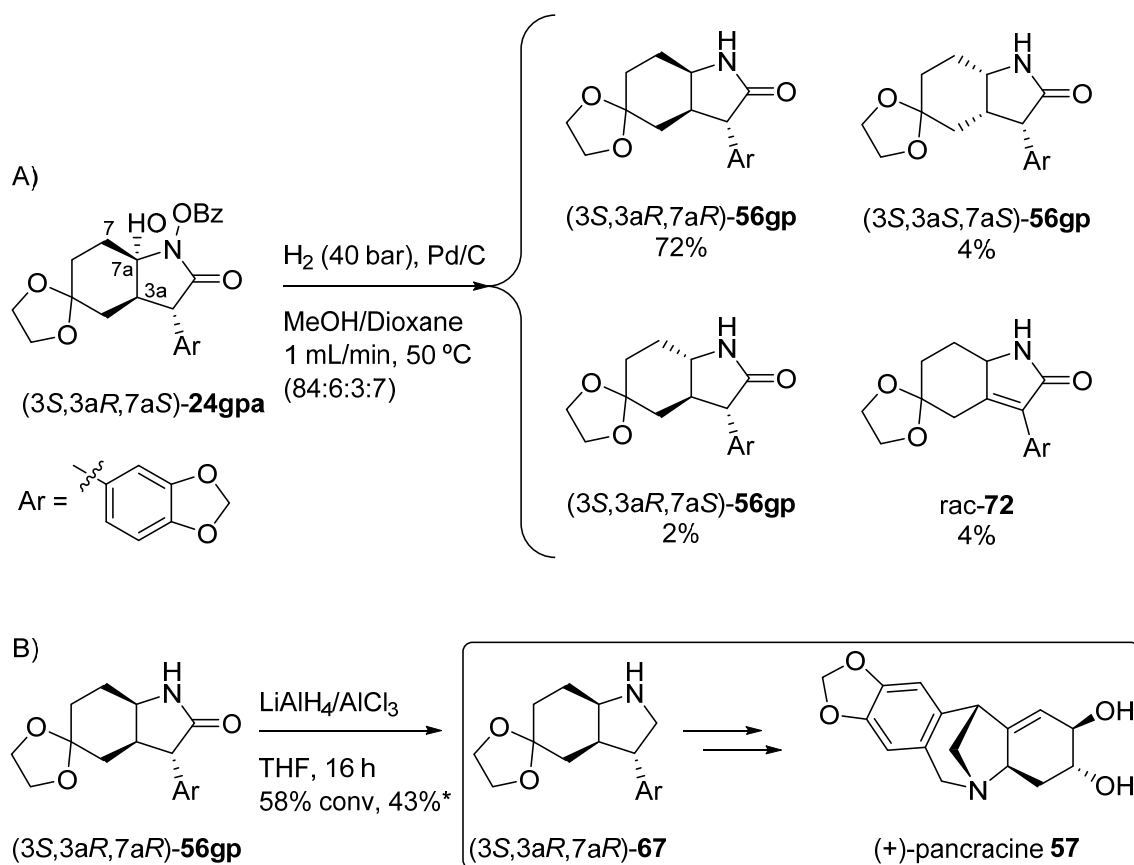
**Table 5.** Cyclization reaction between ketone **11g**, nitroalkene **4p** and benzoic acid **31a** employing NO<sub>2</sub>-X<sub>L</sub>-OMe-**5aa**, NO<sub>2</sub>-X<sub>L</sub>X<sub>L</sub>-OMe-**25a** and NO<sub>2</sub>-X<sub>D</sub>X<sub>L</sub>-OMe-**25a** catalysts.<sup>a</sup>



entry	catalyst	load (mol %)	T (°C)	conv (%) <sup>b</sup>	yield (%) <sup>c</sup>	ee (%) <sup>d</sup>
1	NO <sub>2</sub> -X <sub>L</sub> -OMe- <b>5aa</b>	30	25	28 <sup>e</sup>	-	-
2	NO <sub>2</sub> -X <sub>L</sub> -OMe- <b>5aa</b>	30	45	80 <sup>e</sup>	64	>99
3	NO <sub>2</sub> -X <sub>L</sub> X <sub>L</sub> -OMe- <b>25a</b>	20	45	>99	82	>99
4	NO <sub>2</sub> -X <sub>D</sub> X <sub>L</sub> -OMe- <b>25a</b>	20	70	80	27	-60

<sup>a</sup>Reactions were monitored by <sup>1</sup>H NMR. <sup>b</sup>Conversions were measured by <sup>1</sup>H NMR. <sup>c</sup>Yields refer to isolated pure lactam. <sup>d</sup>Enantiomeric excesses measured by HPLC correspond to the major lactam (3*S*,3*aR*,7*aS*)-**24gpa**. <sup>e</sup>Conversion measured after four days.

Once (3*S*,3*aR*,7*aS*)-**24gpa** was obtained, the formal synthesis of (+)-pancracine **57** alkaloid was pursued (Scheme 27A). The first step consisted of the catalytic hydrogenation of *N*-benzoyloxylactam (3*S*,3*aR*,7*aS*)-**24gpa**. This reaction was carried out in a hydrogenation flow reactor at 50 °C employing a Pd/C catalyst cartridge. Also, methanol/dioxane 1:1 solvent mixture was necessary due to the insolubility of (3*S*,3*aR*,7*aS*)-**24gpa** in pure methanol. In this case, the major desired lactam (3*S*,3*aR*,7*aR*)-**56gp** was successfully achieved. However, other three minor products were observed: (3*S*,3*aS*,7*aS*)-**56gp**, (3*S*,3*aR*,7*aS*)-**56gp** and racemic lactam **72** in 84:6:3:7 ratio (Scheme 27A).



**Scheme 27.** Formal synthesis of (+)-pancracine **57**: A) hydrogenation step and B) reduction step. \*38% of (3S,3aR,7aR)-**56gp** was recovered from the reaction mixture.

The presence of these isomers may indicate the transient formation of a double bond between C3a–C7a, C7–C7a or C7a–N atom pairs during the reaction course. On the other side, lactam **72** could arise from a previous pyrrole formation. The purification was carried out by means of semipreparative HPLC technique due to the failure of isomers separation under standard column chromatography conditions. The performed HPLC filled with a chiral column (see experimental section) provided lactam (3S,3aR,7aR)-**56gp** in 72% yield. The chief geometric features and stereochemistries of compounds (3S,3aS,7aS)-**56gp**, (3S,3aR,7aS)-**56gp** and **72** were verified by X ray diffraction analysis (Figure 6).

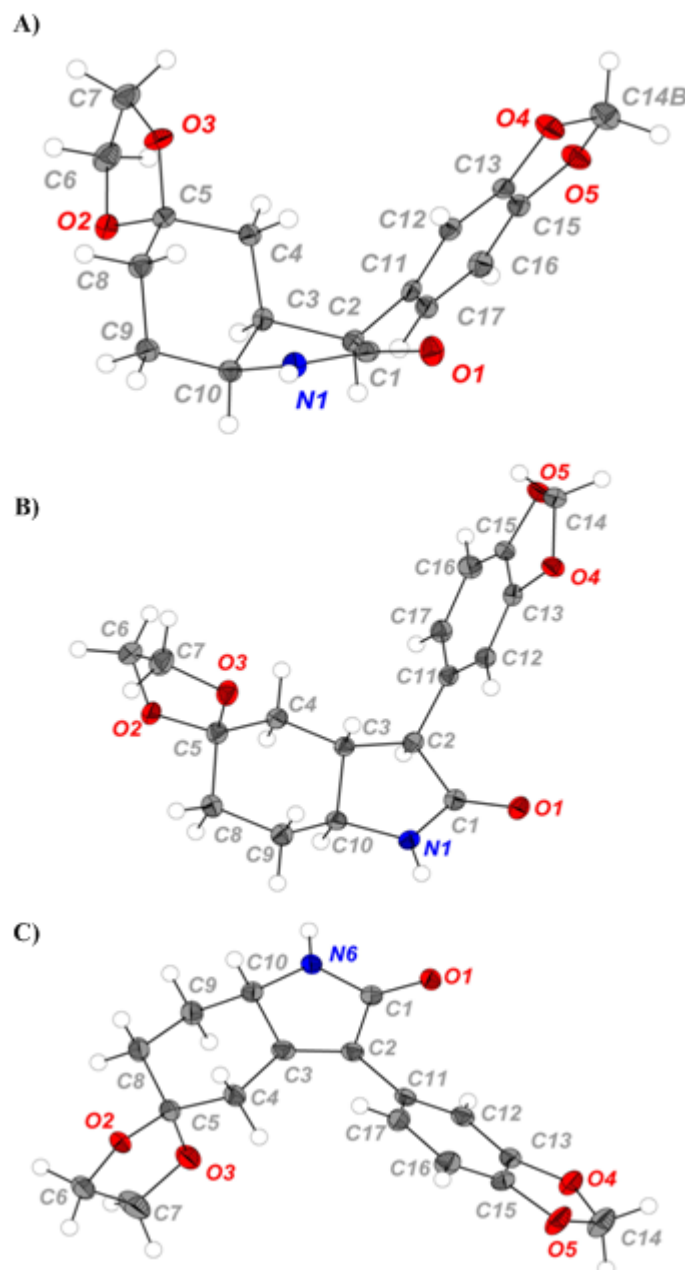


**Figure 6.** ORTEP drawings of: A) (3*S*,3*aS*,7*aS*)-**56gp**, B) (3*S*,3*aR*,7*aS*)-**56gp** and C) *rac*-**72**.

Once lactam (3*S*,3*aR*,7*aR*)-**56gp** was isolated, it was reduced with the  $\text{LiAlH}_4/\text{AlCl}_3$  system (Scheme 27B).<sup>36</sup> Amine (3*S*,3*aR*,7*aR*)-**67** was obtained in 43% yield and 58% conversion after 16 hours of reaction at room temperature. Longer reaction times produced a degradation of the final product. Nevertheless, the starting (3*S*,3*aR*,7*aR*)-**56gp** amide could be recovered in 38% yield, which allows to be used in a second reduction reaction. The obtained  $^1\text{H}$  NMR spectrum of amine (3*S*,3*aR*,7*aR*)-**67** was coincident with the published data for its enantiomer (3*R*,3*aS*,7*aS*)-**67**.<sup>35</sup> Therefore, this organocatalytic reaction permits the formal total synthesis of (+)-panpracine **57**. The only formal synthesis towards (+)-panpracine **57** described till date was proposed by Chang,<sup>33</sup> in which *trans*-4-hydroxyproline was used as chiral template.

#### 4.7. Conclusions

From the experimental studies discussed along this chapter, the following conclusions can be drawn:

- An unprecedented multicomponent organocatalytic reaction consisting of cyclization between cyclohexanone **11a**, nitrostyrene **4a**, and benzoic acid **31a** to provide 7a-hydroxy-2-oxo-3-phenyloctahydro-1*H*-indol-1-yl benzoate as a product.
- 4-Nitro densely substituted monomeric NO<sub>2</sub>-X<sub>L</sub>-OMe-**5aa**, NO<sub>2</sub>-X<sub>L</sub>X<sub>L</sub>-OMe-**25a** and NO<sub>2</sub>-X<sub>D</sub>X<sub>L</sub>-OMe-**25a** dimeric compounds resulted to be the most efficient organocatalysts in this novel cyclization reaction.
- While NO<sub>2</sub>-X<sub>L</sub>-OMe-**5aa** provided exclusively the lactamization product with high enantiomeric excesses, NO<sub>2</sub>-X<sub>L</sub>X<sub>L</sub>-OMe-**25a** and NO<sub>2</sub>-X<sub>D</sub>X<sub>L</sub>-OMe-**25a** dimers provided the lactam product with total enantiocontrol (except in the case of **24aga**) always in the presence of the corresponding Michael adducts.
- The stereocontrol at C3 and C3a centres match those found for the corresponding Michael adduct using the same catalyst.
- A wide range of acids were tested in the reaction such as mono and double carboxylic acids, thiobenzoic acid, phenol, phosphinic, phosphonic acids and phosphonates. Among these, aromatic and aliphatic carboxylic acids were able to promote the lactamization reaction.
- Heteroatom-containing aromatic nitroalkenes were tested giving lactams in different ratios with respect to the Michael adduct.
- Several cyclohexanones and related (thio)tetrahydropyranones were the most satisfactory nucleophiles in the process. Acyclic ketones or other cyclic ketones such as pentanone and cyclopentanone provided the corresponding Michael products only.
- Hydrogenation onto Pd/C catalyst of 7a-hydroxy-2-oxo-3-aryloctahydro-1*H*-indol-1-yl benzoates permits their transformation into *cis*-3-aryloctahydroindoles, as both the hydroxy at C7a position and benzoate groups are removed in one preparative step.
- This reaction allowed the first organocatalytic concise formal synthesis of an advanced intermediate towards (+)-pancracine **57**.

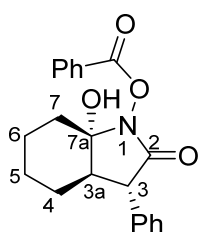
## 4.8. Experimental section

**General Remarks.** See Chapter 2 section 2.8.

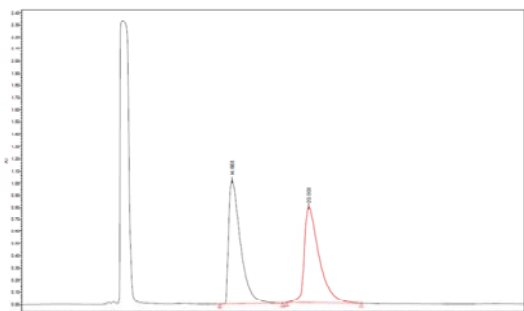
### Synthesis of lactams

A reaction mixture of nitroalkene **4** (0.1 mmol), ketone **11** (0.8 mmol), the corresponding carboxylic acid **31** (0.11 mmol) and catalyst NO<sub>2</sub>-X<sub>L</sub>-OMe-**5aa** (6.5 mg, 0.02 mmol) NO<sub>2</sub>-X<sub>L</sub>X<sub>L</sub>-OMe-**25a** or NO<sub>2</sub>-X<sub>D</sub>X<sub>L</sub>-OMe-**25a** (6.05 mg, 0.01 mmol) was stirred at room temperature or 45 °C (for NO<sub>2</sub>-X<sub>L</sub>-OMe-**5aa** catalyst). The progress of the reactions were monitored by TLC with EtOAc:Hexane elution mixtures. After consumption of the nitroalkene, the crude product was purified by column chromatography over silica gel using EtOAc:Hexane system as eluent to provide the Michael addition product first followed by the lactam product (elution order). TLC plates were stained with vanillin. Michael products showed blue colour and lactam products produced pink spots.

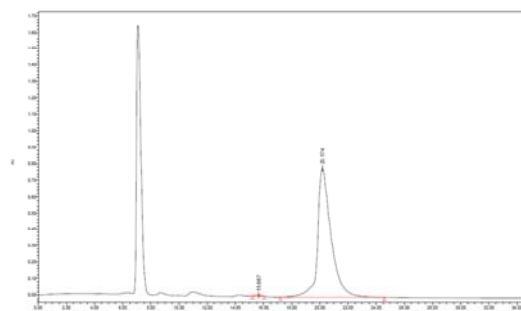
**Nomenclature:** For a better assignment of protons on NMR spectra, the IUPAC carbon order in octahydroindole-type rings has been used. The following lactam structures follow the same pattern.



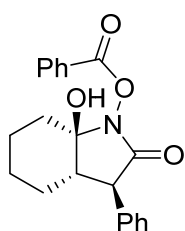
(3*S*,3*aR*,7*aS*)-7*a*-Hydroxy-2-oxo-3-phenyloctahydro-1*H*-indol-1-yl benzoate (**24aaa**). NO<sub>2</sub>-X<sub>L</sub>X<sub>L</sub>-OMe-**1a** was employed as catalyst. Yield: 21.77 mg, 62%, white solid. *m<sub>p</sub>* = 148-149 °C. [α]<sub>D</sub><sup>25</sup> = -36.05 (c 0.35, CHCl<sub>3</sub>). FTIR (neat, cm<sup>-1</sup>) 3313, 1761, 1698, 1234, 1068, 1052, 1011, 702. <sup>1</sup>H NMR (400 MHz, CDCl<sub>3</sub>) δ 8.11 (d, *J* = 7.8 Hz, 2H, ArH), 7.64 (t, *J* = 7.4 Hz, 1H, ArH), 7.48 (t, *J* = 7.7 Hz, 2H, ArH), 7.34 (dq, *J* = 15.2, 7.7 Hz, 5H, ArH), 3.53 (d, *J* = 9.7 Hz, 1H, C<sup>3</sup>H), 3.17 (s, 1H, OH), 2.45 (t, *J* = 7.3 Hz, 1H, C<sup>3*a*</sup>H), 2.22 (q, *J* = 5.3 Hz, 1H, C<sup>7</sup>H), 1.88 – 1.78 (m, 1H, C<sup>4</sup>H), 1.67 (m, 4H, C<sup>4</sup>H, C<sup>5</sup>H, C<sup>6</sup>H and C<sup>7</sup>H), 1.51 (m, 2H, C<sup>5</sup>H and C<sup>6</sup>H). <sup>13</sup>C NMR (101 MHz, CDCl<sub>3</sub>) δ 169.5, 165.2, 136.9, 134.4, 130.4, 129.0, 128.8, 128.7, 127.7, 126.8, 88.9, 49.7, 47.5, 32.6, 23.7, 21.1 (2 signals). HRMS (ESI) for C<sub>21</sub>H<sub>20</sub>NO<sub>3</sub>: calculated [M - H<sub>2</sub>O + H]<sup>+</sup>: 334.11443. Found: 334.1440. HPLC (Daicel Chiralpak IB, hexane/PrOH = 90:10, flow rate 1.0 mL/min, λ = 210 nm), *t<sub>R</sub>* (minor) = 15.67 min, *t<sub>R</sub>* (major) = 20.17 min; ee = >99%.



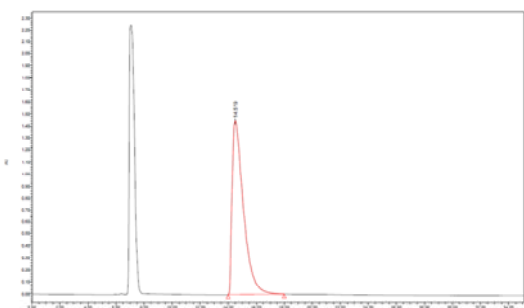
	Time	Area	% Height	% Area
1	14.668	57664653	56.30	50.74
2	20.003	55991546	43.70	49.26



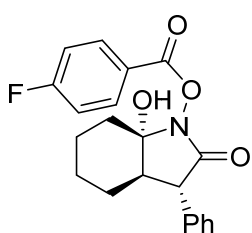
	Time	Area	% Height	% Area
1	15.667	1141110	0.59	0.22
2	20.174	51671567	99.41	99.78



(3*R*,3*aS*,7*aR*)-7*a*-Hydroxy-2-oxo-3-phenyloctahydro-1*H*-indol-1-yl benzoate (*ent*-**24aaa**). NO<sub>2</sub>-X<sub>D</sub>X<sub>L</sub>-OMe-**4a** was employed as catalyst. Analytical and spectroscopic properties were coincident with the previously reported data. Yield: 22.47 mg, 64%. [α]<sub>D</sub><sup>25</sup> = +41.13 (c 0.15, CHCl<sub>3</sub>). HPLC (Daicel Chiralpak IB, hexane/<sup>i</sup>PrOH = 90:10, flow rate 1 mL/min, λ = 210 nm), t<sub>R</sub> (major) = 14.52 min; ee = <-99%.

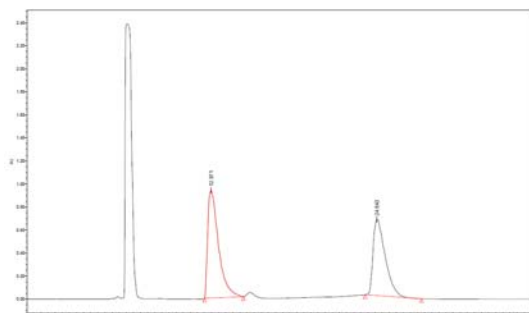


	Time	Area	% Height	% Area
1	14.519	81153019	100.00	100.00

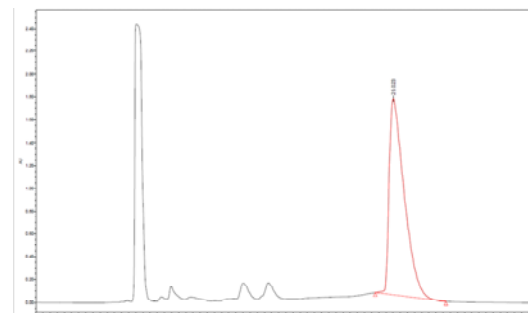


(3*S*,3*aR*,7*aS*)-7*a*-Hydroxy-2-oxo-3-phenyloctahydro-1*H*-indol-1-yl 4-fluorobenzoate (**24aab**). NO<sub>2</sub>-X<sub>L</sub>X<sub>L</sub>-OMe-**1a** was employed as catalyst. Yield: 18.46 mg, 50%, white solid. m<sub>p</sub> = 159-160 °C. [α]<sub>D</sub><sup>25</sup> = -28.34 (c 0.45, CHCl<sub>3</sub>). FTIR (neat, cm<sup>-1</sup>) 3314, 1763, 1701, 1238, 1068, 1051, 755. <sup>1</sup>H NMR (400 MHz, CDCl<sub>3</sub>) δ 8.16 (dd, *J* = 8.4, 5.2 Hz, 2H, ArH), 7.46 – 7.26 (m, 5H, ArH), 7.18 (t, *J* = 8.5 Hz, 2H, ArH), 3.56 (d, *J* = 9.7 Hz, 1H, C<sup>3</sup>H), 3.23 (s, 1H, OH), 2.47 (t, *J* = 7.0 Hz, 1H, C<sup>3a</sup>H), 2.32 – 2.17 (m, 1H, C<sup>7</sup>H), 1.95 – 1.80 (m, 1H, C<sup>4</sup>H), 1.80 – 1.63 (m, 4H, C<sup>4</sup>H, C<sup>5</sup>H, C<sup>6</sup>H and C<sup>7</sup>H), 1.61 – 1.48 (m, 2H, C<sup>5</sup>H and C<sup>6</sup>H). <sup>13</sup>C NMR (101 MHz, CDCl<sub>3</sub>) δ 169.6, 166.63 (d, <sup>1</sup>J<sub>CF</sub> = 256.3 Hz), 164.2, 136.8, 133.16 (d, <sup>3</sup>J<sub>CF</sub> = 9.6 Hz), 129.1, 128.7, 127.8, 123.07 (d, <sup>4</sup>J<sub>CF</sub> = 3.2 Hz), 116.16 (d, <sup>2</sup>J<sub>CF</sub> = 22.2 Hz), 88.9, 49.6, 47.5, 32.5, 23.6, 21.0 (2 signals). HRMS (ESI) for C<sub>21</sub>H<sub>20</sub>FNO<sub>4</sub>Na: calculated [M + Na]<sup>+</sup>: 392.1274. Found: 392.1269. HPLC (Daicel Chiralpak IB, hexane/<sup>i</sup>PrOH = 90:10, flow rate 1.0 mL/min, λ = 210 nm), t<sub>R</sub> (major) = 25.02 min; ee = >99%.

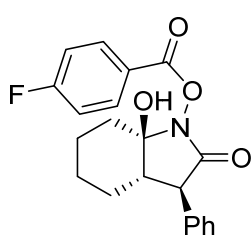
Stereoselective Synthesis of 7a-Hydroxy-2-oxo-aryloctahydro-1H-indol-yl Carboxylates.  
A Concise Formal Synthesis of (+)-Pancracine



	Time	Area	% Height	% Area
1	12.971	49160238	58.59	55.60
2	24.643	39252427	41.41	44.40

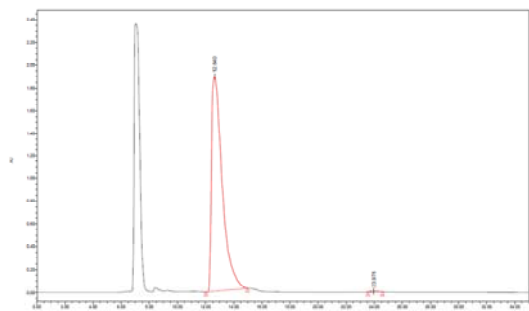


	Time	Area	% Height	% Area
1	25.023	125605278	100.00	100.00

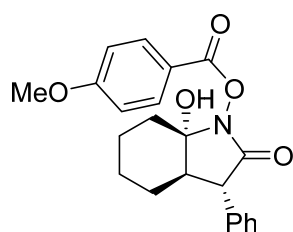


(3R,3aS,7aR)-7a-Hydroxy-2-oxo-3-phenyloctahydro-1H-indol-1-yl 4-fluorobenzoate (*ent*-**24aab**). NO<sub>2</sub>-X<sub>D</sub>X<sub>L</sub>-OMe-**4a** was employed as catalyst. Analytical and spectroscopic properties were coincident with the previously reported data. Yield: 25.47 mg, 69%. [α]<sub>D</sub><sup>25</sup> = +29.86 (c 0.51, CHCl<sub>3</sub>). HPLC (Daicel Chiralpak IB, hexane/*i*PrOH = 90:10, flow rate 1.0 mL/min, λ = 210 nm), t<sub>R</sub> (major) = 12.64 min, t<sub>R</sub> (minor) = 23.98

min; ee = <-99%.



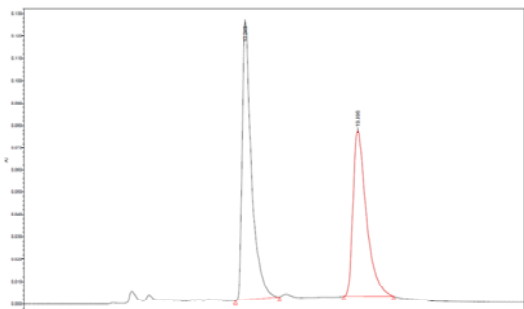
	Time	Area	% Height	% Area
1	12.640	99795596	99.68	99.78
2	23.976	216343	0.32	0.22



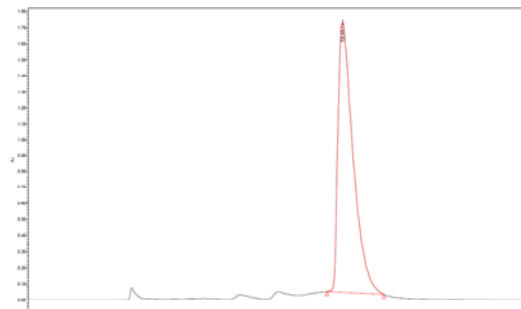
(3S,3aR,7aS)-7a-Hydroxy-2-oxo-3-phenyloctahydro-1H-indol-1-yl 4-methoxybenzoate (**24aac**). NO<sub>2</sub>-X<sub>L</sub>X<sub>L</sub>-OMe-**4a** was employed as catalyst. Yield: 20.20 mg, 53%, white solid. m<sub>p</sub> = 160-161 °C. [α]<sub>D</sub><sup>25</sup> = -47.28 (c 0.54 CHCl<sub>3</sub>). FTIR (neat, cm<sup>-1</sup>) 3302, 1753, 1692, 1246, 1164, 1016, 991. <sup>1</sup>H NMR (400 MHz, CDCl<sub>3</sub>) δ 7.98 (d, *J* = 8.5 Hz, 2H, ArH), 7.43 – 7.09 (m, 5H, ArH), 6.86 (d, *J* = 8.5 Hz, 2H, ArH), 3.80 (s, 3H, OMe), 3.45 (d, *J* = 9.6 Hz, 1H, C<sup>3</sup>H), 3.25 (s, 1H, OH), 2.52 – 2.24 (m, 1H, C<sup>3a</sup>H), 2.23 – 2.08 (m, 1H, C<sup>7</sup>H), 1.82 – 1.70 (m, 1H, C<sup>4</sup>H), 1.69 – 1.53 (m, 4H, C<sup>4</sup>H, C<sup>5</sup>H, C<sup>6</sup>H and C<sup>7</sup>H), 1.53 – 1.33 (m, 2H, C<sup>5</sup>H and C<sup>6</sup>H).

<sup>13</sup>C NMR (101 MHz, CDCl<sub>3</sub>) δ 169.5, 164.9, 164.5, 137.0, 132.7, 129.0, 128.9, 128.8, 127.7, 118.8, 114.1, 88.9, 55.7, 49.7, 47.5, 32.6, 23.7, 21.1 (2 signals). HRMS (ESI) for C<sub>22</sub>H<sub>23</sub>NO<sub>5</sub>Na: calculated [M + Na]<sup>+</sup>: 404.1474. Found: 404.1477.

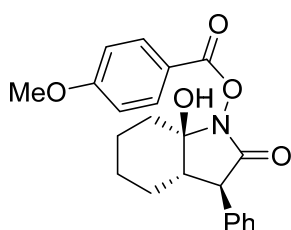
HPLC (Daicel Chiralpak IB, hexane/PrOH = 80:20, flow rate 1.0 mL/min,  $\lambda = 210$  nm),  $t_R$  (major) = 18.67 min; ee = >99%.



	Time	Area	% Height	% Area
1	13.249	4808086	62.56	54.03
2	19.996	4090627	37.44	45.97

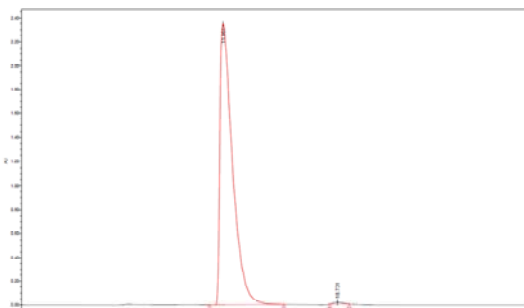


	Time	Area	% Height	% Area
1	18.667	104735105	100.00	100.00

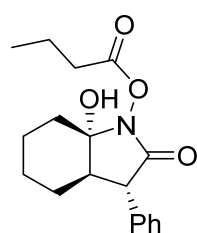


(3*R*,3*aS*,7*aR*)-7*a*-Hydroxy-2-oxo-3-phenyloctahydro-1*H*-indol-1-yl 4-methoxybenzoate (*ent*-**24aac**). NO<sub>2</sub>-X<sub>D</sub>X<sub>L</sub>-OMe-**4a** was employed as catalyst. Analytical and spectroscopic properties were coincident with the previously reported data. Yield: 25.16 mg, 66%.  $[\alpha]_D^{25} = +51.90$  (c 0.85, CHCl<sub>3</sub>). HPLC (Daicel Chiralpak IB, hexane/PrOH = 80:20, flow rate 1.0 mL/min,  $\lambda = 210$  nm),  $t_R$  (major) = 11.96 min,

$t_R$  (minor) = 18.73 min; ee = -99%.



	Time	Area	% Height	% Area
1	11.961	121160691	99.38	99.51
2	18.731	594740	0.62	0.49

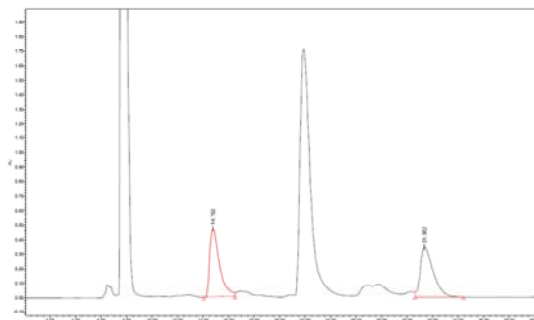


(3*S*,3*aR*,7*aS*)-7*a*-Hydroxy-2-oxo-3-phenyloctahydro-1*H*-indol-1-yl butyrate (**24aad**). NO<sub>2</sub>-X<sub>L</sub>-OMe-**1a** was employed as catalyst with 2 equivalents of benzoic acid. Yield: 12.05 mg, 38%, white solid.  $m_p = 134-135$  °C.  $[\alpha]_D^{25} = +5.06$  (c 0.32 CHCl<sub>3</sub>). FTIR (neat, cm<sup>-1</sup>) 3372, 1784, 1705, 1068. <sup>1</sup>H NMR (400 MHz, CDCl<sub>3</sub>)  $\delta$  7.36 (t,  $J = 7.5$  Hz, 2H, ArH), 7.27 (d,  $J = 10.2$  Hz, 3H, ArH), 3.46 (d,  $J = 9.5$  Hz, 1H, C<sup>3</sup>H), 2.63 (s, 1H, OH), 2.54 (td,  $J = 7.3, 3.2$  Hz, 2H, COCH<sub>2</sub>), 2.35 (t,  $J = 6.7$  Hz, 1H, C<sup>3a</sup>H), 2.12 (d,  $J = 10.2$  Hz, 1H, C<sup>7</sup>H), 1.79 (m, 3H, C<sup>4</sup>H and CH<sub>2</sub>), 1.64 (dt,  $J = 12.9, 7.1$  Hz, 4H, C<sup>4</sup>H, C<sup>5</sup>H, C<sup>6</sup>H and C<sup>7</sup>H), 1.50 (d,  $J = 10.6$

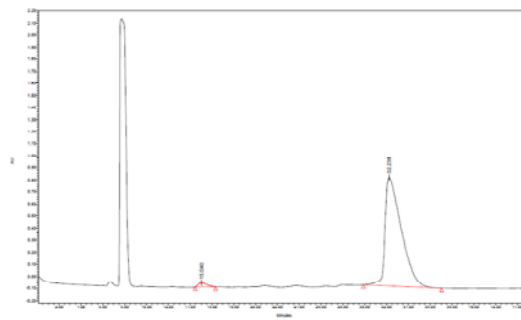


Steroselective Synthesis of 7a-Hydroxy-2-oxo-aryloctahydro-1*H*-indol-yl Carboxylates.  
A Concise Formal Synthesis of (+)-Pancracine

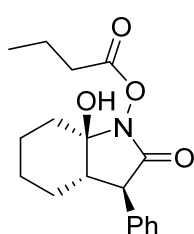
Hz, 2H, C<sup>5</sup>H and C<sup>6</sup>H), 1.04 (t, *J* = 7.4 Hz, 3H, CH<sub>3</sub>). <sup>13</sup>C NMR (101 MHz, CDCl<sub>3</sub>) δ 172.0, 169.1, 136.9, 129.1, 128.7, 127.7, 88.6, 49.7, 47.8, 33.6, 32.4, 23.8, 21.1, 21.0, 18.6, 13.7. HRMS (ESI) for C<sub>18</sub>H<sub>23</sub>NO<sub>4</sub>Na: calculated [M + Na]<sup>+</sup>: 340.1525. Found: 340.1523. HPLC (Daicel Chiralpak IB, hexane/*i*PrOH = 95:5, flow rate 1.0 mL/min, λ = 210 nm), *t*<sub>R</sub> (minor) = 15.040 min, *t*<sub>R</sub> (major) = 32.238 min; ee = 96%.



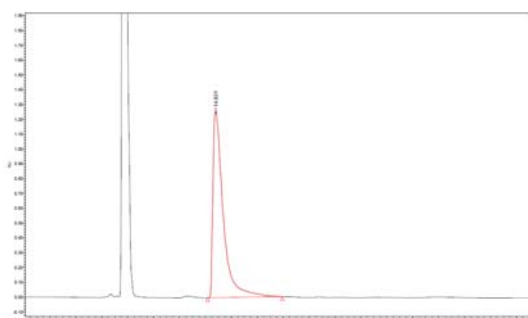
	Time	Area	% Height	% Area
1	14.762	24599776	57.60	51.02
2	31.362	23615305	42.40	48.98



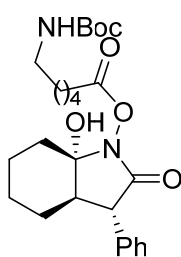
	Time	Area	% Height	% Area
1	15.040	1913841	3.71	2.02
2	32.238	93050340	96.29	97.98



(3*R*,3*aS*,7*aR*)-7*a*-Hydroxy-2-oxo-3-phenyloctahydro-1*H*-indol-1-yl butyrate (*ent*-**24aad**). NO<sub>2</sub>-X<sub>D</sub>X<sub>L</sub>-OMe-**4a** was employed as catalyst. Analytical and spectroscopic properties were coincident with the previously reported data. Yield: 19.66 mg, 62%. [α]<sub>D</sub><sup>25</sup> = -5.44 (c 0.53, CHCl<sub>3</sub>). HPLC (Daicel Chiralpak IB, hexane/*i*PrOH = 95:5, flow rate 1.0 mL/min, λ = 210 nm), *t*<sub>R</sub> (major) = 14.80 min; ee = <-99%.

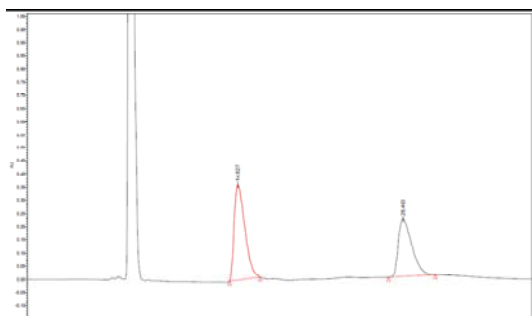


	Time	Area	% Height	% Area
1	14.801	69845608	100.00	100.00

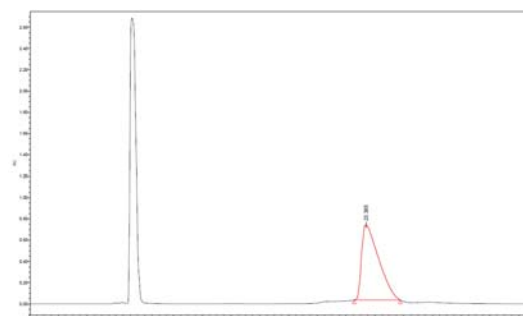


(3*S*,3*aR*,7*aS*)-7*a*-Hydroxy-2-oxo-3-phenyloctahydro-1*H*-indol-1-yl 3-((*tert*-butoxycarbonyl)amino)hexanoate (**24aae**). NO<sub>2</sub>-X<sub>L</sub>X<sub>L</sub>-OMe-**4a** was employed as catalyst. Yield: 22.09 mg, 48%, white solid. *m*<sub>p</sub> = 52-54 °C. [α]<sub>D</sub><sup>25</sup> = +8.17 (c 0.05, CHCl<sub>3</sub>). FTIR (neat, cm<sup>-1</sup>) 3343, 1699, 1684, 1164, 696. <sup>1</sup>H NMR (500 MHz, CDCl<sub>3</sub>) δ 7.40 – 7.31 (m, 2H, ArH), 7.30 – 7.22 (m, 3H, ArH), 4.63 (s, 1H, NH), 3.45 (d, *J* = 9.7 Hz, 1H, C<sup>3</sup>H), 3.18 (s, 1H, OH), 3.14 – 3.05 (m, 2H, NHCH<sub>2</sub>), 2.55 (hept, *J* = 7.9, 7.3 Hz, 2H, COCH<sub>2</sub>), 2.44 – 2.30 (m, 1H, C<sup>3a</sup>H), 2.19 – 2.10

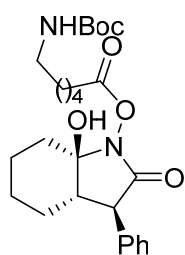
(m, 1H, C<sup>7</sup>H), 1.91 – 1.71 (m, 3H, C<sup>4</sup>H and CH<sub>2</sub>), 1.68 – 1.55 (m, 5H, C<sup>4</sup>H, C<sup>5</sup>H, C<sup>6</sup>H, C<sup>7</sup>H and CH<sub>2</sub>), 1.56 – 1.46 (m, 5H, C<sup>5</sup>H, C<sup>6</sup>H and CH<sub>2</sub>), 1.43 (s, 9H, C(CH<sub>3</sub>)<sub>3</sub>). <sup>13</sup>C NMR (126 MHz, CDCl<sub>3</sub>) δ 171.7, 169.1, 156.2, 136.9, 129.0, 128.7, 127.7, 88.6, 79.3, 49.5, 47.5, 40.5, 32.6, 31.5, 29.6, 28.6, 26.0, 24.5, 23.5, 21.0 (2 signals). HRMS (ESI) for C<sub>25</sub>H<sub>36</sub>N<sub>2</sub>O<sub>6</sub>Na: calculated [M + Na]<sup>+</sup>: 483.2471. Found: 483.2473. HPLC (Daicel Chiralpak IB, hexane/<sup>i</sup>PrOH = 90:10, flow rate 1.0 mL/min, λ = 210 nm), t<sub>R</sub> (major) = 23.38 min; ee = >99%.



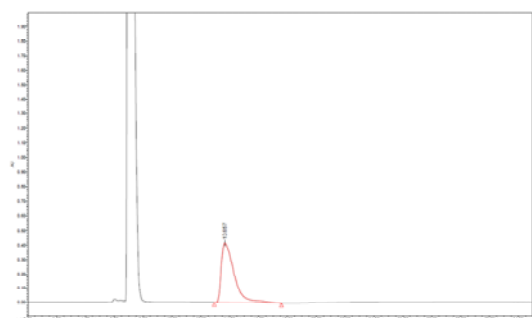
	Time	Area	% Height	% Area
1	14.827	18739372	62.53	56.69
2	26.463	14315018	37.47	43.31



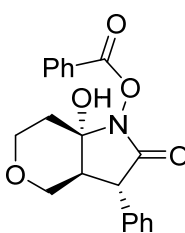
	Time	Area	% Height	% Area
1	23.385	58249025	100.00	100.00



(3*R*,3*aS*,7*aR*)-7*a*-Hydroxy-2-oxo-3-phenyloctahydro-1*H*-indol-1-yl 3-((*tert*-butoxycarbonyl)amino)hexanoate (*ent*-**24aae**). NO<sub>2</sub>-X<sub>D</sub>X<sub>L</sub>-OMe-**4a** was employed as catalyst. Analytical and spectroscopic properties were coincident with the previously reported data. Yield: 24.39 mg, 53%. [α]<sub>D</sub><sup>25</sup> = -6.40 (c 0.25, CHCl<sub>3</sub>). HPLC (Daicel Chiralpak IB, hexane/<sup>i</sup>PrOH = 90:10, flow rate 1.0 mL/min, λ = 210 nm), t<sub>R</sub> (major) = 13.66 min; ee = <-99%.



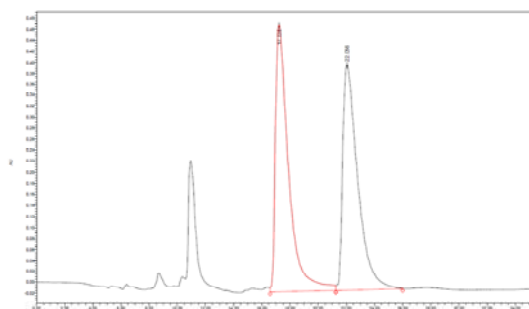
	Time	Area	% Height	% Area
1	13.657	25817624	100.00	100.00



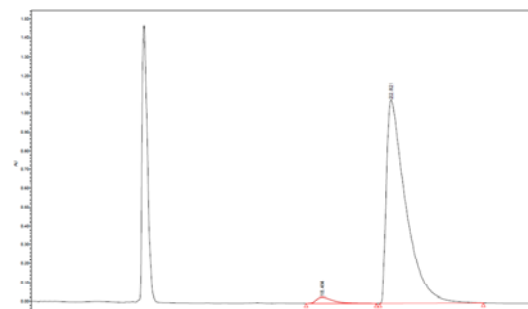
(3*S*,3*aS*,7*aS*)-7*a*-Hydroxy-2-oxo-3-phenylhexahydropyrano[4,3-*b*]pyrrol-1(4*H*)-yl benzoate (**24aea**). NO<sub>2</sub>-X<sub>L</sub>-OMe-**1a** was employed as catalyst. Yield: 19.78 mg, 56%, white solid. m<sub>p</sub> = 156-157 °C. [α]<sub>D</sub><sup>25</sup> = -29.65 (c 0.60, CHCl<sub>3</sub>). FTIR (neat, cm<sup>-1</sup>) 3365, 1770, 1709, 1238, 1041, 699. <sup>1</sup>H NMR (400 MHz, CDCl<sub>3</sub>) δ 8.11 (d, *J* = 7.8 Hz, 2H, ArH), 7.65 (t, *J* = 7.6 Hz, 1H,

Stereoselective Synthesis of 7a-Hydroxy-2-oxo-aryloctahydro-1*H*-indol-yl Carboxylates.  
A Concise Formal Synthesis of (+)-Pancreline

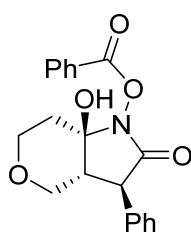
ArH), 7.49 (t,  $J = 7.8$  Hz, 2H, ArH), 7.34 (dq,  $J = 13.7, 7.2, 6.8$  Hz, 5H, ArH), 3.95 (dt,  $J = 11.6, 4.0$  Hz, 1H, C<sup>6</sup>H), 3.87 – 3.79 (m, 2H, C<sup>4</sup>H), 3.75 (d,  $J = 10.0$  Hz, 1H, C<sup>3</sup>H), 3.65 – 3.48 (m, 2H, C<sup>6</sup>H, OH), 2.32 (d,  $J = 9.8$  Hz, 1H, C<sup>3a</sup>H), 2.20 (d,  $J = 14.1$  Hz, 1H, C<sup>7</sup>H), 2.04 (ddd,  $J = 14.6, 11.3, 5.0$  Hz, 1H, C<sup>7</sup>H). <sup>13</sup>C NMR (101 MHz, CDCl<sub>3</sub>)  $\delta$  169.8, 165.3, 136.1, 134.6, 130.5, 129.2, 128.9, 128.8, 128.0, 126.6, 86.4, 64.4, 64.2, 48.2, 47.5, 33.3. HRMS (ESI) for C<sub>20</sub>H<sub>19</sub>NO<sub>5</sub>Na: calculated  $[M + Na]^+$ : 376.1161. Found: 376.1157. HPLC (Daicel Chiralpak IB, hexane/<sup>i</sup>PrOH = 90:10, flow rate 1.0 mL/min,  $\lambda = 210$  nm),  $t_R$  (minor) = 18.45 min,  $t_R$  (major) = 22.82 min; ee = 95%.



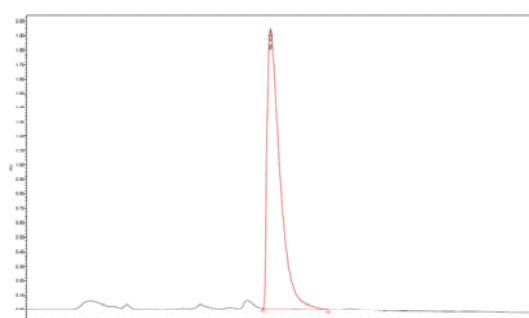
	Time	Area	% Height	% Area
1	17.228	31592149	54.19	50.97
2	22.056	30388854	45.81	49.03



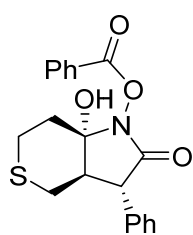
	Time	Area	% Height	% Area
1	18.454	2281962	2.88	2.43
2	22.821	91613693	97.12	97.57



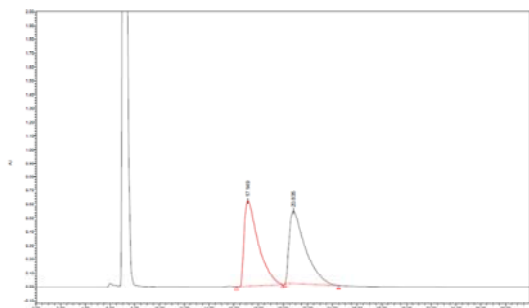
(3*R*,3*aR*,7*aR*)-7*a*-Hydroxy-2-oxo-3-phenylhexahydropyrano[4,3-*b*]pyrrol-1(4*H*)-yl benzoate (*ent*-**24aea**). NO<sub>2</sub>-X<sub>D</sub>X<sub>L</sub>-OMe-**4a** was employed as catalyst. Analytical and spectroscopic properties were coincident with the previously reported data. Yield: 24.01 mg, 68%.  $[\alpha]_D^{25} = +30.51$  ( $c$  0.74, CHCl<sub>3</sub>). HPLC (Daicel Chiralpak IB, hexane/<sup>i</sup>PrOH = 90:10, flow rate 1.0 mL/min,  $\lambda = 210$  nm),  $t_R$  (major) = 16.92 min; ee = <-99%.



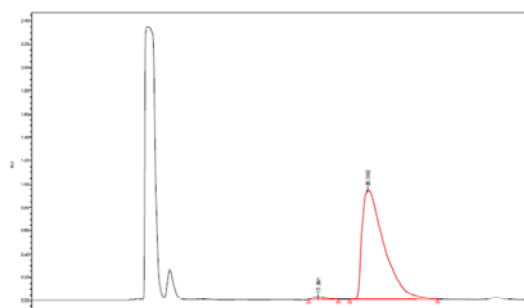
	Time	Area	% Height	% Area
1	16.922	119236811	100.00	100.00



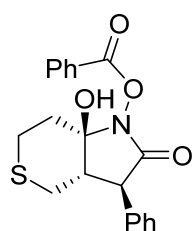
(3*S*,3*aR*,7*aS*)-7*a*-Hydroxy-2-oxo-3-phenylhexahydrothiopyrano [4,3-*b*]pyrrol-1(4*H*)-yl benzoate (**24afa**). NO<sub>2</sub>-X<sub>L</sub>-OMe-**4a** was employed as catalyst. 4 Equivalents of ketone and 100 μL of CH<sub>2</sub>Cl<sub>2</sub> were added. Yield: 26.21 mg, 71%, white solid. *m*<sub>p</sub> = 165-167 °C. [α]<sub>D</sub><sup>25</sup> = -3.65 (c 0.65, CHCl<sub>3</sub>). FTIR (neat, cm<sup>-1</sup>) 3289, 1758, 1700, 1687, 1240, 1068, 703. <sup>1</sup>H NMR (400 MHz, CDCl<sub>3</sub>) δ 8.10 (d, *J* = 7.8 Hz, 2H, ArH), 7.65 (t, *J* = 7.6 Hz, 1H, ArH), 7.48 (t, *J* = 7.8 Hz, 2H, ArH), 7.34 (dt, *J* = 24.3, 7.7 Hz, 5H, ArH), 4.12 (d, *J* = 10.5 Hz, 1H, C<sup>3</sup>H), 3.44 (s, 1H, OH), 3.17 (dd, *J* = 14.4, 4.1 Hz, 1H, C<sup>4</sup>H), 2.82 – 2.68 (m, 1H, C<sup>6</sup>H), 2.66 – 2.44 (m, 4H, C<sup>3a</sup>H, C<sup>4</sup>H, C<sup>6</sup>H and C<sup>7</sup>H), 2.12 – 1.99 (m, 1H, C<sup>7</sup>H). <sup>13</sup>C NMR (101 MHz, CDCl<sub>3</sub>) δ 169.3, 165.4, 136.0, 134.6, 130.5, 129.2, 128.9, 128.9, 128.0, 126.6, 87.6, 47.9, 47.8, 33.9, 25.5, 24.0. HRMS (ESI) for C<sub>20</sub>H<sub>19</sub>NO<sub>4</sub>SNa: calculated [M + Na]<sup>+</sup>: 392.0933. Found: 392.0934. HPLC (Daicel Chiralpak IB, hexane/PrOH = 90:10, flow rate 1.0 mL/min, λ = 210 nm), *t*<sub>R</sub> (minor) = 17.39 min, *t*<sub>R</sub> (major) = 20.39 min; ee = 97%.



	Time	Area	% Height	% Area
1	17.149	49080189	54.07	50.69
2	20.835	47741546	45.93	49.31

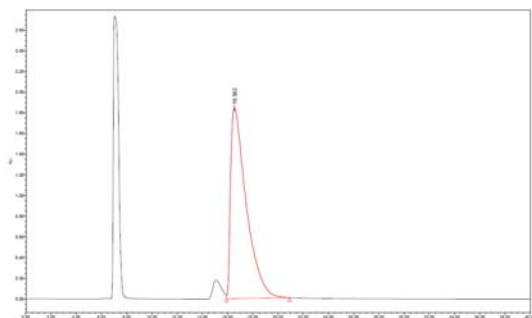


	Time	Area	% Height	% Area
1	17.391	1425824	2.56	1.61
2	20.392	86951843	97.44	98.39

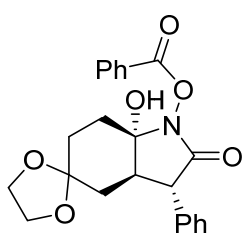


(3*R*,3*aS*,7*aR*)-7*a*-Hydroxy-2-oxo-3-phenylhexahydrothiopyrano [4,3-*b*]pyrrol-1(4*H*)-yl benzoate (*ent*-**24afa**). NO<sub>2</sub>-X<sub>D</sub>X<sub>L</sub>-OMe-**4a** was employed as catalyst. 4 Equivalents of ketone and 100 μL of CH<sub>2</sub>Cl<sub>2</sub> were added. Analytical and spectroscopic properties were coincident with the previously reported data. Yield: 25.10 mg, 68%. [α]<sub>D</sub><sup>25</sup> = +7.27 (c 0.75, CHCl<sub>3</sub>). HPLC (Daicel Chiralpak IB, hexane/PrOH = 90:10, flow rate 1.0 mL/min, λ = 210 nm), *t*<sub>R</sub> (major) = 16.56 min; ee = <-99%.

Stereoselective Synthesis of 7a-Hydroxy-2-oxo-aryloctahydro-1*H*-indol-yl Carboxylates.  
A Concise Formal Synthesis of (+)-Pancreline

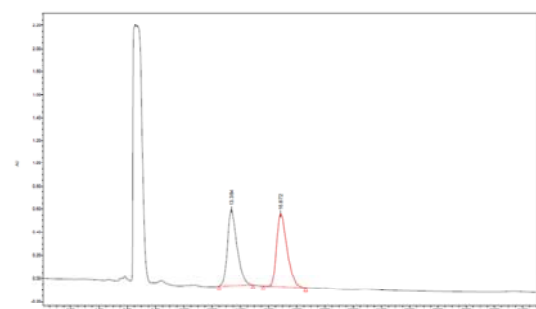


	Time	Area	% Height	% Area
1	16.562	159007291	100.00	100.00

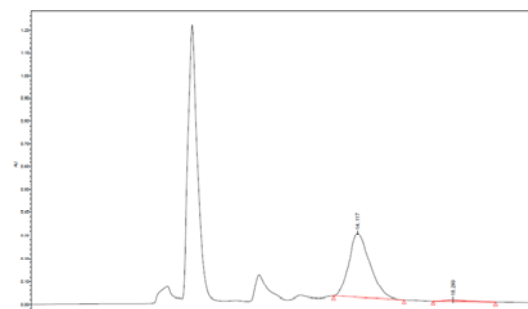


(3*S*,3*aR*,7*aS*)-7*a*-Hydroxy-2-oxo-3-phenylhexahydrospiro [indole-5,2'-[1,3]dioxolan]-1(4*H*)-yl benzoate (**24aga**). NO<sub>2</sub>-X<sub>L</sub>-OMe-**1a** was employed as catalyst. 4 Equivalents of ketone and 100 μL of CH<sub>2</sub>Cl<sub>2</sub> were added.

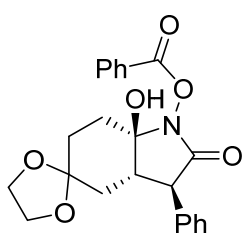
Yield: 25.37 mg, 62%, white solid. *m*<sub>p</sub> = 192-193 °C. [α]<sub>D</sub><sup>25</sup> = -19.37 (c 1.45, CHCl<sub>3</sub>). FTIR (neat, cm<sup>-1</sup>) 3328, 1778, 1698, 988, 696. <sup>1</sup>H NMR (400 MHz, CDCl<sub>3</sub>) δ 8.12 (d, *J* = 7.7 Hz, 2H, ArH), 7.63 (d, *J* = 7.7 Hz, 1H, ArH), 7.49 (t, *J* = 7.7 Hz, 2H, ArH), 7.33 (dd, *J* = 22.6, 7.3 Hz, 5H, ArH), 4.10 (d, *J* = 11.1 Hz, 1H, C<sup>3</sup>H), 4.07 – 3.92 (m, 4H, O(CH<sub>2</sub>)<sub>2</sub>O), 3.10 (s, 1H, OH), 2.56 (t, *J* = 8.3 Hz, 1H, C<sup>3*a*</sup>H), 2.31 (d, *J* = 14.0 Hz, 1H, C<sup>7</sup>H), 2.16 – 1.98 (m, 2H, C<sup>4</sup>H and C<sup>7</sup>H), 1.92 – 1.83 (m, 1H, C<sup>6</sup>H), 1.78 (m, 2H, C<sup>4</sup>H and C<sup>6</sup>H). <sup>13</sup>C NMR (101 MHz, CDCl<sub>3</sub>) δ 169.5, 165.3, 136.7, 134.5, 130.5, 129.1, 128.9, 128.8, 127.8, 126.8, 108.3, 88.1, 64.7, 64.3, 50.2, 48.6, 31.1, 30.3, 29.7. HRMS (ESI) for C<sub>23</sub>H<sub>23</sub>NO<sub>6</sub>Na: calculated [M + Na]<sup>+</sup>: 432.1423. Found: 432.1409. HPLC (Daicel Chiralpak IC, hexane/*i*PrOH = 70:30, flow rate 1.0 mL/min, λ = 210 nm), *t*<sub>R</sub> (major) = 14.12 min, *t*<sub>R</sub> (minor) = 18.25 min; ee = 95%.



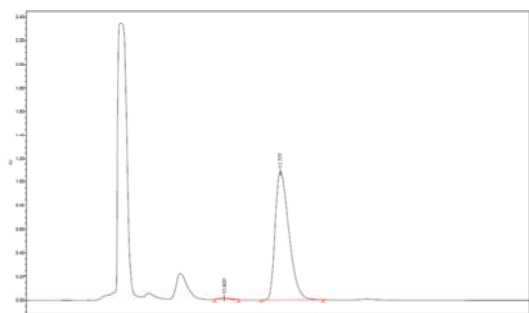
	Time	Area	% Height	% Area
1	13.384	30774155	51.00	48.60
2	16.872	32546748	49.00	51.40



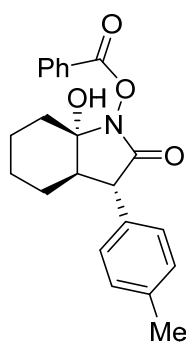
	Time	Area	% Height	% Area
1	14.117	17645855	97.76	97.49
2	18.249	453646	2.24	2.51



(3*R*,3*aS*,7*aR*)-7*a*-Hydroxy-2-oxo-3-phenylhexahydrospiro [indole-5,2'-[1,3]dioxolan]-1(4*H*)-yl benzoate (*ent*-**24aga**). NO<sub>2</sub>-X<sub>D</sub>X<sub>L</sub>-OMe-**4a** was employed as catalyst. 4 Equivalents of ketone and 100 μL of CH<sub>2</sub>Cl<sub>2</sub> were added. Analytical and spectroscopic properties were coincident with the previously reported data. Yield: 29.87 mg, 73%. [α]<sub>D</sub><sup>25</sup> = +20.56 (c 0.64, CHCl<sub>3</sub>); HPLC (Daicel Chiralpak IC, hexane/*i*PrOH = 70:30, flow rate 1.0 mL/min, λ = 210 nm), *t*<sub>R</sub> (major) = 17.78 min; ee = -98%.

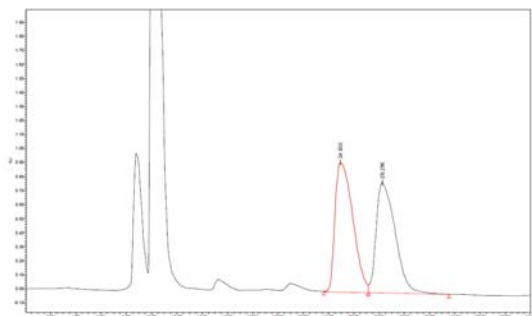


	Time	Area	% Height	% Area
1	13.901	727519	1.33	1.01
2	17.777	71443426	98.67	98.99

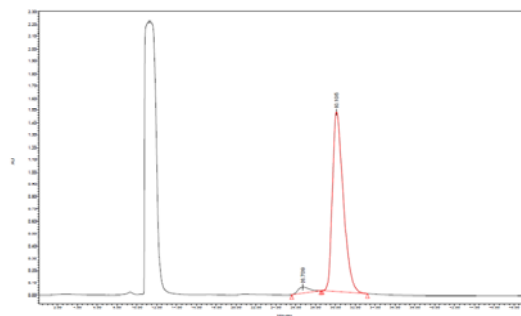


(3*S*,3*aR*,7*aS*)-7*a*-Hydroxy-2-oxo-3-(*p*-tolyl)octahydro-1*H*-indol-1-yl benzoate (**24baa**). NO<sub>2</sub>-X<sub>L</sub>-OMe-**1a** was employed as catalyst. Yield: 23.75 mg, 65%, brown solid. *m*<sub>p</sub> = 135-136 °C. [α]<sub>D</sub><sup>25</sup> = -17.22 (c 1.00, CHCl<sub>3</sub>). FTIR (neat, cm<sup>-1</sup>) 3363, 1765, 1698, 1238, 1062, 706. <sup>1</sup>H NMR (400 MHz, CDCl<sub>3</sub>) δ 8.12 (t, *J* = 7.9 Hz, 2H, ArH), 7.74 – 7.57 (m, 1H, ArH), 7.48 (td, *J* = 7.5, 4.2 Hz, 2H, ArH), 7.19 (q, *J* = 7.8 Hz, 4H, ArH), 3.51 (d, *J* = 9.6 Hz, 1H, C<sup>3</sup>H), 2.48 – 2.39 (m, 1H, C<sup>3a</sup>H), 2.33 (s, 3H, Me), 2.28 – 2.14 (m, 1H, C<sup>7</sup>H), 1.85 (dt, *J* = 11.1, 5.8 Hz, 1H, C<sup>4</sup>H), 1.82 – 1.59 (m, 4H, C<sup>4</sup>H, C<sup>5</sup>H, C<sup>6</sup>H and C<sup>7</sup>H), 1.53 (d, *J* = 10.2 Hz, 2H, C<sup>5</sup>H and C<sup>6</sup>H)- <sup>13</sup>C NMR (101 MHz, CDCl<sub>3</sub>) δ 171.1, 169.8, 137.5, 134.4, 133.8, 130.5, 130.3, 129.7, 128.8, 128.6, 89.0, 49.4, 47.6, 32.5, 23.7, 21.2, 21.1 (2 signals)- HRMS (ESI) for C<sub>22</sub>H<sub>23</sub>NO<sub>4</sub>Na: calculated [M + Na]<sup>+</sup>: 388.1525. Found: 388.1528- HPLC (Daicel Chiralpak IC, hexane/*i*PrOH = 70:30, flow rate 1.0 mL/min, λ = 210 nm), *t*<sub>R</sub> (minor) = 26.71 min, *t*<sub>R</sub> (major) = 30.19 min; ee = 95%.

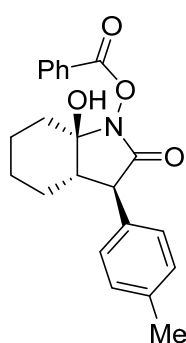
Steroselective Synthesis of 7a-Hydroxy-2-oxo-aryloctahydro-1*H*-indol-yl Carboxylates.  
A Concise Formal Synthesis of (+)-Pancracine



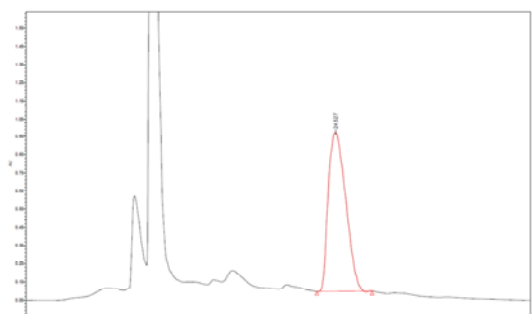
	Time	Area	% Height	% Area
1	24.930	90624709	53.90	52.29
2	28.256	82672456	46.10	47.71



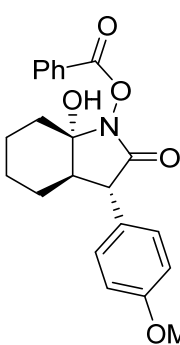
	Time	Area	% Height	% Area
1	26.709	2835873	2.77	2.49
2	30.105	110929143	97.23	97.51



(3*R*,3*aS*,7*aR*)-7*a*-Hydroxy-2-oxo-3-(*p*-tolyl)octahydro-1*H*-indol-1-yl benzoate (*ent*-**24baa**). NO<sub>2</sub>-X<sub>D</sub>X<sub>L</sub>-OMe-**4a** was employed as catalyst. Analytical and spectroscopic properties were coincident with the previously reported data. Yield: 21.91 mg, 60%. [α]<sub>D</sub><sup>25</sup> = +18.63 (c 0.6, CHCl<sub>3</sub>). HPLC (Daicel Chiralpak IC, hexane/PrOH = 70:30, flow rate 1.0 mL/min, λ = 210 nm), t<sub>R</sub> (major) = 24.53 min; ee = <-99%.

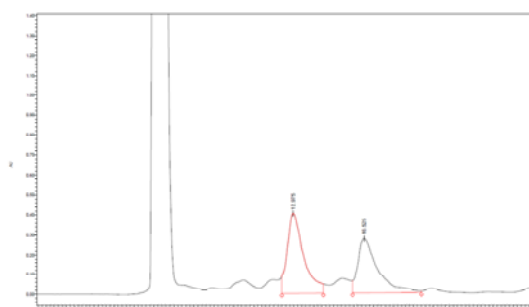


	Time	Area	% Height	% Area
1	24.527	83469903	100.00	100.00

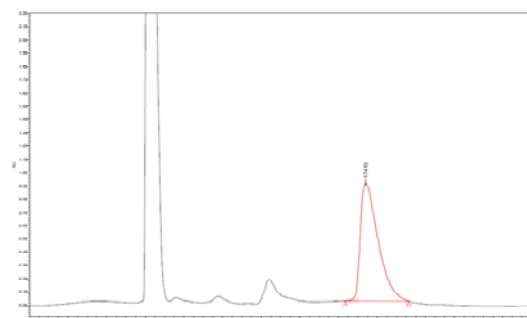


(3*S*,3*aR*,7*aS*)-7*a*-Hydroxy-3-(4-methoxyphenyl)-2-oxooctahydro-1*H*-indol-1-yl benzoate (**24caa**). NO<sub>2</sub>-X<sub>L</sub>X<sub>L</sub>-OMe-**4a** was employed as catalyst. Yield: 18.30 mg, 48%, white solid. m<sub>p</sub> = 106-107 °C. [α]<sub>D</sub><sup>25</sup> = -12.13 (c 0.15, CHCl<sub>3</sub>). FTIR (neat, cm<sup>-1</sup>) 3360, 1761, 1695, 1252, 1237, 1069, 1052, 1010, 828, 706. <sup>1</sup>H NMR (400 MHz, CDCl<sub>3</sub>) δ 8.13 (d, *J* = 7.8 Hz, 2H, ArH), 7.64 (t, *J* = 7.4 Hz, 1H, ArH), 7.49 (t, *J* = 7.7 Hz, 2H, ArH), 7.25 (d, *J* = 8.9 Hz, 2H, ArH), 6.91 (d, *J* = 8.3 Hz, 2H, ArH), 3.80 (s, 3H, OMe), 3.49 (d, *J* = 9.5 Hz, 1H, C<sup>3</sup>H), 2.88 (s, 1H, OH), 2.40 (t, *J* = 7.5 Hz, 1H, C<sup>3a</sup>H), 2.20 (t, *J* = 9.0 Hz, 1H, C<sup>7</sup>H), 1.85 (dd, *J* = 10.7, 5.9 Hz, 1H, C<sup>4</sup>H), 1.67 (dd, *J* = 26.9, 15.2 Hz, 4H, C<sup>4</sup>H, C<sup>5</sup>H, C<sup>6</sup>H and C<sup>7</sup>H), 1.53 (d, *J* = 10.3 Hz, 2H, C<sup>5</sup>H and C<sup>6</sup>H). <sup>13</sup>C NMR (101 MHz, CDCl<sub>3</sub>) δ 169.7, 165.2, 159.2, 134.4, 130.5, 129.8, 128.9, 128.8, 126.9, 114.5, 88.9, 55.5, 49.0, 47.8,

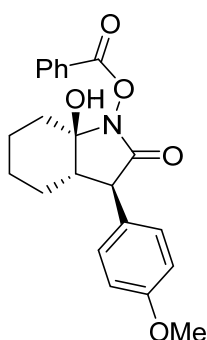
32.5, 23.8, 21.2, 21.1. HRMS (ESI) for  $C_{22}H_{23}NO_5Na$ : calculated  $[M + Na]^+$ : 404.1474. Found: 404.1473. HPLC (Daicel Chiralpak IB, hexane/ $i$ PrOH = 80:20, flow rate 1.0 mL/min,  $\lambda$  = 210 nm),  $t_R$  (major) = 17.41 min; ee = >99%.



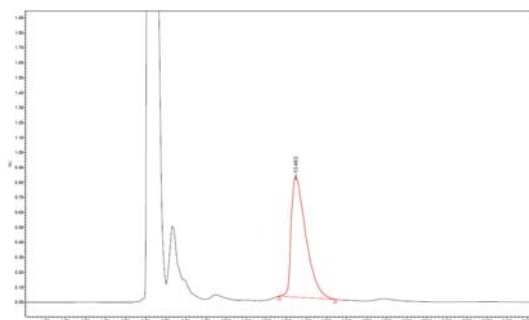
	Time	Area	% Height	% Area
1	12.975	23251604	59.28	54.93
2	16.525	19078763	40.72	45.07



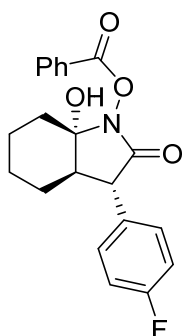
	Time	Area	% Height	% Area
1	17.413	56550758	100.00	100.00



(3*R*,3*aS*,7*aR*)-7*a*-Hydroxy-3-(4-methoxyphenyl)-2-oxooctahydro-1*H*-indol-1-yl benzoate (**ent-24caa**).  $NO_2$ - $X_D$  $X_L$ -OMe-**4a** was employed as catalyst. Analytical and spectroscopic properties were coincident with the previously reported data. Yield: 22.87 mg, 60%.  $[\alpha]_D^{25} = +9.98$  ( $c$  0.50,  $CHCl_3$ ). HPLC (Daicel Chiralpak IB, hexane/ $i$ PrOH = 80:20, flow rate 1.0 mL/min,  $\lambda$  = 210 nm),  $t_R$  (major) = 13.46 min; ee = <-99%.



	Time	Area	% Height	% Area
1	13.463	40984009	100.00	100.00

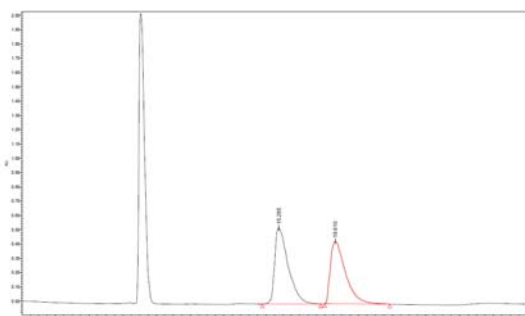


(3*S*,3*aR*,7*aS*)-3-(4-Fluorophenyl)-7*a*-hydroxy-2-oxooctahydro-1*H*-indol-1-yl benzoate (**24naa**).  $NO_2$ - $X_L$  $X_L$ -OMe-**4a** was employed as catalyst. Yield: 16.24 mg, 44%, white solid.  $m_p = 154$ -155 °C.  $[\alpha]_D^{25} = -17.57$  ( $c$  0.39,  $CHCl_3$ ). FTIR (neat,  $cm^{-1}$ ) 3337, 1757, 1696, 1510, 1234, 1050, 1011, 701.  $^1H$  NMR (400 MHz,  $CDCl_3$ )  $\delta$  8.11 (d,  $J = 7.8$  Hz, 2H, ArH), 7.65 (t,  $J = 7.6$  Hz, 1H, ArH), 7.49 (t,  $J = 7.7$  Hz, 2H, ArH), 7.29 (dd,  $J = 8.1, 5.1$  Hz, 2H, ArH), 7.05 (t,  $J = 8.5$  Hz, 2H, ArH), 3.51 (d,  $J = 9.3$  Hz, 1H,  $C^3H$ ), 3.06 (s, 1H, OH), 2.53 –

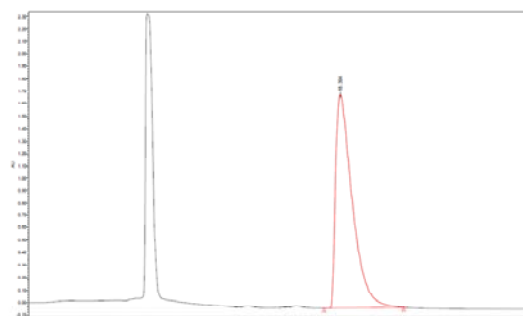


Stereoselective Synthesis of 7a-Hydroxy-2-oxo-aryloctahydro-1*H*-indol-yl Carboxylates.  
A Concise Formal Synthesis of (+)-Pancracine

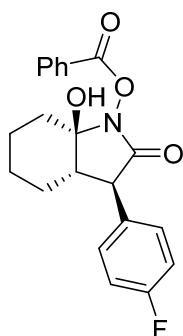
2.36 (m, 1H, C<sup>3a</sup>H), 2.30 – 2.13 (m, 1H, C<sup>7</sup>H), 1.96 – 1.81 (m, 1H, C<sup>4</sup>H), 1.68 (q, *J* = 13.6 Hz, 4H, C<sup>4</sup>H, C<sup>5</sup>H, C<sup>6</sup>H and C<sup>7</sup>H), 1.51 (q, *J* = 9.9, 9.3 Hz, 2H, C<sup>5</sup>H and C<sup>6</sup>H). <sup>13</sup>C NMR (101 MHz, CDCl<sub>3</sub>) δ 169.4, 165.2, 162.40 (d, <sup>1</sup>*J*<sub>CF</sub> = 246.0 Hz), 134.5, 132.6 (d, <sup>4</sup>*J*<sub>CF</sub> = 3.5 Hz), 130.5, 130.4 (d, <sup>3</sup>*J*<sub>CF</sub> = 8.0 Hz), 128.8, 126.7, 115.9 (d, <sup>2</sup>*J*<sub>CF</sub> = 21.5 Hz), 88.9, 49.0, 47.5, 32.6, 23.8, 21.1, 21.0. HRMS (ESI) for C<sub>21</sub>H<sub>20</sub>FNO<sub>4</sub>Na: calculated [M + Na]<sup>+</sup>: 392.1274. Found: 392.1274. HPLC (Daicel Chiralpak IB, hexane/<sup>i</sup>PrOH = 90:10, flow rate 1.0 mL/min, λ = 210 nm), *t*<sub>R</sub> (major) = 18.39 min; ee = >99%.



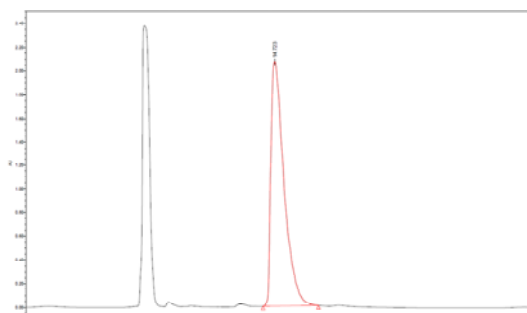
	Time	Area	% Height	% Area
1	15.265	29836339	54.94	52.24
2	18.610	27274302	45.06	47.76



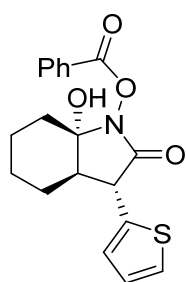
	Time	Area	% Height	% Area
1	18.394	117559812	100.00	100.00



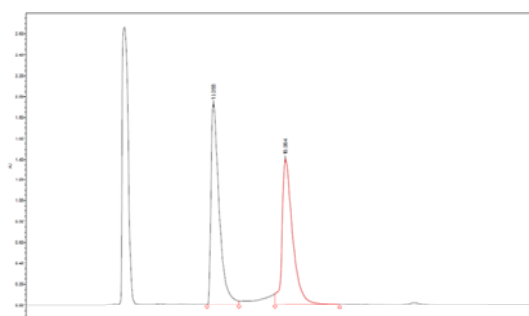
(3*R*,3*aS*,7*aR*)-3-(4-Fluorophenyl)-7*a*-hydroxy-2-oxooctahydro-1*H*-indol-1-yl benzoate (*ent*-**24naa**). NO<sub>2</sub>-X<sub>D</sub>X<sub>L</sub>-OMe-**4a** was employed as catalyst. Analytical and spectroscopic properties were coincident with the previously reported data. Yield: 19.93 mg, 54%. [α]<sub>D</sub><sup>25</sup> = +21.18 (*c* 0.69, CHCl<sub>3</sub>). HPLC (Daicel Chiralpak IB, hexane/<sup>i</sup>PrOH = 90:10, flow rate 1.0 mL/min, λ = 210 nm), *t*<sub>R</sub> (major) = 14.72 min; ee = <-99%.



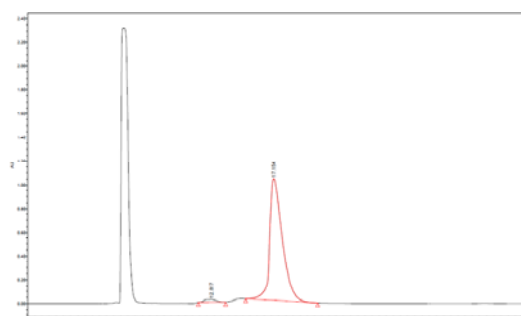
	Time	Area	% Height	% Area
1	14.723	110997142	100.00	100.00



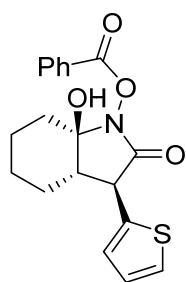
(3*R*,3*aR*,7*aS*)-7*a*-Hydroxy-2-oxo-3-(thiophen-2-yl)octahydro-1*H*-indol-1-yl benzoate (**24oaa**). NO<sub>2</sub>-X<sub>L</sub>-OMe-**1a** was employed as catalyst. Yield: 23.91 mg, 67%, brown solid. *m*<sub>p</sub> = 154-156 °C. [α]<sub>D</sub><sup>25</sup> = -24.86 (*c* 1.10, CHCl<sub>3</sub>). FTIR (neat, cm<sup>-1</sup>) 3338, 1760, 1699, 1039, 700. <sup>1</sup>H NMR (400 MHz, CDCl<sub>3</sub>) δ 8.11 (d, *J* = 7.6 Hz, 2H, ArH), 7.64 (t, *J* = 7.4 Hz, 1H, ArH), 7.48 (t, *J* = 7.7 Hz, 2H, ArH), 7.26 (d, *J* = 4.4 Hz, 1H, ArH), 7.10 (d, *J* = 3.6 Hz, 1H, ArH), 7.00 (t, *J* = 4.4 Hz, 1H, ArH), 3.78 (d, *J* = 8.3 Hz, 1H, C<sup>3</sup>H), 3.21 (s, 1H, OH), 2.59 (t, *J* = 6.7 Hz, 1H, C<sup>3a</sup>H), 2.13 (dd, *J* = 14.3, 5.8 Hz, 1H, C<sup>7</sup>H), 1.98 (dt, *J* = 8.9, 5.0 Hz, 1H, C<sup>4</sup>H), 1.75 (m, 2H, C<sup>4</sup>H and C<sup>7</sup>H), 1.69 – 1.58 (m, 2H, C<sup>5</sup>H and C<sup>6</sup>H), 1.55 (m, 2H, C<sup>5</sup>H and C<sup>6</sup>H). <sup>13</sup>C NMR (101 MHz, CDCl<sub>3</sub>) δ 168.4, 164.9, 138.7, 134.5, 130.5, 128.8, 127.2, 126.7, 126.4, 125.4, 89.1, 47.2, 45.0, 32.5, 25.2, 21.5, 21.1. HRMS (ESI) for C<sub>19</sub>H<sub>19</sub>NO<sub>4</sub>SNa: calculated [M + Na]<sup>+</sup>: 380.0933. Found: 380.0934. HPLC (Daicel Chiralpak IB, hexane/<sup>i</sup>PrOH = 85:15, flow rate 1.0 mL/min, λ = 210 nm), *t*<sub>R</sub> (minor) = 12.82 min, *t*<sub>R</sub> (major) = 17.15 min; ee = 96%.



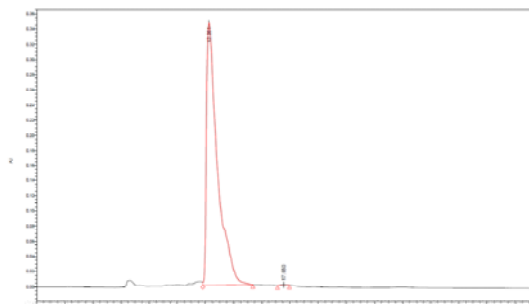
	Time	Area	% Height	% Area
1	13.055	76196939	57.92	51.90
2	18.064	70606416	42.08	48.10



	Time	Area	% Height	% Area
1	12.817	1266588	2.39	1.98
2	17.154	62779425	97.61	98.02



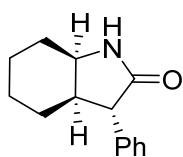
(3*S*,3*aS*,7*aR*)-7*a*-hydroxy-2-oxo-3-(thiophen-2-yl)octahydro-1*H*-indol-1-yl benzoate (*ent*-**24oaa**). NO<sub>2</sub>-X<sub>D</sub>X<sub>L</sub>-OMe-**4a** was employed as catalyst. Analytical and spectroscopic properties were coincident with the previously reported data. Yield: 23.93 mg, 67%. [α]<sub>D</sub><sup>25</sup> = +25.26 (*c* 0.92, CHCl<sub>3</sub>). HPLC (Daicel Chiralpak IB, hexane/<sup>i</sup>PrOH = 85:15, flow rate 1.0 mL/min, λ = 210 nm), *t*<sub>R</sub> (major) = 12.26 min, *t*<sub>R</sub> (minor) = 17.55 min; ee = <-99%.



	Time	Area	% Height	% Area
1	12.261	18720230	99.69	99.84
2	17.550	30627	0.31	0.16

### Hydrogenation procedure

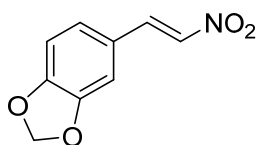
A solution of  $\gamma$ -lactam **24aaa** (180 mg, 0.51 mmol) in 10 mL of methanol was pumped at 1.0 mL/min through a H-Cube® Hydrogenation Reactor using a Palladium/Carbon CatCart® as catalyst. The pressure of the system was set to 30 bars and the temperature to 50 °C. After all the reaction mixture had passed through the flow reactor, the reaction mixture was washed twice with an aqueous solution of sodium carbonate. Then, the solvent was evaporated and the crude mixture was purified by column chromatography eluting with ethyl acetate/hexanes (1:2) to provide the desired product **56aa**.



(3*S*,3*aR*,7*aR*)-3-Phenyloctahydro-2*H*-indol-2-one (**56aa**). Yield: 83.38 mg, 76%, white solid.  $m_p$  = 163-164 °C.  $[\alpha]_D^{25}$  = -22.86 ( $c$  0.75,  $\text{CHCl}_3$ ). FTIR (neat,  $\text{cm}^{-1}$ ) 3303, 1696, 1656, 698.  $^1\text{H}$  NMR (400 MHz,  $\text{CDCl}_3$ )  $\delta$  7.35 (t,  $J$  = 7.5 Hz, 2H, ArH), 7.30 – 7.19 (m, 3H, ArH), 6.69 (s, 1H, NH), 3.60 (q,  $J$  = 6.8 Hz, 1H,  $\text{C}^{7a}\text{H}$ ), 3.46 (d,  $J$  = 10.3 Hz, 1H,  $\text{C}^3\text{H}$ ), 2.50 (dd,  $J$  = 10.6, 5.3 Hz, 1H,  $\text{C}^{3a}\text{H}$ ), 1.97 – 1.86 (m, 1H,  $\text{C}^7\text{H}$ ), 1.79 – 1.60 (m, 2H,  $\text{C}^4\text{H}$  and  $\text{C}^5\text{H}$ ), 1.60 – 1.49 (m, 2H,  $\text{C}^4\text{H}$  and  $\text{C}^6\text{H}$ ), 1.44 (t,  $J$  = 10.9 Hz, 2H,  $\text{C}^6\text{H}$  and  $\text{C}^7\text{H}$ ), 1.25 (t,  $J$  = 11.9 Hz, 1H,  $\text{C}^5\text{H}$ ).  $^{13}\text{C}$  NMR (101 MHz,  $\text{CDCl}_3$ )  $\delta$  178.5, 138.1, 128.8, 128.8, 127.2, 51.9, 51.0, 43.8, 30.8, 25.4, 22.4, 21.3. HRMS (ESI) for  $\text{C}_{14}\text{H}_{18}\text{NO}$ : calculated  $[\text{M} + \text{H}]^+$ : 216.1388. Found: 216.1382.

### Formal synthesis of (+)-Pancracine

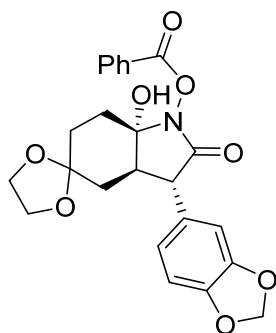
Piperonal (1.0 g, 6.66 mmol), nitromethane (1.5 mL, 26.64 mmol), sodium acetate (547 mg, 6.66 mmol) and methylammonium chloride (450 mg, 6.66 mmol) were dissolved in 40 mL of methanol and stirred for 16 hours at room temperature. After this time, the bright yellow heterogeneous solution was washed with brine and dried onto  $\text{Na}_2\text{SO}_4$  to provide **4p** (1.21 g, 94%) as a bright yellow solid.



(*E*)-5-(2-Nitrovinyl)benzo[*d*][1,3]dioxole (**4p**). Analytical and spectroscopic properties were coincident with the previously reported data.<sup>37</sup>  $^1\text{H}$  NMR (400 MHz,  $\text{CDCl}_3$ )  $\delta$  7.93 (d,  $J$  = 13.4 Hz, 1H,  $\text{NO}_2\text{CH}$ ), 7.47 (d,  $J$  = 13.4 Hz, 1H, ArCH), 7.08 (d,  $J$  = 7.9 Hz, 1H, ArH), 7.00 (s, 1H, ArH), 6.87 (d,  $J$  = 7.9 Hz, 1H, ArH), 6.07 (s, 2H,  $\text{OCH}_2\text{O}$ ).

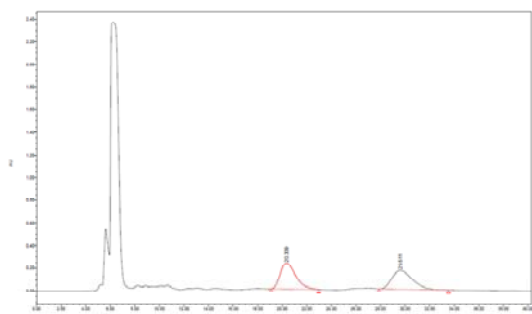
1,4-Cyclohexanedione monoethylene acetal **11g** (124.96 mg, 0.8 mmol), (*E*)-5-(2-nitrovinyl)benzo[*d*][1,3]dioxole **4p** (38.64 mg, 0.2 mmol), benzoic acid (36.64 mg, 0.3 mmol) and  $\text{NO}_2\text{-X}_L\text{X}_L\text{-OMe-25a}$  (24.20 mg, 0.04 mmol) were dissolved in 600  $\mu\text{L}$  of toluene and stirred for 72 hours at 45 °C. Then, the solvent was evaporated and the afforded crude mixture was purified by column chromatography over silica gel using EtOAc:Hexanes (1:3) as eluent to provide **24gpa** as a white solid (70.8 mg, 78%). Once the enantiomeric excess (>99% ee) was

verified after column chromatography the solvent was evaporated and the product precipitated and filtered from a solution of ethyl acetate enhancing the yield of the process to 82%.

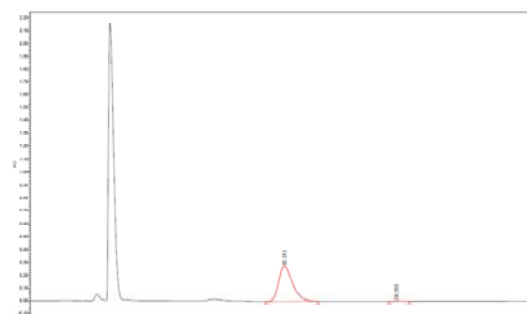


(3*S*,3*aR*,7*aS*)-3-(Benzo[*d*][1,3]dioxol-5-yl)-7*a*-hydroxy-2-oxohexahydrospiro[indole-5,2'-[1,3]dioxolan]-1(4*H*)-yl benzoate (**24gpa**). Yield: 74.0 mg, 82%, white solid.  $m_p = 218-219$  °C.  $[\alpha]_D^{25} = -15.45$  (c 0.18,  $\text{CHCl}_3$ ). FTIR (neat,  $\text{cm}^{-1}$ ) 3313, 1775, 1697, 1236, 1036, 1010, 706.  $^1\text{H}$  NMR (400 MHz,  $\text{CDCl}_3$ )  $\delta$  8.13 (d,  $J = 7.7$  Hz, 2H, ArH), 7.65 (t,  $J = 7.6$  Hz, 1H, ArH), 7.50 (t,  $J = 7.6$  Hz, 2H, ArH), 6.78 (q,  $J = 8.1$  Hz, 3H, ArH), 5.96 (s, 2H,  $\text{OCH}_2\text{O}$ ), 4.15 – 3.90 (m, 5H,  $\text{C}^3\text{H}$  and  $\text{O}(\text{CH}_2)_2\text{O}$ ), 2.81 (s, 1H, OH), 2.48 (t,  $J = 8.4$

Hz, 1H,  $\text{C}^{3a}\text{H}$ ), 2.28 (d,  $J = 13.8$  Hz, 1H,  $\text{C}^7\text{H}$ ), 2.03 (dd,  $J = 14.7, 6.7$  Hz, 2H,  $\text{C}^4\text{H}$  and  $\text{C}^7\text{H}$ ), 1.86 (td,  $J = 13.5, 4.0$  Hz, 1H,  $\text{C}^6\text{H}$ ), 1.77 (dd,  $J = 14.0, 8.1$  Hz, 2H,  $\text{C}^4\text{H}$  and  $\text{C}^6\text{H}$ ).  $^{13}\text{C}$  NMR (101 MHz,  $\text{CDCl}_3$ )  $\delta$  169.4, 165.3, 148.3, 147.3, 134.5, 130.5, 130.3, 128.9, 126.8, 122.5, 109.2, 108.8, 108.3, 101.3, 88.0, 64.8, 64.3, 50.0, 48.9, 31.1, 30.3, 29.7. HRMS (ESI) for  $\text{C}_{24}\text{H}_{23}\text{NO}_8\text{Na}$ : calculated  $[\text{M} + \text{Na}]^+$ : 476.1321. Found: 476.1316. HPLC (Daicel Chiralpak IC, hexane/ $i$ PrOH = 60:40, flow rate 1.0 mL/min,  $\lambda = 210$  nm),  $t_R$  (major) = 20.31 min,  $t_R$  (minor) = 29.25 min; ee = >99%.



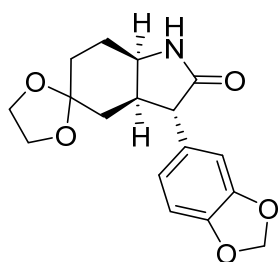
	Time	Area	% Height	% Area
1	20.339	19952866	57.98	50.89
2	29.611	19254902	42.02	49.11



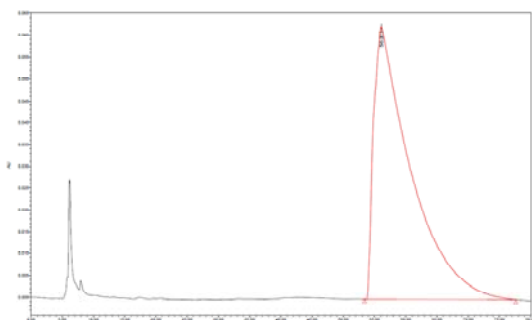
	Time	Area	% Height	% Area
1	20.312	21166513	99.98	99.96
2	29.250	3671	0.02	0.04

A solution of lactam **24gpa** (360 mg, 0.79 mmol) in 500 mL of methanol/dioxane (1:1) was pumped at 1 mL/min through the H-Cube® Hydrogenation Reactor using a Palladium/Carbon CatCart® cartridge as catalyst. The pressure of the system was set to 40 bars and the temperature to 50 °C. After all the reaction mixture had passed through the reactor, the reaction mixture was washed twice with an aqueous solution of sodium carbonate. The solvent was evaporated providing the mixture (205 mg) of diastereoisomers. The semipreparative resolution of **56gp** and **72** was carried out on a Waters 600 Delta Prep 4000 system equipped with a 2487 dual wavelength absorbance detector. The semipreparative HPLC was carried out on a 250 x 20 mm Chiralpak® IA column eluting with Hex/ $i$ PrOH 80:20 at a flow rate of 15 mL/min. The process was monitored by UV absorption at 210 nm. The crude mixture was dissolved in

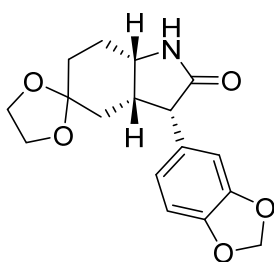
Hex<sup>i</sup>PrOH 80:20 (10 mL) and injected in one portion. Firstly, rac-**72** was eluted followed by (3*S*,3*aR*,7*aS*)-**56gp**, (3*S*,3*aS*,7*aS*)-**56gp** and (3*S*,3*aR*,7*aR*)-**56gp**.



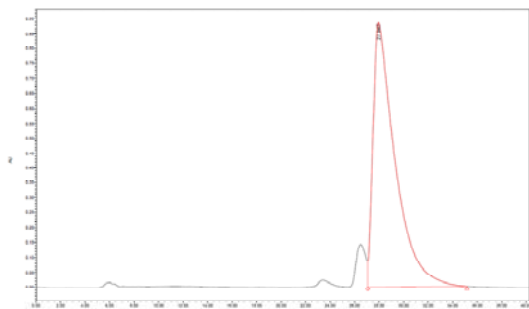
(3*S*,3*aR*,7*aR*)-3-(Benzo[d][1,3]dioxol-5-yl)hexahydrospiro[indole-5,2'-[1,3]dioxolan]-2(3*H*)-one [(3*S*,3*aR*,7*aR*)-**56gp**]. Yield: 180 mg, 72%, white foam.  $m_p = 155-156$  °C.  $[\alpha]_D^{25} = +32.26$  (*c* 1.6, CHCl<sub>3</sub>). FTIR (neat, cm<sup>-1</sup>) 3225, 1690. <sup>1</sup>H NMR (400 MHz, CDCl<sub>3</sub>)  $\delta$  7.50 (s, 1H, NH), 6.77 (d, *J* = 7.9 Hz, 1H, ArH), 6.72 – 6.64 (m, 2H, ArH), 5.91 (d, *J* = 2.9 Hz, 2H, OCH<sub>2</sub>O), 3.94 (dt, *J* = 29.8, 6.3 Hz, 4H, O(CH<sub>2</sub>)<sub>2</sub>O), 3.83 (d, *J* = 10.5 Hz, 1H, C<sup>3</sup>H), 3.59 (dt, *J* = 10.3, 6.1 Hz, 1H, C<sup>7a</sup>H), 2.55 (dd, *J* = 10.8, 5.4 Hz, 1H, C<sup>3a</sup>H), 1.95 (dd, *J* = 13.5, 5.1 Hz, 1H, C<sup>7</sup>H), 1.85 – 1.64 (m, 4H, C<sup>4</sup>H, C<sup>6</sup>H and C<sup>7</sup>H), 1.54 (td, *J* = 13.1, 3.8 Hz, 1H, C<sup>6</sup>H). <sup>13</sup>C NMR (101 MHz, CDCl<sub>3</sub>)  $\delta$  178.8, 148.0, 146.8, 131.6, 122.4, 109.1, 108.5, 108.1, 101.1, 64.6, 64.1, 51.2, 50.9, 44.6, 33.1, 31.3, 27.8. HRMS (ESI) for C<sub>17</sub>H<sub>20</sub>NO<sub>5</sub>: calculated [M + H]<sup>+</sup>: 318.1341. Found: 318.1332. HPLC (Daicel Chiralpak IA, hexane/<sup>i</sup>PrOH = 80:20, flow rate 1.0 mL/min,  $\lambda = 210$  nm),  $t_R = 56.07$  min.



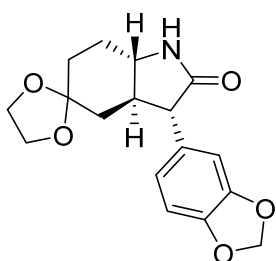
	Time	Area	% Height	% Area
1	56.073	25693894	100.00	100.00



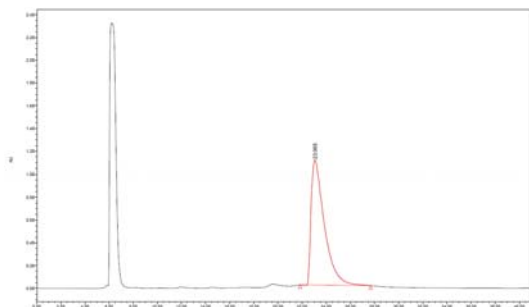
(3*S*,3*aS*,7*aS*)-3-(Benzo[d][1,3]dioxol-5-yl)hexahydrospiro[indole-5,2'-[1,3]dioxolan]-2(3*H*)-one [(3*S*,3*aS*,7*aS*)-**56gp**]. Yield: 10 mg, 4%, white solid.  $m_p = 186-187$  °C.  $[\alpha]_D^{25} = -69.21$  (*c* 0.48, CHCl<sub>3</sub>). FTIR (neat, cm<sup>-1</sup>) 3235, 1693, 1252, 1036, 1025, 728. <sup>1</sup>H NMR (400 MHz, CDCl<sub>3</sub>)  $\delta$  6.78 (d, *J* = 15.6 Hz, 3H, ArH), 5.92 (d, *J* = 4.0 Hz, 2H, OCH<sub>2</sub>O), 3.98 – 3.70 (m, 6H, O(CH<sub>2</sub>)<sub>2</sub>O, C<sup>3</sup>H and C<sup>7a</sup>H), 2.73 (dd, *J* = 12.0, 6.0 Hz, 1H, C<sup>3a</sup>H), 2.07 – 1.86 (m, 2H, C<sup>7</sup>H), 1.68 (m, 1H, C<sup>6</sup>H), 1.62 – 1.47 (m, 1H, C<sup>6</sup>H), 1.41 (t, *J* = 13.1 Hz, 1H, C<sup>4</sup>H), 1.14 – 0.98 (m, 1H, C<sup>4</sup>H). <sup>13</sup>C NMR (101 MHz, CDCl<sub>3</sub>)  $\delta$  177.7, 147.6, 146.6, 128.1, 123.0, 110.1, 108.4, 108.3, 101.1, 64.5, 64.3, 53.8, 50.3, 41.0, 32.4, 28.8, 25.4. HRMS (ESI) for C<sub>17</sub>H<sub>20</sub>NO<sub>5</sub>: calculated [M + H]<sup>+</sup>: 318.1341. Found: 318.1333. HPLC (Daicel Chiralpak IA, hexane/<sup>i</sup>PrOH = 80:20, flow rate 1.0 mL/min,  $\lambda = 210$  nm),  $t_R = 29.95$  min.



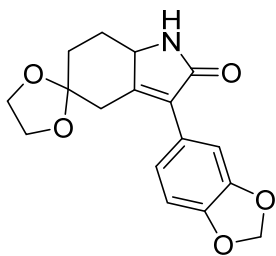
	Time	Area	% Height	% Area
1	29.947	110763599	100.00	100.00



(3*S*,3*aR*,7*aS*)-3-(Benzo[d][1,3]dioxol-5-yl)hexahydrospiro[indole-5,2'-[1,3]dioxolan]-2(3*H*)-one [(3*S*,3*aR*,7*aS*)-**56gp**]. Yield: 5 mg, 2%, white solid.  $m_p = 191-192$  °C.  $[\alpha]_D^{25} = +32.75$  (c 0.6, CHCl<sub>3</sub>). FTIR (neat, cm<sup>-1</sup>) 3245, 1691, 1234, 1035. <sup>1</sup>H NMR (400 MHz, CDCl<sub>3</sub>)  $\delta$  6.78 (d,  $J = 8.0$  Hz, 1H, ArH), 6.70 (s, 1H, ArH), 6.66 (d,  $J = 7.8$  Hz, 1H, ArH), 6.41 (s, 1H, NH), 5.99 – 5.89 (m, 2H, OCH<sub>2</sub>O), 4.01 – 3.77 (m, 4H, O(CH<sub>2</sub>)<sub>2</sub>O), 3.17 (d,  $J = 12.3$  Hz, 1H, C<sup>3</sup>H), 3.15 – 3.07 (m, 1H, C<sup>7a</sup>H), 2.21 – 2.10 (m, C<sup>3a</sup>H), 2.05 (d,  $J = 8.6$  Hz, 1H, C<sup>7</sup>H), 1.87 (d,  $J = 10.8$  Hz, 1H, C<sup>6</sup>H), 1.79 (d,  $J = 12.6$  Hz, 1H, C<sup>4</sup>H), 1.62 (dd,  $J = 15.0, 11.0$  Hz, 3H, C<sup>4</sup>H, C<sup>6</sup>H and C<sup>7</sup>H). <sup>13</sup>C NMR (101 MHz, CDCl<sub>3</sub>)  $\delta$  178.9, 148.1, 147.0, 130.2, 122.3, 109.0, 108.6, 108.4, 101.1, 64.7, 64.5, 57.4, 54.7, 49.7, 36.8, 33.9, 27.8. HRMS (ESI) for C<sub>17</sub>H<sub>20</sub>NO<sub>5</sub>: calculated  $[M + H]^+$ : 318.1341. Found: 318.1332. HPLC (Daicel Chiralpak IA, hexane/<sup>i</sup>PrOH = 80:20, flow rate 1.0 mL/min,  $\lambda = 210$  nm),  $t_R = 23.06$  min.

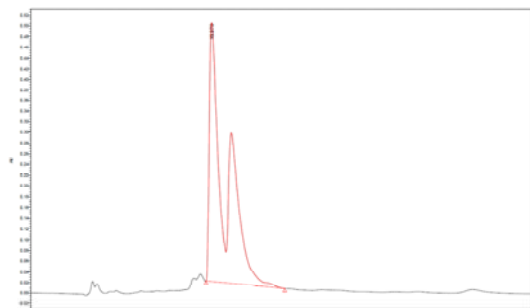


	Time	Area	% Height	% Area
1	23.065	83516501	100.00	100.00



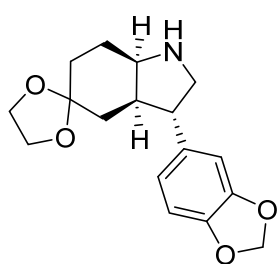
3-(Benzo[d][1,3]dioxol-5-yl)-1,6,7,7*a*-tetrahydrospiro[indole-5,2'-[1,3]dioxolan]-2(4*H*)-one (rac--**72**). Yield: 10 mg, 4%, white solid.  $m_p = 233-234$  °C. FTIR (neat, cm<sup>-1</sup>): 3234, 1681, 1244, 1037. <sup>1</sup>H NMR (400 MHz, CDCl<sub>3</sub>)  $\delta$  6.99 (s, 1H, ArH), 6.94 (d,  $J = 8.1$  Hz, 1H, ArH), 6.86 (d,  $J = 8.0$  Hz, 1H, ArH), 6.35 (s, 1H, NH), 5.97 (s, 2H, OCH<sub>2</sub>O), 3.95 (dq,  $J = 11.5, 5.7, 5.1$  Hz, 5H, O(CH<sub>2</sub>)<sub>2</sub>O and C<sup>7a</sup>H), 3.10 (d,  $J = 13.9$  Hz, 1H, C<sup>4</sup>H), 2.55 (d,  $J = 14.0$  Hz, 1H, C<sup>4</sup>H), 2.28 (m, 1H, C<sup>7</sup>H), 1.83 (m, 2H,

C<sup>6</sup>H), 1.52 (qd,  $J = 12.8, 4.6$  Hz, 1H, C<sup>7</sup>H). <sup>13</sup>C NMR (101 MHz, CDCl<sub>3</sub>)  $\delta$  173.7, 153.4, 147.6, 147.4, 130.7, 124.8, 123.2, 109.8, 109.8, 108.5, 101.1, 64.9, 64.7, 56.5, 36.9, 32.2, 29.8. HRMS (ESI) for C<sub>17</sub>H<sub>18</sub>NO<sub>5</sub>: calculated  $[M + H]^+$ : 316.1185. Found: 316.1182. HPLC (Daicel Chiralpak IA, hexane/<sup>i</sup>PrOH = 80:20, flow rate 1.0 mL/min,  $\lambda = 210$  nm),  $t_R = 16.98$  min.



	Time	Area	% Height	% Area
1	16.979	47152410	100.00	100.00

LiAlH<sub>4</sub> 1.0 M in THF (3.2 mL) was cooled under argon atmosphere to -20 °C and a previously dissolved and well-stirred, solution of AlCl<sub>3</sub> in THF (426.7 mg in 4 mL) was slowly added. The mixture was then allowed to reach room temperature and stirred for 30 minutes. Then, it was cooled to -20 °C and a solution of amide (3*S*,3*aR*,7*aR*)-**56gp** in THF (0.2 mmol, 63.4 mg in 3.5 mL) was added dropwise. The resulting mixture reaction was allowed to reach room temperature and stirred for 16 hours. Then, the reaction mixture was quenched at 0 °C with 5% aq. NH<sub>3</sub>. The precipitates were filtered and the filtrate evaporated. Then, the crude residue was dissolved in DCM and washed with brine, dried onto Na<sub>2</sub>SO<sub>4</sub> and concentrated. The oily residue thus obtained was chromatographed on silica gel with 1:1 DCM/MeOH to give starting material (3*S*,3*aR*,7*aR*)-**56gp** (25 mg, 38%) and (3*S*,3*aR*,7*aR*)-**67** (26.1 mg, 43%) as colorless oil.



(3*S*,3*aR*,7*aR*)-3-(Benzo[d][1,3]dioxol-5-yl) octahydrospiro [indole-5,2'-[1,3]dioxolane] [(3*S*,3*aR*,7*aR*)-**67**]. Analytical and spectroscopic properties were coincident with the previously reported data. Yield: 26.1 mg, 43%, colorless oil.  $[\alpha]_D^{25} = +57.07$  ( $c$  0.75, CHCl<sub>3</sub>). <sup>1</sup>H NMR (400 MHz, CDCl<sub>3</sub>)  $\delta$  6.71 (m, 3H, ArH), 5.92 (s, 2H, OCH<sub>2</sub>O), 4.05 – 3.76 (m, 4H, O(CH<sub>2</sub>)<sub>2</sub>O), 3.57 – 3.43 (m, 1H, C<sup>2</sup>H), 3.36 (q,  $J = 5.9$  Hz, 1H, C<sup>7a</sup>H), 3.27 (q,  $J = 8.3$  Hz, C<sup>3</sup>H), 2.96 (dd,  $J = 11.0, 8.0$  Hz, 1H, C<sup>2</sup>H), 2.24 (m, 1H, C<sup>3a</sup>H), 1.89 – 1.52 (m, 6H, CH<sub>2</sub>).

<sup>1</sup> (a) Kakeya, H.; Zhang, H. P.; Kobinata, K.; Onose, R.; Onozawa, C.; Kudo, T.; Osada, H. *J. Antibiot.* **1997**, *50*, 370-372. (b) Osada, H.; Kakeya, H.; Zhang, H. P.; Kobinata, K. WO 9823594. 1998 Jun 04. (c) Zhang, H. P.; Kakeya, H.; Osada, H. *Tetrahedron Lett.* **1998**, *39*, 6947-6948. (d) Kakeya, H.; Onose, R.; Osada, H. *Cancer Res.* **1998**, *58*, 4888-4894.

<sup>2</sup> Hayashi, Y.; Shoji, M.; Ishikawa, H.; Yamaguchi, J.; Imai, H.; Nishigaya, Y.; Takabe, K.; Kakeya, H.; Osada, H. *Angew. Chem. Int. Ed.* **2008**, *47*, 6657-6660.

<sup>3</sup> Northup, A. B.; MacMillan, D. W. C. *J. Am. Chem. Soc.* **2002**, *124*, 6798-6799.

- <sup>4</sup> (a) Kamano, Y.; Zhang, H.-P.; Ichihara, Y.; Kizu, H.; Komiyama, K.; Pettit, G. R. *Tetrahedron Lett.* **1995**, *36*, 2783-2784. (b) Zhang, H.-P.; Kamano, Y.; Ichihara, Y.; Kizu, H.; Komiyama, K.; Itokawa, H.; Pettit, G. R. *Tetrahedron* **1995**, *51*, 5523-5528. (c) Kamano, Y.; Kotake, A.; Hashima, H.; Hayakawa, I.; Hiraide, H.; Zhang, H.-P.; Kizu, H.; Komiyama, K.; Hayashi, M.; Pettit, G. R. *Collect. Czech. Chem. Commun.* **1999**, *64*, 1147-1153.
- <sup>5</sup> Chen, J. R.; Liu, X. P.; Zhu, X. Y.; Li, L.; Qiao, Y. F.; Zhang, J. M.; Xiao, W. J. *Tetrahedron*, **2007**, *63*, 10437-10444.
- <sup>6</sup> (a) Kaufman, T. S.; Rúveda, E. A. *Angew. Chem. Int. Ed.* **2005**, *44*, 854-885. (b) Song, C. E. *Cinchona Alkaloids in Synthesis and Catalysis: Ligands, Immobilization and Organocatalysis*, **2009**, Weinheim: Wiley-VCH. (c) Marcelli, T.; Hiemstra, H. *Synthesis*, **2010**, 1229-1279.
- <sup>7</sup> Sarkar, S. M.; Taira, Y.; Nakano, A.; Takahashi, K.; Ishihara, J. Hatakeyama, S. *Tetrahedron Lett.* **2011**, *52*, 923-927.
- <sup>8</sup> (a) Raheem, I. T.; Goodman, S. N.; Jacobsen, E. N. *J. Am. Chem. Soc.* **2004**, *126*, 706-707. (b) Igarashi, J.; Katsukawa, M.; Wang, Y. G.; Acharaya, H. P.; Kobayashi, Y. *Tetrahedron Lett.* **2004**, *45*, 3783-3786. (c) Igarashi, J.; Kobayashi, Y. *Tet. Lett.* **2005**, *46*, 6381-6384.
- <sup>9</sup> (a) Austin, J. F.; MacMillan, D. W. C. *J. Am. Chem. Soc.* **2002**, *124*, 1172-1173. (b) Paras, N. A.; *J. Am. Chem. Soc.* **2002**, *124*, 7894-7895.
- <sup>10</sup> Hanessian, S.; Stoffman, E.; Mi, X.; Renton, P. *Org. Lett.* **2011**, *13*, 840-843.
- <sup>11</sup> Jakubec, P.; Cockfield, D. M.; Dixon, D. J. *J. Am. Chem. Soc.* **2009**, *131*, 16632-16633.
- <sup>12</sup> (a) Magnier, E.; Langlois, Y. *Tetrahedron*, **1998**, *54*, 6201-6258. (b) Kobayashi, J.; Watanabe, D.; Kawasaki, N.; Tsuda, M. *J. Org. Chem.* **1997**, *62*, 9236-9239. (c) Kobayashi, J.; Tsuda, M.; Ishibashi, M. *Pure. Appl. Chem.* **1999**, *71*, 1123-1126.
- <sup>13</sup> Hoashi, Y.; Yabuta, T.; Takemoto, Y. *Tetrahedron Lett.* **2004**, *45*, 9185-9188.
- <sup>14</sup> Bui, T.; Syed, S. Barbas III, C. F. *J. Am. Chem. Soc.* **2009**, *131*, 8758-8759.
- <sup>15</sup> (a) Matsuura, T.; Overman, L. E.; Poon, D. J. *J. Am. Chem. Soc.* **1998**, *120*, 6500-6503. (b) Asakawa, K.; Noguchi, N.; Takashima, S.; Nakada, M. *Tetrahedron: Asymm.* **2008**, *19*, 2304-2309.
- <sup>16</sup> Witherup, K. M.; Ranson, R. W.; Graham, A. C.; Bernand, A. M.; Salvatore, M. J.; Lumma, W. C.; Anderson, R. P. S.; Pitzewberger, S. M.; Verga, S. L. *J. Am. Chem. Soc.* **1995**, *117*, 6682-6685.
- <sup>17</sup> Yoshitomi, Y.; Arai, H.; Makino, K.; Hamada, Y. *Tetrahedron*, **2008**, *64*, 11568-11579.
- <sup>18</sup> (a) Bowman, W. R.; Brown, D. S.; Chaffin, J. D. E.; Symons, M. C. R.; Jackson, S. W.; Willcocks, N. A. *Tetrahedron Lett.* **1991**, *32*, 2285-2288. (b) Symons, M. C. R.; Bowman, W. R.; Bradley, G. W.; Morris, D. G. *J. Chem. Soc. Perkin Trans 2*, **1992**, 545-547.
- <sup>19</sup> Berrocal, M. V.; Gil, M. V.; Román, E.; Serrano, J. A. *Tetrahedron* **2002**, 5327-5333.
- <sup>20</sup> Zhong, J. *Nat. Prod. Rep.* **2009**, *26*, 363-381.
- <sup>21</sup> Dry, L. G.; Poynton, M. E.; Thompson, M. E.; Warren, F. L. *J. Chem. Soc.* **1958**, 4701-4704.
- <sup>22</sup> (a) Wildman, W. C.; Kaufman, C. J. *J. Am. Chem. Soc.* **1955**, *77*, 1248-1252. (b) Inubushi, Y.; Fales, H. M.; Warnhoff, E. W.; Wildman, W. C. *J. Org. Chem.* **1960**, *25*, 2153-2164. (c) Wildman, W. C.; Brown, C. L. *J. Am. Chem. Soc.* **1968**, *90*, 6439-6446.
- <sup>23</sup> Southon, I.; Buckingham, J. *Dictionary of the Alkaloids*, **1989**, Chapman & Hall: New York.
- <sup>24</sup> Overman, L. E.; Shim, J. *J. Org. Chem.* **1991**, *56*, 5005-5007.
- <sup>25</sup> Ishizaki, M.; Hoshino, O.; Iitaka, Y. *Tetrahedron Lett.* **1991**, *32*, 7079-7082.
- <sup>26</sup> Overman, L. E.; Shim, J. *J. Org. Chem.* **1993**, *58*, 4662-4672.
- <sup>27</sup> Jin, J.; Weinreb, S. M. *J. Am. Chem. Soc.* **1997**, *119*, 2050-2051. (b) Jin, J.; Weinreb, S. M. *J. Am. Chem. Soc.* **1997**, *119*, 5773-5784.
- <sup>28</sup> Bao, X.; Cao, Y.-X.; Chu, W.-D.; Qu, H.; Du, J.-Y.; Zhao, X.-H.; Ma, X.-Y.; Wang, C.-T.; Fan, C.-A. *Angew. Chem. Int. Ed.* **2013**, *52*, 14167-14172.
- <sup>29</sup> Ishizaki, M.; Kurihara, K.-I.; Tanazawa, E.; Hoshino, O. *J. Chem. Soc. Perkin Trans 1* **1993**, 101-110.
- <sup>30</sup> Ikeda, M.; Hamada, M.; Yamashita, T.; Matsui, K.; Sato, T.; Ishibashi, H. *J. Chem. Soc. Perkin Trans 1* **1999**, 1949-1956.
- <sup>31</sup> Banwell, M. G.; Edwards, A. J.; Jolliffe, K. A.; Kemmler, M. *J. Chem. Soc. Perkin Trans 1*, **2001**, 1345-1348.
- <sup>32</sup> Pandey, G.; Banerjee, P.; Kumar, R.; Puranik, V. G. *J. Org. Lett.* **2005**, *7*, 3713-3716.
- <sup>33</sup> Chang, M.-Y.; Chen, H.-P.; Lin, C.-Y.; Pai, C.-L. *Heterocycles* **2005**, *65*, 1999-2004.
- <sup>34</sup> Anada, M.; Tanaka, M.; Shimada, N.; Nambu, H.; Yamawaki, M.; Hashimoto, S. *Tetrahedron*, **2009**, *65*, 3069-3077.
- <sup>35</sup> Pansare, S. V.; Lingampally, R.; Kirby, R. L. *Org. Lett.* **2010**, *12*, 556-559.

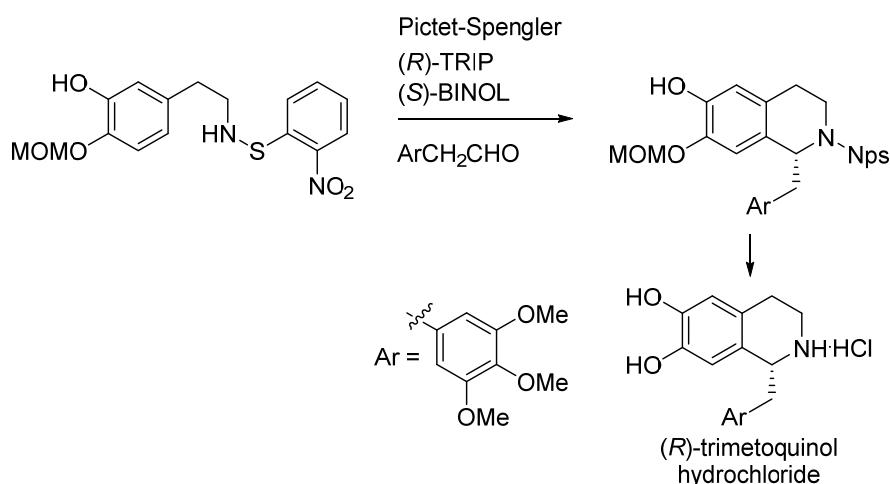


<sup>36</sup> Ikeda, M.; Hamada, M.; Yamashita, T.; Matsui, K.; Sato, T.; Ishibashi, H. *J. Chem. Soc. Perkin Trans 1* **1999**, 1949-1956.

<sup>37</sup> Revial, G.; Lim, S.; Viossat, B.; Lemoine, P.; Tomas, A.; Duprat, A. F.; Pfau, M. *J. Org. Chem.* **2000**, *65*, 4593-4600.



# Chapter 5. Organocatalyzed Pictet-Spengler Reaction for the Synthesis of 1-Benzyl-1,2,3,4-Tetrahydroisoquinolines and Total Synthesis of (*R*)-Trimetoquinol Hydrochloride



## Abstract.

A new phenylethylamine derived substrate was prepared for the organocatalyzed Pictet-Spengler reaction with substituted phenylacetaldehydes. (*R*)-TRIP, a BINOL-derived chiral phosphoric acid, was employed in junction with (*S*)-BINOL as co-catalyst. After some optimization studies, the synthetic route towards enantiopure (*R*)-trimetoquinol hydrochloride was achieved.

Part of this chapter has been published as: Ruiz-Olalla, A.; Würdemann, M. A.; Wanner, M. J.; Ingemann, S.; van Maarseveen, J. H.; Hiemstra, H. *J. Org. Chem.* **2015**, *80*, 5125-5132.

Article also selected by the ACS Catalysis Journal: Ooi, T. Virtual Issue Posts on Organocatalysis: Design, Applications, and Diversity. *ACS Catal.* **2015**, *5*, 6980-6988.



## 5.1. Introduction

1-Substituted 1,2,3,4-tetrahydroisoquinoline (THIQ) alkaloids such as (+)-crispine **I**<sup>1</sup>, (-)-norcoclaurine **II**<sup>2</sup> or (+)-sinomenine **III**<sup>3</sup> and their derivatives as morphine **IV**<sup>4</sup> or aporphine alkaloids **V**<sup>5</sup> are receiving enhancing attention in both medicinal and synthetic chemistry due to their large pharmacological applications (Figure 1).<sup>6</sup>

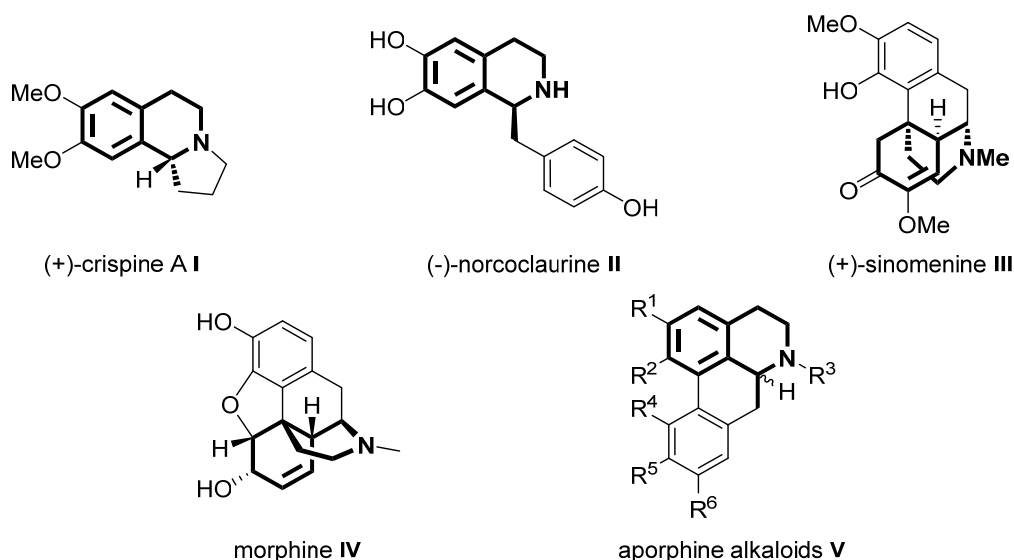
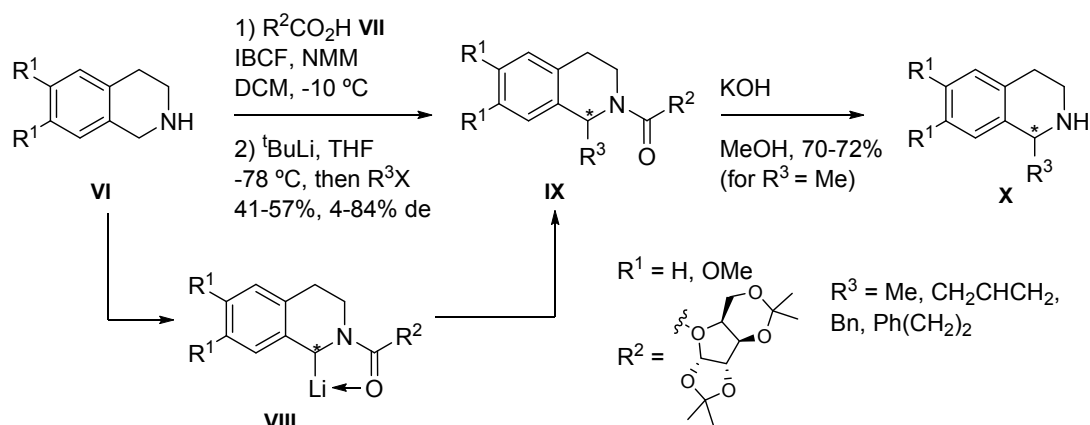


**Figure 1.** Relevant THIQ's and derived structures.

Due to their different biological activities of both enantiomers in some cases,<sup>7</sup> the search of efficient methodologies for the stereoselective synthesis is becoming a challenge for the synthetic field.

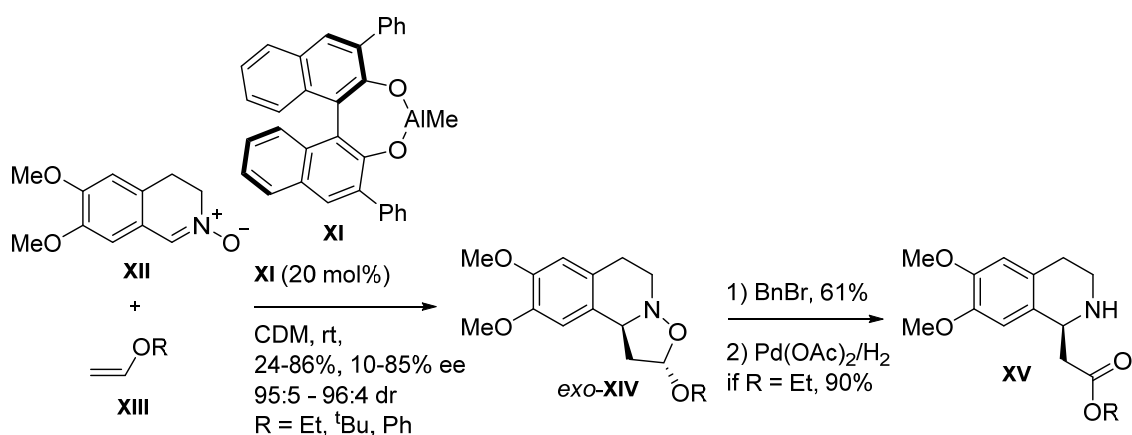
### 5.1.1. Asymmetric synthesis of 1-substituted-1,2,3,4-tetrahydroisoquinolines

Intense efforts have been made in order to reach successful synthetic approaches towards 1-substituted 1,2,3,4-tetrahydroisoquinoline structures.<sup>8</sup> Resolution of racemate mixtures of 1-benzyltetrahydroisoquinolines by cocrystallization with tartaric acid has been reported.<sup>9</sup> Other methods also allow the synthesis of enantiopure 1-substituted THIQ's in two steps: cyclization and then the formation of the stereocenter, for instance by  $\alpha$ -lithiation of amides (Scheme 1).<sup>10</sup> As a representative example, Quirion reported the alkylation of amides **VIII** derived from gulonic acid derivative **VII** where the stereochemistry was assigned at the alkylation stage. Nevertheless, the value of enantiomeric excesses reported for few non-functionalized electrophiles **X** were moderate.



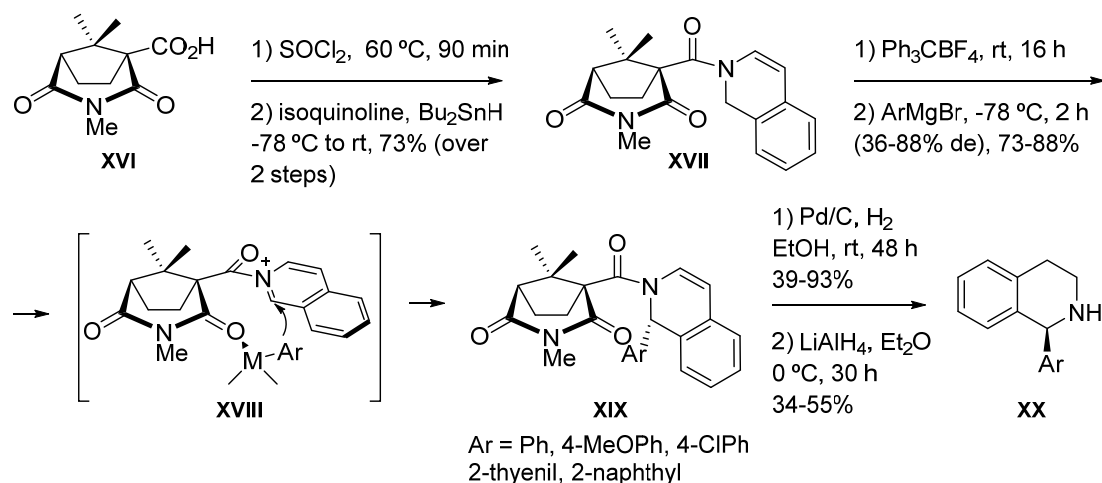
**Scheme 1.** Introduction of stereocenter by means of  $\alpha$ -lithiation of amides.

Also, (3+2) cycloaddition of cyclic nitrones **XII** derived from isoquinolines with electron-rich alkenes as **XIII** in presence of the suitable BINOL-derived AlMe complex **XI** functionalizes the position 1 of the alkaloid (Scheme 2).<sup>11</sup> The major diastereoisomer turned to be *exo*-**XIV** in all cases in high yields and ee's up to 85%. Also, they showed that reaction with benzyl bromide followed by reduction gave aminoester **XV** in high yield, thus, being able to assign the stereochemistry by comparison.



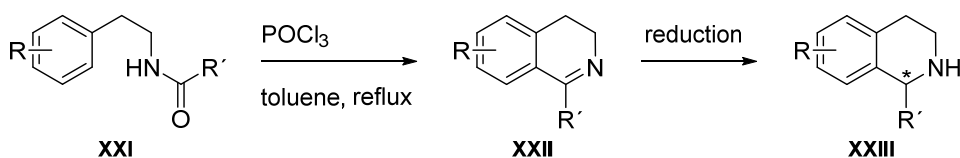
**Scheme 2.** (3+2) cycloaddition of isoquinoline derived cyclic nitrones.

1-substituted 1,2,3,4-THIQ's can also be obtained by stereoselective addition of organozinc compounds to the *N*-acyl isoquinolinium intermediate **XVIII** as for the work reported by Wanner et al.<sup>12</sup> In this case, the stereochemical induction was rationalized by the induction created by the chiral auxiliary **XVI** which properly produced complexation to the ambiphilic organoreagent (**XVIII** in Scheme 3). The process provided good diastereoselectivities, but the aryl-magnesium chloride nucleophiles provided better yields than their alkyl counterparts. Following hydrogenation and reduction allowed 1-substituted 1,2,3,4-THIQ's **XX**.



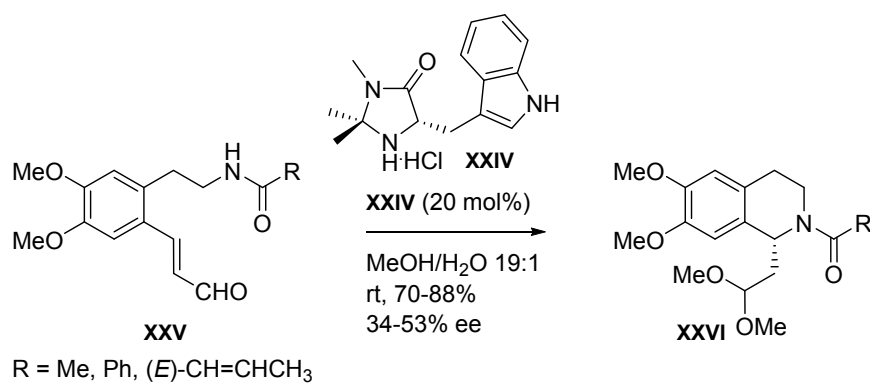
**Scheme 3.** Asymmetric addition of an organometallic compound to *N*-acyl isoquinolinium intermediate.

Other reaction such as the Bischler-Napieralski/reduction cyclization is also known as a powerful method for the construction of the isoquinoline core.<sup>13</sup> It allows the synthesis of 3,4-dihydroisoquinolines **XXIII** starting from electron rich phenylethylamides **XXI** aided by condensation reagents as  $\text{POCl}_3$  or  $\text{P}_2\text{O}_5$  (Scheme 4). These products **XXII** are often further reduced via hydride reduction<sup>14</sup> or asymmetric hydrogenation to provide 1-substituted 1,2,3,4-THIQ derivatives **XXIII**. For this stage, several metal complexes have been applied such as diphosphine-iridium (I)<sup>15</sup>, diamine ruthenium<sup>16</sup> or even Lewis acid thiazazincolidine complexes in junction with borane complexes<sup>17</sup> have been used.



**Scheme 4.** Bischler-Napieralski cyclization and reduction.

Lastly, the group the Takasu and Ihara published in 2003 the first intramolecular aza-Michael reaction with enals (Scheme 5).<sup>18</sup> The reaction of bifunctional dopamine derivatives **XXV** occurred through nucleophilic attack of the amide moiety on the iminium-ion formed with the chiral oxazolidinone **XXIV**. This process gave access to a range of 1,2,3,4-tetrahydroisoquinolines **XXVI** in good yield but with low enantiomeric excesses. However, the reaction was limited to 3,4-dimethylated 1-substituted dimethoxyethyl tetrahydroisoquinolines, hampering its use towards total synthetic purposes.

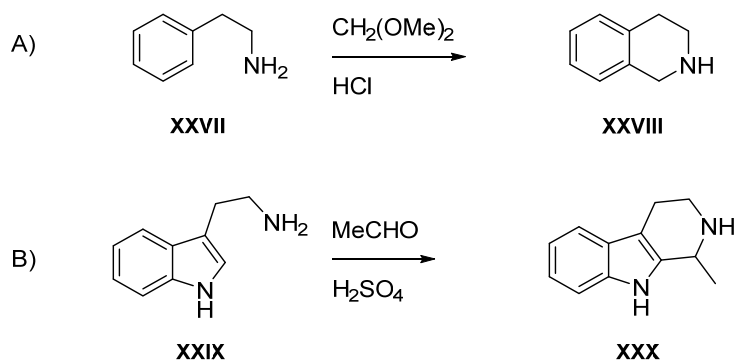


**Scheme 5.** Intramolecular aza-Michael addition of amides to enals.

Therefore, none of these methodologies are able to generate the stereogenic carbon at C-1 with simultaneous ring closure in decent enantioselectivities with assortment at the hydroxyl groups of the dopamine scaffold neither different functionalities at the C-1 carbon. Additionally, most of the reported procedures are not metal-free and a more desirable synthesis would be required in view of pharmaceutical applications for instance the bio-mimetic Pictet-Spengler condensation.

### 5.1.2. Pictet-Spengler reaction

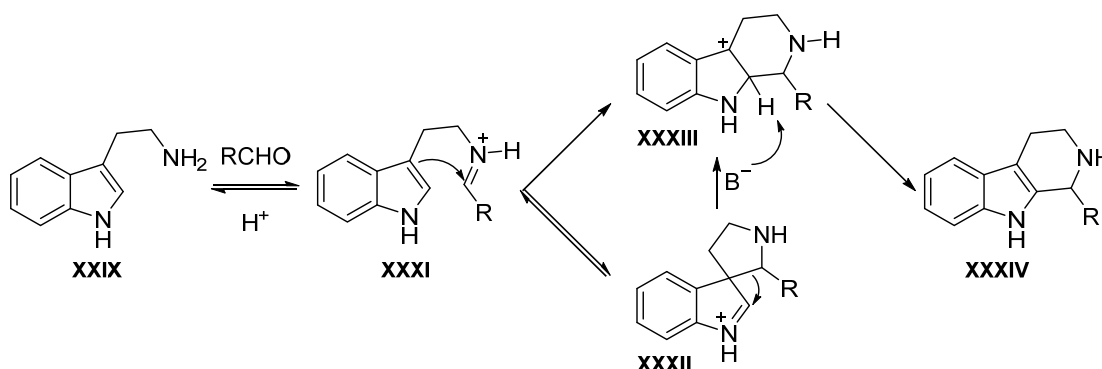
In early 1900, Amè Pictet and Theodor Spengler heated a reaction mixture containing  $\beta$ -phenylethylamine **XXVII** and formaldehyde dimethylacetal in the presence of hydrochloric acid producing 1,2,3,4-tetrahydroisoquinoline alkaloid **XXVIII** (Scheme 6A).<sup>19</sup> It was 20 years later when Tatsui performed the same reaction this time in the presence of tryptamine **XXIX** (Scheme 6B) as the amine skeleton and acetaldehyde to produce for the first time the structure of 1-methyl-1,2,3,4-tetrahydro- $\beta$ -carboline (THBC) **XXX**.<sup>20</sup>



**Scheme 6.** First Pictet-Spengler reactions towards A) tetrahydroisoquinolines and B) tetrahydro- $\beta$ -carbolines.

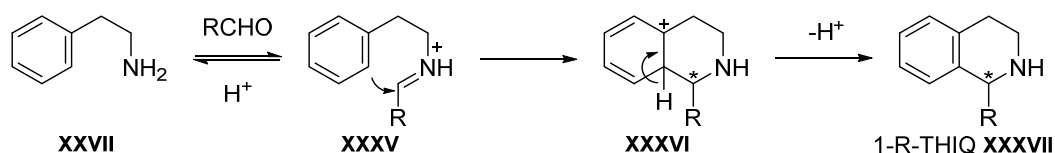


The validated mechanism for the Pictet-Spengler reaction with tryptamine as nucleophile is shown in Scheme 7.<sup>21</sup> The reaction commences with the formation of an iminium intermediate **XXXI** by condensation between the amine moiety of **XXIX** and the aldehyde. It is then followed by a nucleophilic addition from the position C-3 which produces the spiro intermediate **XXXII**.<sup>22</sup> The formation of this intermediate is fast and reversible and lastly, the further rearrangement or the formation of the pentahydro- $\beta$ -carboline carbonium ion **XXXIII** (which is still unclear the exact mechanism<sup>23</sup>) through the attack from the position 2 produces the final product **XXXIV**.



**Scheme 7.** The mechanism of the Pictet-Spengler reaction with indole as nucleophile.

The accepted mechanism for the Pictet-Spengler reaction with phenylethylamines **XXVII** occurs in a similar manner (Scheme 8).<sup>24</sup> The difference resides in the addition step **XXXV** in which the nucleophilic moiety is the phenyl group and, therefore, less nucleophilic scaffold when compared to the indole group in tryptamine (**XXXI** vs. **XXXV**).

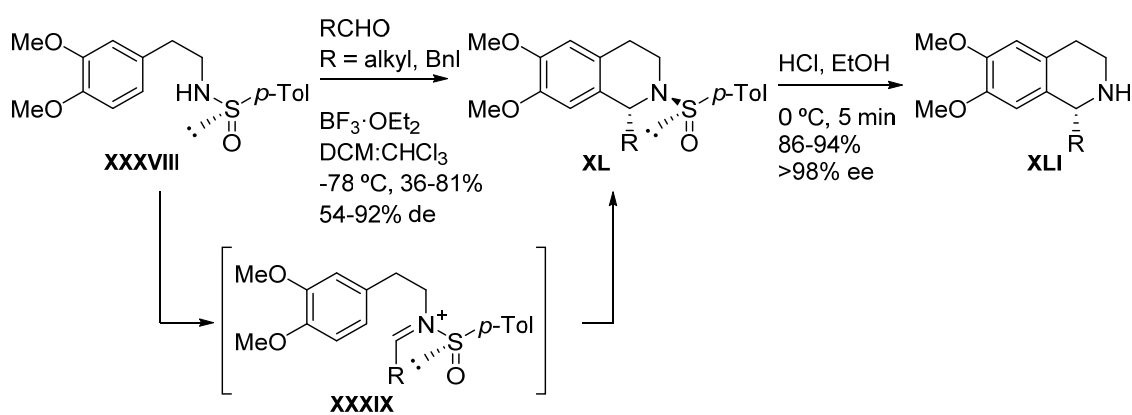


**Scheme 8.** The mechanism of the Pictet-Spengler reaction with a phenyl group as nucleophile.

There is a wide range of reported enantioselective Pictet-Spengler reactions which are focused in the nucleophilic tryptamine and its derivatives towards the synthesis of tetrahydro- $\beta$ -carbolines.<sup>21a</sup> This is due to its high nucleophilic indole, the presence of the nitrogen atom, which may interact by hydrogen bond network with Brønsted acids<sup>25</sup> or chiral thiourea catalysts<sup>26</sup>, and the electronic properties which are able to promote secondary interactions with, for instance, aromatic substituents of chiral organocatalysts. In these cases, also the electrophilicity is increased by activating the iminium moiety with *N*-acyl<sup>26b</sup> or *N*-sulfonyl<sup>27</sup> scaffolds. By using this methodology, the

synthesis of a wide array of natural molecules has been achieved such as yohimbine<sup>25</sup>, mitragynine, paynantheine, speciogynine<sup>26c</sup> and arboricine<sup>28</sup>.

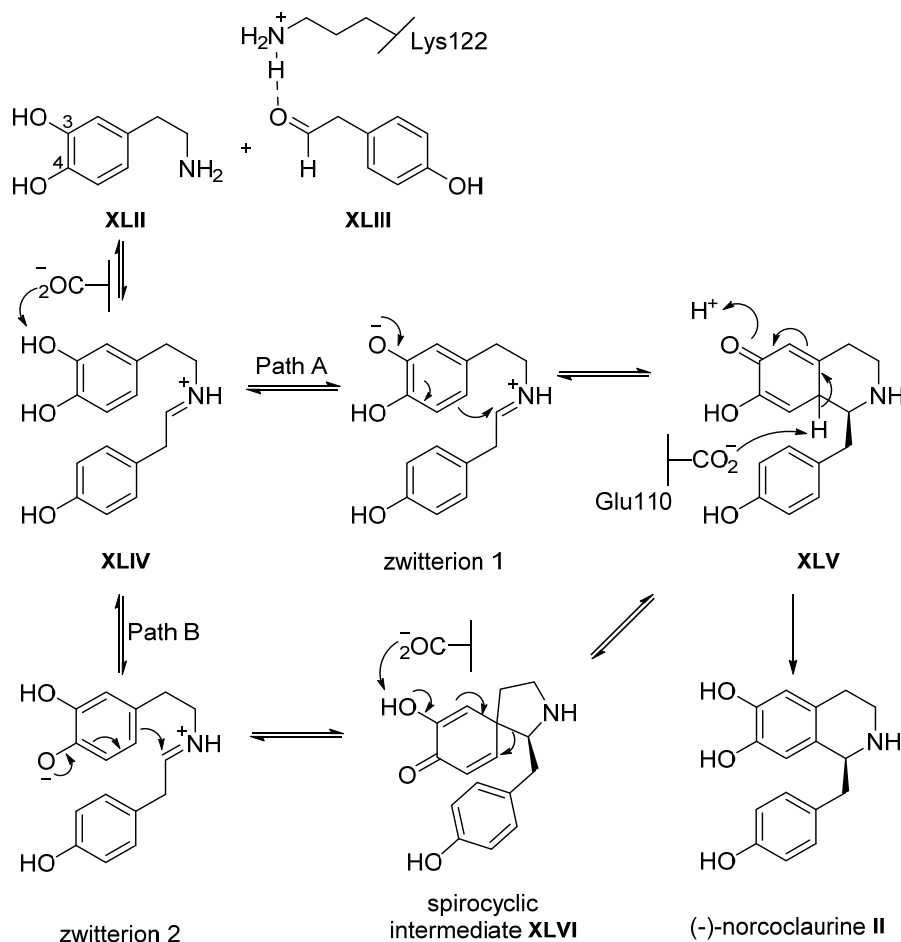
However, efforts are being made in order to obtain enantioenriched THIQ's. For example, there are numerous reported approaches that employ chiral auxiliaries.<sup>29</sup> For instance, in 2001 the group of Koomen proposed a diastereoselective method to obtain 1-alkyl- and 1-benzyl- substituted THIQ's **XLI** by placing a chiral *p*-tolylsulfinyl auxiliary.<sup>30</sup> The corresponding products **XL** were achieved with diastereoselectivities up to 92% de (Scheme 9) and later, the chiral auxiliary could be removed by treatment with HCl in ethanol at 0 °C without racemization.



**Scheme 9.** Diastereoselective Pictet-Spengler reaction.

Some other chiral auxiliaries that have been reported apart from sulfoxide groups<sup>31</sup> for the synthesis of 1-substituted THIQ via Pictet-Spengler cyclizations are galactosyl bromide<sup>32</sup> or trans-2-( $\alpha$ -cumyl)cyclohexanol<sup>33</sup> among others<sup>34</sup>.

Taking into the account mechanistic aspects of the enzymatic process catalyzed by norcoclaurine synthase (NCS) between dopamine **XLII** with 4-hydroxyphenyl acetaldehyde **XLIII**, it is stated that the reaction mechanism can occur according to a bifunctional catalytic process in both reaction sequences.<sup>35</sup> According to X ray analyses and as illustrated in Scheme 10, the key catalytic residue Lys122 may interact with the aldehyde **XLIII** thus, forming a Schiff base with dopamine which protonates to give iminium ion **XLIV**.

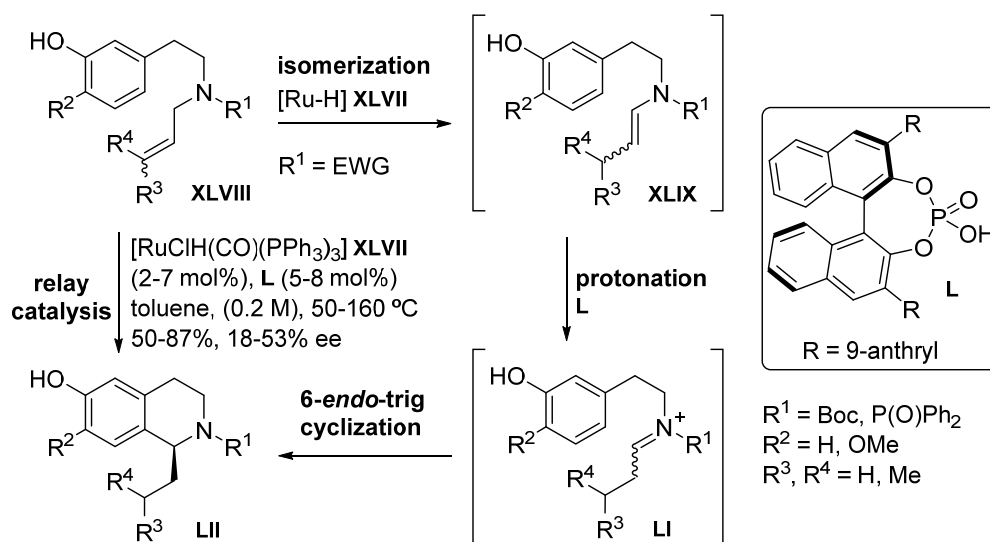


**Scheme 10.** The norcoclaurine synthase-catalyzed reaction between dopamine **XLII** and 4-hydroxyphenylacetaldehyde **XLIII**.

After condensation, the cyclization of zwitterion 1 (assisted by deprotonation of the hydroxyl group at the 3 position in Path A) could also be supported by Glu110 residue helping the aromatization process towards the formation of (-)-norcoclaurine II. Path B (less probable<sup>36</sup>) includes again the formation of the spiro intermediate **XLVI** in similar manner to the example showed in Scheme 7. Also, these studies showed that both 4-methoxy- and 4-deoxydopamine still are good NCS substrates with good activity comparable to dopamine. Nevertheless, these precursors would not allow the reaction to proceed through pathway B. Additional results stated that 3-methoxy- and 3-deoxydopamine were not accepted by the enzyme, probably due to the absence of the acidic OH group at C-3 position which would be necessary for the ring closing step (of the spirocyclic intermediate **XLVI**).

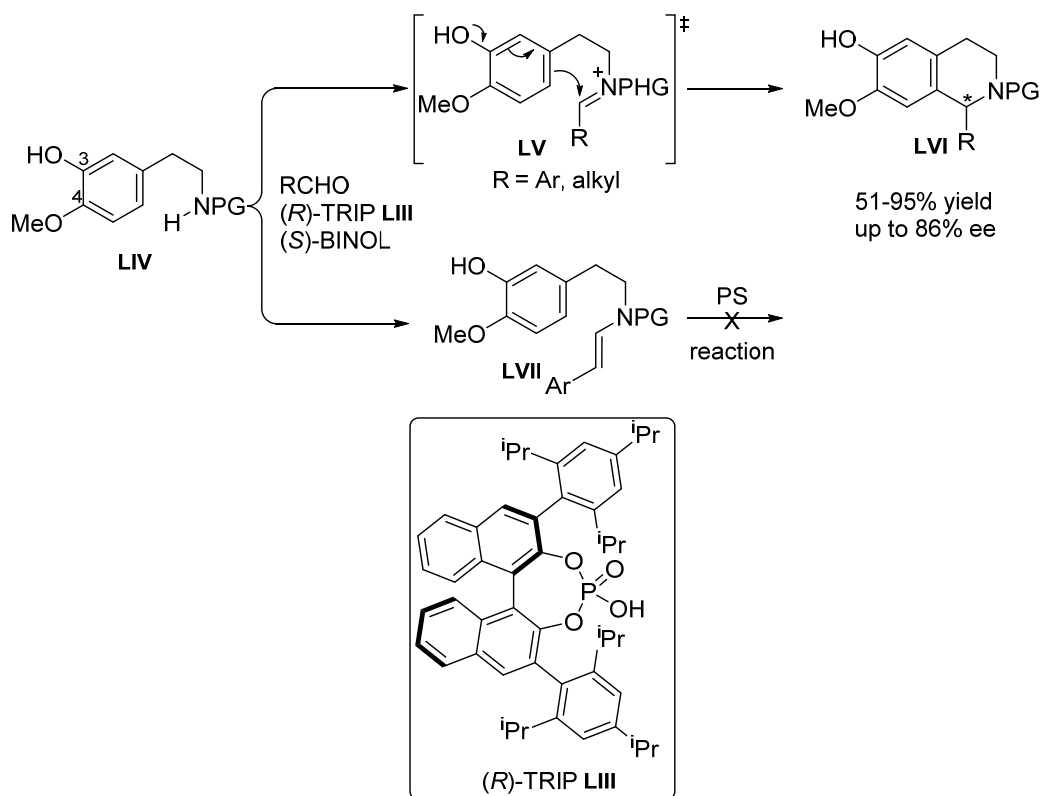
### 5.1.3. Organocatalyzed Pictet-Spengler reaction towards 1-substituted THIQs

The first example of a pseudo-organocatalyzed reaction towards THIQ's as final products was published by Toda and Terada in 2013.<sup>37</sup> They reported a ruthenium **XLVII**-catalyzed isomerisation of the allylamide substrate **XLVIII** to enamide **XLIX** (Scheme 11). It was then protonated by the chiral phosphoric acid **L** to provide the iminium intermediate **LI** which was followed by an enantioselective organocatalyzed Pictet-Spengler reaction towards **LII** (through a 6-*endo*-trig type cyclization) under the effect of the chiral environment provided by the chiral Brønsted acid. This became the first example of the simultaneous cyclization and introduction of the stereocenter. However, the obtained enantiomeric induction reached moderate values and also, the scope of the reaction was limited to allylamides.



**Scheme 11.** Relay catalytic approach reported by Toda and Terada.

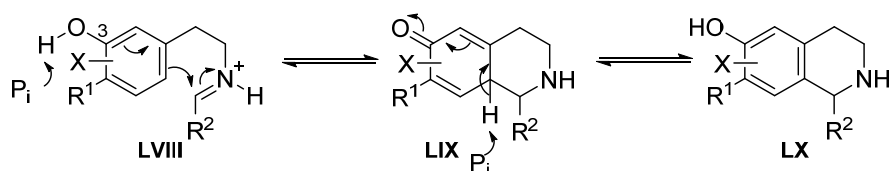
Shortly after, the group published a pioneering work describing the metal-free organocatalyzed PS reaction leading to 1-substituted THIQ's **LVI** (Scheme 12).<sup>11</sup> The reaction was assisted by (*R*)-TRIP **LIII**, a BINOL- derived phosphoric acid, with phenylethyl protected amines **LIV** in ee's up to 86% with aromatic and aliphatic aldehydes. Previous experimental work in the group showed that the conditions established for this reaction did not success when phenylacetaldehydes were used as electrophiles due to, probably, a dead end of the strongly stabilized enamine intermediate **LVII**. If the reactivity and enantioselectivity of this process could be controlled, the obtained PS products would be easily transformed to a large number of biologically active natural products such as norcoclaurine **II** in Figure 1 (vide supra).



**Scheme 12.** Enantioselective PS approach with phenylethylamine as precursor towards 1-substituted THIQs.

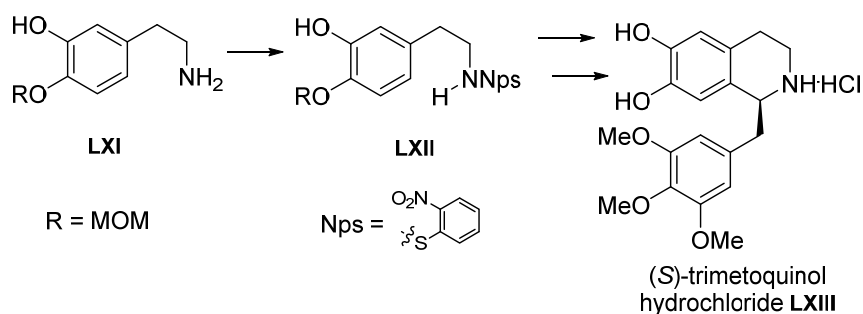
#### 5.1.4. Objectives

Earlier experimental studies in the group on the PS reaction using BINOL-based phosphoric acids as catalysts showed that the 3-methoxy electron donating group in 3,4-dimethoxyphenylethylamine was not sufficiently activating at the *para*- position for the ring closure to occur. Additionally, this result was in agreement with the work described by Hailes *et al.* in which they identified the reaction conditions for the  $\text{KH}_2\text{PO}_4$  mediated Pictet-Spengler cyclization (Scheme 13).<sup>38</sup> When they tested an array of different phenylethylamines, the obtained results suggested that a hydroxyl (or amine) electron donating group at *meta*- to the ethylamine group was required for the cyclization. Also, it was suggested that the mechanism involved the formation of the 6-membered isoquinoline ring **LX** instead of the 5-membered spirocyclic intermediate.<sup>35b</sup>



**Scheme 13.** Proposed phosphate mediated mechanism for the Pictet-Spengler reaction.  $P_i$  = phosphate.

Another important matter is the nature of the substituent on the adjacent phenolic oxygen atom. The 4-OH has always been methylated in the previous work<sup>11</sup>, as it is present in many natural products such as (*S*)-calycotomine and (*R*)-crispine A (see **LIV** in Scheme 12). Changing this substituent also influenced the PS reaction as was observed in preliminary studies: A large group such as OTBS slowed down the reaction drastically. Further functionalization of the 4-OH with other containing heteroatoms groups (e.g. methyloxymethyl, MOM), which could activate the 3-OH intramolecularly by hydrogen bonding may give improvement. Additional advantage of a removable protecting group at the 4-OH is the entry to a large group of alkaloids with a free 4-OH such as (*S*)-trimetoquinol **LXIII**.



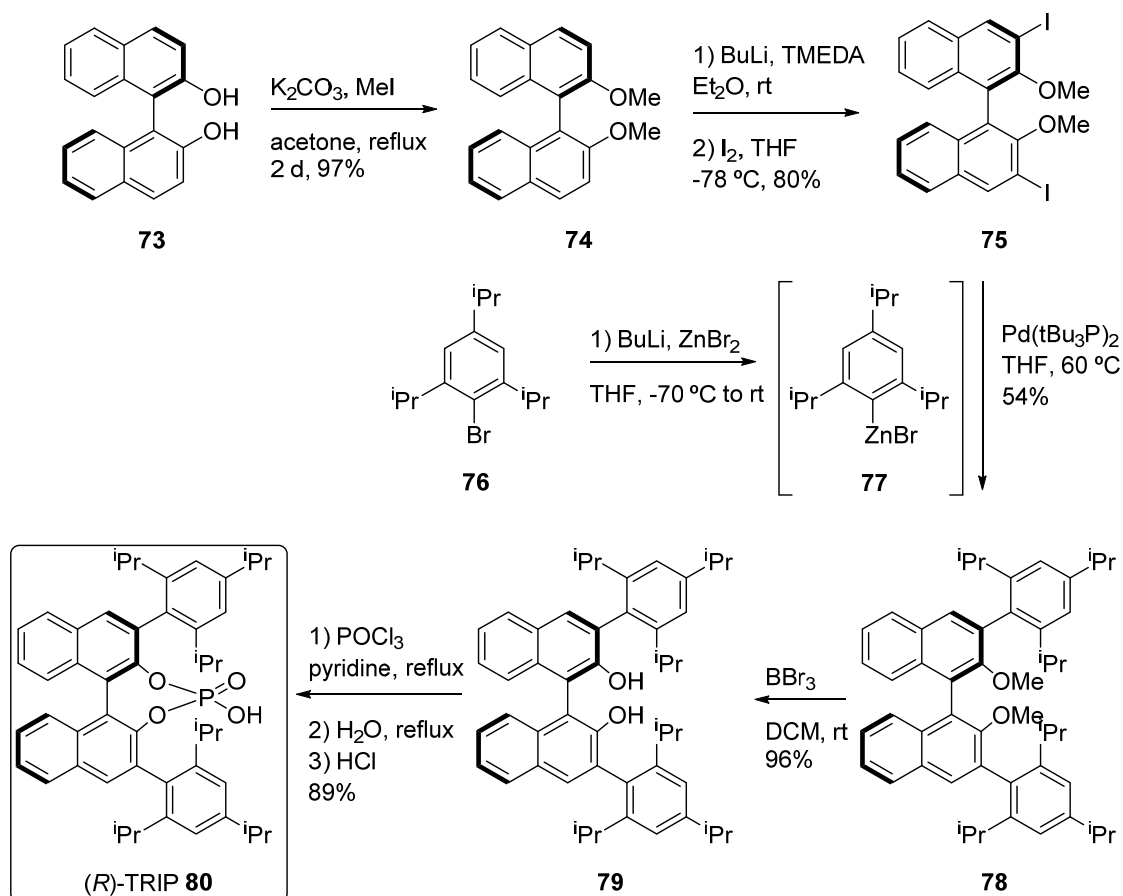
**Scheme 14.** Precursor **LXI** towards (*S*)-trimetoquinol hydrochloride **LXIII** natural products.

Thus, the aim of the project laid in finding the proper method to produce a decent enantioselective Pictet-Spengler reaction to synthesize 1-benzyl 1,2,3,4-tetrahydroisoquinoline derivatives. Lastly, the sequence to achieve these purposes are the 1) synthesis of the 4-MOM protected PS precursor **LXII**. Then, 2) analysis of the MOM- role at the *ortho*-nitrophenylsulfenyl (Nps) protected phenylethyl amine **LXII** for the PS reaction will be explored when the reaction is organocatalyzed by BINOL-based phosphoric acids (Figure 2).

If successful, this easily removable group, together with the removal of the acid labile Nps protecting group, would lead to the conversion of the Pictet-Spengler products (and optional functionalizations) into natural THIQ's.

## 5.2. Synthesis of (*R*)-TRIP 80 catalyst and analogues

(*R*)-TRIP **80** organocatalyst is one of the most common Brønsted acids employed nowadays. It is commercially available but due to its high price (333€/100 mg, on December 2015), its synthesis is recommendable. The readily accessible catalyst in the laboratory was synthesized according to a modified procedure of List's work<sup>39</sup> in which a palladium-catalyzed Negishi coupling had been introduced (Scheme 15).<sup>40</sup>



**Scheme 15.** Total synthesis of (*R*)-TRIP **80** from (*R*)-BINOL **73** established in the hosting group.

It consisted of a 5 steps procedure providing (*R*)-TRIP **80** in 36% in gram scale. The synthetic route commenced with the protecting of the OH groups, to give dimethyl ester **74** quantitatively. Then, C3 and C3' positions were functionalized by a directed *ortho*-lithiation and iodination providing **75** in good yield. Next, the palladium-catalyzed Negishi coupling between **75** and zinc bromide **77** provided **78** in moderate yield due to low conversion of the reaction. Finally, and as described by List, (*R*)-TRIP **80** was obtained by a 2 step -deprotection followed by phosphorylation- procedure. More acidic phosphoric acids were also employed in this work which were already available in the laboratory. These are (*R*)- $\text{CF}_3$ -TRIP **81**, where C3 and C3' positions bear

3,5-bistrifluoromethyl phenyl groups, (*R*)-super-TRIP<sup>i</sup> **82**, where the hydroxyl is replaced by the *N*-triflyl group<sup>41</sup> and (*S*)-STRIP **83**, which may give some improvement as in some reactions catalyzed by Brønsted acids based on BINOL backbone showed limitations.<sup>42</sup>

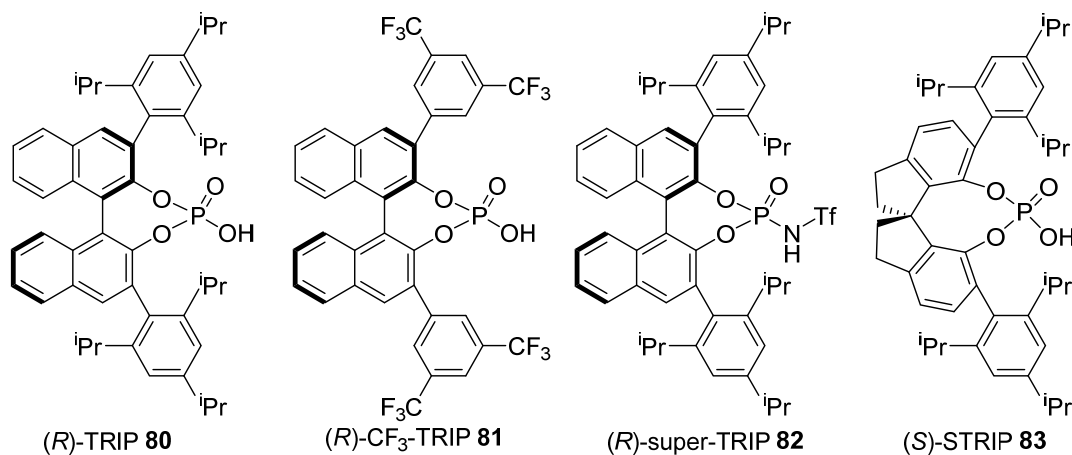
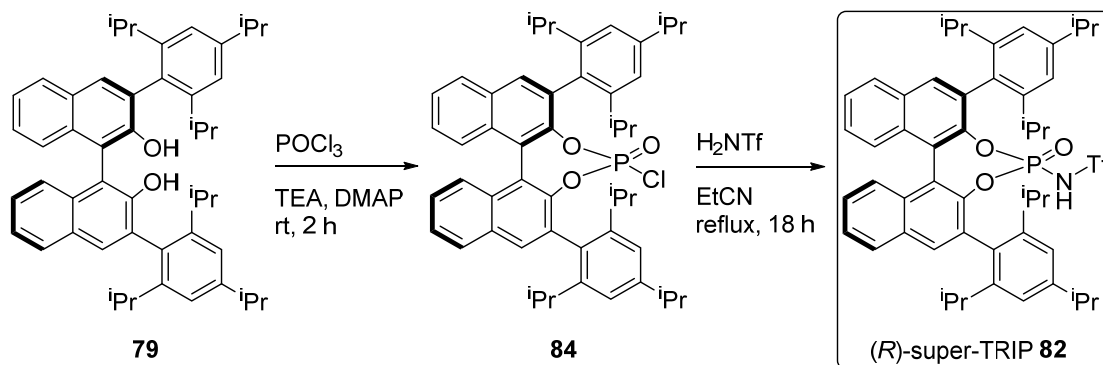


**Figure 2.** Used organocatalysts derived from BINOL- and SPINOL- based phosphoric acids.

The more acidic catalyst phosphoramidate (*R*)-super-TRIP **82** was synthesized according to the work described by Yamamoto.<sup>41</sup> In the work, **79** was reacted with phosphoryl chloride and the resulting chlorophosphate **84** was substituted with trifluoromethylsulfonamide to provide in (*R*)-super-TRIP **82** in 77% yield.



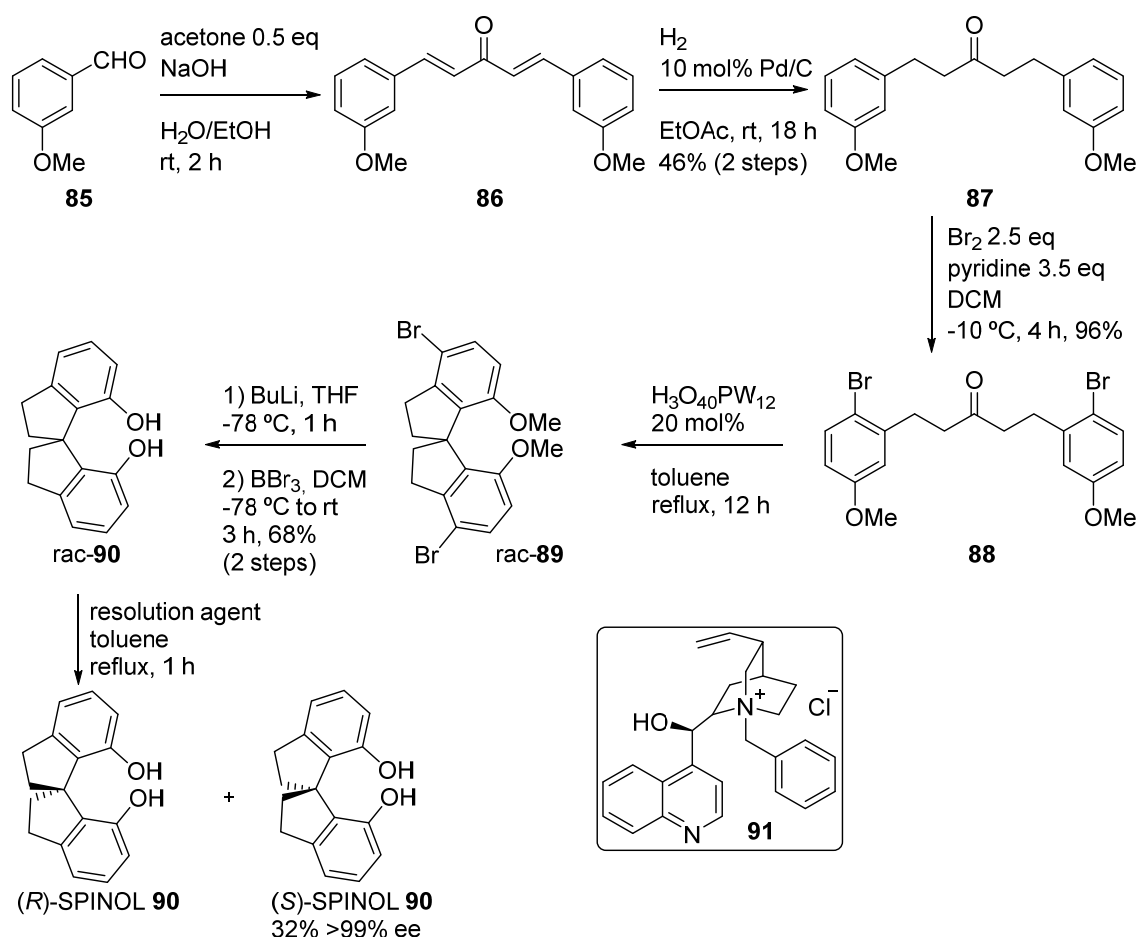
**Scheme 16.** (*R*)-super-TRIP **82** synthesis.

In order to get (*S*)-STRIP **83** catalyst, first SPINOL **90** diol had to be synthesized in advance as it is still not commercially available. According to reported procedures<sup>43</sup> the route commenced with the condensation between *meta*-anisaldehyde **85** and acetone to give pentadienone **86** which was later hydrogenated to yield **87** (Scheme 17). Then, in order to get the proper cyclization product, pentanone **87** was firstly brominated as **88** prior to the cyclization step in the presence of phosphotungstic acid (which had

<sup>i</sup> “super” prefix was adopted for convenience.

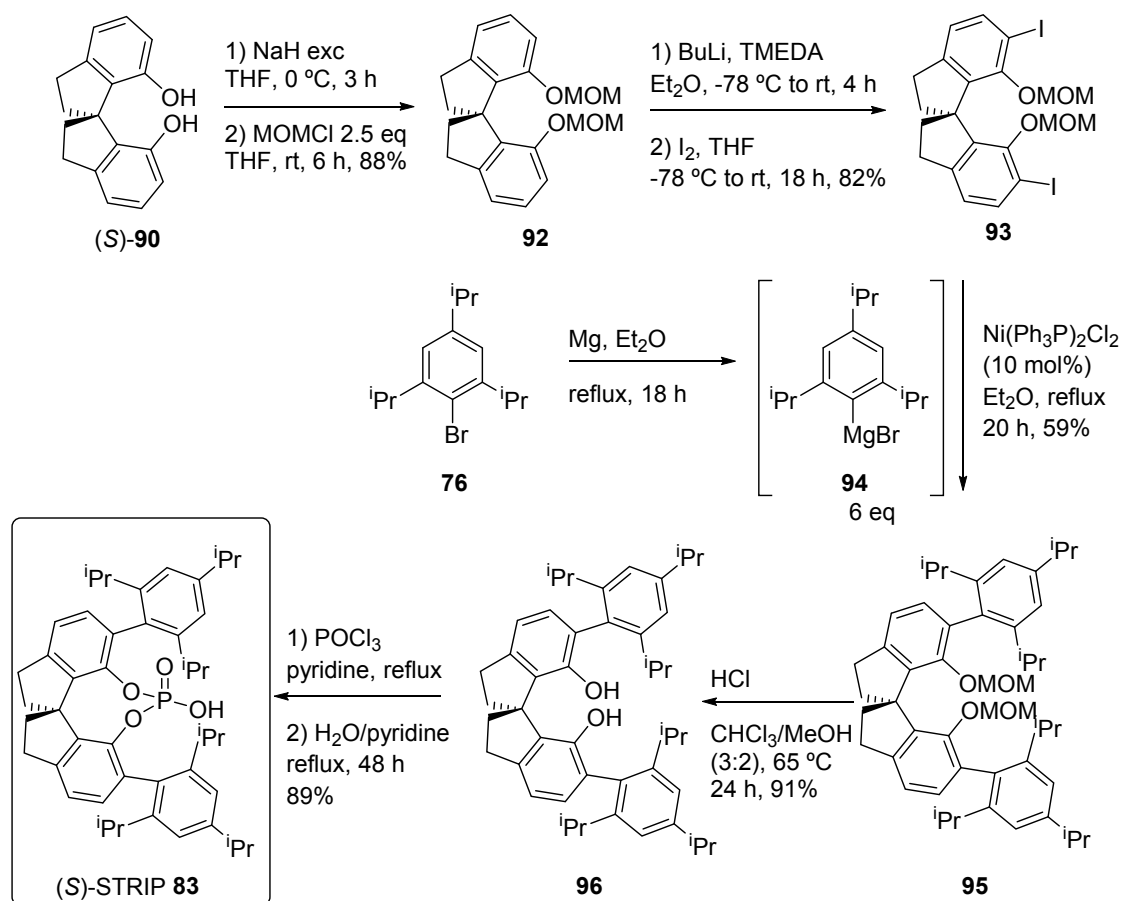


been reported as easy to handle compound allowing high yields<sup>44</sup>). Lastly, debromination and demethylation of **89** allowed racemic SPINOL **90**, which was resolved by forming a complex with *N*-benzylcinchonidium chloride **91** providing after acidification enantiopure (*S*)-SPINOL **90**.



**Scheme 17** Synthesis of *rac*-SPINOL **90** and resolution to give (*S*)-SPINOL **90**.

The synthesis of (*S*)-STRIP-**83** was achieved following the procedure reported by List (Scheme 18).<sup>45</sup> Protection of diol **90** and *ortho*-halogenation<sup>46</sup> allowed **93** for the nickel catalyzed Kumada coupling with **94** Grignard reagent previously prepared from triisopropyl bromobenzene **76**. The coupled product **95** was then deprotected in high yield and lastly, slow phosphorylation of **96** (due to the dense steric hindrance) provided the desired (*S*)-STRIP **83** catalyst.

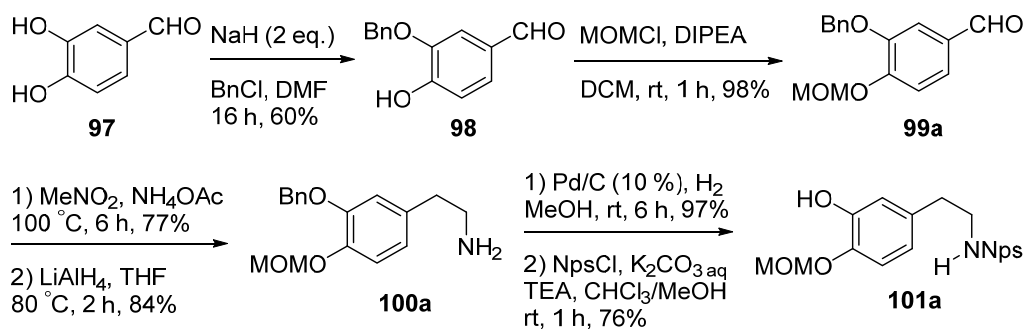


Scheme 18. Synthesis of (S)-STRIP 83.

### 5.3. Synthesis of the precursors for the Pictet-Spengler reaction

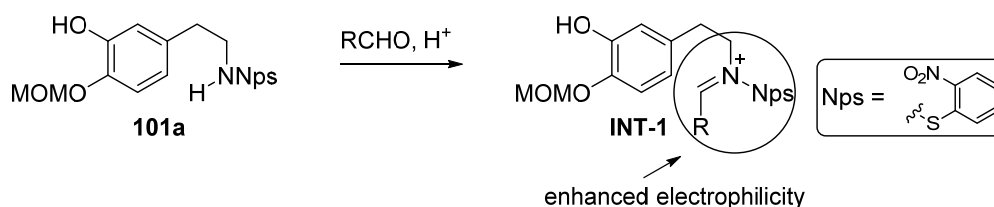
#### 5.3.1. *N*-protected dopamine analogue

The synthesis of the 4-MOM protected *ortho*-nitrophenylsulfenyl phenylethyl amine **101a** was successfully achieved (Scheme 19).<sup>ii</sup>

Scheme 19. Synthesis of the Nps-protected dopamine derivative **101a**.

<sup>ii</sup> In the publication, the MOM group is directly introduced in the diol.

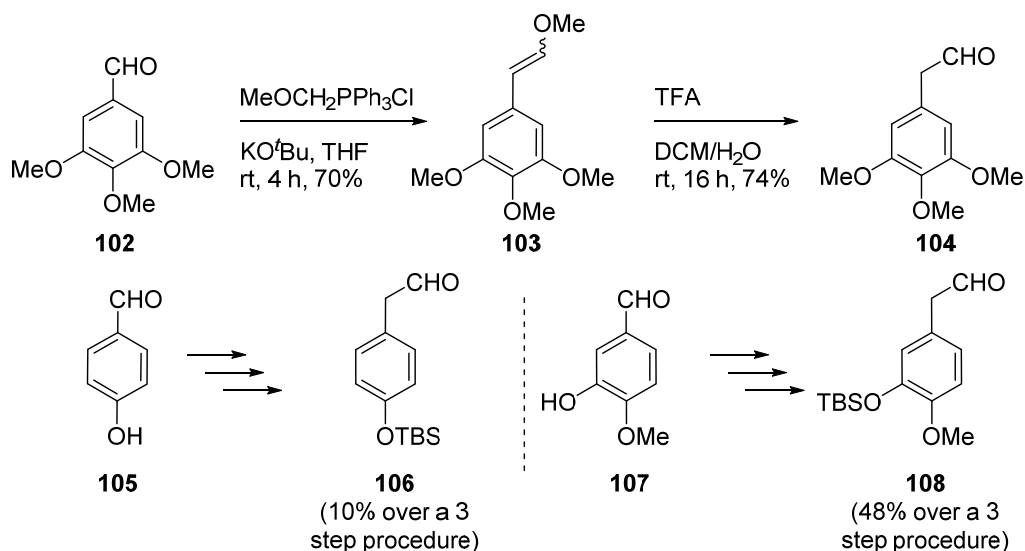
Amine **100a** was prepared from commercially available 3,4-dihydroxybenzaldehyde **97**, which was selectively protected with orthogonal groups at the 3- and 4- position with benzyl (**98** in 60% yield) and methyloxymethyl groups (**99a** in 98% yield), respectively. The Henry reaction (followed by dehydration) was performed in neat nitromethane (usual conditions are performed in refluxing acetic acid) in order to avoid possible cleavage of the acid-labile MOM group. This reaction provided the corresponding alkene in 77% yield which was later reduced with LiAlH<sub>4</sub> in high yield to produce primary amine **100a**. The product was subjected to hydrogenolysis to remove the benzyl protecting group in 97% yield. The final *ortho*-nitrophenyl sulfenyl protection step afforded the PS precursor **101a** in 76%. As it has already been described in the previous work, the primary amine was protected with the electron withdrawing Nps group. This is due to the proper ability to activate the iminium ion towards the PS cyclization by enhancing its electrophilicity.



**Scheme 20.** Effect of the Nps group on **101a**'s electrophilicity.

### 5.3.2. Phenylacetaldehydes

The model 2-(3,4,5-trimethoxyphenyl)acetaldehyde **104** was synthesized according to the described route (Scheme 21).<sup>47</sup> It proceeds via Wittig reaction with the ylide generated from **102** and (methoxymethyl) triphenyl phosphonium chloride forming the enol ether **103** in a 1:1 mixture of E/Z isomers in 70% yield. Acid hydrolysis afforded phenylacetaldehyde **104** in 74% yield.



**Scheme 21.** Synthesis of phenylacetaldehydes **104**, **106** and **108**.

Mono- and di- substituted phenylacetaldehydes **106** and **108** were also synthesized with the purpose of broadening the scope of the PS reaction once this had been optimized. Yields for **106** and **108** are expressed as overall yield over the 3 step procedure: OH- protection, Wittig and hydrolysis.

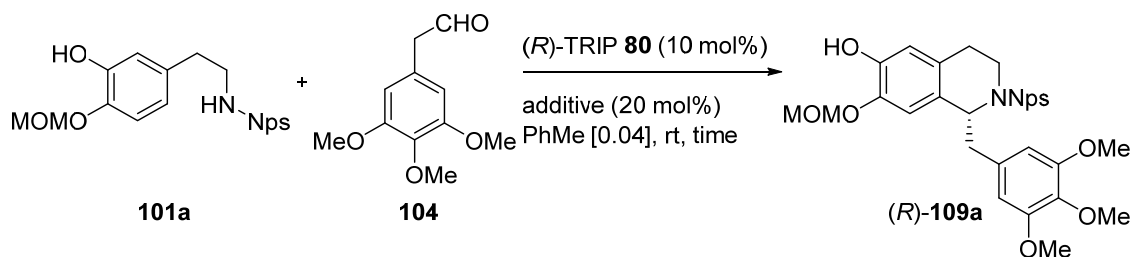
#### 5.4. Optimization screenings: Additives, concentration/temperature dependence and catalysts screening

The reaction between **101a** and 2-(3,4,5-trimethoxyphenyl)acetaldehyde **104** was chosen for optimizing the reaction conditions as its PS product **109a** would straightforwardly provide trimetoquinol hydrochloride **LXIII** via acidic hydrolysis (see Scheme 14). All the following reactions showed from here on to optimize the reaction conditions were performed on milligram scale. Therefore, no purification of the final products was attempted in order to reduce the processing time. Reaction conversions were appropriately followed using HPLC analysis as TLC analysis method resulted unsuccessful (see the experimental section).

First of all, an additive screening was performed in 0.04 M dilution of amine **101a** with two equivalents of aldehyde **xx** (Table 1). The almost racemic analytical sample was accomplished by using the acidic catalyst (*R*)-CF<sub>3</sub>-TRIP **81** at 70 °C providing 16% of enantiomeric excess (entry 1). (*R*)- configuration was firstly assigned in agreement with the enantioinduction obtained in the previous work for aliphatic aldehydes (later in the research, the total synthesis of (+)-trimetoquinol hydrochloride **LXIII** confirmed the

absolute configuration by comparison of the obtained optical rotation with literature values).<sup>1j</sup> According to the previous work, (*R*)-TRIP **80** (Figure 2) was the catalyst of choice for the initial reaction conditions screening. This screening showed that (*S*)-BINOL (entry 2) promoted the highest enantioselectivity of 91% ee when compared to (*R*)-BINOL, PNBA or in the absence of any additive (entries 3 to 5). All these cases provided the product in low conversions.

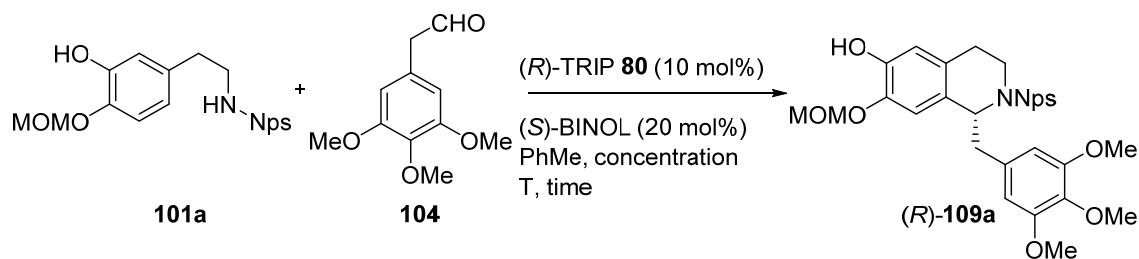
**Table 1.** Optimization of the reaction conditions with **104**.<sup>a</sup> Additive screening.



entry	additive	time (h)	conv <sup>b</sup> (%)	ee <sup>c</sup> (%)
1 <sup>d</sup>	( <i>S</i> )-BINOL	16	>99	16
2	( <i>S</i> )-BINOL	3 d	57	91
3	( <i>R</i> )-BINOL	17	25	83
4 <sup>e</sup>	PNBA	20	20	87
5	no additive	20	17	79

<sup>a</sup>The reaction condition screening was carried out in small scale: amine **101a** (0.014 mmol, 5.0 mg), aldehyde **104** (0.028 mmol, 5.8 mg), (*R*)-TRIP **80** (0.0014 mmol, 1.0 mg), additive (0.0028 mmol) in 350  $\mu$ L of toluene. <sup>b</sup>Reactions were monitored by HPLC using ChiralPack AD (80:20 Heptane:<sup>i</sup>PrOH, 0.5 mL/min, 220 nm). <sup>c</sup>Enantiomeric excesses measured by HPLC using ChiralPack AD. <sup>d</sup>(*R*)-CF<sub>3</sub>-TRIP **81** was used as catalyst at 70 °C. <sup>e</sup>PNBA = *para*-nitro benzoic acid.

Later, in order to improve the conversion, the concentration and temperature dependency was analyzed (Table 2). Thus, reactions in concentrations 0.1 and 0.3 M (entries 2 and 3) of **101a** were set up, and the reaction at 0.3 M (entry 3) provided the best conversion with a comparable enantioselectivity of 89% ee. Also, according to total synthesis purposes, a reduction of the catalytic load to 5 mol% (and corresponding load of 10 mol% of (*S*)-BINOL) strongly affected the activity of the catalyst in sense of conversion as the enantioselectivity of the process remained. Any trial in order to increase the enantiocontrol by means of the temperature failed (entries 5 and 6). However, it was possible to reach the reaction to completion at the expense of decreasing the enantiomeric excess (entry 6).

**Table 2.** Optimization of the reaction conditions with **104**.<sup>a</sup> Concentration/temperature dependency.

entry	[amine] (M)	T (°C)	time (h)	conv <sup>b</sup> (%)	ee <sup>c</sup> (%)
1	0.04	rt	3 d	57	91
2	0.1	rt	23	61	90
3 <sup>d</sup>	0.3	rt	22	72	89
4 <sup>e,d</sup>	0.3	rt	4 d	68	91
5	0.3	40	2 d	91	85
6	0.3	60	24	>99	81

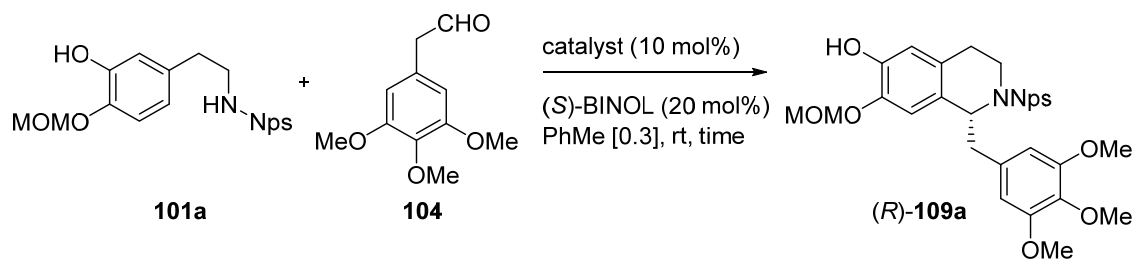
<sup>a</sup>Reaction conditions: see table 1. <sup>b</sup>Reactions were monitored by HPLC: see table 1. <sup>c</sup>Enantiomeric excesses measured by HPLC: see table 1.

<sup>d</sup>Longer reaction times did not complete the reaction. <sup>e</sup>The reaction was carried out with (*R*)-TRIP **80** (5 mol%) and (*S*)-BINOL (10 mol%).

The use of other more acidic BINOL- or SPINOL- based phosphoric acid organocatalysts (Figure 2) such as (*R*)-superTRIP **82** or (*S*)-STRIP **83** (Note: the (*S*)-configuration of the SPINOL backbone in **83** provides the same enantiomeric induction as the (*R*)- configuration of BINOL backbone based organocatalysts<sup>48</sup>) did not provide higher enantiocontrol (Table 3, entries 2 and 3).

A higher catalyst load of 20 mol% of (*R*)-TRIP **80** provided full conversion in 84% ee after two days of reaction (entry 4) but such a high load is not adequate for total synthetic purposes. When the reaction was carried out with the preformed enamine, it provided a higher conversion but lower enantiocontrol, though (entry 5). In contrast to the previous work, the addition of MgSO<sub>4</sub> as drying agent together with more strict dry conditions (oven dried glassware and reaction under argon atmosphere) had a positive effect on the enantiomeric excess which was raised up to 91% ee and the conversion raised to 94% after 3 days (entry 6). Additionally, reduction in the number of aldehyde equivalents **104** from 2 to 1.1 increased the reactivity of the catalyst in this process allowing full conversion (entry 7).

**Table 3.** Optimization of the Reaction Conditions with **104**.<sup>a</sup> Catalyst and further conditions screening.

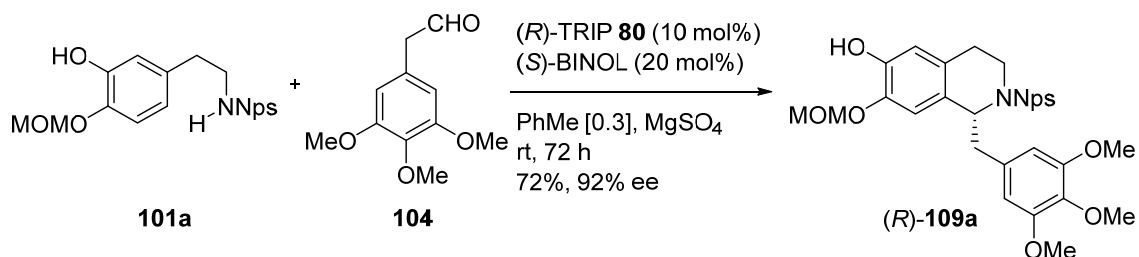


entry	catalyst	time (h)	conv <sup>b</sup> (%)	ee <sup>c</sup> (%)
1	( <i>R</i> )-TRIP <b>80</b>	22	72	89
2	( <i>R</i> )-superTRIP <b>82</b>	4 d	38	73
3	( <i>S</i> )-STRIP <b>83</b>	24	<50	82
4 <sup>d</sup>	( <i>R</i> )-TRIP <b>80</b>	48	99	84
5 <sup>e</sup>	( <i>R</i> )-TRIP <b>80</b>	24	84	72
6 <sup>f</sup>	( <i>R</i> )-TRIP <b>80</b>	3 d	94	91
7 <sup>g</sup>	( <i>R</i> )-TRIP <b>80</b>	3 d	99	92

<sup>a</sup>Reaction conditions: see table 1. <sup>b</sup>Reactions were monitored by HPLC.

<sup>c</sup>Enantiomeric excesses measured by HPLC. <sup>d</sup>20 mol% and 40 mol% of (*R*)-TRIP and (*S*)-BINOL were used, respectively. <sup>e</sup>The reaction was carried out with the preformed enamine. <sup>f</sup>MgSO<sub>4</sub> as drying agent under Ar. <sup>g</sup>MgSO<sub>4</sub> as drying agent and 1.1 equivalents of aldehyde, under Ar.

Finally, when the organocatalyzed Pictet-Spengler reaction was carried out in a 100 mg scale with the conditions described in Table 3 entry 7, it successfully provided the product **109a** in 92% ee and 72% yield (Scheme 22).



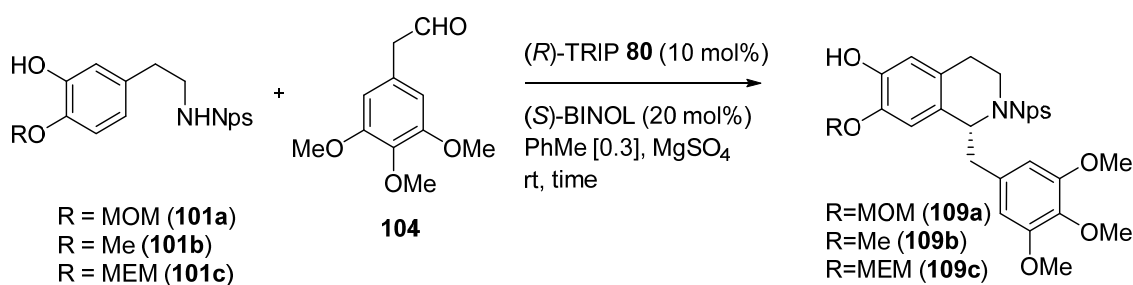
**Scheme 22.** Large scale Pictet-Spengler reaction.

This momylated PS product **109a** was of glass solid nature. In accordance to the previous work, **109a** was attempted to recrystallization in order to obtain enantioenriched product as happened with methylated adducts. Nevertheless, all efforts failed.

### 5.5. Proposed reaction mechanism. Influence of the protecting group

Additional evidences aided the theory of the intramolecular activation generated by MOM (Table 4). The reaction where MOM- protecting group was replaced by a methyl group as in **101b** was also run yielding, in this case, the product **109b** in lower yield and ee but the reaction time was reduced (entry 2). This could be due to a less steric hindrance of Me with respect to MOM allowing the reaction to perform faster. Also, when MOM was replaced by 2-methoxyethoxymethyl ether, MEM, protecting group **xx**, the enantiocontrol of the process decreased (entry 3).

**Table 4.** Influence of the protecting group at the *para*- position of the amine precursor.<sup>a</sup>

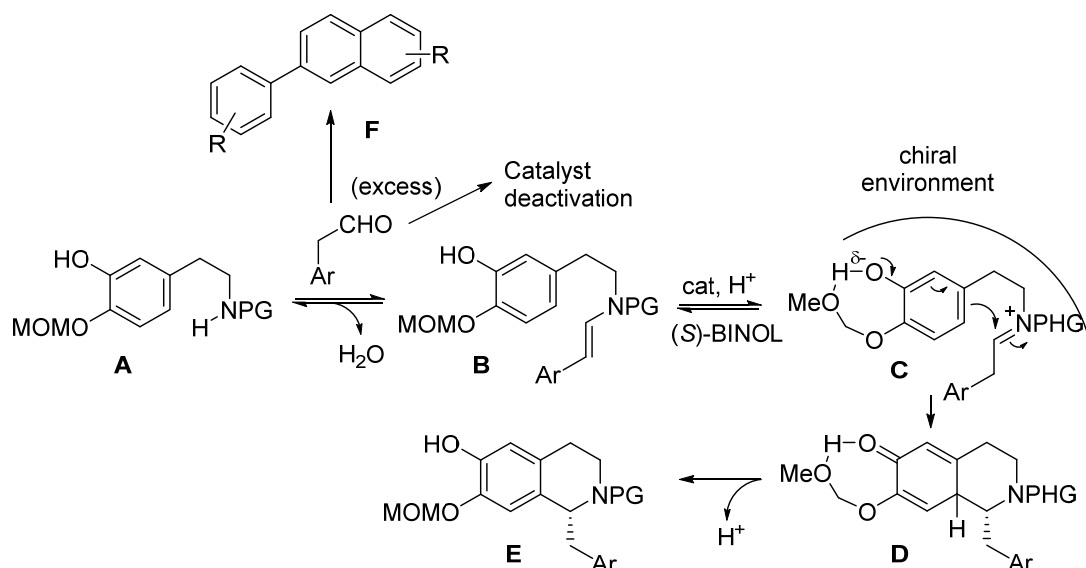


entry	R	time (d)	yield <sup>b</sup> (%)	ee <sup>c</sup> (%)
1	MOM	3	70	92
2	Me	2	79	85
3 <sup>d</sup>	MEM	3	nd <sup>e</sup>	85

<sup>a</sup>Reaction conditions: see table 3 entry 7. <sup>b</sup>Isolated product.  
<sup>c</sup>Enantiomeric excesses measured by HPLC. <sup>d</sup>Test reaction on 5 mg scale. <sup>e</sup>nd = not determined.

The reaction mechanism (Scheme 23) was suggested to go stepwise through a first formation of the enamine species **B**. It tautomerizes to the active iminium ion **C** assisted both by the acidic medium and the electron-withdrawing properties of the *ortho*-nitrophenylsulfenyl protecting group. Then, the cyclization occurs to **D** in an enantioselective manner aided by the chiral environment provided by the phosphoric acid-BINOL catalyst system and the suggested intramolecular activation from MOM to the OH at the 3 position. Finally, the loss of a proton regenerates the aromatic system providing the final product **E**. Due to acidic medium and the reversible nature of the enamine-iminium formation reactions, the enamine is additionally prone to be hydrolyzed to the starting materials. Moreover, the aldehyde may follow a dimerizing reaction to form phenylnaphthalene **F**<sup>49</sup> in addition to deactivation of the catalyst. These facts were consistent with the non-completed reactions, e.g. Table 1 entry 2.



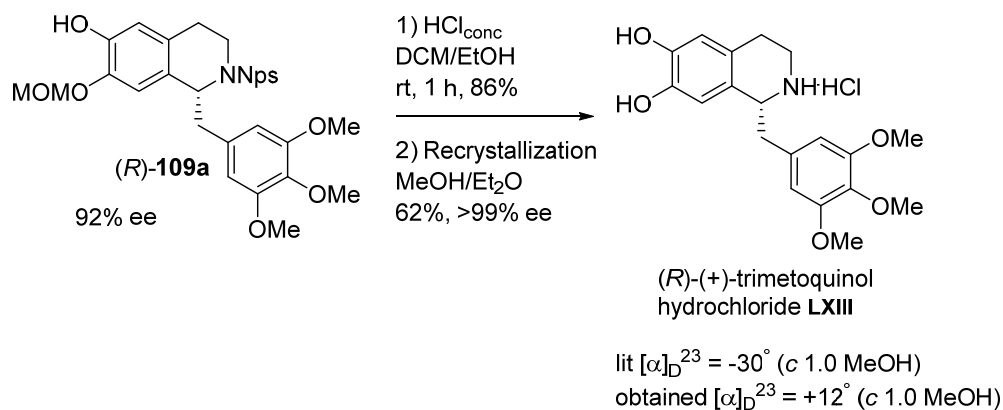


**Scheme 23.** Suggested reaction mechanism.

### 5.6. Total synthesis of (+)-trimetoquinol hydrochloride

(*S*)-(-)-Trimetoquinol hydrochloride is a kind of sympathomimetic drug which act as  $\beta$ -adrenergic agonist affecting the muscles of the airways.<sup>50</sup> It is marketed in Japan under the name of Inolin as an oral bronchodilator for the treatment of respiratory conditions as asthma. On the other hand, the (*R*)-(+)- isomer has thromboxane A<sub>2</sub>/prostaglandin H<sub>2</sub> antagonist activity.<sup>51</sup>

In order to complete the total synthesis of (*R*)-trimetoquinol hydrochloride **LXIII**, the Pictet-Spengler product **109a** was subjected to the direct hydrolysis in a 1/1/1 mixture of HCl<sub>conc</sub>/DCM/EtOH which excised both MOM and Nps protecting groups in 86% yield (Scheme 24). The stereocontrol towards the (*R*)- enantiomer was verified by means of optical rotation and comparison with the reported <sup>1</sup>H NMR literature data supported the success of the total synthesis.<sup>52</sup>



**Scheme 24.** Follow up chemistry: Synthesis of (*R*)-(+)-trimetoquinol hydrochloride **LXIII** by means of hydrolysis and recrystallization.

Fortunately at this stage it was possible to perform recrystallization out of a MeOH/Et<sub>2</sub>O mixture, from with the racemate crystallized first allowing the mother liquors enantioenriched (ee >99%) in 62% yield (see experimental section).

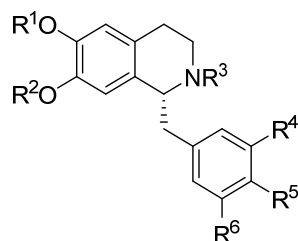
Nevertheless, as it can be observed in Scheme 24 the obtained value for the optical rotation did not match with the reported in literature. Although the NMR spectrum was clean, some impurities may had affected the measurements giving the above reported value. Further optimization of the hydrolysis process identified the 0.1/1/1 mixture of  $\text{HCl}_{\text{conc}}$ /DCM/EtOH as the proper reaction mixture in addition of a stirring for 24 hours at room temperature rather than 1 hour. However, this refinement did not improve the optical rotation reading.

## 5.7. Follow up chemistry

Once seen the viability of the organocatalytic Pictet-Spengler transformation between **101a** and 2-(3,4,5-trimethoxyphenyl)acetaldehyde **104** catalyzed by (*R*)-TRIP **80**, the method was continued in the research group, showing its effectiveness by the synthesis of a large family of 1-benzyl-1,2,3,4-tetrahydroisoquinolines.<sup>53</sup> 9 other pharmaceutically relevant alkaloids were uneventfully synthesized starting from either **101a** or **101b** amines (Table 5) retaining the (*R*)- configuration in all cases: (*R*)-norcoclaurine, (*R*)-coclaurine, (*R*)-norreticuline, (*R*)-reticuline, (*R*)-armepavine, (*R*)-norprotosimomenine, (*R*)-laudanosine and (*R*)-5-methoxylaundanosine in addition to (*R*)-nor-armepavine, (*R*)-norlaudanosine, (*R*)-nor-5-methoxylaundanosine and (*R*)-5-methoxylaundanosine. The enantiomeric excesses ranged in high values between 86 and 92% ee for the organocatalytic Pictet-Spengler reaction, and the obtained ee's

for the final products varied between 83 and >99% ee for those products that could be crystallized.

**Table 5.** Achieved end products.



entry	R <sup>1</sup>	R <sup>2</sup>	NR <sup>3</sup>	R <sup>4</sup>	R <sup>5</sup>	R <sup>6</sup>	alkaloid
<b>Starting from amine 101a</b>							
1	H	H	H	H	OH	H	( <i>R</i> )-(+)-norcoclaurine
2	Me	H	H	H	OH	H	( <i>R</i> )-(+)-coclaurine
3	Me	H	H	OH	OMe	H	( <i>R</i> )-(+)-norreticuline
4	Me	H	Me	OMe	OMe	H	( <i>R</i> )-(-)-reticuline
<b>Starting from amine 101b</b>							
5	Me	Me	H	H	OH	H	( <i>R</i> )-(+)-nor-armepavine
6	Me	Me	Me	H	OH	H	( <i>R</i> )-(-)-armepavine
7	H	Me	H	OH	OMe	H	( <i>R</i> )-(+)-norprotosinomenine
8	H	Me	Me	OH	OMe	H	( <i>R</i> )-(-)-protosinomenine
9	Me	Me	H	OMe	OMe	H	( <i>R</i> )-(-)-norlaudanosine
10	Me	Me	Me	OMe	OMe	H	( <i>R</i> )-(-)-laudanosine
11	Me	Me	H	OMe	OMe	OMe	( <i>R</i> )-(-)-nor-5-methoxylaudanosine
12	Me	Me	Me	OMe	OMe	OMe	( <i>R</i> )-(-)-5-methoxylaudanosine

Some of the products needed to be O-methylated at the OH positions with standard MeI/K<sub>2</sub>CO<sub>3</sub> conditions prior to the Nps deprotection. Also, when *N*-methyl group was necessary (entries 4, 6, 8, 10 and 12), a reductive amination was applied with NaBH<sub>3</sub>CN, formaldehyde and zinc chloride.

## 5.8. Conclusions

From the experimental studies reported and discussed along this chapter, the following conclusions can be drawn:

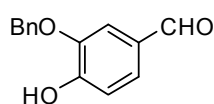
- The 3-Hydroxy-4-methoxymethyl derivative with an *ortho*-nitrophenylsulfenyl group on the amine moiety **101a** was achieved via seven step procedure with a 28% overall yield.
- 2-(3,4,5-Trimethoxyphenyl)acetaldehyde **104** was accomplished via two step homologation procedure with a 52% overall yield.
- The Pictet-Spengler reaction between **101a** and **104** produced enantioenriched (*R*)-1-substituted tetrahydroisoquinoline **109a** when it was organocatalyzed by (*R*)-TRIP **80**.
- A matching effect was observed when the reaction was assisted in the presence of (*S*)-BINOL.
- The conversion of the process was strongly dependant on the concentration of the reaction.
- The employment of other more acidic phosphoric acids as organocatalysts did not improve the outcome of the process.
- An almost equimolecular amount of aldehyde and excess of MgSO<sub>4</sub> as drying agent were needed in order to avoid dimerization or catalysts deactivation.
- An intramolecular activation from MOM towards the C3 hydroxy group in the phenylethylamine counterpart was suggested and was additionally, supported by the results of the reactions carried out with Me and MEM protecting groups.
- The hydrolysis of the Pictet-Spengler product **109a** allowed the straightforward synthesis of enantioenriched (*R*)-trimetoquinol hydrochloride **LXIII**, which was achieved with >99% ee of purity after removal of crystalline racemate by recrystallization.
- This method turns to be a general procedure for the synthesis of a wide range of enantioenriched biologically relevant 1-benzyl-1,2,3,4-tetrahydroisoquinoline alkaloids. In addition, it allows to prepare all four OH/OMe possible substituents at C6 and C7 positions of the isoquinoline ring.

## 5.9. Experimental section

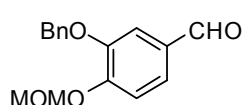
**General Remarks.** All <sup>1</sup>H NMR and <sup>13</sup>C NMR (APT) were recorded (<sup>1</sup>H 500, 400, 300 MHz, <sup>13</sup>C 500 MHz, 100 MHz) at room temperature (otherwise noted) in CDCl<sub>3</sub>, D<sub>2</sub>O, and deuterated toluene or methanol. Accurate mass measurements were performed on Accutof with electron spray ionization (EI) or field desorption (FD +) techniques. The required reactions were carried out in oven-dried glassware with magnetic stirring under nitrogen atmosphere. THF was freshly distilled from sodium and benzophenone. Toluene was distilled over calcium hydride and stored

on 4 Å molecular sieves. Aldehydes were purified by recrystallization or chromatography on silica gel. Nps-protected tetrahydroisoquinoline **101a** was bright orange stable compound. The  $^1\text{H}$  and  $^{13}\text{C}$  NMR spectra, however, showed line broadening for the atoms in the vicinity of the nitrogen-sulfur bond.<sup>54</sup>

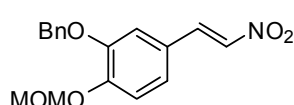
### General procedure for the synthesis of the precursor



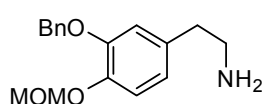
**3-(Benzyloxy)-4-hydroxybenzaldehyde (98)** It was synthesized according to previously reported experimental procedure and  $^1\text{H}$  NMR agrees with the reported data.<sup>55</sup>  $^1\text{H}$  NMR (400 MHz,  $\text{CDCl}_3$ )  $\delta$  9.83 (s, 1H), 7.52 (d,  $J$  = 1.8 Hz, 1H), 7.49 – 7.36 (m, 5H), 7.07 (d,  $J$  = 8.1 Hz, 1H), 6.21 (d,  $J$  = 3.5 Hz, 1H), 5.18 (s, 2H).



**3-(Benzyloxy)-4-(methoxymethoxy)benzaldehyde (99a)** Aldehyde **98** (1 g, 4.38 mmol), was dissolved in 50 mL of DCM along with diisopropylethylamine (3 mL, 17.52 mmol) and the resulting solution was cooled to 0 °C. Chloromethyl methyl ether (1.33 mL, 17.52 mmol) was added dropwise over 5 min, and the solution was stirred for one hour at which time the reaction appeared completed according to TLC. The reaction mixture was extracted 3 times with water and once with brine, dried onto  $\text{MgSO}_4$  and concentrated under reduced pressure. The resulting residue was purified by column chromatography in silica gel with 1/8 (EtOAc/PE) mixture to produce **99a**. Yield: 1.18 g, 98%, colorless oil. FTIR (neat,  $\text{cm}^{-1}$ ) 3335, 1688, 1258, 1150, 1127, 962, 736, 696.  $^1\text{H}$  NMR (400 MHz,  $\text{CDCl}_3$ )  $\delta$  9.83 (s, 1H), 7.52 – 7.42 (m, 4 H), 7.42 – 7.36 (m, 2H), 7.34 (d,  $J$  = 7.3 Hz, 1H), 7.28 (d,  $J$  = 8.2 Hz, 1H), 5.33 (s, 2H), 5.21 (s, 2H), 3.53 (s, 3H).  $^{13}\text{C}$  NMR (101 MHz,  $\text{CDCl}_3$ )  $\delta$  190.9, 152.3, 149.1, 136.2, 130.9, 128.5, 128.0, 127.3, 126.3, 115.2, 111.8, 94.8, 70.7, 56.4. HRMS (EI) for  $\text{C}_{16}\text{H}_{16}\text{O}_4$ : calculated  $[\text{M}]^+$ : 272.1052. Found  $[\text{M}]^+$ : 272.1049.

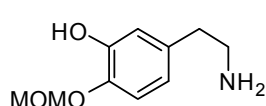


**(E)-2-(Benzyloxy)-1-(methoxymethoxy)-4-(2-nitrovinyl)benzene** A mixture of **99a** (1.48 g, 4.33 mmol),  $\text{CH}_3\text{NO}_2$  (22 mL) and  $\text{NH}_4\text{OAc}$  (329 mg, 4.27 mmol) was stirred at 100 °C for 4 hours, at which time it was cooled down to room temperature and poured into ice cold water (75 mL). The aqueous mixture was extracted with  $\text{Et}_2\text{O}$  (2 x 50 mL) and the combined organic extracts were washed with brine and dried over  $\text{MgSO}_4$ . Purification with flash chromatography eluted with a 1:6 mixture of EtOAc:PE afforded the alkene. Yield: 3.30 g, 77%, bright yellow solid.  $m_p$  = 69-70 °C. FTIR (neat,  $\text{cm}^{-1}$ ) 2896, 1504, 1332, 1255.  $^1\text{H}$  NMR (400 MHz,  $\text{CDCl}_3$ )  $\delta$  7.90 (d,  $J$  = 13.6 Hz, 1H), 7.58 – 7.37 (m, 5H), 7.37 – 7.32 (m, 1H), 7.20 (d,  $J$  = 8.3 Hz, 1H), 7.14 (dd,  $J$  = 8.4, 2.0 Hz, 1H), 7.05 (d,  $J$  = 2.1 Hz, 1H), 5.30 (s, 2H), 5.19 (s, 2H), 3.52 (s, 3H).  $^{13}\text{C}$  NMR (101 MHz,  $\text{CDCl}_3$ )  $\delta$  150.7, 149.2, 139.0, 136.2, 135.5, 128.6, 128.2, 127.2, 124.2, 124.0, 116.5, 114.0, 95.0, 71.1, 56.4. HRMS (EI) for  $\text{C}_{17}\text{H}_{17}\text{NO}_5$ : calculated  $[\text{M}]^+$ : 315.1101. Found  $[\text{M}]^+$ : 315.1101.



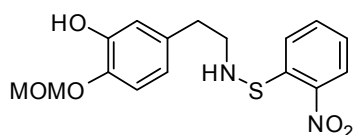
**2-(3-(Benzyloxy)-4-(methoxymethoxy)phenyl)ethanamine (100a)**  $\text{LiAlH}_4$  (482 mg, 12.68 mmol) was dissolved in 15 mL of dry THF and cooled to

0 °C. Nitroalkene (1 g, 3.17 mmol) previously dissolved in 15 mL of THF was added dropwise and the resulting mixture was heated up to reflux for 2 hours. After this time, the reaction was allowed to room temperature and cooled down to 0 °C. The reaction mixture was then quenched following by stepwise addition of 0.65 mL H<sub>2</sub>O, 1 mL 10% NaOH, 1.63 mL H<sub>2</sub>O and allowed to stir for 30 minutes. It was then filtered through a pad of celite and the solvent evaporated afford **100a**. The product was taken to the next step without further purification. Yield: 758 mg, 84%, brown oil. FTIR (neat, cm<sup>-1</sup>) 3371, 1510, 907, 725, 696. <sup>1</sup>H NMR (400 MHz, CDCl<sub>3</sub>) δ 7.42 (d, *J* = 7.2 Hz, 2H), 7.35 (t, *J* = 7.4 Hz, 2H), 7.29 (d, *J* = 7.1 Hz, 1H), 7.06 (d, *J* = 8.1 Hz, 1H), 6.76 (d, *J* = 2.0 Hz, 1H), 6.71 (dd, *J* = 8.1, 2.0 Hz, 1H), 5.18 (s, 2H), 5.12 (s, 2H), 3.50 (s, 3H), 2.85 (t, *J* = 6.8 Hz, 2H), 2.61 (t, *J* = 6.8 Hz, 2H). <sup>13</sup>C NMR (101 MHz, CDCl<sub>3</sub>) δ 148.9, 145.1, 136.9, 134.2, 128.3, 127.6, 127.1, 121.4, 117.64, 115.2, 95.6, 70.8, 55.9, 43.2, 39.2. HRMS (EI) for C<sub>17</sub>H<sub>21</sub>NO<sub>3</sub>: calculated [M]<sup>+</sup>: 287.1519. Found [M]<sup>+</sup>: 287.1521.



*5-(2-Aminoethyl)-2-(methoxymethoxy)phenol* Phenylethylamine **100a**

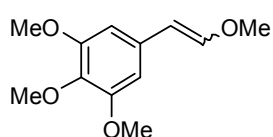
(728 mg, 2.63 mmol) was dissolved in 15 mL of methanol and Pd/C 10% (76 mg) was added. The mixture was stirred under an atmosphere of H<sub>2</sub> until completion of the reaction. The reaction mixture was filtered through a plug of celite and the solvent evaporated under reduced pressure to provide the deprotected primary amine. Yield: 513 mg, 97%, dark oil. FTIR (neat, cm<sup>-1</sup>) 2938, 1507, 1151, 982. <sup>1</sup>H NMR (400 MHz, MeOD) 6.96 (d, *J* = 8.2 Hz, 1H), 6.68 (s, 1H), 6.61 – 6.56 (m, 1H), 5.10 (s, 2H), 3.43 (s, 3H), 3.27 (s, 1H), 2.87 (t, *J* = 7.3 Hz, 2H), 2.65 (t, *J* = 7.2 Hz, 2H). <sup>13</sup>C NMR (101 MHz, MeOD) δ 148.0, 144.2, 133.7, 119.9, 117.2, 116.5, 95.8, 55.5, 42.6, 36.7. HRMS (EI) for C<sub>10</sub>H<sub>15</sub>NO<sub>3</sub>: calculated [M]<sup>+</sup>: 197.1053. Found [M]<sup>+</sup>: 197.1052.



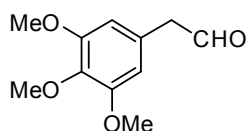
*2-(Methoxymethoxy)-5-(2-((2-nitrophenyl)thio)amino)*

*ethyl)phenol* (**101a**) The hydrogenated amine (513 mg, 2.59

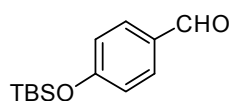
mmol) was dissolved in a mixture of CHCl<sub>3</sub> (25 mL), methanol (1.5 mL) and triethylamine (130 μL) in a flask of 100 mL with stirring and heating until fully dissolved. The solution was cooled to 0 °C, 25 mL of aqueous saturated K<sub>2</sub>CO<sub>3</sub> solution was added and allowed to stir for 5 minutes. Then, 2-nitrophenylsulfenyl chloride (589 mg, 3.11 mmol) was added in three portions. The reaction was finished after one hour (confirmed by TLC). The reaction mixture was extracted with CHCl<sub>3</sub>, dried over MgSO<sub>4</sub> and evaporated under reduced pressure. The crude product was then purified by flash chromatography with DCM/PE/EtOAc 50/50/2 eluent system providing the desired product **101a**. Yield: 694 mg, 76%, bright orange thick oil. FTIR (neat, cm<sup>-1</sup>) 3348, 1504, 906, 726. <sup>1</sup>H NMR (400 MHz, CDCl<sub>3</sub>) δ 8.26 (dd, *J* = 8.3, 1.4 Hz, 1H), 7.79 (dd, *J* = 8.3, 1.3 Hz, 1H), 7.57 (ddd, *J* = 8.3, 7.1, 1.4 Hz, 1H), 7.23 (ddd, *J* = 8.3, 7.1, 1.3 Hz, 1H), 7.03 (d, *J* = 8.2 Hz, 1H), 6.84 (d, *J* = 2.1 Hz, 1H), 6.69 (dd, *J* = 8.3, 2.2 Hz, 1H), 5.96 (s, 1H), 5.19 (s, 2H), 3.53 (s, 3H), 3.24 – 3.18 (m, 2H), 2.83 (t, *J* = 6.8 Hz, 2H), 2.71 (s, 1H). <sup>13</sup>C NMR (101 MHz, CDCl<sub>3</sub>) δ 146.4, 145.6, 143.0, 142.4, 133.8, 133.6, 125.6, 124.3, 124.2, 120.4, 115.7, 95.9, 56.2, 52.4, 36.09, 36.1. HRMS (EI) for C<sub>16</sub>H<sub>18</sub>N<sub>2</sub>O<sub>5</sub>S: calculated [M]<sup>+</sup>: 350.0940. Found [M]<sup>+</sup>: 350.0936.



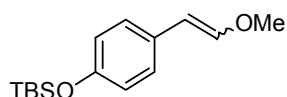
**1,2,3-Trimethoxy-5-(2-methoxyvinyl)benzene (103)** It was synthesized according to previously reported experimental procedure and  $^1\text{H}$  NMR agrees with the reported data.<sup>56</sup> (E/Z 58:42).  $^1\text{H}$  NMR (400 MHz,  $\text{CDCl}_3$ )  $\delta$  7.01 (d,  $J = 12.9$  Hz, 1H), 6.86 (s, 2H), 6.47 (s, 2H), 6.13 (d,  $J = 7.05$  Hz, 1H), 5.79 (d,  $J = 12.9$  Hz, 1H), 5.17 (d,  $J = 7.05$  Hz, 1H), 3.88 (s, 6H), 3.88 (s, 6H), 3.85 (s, 3H), 3.85 (s, 3H), 3.81 (s, 3H), 3.71 (s, 3H).



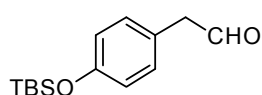
**2-(3,4,5-Trimethoxyphenyl)acetaldehyde (104)** It was synthesized according to previously reported experimental procedure and  $^1\text{H}$  NMR agrees with the reported data.<sup>56</sup>  $^1\text{H}$  NMR (400 MHz,  $\text{CDCl}_3$ )  $\delta$  9.57 (t,  $J = 2.3$  Hz, 1H), 6.31 (s, 2H), 3.70 (s, 6H), 3.69 (s, 3H), 3.57 (d,  $J = 2.3$  Hz, 2H).



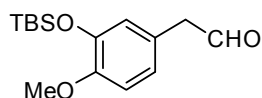
**4-((tert-Butyldimethylsilyl)oxy)benzaldehyde<sup>57</sup> Phenol 105** (5 g, 40.9 mmol) was dissolved in 150 mL of dichloromethane and cooled down to 0 °C. To the solution was added imidazole (5.5 g, 81.8 mmol), DMAP (250 mg, 2.05 mmol) and TBSCl (7.4 g, 49.08 mmol). The reaction mixture was allowed to reach room temperature and stirred for 16 hours. Then, the mixture was quenched with  $\text{NH}_4\text{Cl}$  and extracted with DCM. The organic layers were combined, washed with brine, dried over  $\text{Na}_2\text{SO}_4$  and concentrated under reduced pressure. The crude mixture was filtered through a plug of silica using a 1:1 (DCM:PE) mixture to afford the protected aldehyde as a colorless oil (8.41 g, 87%).  $^1\text{H}$  NMR (300 MHz,  $\text{CDCl}_3$ )  $\delta$  9.89 (s, 1H), 7.79 (d,  $J = 8.5$  Hz, 2H), 6.94 (d,  $J = 8.5$  Hz, 2H), 0.99 (s, 9H), 0.25 (s, 6H).



**tert-Butyl(4-(2-methoxyvinyl)phenoxy)dimethylsilane Aldehyde** (8.41 g, 35.62 mmol) and (methoxymethyl) triphenyl phosphonium chloride (14.65 g, 42.74 mmol) were dissolved in 150 mL of THF. The reaction mixture was cooled to 0 °C after which  $\text{KO}^t\text{Bu}$  (4.79 g, 42.74 mmol) was added in one portion. The reaction was stirred for 10 minutes and the allowed to room temperature. The reaction was stirred for 4 hours more. Then, it was quenched with  $\text{NH}_4\text{Cl}$  and the aqueous layer was extracted with  $\text{Et}_2\text{O}$ . The organic layers were combined, washed with brine, dried onto  $\text{MgSO}_4$  and concentrated under reduced pressure. The crude was purified by flash chromatography in silica using a 1:20 (EtOAc:PE) system to provide the enol in a E/Z 1/1 relationship. Yield: 5.89 g, 63%, colorless oil. FTIR (neat,  $\text{cm}^{-1}$ ) 2929, 1507, 1250, 908, 835, 777.  $^1\text{H}$  NMR (400 MHz,  $\text{CDCl}_3$ )  $\delta$  7.45 (d,  $J = 8.6$  Hz, 2H), 7.10 (d,  $J = 8.5$  Hz, 2H), 6.93 (d,  $J = 13.0$  Hz, 1H), 6.76 (dd,  $J = 8.7, 7.3$  Hz, 4H), 6.05 (d,  $J = 7.0$  Hz, 1H), 5.78 (d,  $J = 12.9$  Hz, 1H), 5.17 (d,  $J = 6.9$  Hz, 1H), 3.76 (s, 3H), 3.66 (s, 3H), 0.98 (s, 18H), 0.19 (s, 12H).  $^{13}\text{C}$  NMR (101MHz,  $\text{CDCl}_3$ )  $\delta$  153.4, 153.2, 147.2, 145.9, 129.1, 129.0, 125.7, 119.9, 119.5, 105.0, 104.3, 60.0, 55.9, 25.3, 17.8, -4.8. HRMS (FD +) for  $\text{C}_{15}\text{H}_{24}\text{O}_2\text{Si}$ : calculated  $[\text{M}]^+$ : 264.1546. Found  $[\text{M}]^+$ : 264.1530.



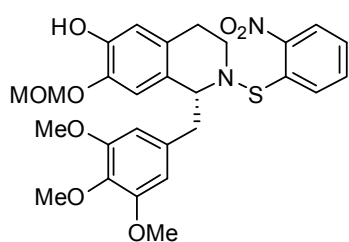
*2-(4-((tert-Butyldimethylsilyl)oxy)phenyl)acetaldehyde (106)* It was synthesized from the corresponding enol ether according to previously reported experimental procedure and  $^1\text{H}$  NMR agrees with the reported data.<sup>58</sup>  $^1\text{H}$  NMR (400 MHz,  $\text{CDCl}_3$ )  $\delta$  9.74 (m, 1H), 7.09 (d,  $J = 8.4$  Hz, 2H), 6.86 (d,  $J = 8.4$  Hz, 2H), 3.63 (s, 2H), 1.0 (s, 9H), 0.22 (s, 6H).



*2-(3-((tert-Butyldimethylsilyl)oxy)-4-methoxyphenyl)acetaldehyde (108)* It was synthesized from **107** according to previously reported experimental procedure.  $^1\text{H}$  NMR agrees with the reported data.<sup>59</sup>  $^1\text{H}$  NMR (400 MHz,  $\text{CDCl}_3$ )  $\delta$  9.69 (t,  $J = 2.5$  Hz, 1H), 6.84 (d,  $J = 8.2$  Hz, 1H), 6.75 (dd,  $J = 8.2$  Hz,  $J = 2.1$  Hz, 1H), 6.71 (d,  $J = 2.1$  Hz, 1H), 3.80 (s, 3H), 3.55 (d,  $J = 2.5$  Hz, 2H), 0.99 (s, 9H), 0.15 (s, 6H);

### Pictet-Spengler Reactions of 2-(3,4,5-trimethoxyphenyl)acetaldehyde **15** with 2-Nitrophenylsulfenyl Substituted Phenylethylamine **2**: Optimization Studies

Reactions were performed with amine **101a** (0.014 mmol, 5 mg) and 2-(3,4,5-trimethoxyphenyl)acetaldehyde **104** (0.028 mmol, 5.9 mg), catalyst (10 mol%) and additive (20 mol%) in dry toluene in the cited concentrations. Argon atmosphere was applied when cited.  $\text{MgSO}_4$  was added when cited. The conversion of the Nps-derivative was followed using HPLC [ChiralPack AD, 20%  $^i\text{PrOH}$ /Heptane, 0.5 mL/min, 220 nm] due to the same retention time on the TLC plates of the instantly formed enamine and the final product. HPLC samples for conversion and ee determination were prepared by scratching the enamine-product spot from the TLC-plate, followed by extraction of the silica gel with a mixture of 15%  $^i\text{PrOH}$ /Heptane, filtration and direct analysis. Conversion are reported as  $\text{Conv} = 100 \times [(\%A_M) + (\%A_m)] / [(\%A_M) + (\%A_m) + (\%A_{\text{enamine}})]$  where:  $t_R$  (*R*) 26.30 min,  $t_R$  (*S*) 40.65 min, and  $t_R$  (enamine) 57.63 min.

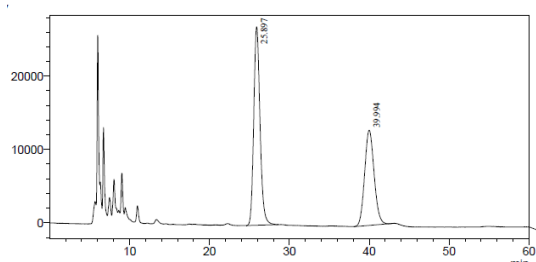


*(R)-7-(Methoxymethoxy)-2-((2-nitrophenyl)thio)-1-(3,4,5-trimethoxybenzyl)-1,2,3,4-tetrahydroisoquinolin-6-ol (109a)* In an oven dried flask Nps-protected amine **101a** (100 mg, 0.29 mmol), aldehyde **104** (66 mg, 0.31 mmol), (*R*)-TRIP **80** (20.6 mg, 0.03 mmol), (*S*)-BINOL (15.7 mg, 0.06 mmol) and  $\text{MgSO}_4$  (4.48 mmol, 540 mg) were dissolved in dry toluene under argon atmosphere and stirred at room temperature vigorously for 3 days. Then, the reaction mixture was concentrated under reduced pressure and the crude mixture was purified by flash chromatography using a DCM/PE/EtOAc 50/50/2 (then increased to 50/50/4) eluent system to produce **109a**. Yield: 107 mg, 72%, orange glass solid.  $[\alpha]_D^{25} = -3.5$  (c 1.00,  $\text{CHCl}_3$ ), 92% ee. FTIR (neat,  $\text{cm}^{-1}$ ) 3398, 2925, 1503, 1235, 1122, 734.  $^1\text{H}$  NMR (500 MHz, Toluene- $d_8$ , 90  $^\circ\text{C}$ )  $\delta$  7.95 (d,  $J = 8.1$  Hz, 1H), 7.52 (d,  $J = 8.1$  Hz, 1H), 7.05 (m, 1H), 6.70 (m, 2H), 6.56 (s, 1H), 6.27

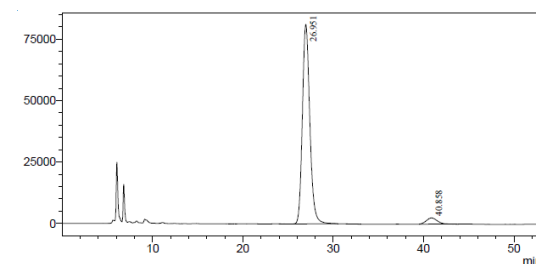


## Organocatalyzed Pictet-Spengler Reaction for the Synthesis of 1-Benzyl-1,2,3,4-tetrahydroisoquinolines and Total Synthesis of (*R*)-Trimetoquinol Hydrochloride

(m, 2H), 5.87 (bs, 1H), 4.75 (m, 2H), 4.35 (t,  $J = 6.8$  Hz, 1H), 3.80 (s, 3H), 3.46 (m, 6H), 3.36 (m, 1H), 3.17 (m, 3H), 3.05 (m, 1H), 2.98 (m, 2H), 2.82 (bs, 1H), 2.42 (dt,  $J = 14.6, 4.3$  Hz, 1H).  $^{13}\text{C}$  NMR (126 MHz, Toluene- $d_8$ , 90 °C)  $\delta$  154.1, 146.4, 143.5, 143.0, 139.0, 134.3, 133.5, 133.3, 129.6, 129.2, 125.7, 124.9, 124.3, 116.0, 115.6, 108.7, 96.8, 96.2, 60.4, 56.5, 56.2, 55.9, 55.3. HRMS (FD +) for  $\text{C}_{27}\text{H}_{30}\text{N}_2\text{O}_8\text{S}$ : calculated  $[\text{M}]^+$ : 542.1723. Found  $[\text{M}]^+$ : 542.1838; HPLC (Chiralcel AD, heptane/ $i$ PrOH = 80/20, flow rate 0.5 mL/min,  $\lambda = 220$  nm),  $t_{\text{R}}$  (major) = 26.9 min,  $t_{\text{R}}$  (minor) = 40.9 min; ee = 92%.



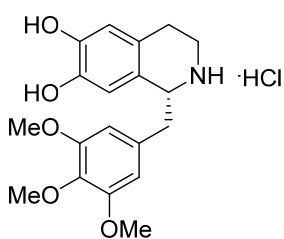
	Time	Area	% Height	% Area
1	25.897	1475341	67.58	57.97
2	39.994	1069453	32.42	42.02



	Time	Area	% Height	% Area
1	26.951	4644231	97.03	95.79
2	40.858	203925	2.97	4.21

### Hydrolysis procedure

The corresponding Pictet-Spengler product (0.19 mmol) was dissolved in a 1:1 mixture of DCM:EtOH (2 mL).  $\text{HCl}_{\text{conc}}$  (1 mL) was added and the reaction was stirred at room temperature for one hour. After this time, the aqueous layer extracted with DCM until the organic phase remained clear. Then, the aqueous layers was evaporated under reduce pressure to afford pure hydrochloric salts as stable solids. The products were further recrystallized from MeOH/Et<sub>2</sub>O mixtures.

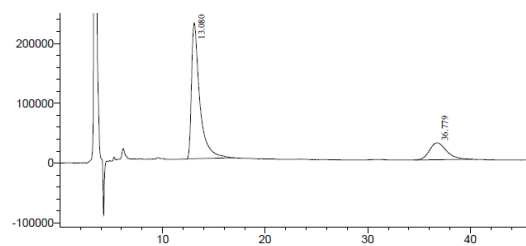


(*R*)-1-(3,4,5-trimethoxybenzyl)-1,2,3,4-tetrahydroisoquinoline-6,7-diol hydrochloride or (*R*)-Trimetoquinol Hydrochloride (LXIII) Hydrolysis produced pure compound LXIII as a stable brownish solid (62 mg, 86%). The racemate crystallized allowing the mother liqueurs enantiopure (43 mg, 62%, >99% ee) Note: HPLC chromatograms were performed after the hydrochloride salt had been neutralized with

a concentrated solution of  $\text{K}_2\text{CO}_3$ . Chiral HPLC: Chiralcel AD, <sup>n</sup>heptane/ isopropanol/Diethyl amine (v/v/v = 70/30/0.1) as eluent, flow 0.8 mL/min, 254 nm.  $t_{\text{R}}$  (major) = 13.2 min,  $t_{\text{R}}$  (minor) = 36.4 min. Data:  $[\alpha]_{\text{D}}^{25}$  = no transmission, literature:  $[\alpha]_{\text{D}}^{25}$  = -30 ( $c$  1.0, MeOH).  $m_{\text{p}}$  = 157-158 °C, literature: 151-153 °C. IR (neat,  $\text{cm}^{-1}$ ) 3367, 3212, 1592, 1452, 1423, 1116.<sup>60</sup>  $^1\text{H}$  NMR (400 MHz, Deuterium Oxide)  $\delta$  6.76 (s, 1H), 6.54 (s, 3H), 4.74 – 4.65 (m, 1H), 3.79 (s, 6H), 3.77 (s, 3H), 3.52 – 3.40 (m, 1H), 3.31 (m, 2H), 3.07 (m, 1H), 2.95 (m, 2H).  $^{13}\text{C}$  NMR (75 MHz, Deuterium Oxide)  $\delta$  152.5, 144.0, 142.8, 135.9, 131.5, 123.6, 122.7, 115.6, 113.7, 106.9, 60.8,

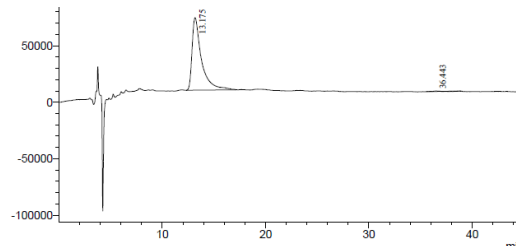
55.9, 55.6, 39.5, 39.1, 23.9. HRMS (FD +) for C<sub>19</sub>H<sub>24</sub>NO<sub>5</sub>: calculated [M + H]<sup>+</sup>: 346.1654. Found [M + H]<sup>+</sup>: 346.1646.

1<sup>st</sup> batch recrystallization: 59% ee



	Time	Area	% Height	% Area
1	13.080	12664987	88.90	79.31
2	36.779	3303675	11.10	20.69

1<sup>st</sup> batch mother liqueurs: >99% ee



	Time	Area	% Height	% Area
1	13.175	4065254	99.33	99.79
2	36.443	8711	0.67	0.21

<sup>1</sup> (a) Wu, T. R.; Chong, J. M. *J. Am. Chem. Soc.* **2006**, *128*, 9646-9647. (b) Kanemitsu, T.; Yamashita, Y.; Nagata, K.; Itoh, T. *Heterocycles* **2007**, *74*, 199-203. (c) Allin, S. M.; Gaskell, S. N.; Towler, J. M. R.; Page, P. C. B.; Saha, B.; McKenzie, M. J.; Martin, W. P. *J. Org. Chem.* **2007**, *72*, 8972-8975. (d) Bailey, K. R.; Ellis, A. J.; Reiss, R.; Snape, T. J.; Turner, N. J. *Chem. Commun.* **2007**, *43*, 3640-3642. (e) Hou, G.-H.; Xie, J.-H.; Yan, P.-C.; Zhou, Q.-L. *J. Am. Chem. Soc.* **2009**, *131*, 1366-1367. (f) Miyazaki, M.; Ando, N.; Sugai, K.; Seito, Y.; Fukuoka, H.; Kanemitsu, T.; Nagata, K.; Odanaka, Y.; Nakamura, K. T.; Itoh, T. *J. Org. Chem.* **2011**, *76*, 534-542. (g) Gurram, M.; Gyimothy, B.; Wang, R.; Lam, S. Q.; Ahmed, F.; Herr, R. J. *J. Org. Chem.* **2011**, *76*, 1605-1613. (h) Louafi, F.; Moreau, J.; Shahane, S.; Golhen, S.; Roisnel, T.; Sinbandhit, S.; Hurvois, J.-P. *J. Org. Chem.* **2011**, *76*, 9720-9732. (i) Mons, E.; Wanner, J. M.; Ingemann, S.; van Maarseveen, J. H.; Hiemstra, H. *J. Org. Chem.* **2014**, *79*, 7380-7390. (j) Battersby, A. R.; Edwards, T. P. *J. Chem. Soc.* **1960**, 1214-1221.

<sup>2</sup> (a) Hagel, J. M.; Facchini, P. *J. Plant Cell Physiol.* **2013**, *54*, 647-672. (b) Stöckigt, J.; Antonchick, A. P.; Wu, F.; Waldmann, H. *Angew. Chem. Int. Ed.* **2011**, *50*, 8538-8564. (c) Yoshiki Kashiwada, Y.; Aoshima, A.; Ikeshiro, Y.; Chen, Y.-C.; Furukawa, H.; Itoigawa, M.; Fujioka, T.; Mihashi, K.; L. Cosentino, M.; Morris-Natschke, S. L.; Leeg, K.-H. *Bioorg. Med. Chem.* **2005**, *13*, 443-448. (d) Pesnot, T.; Gershter, M. C.; Ward, J. M.; Hales, H. C. *Adv. Synth. Catal.* **2012**, *354*, 2997-3008. (e) Pyo, M. K.; Lee, D.-H.; Kim, D.-H.; Lee, J.-H.; Moon, J.-C.; Chang, K. C.; Yun-Choi, H. S. *Bioorg. Med. Chem. Lett.* **2008**, 4110-4114.

<sup>3</sup> (a) Kok, T. W.; Yue, P. Y. K.; Mak, N. K.; Fan, T. P. D. Liu, L.; Wong, N. S. *Angiogenesis*, **2005**, *8*, 3-12. (b) Wang, Y.; Fang, Y.; Huang, W.; Zhou, X.; Wang, M.; Zhong, B.; Peng, D. *J. Ethnopharmacol.* **2005**, *98*, 37-43. (c) Liu, L.; Buchner, E.; Beitze, D.; Schmidt-Weber, C. B.; Kaefer, V.; Emmrich, F.; Kinne, R. W. *Int. J. Immunopharmac.* **1996**, *18*, 529-543. (d) Song, L.; Liu, D.; Zhao, Y.; He, J.; Kang, H.; Dai, Z.; Wang, X.; Zhang, S.; Zan, Y. *Biochem. Biophys. Res. Commun.* **2015**, *464*, 705-710. (e) Kametani, T.; Ihara, M.; Fukumoto, K.; Yagi, H. *J. Chem. Soc. C.* **1996**, *15*, 2030-2033.

<sup>4</sup> Onoyovwe, A.; Hagel, J. M.; Chen, X.; Khan, M. F.; Schriemer, D. C.; Facchini, P. *J. The Plant Cell* **2013**, 4110-4122.

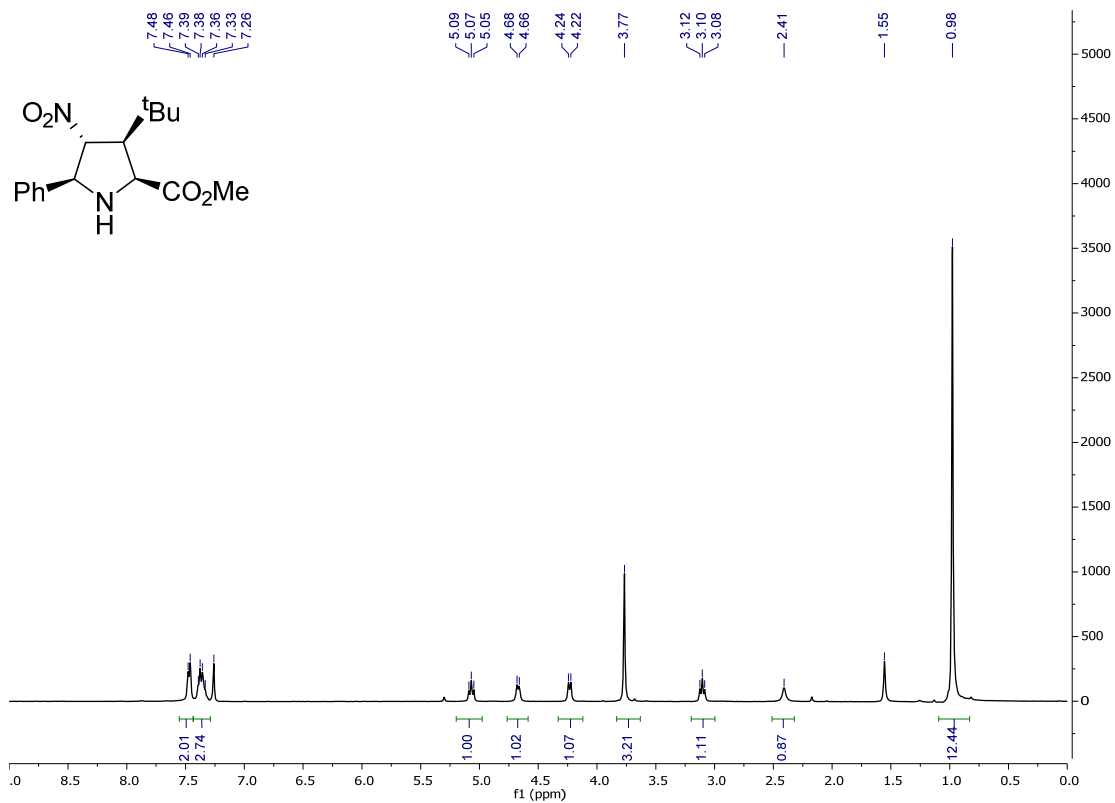
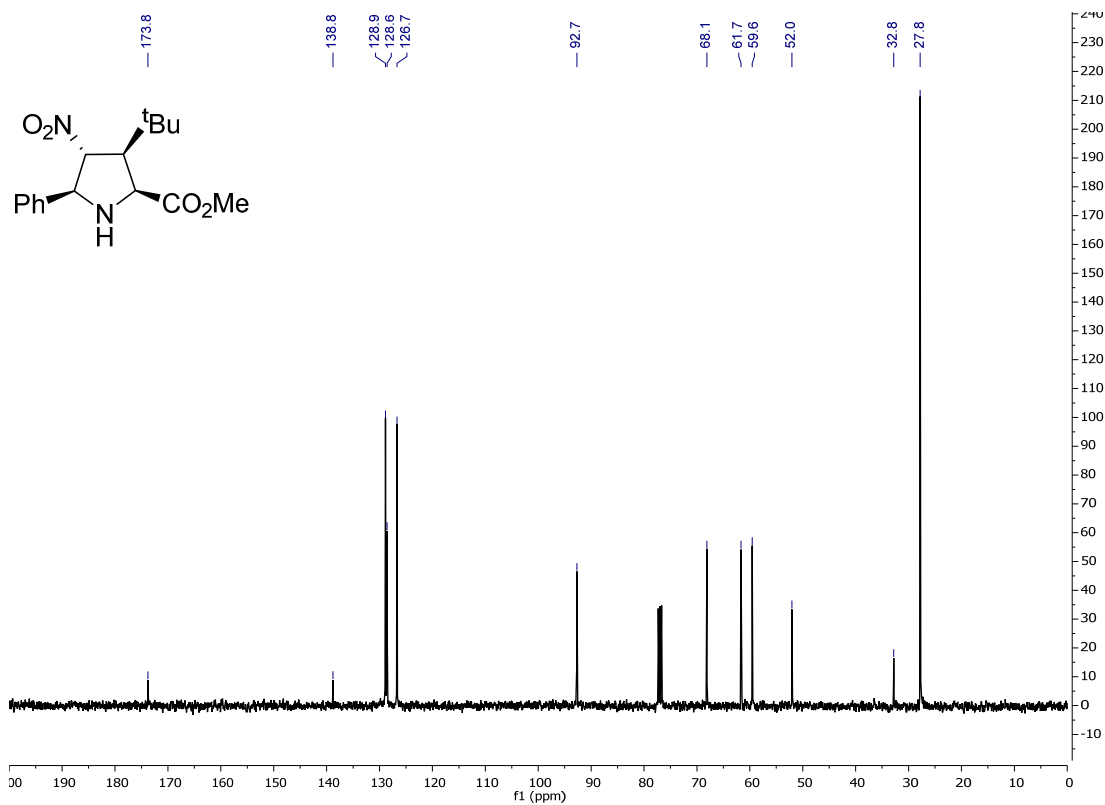
<sup>5</sup> (a) Guinaudeau, H.; Leboeuf, M.; Cave, A. *Lloydia*, **1975**, *38*, 275-338. (b) Guinaudeau, H.; Leboeuf, M.; Cave, A. *Lloydia*, **1979**, *42*, 325-360. (c) Stevigny, C.; Bailly, C.; Quetin-Leclercq, J. *Curr Med Chem Anticancer Agents* **2005**, *5*, 173-182. (d) Likhitwitayawuid, K.; Angerhofer, C. K.; Chai, H.; Pezzuto, J. M.; Cordell, G. A.; Ruangrunsi, N. *J. Nat. Prod.* **1993**, *56*, 1468-1478. (e) Montanha, J. A.; Amoros, M.; Boustie, J.; Girre, L. *Planta Medica* **1995**, *61*, 419-424.

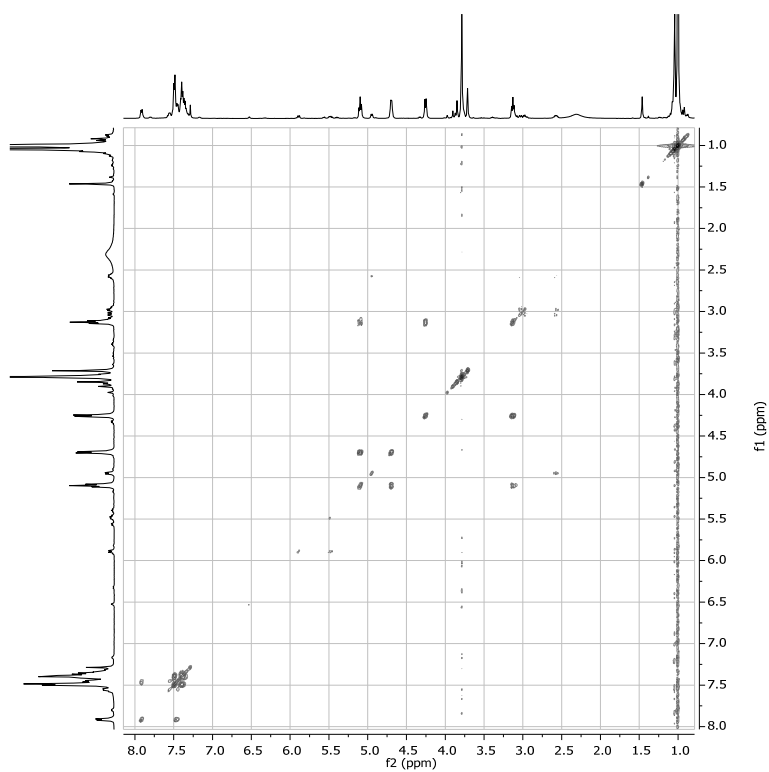
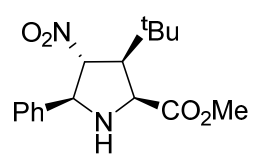
<sup>6</sup> (a) Jack, D.; Williams, R. *Chem. Rev.* **2002**, *102*, 1669-1730. (b) Bentley, K. W. *Nat. Prod. Rep.* **2006**, *23*, 444-463. (c) Aladesanmi, A. J.; Kelly, C. J.; Leary, J. D. *J. Nat. Prod.* **1983**, *46*,

- 127-131. (d) Zhang, A.; Neumeyer, J. L.; Baldessarini, R. J. *Chem. Rev.* **2007**, *107*, 274-302. (e) Perrey, D. A.; German, N. A.; Gilmour, B. P.; Li, J. X.; Harris, D. L.; Thomas, B. F.; Zhang, Y. *J. Med. Chem.* **2013**, *56*, 6901-6916. (f) Wu, H.-P.; Lu, T.-N.; Hsu, N.-Y.; Chang, C.-C. *Eur. J. Org. Chem.* **2013**, 2898-2905.
- <sup>7</sup> (a) Tatton, W. G.; Ju, W. Y. L.; Holland, D. P.; Tai, C.; Kwan, M. *J. Neurochem.* **1994**, *63*, 1572-1575. (b) Mayuyama, W.; Naoi, M.; Kasamatsu, T.; Hashizume, Y.; Takahashi, T.; Kohda, K.; Dostert, P. *J. Neurochem.* **1997**, *69*, 322-329.
- <sup>8</sup> Liu, W.; Liu, S.; Jin, R.; Guo, H.; Zhao, J. *Org. Chem. Front.* **2015**, *2*, 288-299.
- <sup>9</sup> Vilhanova, B.; Matousek, V.; Vaclavik, J.; Syslova, K.; Prech, J.; Pechacek, J.; Sot, P.; Januscak, J.; Toman, J.; Zapal, J.; Kuzma, M.; Kacer, P. *Tetrahedron Asymm.* **2013**, *24*, 50-55.
- <sup>10</sup> Adam, S.; Pannecoucke, X.; Combret, J.-C.; Quirion, J.-C. *J. Org. Chem.* **2001**, *66*, 8744-8750.
- <sup>11</sup> Jensen, K. B.; Roberson, M.; Jørgensen, K. A. *J. Org. Chem.* **2000**, *65*, 9080-9084.
- <sup>12</sup> Wanner, K. T.; Beer, H.; Höfner, G.; Ludwig, M. *Eur. J. Org. Chem.* **1998**, 2019-2029.
- <sup>13</sup> (a) Djerassi, C.; Markley, F. X.; Ehrlich, R. *J. Org. Chem.* **1956**, *21*, 975-978. (b) Fodor, G.; Nagubandi, S. *Tetrahedron* **1980**, *36*, 1279-1300. (c) Capilla, A. S.; Romero, M.; Pujol, M. D.; Caignard, D. H.; Renard, P. *Tetrahedron* **2001**, *57*, 8297-8303.
- <sup>14</sup> (a) Czarnocki, Z.; Mieczkowski, J. B. *Pol. J. Chem.* **1995**, *69*, 1447-1450. (b) Jullian, V.; Quirion, J.-C.; Husson, H.-P. *Eur. J. Org. Chem.* **2000**, 1319-1325.
- <sup>15</sup> Morimoto, T.; Achiwa, K. *Tetrahedron: Asymm.* **1995**, *6*, 2661-2664.
- <sup>16</sup> (a) Noyori, R.; Hashiguchi, S. *Acc. Chem. Res.* **1997**, *30*, 97-102. (b) Tietze, L. F.; Zhou, Y.; Töpken, E. *Eur. J. Org. Chem.* **2000**, 2247-2252. (c) Wu, Z.; Perez, M.; Scalone, M.; Ayad, T.; Ratovelomanana-Vidal, V. *Angew. Chem. Int. Ed.* **2013**, *52*, 4925-4928.
- <sup>17</sup> Kang, J.; Kim, J. B.; Cho, K. H.; Cho, B. T. *Tetrahedron: Asymm.* **1997**, *8*, 657-660.
- <sup>18</sup> Takasu, K.; Maiti, S.; Ihara, M. *Heterocycles* **2003**, *59*, 51-55.
- <sup>19</sup> Pictet, A.; Spengler, T. *Ber. Disch. Chem. Ges.* **1911**, *44*, 2030-2036.
- <sup>20</sup> Tatsui, G. *J. Pharm. Soc. Jpn.* **1928**, *48*, 92.
- <sup>21</sup> (a) Stöckigt, J.; Antonchick, A. P.; Wu, F.; Waldmann, H. *Angew. Chem. Int. Ed.* **2011**, *50*, 8538-8564; (b) Cox, E. D.; Cook, J. M. *Chem. Rev.* **1995**, *95*, 1797-1842.
- <sup>22</sup> (a) Jackson, A. H.; Smith, A. E. *Tetrahedron* **1968**, *24*, 403-413. (b) Ungemach, F.; Cook, J. M. *Heterocycles* **1978**, *9*, 1089-1119. (c) Bailey, P. D. *J. Chem. Res.* **1987**, 202-203.
- <sup>23</sup> (a) Cox, E. D.; Cook, J. M. *Chem. Rev.* **1995**, *95*, 1797-1842. (b) Liu, J. J.; Nakagawa, M.; Ogata, K.; Hino, T. *Chem. Pharm. Bull.* **1991**, *39*, 1672-1676. (c) Czerwinski, K. M.; Deng, L.; Cook, J. M. *Tetrahedron Lett.* **1992**, *33*, 4721-4724.
- <sup>24</sup> Li, J. *Pictet-Spengler tetrahydroisoquinoline synthesis; Name reactions – A collection of detailed mechanisms and synthetic applications*, **2009**, Springer Berlin Heidelberg, 434-435.
- <sup>25</sup> (a) Herlé, B.; Wanner, M. J.; van Maarseveen, J. H.; Hiemstra, H. *J. Org. Chem.* **2011**, *76*, 8907-8912. (b) Sewgobind, N.; Wanner, M. J.; Ingemann, S.; de Gelder, R.; van Maarseveen, J. H.; Hiemstra, H. *J. Org. Chem.* **2011**, *76*, 8907-8912.
- <sup>26</sup> (a) Klausen, R. S.; Jacobsen, E. N. *Org. Lett.* **2009**, *11*, 887-890. (b) Taylor, M. S.; Jacobsen, E. N. *J. Am. Chem. Soc.* **2004**, *126*, 10558-10559. (c) Kerschgens, I. P.; Claveau, E.; Wanner, M. J.; Ingemann, S.; van Maarseveen, J. H.; Hiemstra, H. *Chem. Commun.* **2012**, *48*, 12243-12245.
- <sup>27</sup> Wanner, M. J.; van der Haas, R. N. S.; de Cuba, K. R.; van Maarseveen, J. H.; Hiemstra, H. *Angew. Chem. Int. Ed.* **2007**, *46*, 7485-7487.
- <sup>28</sup> Wanner, M. J.; Boots, R. A.; Eradus, B.; de Gelder, R.; van Maarseveen, J. H.; Hiemstra, H. *Org. Lett.* **2009**, *11*, 2579-2581.
- <sup>29</sup> Chrzanowska M.; Rozwadowska, M. D. *Chem. Rev.* **2004**, *104*, 3341-3370.
- <sup>30</sup> Gremmen, C.; Wanner, M. J.; Koomen, G. J. *Tetrahedron Lett.* **2001**, *42*, 8885-8888.
- <sup>31</sup> (a) Chan, W.; Lee, A. W. M.; Jiang, L. *Tetrahedron Lett.* **1995**, *36*, 715-718. (b) Bravo, P.; Crucianelly, M.; Farina, A.; Meille, S. V.; Volonterio, A.; Zanda, M. *Eur. J. Org. Chem.* **1998**, 435-440.
- <sup>32</sup> Allef, P.; Kunz, H. *Heterocycles* **2007**, *74*, 421-436.
- <sup>33</sup> Commins, D. L.; Thakker, P. M.; Baevsky, M. F.; Badawi, M. M. *Tetrahedron* **1997**, *53*, 16327-16340.
- <sup>34</sup> Schmidt, G.; Herbert Waldmann, H.; Dr. Henning Henke, H.; Burkard, M. *Chem. Eur. J.* **1996**, *2*, 1566-1571.
- <sup>35</sup> (a) Samanani, N.; Liscombe, D. K.; Facchini, P. J. *Plant J.* **2004**, *40*, 302-313. (b) Luk, L. Y. P.; Bunn, S.; Liscombe, D. K.; Facchini, P. J. Tanner, M. E. *Biochemistry*, **2007**, *46*,

- 10153-10161. (c) Ilari, A.; Franceschini, S.; Bonamore, A.; Arengi, F.; Botta, B.; Macone, A.; Pasquo, A.; Belluci, L.; Boffi, A. *J. Biol. Chem.* **2009**, *284*, 897-904. (d) Bonamore, A.; Barba, M.; Botta, B.; Boffi, A.; Macone, A. *Molecules* **2010**, *15*, 2070-2078.
- <sup>36</sup> Maresh, J. J.; Giddings, L. A.; Friedrich, A.; Loris, E. A.; Panjikar, S.; Trout, B. L.; Stöckigt, J.; Peters, B.; O'Connor, S. E.; *J. Am. Chem. Soc.* **2008**, *130*, 710-723.
- <sup>37</sup> Toda, Y.; Terada, M. *Synlett.* **2013**, 752-756.
- <sup>38</sup> Pesnot, T.; Gershater, M. C.; Ward, J. M.; Hailes, H. C. *Chem. Commun.* **2011**, *47*, 3242-3244.
- <sup>39</sup> Klussmann, M.; Ratjen, L.; Hoffmann, S.; Wakchaure, V.; Goddard, R.; List, B. *Synlett* **2010**, 2189-2192.
- <sup>40</sup> Gribkov, D. V.; Hultsch, K. C.; Hampell, F. *Chem. Eur. J.* **2003**, *9*, 4796-4810.
- <sup>41</sup> Nakashima, D.; Yamamoto, H. *J. Am. Chem. Soc.* **2006**, *128*, 9326-9627.
- <sup>42</sup> Xie, J.; Zhou, Q. *Acc. Chem. Res.* **2008**, *41*, 581-593.
- <sup>43</sup> (a) Birman, V. B.; Rheingold, A.; Lam, K. *Tetrahedron: Asymm.* **1999**, *10*, 125-131. (b) Zhang, J.; Liao, J.; Cui, X.; Yu, K.; Zhu, J.; Deng, J.; Zhu, S.; Wang, L.; Zhou, Q.; Chung, L. W.; Ye, T. *Tetrahedron: Asymm.* **2002**, *13*, 1363-1366.
- <sup>44</sup> Lan, K.; Shan, Z.; Fan, S. *Tetrahedron Lett.* **2006**, *47*, 4343-4345.
- <sup>45</sup> Čorić, I.; Müller, S.; List, B. *J. Am. Chem. Soc.* **2010**, *132*, 17370-17373.
- <sup>46</sup> Yang, Y.; Zhu, S.; Duan, H.; Zhou, C.; Wang, L.; Zhou, Q. *J. Am. Chem. Soc.* **2007**, *129*, 2248-2249.
- <sup>47</sup> Li, Q.; Jiang, J.; Fan, A.; Cui, Y.; Jia, Y. *Org. Lett.* **2011**, *13*, 312-315.
- <sup>48</sup> Guin, J.; Varseev, G.; List, B. *J. Am. Chem. Soc.* **2013**, *135*, 2100-2103.
- <sup>49</sup> Maurin, C.; Bailly, F.; Cotelle, P. *Tetrahedron* **2005**, *61*, 7054-7058.
- <sup>50</sup> Iwasawa, Y.; Kiyomoto, A. *Jpn. J. Pharmacol.* **1967**, *17*, 143-152.
- <sup>51</sup> Romstedt, K. J.; Shin, Y.; Shams, G.; Doyle, K.; Tantishaiyakul, V.; Clark, M.; Adejare, A.; Hamada, A.; Miller, D. D.; Feller, D. R. *Biochem. Pharmacol.* **1993**, *46*, 2051-2059.
- <sup>52</sup> (a) Hashigaki, K.; Kan, K.; Qais, N.; Takeucki, Y.; Yamoto, M. *Chem. Pharm. Bull.* **1991**, *39*, 1126-1131. (b) Mashimo, K.; Yamato, E.; Kiyomoto, A.; Nakayima, H.; Africa, S. Patent 68 02416 **1968** [*Chem. Abstr.* **1969**, *70*, 68198w.]
- <sup>53</sup> Ruiz-Olalla, A.; Würdemann, M. A.; Wanner, M. J.; Ingemann, S.; van Maarseveen, J. H.; Hiemstra, H. *J. Org. Chem.* **2015**, *80*, 5125-5132
- <sup>54</sup> See 1i; Craine, L.; Raban, M. *Chem. Rev.* **1989**, *89*, 689-712.
- <sup>55</sup> Zhang, M.; Jagdmann Jr., G. E.; Van Zandt, M.; Beckett, P.; Schroeter, H. *Tetrahedron: Asymm.* **2013**, 362-373.
- <sup>56</sup> Gemma, S.; Brogi, S.; Patil, P. R.; Giovani, S.; Lamponi, S.; Cappelli, A.; Novellino, E.; Brown, A.; Higgins, M. K.; Mustafa, K.; Szeszak, T.; Craig, A. G.; Campiani, G.; Butini, S.; Brindisi, M. *R. S. C. Adv.* **2014**, *4*, 4769-4781.
- <sup>57</sup> Swenton, J. S.; Carpenter, K.; Chen, Y.; Kerns, M. L.; Morrow, G. W. *J. Org. Chem.* **1993**, *58*, 3308-3316.
- <sup>58</sup> Takashima, Y.; Kobayashi, Y. *J. Org. Chem.* **2009**, *74*, 5920-5926.
- <sup>59</sup> Master Thesis, Martien A. Würdemann, **2014** "Enantioselective phosphoric acid catalysed Pictet-Spengler reactions towards 1-benzyltetrahydroisoquinolines".
- <sup>60</sup> Japanese Pharmacopoeia 16<sup>th</sup> Edition, **2011**, pg 1955.

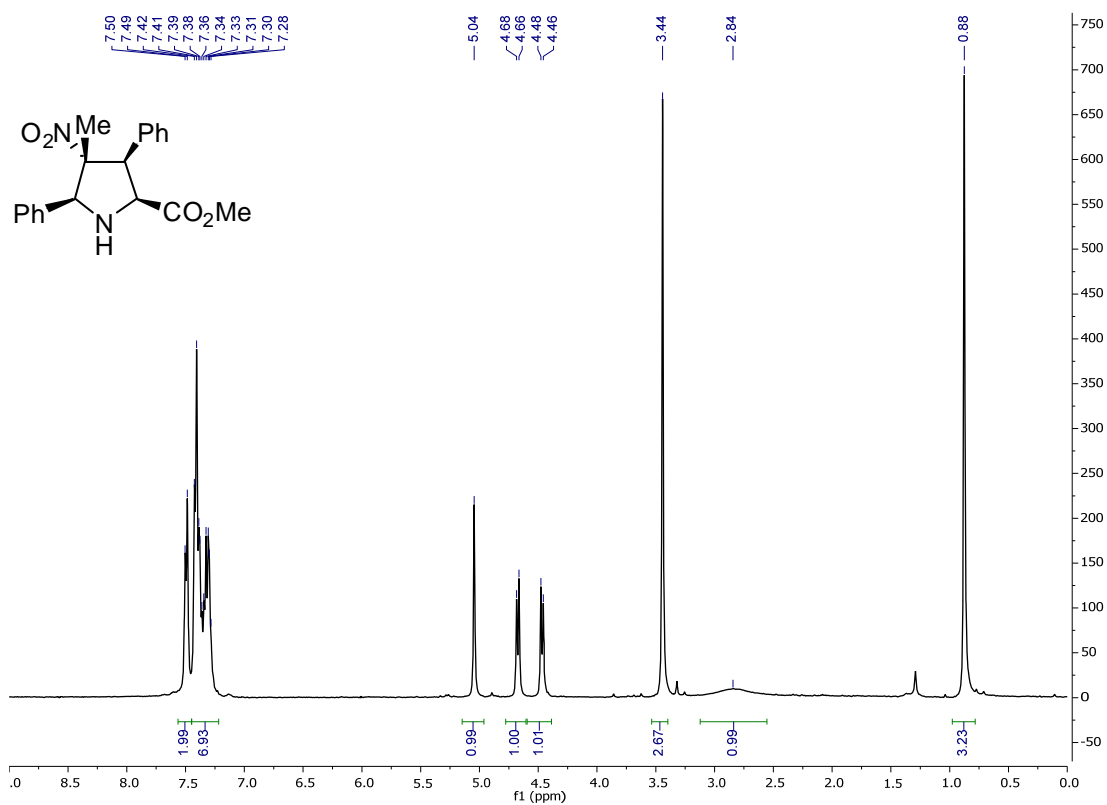
## Annex I-a. NMR spectra selection for Chapter 2

Compound NO<sub>2</sub>-X<sub>L</sub>-OMe-5aI<sup>1</sup>H NMR (CDCl<sub>3</sub>)<sup>13</sup>C NMR (CDCl<sub>3</sub>)

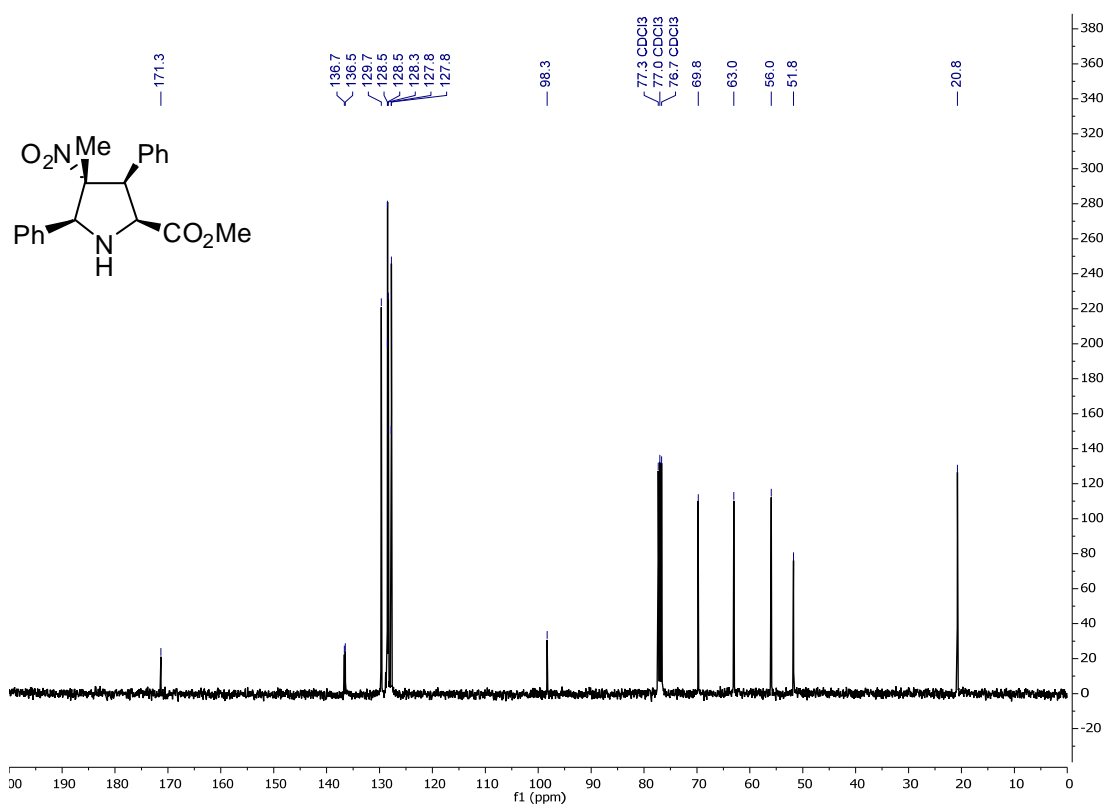
COSY (CDCl<sub>3</sub>)

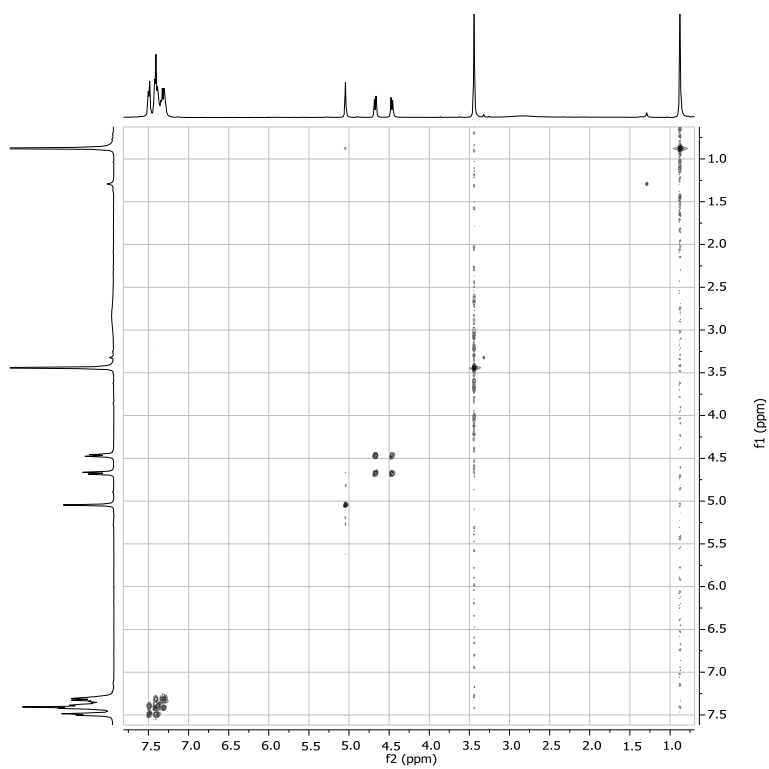
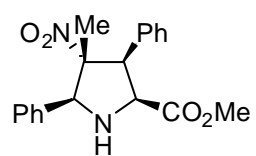
Compound NO<sub>2</sub>-X<sub>L</sub>-OMe-5am

<sup>1</sup>H NMR (CDCl<sub>3</sub>)

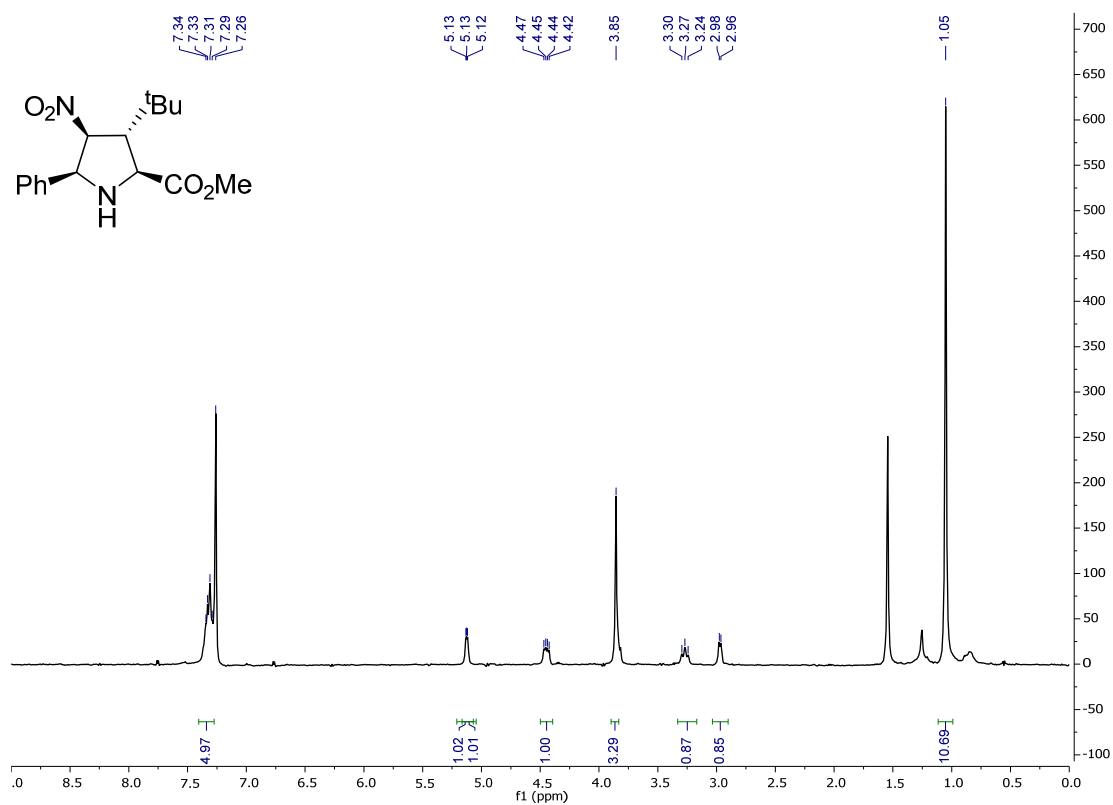
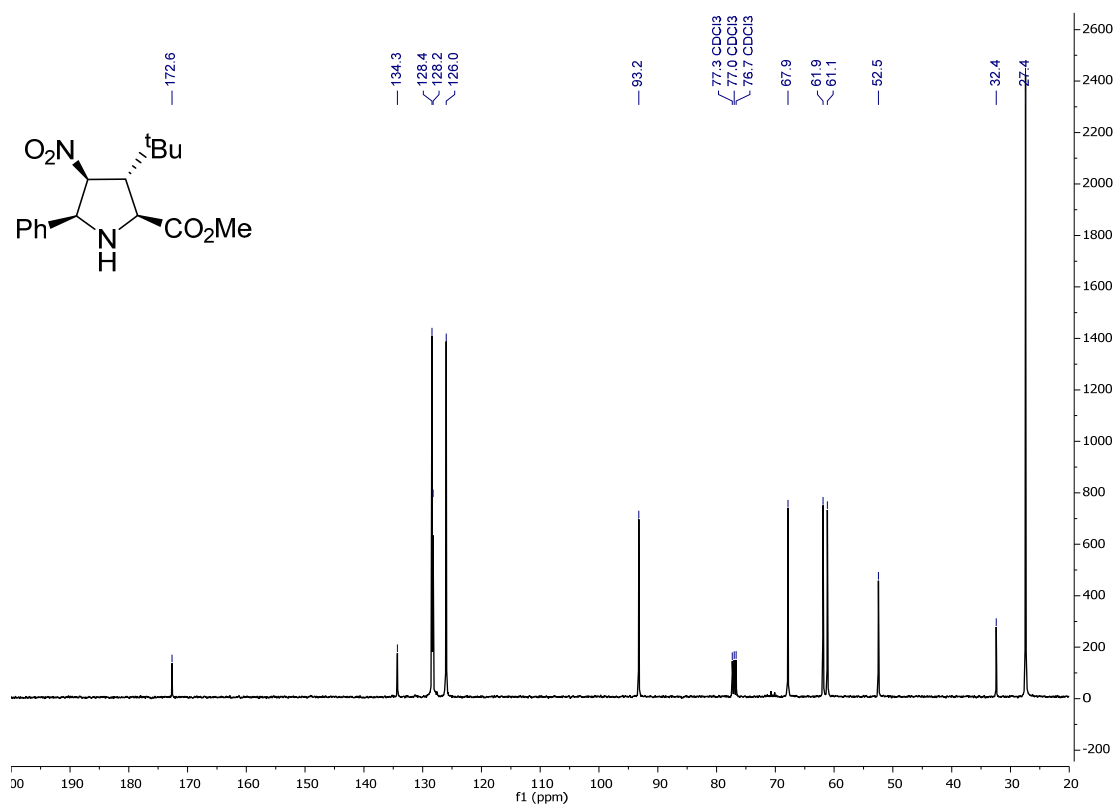


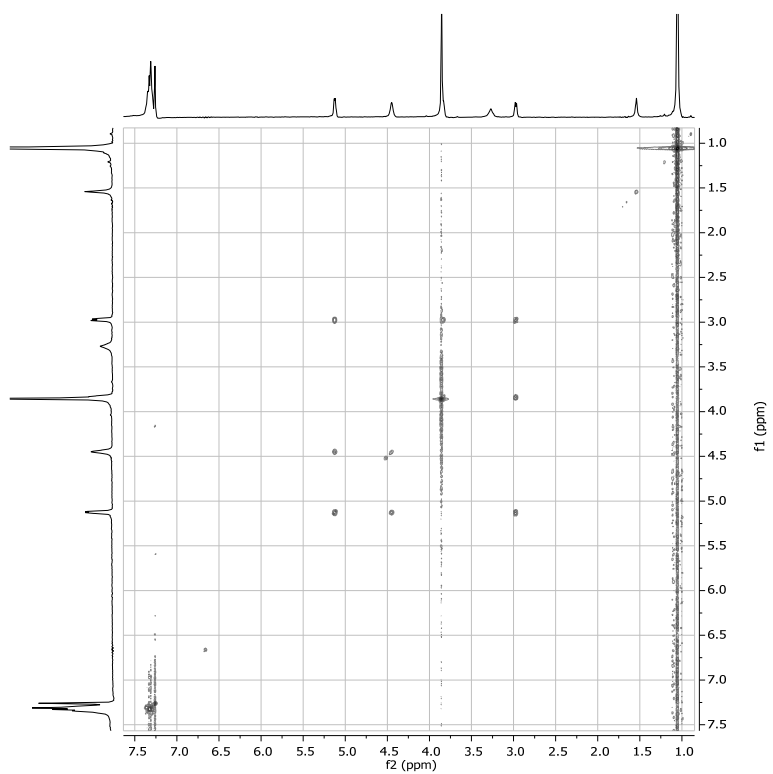
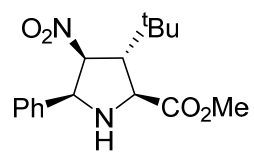
<sup>13</sup>C NMR (CDCl<sub>3</sub>)

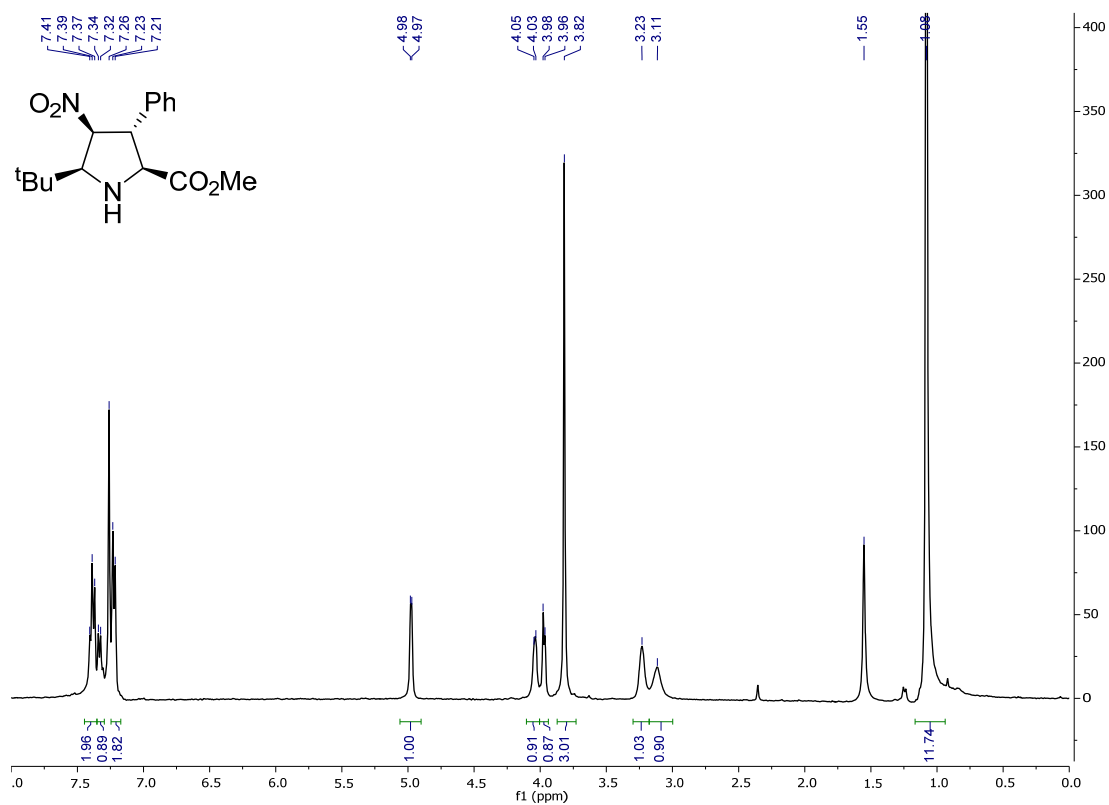
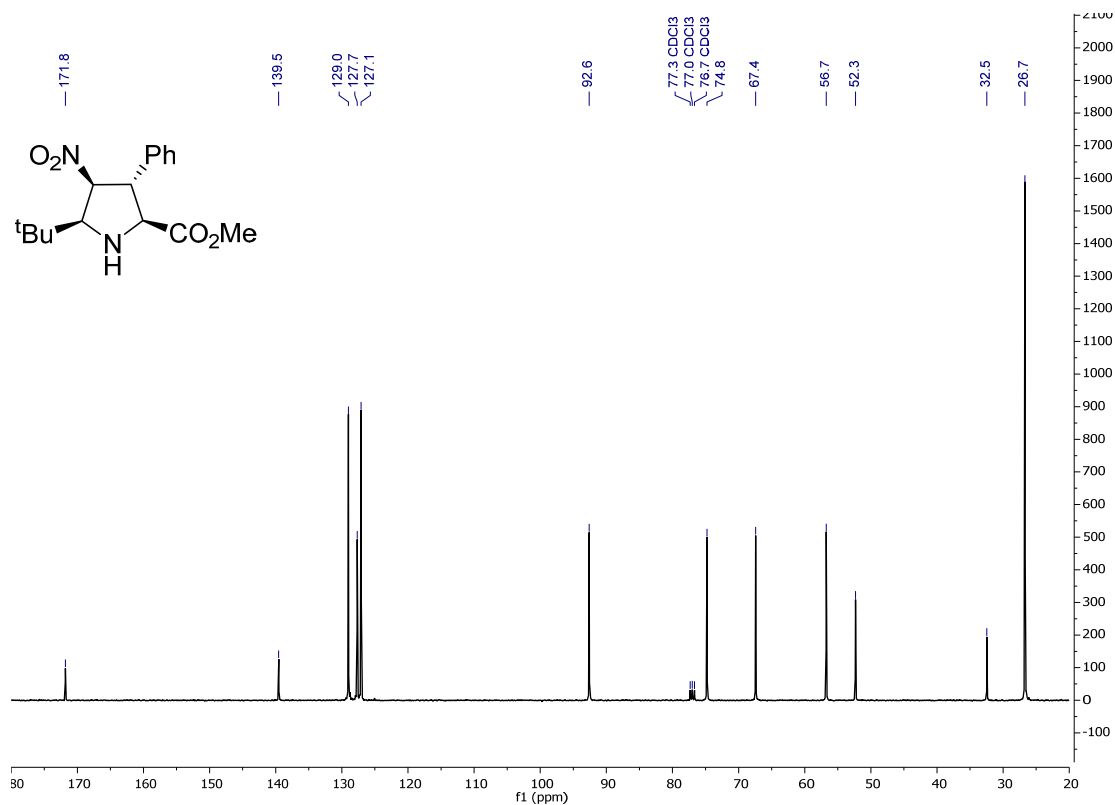


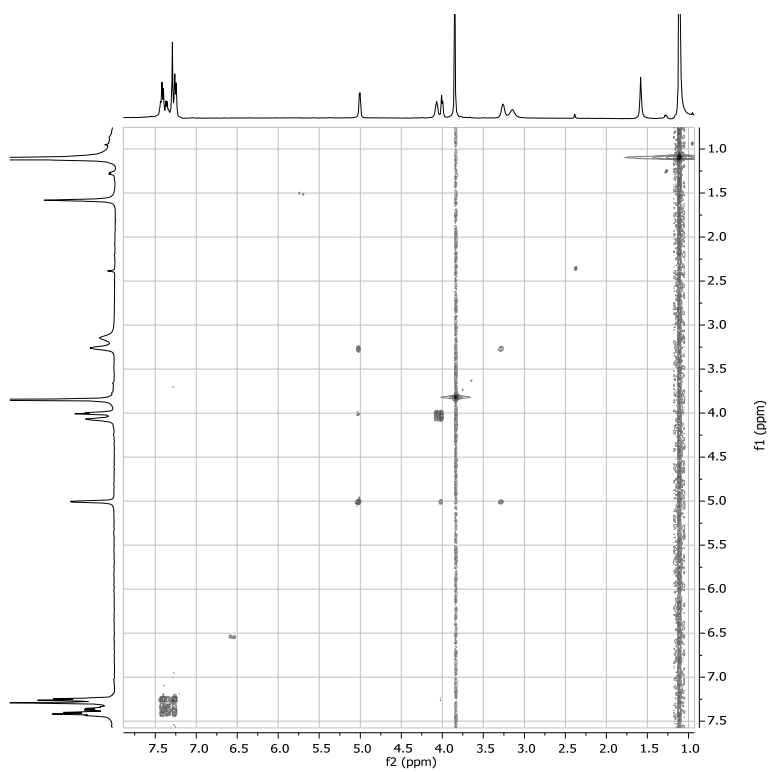
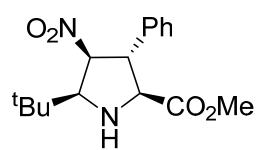
COSY (CDCl<sub>3</sub>)

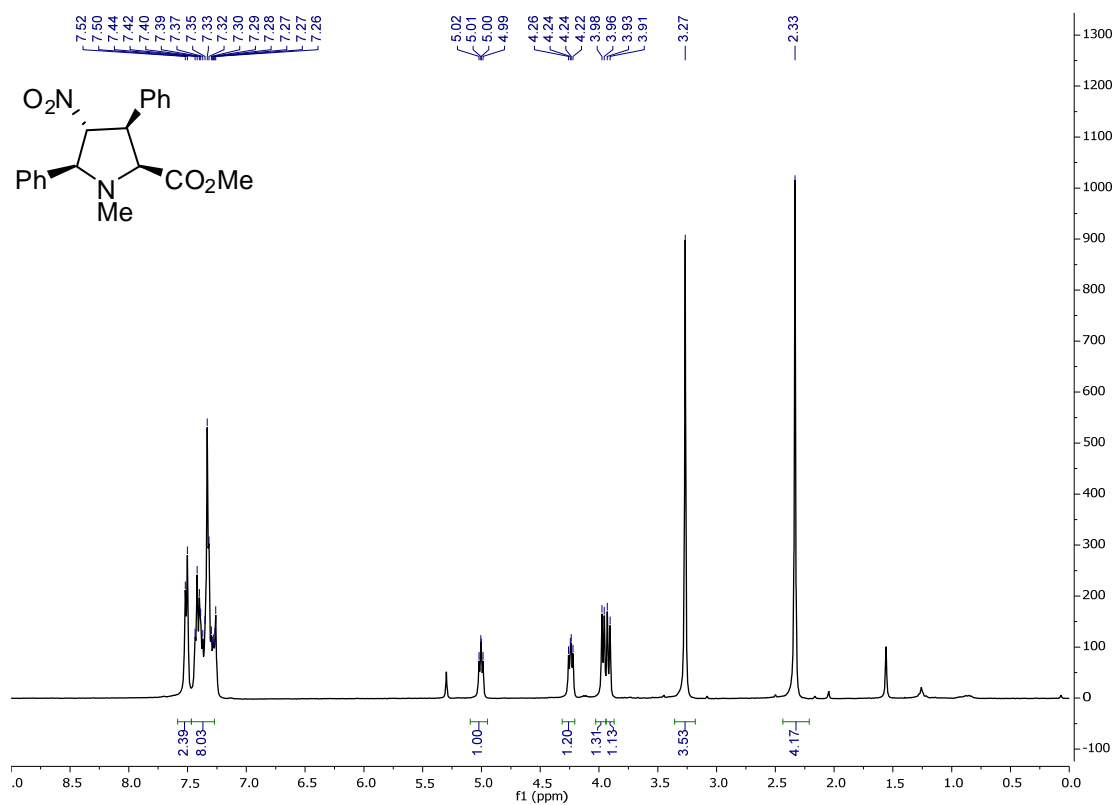
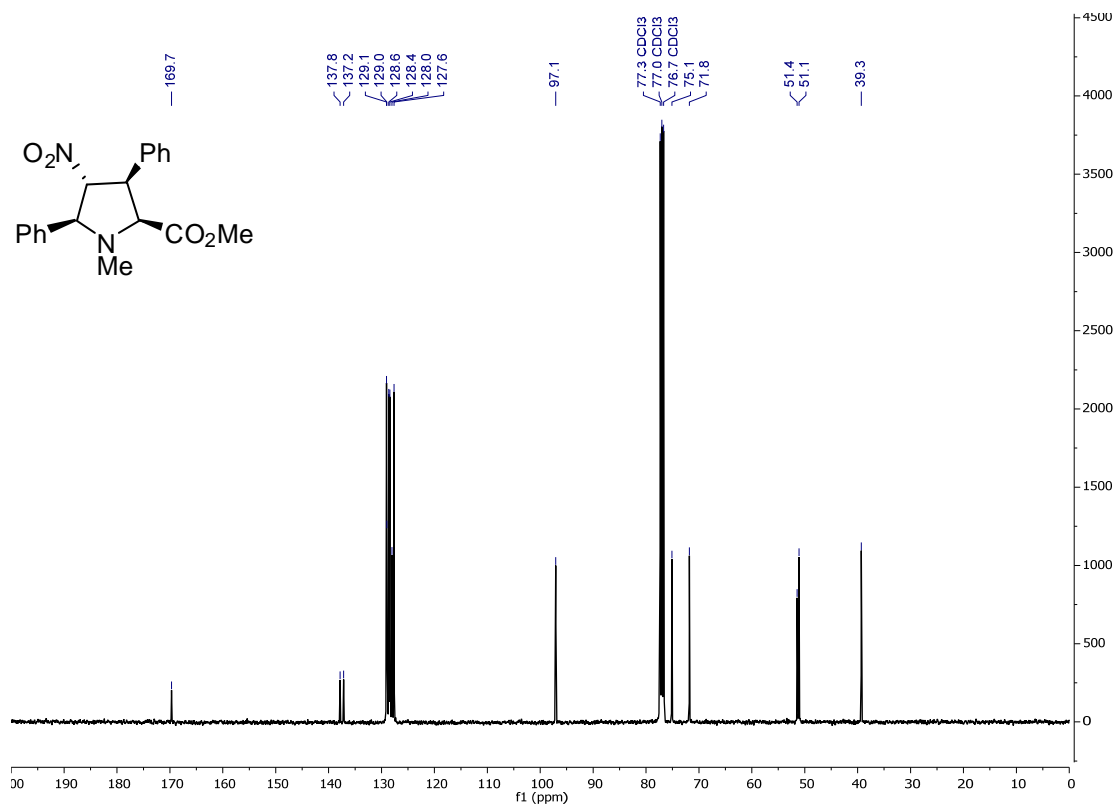


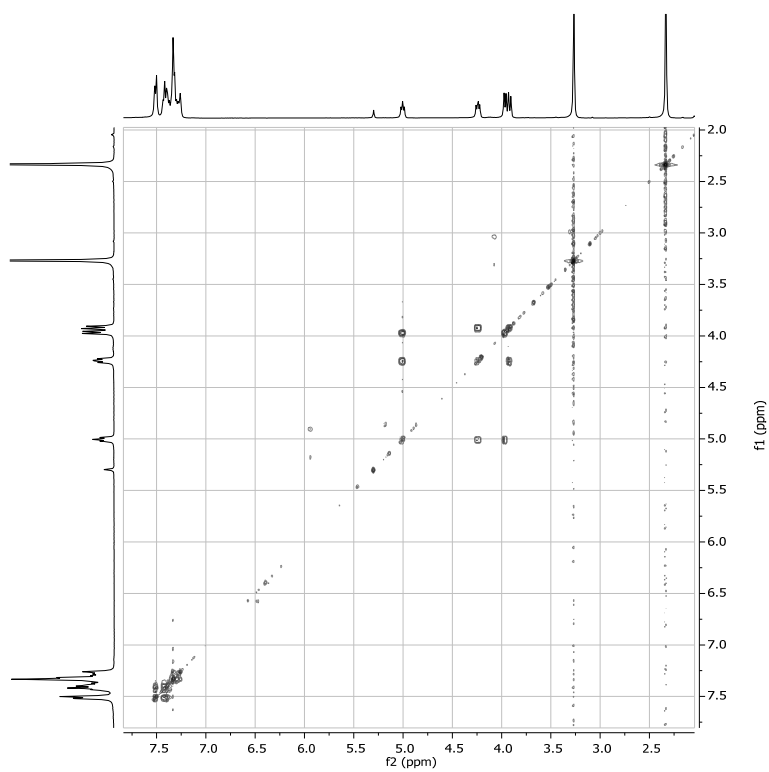
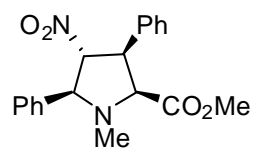
Compound NO<sub>2</sub>-N<sub>L</sub>-OMe-5aI<sup>1</sup>H NMR (CDCl<sub>3</sub>)<sup>13</sup>C NMR (CDCl<sub>3</sub>)

COSY (CDCl<sub>3</sub>)

Compound NO<sub>2</sub>-N<sub>L</sub>-OMe-51a<sup>1</sup>H NMR (CDCl<sub>3</sub>)<sup>13</sup>C NMR (CDCl<sub>3</sub>)

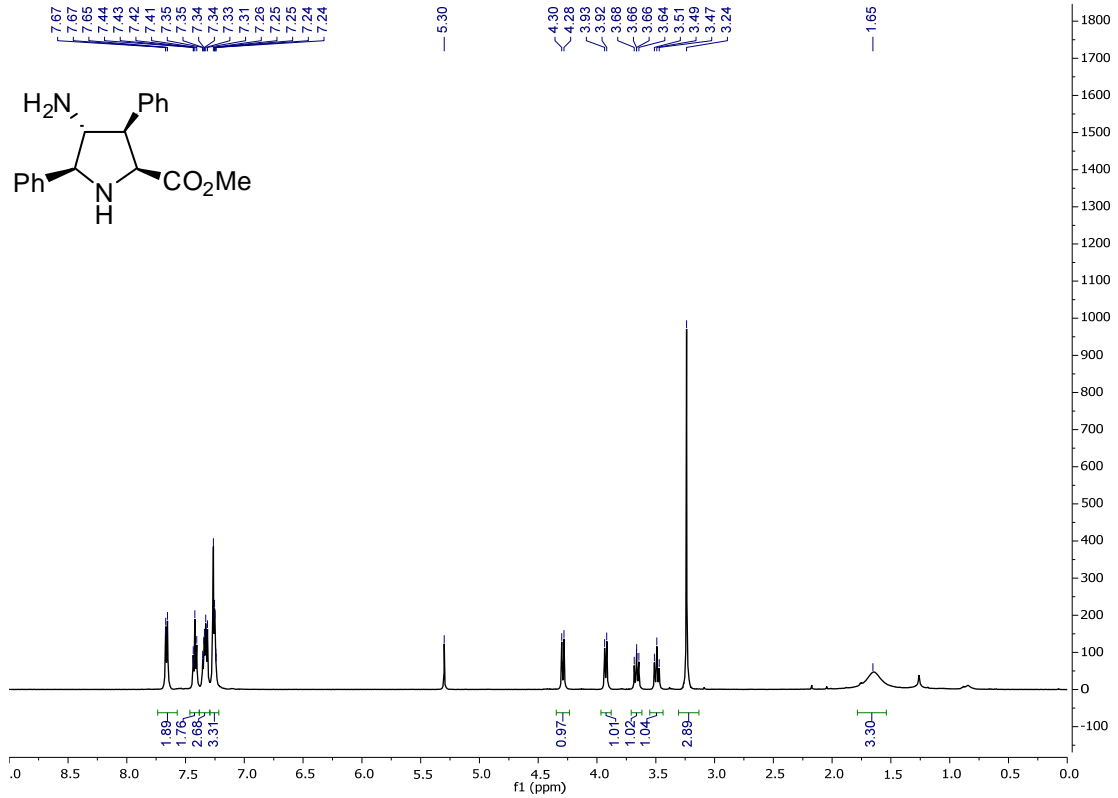
COSY (CDCl<sub>3</sub>)

Compound NO<sub>2</sub>-X<sub>L</sub>-OMe-5c<sup>1</sup>H NMR (CDCl<sub>3</sub>)<sup>13</sup>C NMR (CDCl<sub>3</sub>)

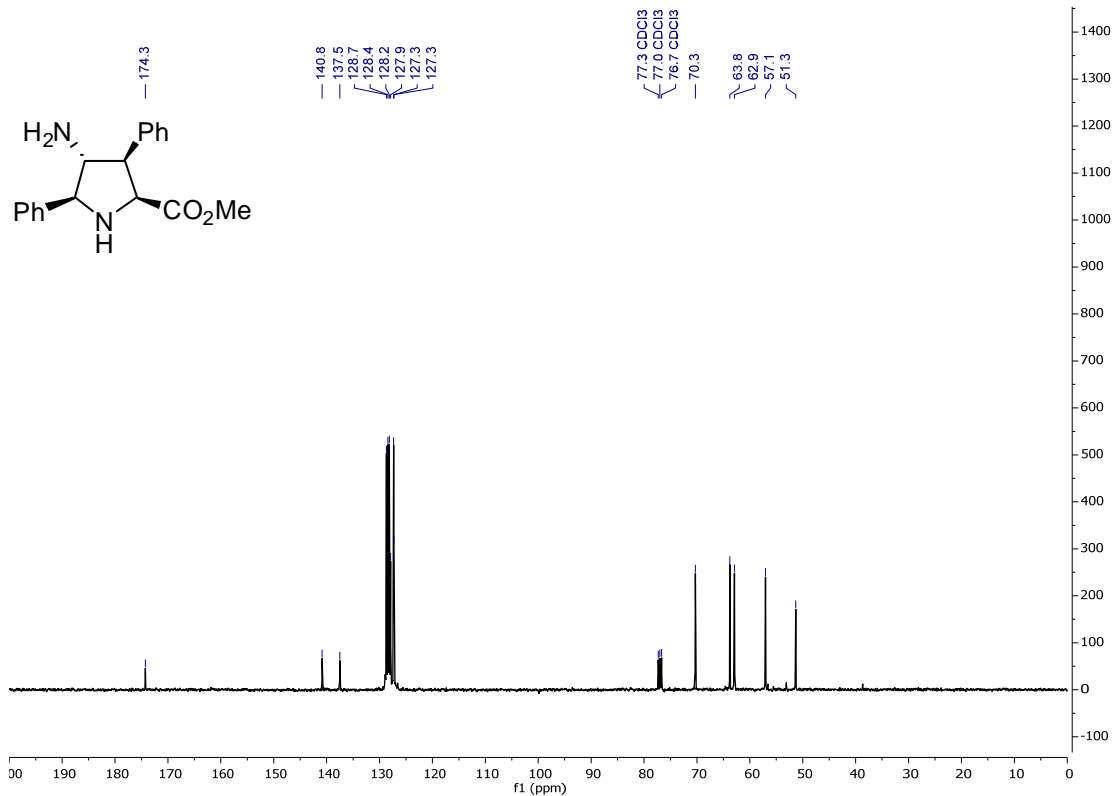
COSY (CDCl<sub>3</sub>)

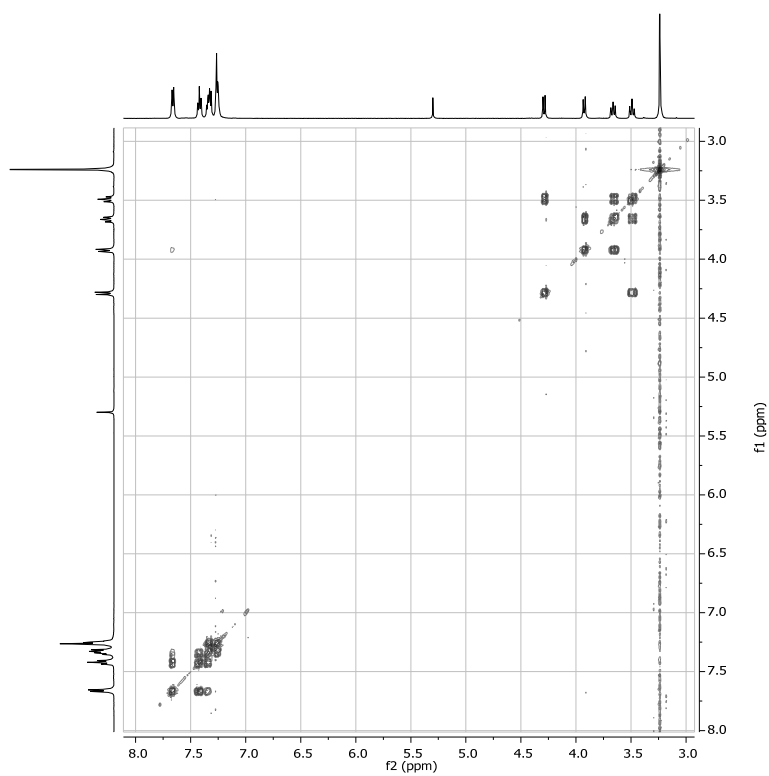
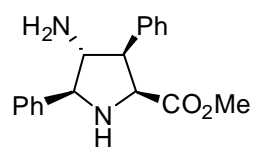
Compound NH<sub>2</sub>-X<sub>L</sub>-OMe-10aa

<sup>1</sup>H NMR (CDCl<sub>3</sub>)

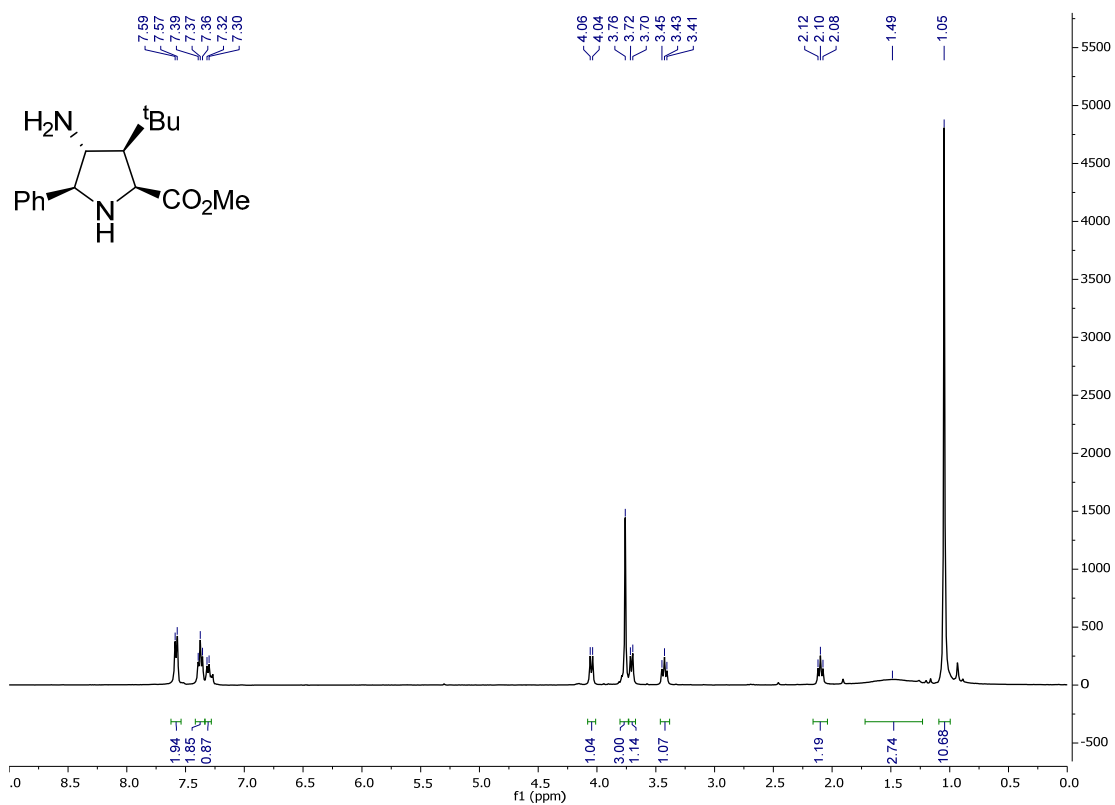
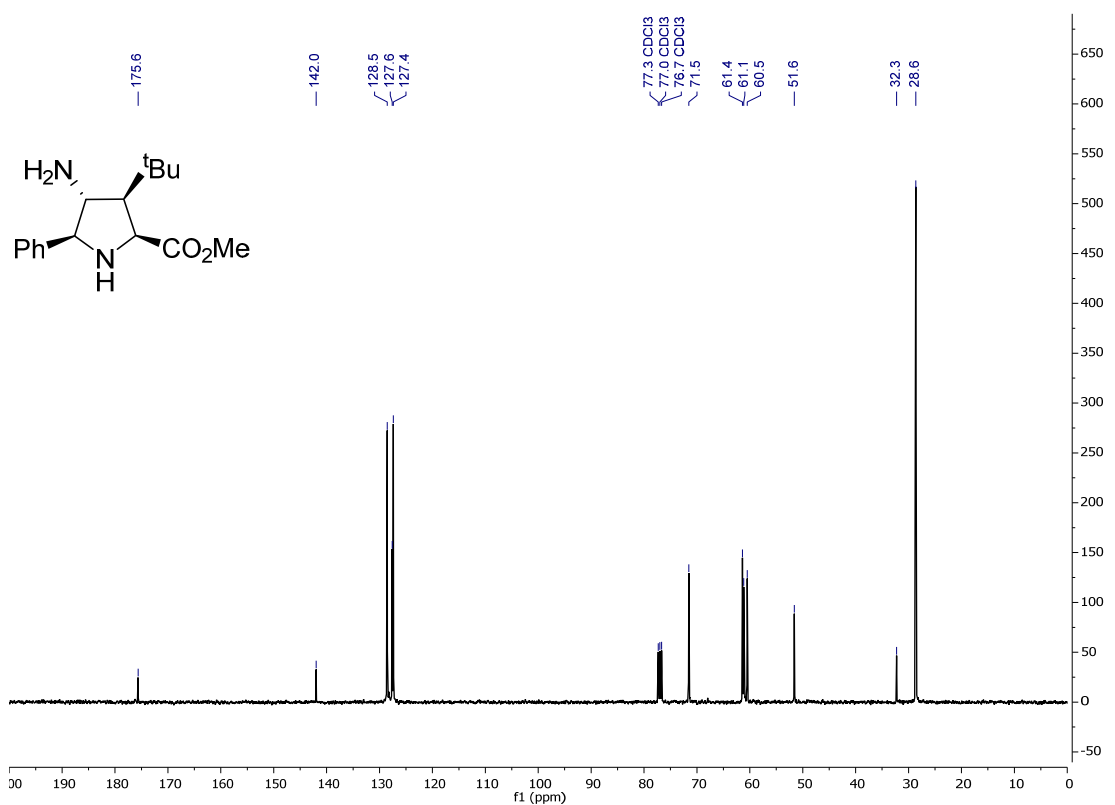


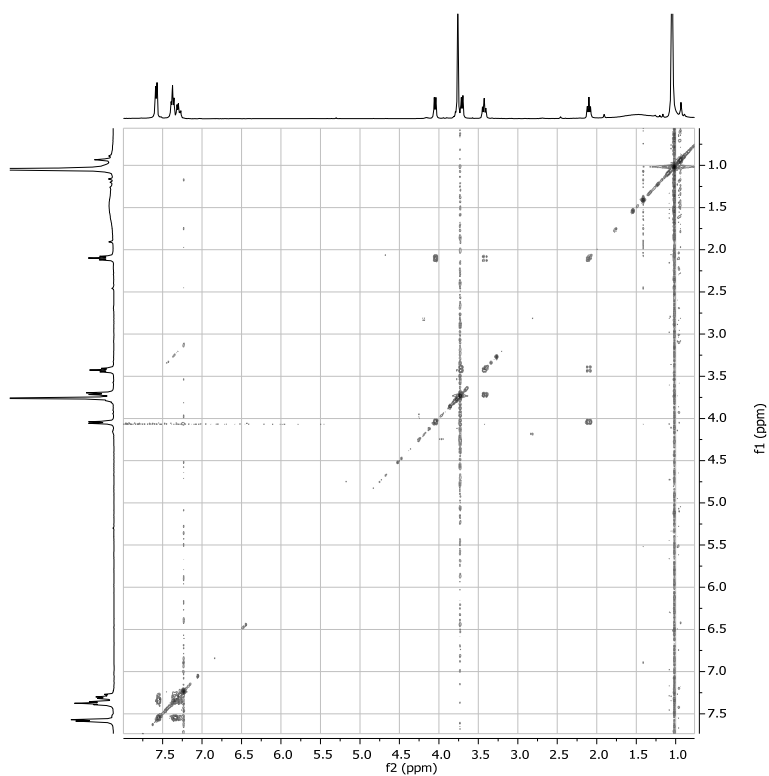
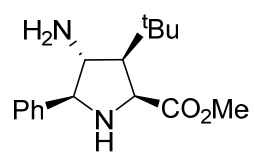
<sup>13</sup>C NMR (CDCl<sub>3</sub>)

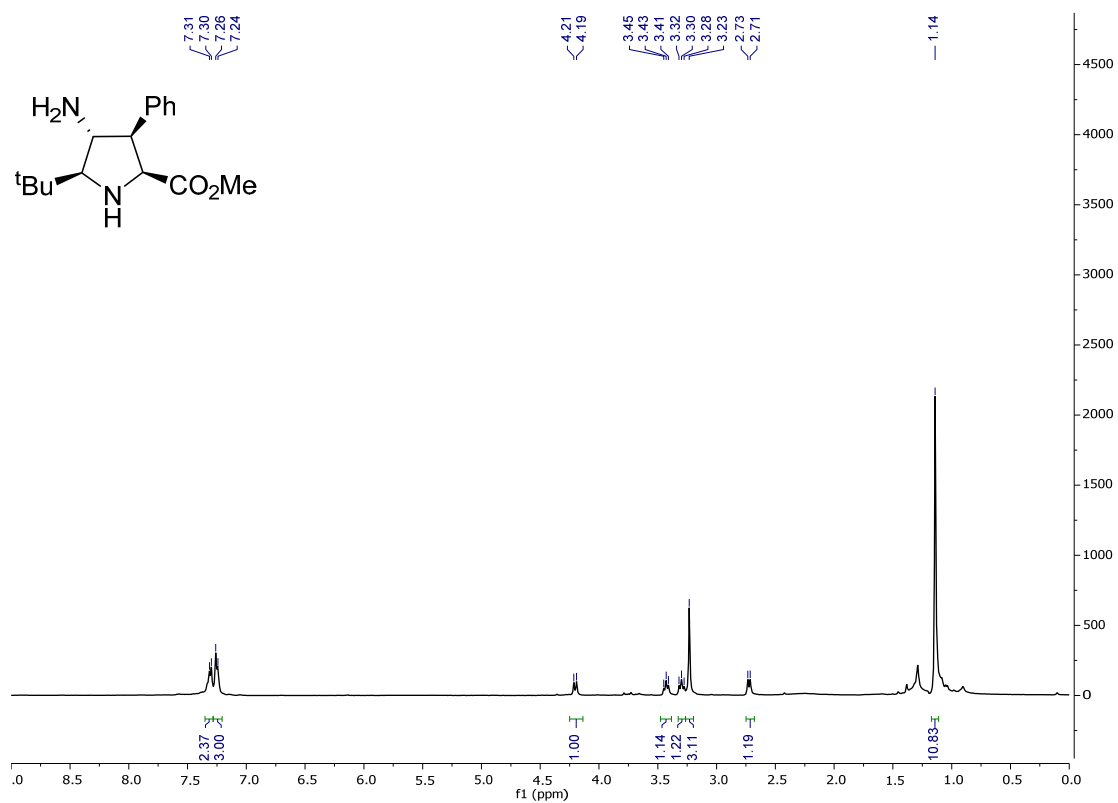
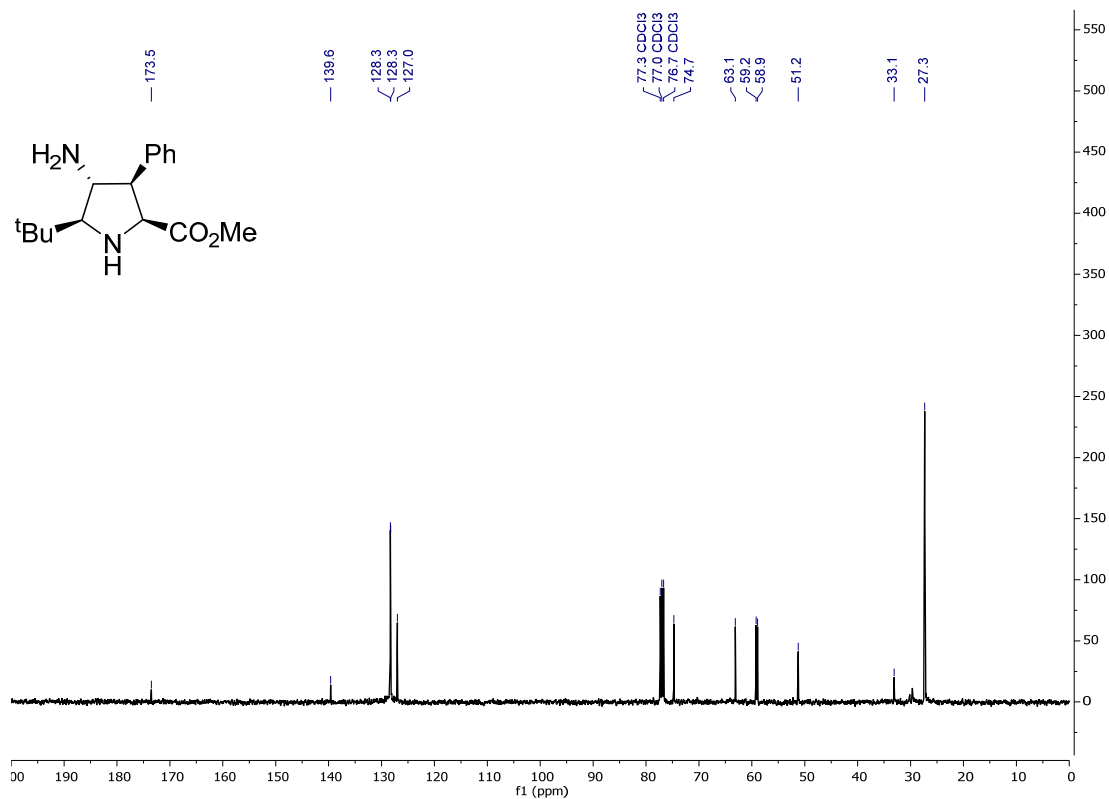


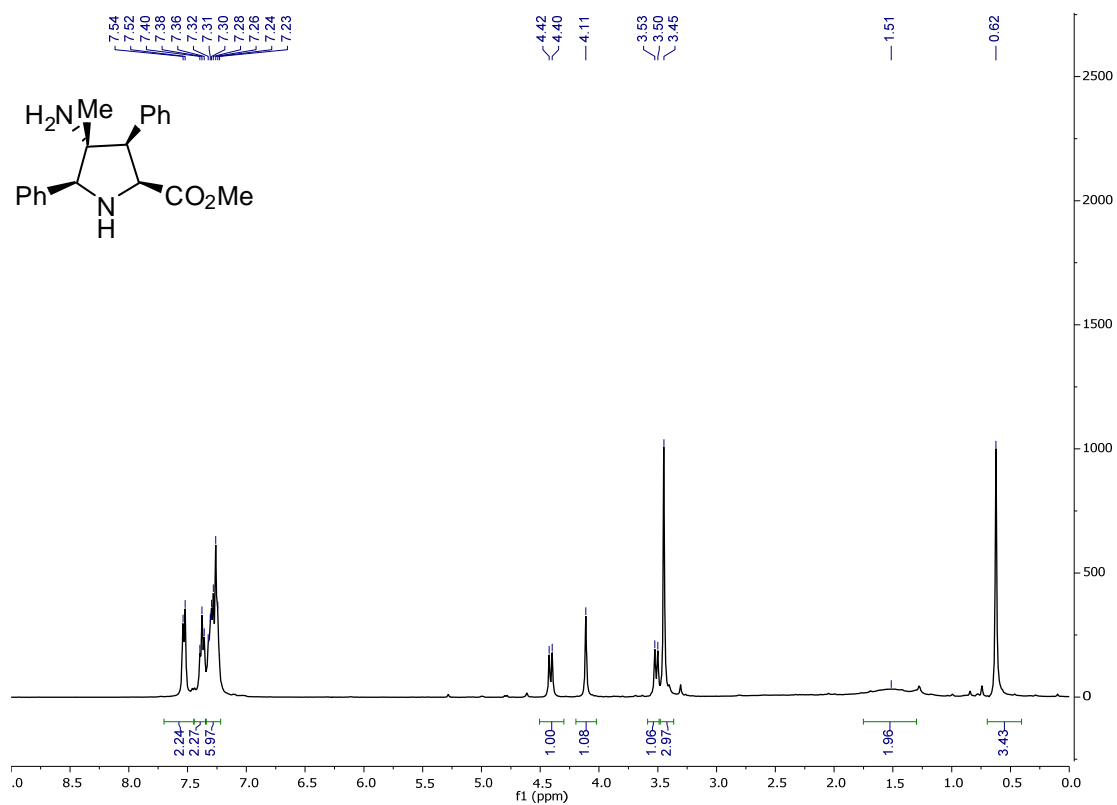
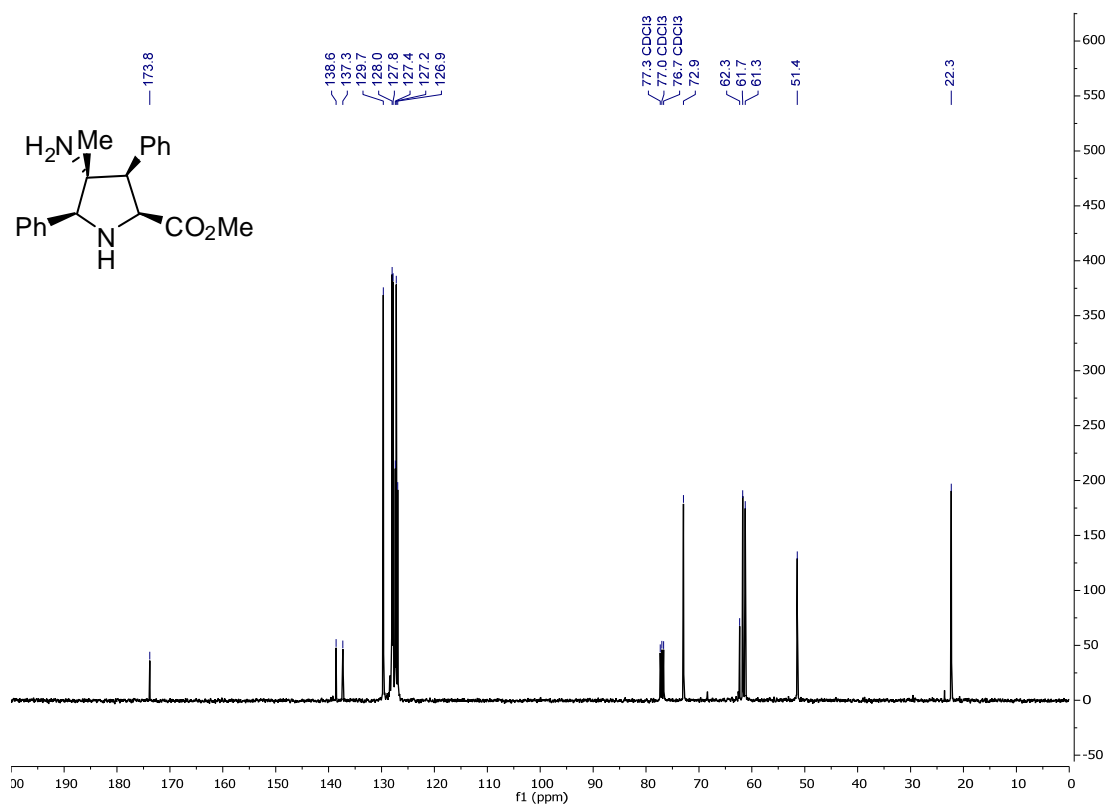
COSY (CDCl<sub>3</sub>)

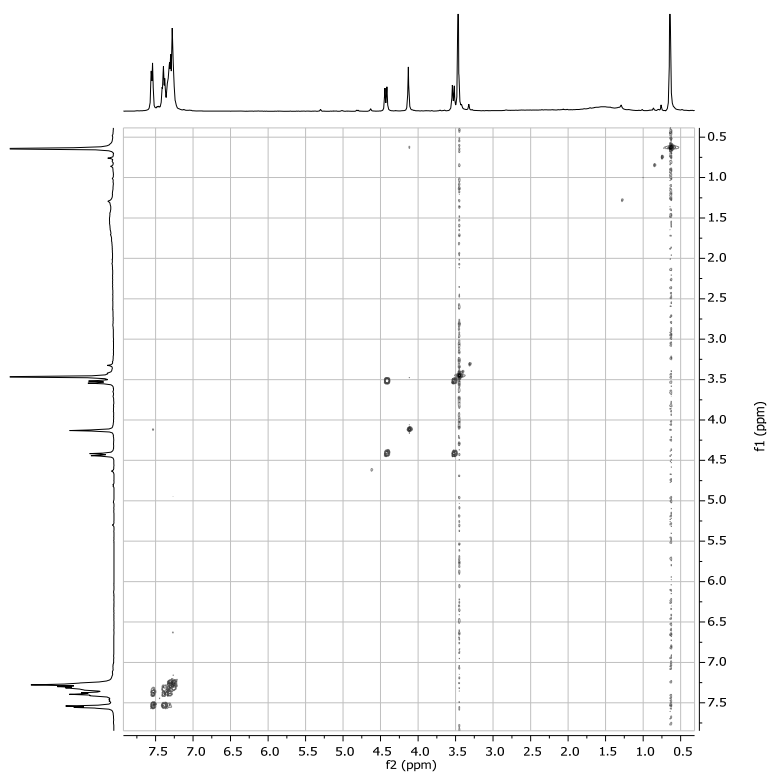
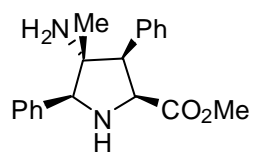


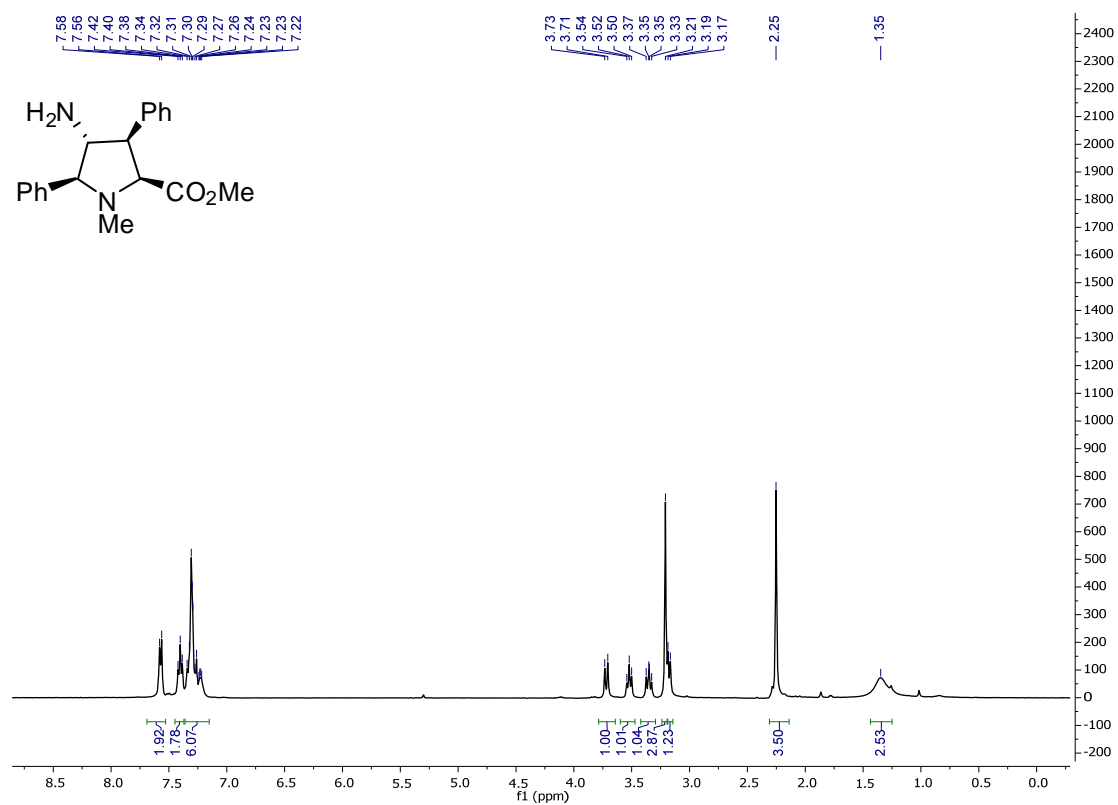
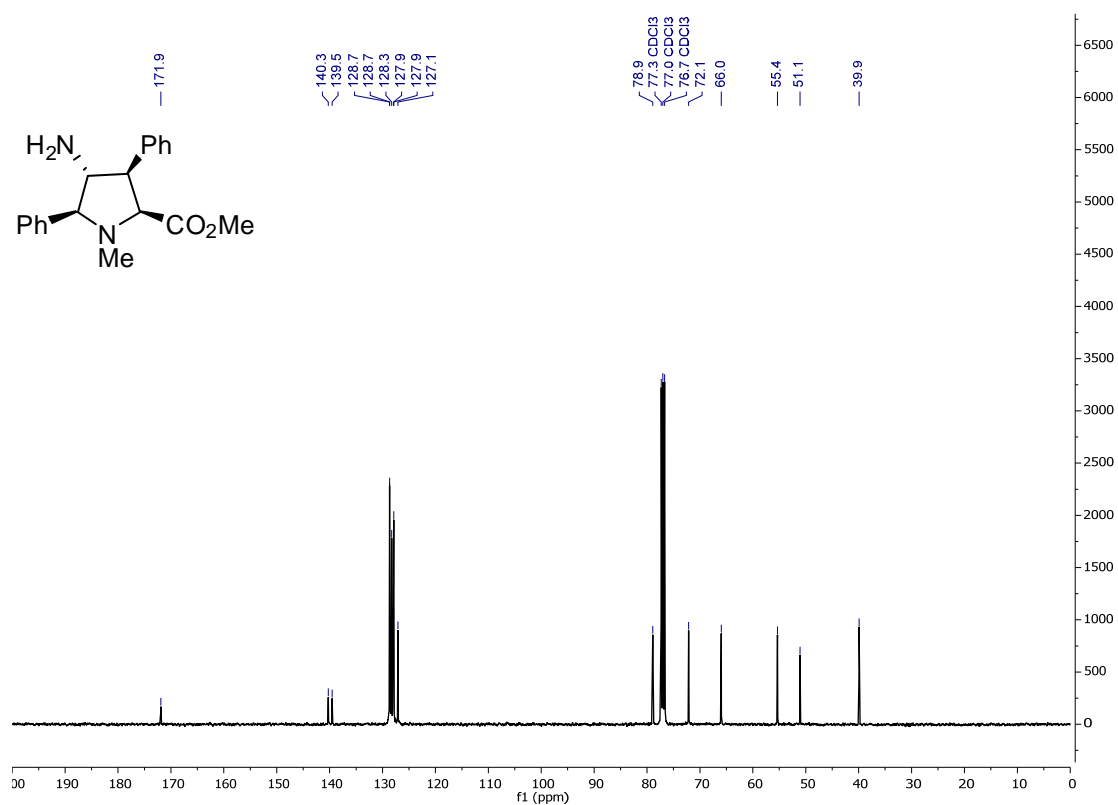
Compound NH<sub>2</sub>-X<sub>L</sub>-OMe-10aI<sup>1</sup>H NMR (CDCl<sub>3</sub>)<sup>13</sup>C NMR (CDCl<sub>3</sub>)

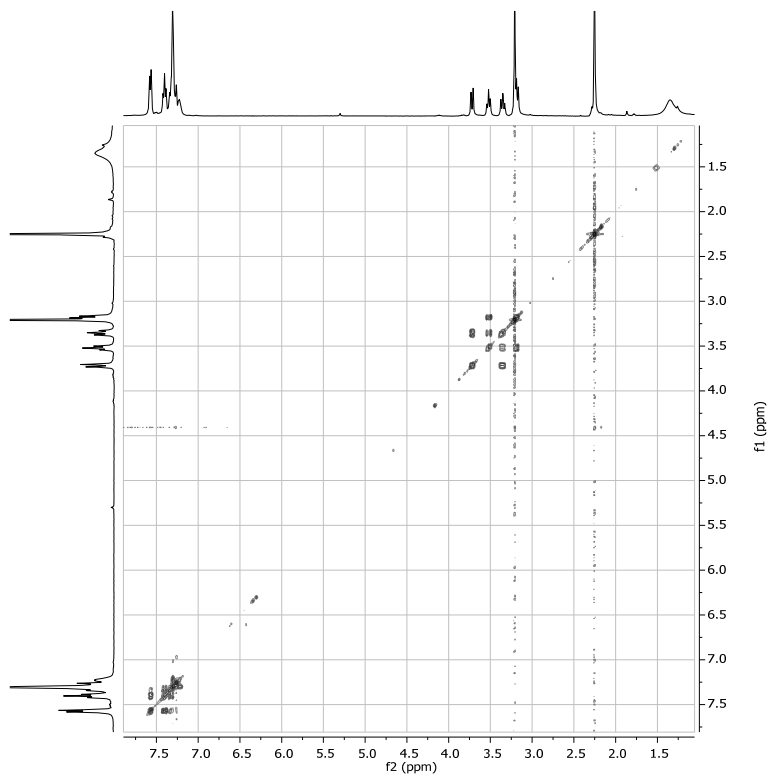
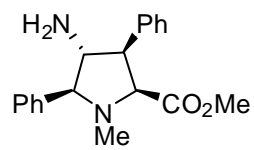
COSY (CDCl<sub>3</sub>)

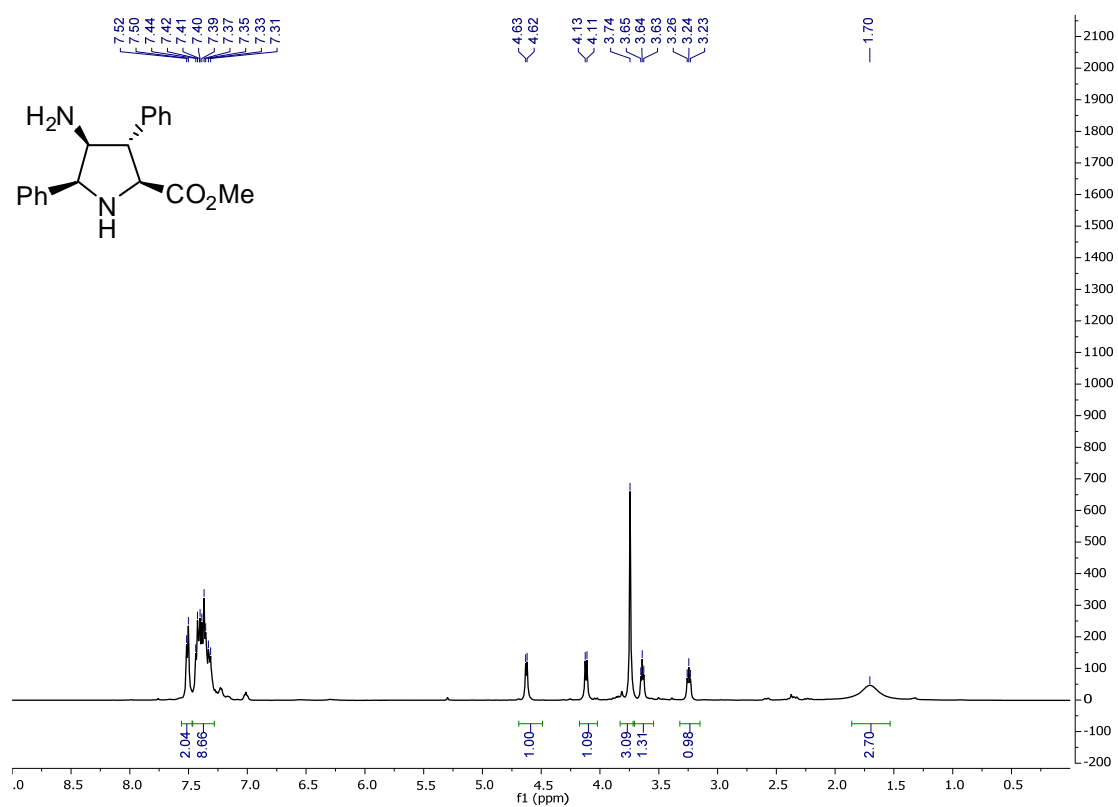
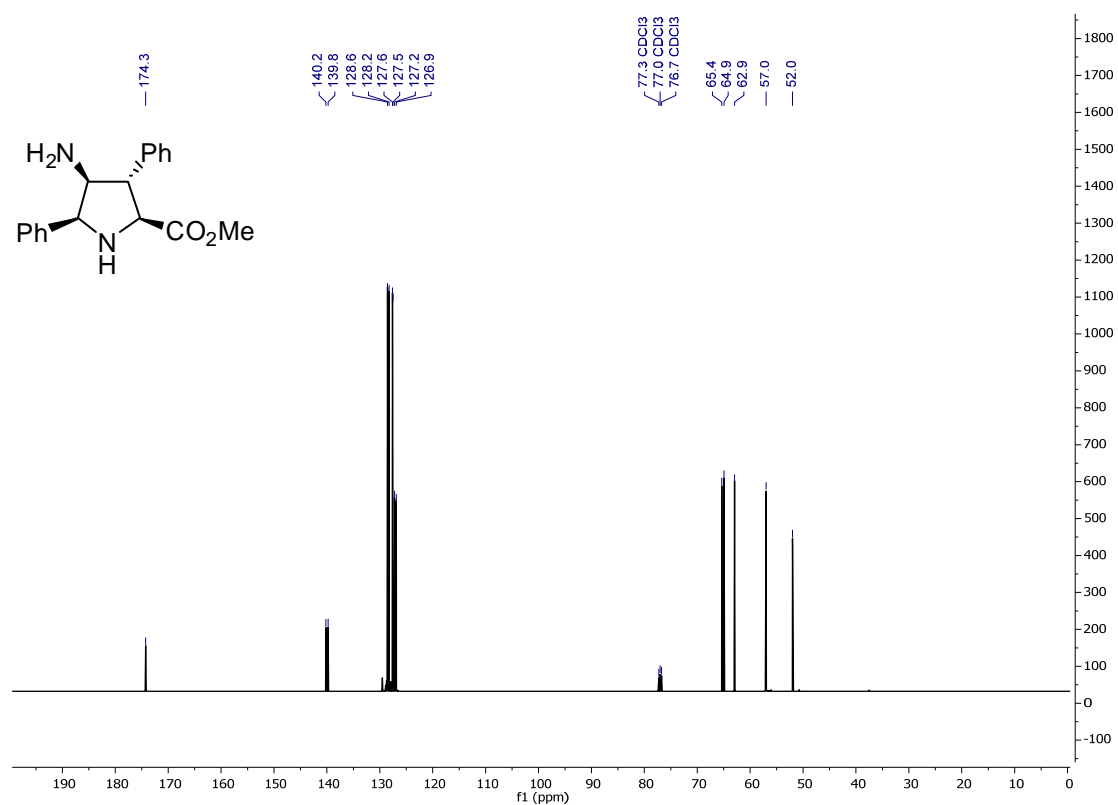
Compound NH<sub>2</sub>-X<sub>L</sub>-OMe-10la<sup>1</sup>H NMR (CDCl<sub>3</sub>)<sup>13</sup>C NMR (CDCl<sub>3</sub>)

Compound NH<sub>2</sub>-X<sub>L</sub>-OMe-10am<sup>1</sup>H NMR (CDCl<sub>3</sub>)<sup>13</sup>C NMR (CDCl<sub>3</sub>)

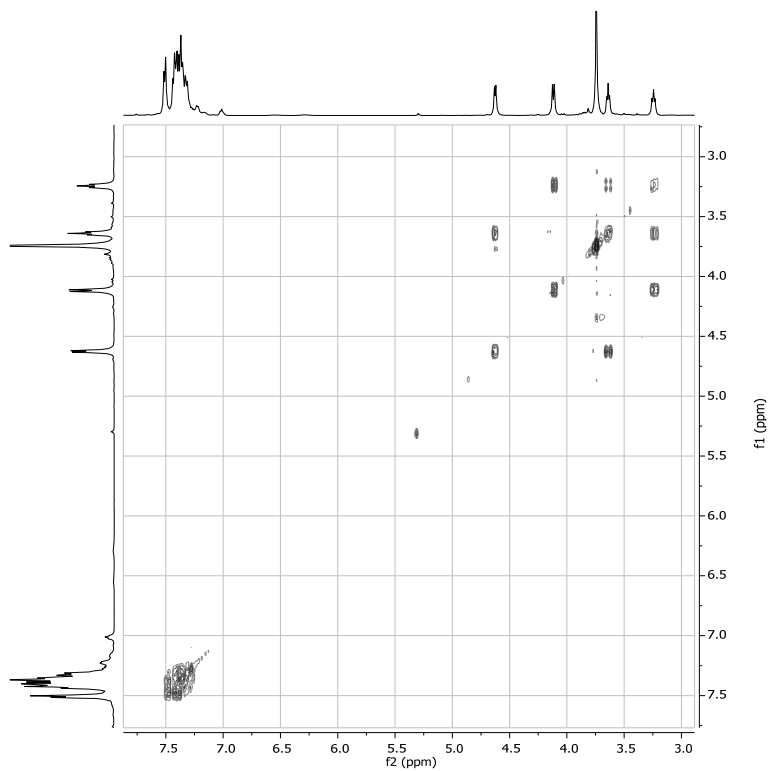
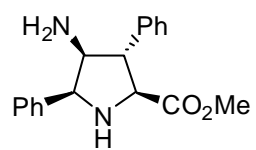
COSY (CDCl<sub>3</sub>)

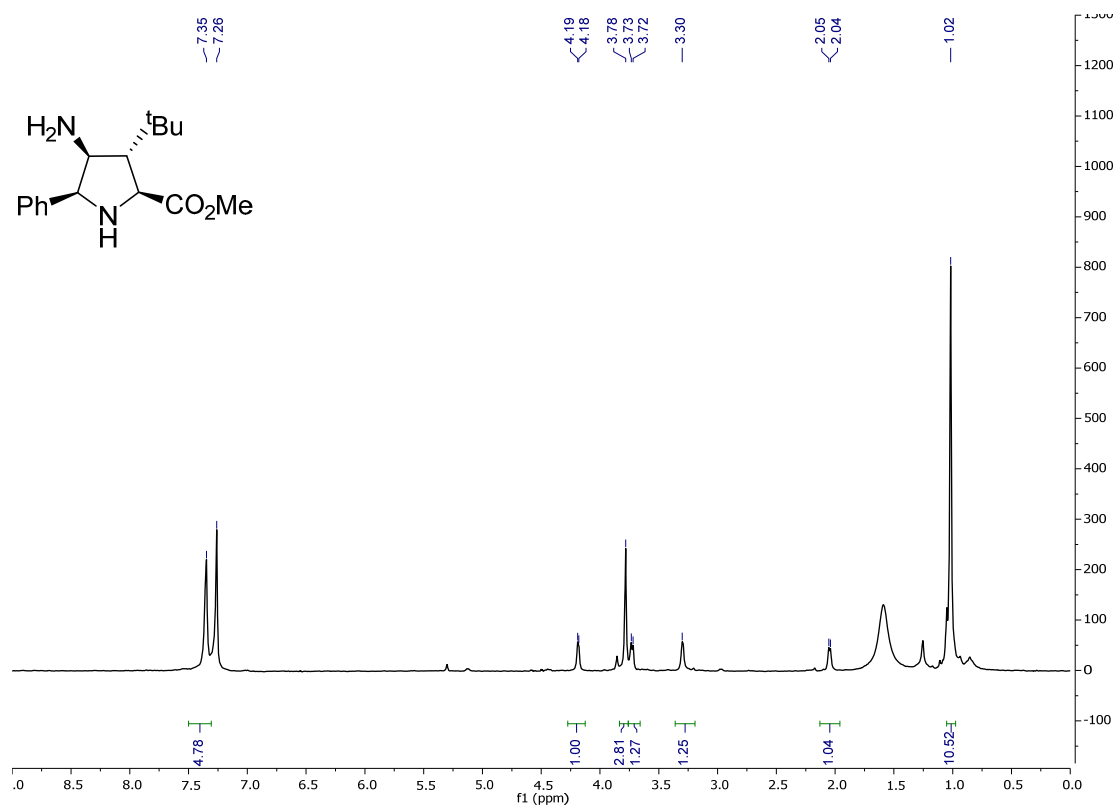
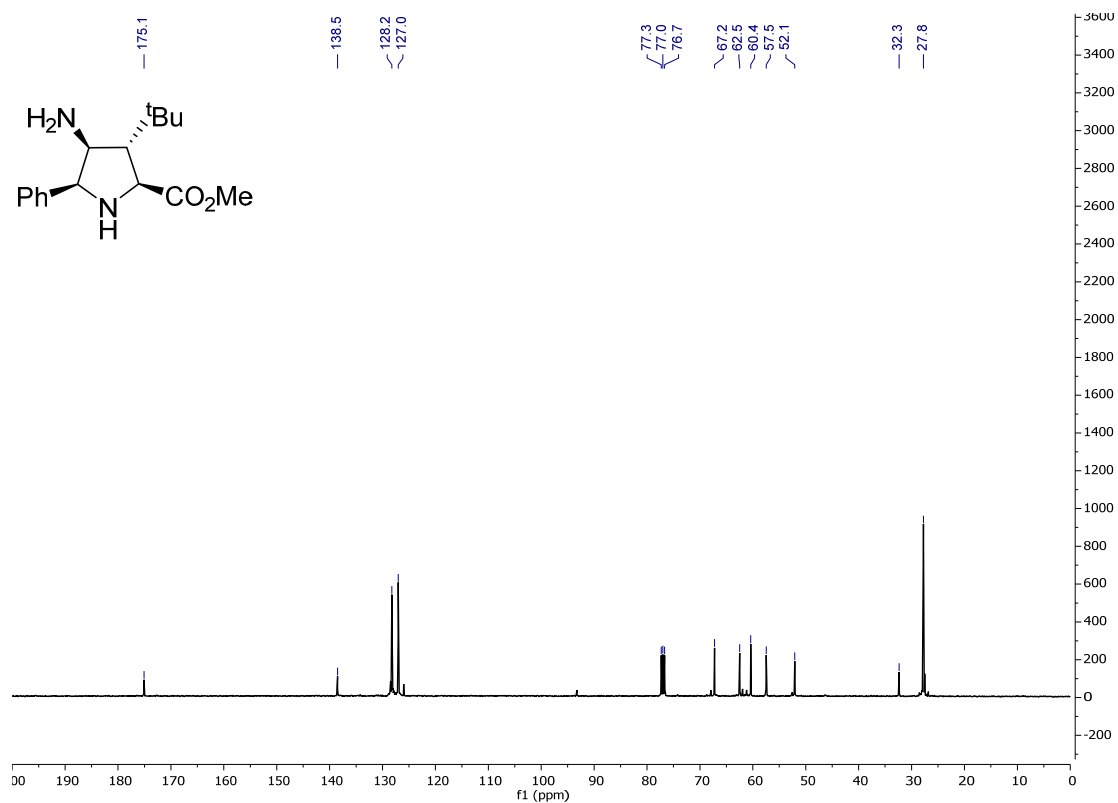
Compound NH<sub>2</sub>-X<sub>L</sub>-OMe-10c<sup>1</sup>H NMR (CDCl<sub>3</sub>)<sup>13</sup>C NMR (CDCl<sub>3</sub>)

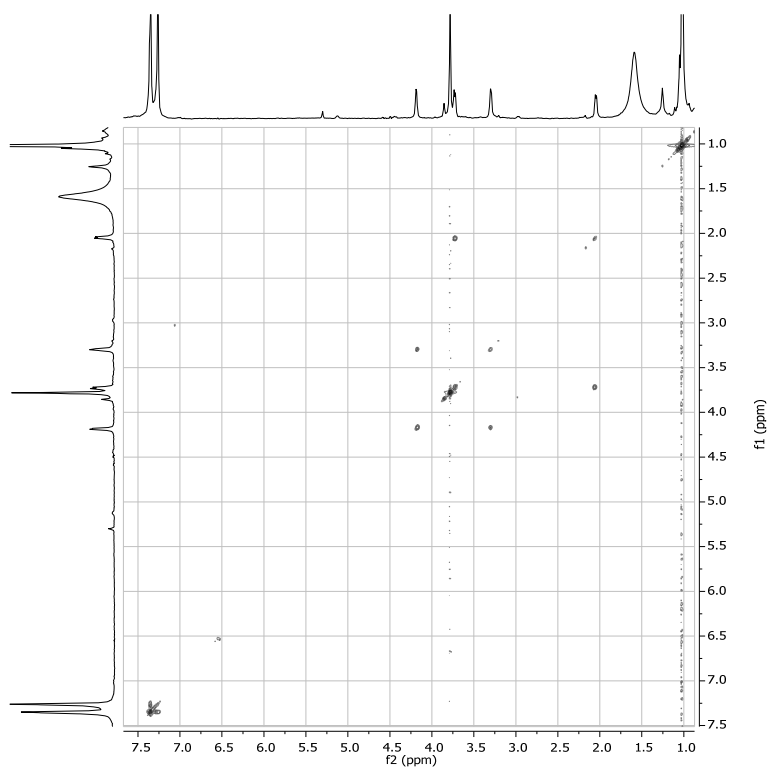
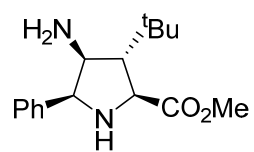
COSY (CDCl<sub>3</sub>)

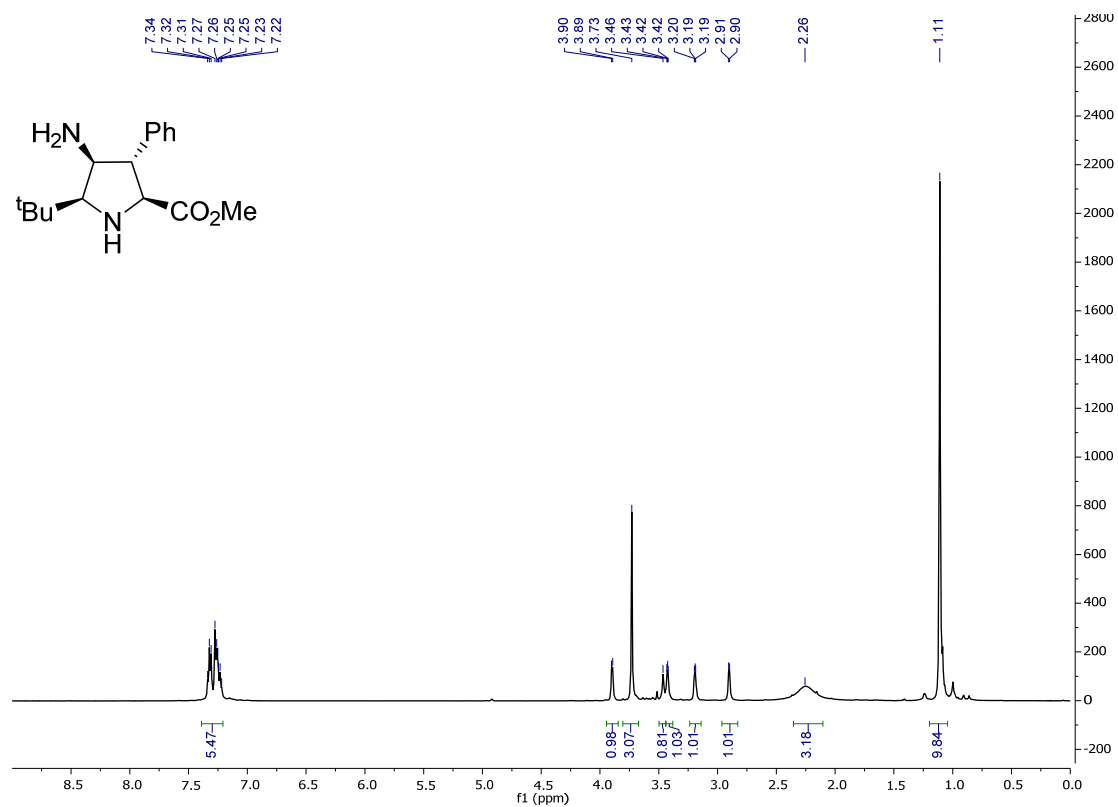
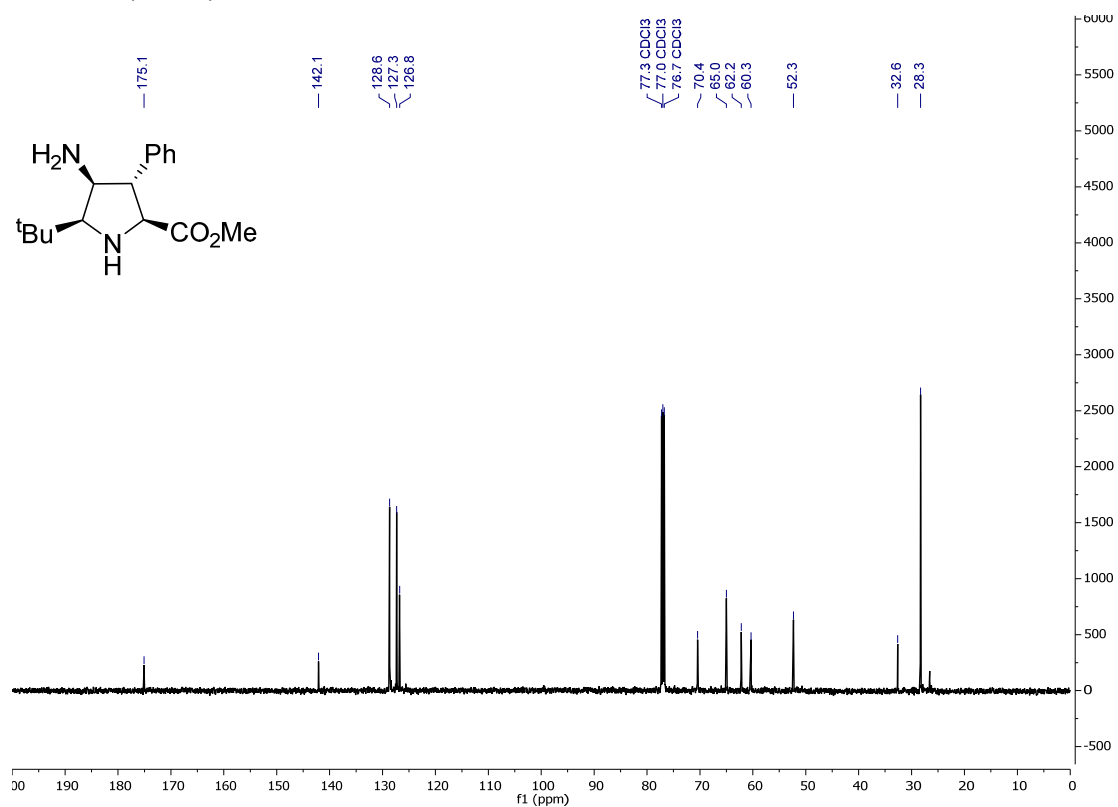
Compound NH<sub>2</sub>-N<sub>L</sub>-OMe-10aa<sup>1</sup>H NMR (CDCl<sub>3</sub>)<sup>13</sup>C NMR (CDCl<sub>3</sub>)

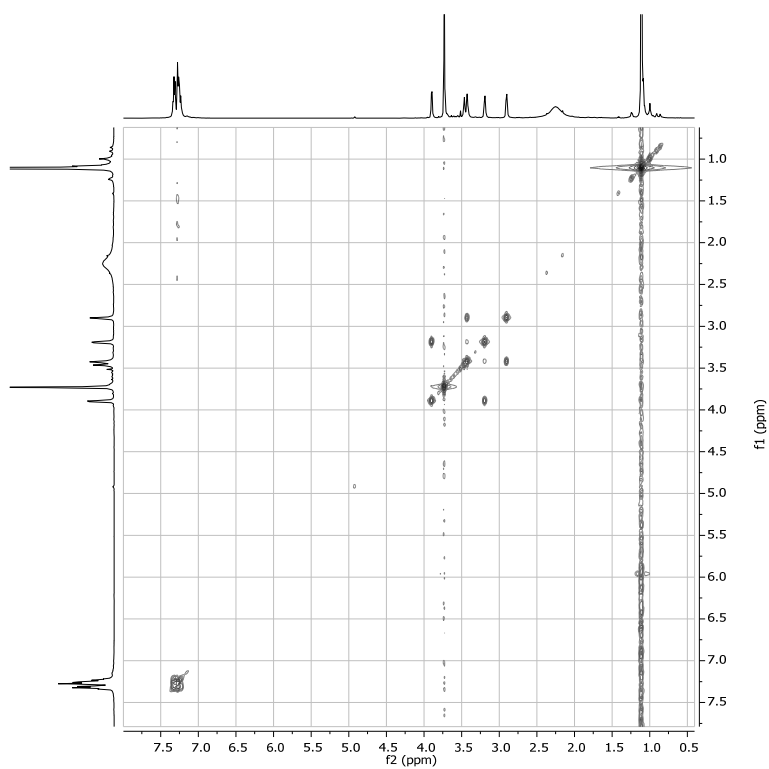
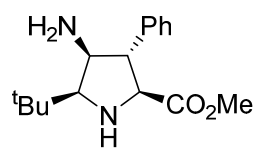


COSY (CDCl<sub>3</sub>)

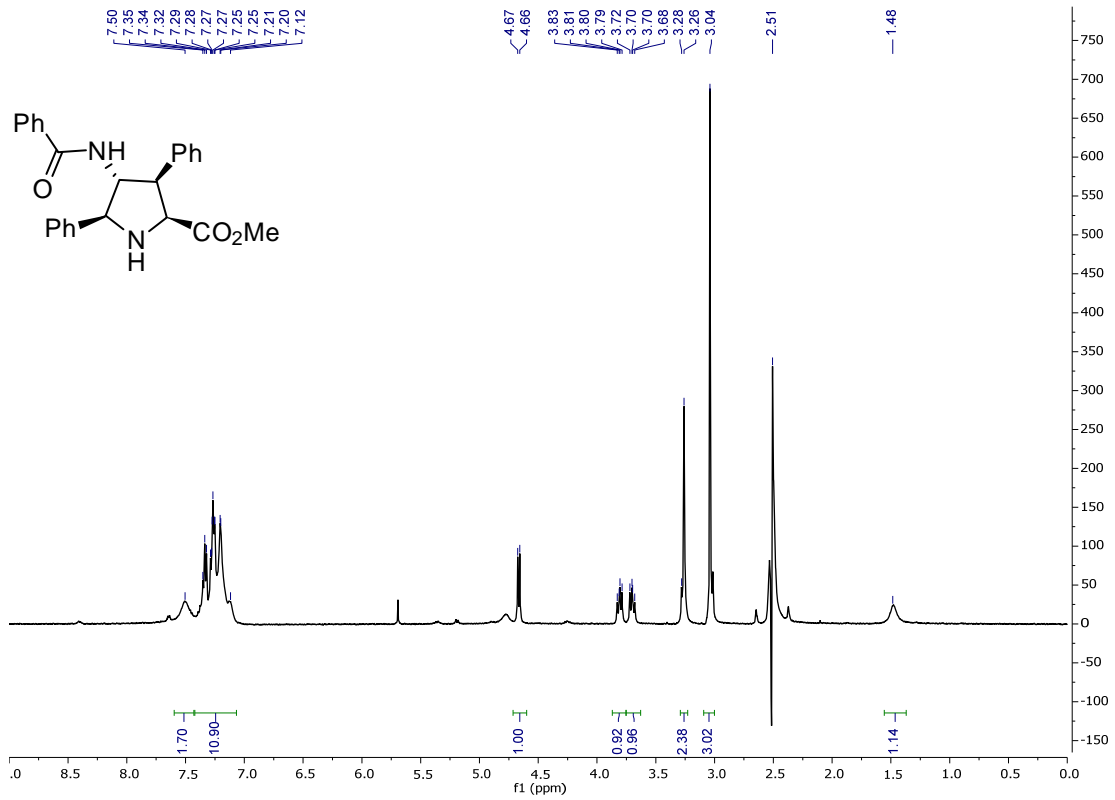
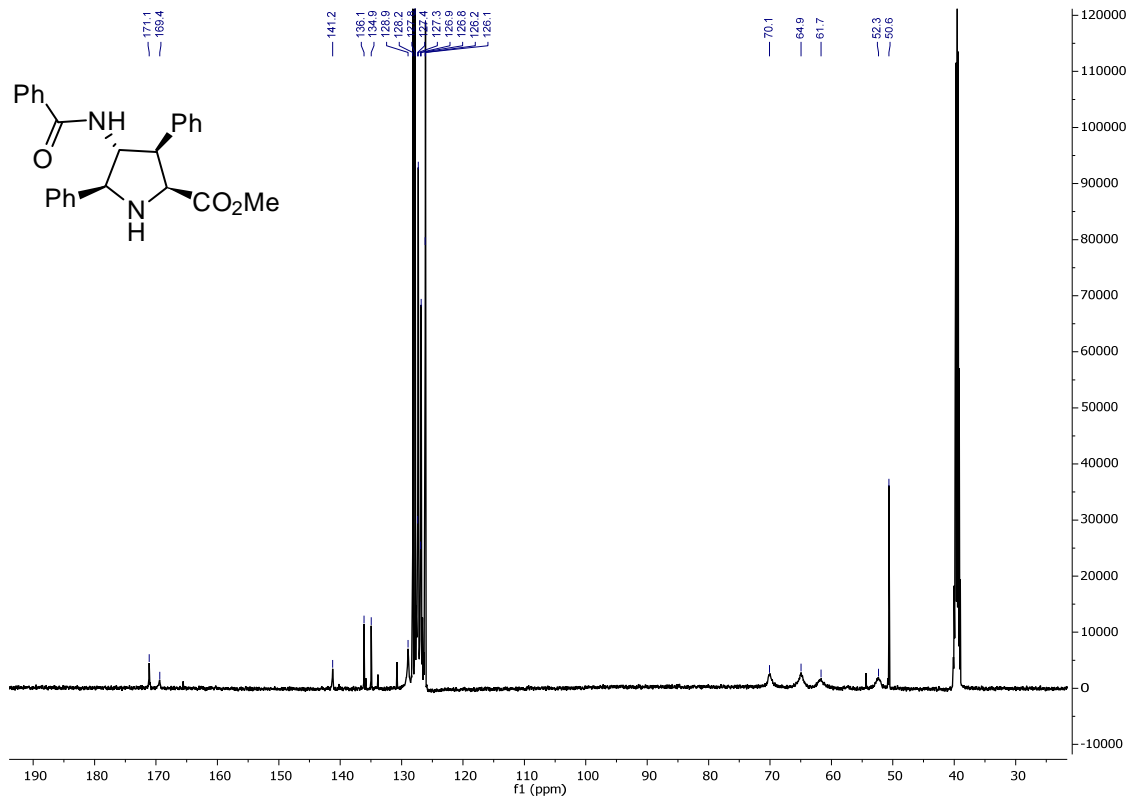
Compound NH<sub>2</sub>-N<sub>L</sub>-OMe-10aI<sup>1</sup>H NMR (CDCl<sub>3</sub>)<sup>13</sup>C NMR (CDCl<sub>3</sub>)

COSY (CDCl<sub>3</sub>)

Compound NH<sub>2</sub>-N<sub>L</sub>-OMe-10la<sup>1</sup>H NMR (CDCl<sub>3</sub>)<sup>13</sup>C NMR (CDCl<sub>3</sub>)

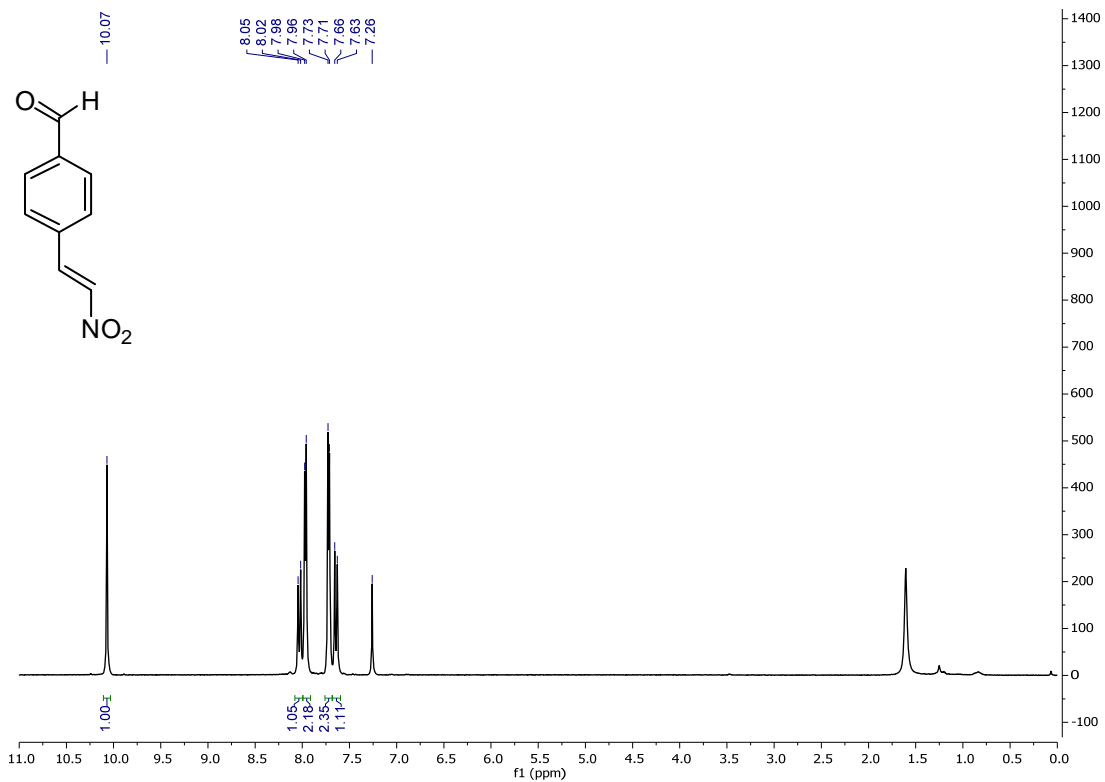
COSY (CDCl<sub>3</sub>)

## Compound 17

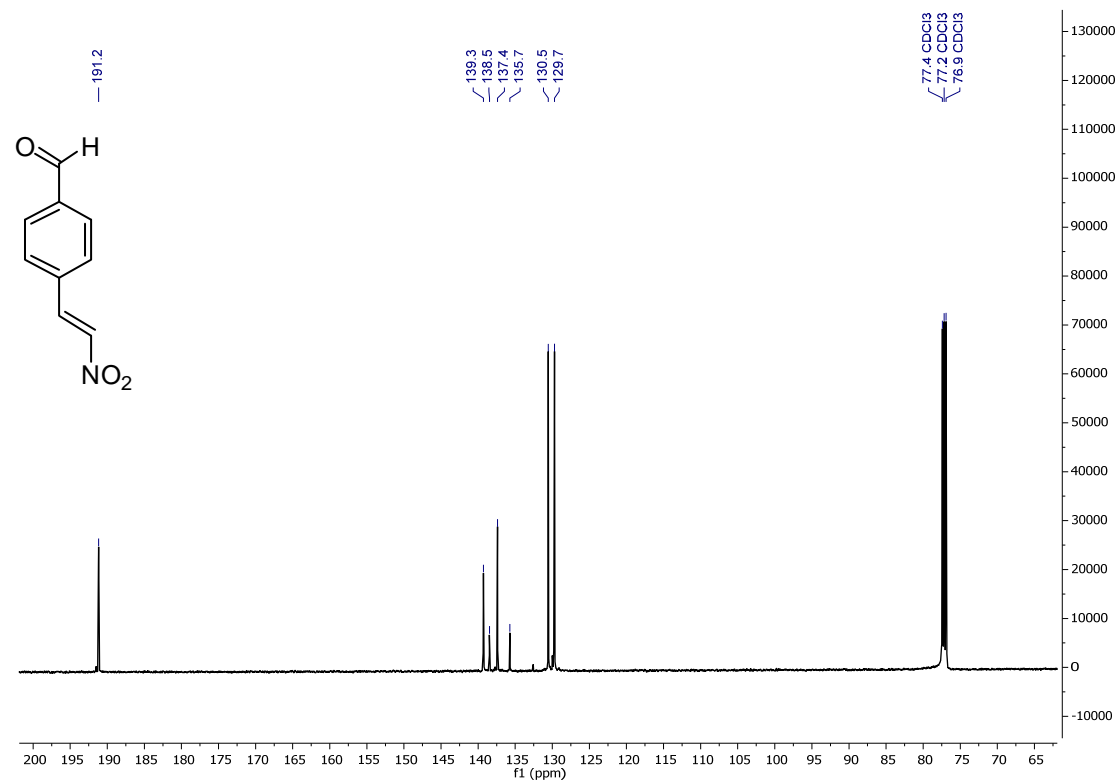
 $^1\text{H}$  NMR (DMSO- $d_6$ , 70°C) $^{13}\text{C}$  NMR (DMSO- $d_6$ , 70°C)

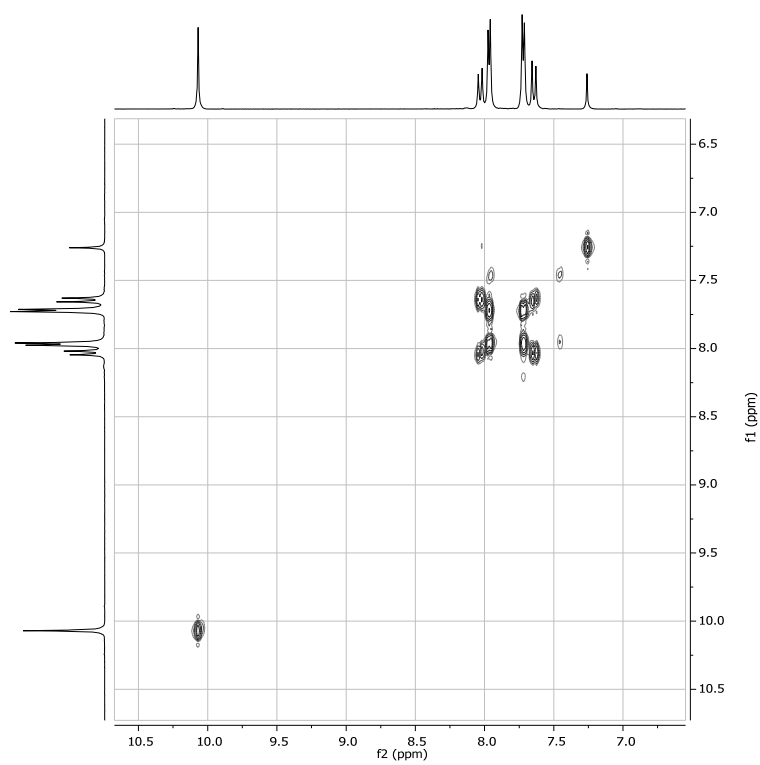
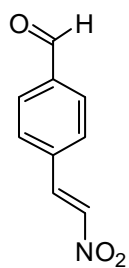
Compound **12b**

$^1\text{H}$  NMR ( $\text{CDCl}_3$ )



$^{13}\text{C}$  NMR ( $\text{CDCl}_3$ )

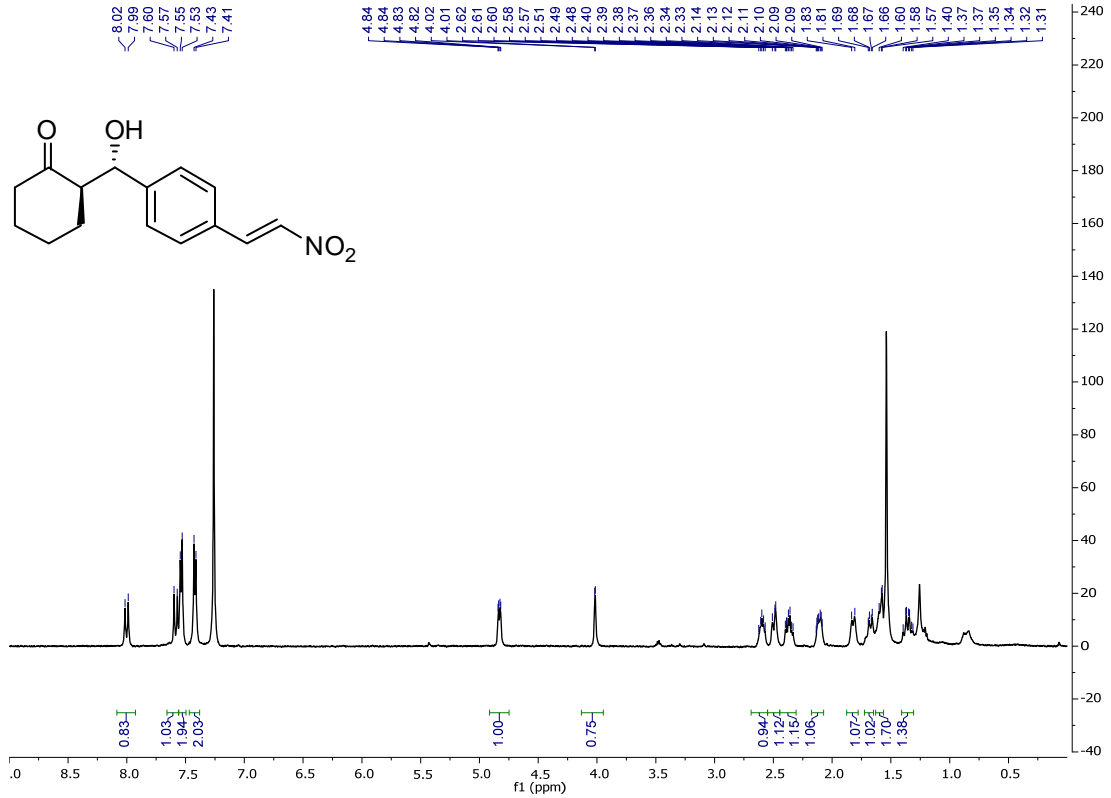


COSY (CDCl<sub>3</sub>)

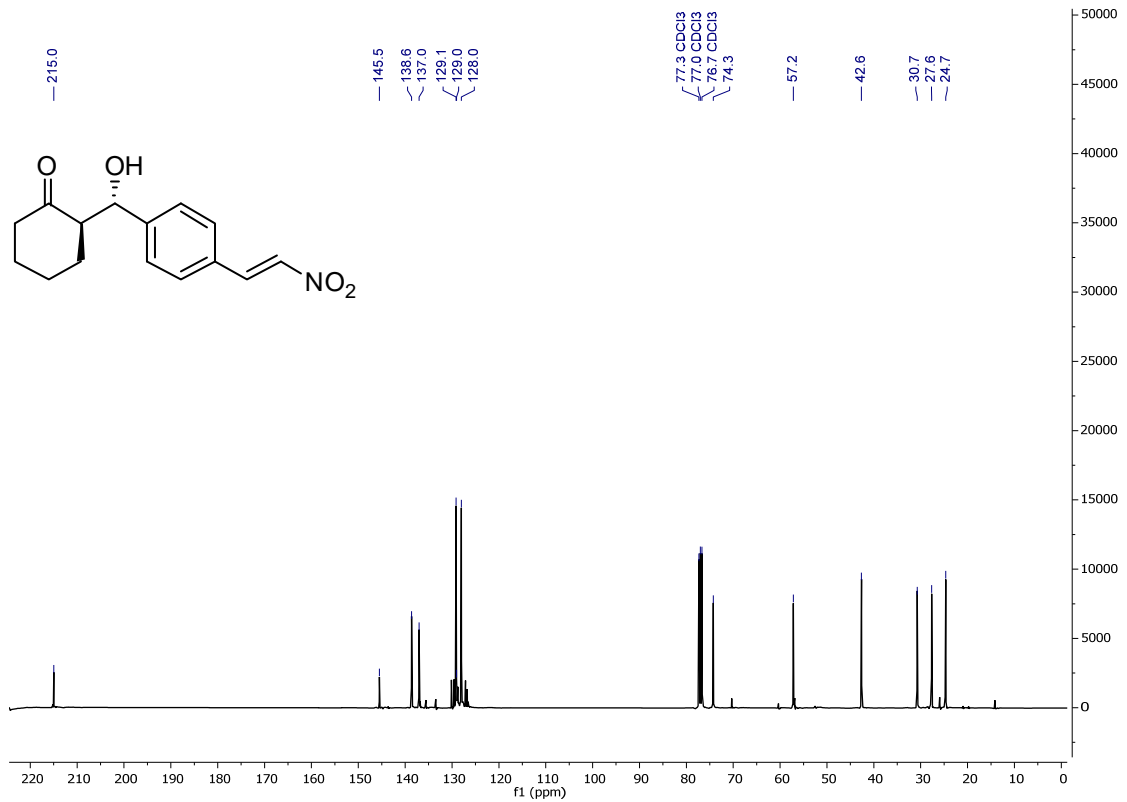


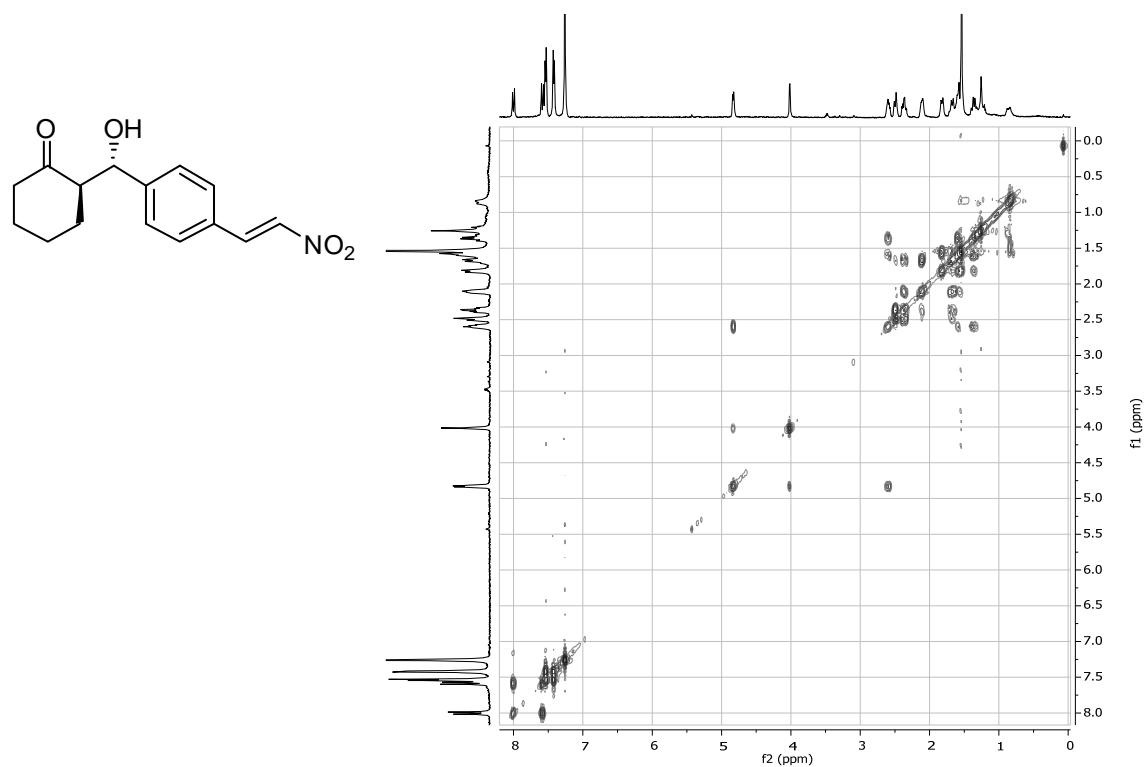
Compound **13ab**

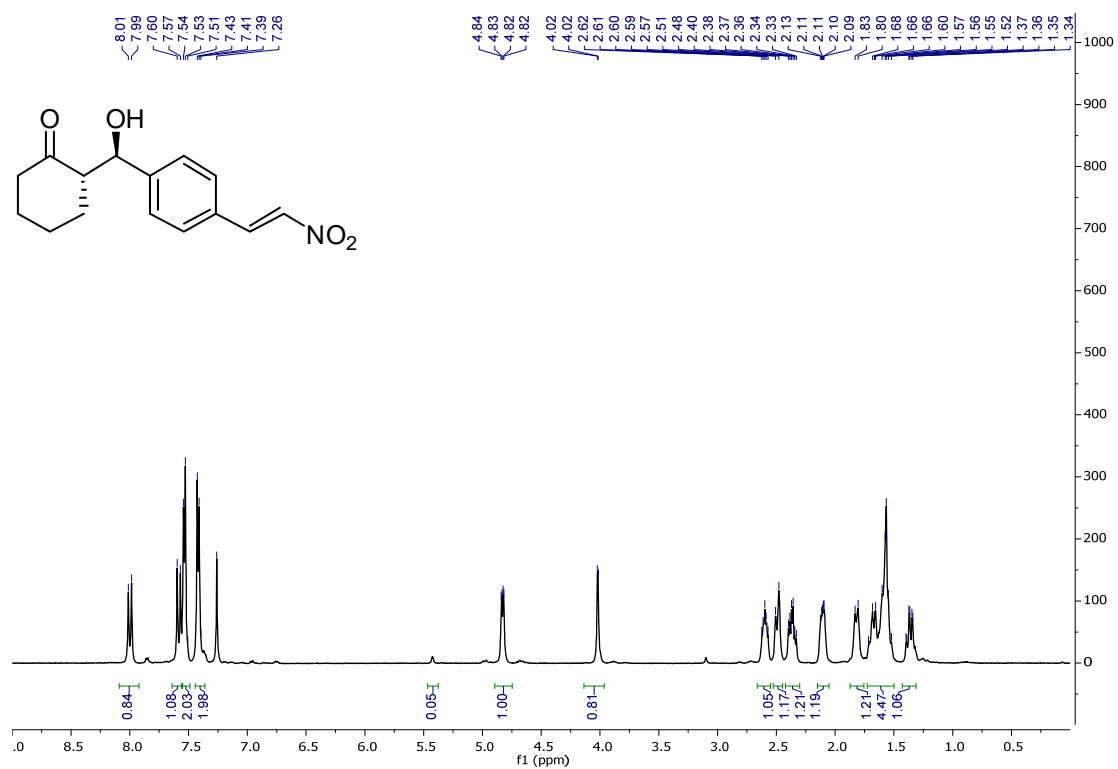
$^1\text{H}$  NMR ( $\text{CDCl}_3$ )

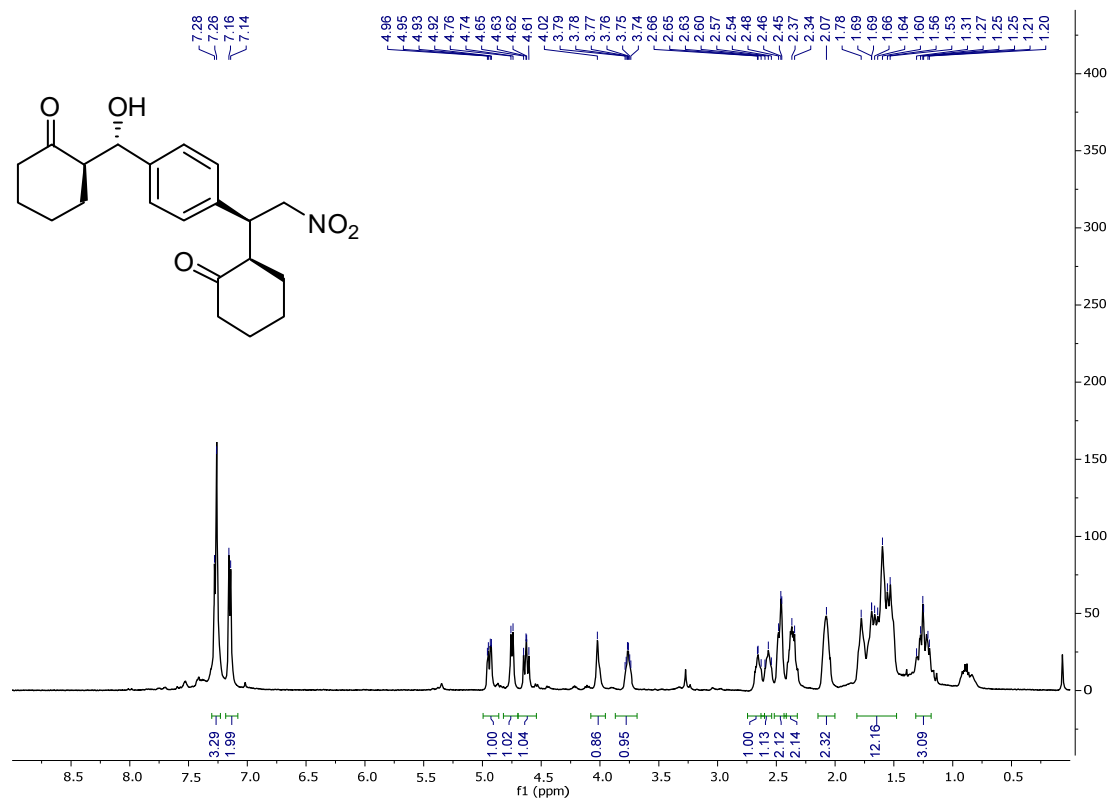
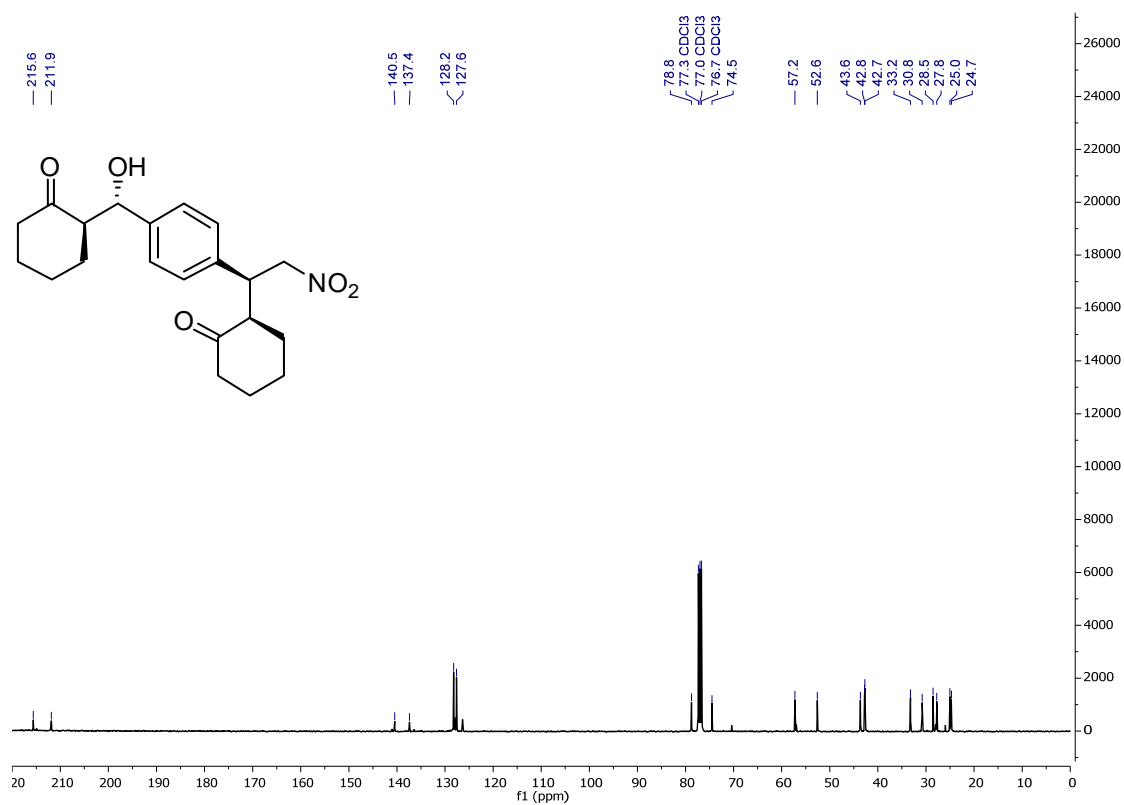


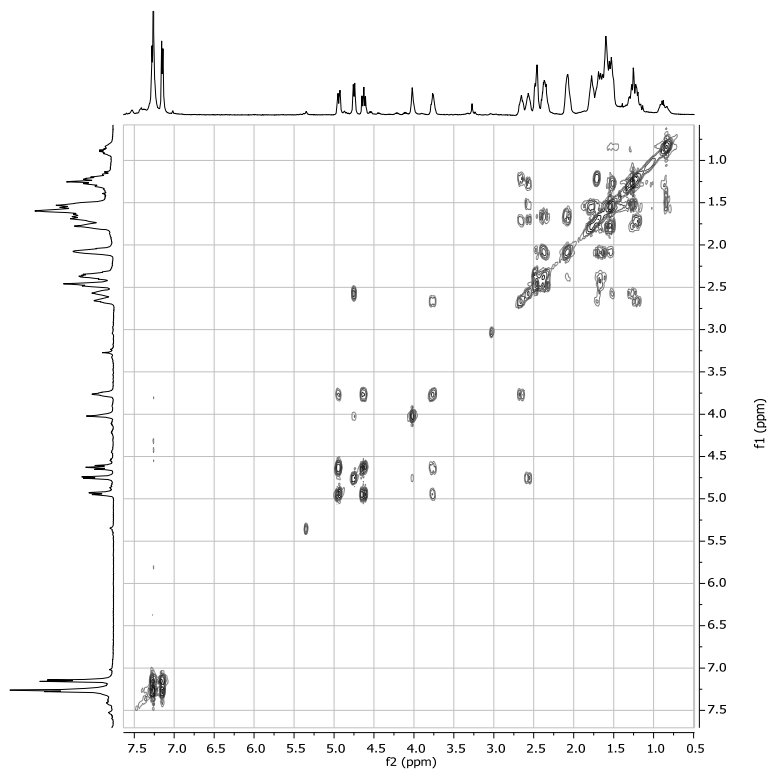
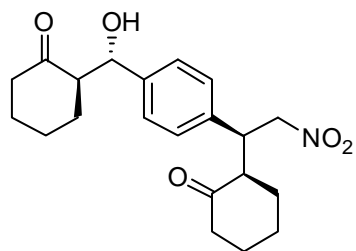
$^{13}\text{C}$  NMR ( $\text{CDCl}_3$ )

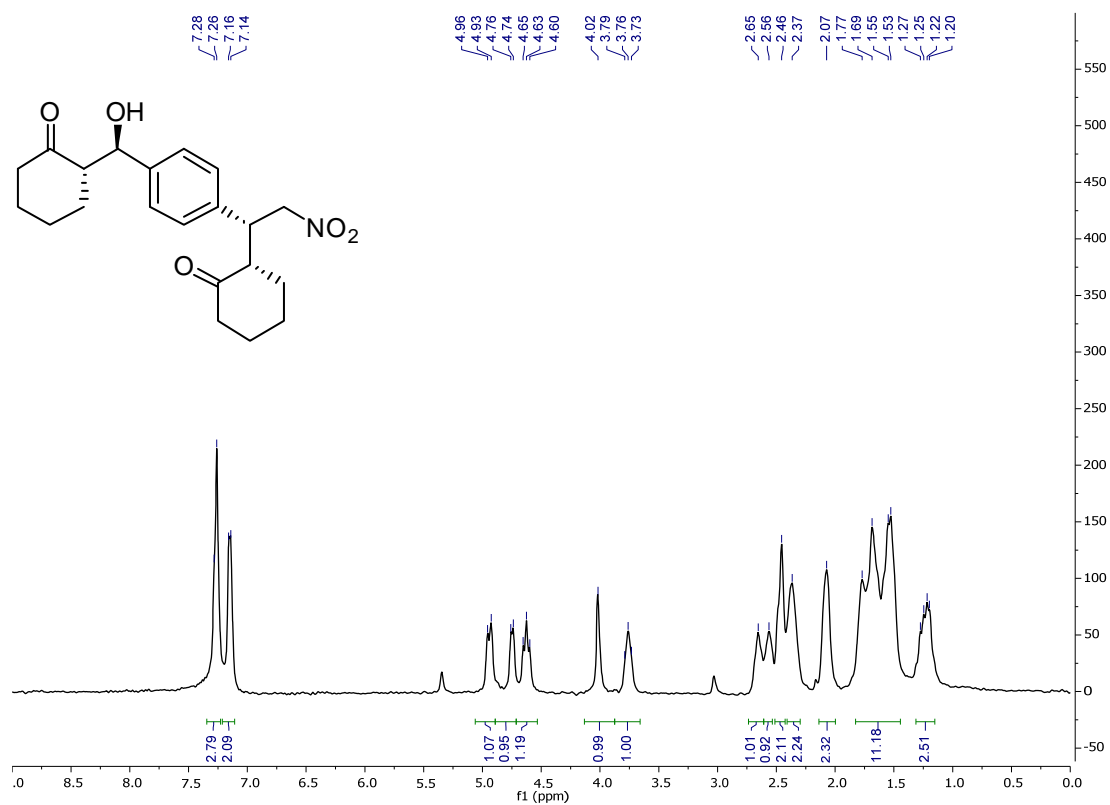


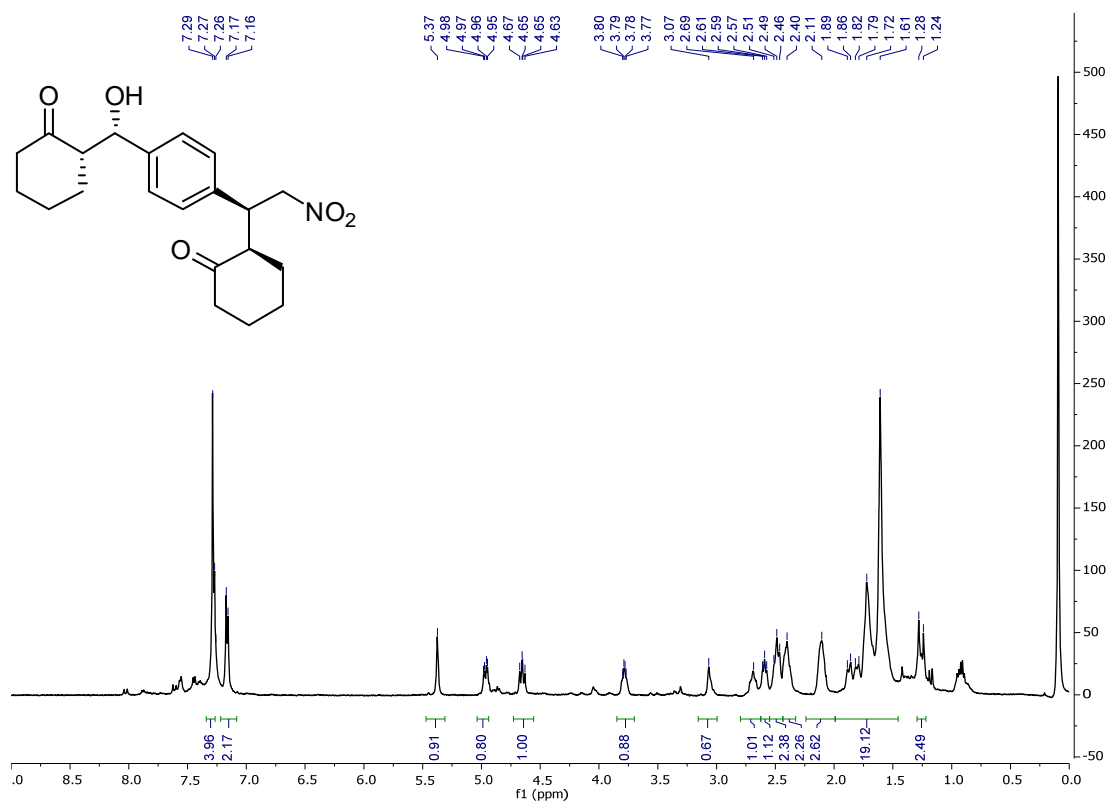
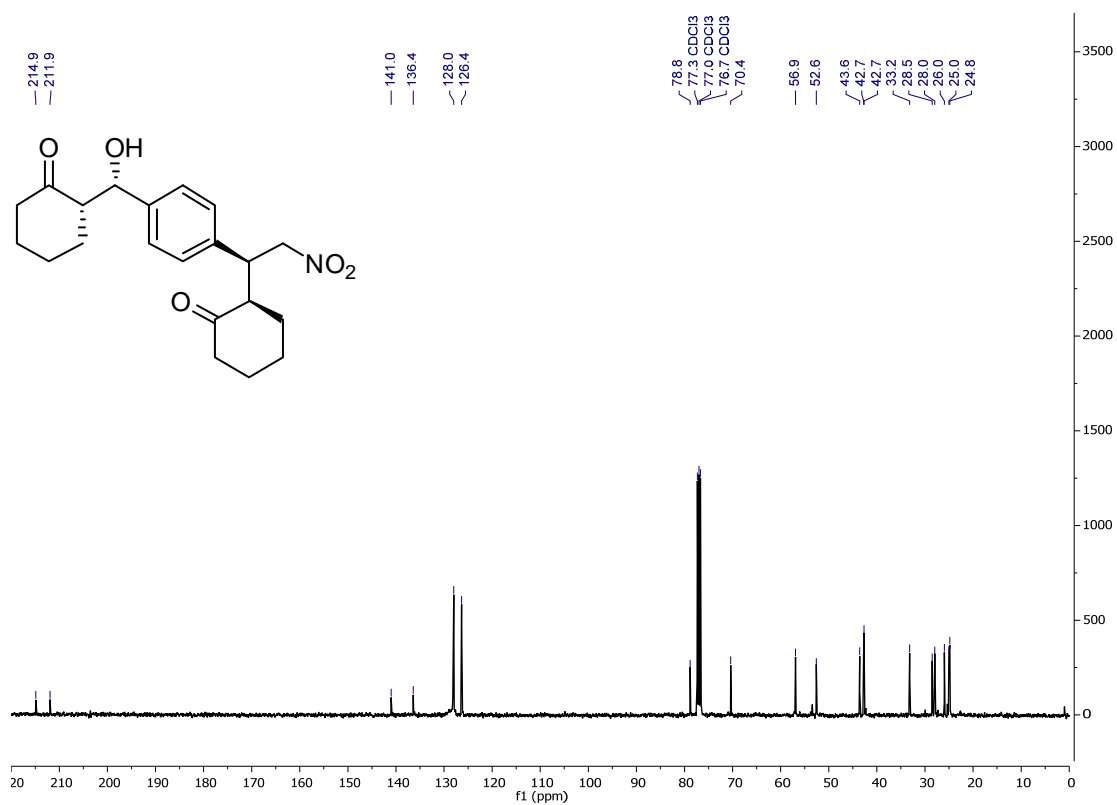
COSY (CDCl<sub>3</sub>)

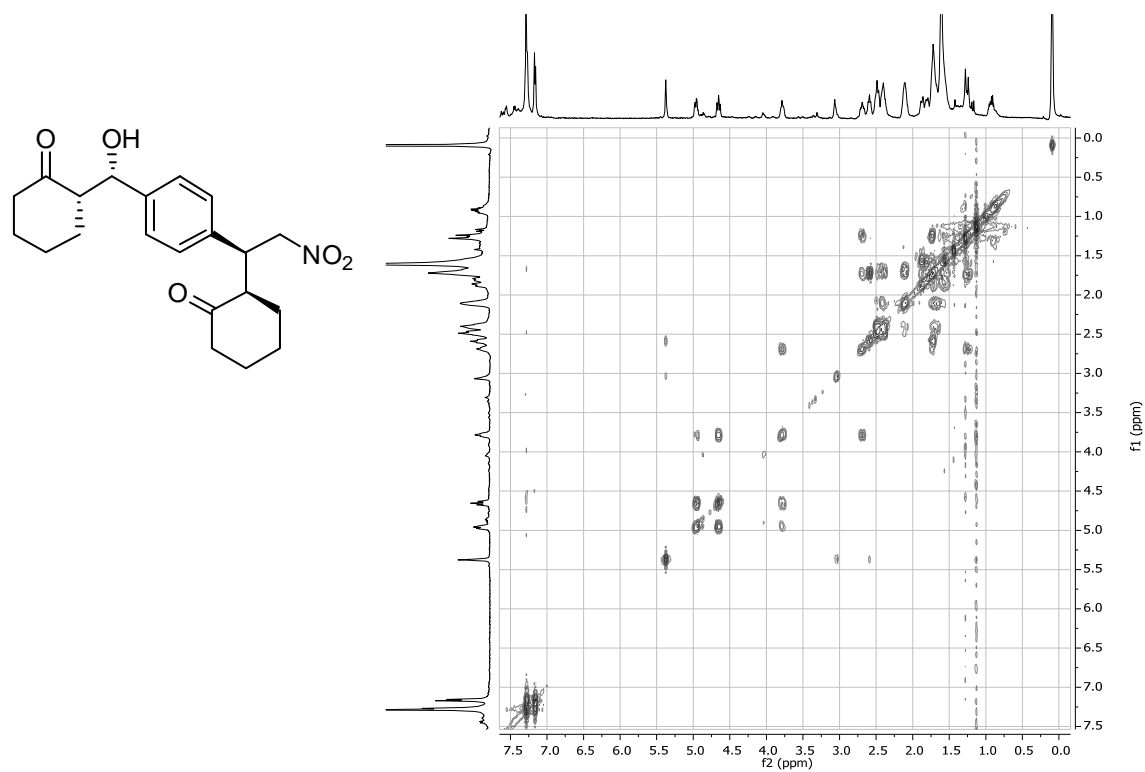
Compound *ent*-13ab $^1\text{H}$  NMR ( $\text{CDCl}_3$ )

Compound *anti*-21 $^1\text{H}$  NMR ( $\text{CDCl}_3$ ) $^{13}\text{C}$  NMR ( $\text{CDCl}_3$ )

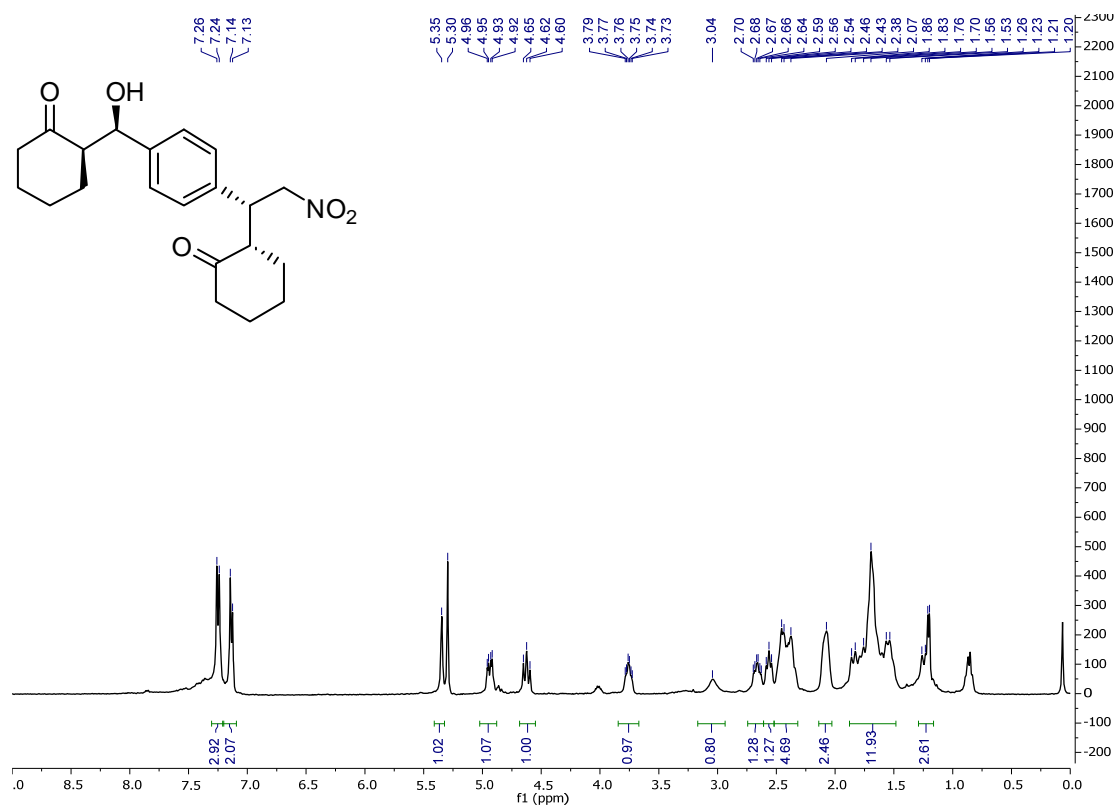
COSY (CDCl<sub>3</sub>)

Compound *ent-anti*-21 $^1\text{H}$  NMR ( $\text{CDCl}_3$ )

Compound *syn-21* $^1\text{H}$  NMR ( $\text{CDCl}_3$ ) $^{13}\text{C}$  NMR ( $\text{CDCl}_3$ )

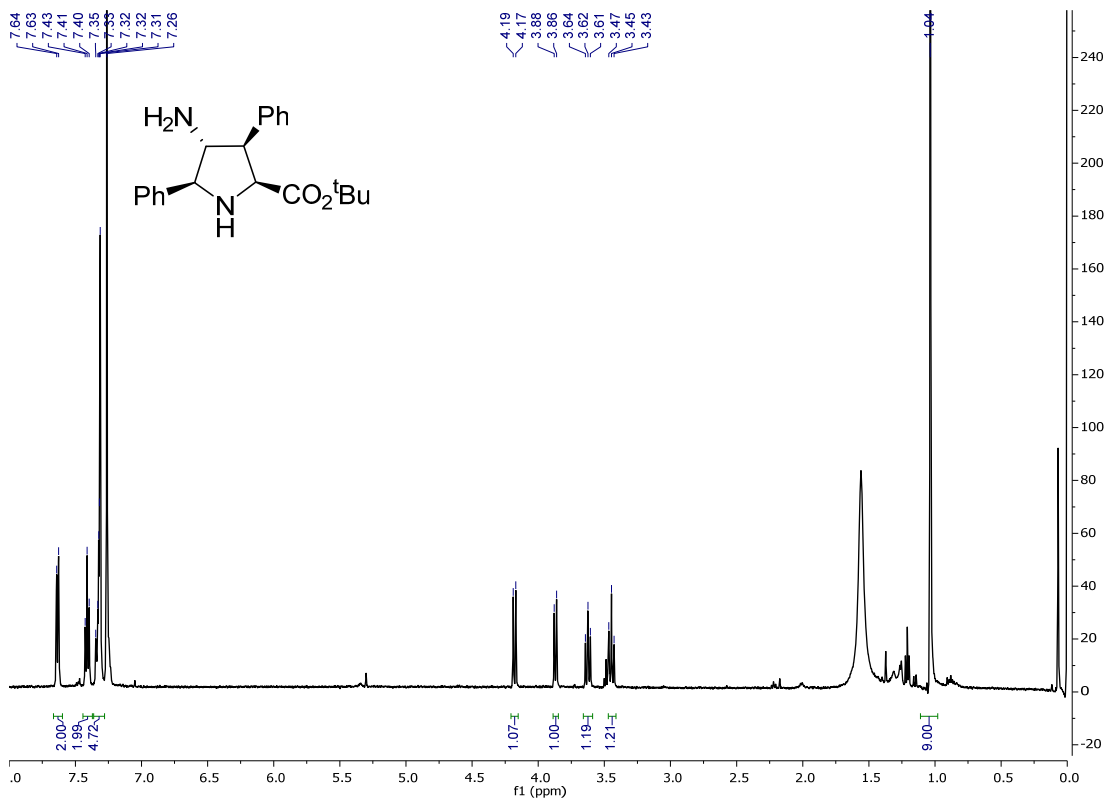
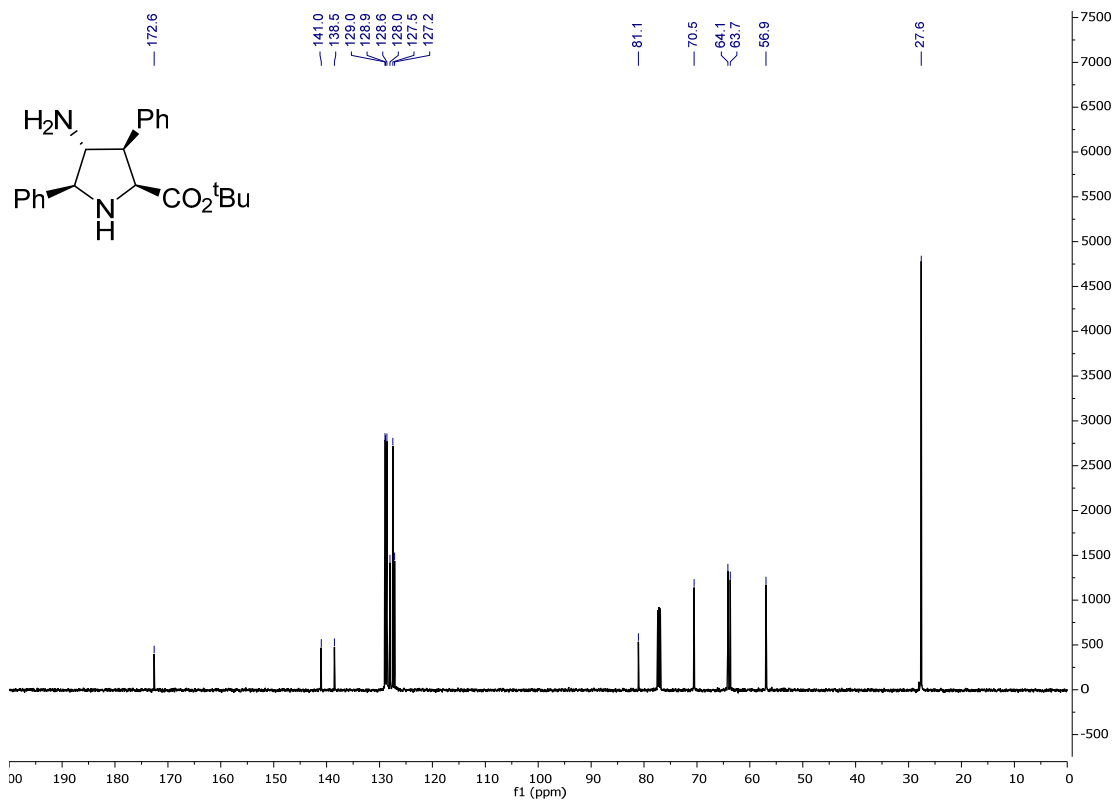
COSY (CDCl<sub>3</sub>)

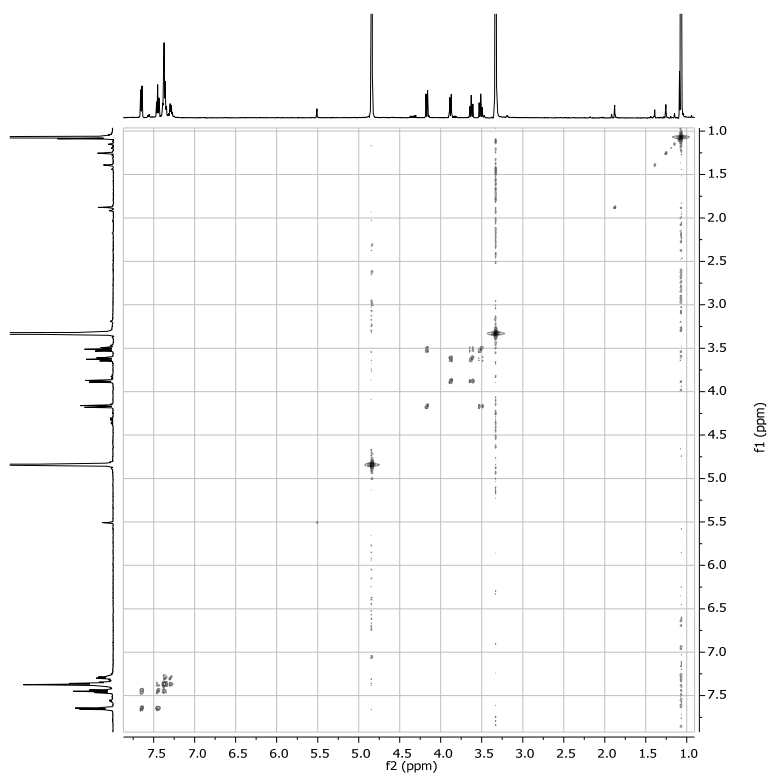
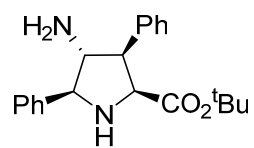


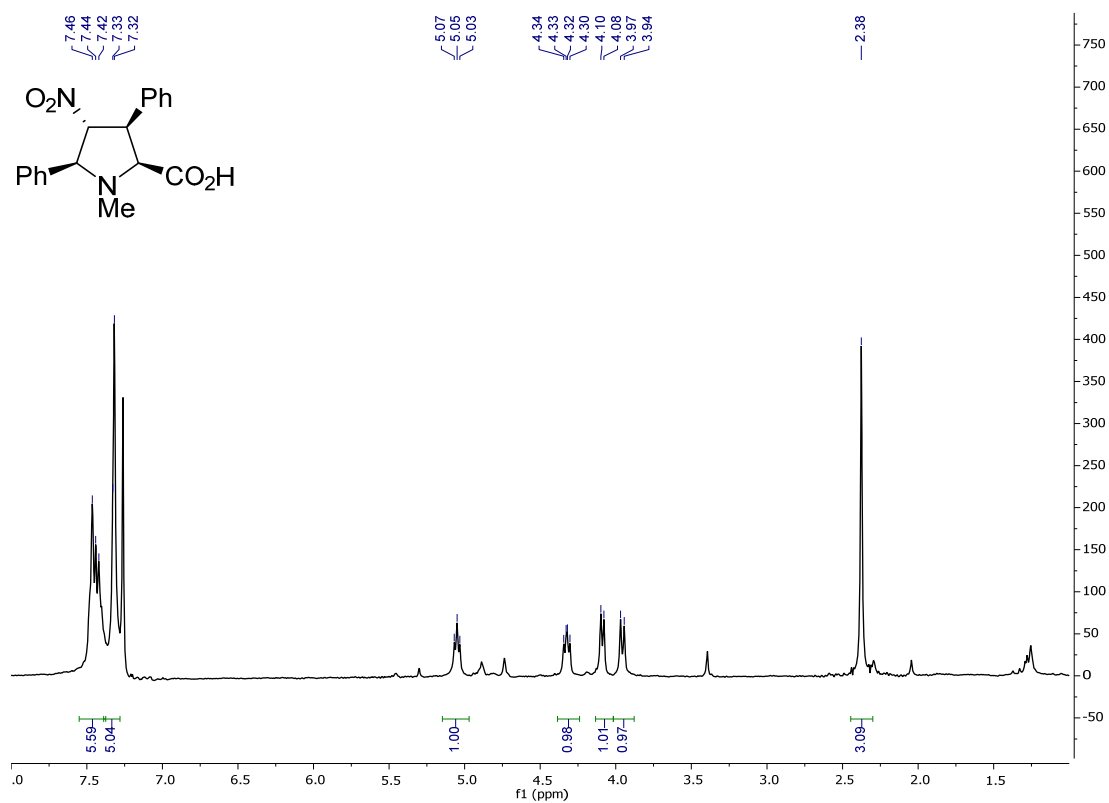
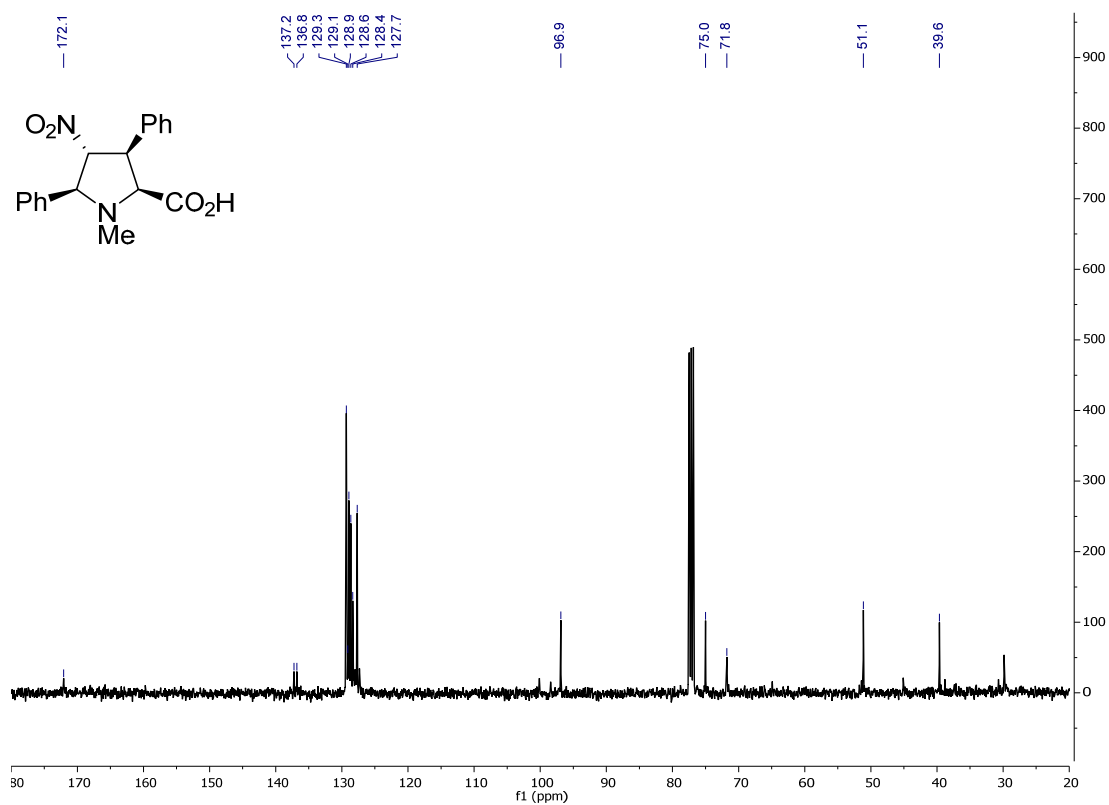
Compound *ent-syn-21* $^1\text{H}$  NMR ( $\text{CDCl}_3$ )

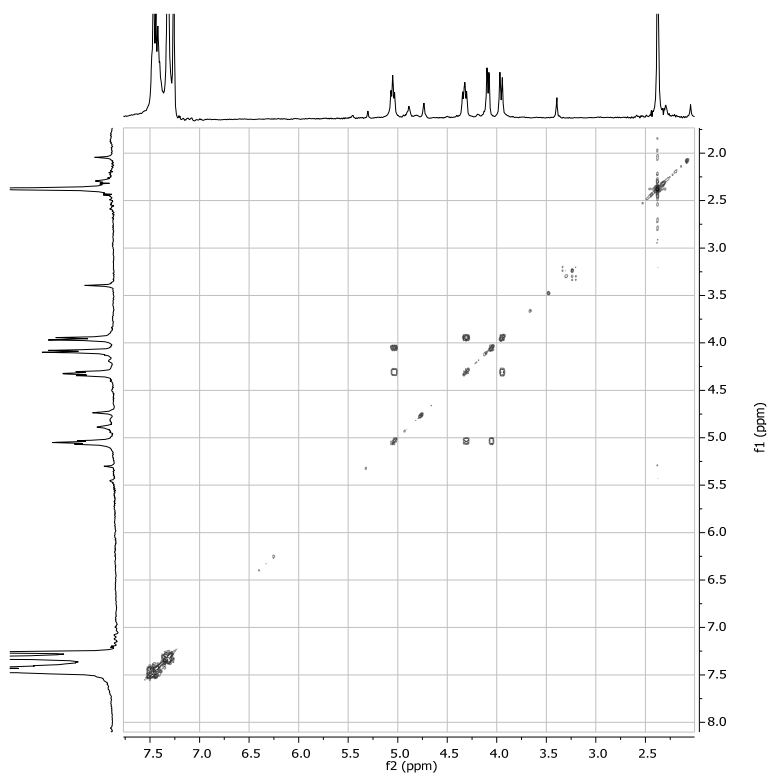
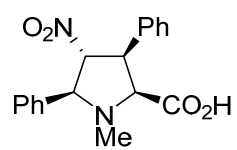


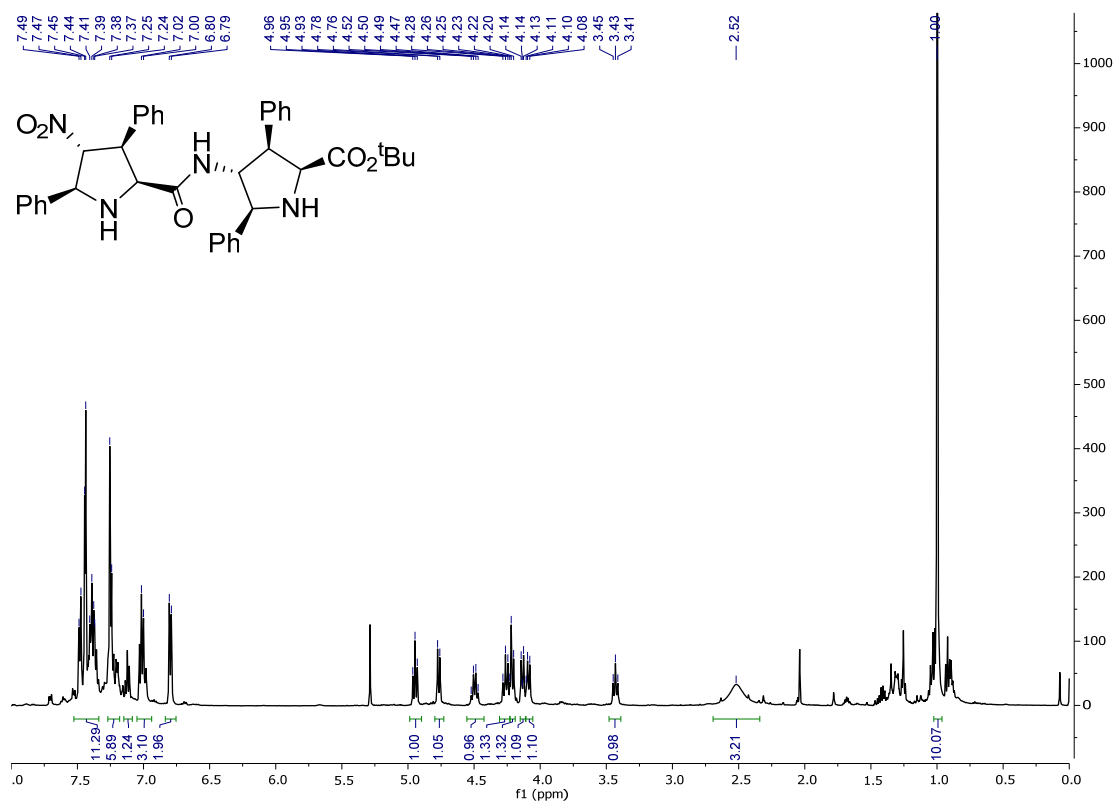
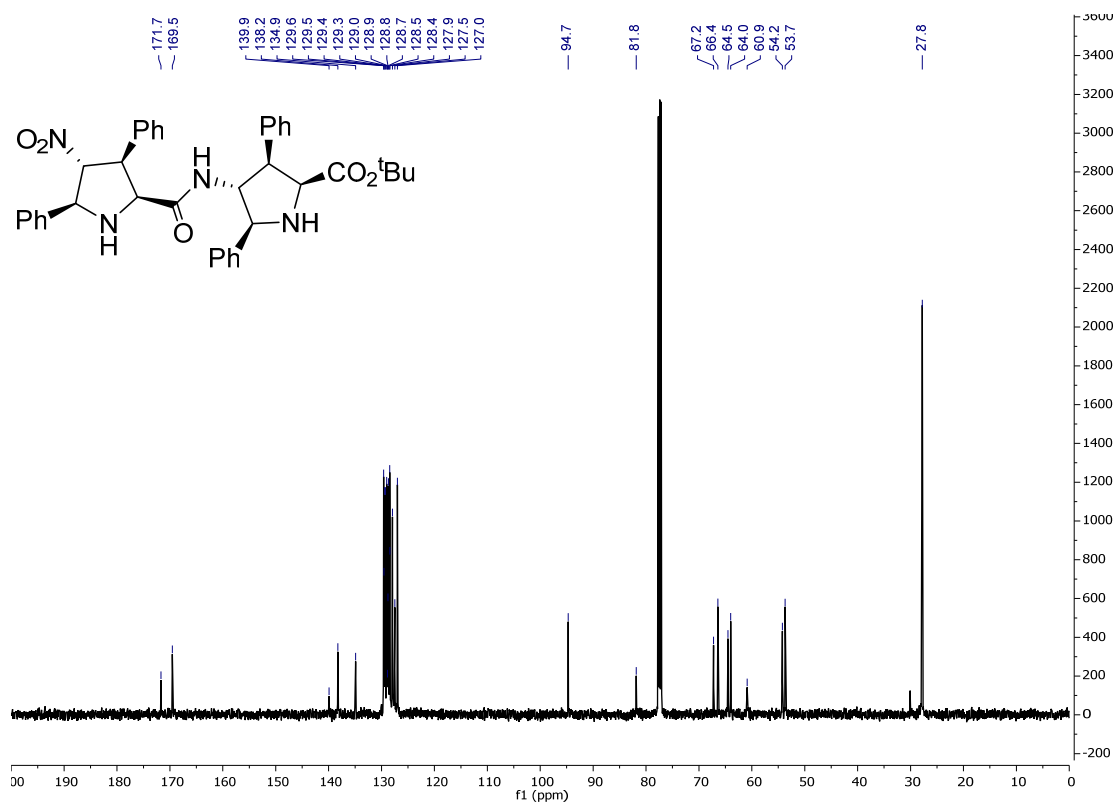
## Annex I-b. NMR spectra selection for Chapter 3

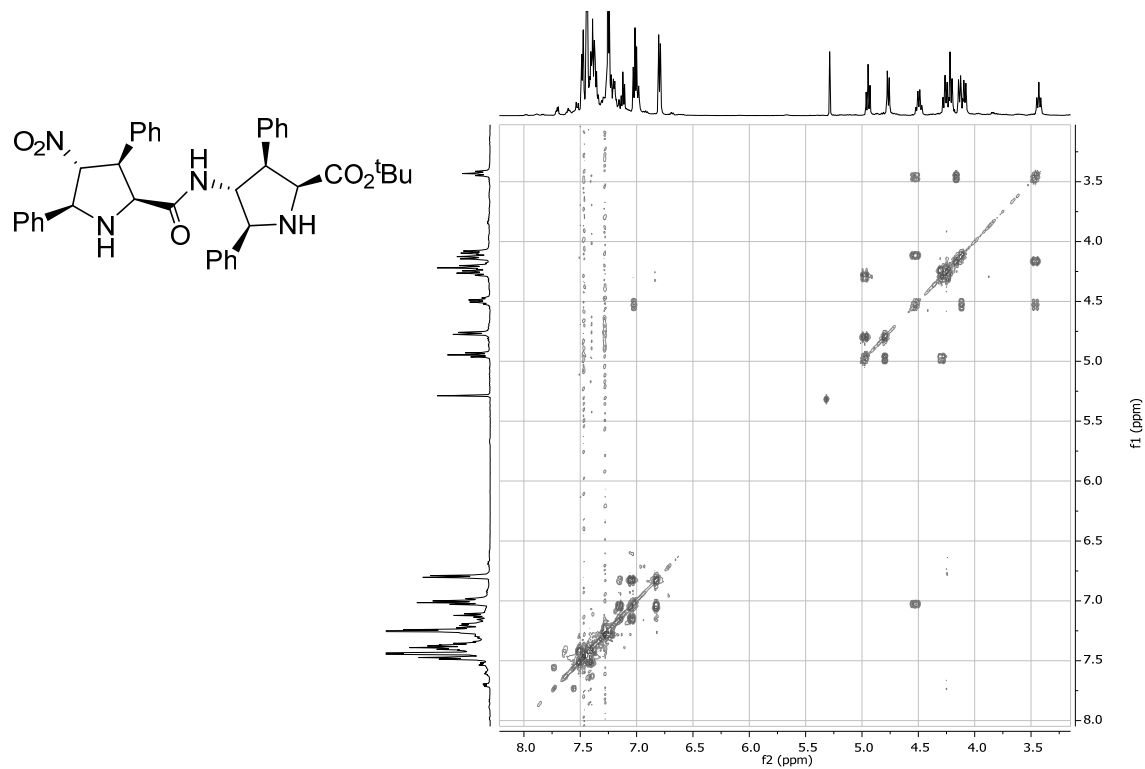
Compound NH<sub>2</sub>-X<sub>L</sub>-O<sup>t</sup>Bu-10ba<sup>1</sup>H NMR (CDCl<sub>3</sub>)<sup>13</sup>C NMR (CDCl<sub>3</sub>)

COSY (CDCl<sub>3</sub>)

Compound NO<sub>2</sub>-X<sub>L</sub>-OMe-5e<sup>1</sup>H NMR (CDCl<sub>3</sub>)<sup>13</sup>C NMR (CDCl<sub>3</sub>)

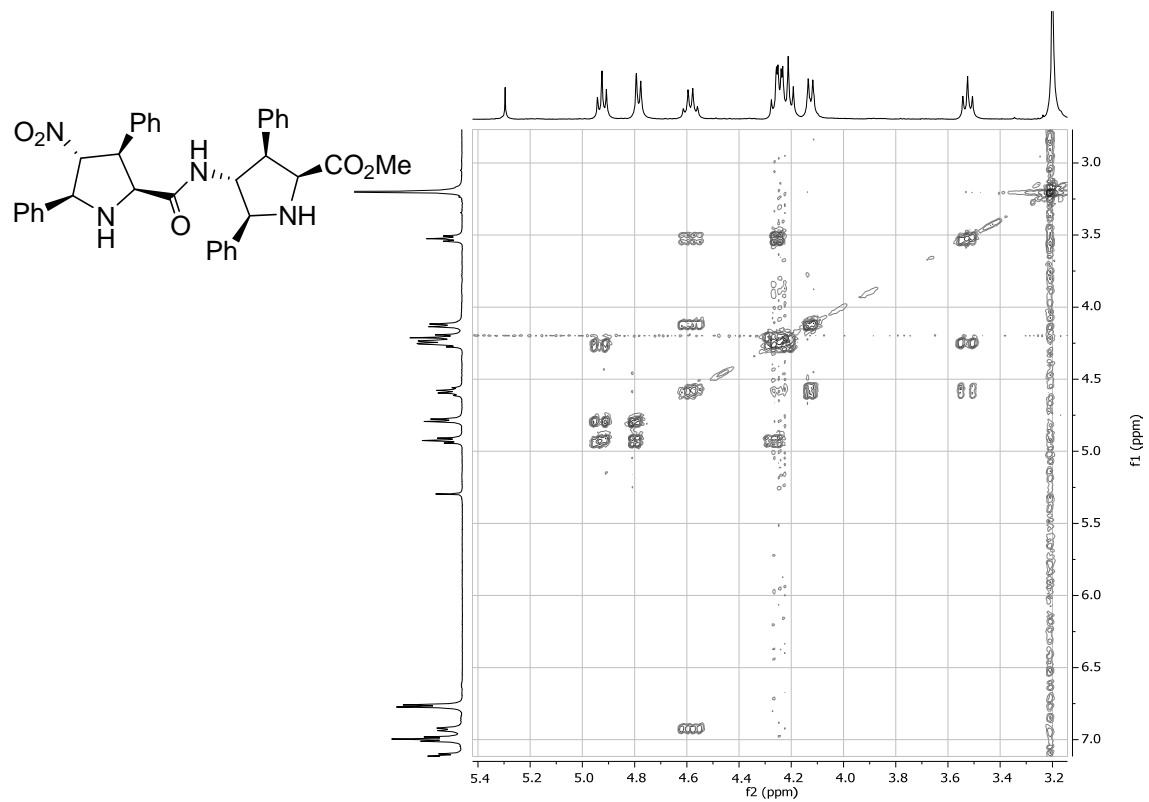
COSY (CDCl<sub>3</sub>)

Compound NO<sub>2</sub>-X<sub>L</sub>X<sub>L</sub>-O<sup>t</sup>Bu-23b<sup>1</sup>H NMR (CDCl<sub>3</sub>)<sup>13</sup>C NMR (CDCl<sub>3</sub>)

COSY (CDCl<sub>3</sub>)

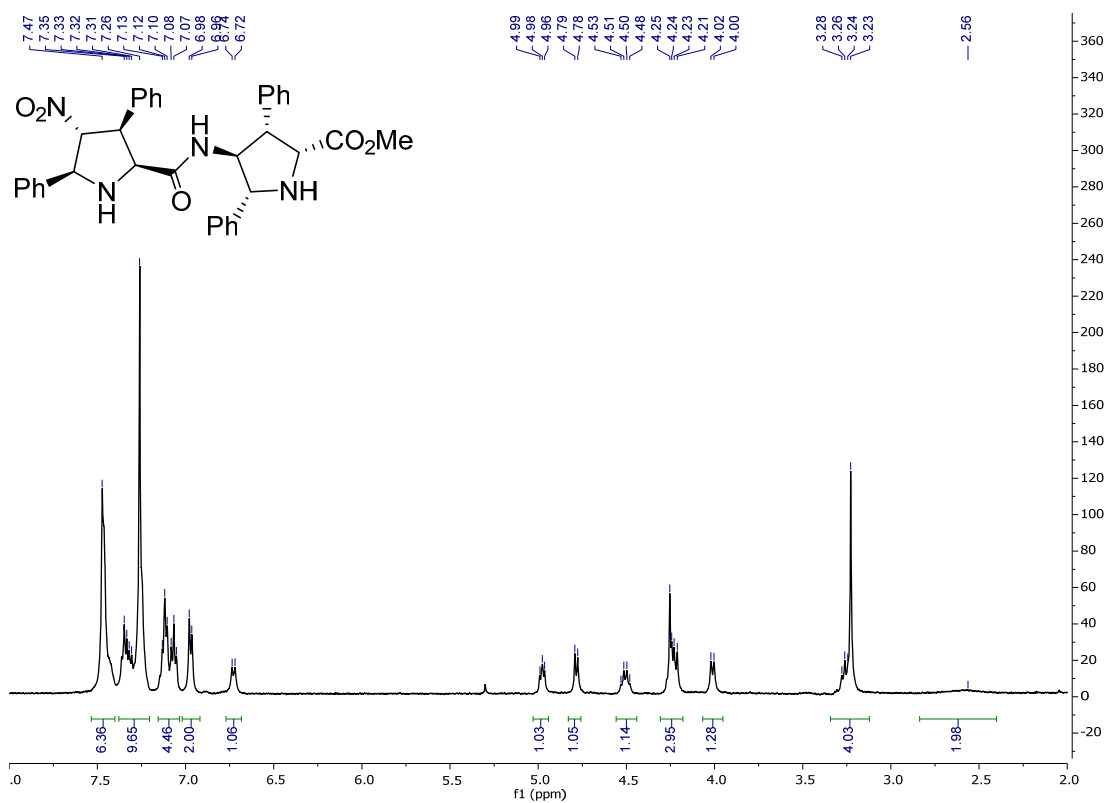




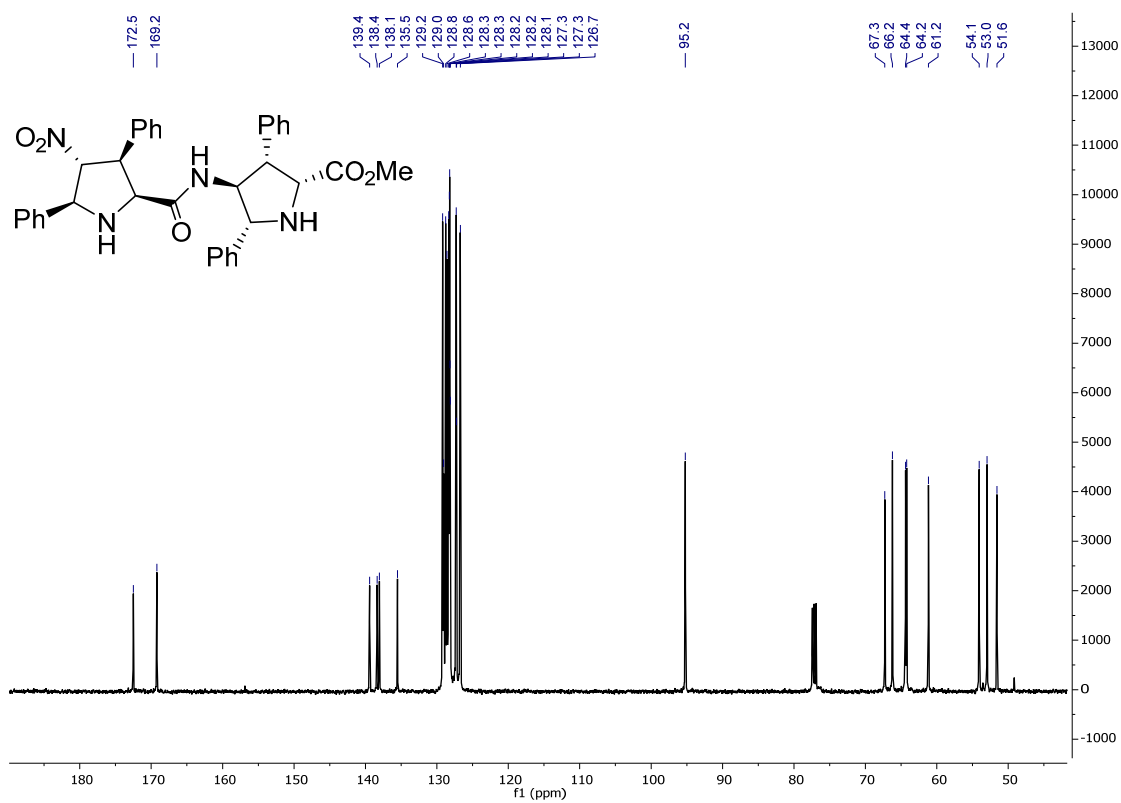
COSY (CDCl<sub>3</sub>)

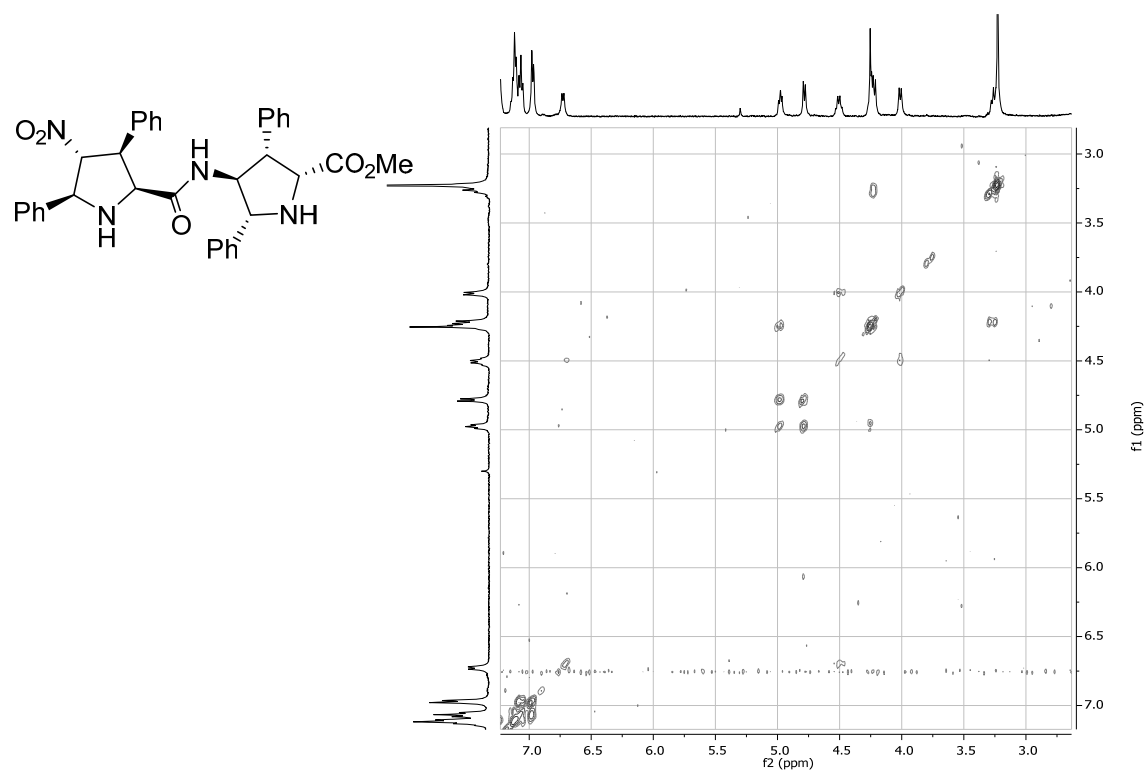
Compound NO<sub>2</sub>-X<sub>L</sub>X<sub>D</sub>-OMe-23a

<sup>1</sup>H NMR (CDCl<sub>3</sub>)



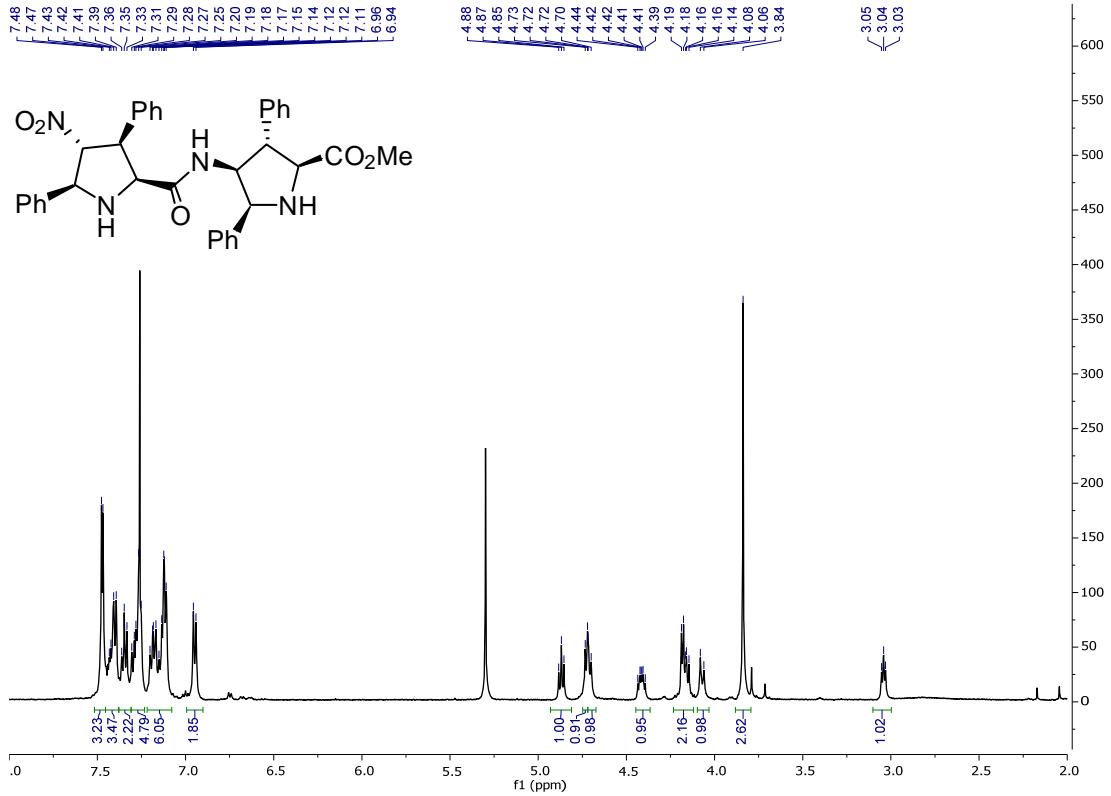
<sup>13</sup>C NMR (CDCl<sub>3</sub>)



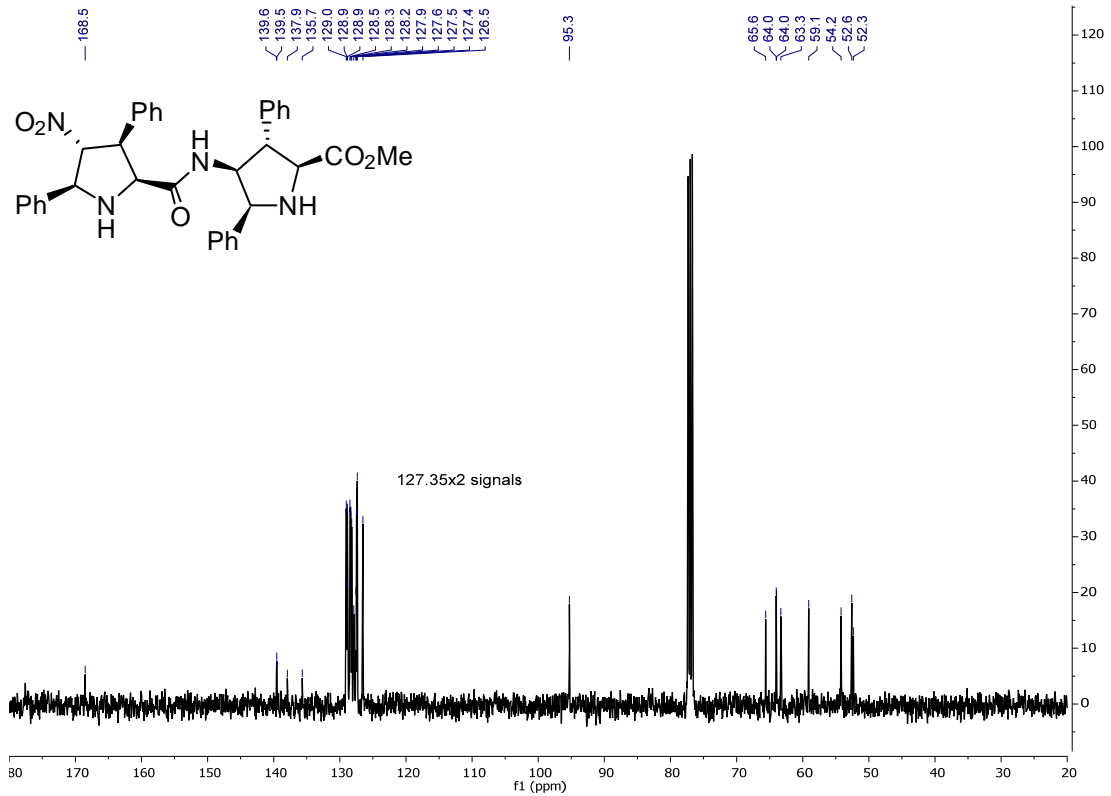
COSY (CDCl<sub>3</sub>)

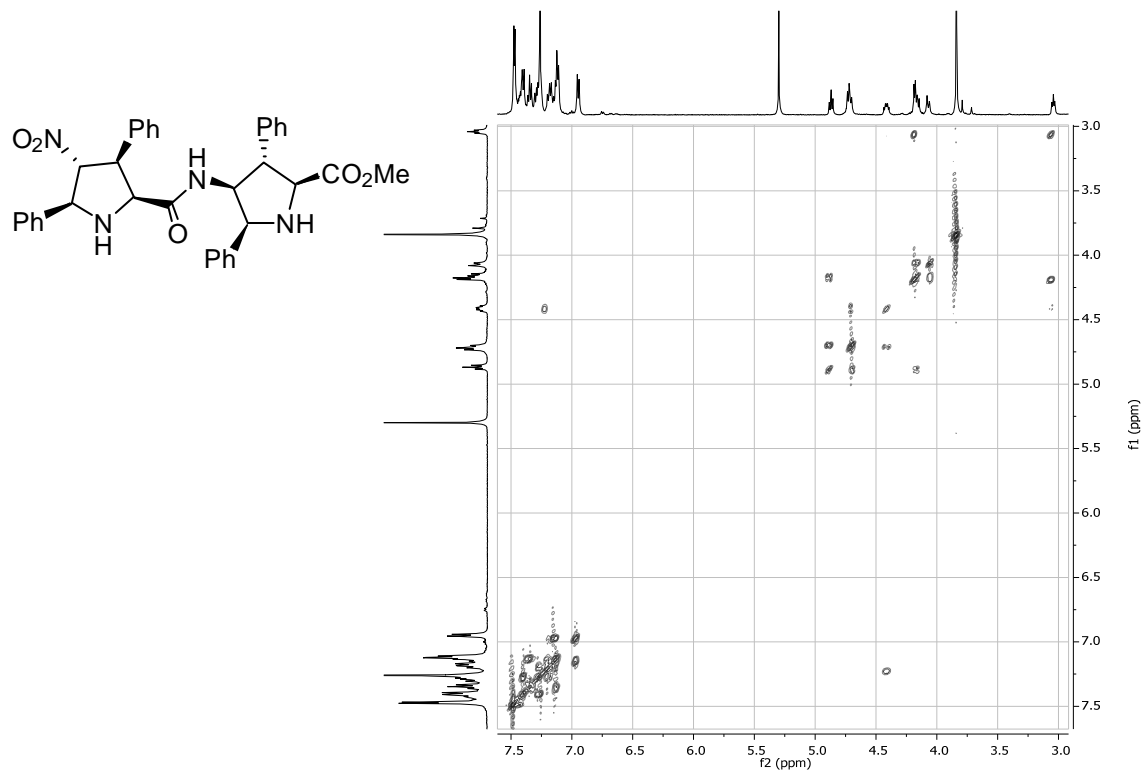
Compound NO<sub>2</sub>-X<sub>L</sub>N<sub>L</sub>-OMe-23a

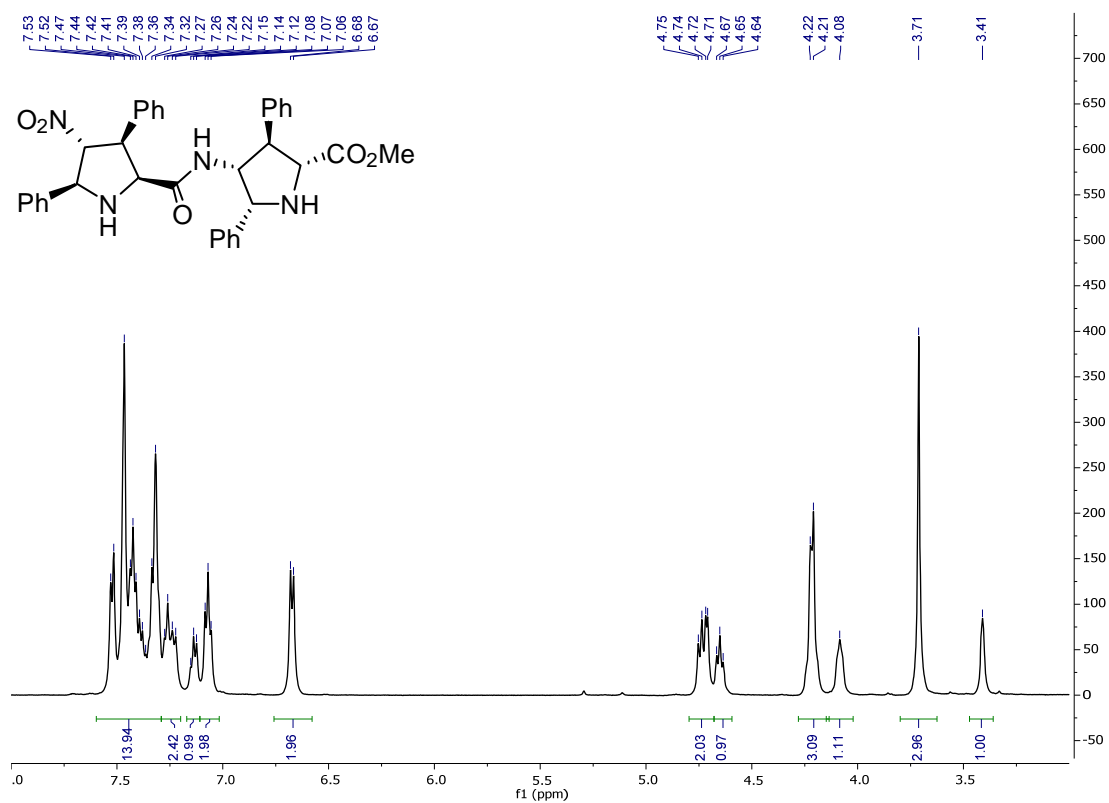
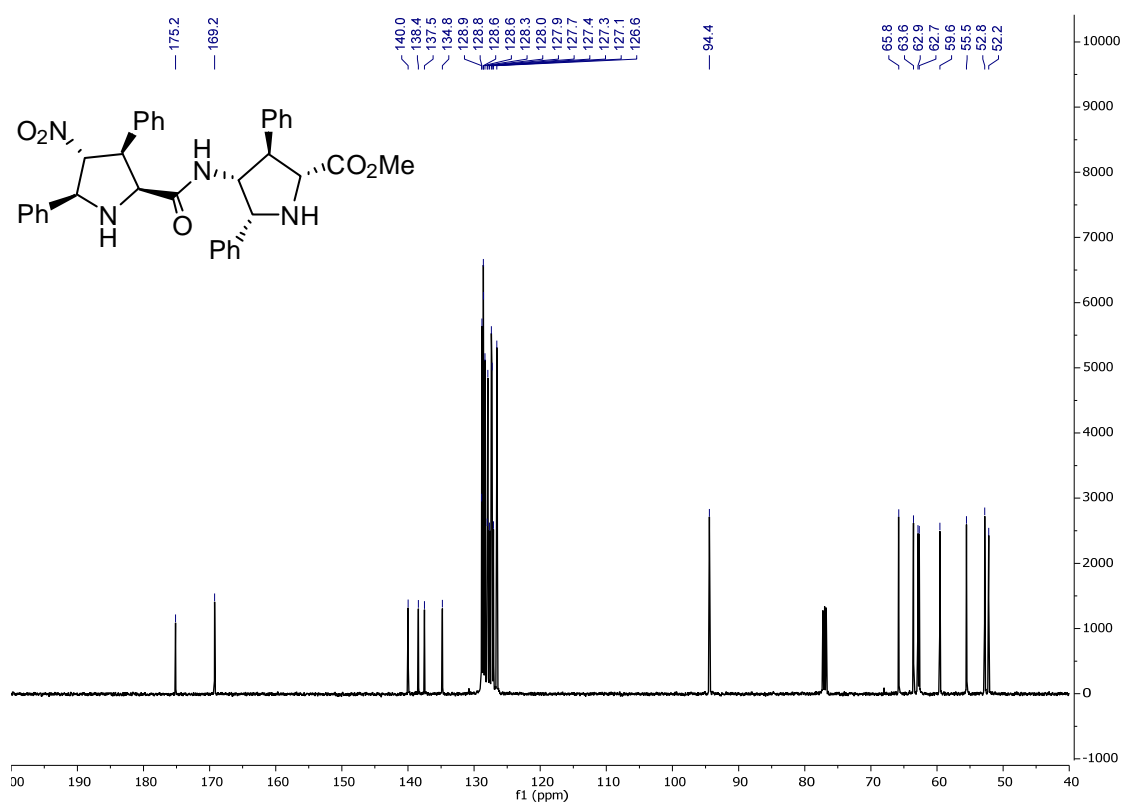
<sup>1</sup>H NMR (CDCl<sub>3</sub>)

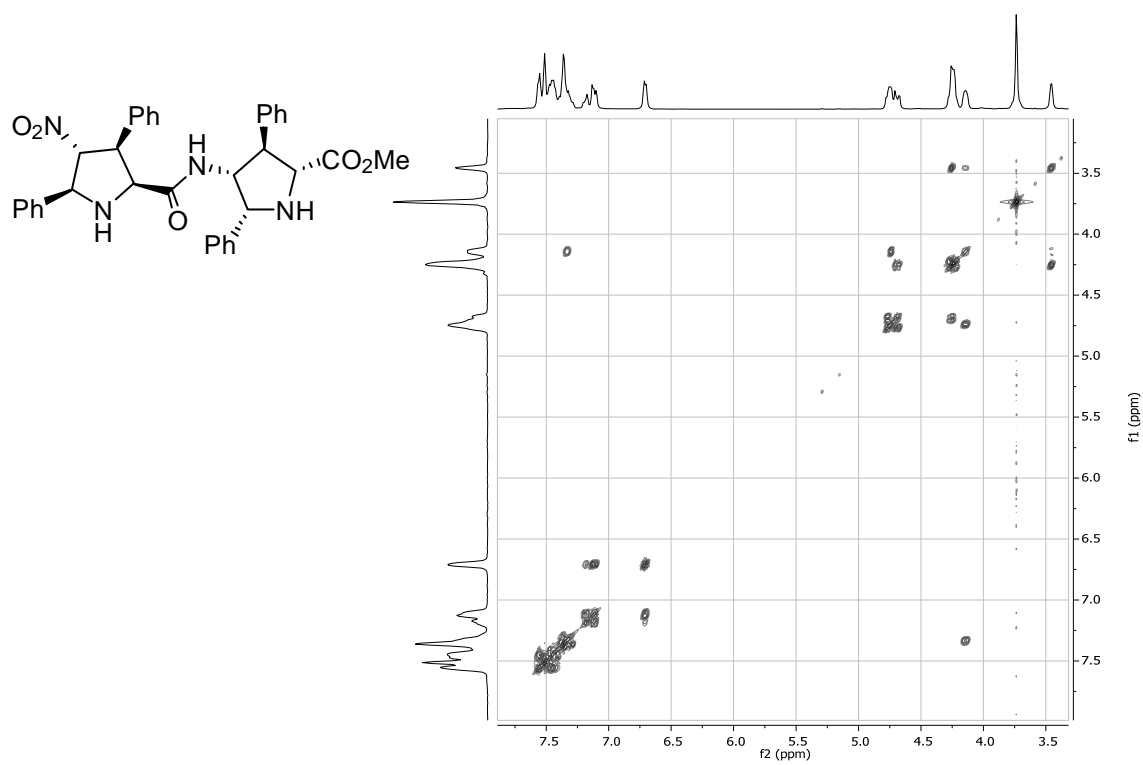


<sup>13</sup>C NMR (CDCl<sub>3</sub>)

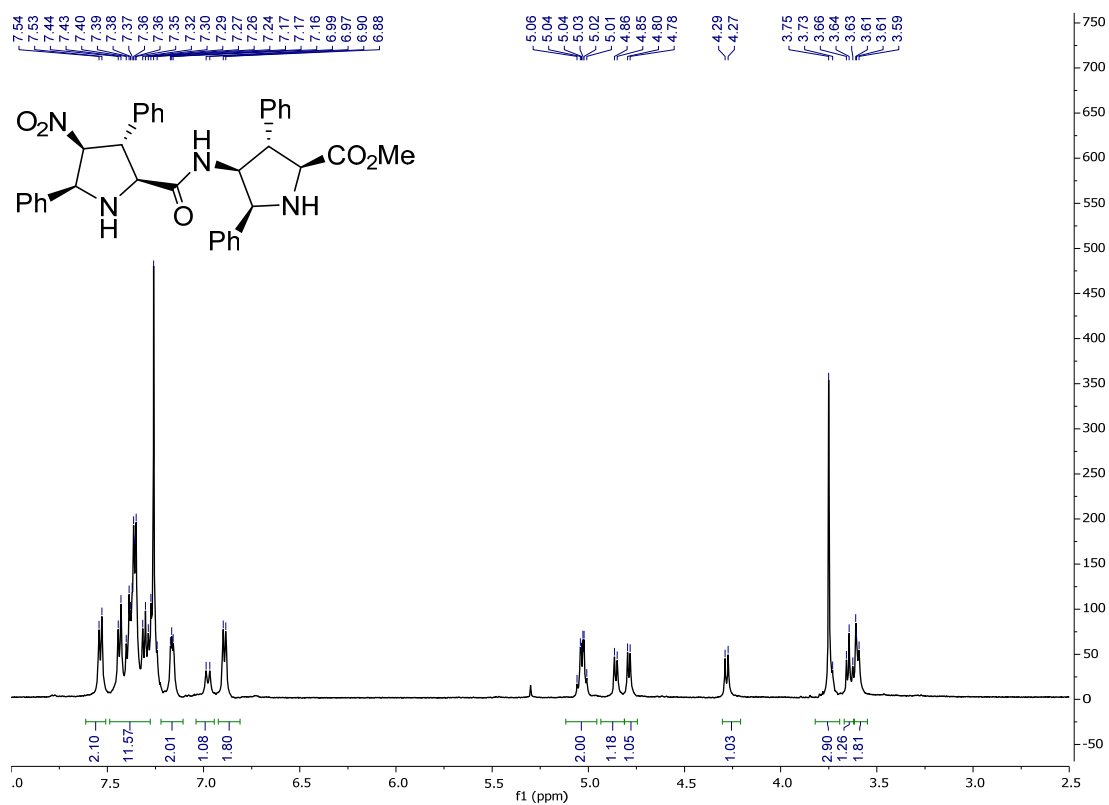
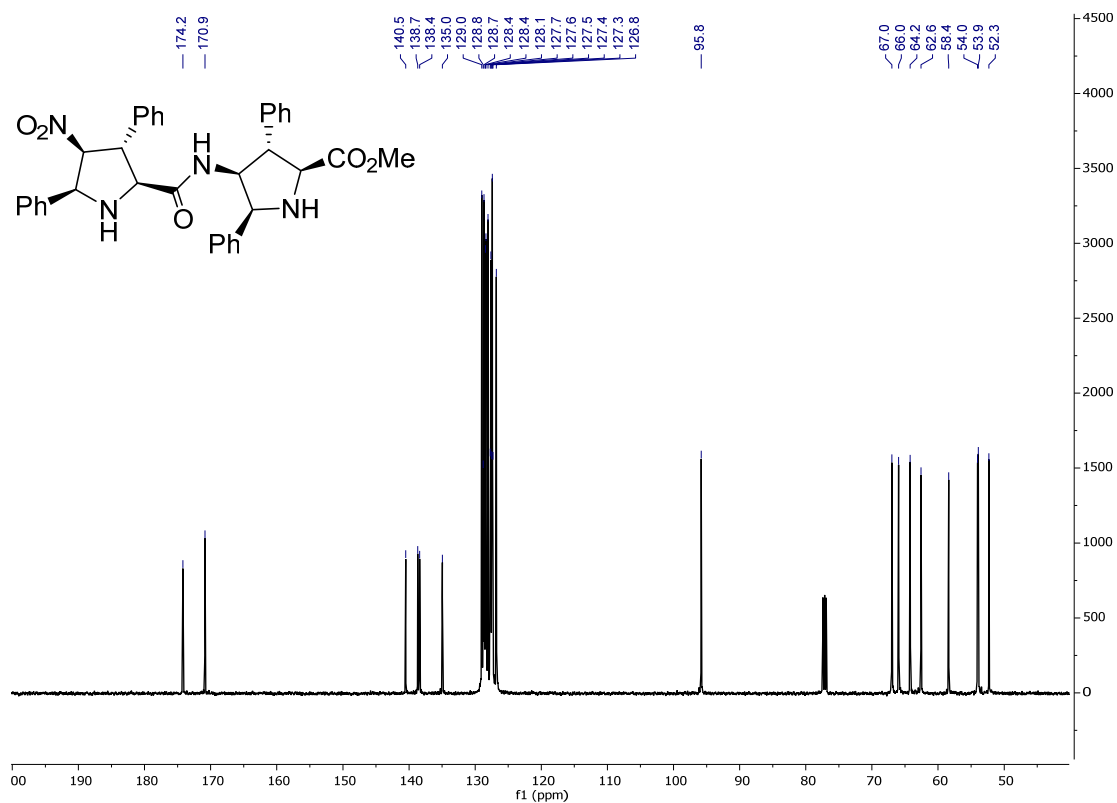


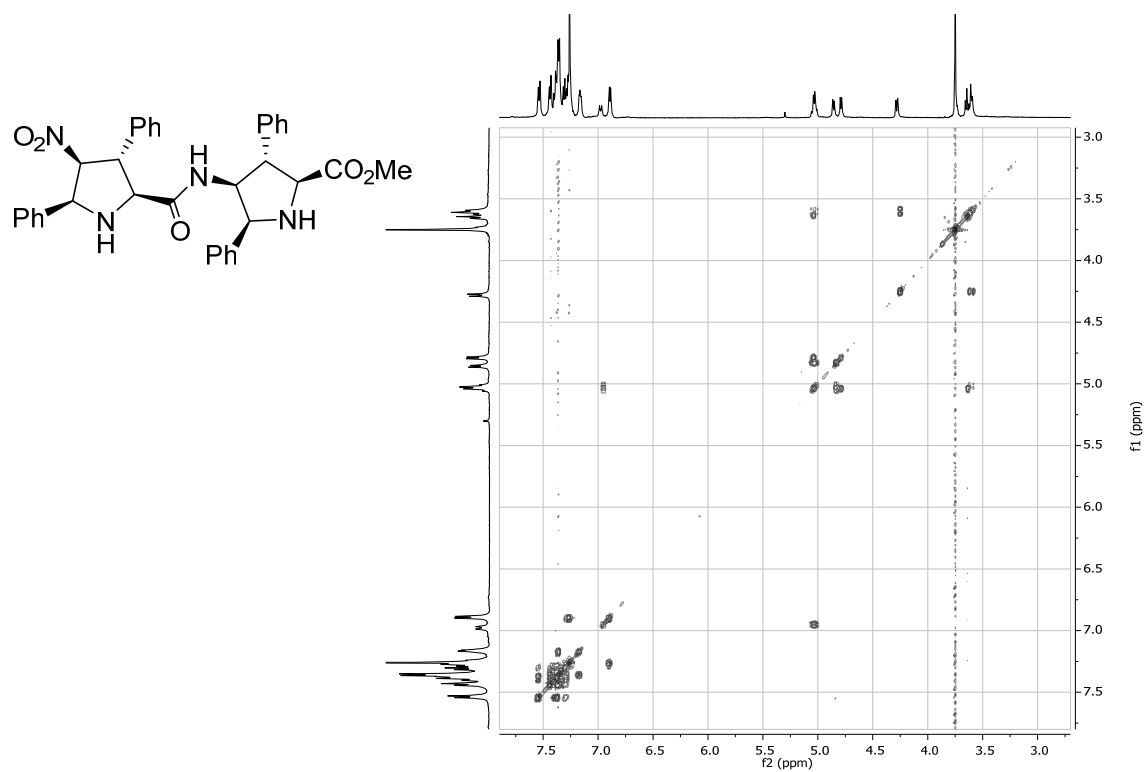
COSY (CDCl<sub>3</sub>)

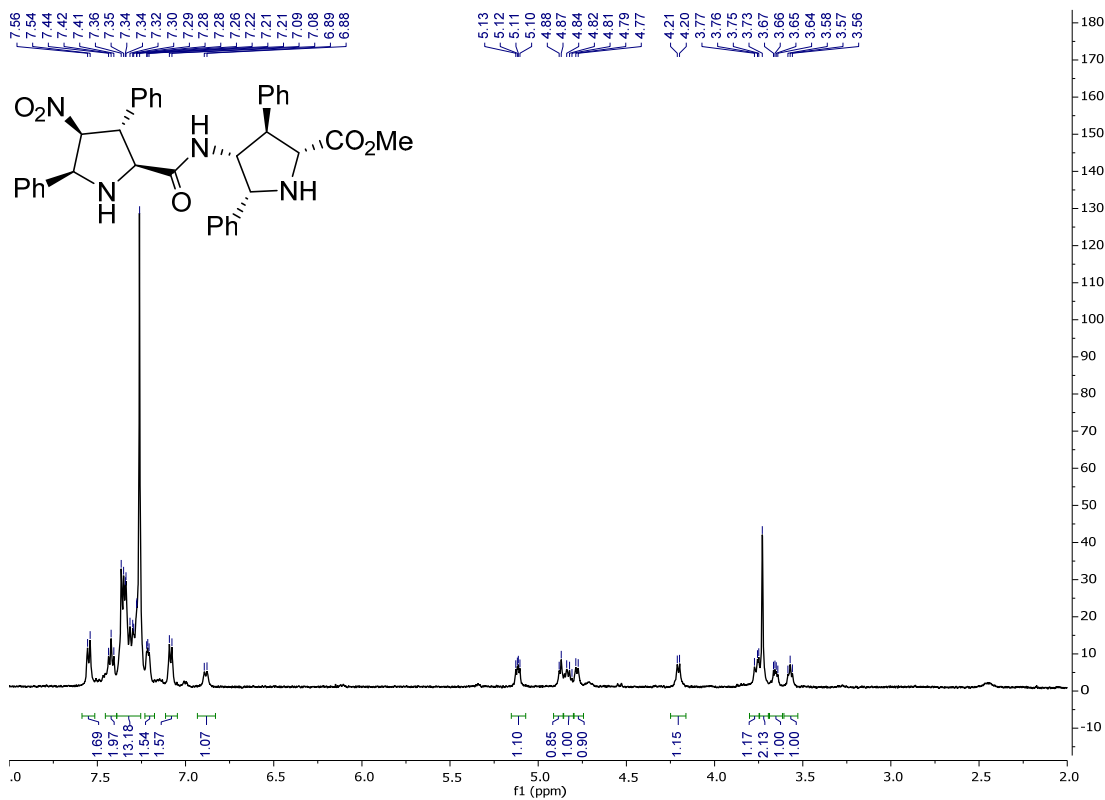
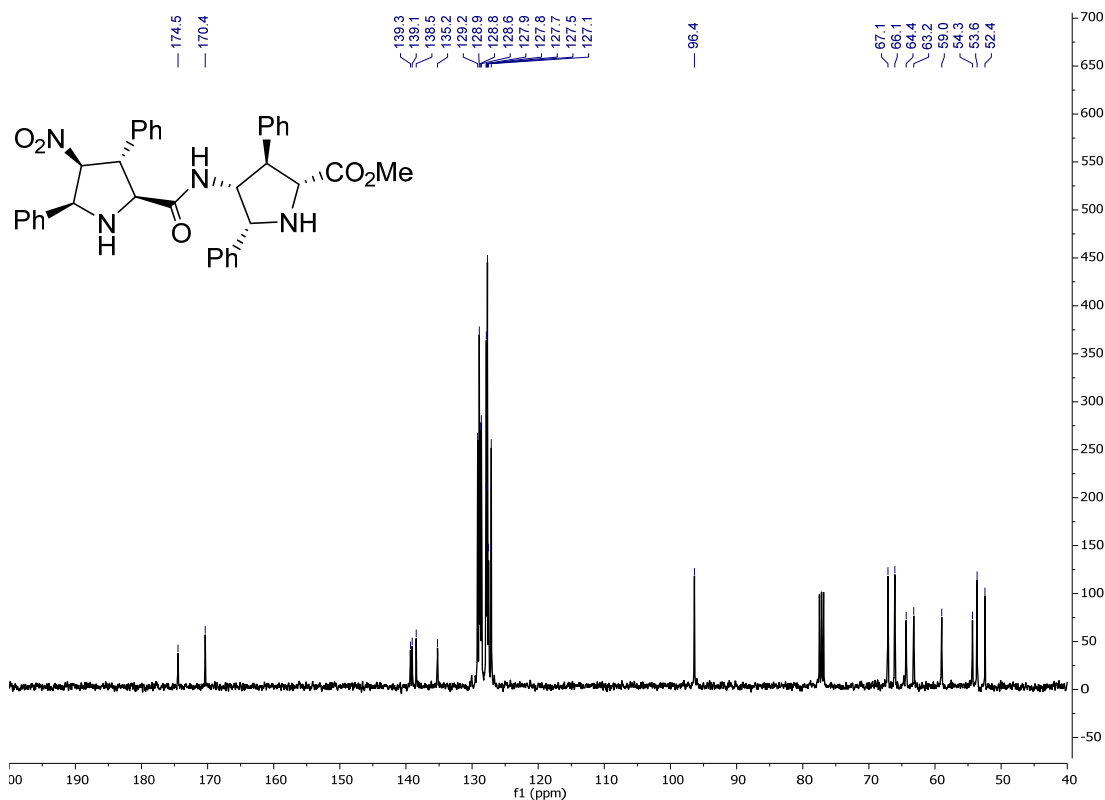
Compound NO<sub>2</sub>-X<sub>L</sub>N<sub>D</sub>-OMe-23a<sup>1</sup>H NMR (CDCl<sub>3</sub>)<sup>13</sup>C NMR (CDCl<sub>3</sub>)

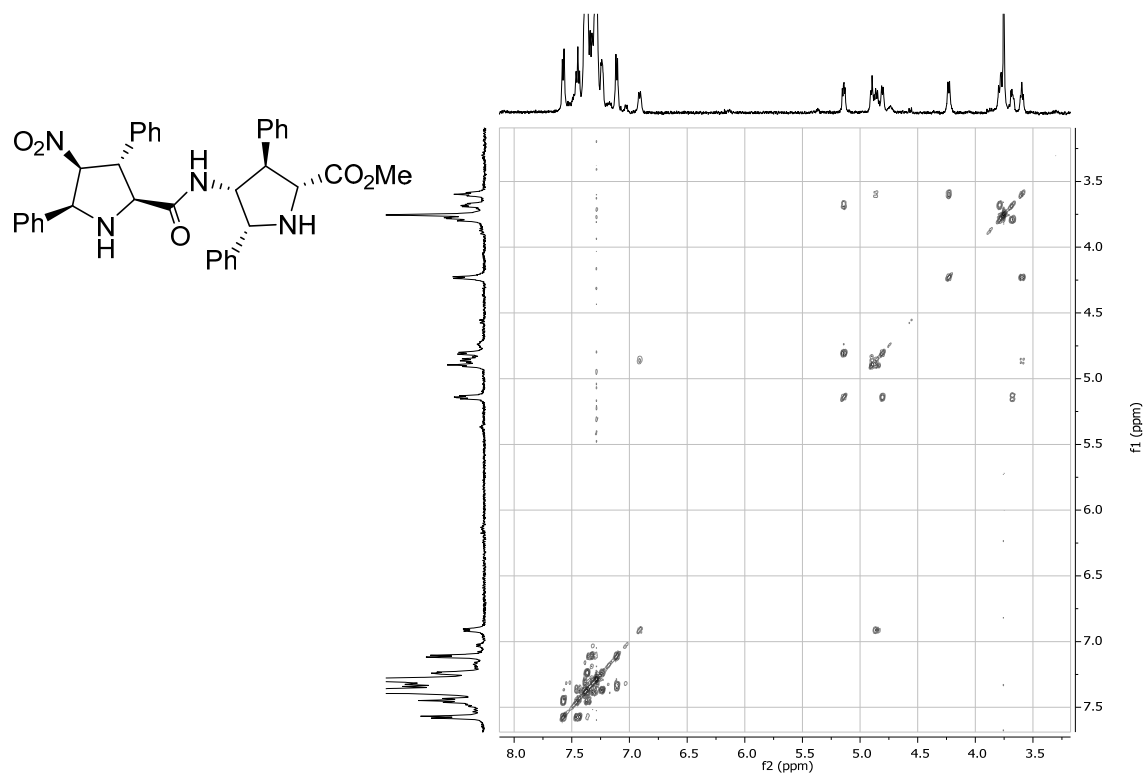
COSY (CDCl<sub>3</sub>)



Compound NO<sub>2</sub>-N<sub>L</sub>N<sub>L</sub>-OMe-23a<sup>1</sup>H NMR (CDCl<sub>3</sub>)<sup>13</sup>C NMR (CDCl<sub>3</sub>)

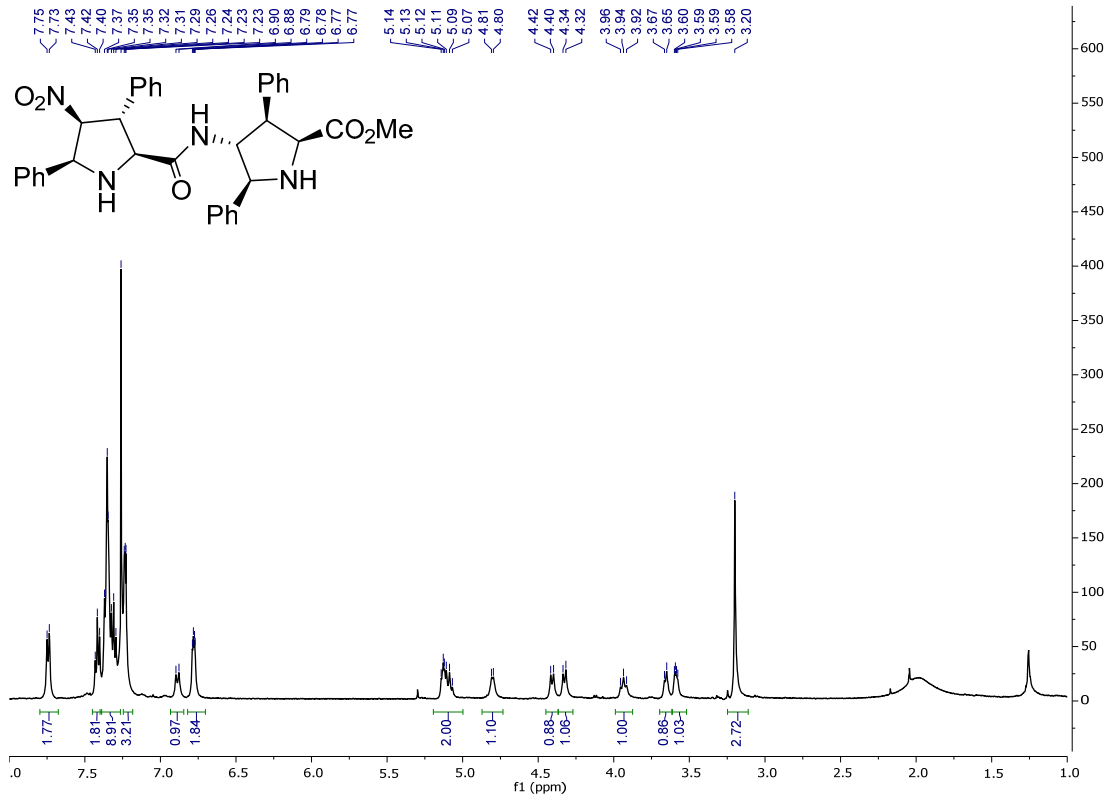
COSY (CDCl<sub>3</sub>)

Compound NO<sub>2</sub>-N<sub>L</sub>N<sub>D</sub>-OMe-23a<sup>1</sup>H NMR (CDCl<sub>3</sub>)<sup>13</sup>C NMR (CDCl<sub>3</sub>)

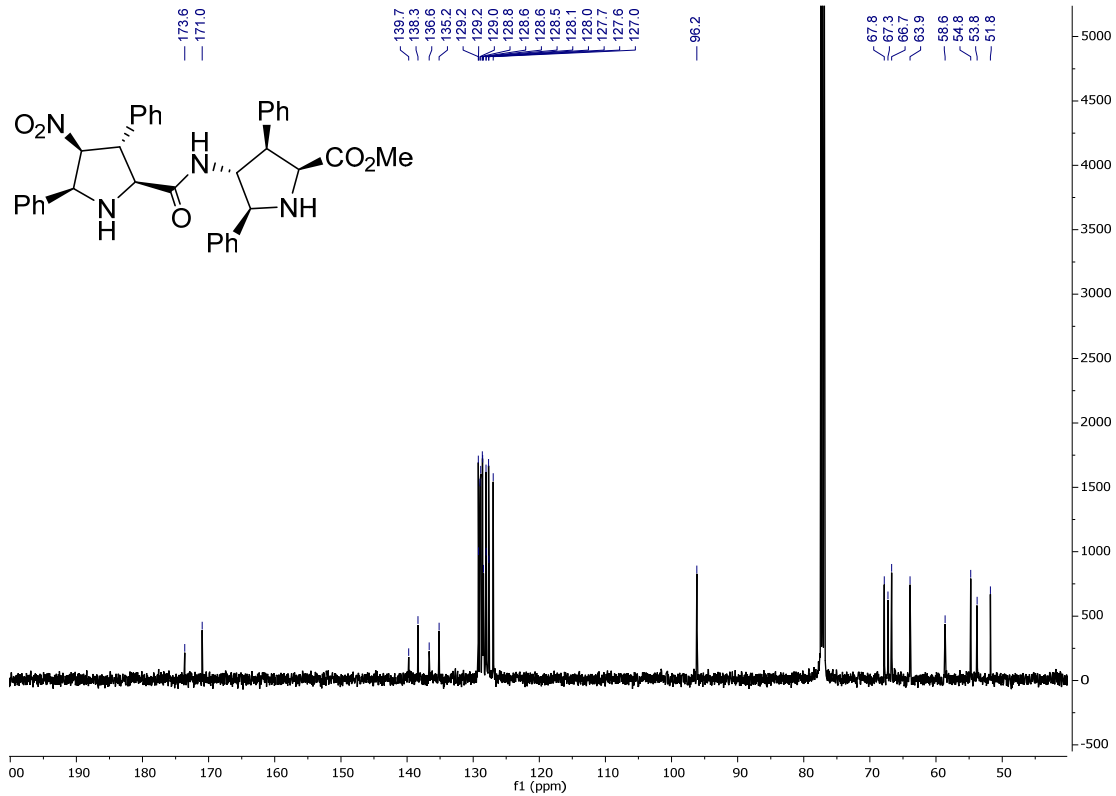
COSY (CDCl<sub>3</sub>)

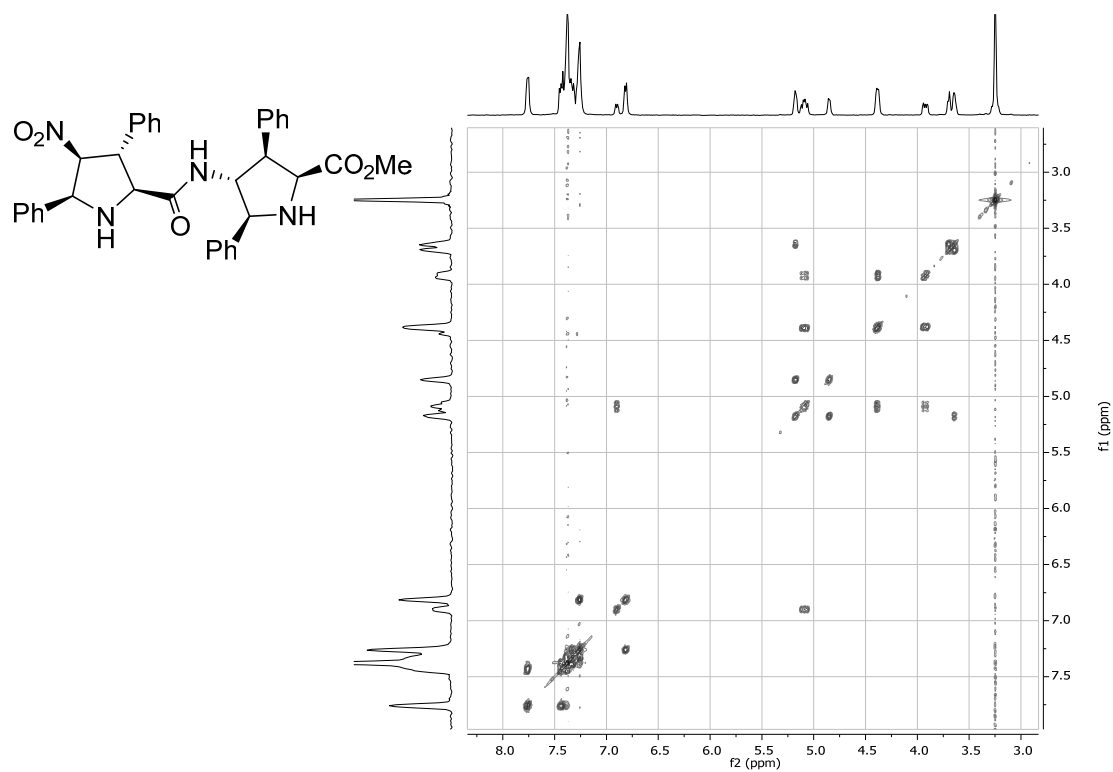
Compound NO<sub>2</sub>-N<sub>L</sub>X<sub>L</sub>-OMe-23a

<sup>1</sup>H NMR (CDCl<sub>3</sub>)



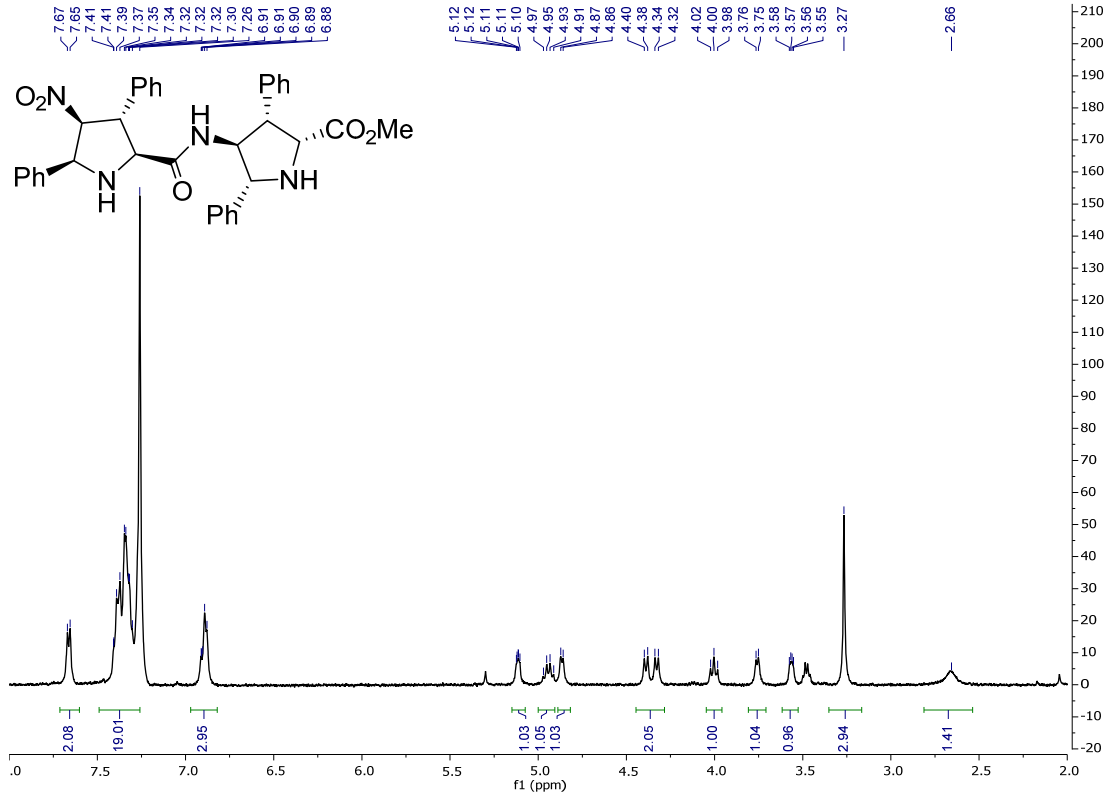
<sup>13</sup>C NMR (CDCl<sub>3</sub>)



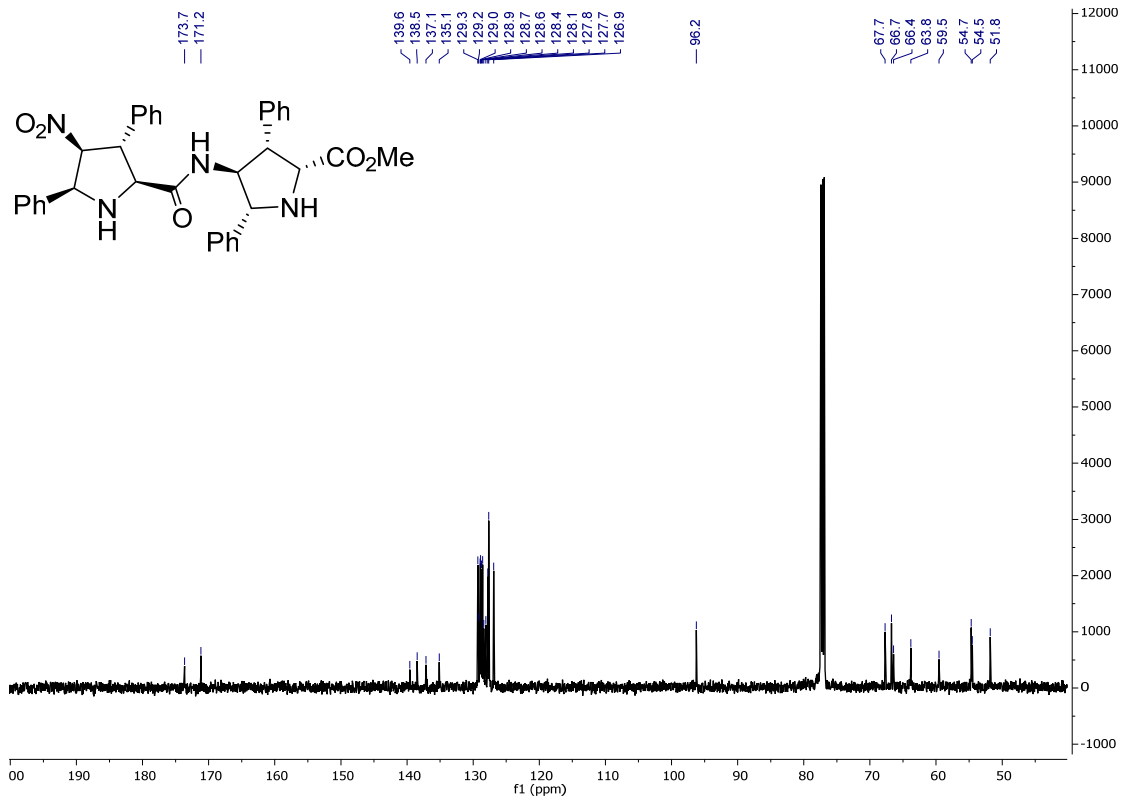
COSY (CDCl<sub>3</sub>)

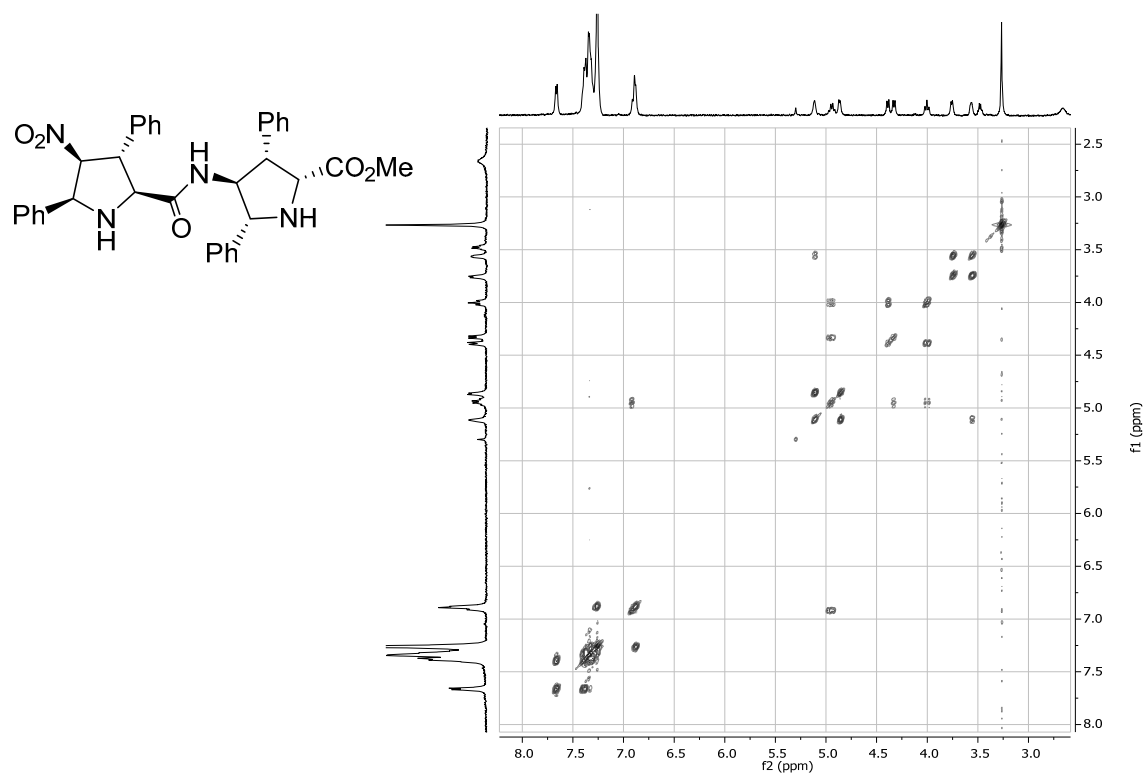
Compound NO<sub>2</sub>-N<sub>L</sub>X<sub>D</sub>-OMe-23a

<sup>1</sup>H NMR (CDCl<sub>3</sub>)



<sup>13</sup>C NMR (CDCl<sub>3</sub>)

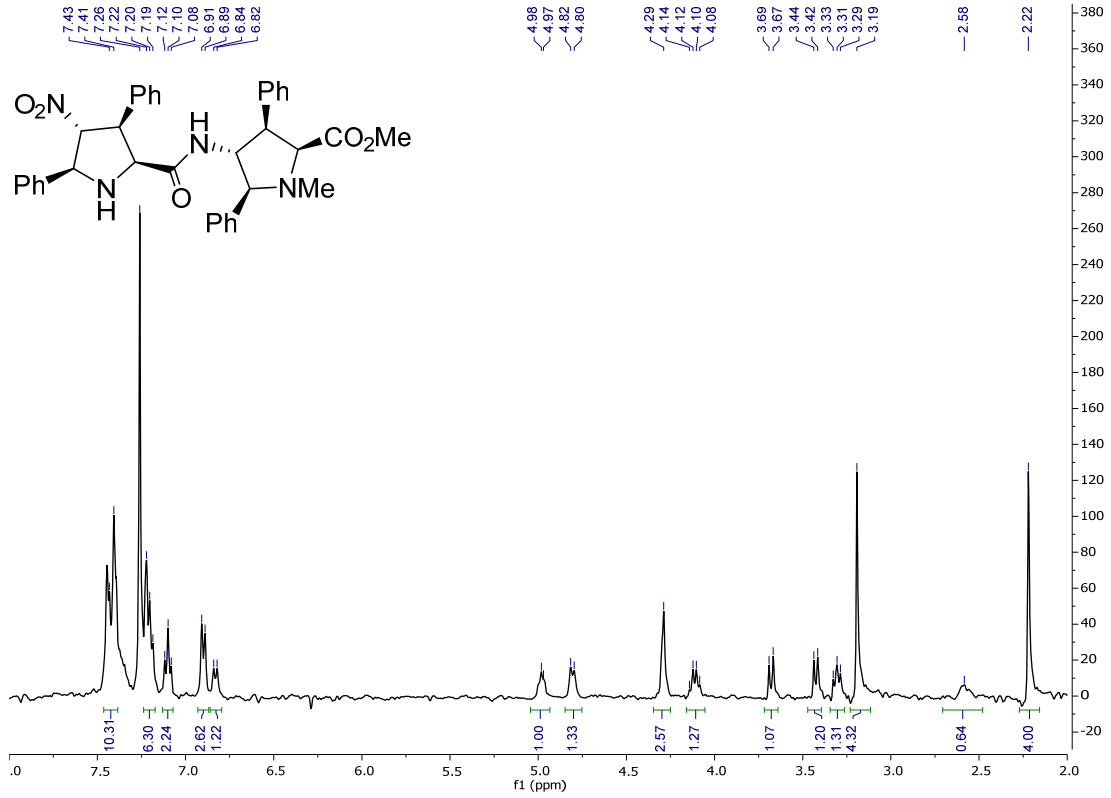


COSY (CDCl<sub>3</sub>)

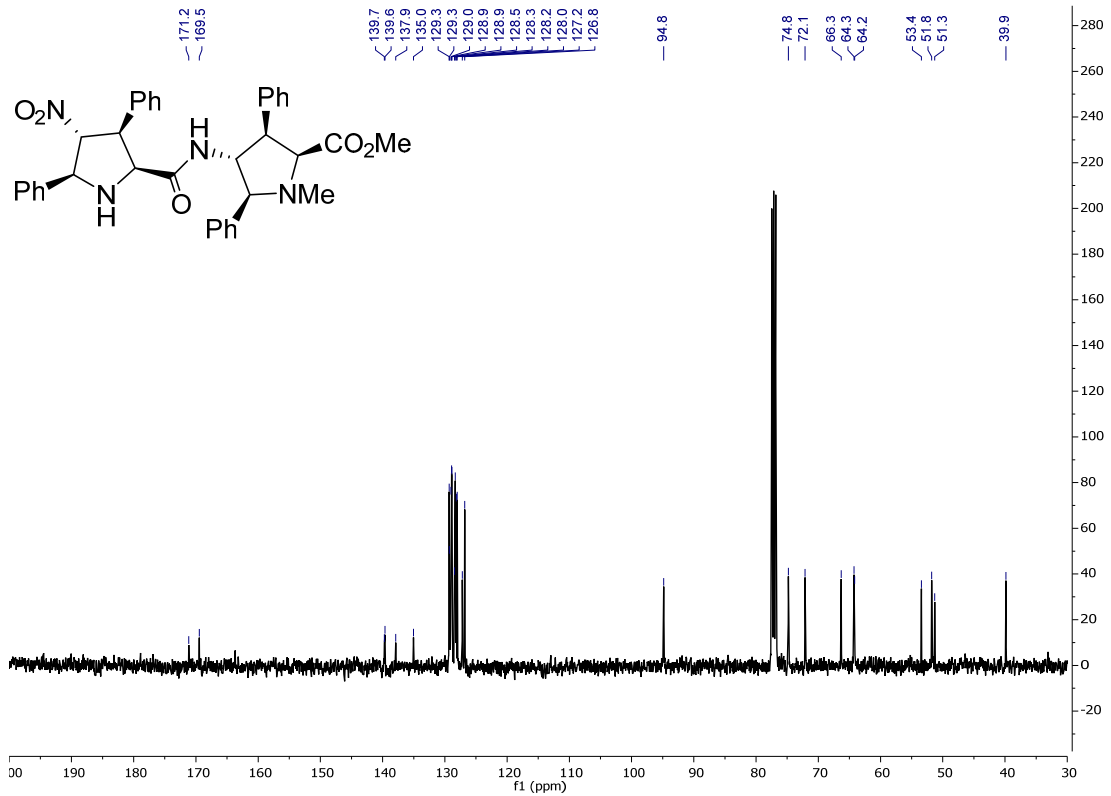


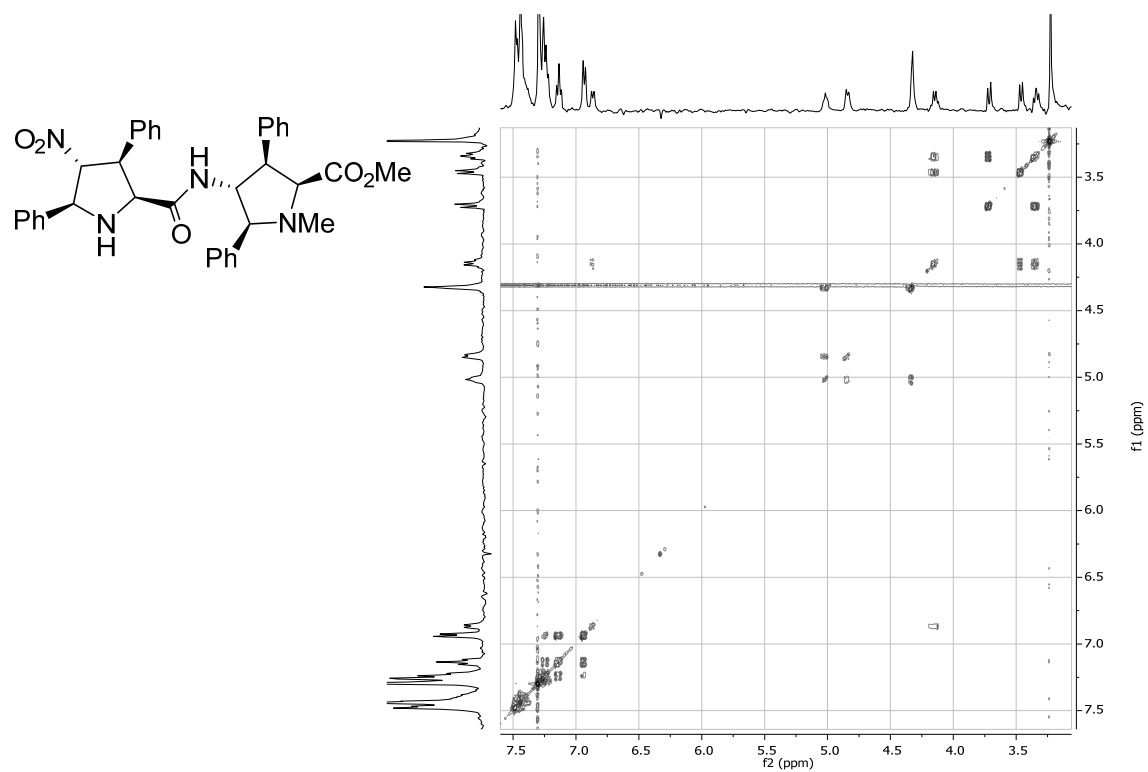
Compound NO<sub>2</sub>-X<sub>L</sub>X<sub>L</sub>-OMe-25a

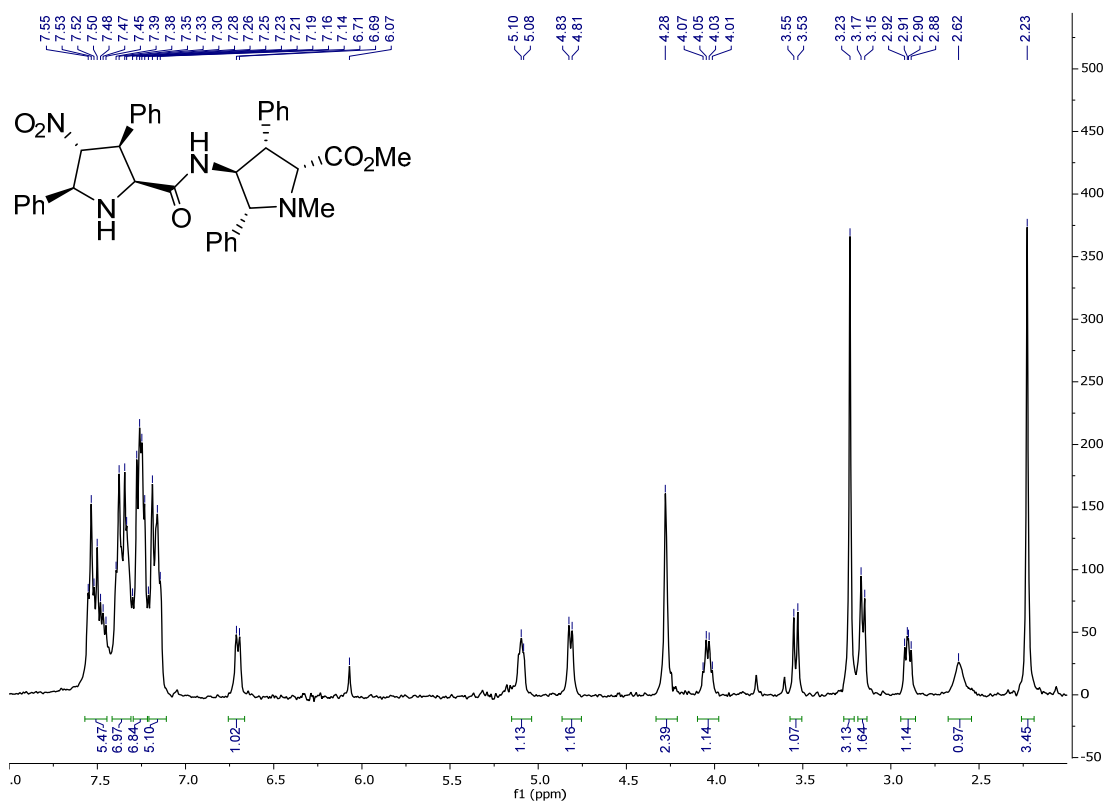
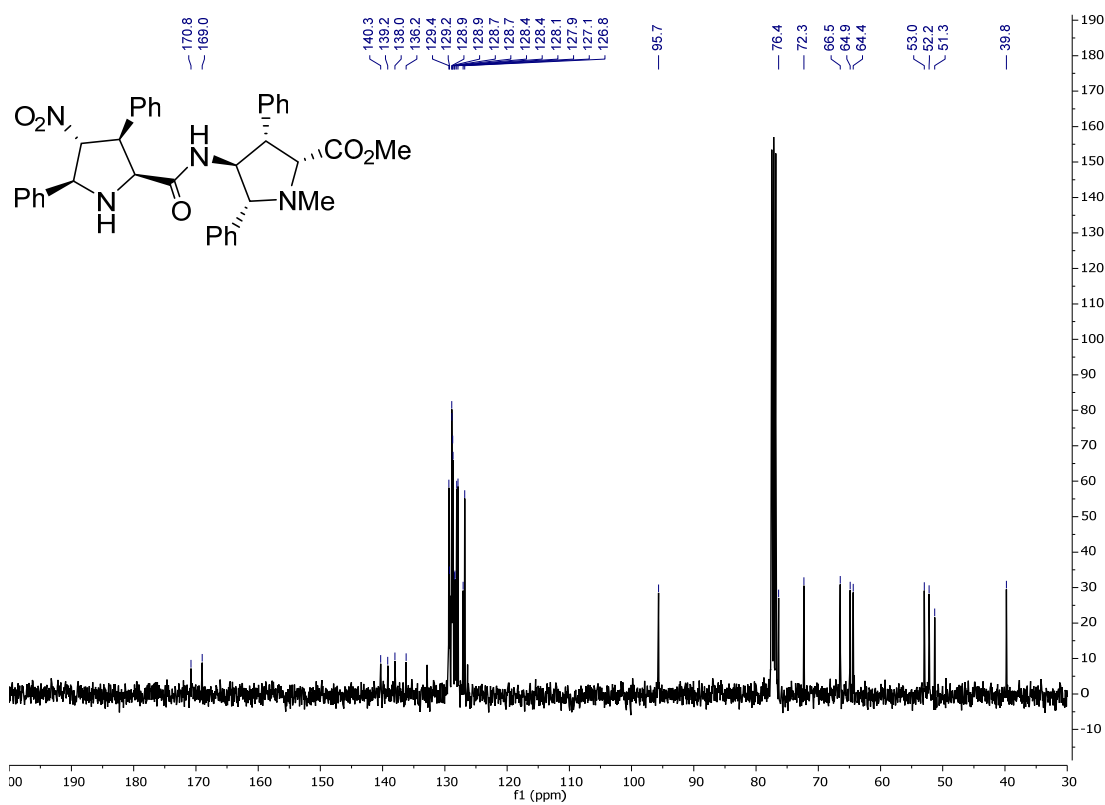
<sup>1</sup>H NMR (CDCl<sub>3</sub>)

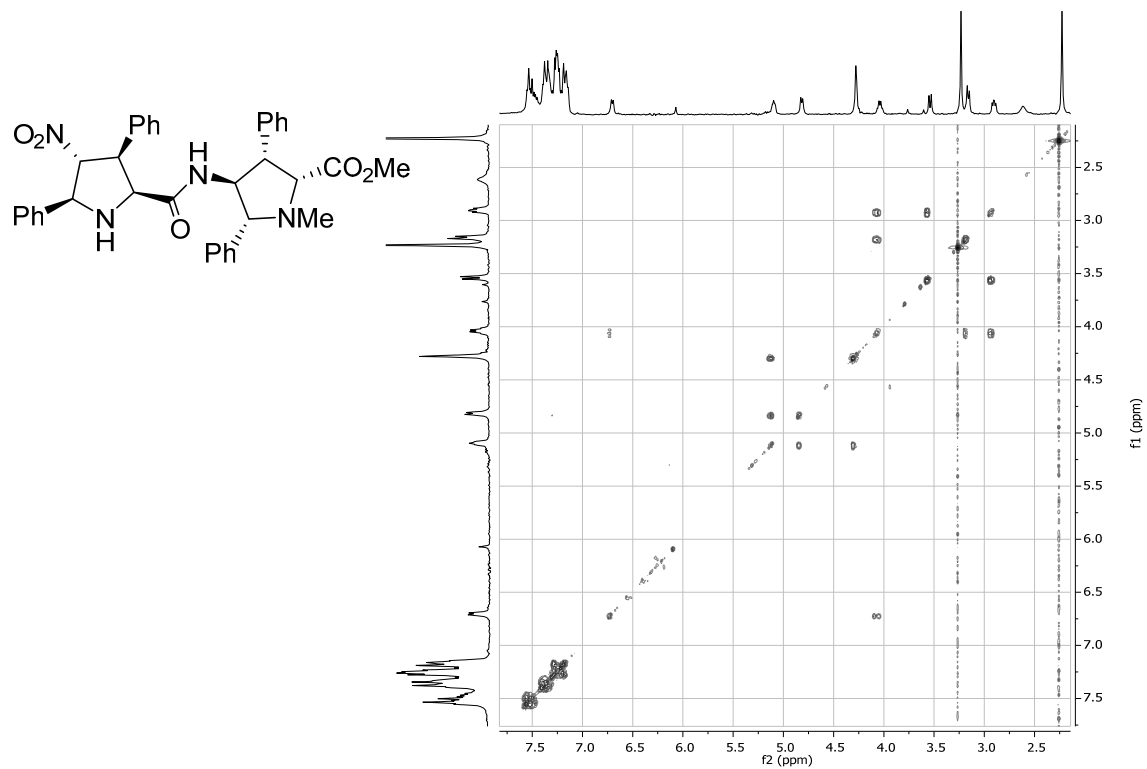


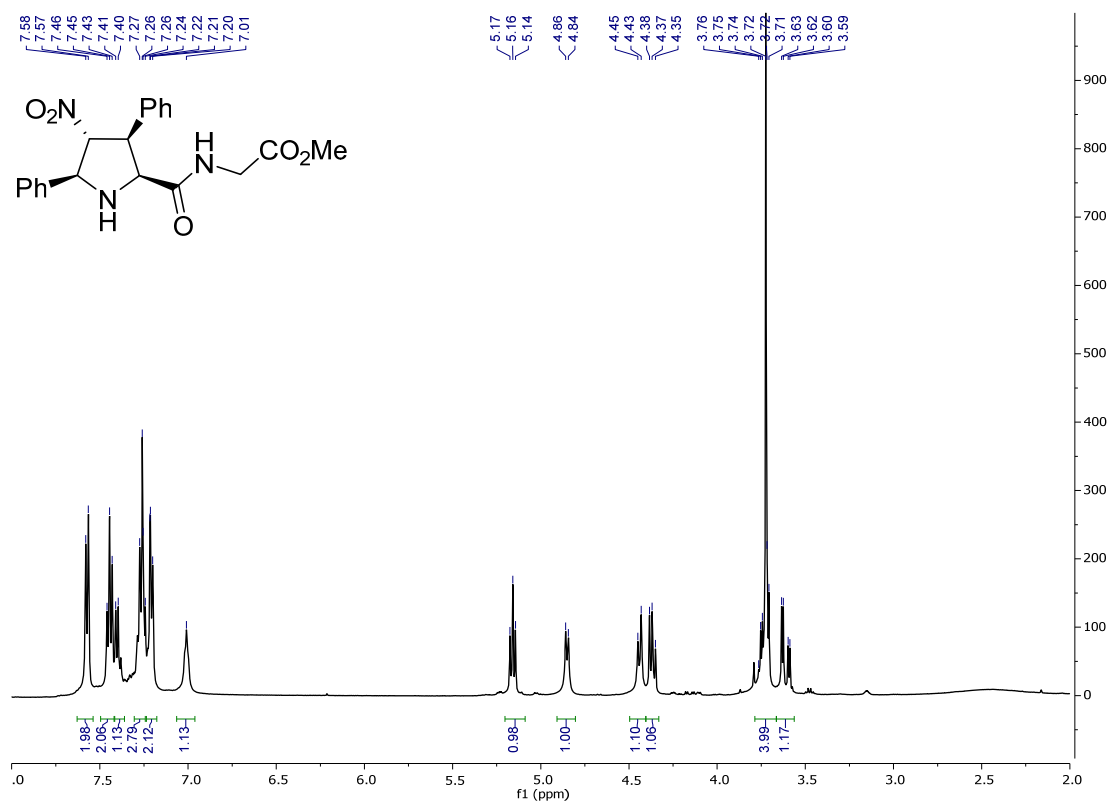
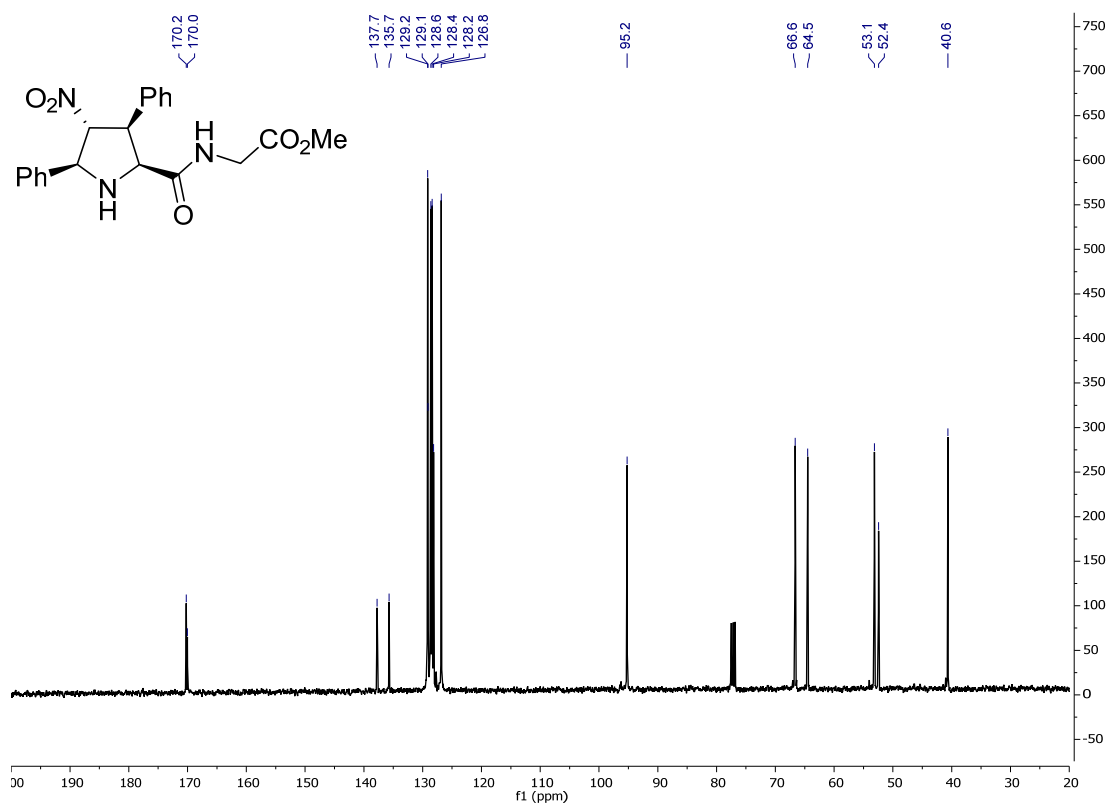
<sup>13</sup>C NMR (CDCl<sub>3</sub>)

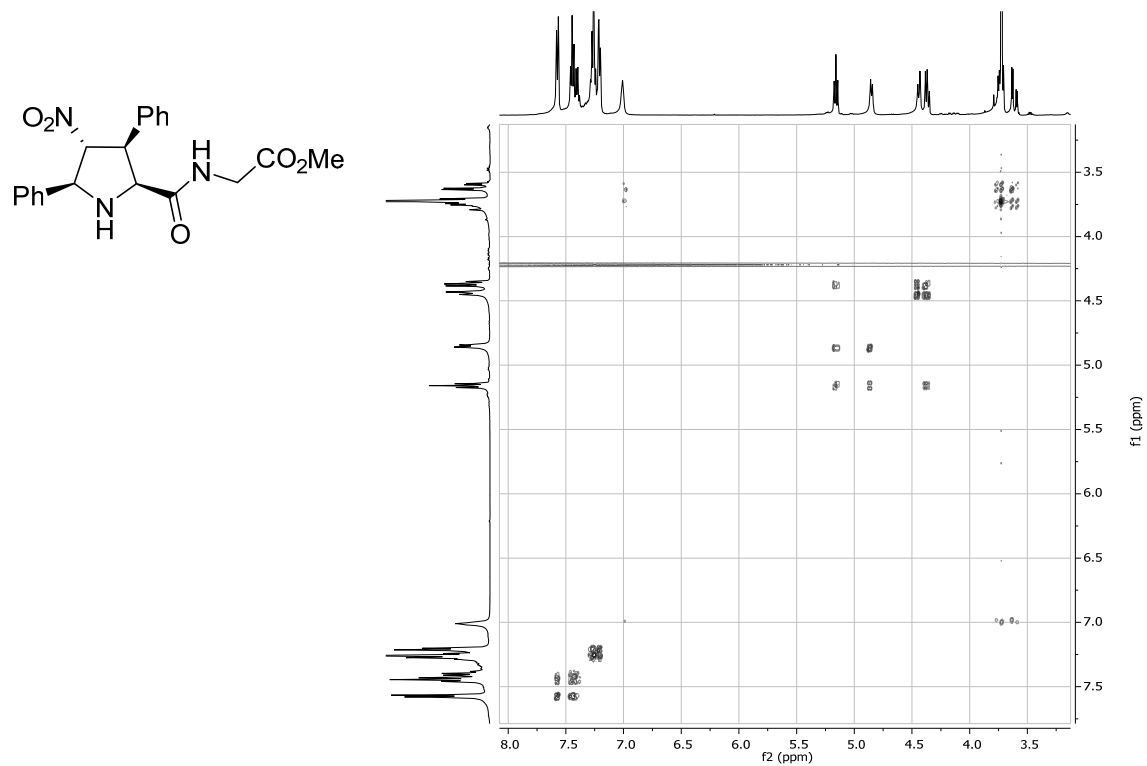


COSY (CDCl<sub>3</sub>)

Compound NO<sub>2</sub>-X<sub>L</sub>X<sub>D</sub>-OMe-25a<sup>1</sup>H NMR (CDCl<sub>3</sub>)<sup>13</sup>C NMR (CDCl<sub>3</sub>)

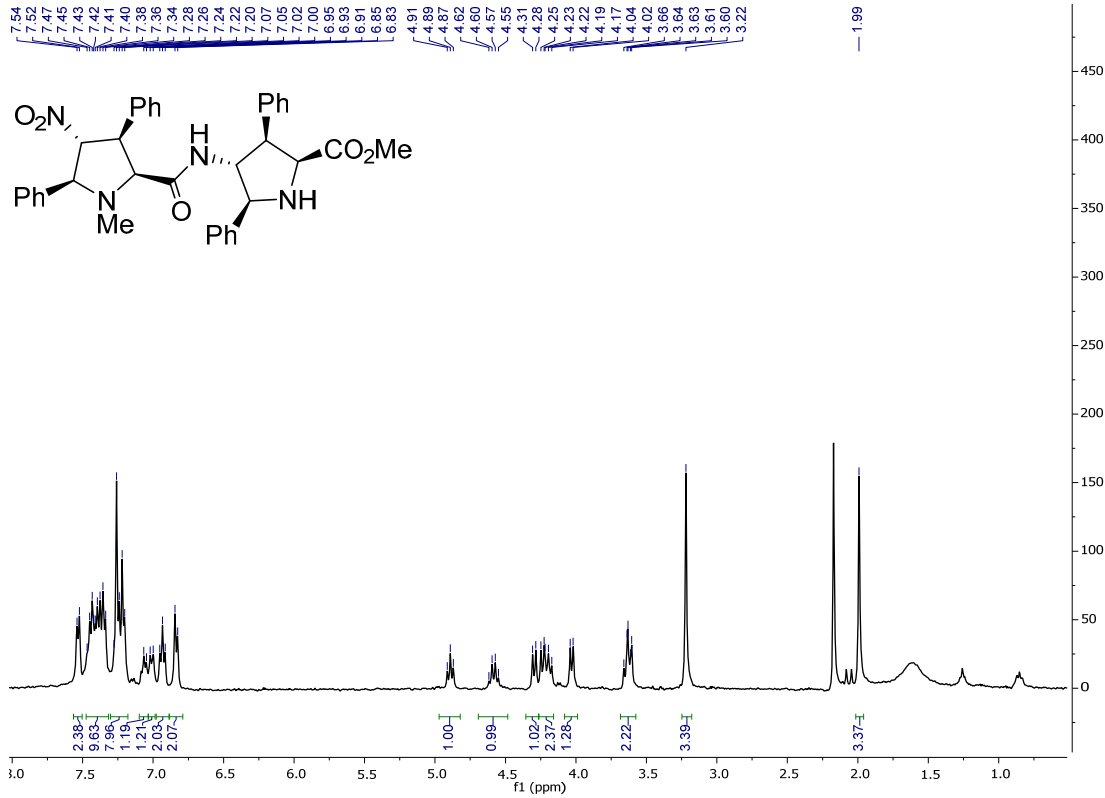
COSY (CDCl<sub>3</sub>)

Compound NO<sub>2</sub>-X<sub>L</sub>Gly-OMe-29<sup>1</sup>H NMR (CDCl<sub>3</sub>)<sup>13</sup>C NMR (CDCl<sub>3</sub>)

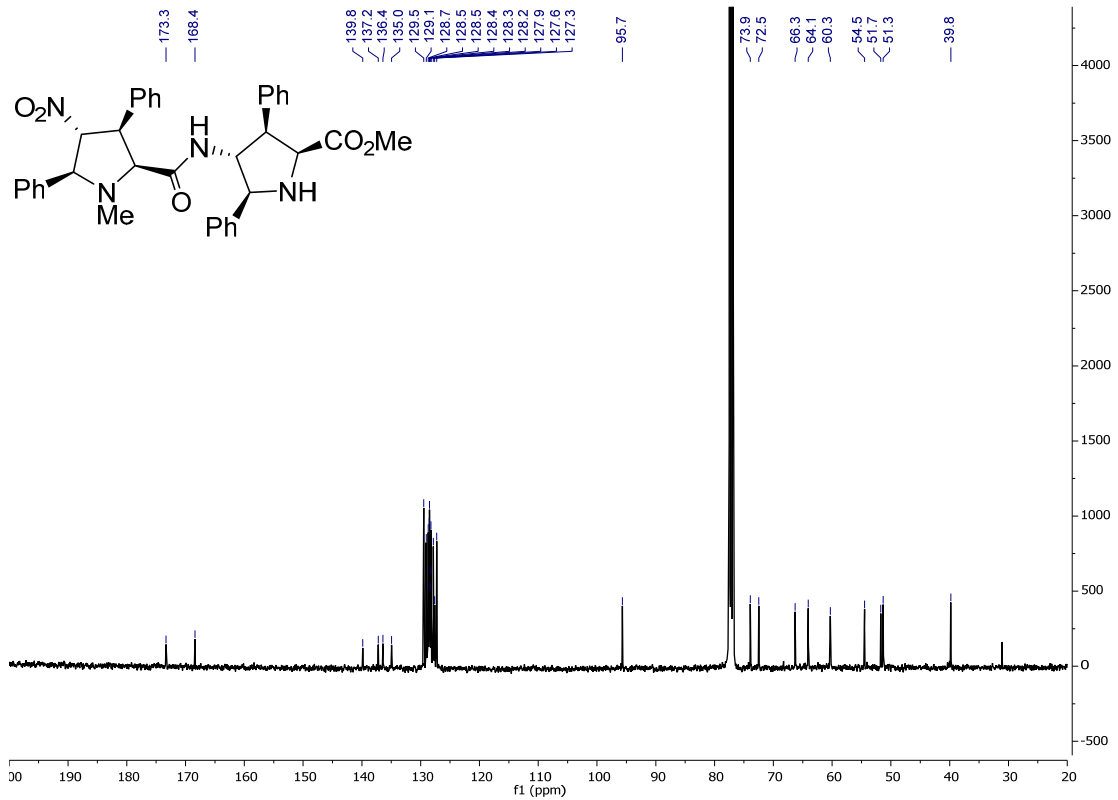
COSY (CDCl<sub>3</sub>)

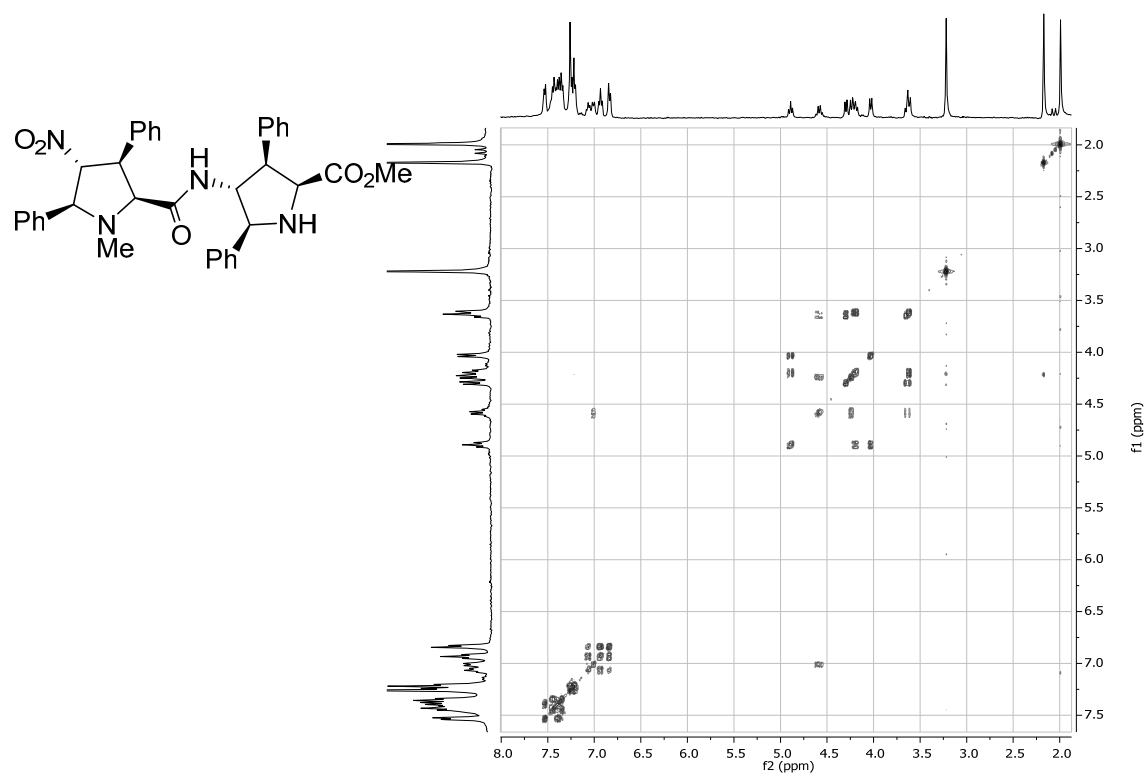
Compound NO<sub>2</sub>-X<sub>L</sub>X<sub>L</sub>-OMe-26a

<sup>1</sup>H NMR (CDCl<sub>3</sub>)



<sup>13</sup>C NMR (CDCl<sub>3</sub>)

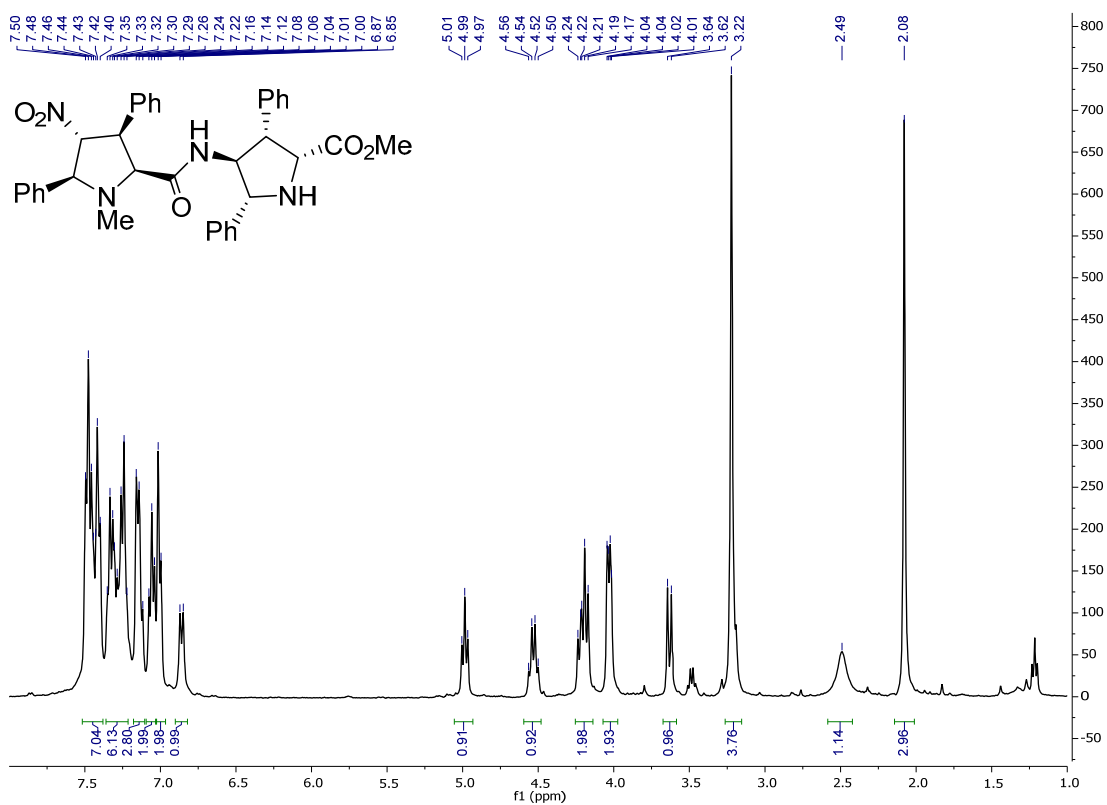


COSY (CDCl<sub>3</sub>)

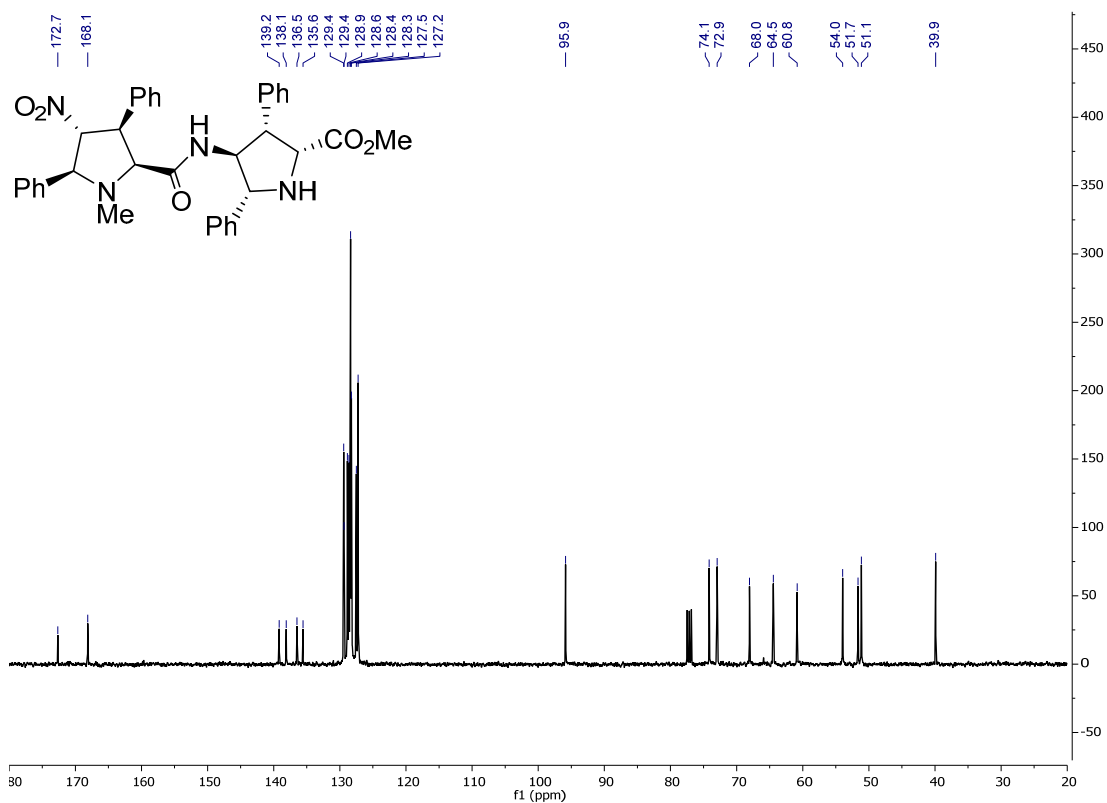


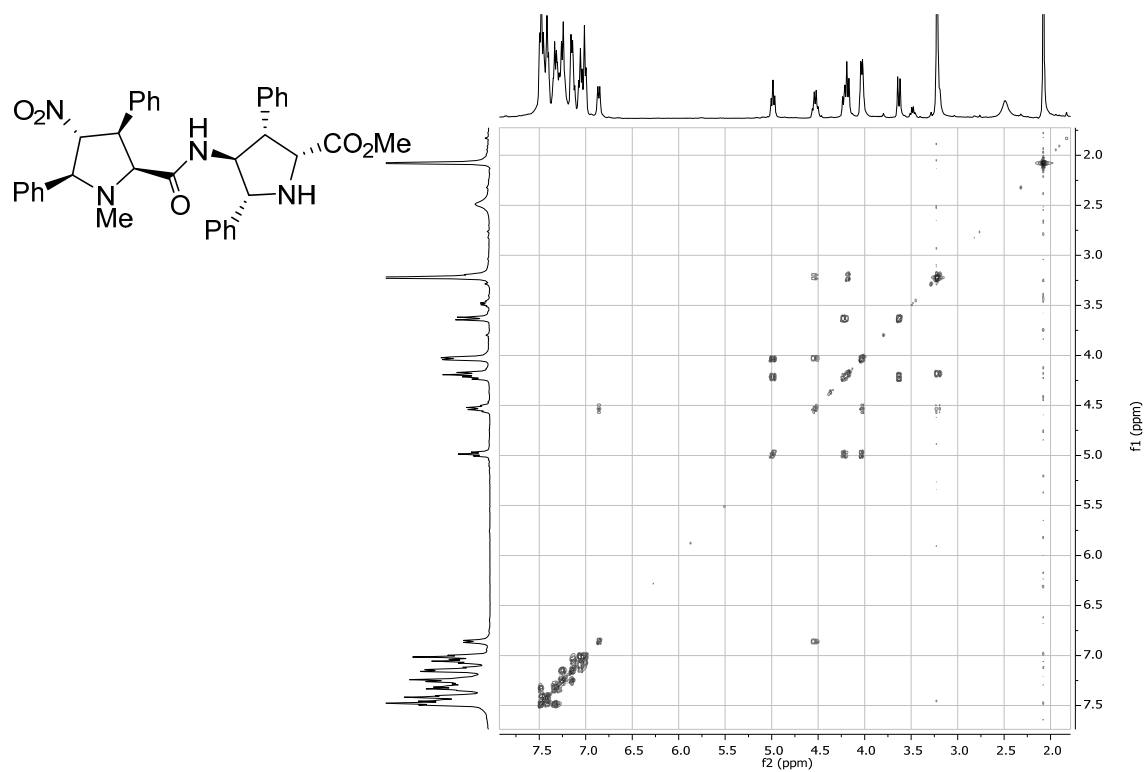
Compound NO<sub>2</sub>-X<sub>L</sub>X<sub>d</sub>-OMe-26a

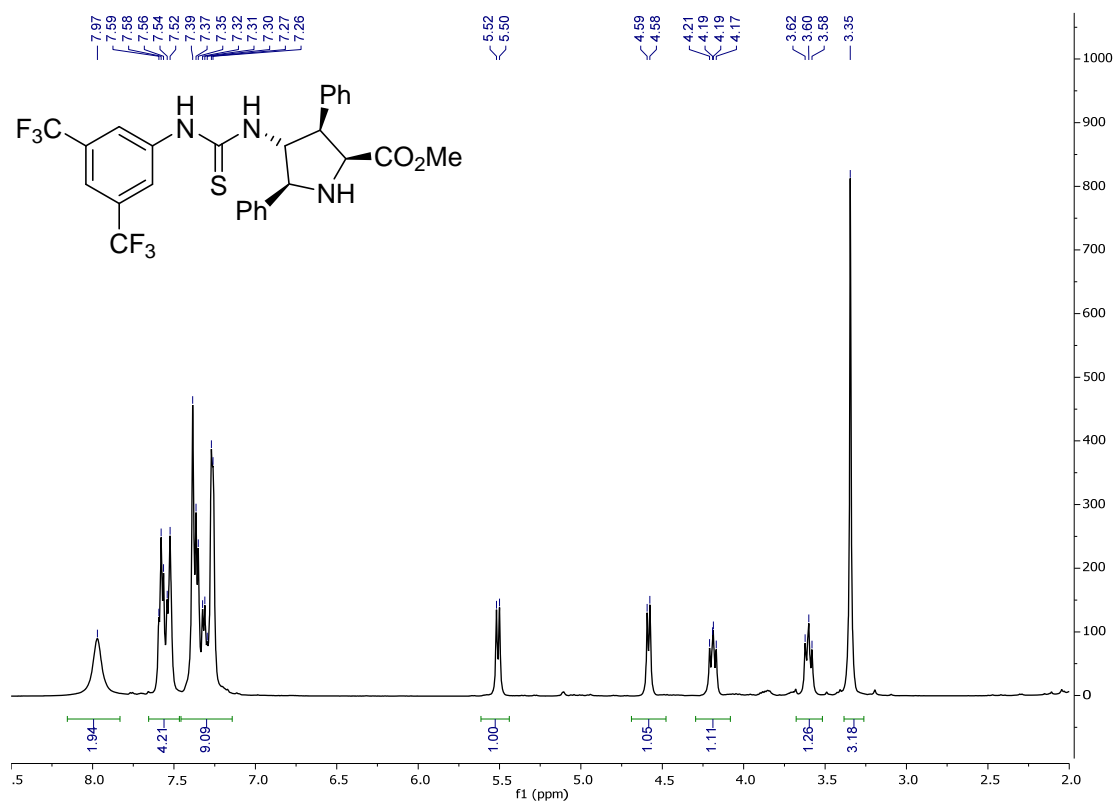
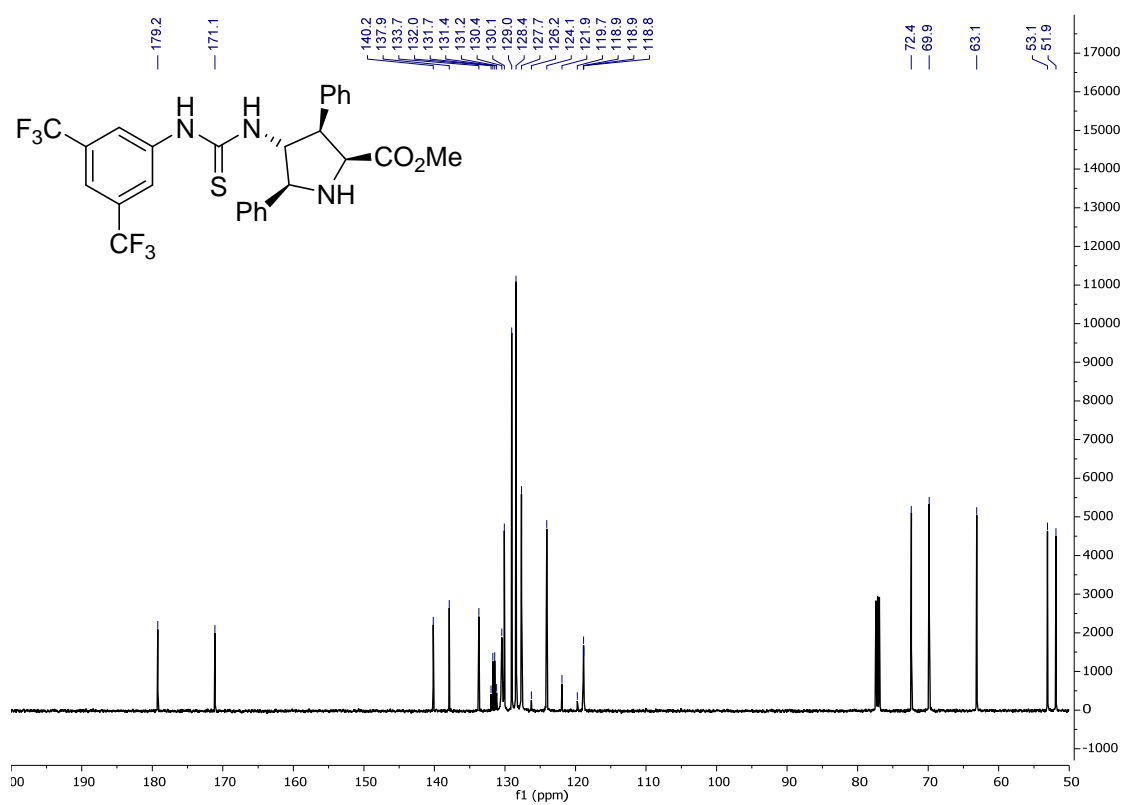
<sup>1</sup>H NMR (CDCl<sub>3</sub>)

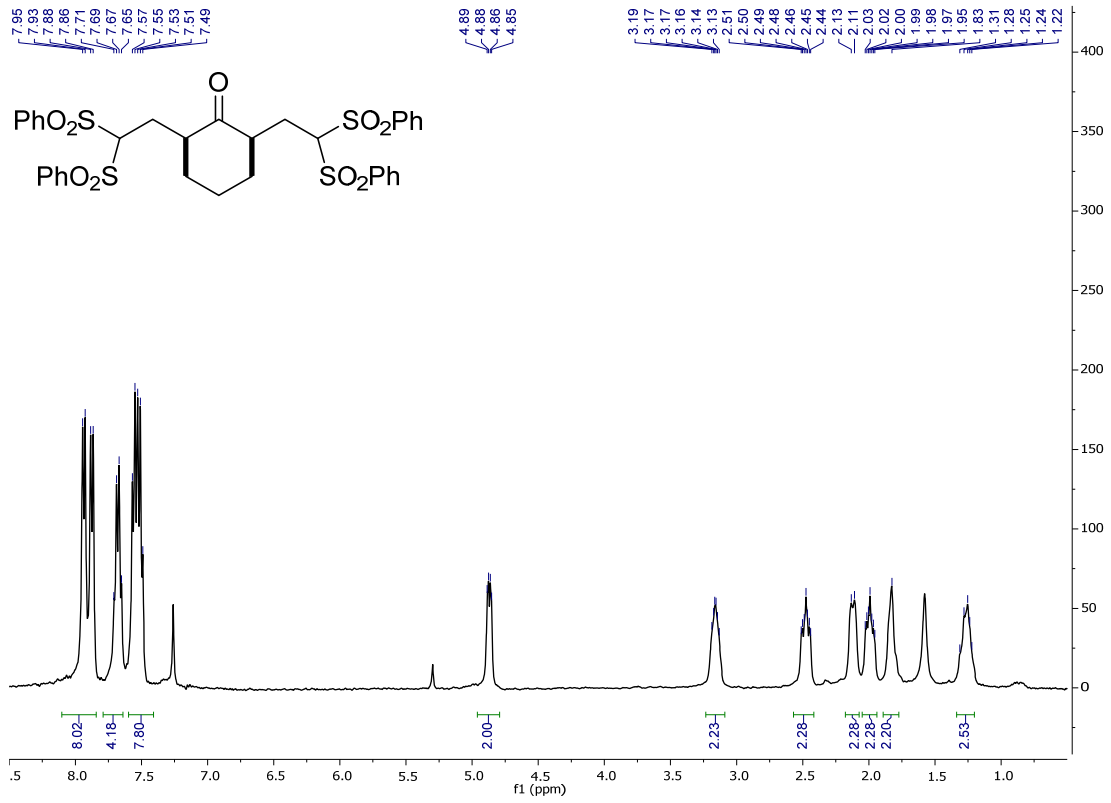
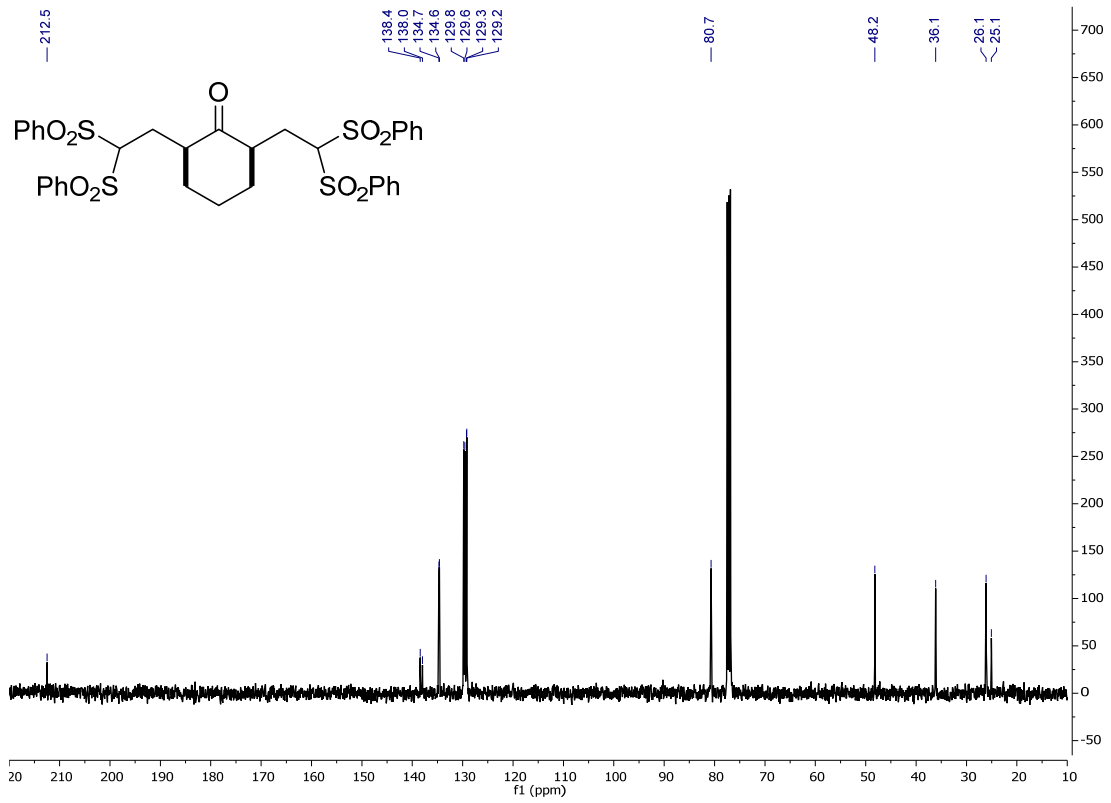


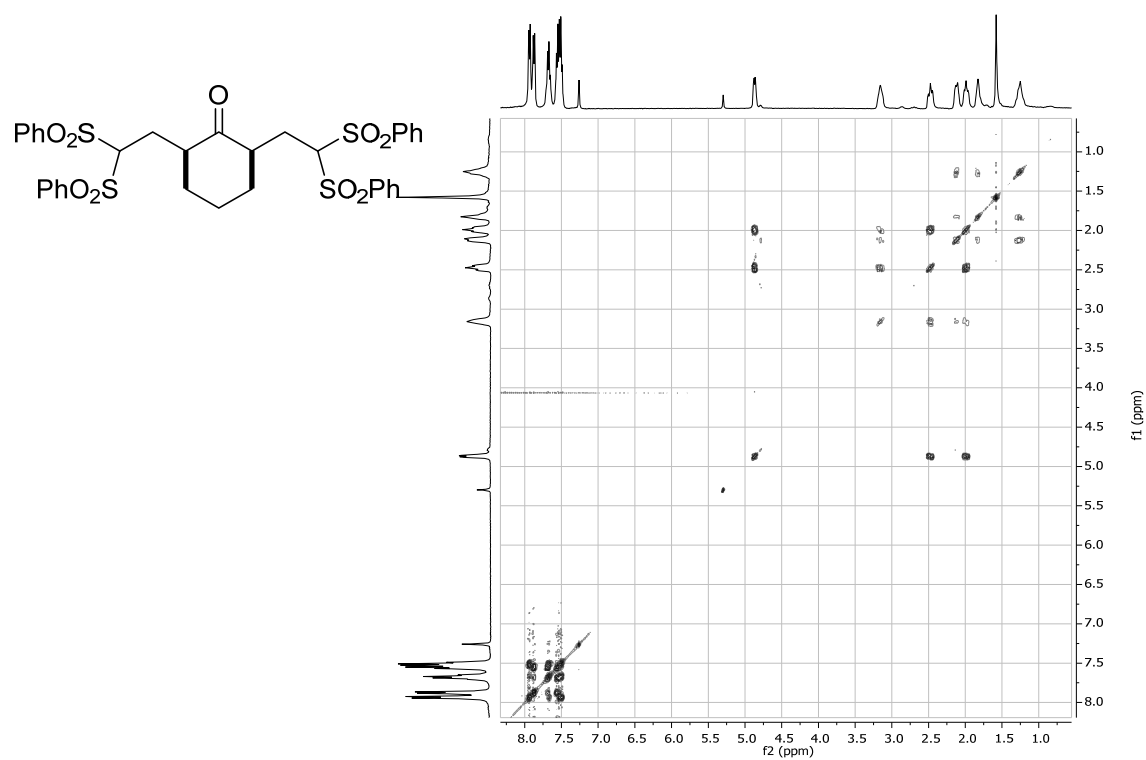
<sup>13</sup>C NMR (CDCl<sub>3</sub>)



COSY (CDCl<sub>3</sub>)

Compound **28** $^1\text{H}$  NMR ( $\text{CDCl}_3$ ) $^{13}\text{C}$  NMR ( $\text{CDCl}_3$ )

Compound **16bis** $^1\text{H}$  NMR ( $\text{CDCl}_3$ ) $^{13}\text{C}$  NMR ( $\text{CDCl}_3$ )

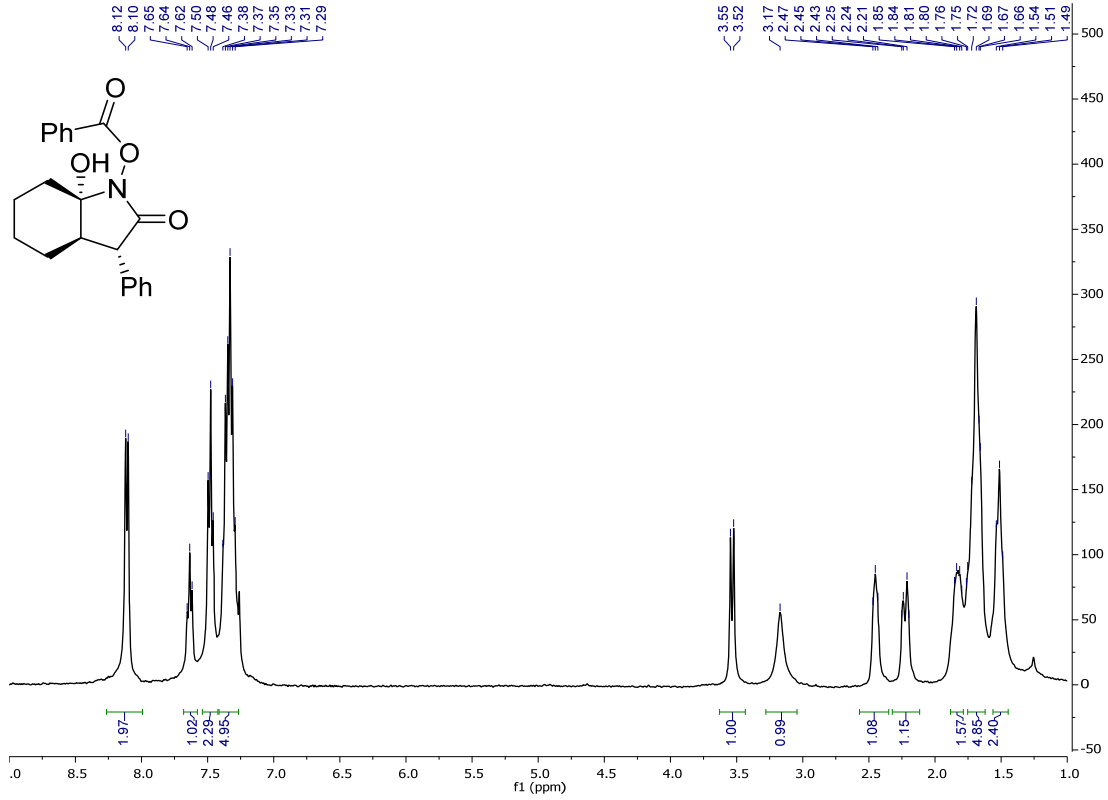
COSY (CDCl<sub>3</sub>)



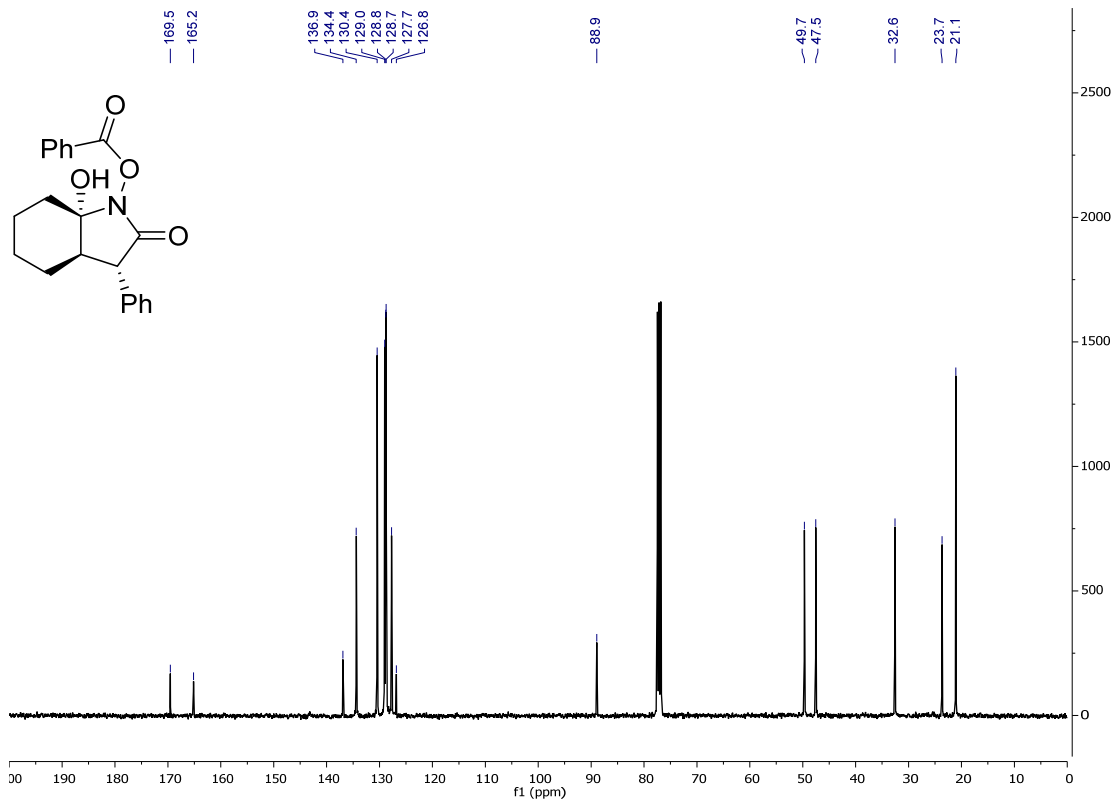
## Annex I-c. NMR spectra selection for Chapter 4

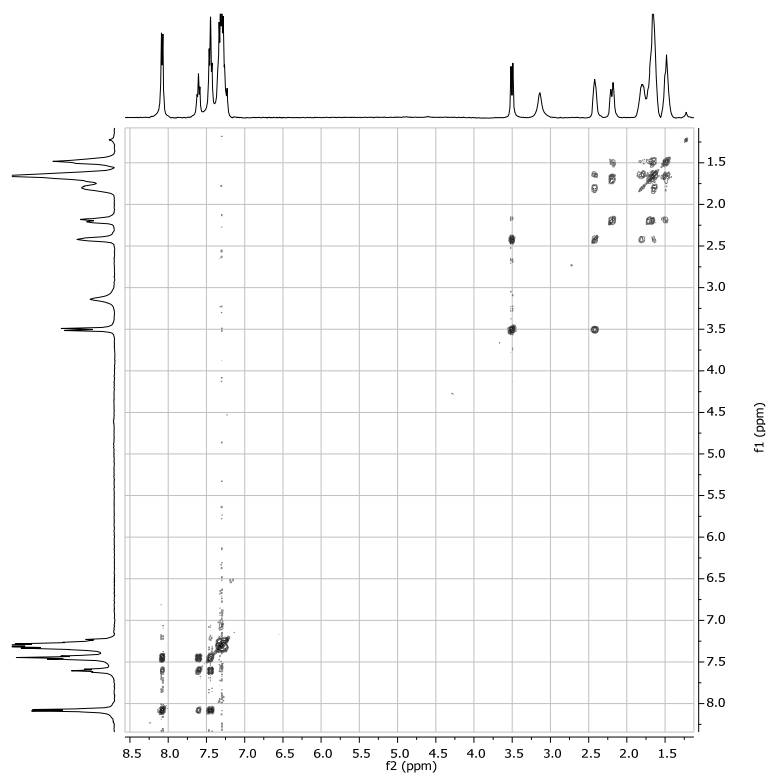
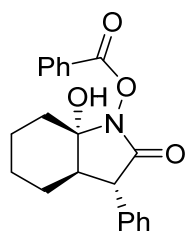
Compound **24aaa**

$^1\text{H}$  NMR ( $\text{CDCl}_3$ )



$^{13}\text{C}$  NMR ( $\text{CDCl}_3$ )

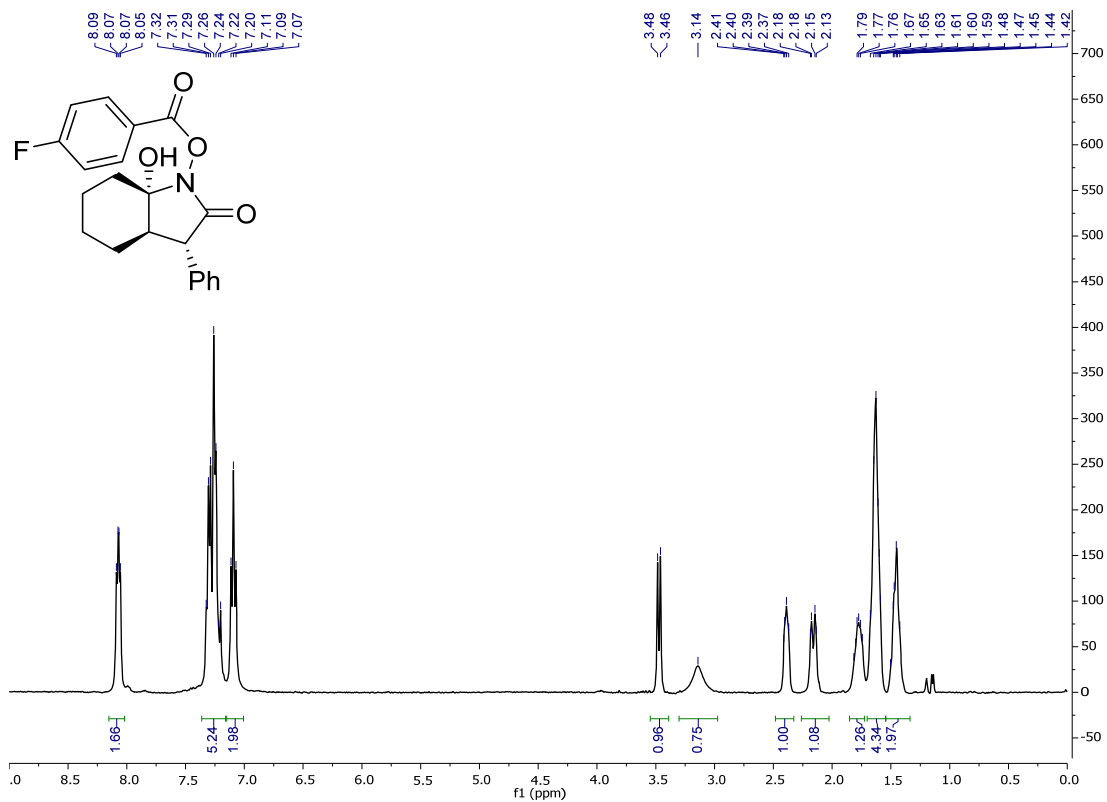


COSY (CDCl<sub>3</sub>)

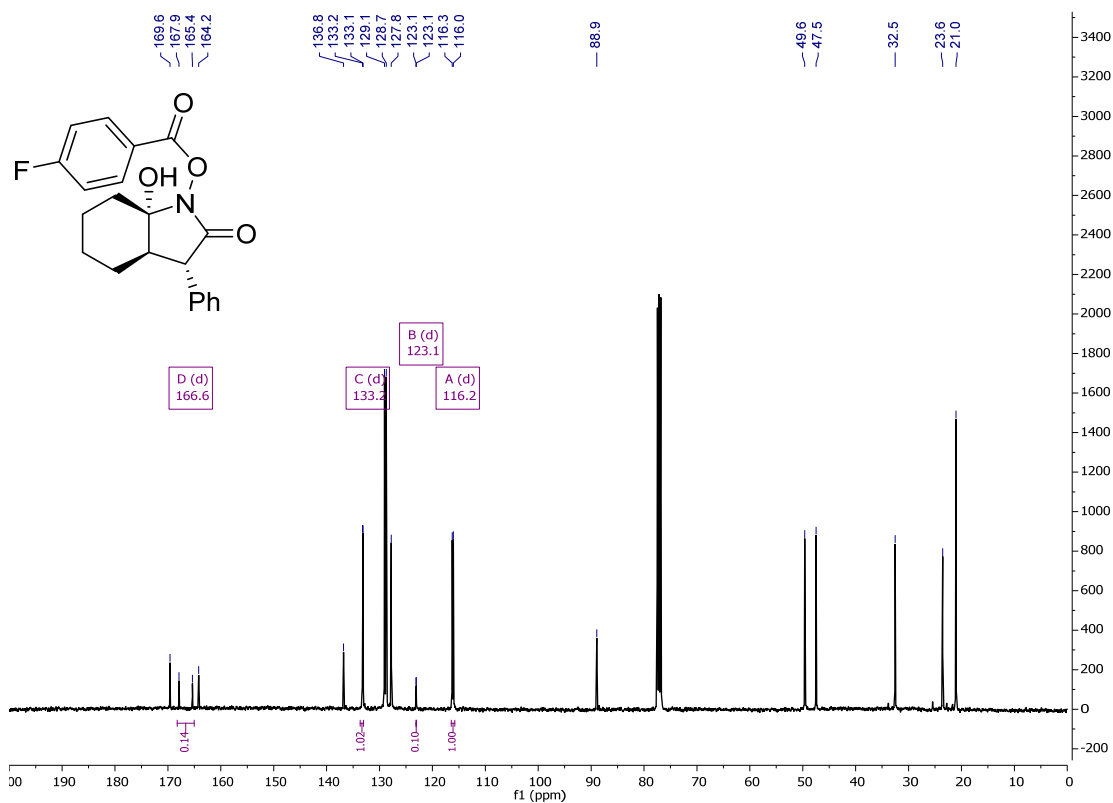


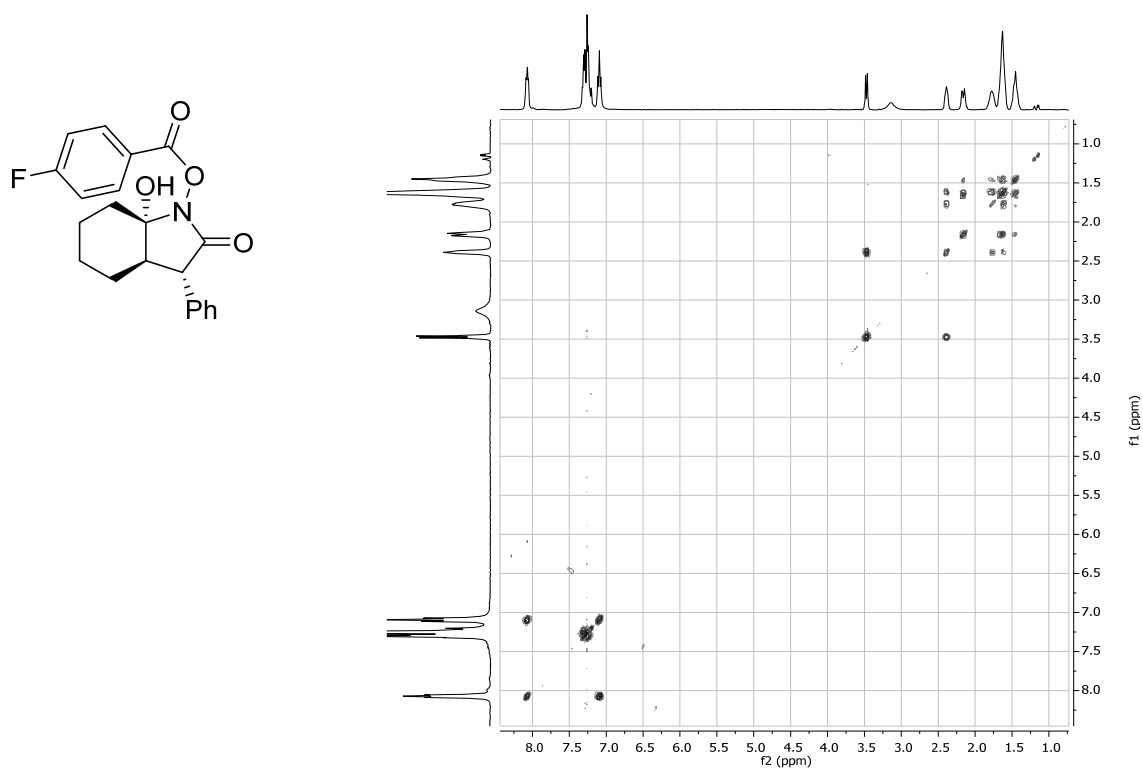
Compound **24aab**

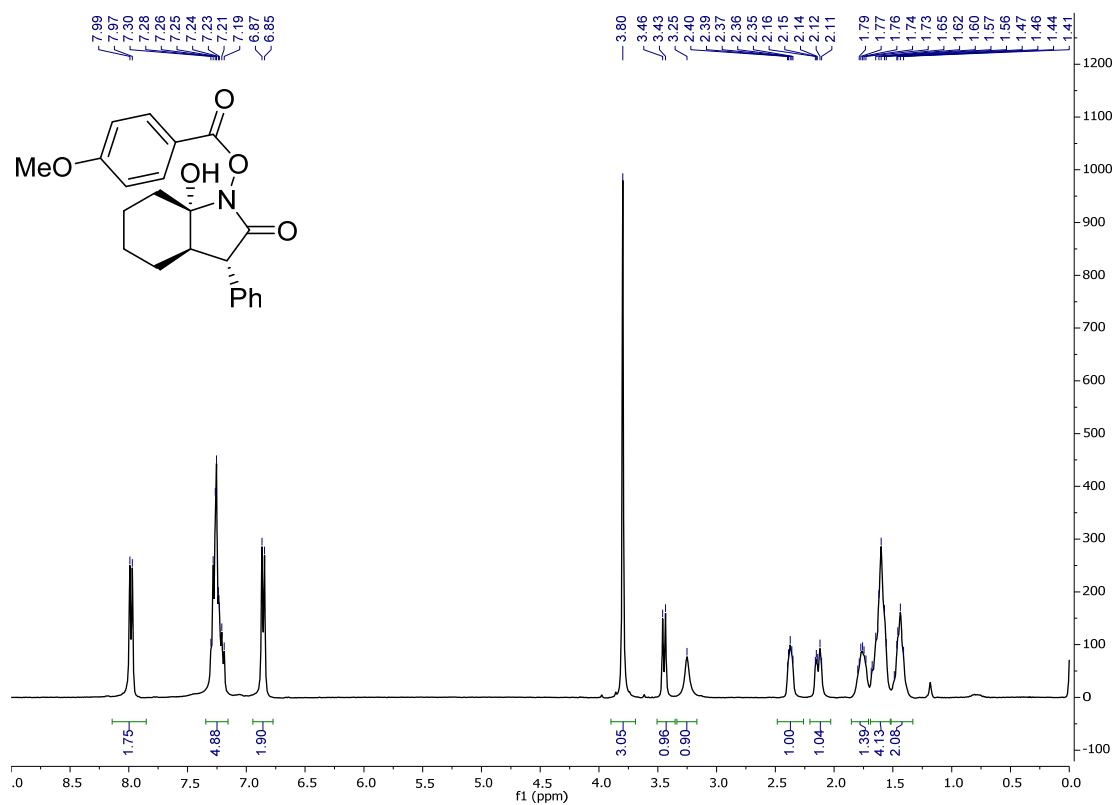
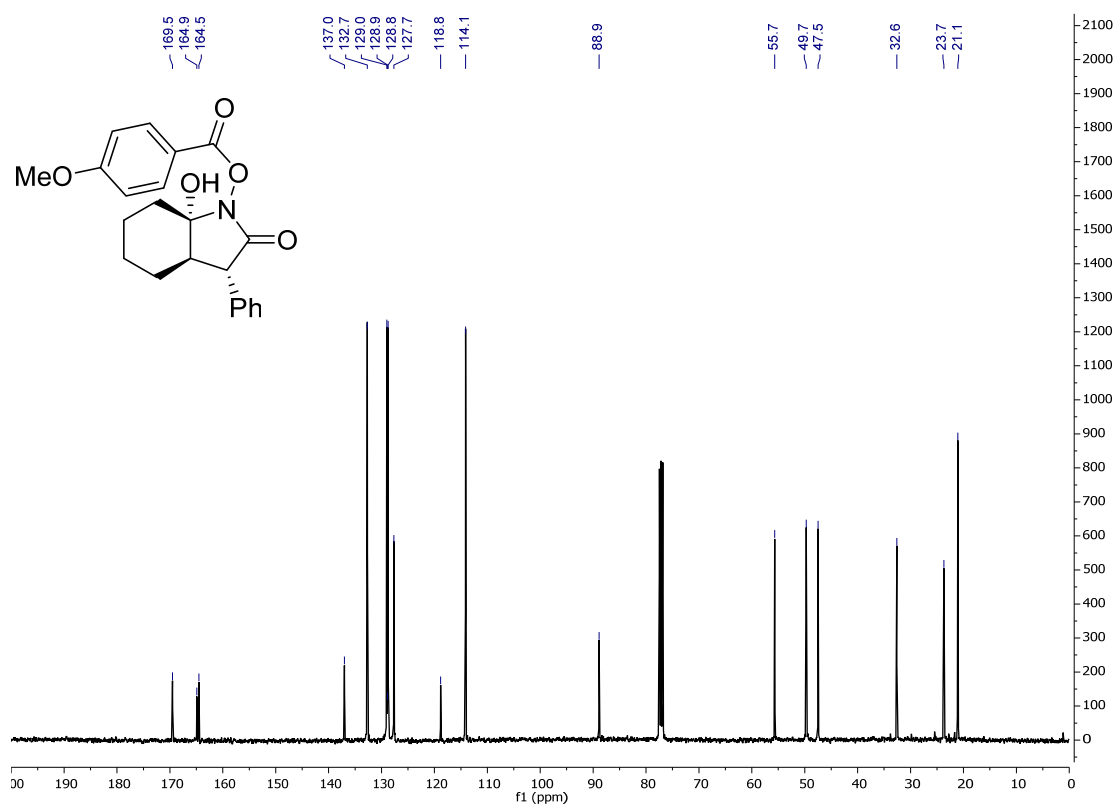
$^1\text{H}$  NMR ( $\text{CDCl}_3$ )

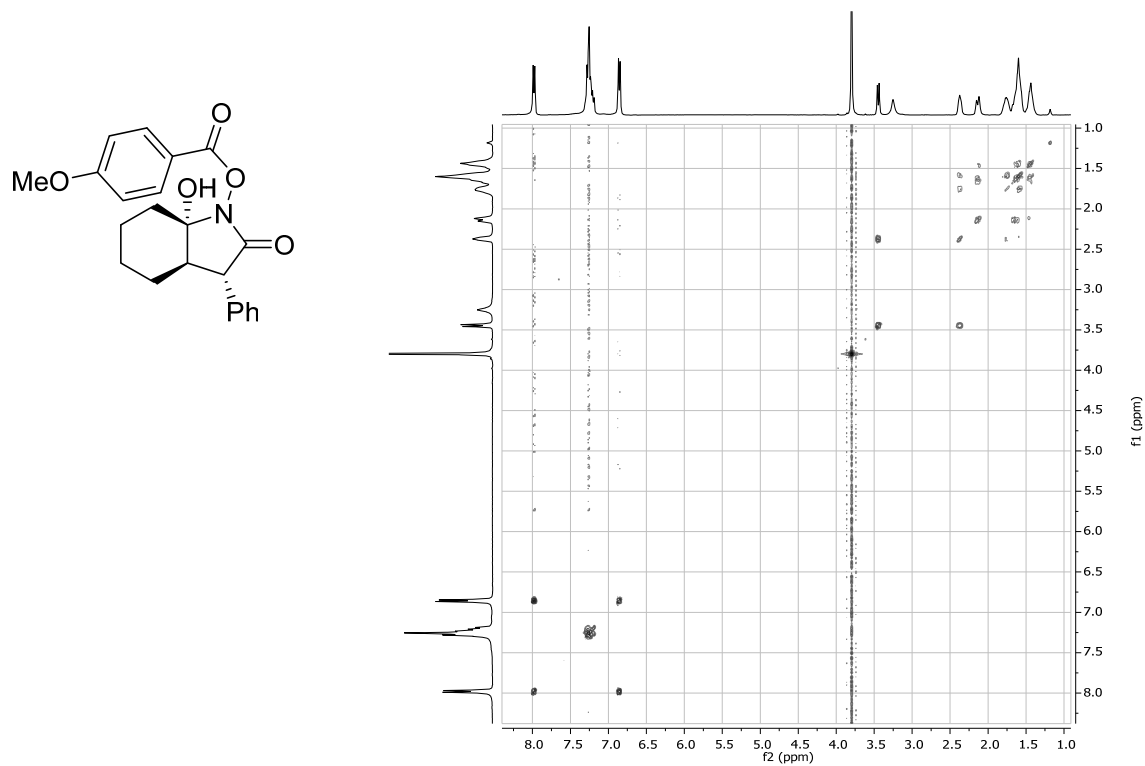


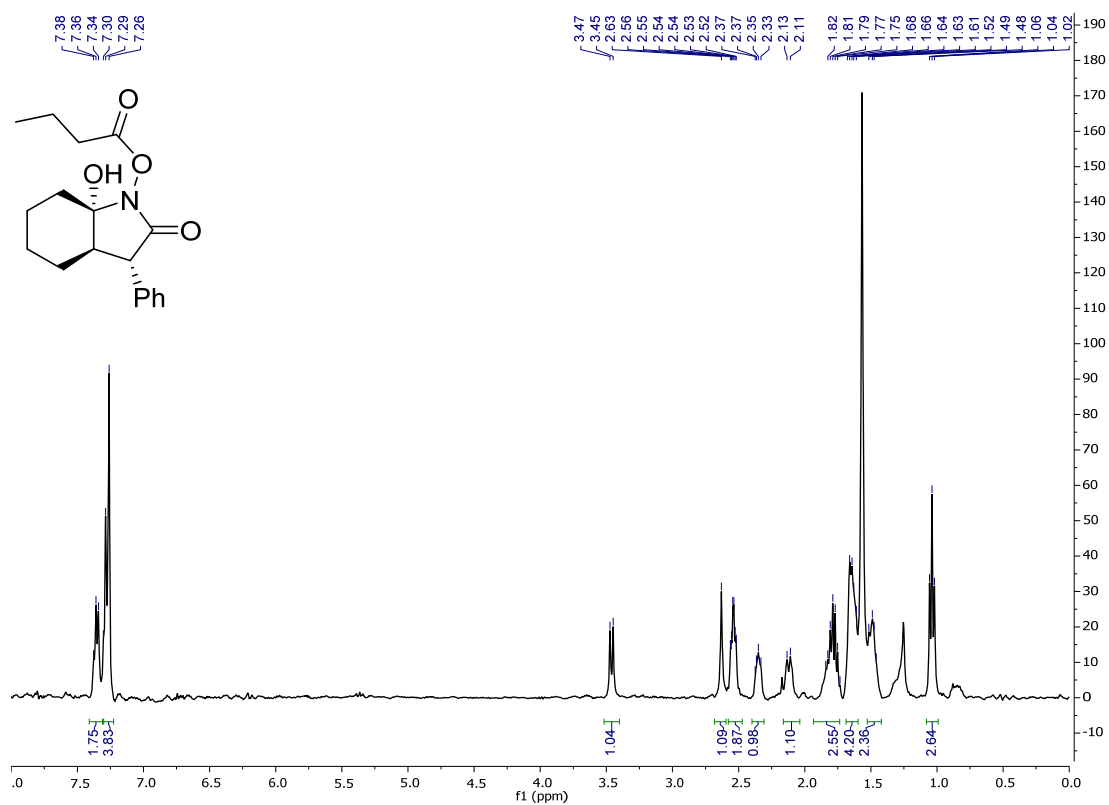
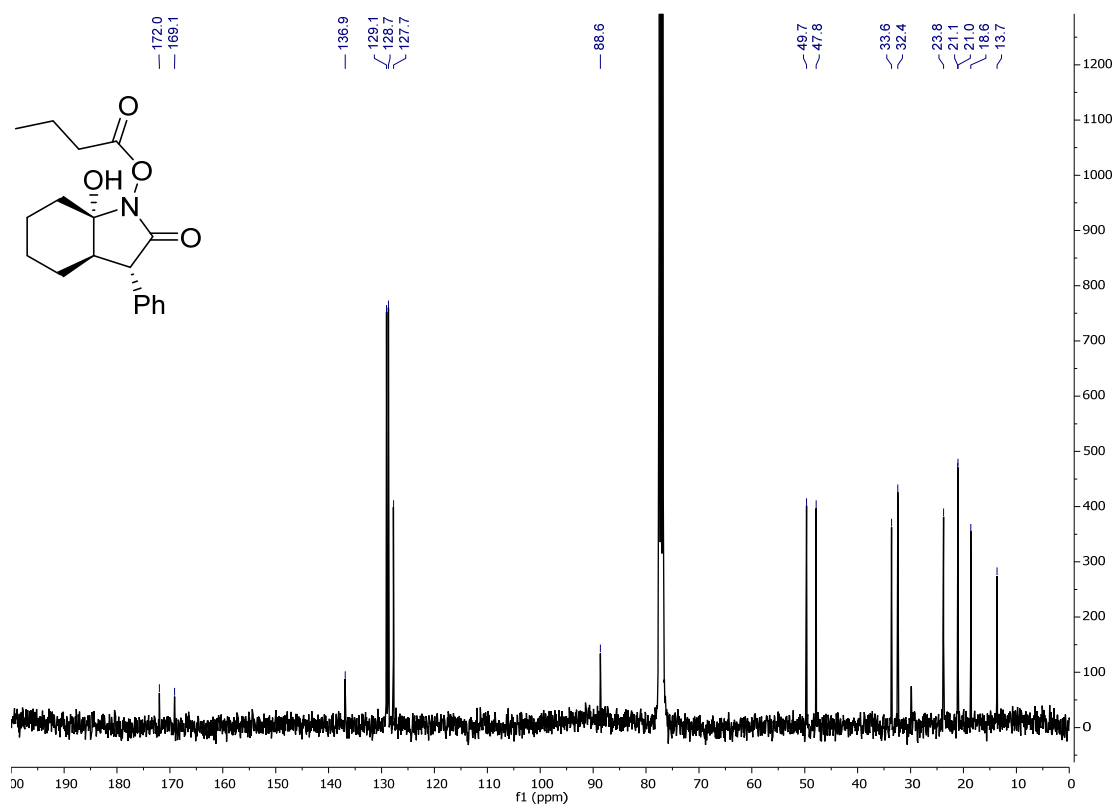
$^{13}\text{C}$  NMR ( $\text{CDCl}_3$ )

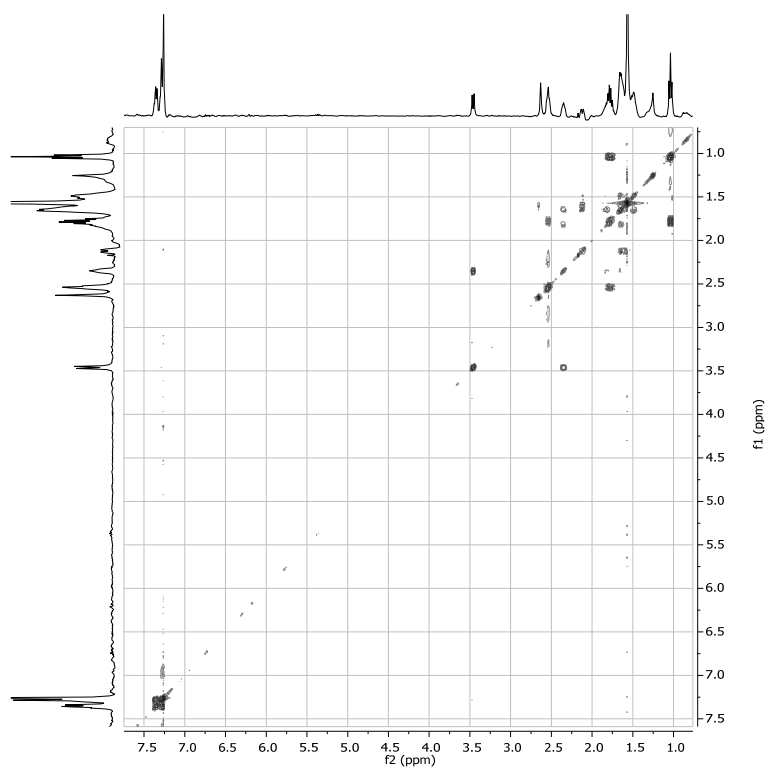
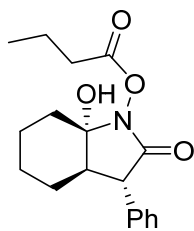


COSY (CDCl<sub>3</sub>)

Compound **24aac** $^1\text{H}$  NMR ( $\text{CDCl}_3$ ) $^{13}\text{C}$  NMR ( $\text{CDCl}_3$ )

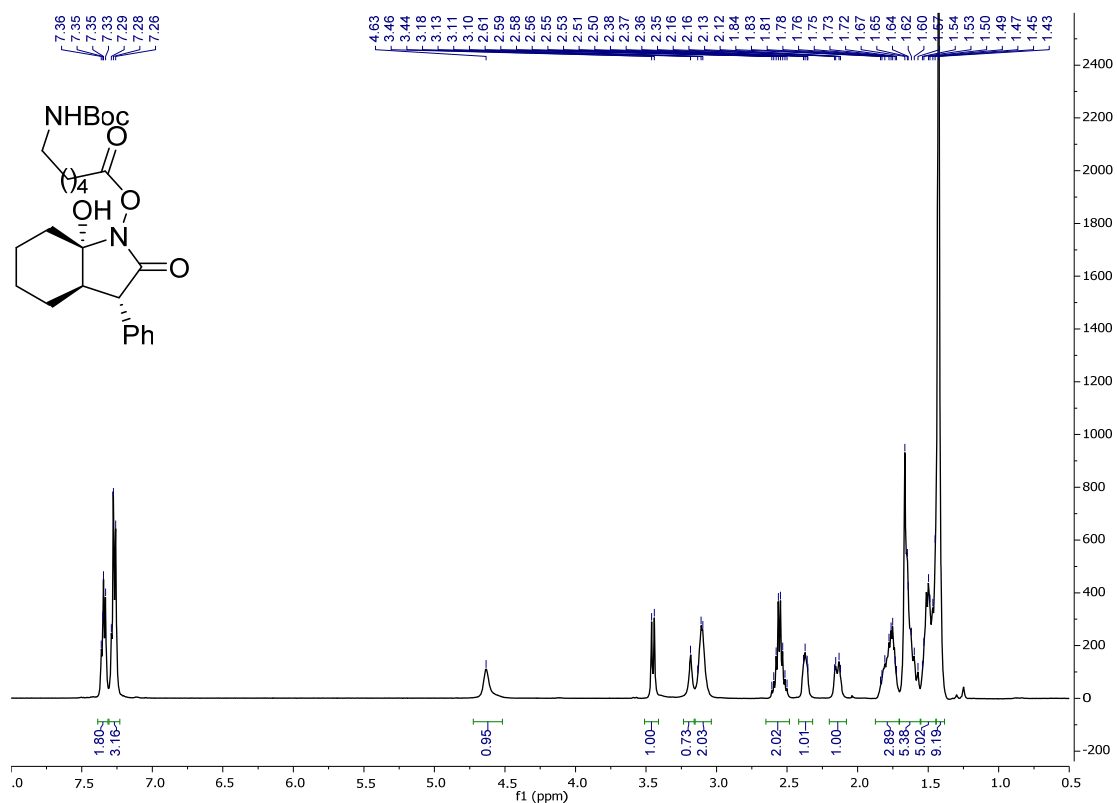
COSY (CDCl<sub>3</sub>)

Compound **24aad** $^1\text{H}$  NMR ( $\text{CDCl}_3$ ) $^{13}\text{C}$  NMR ( $\text{CDCl}_3$ )

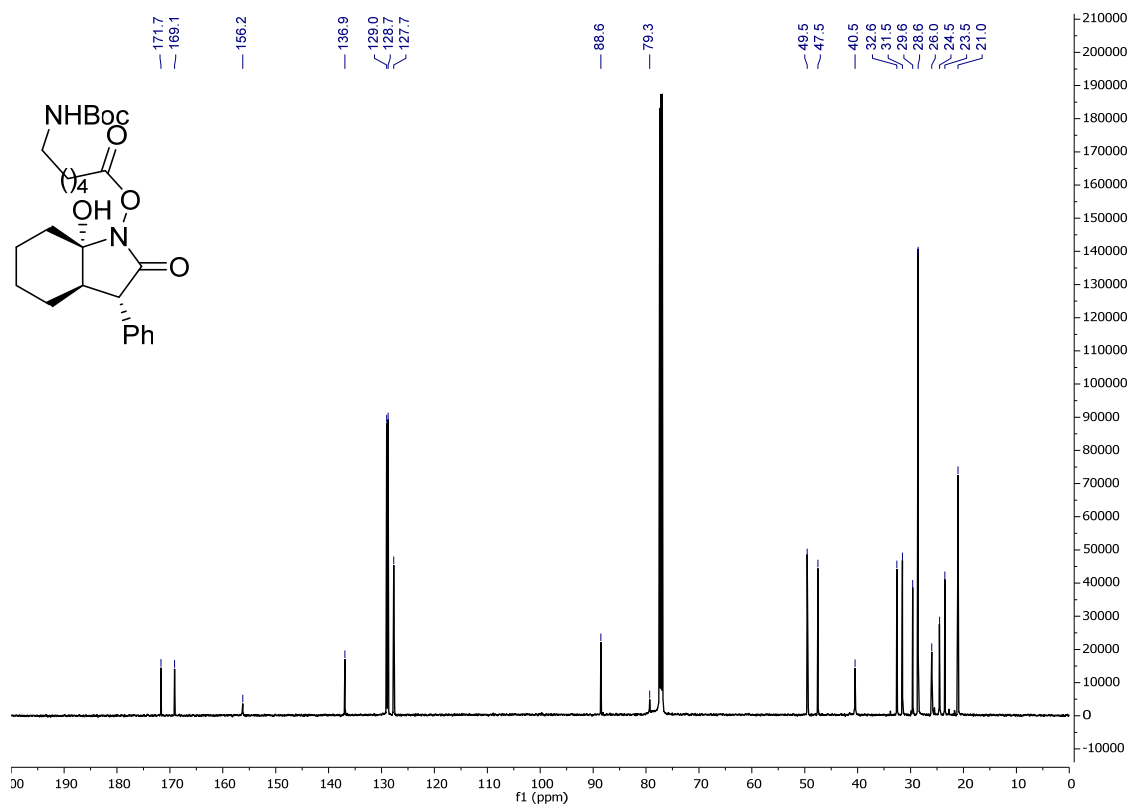
COSY (CDCl<sub>3</sub>)

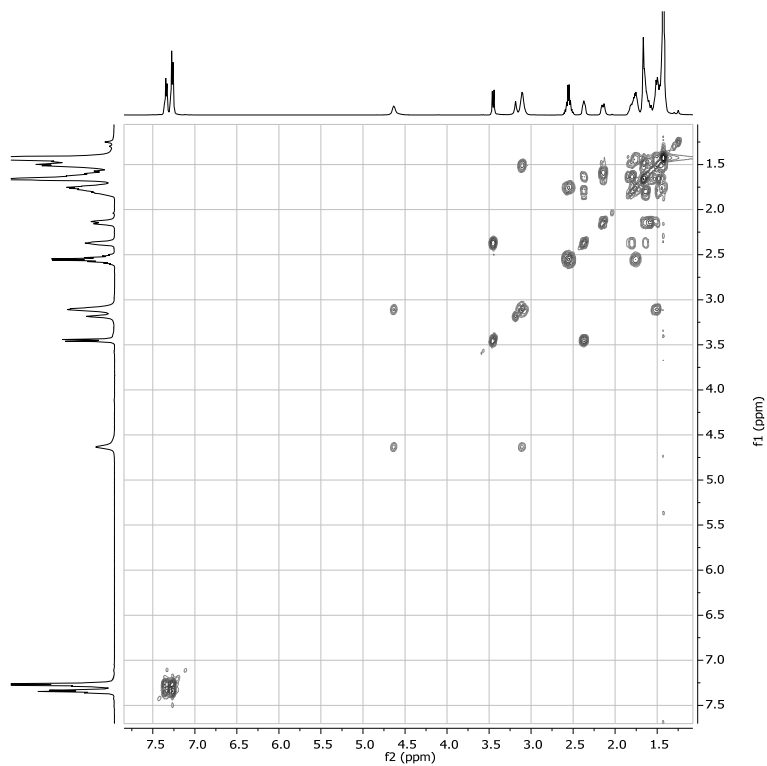
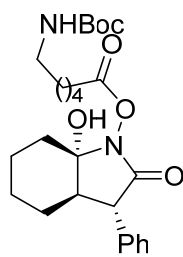
Compound **24aae**

$^1\text{H}$  NMR ( $\text{CDCl}_3$ )

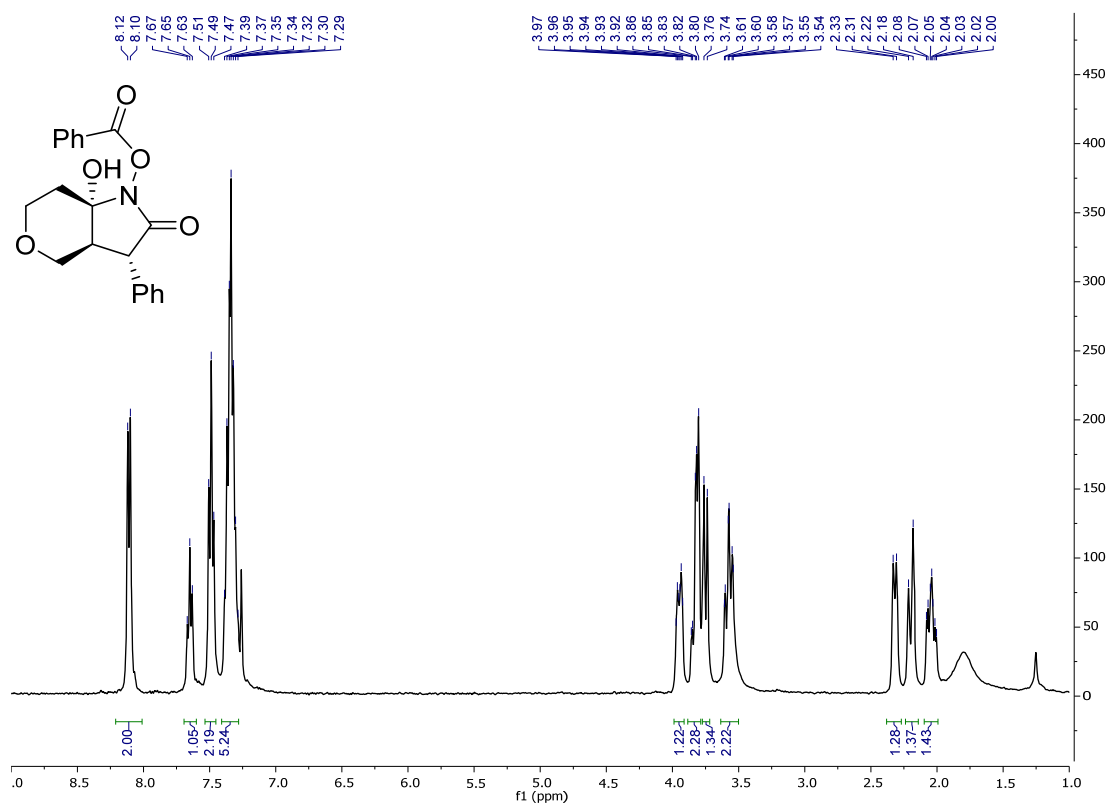
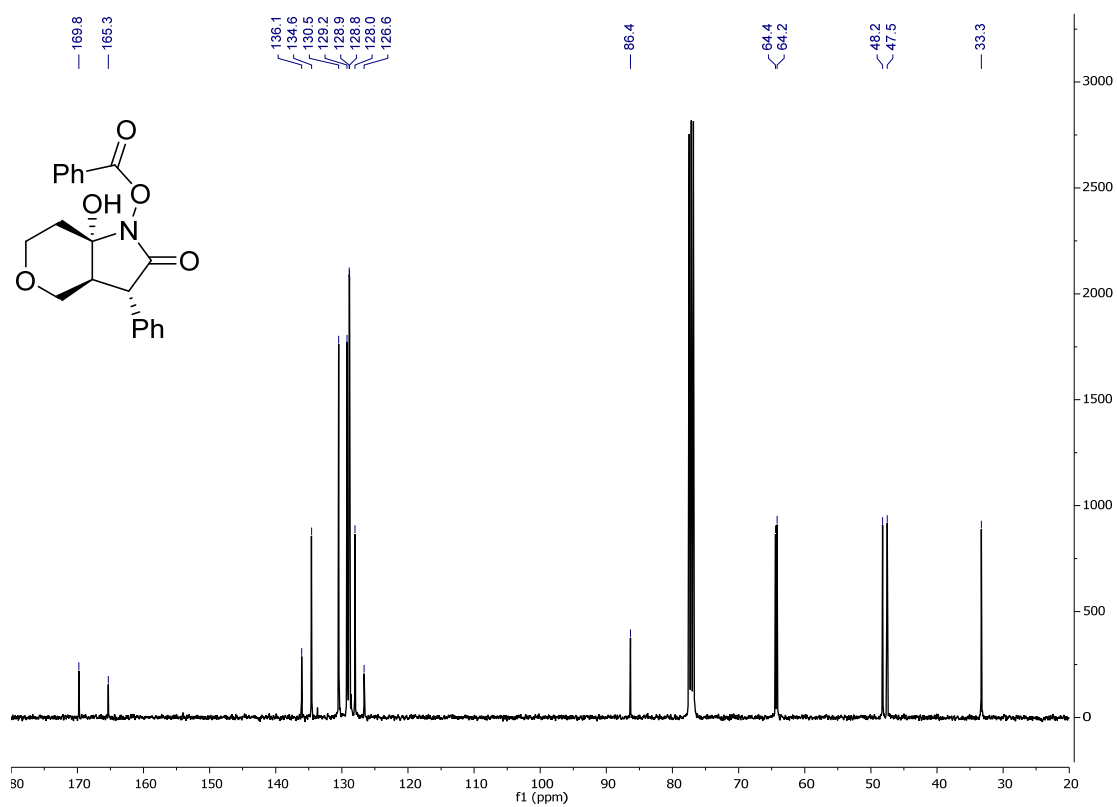


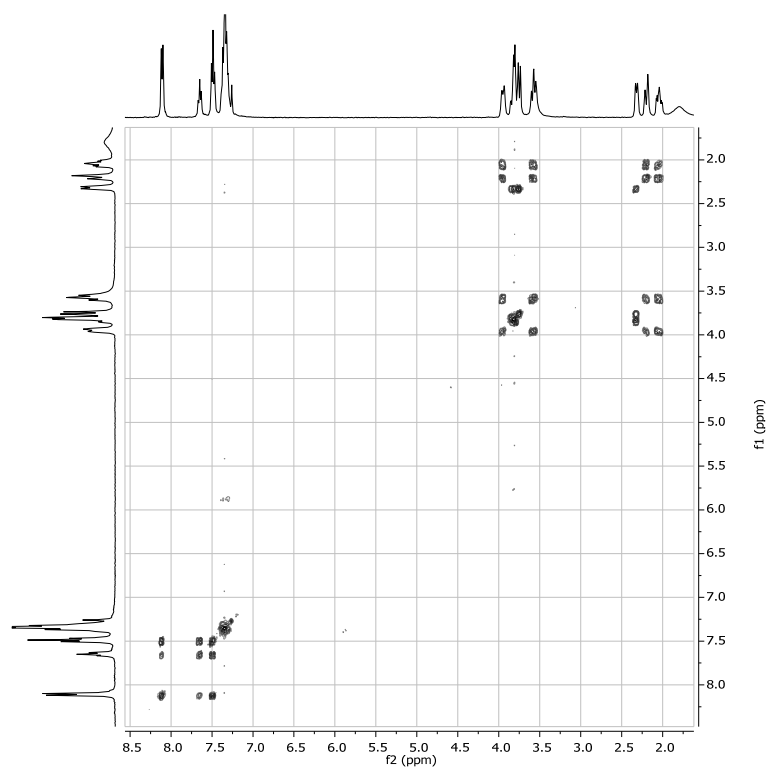
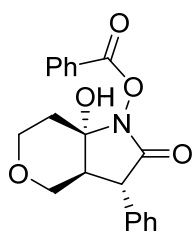
$^{13}\text{C}$  NMR ( $\text{CDCl}_3$ )

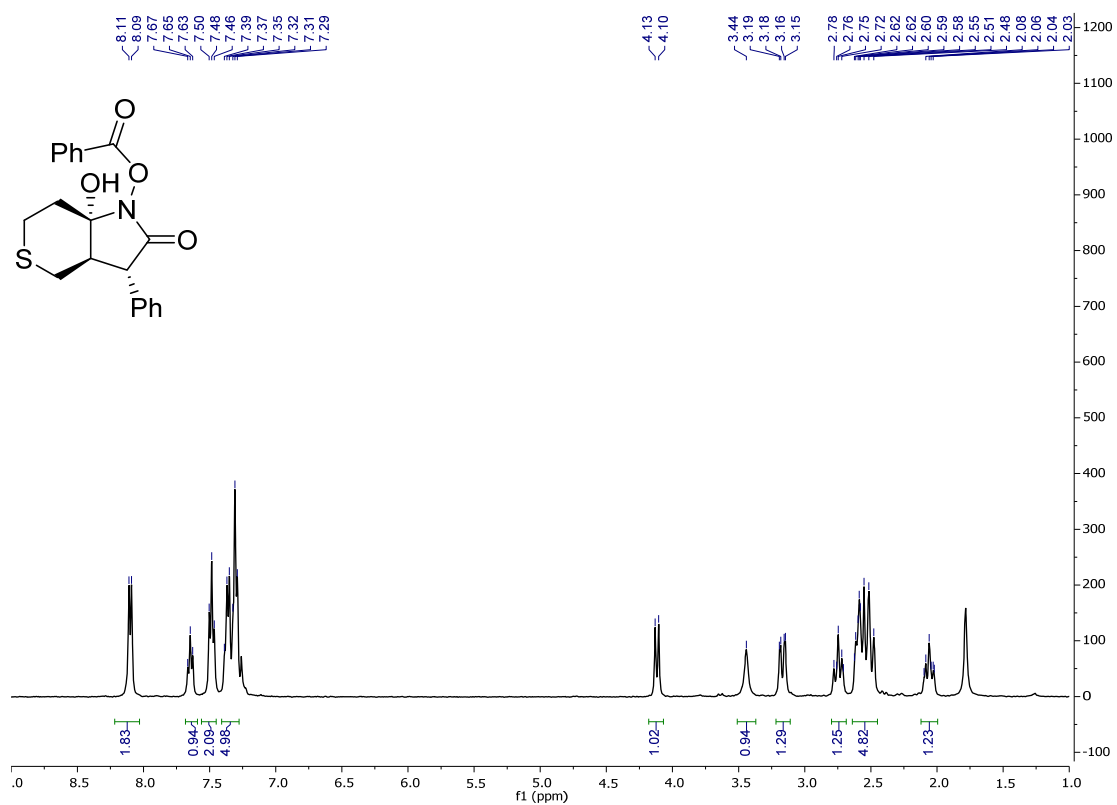
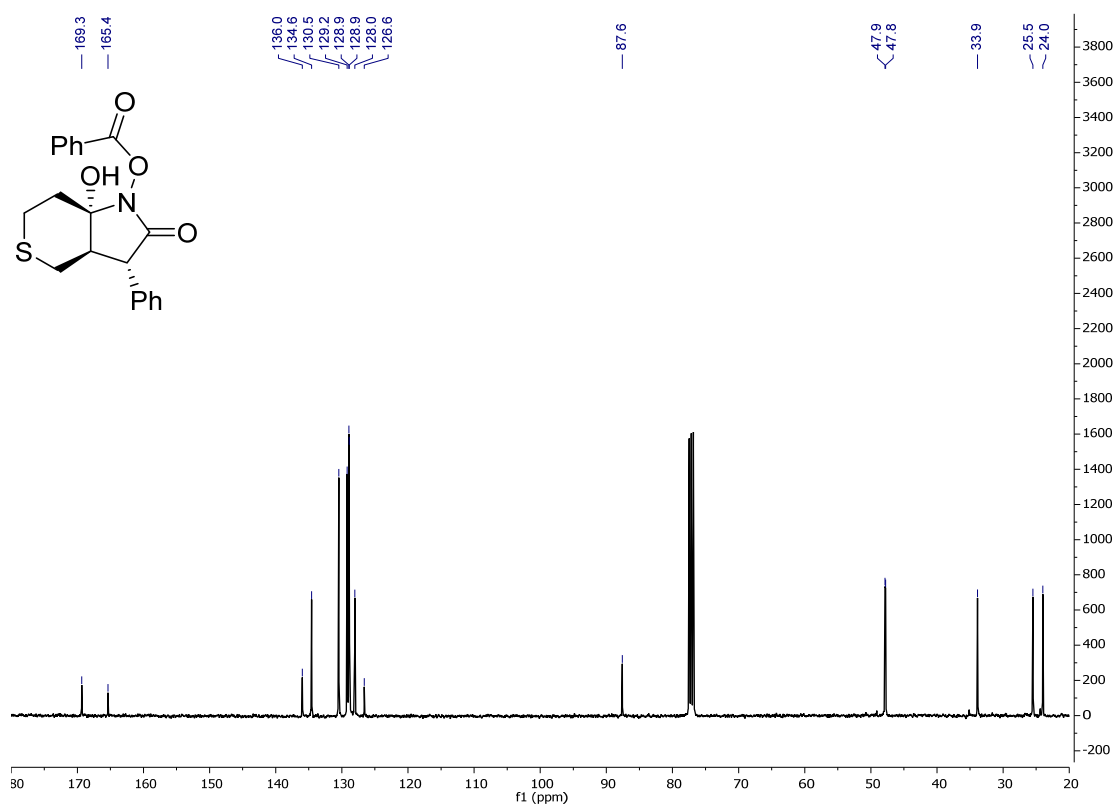


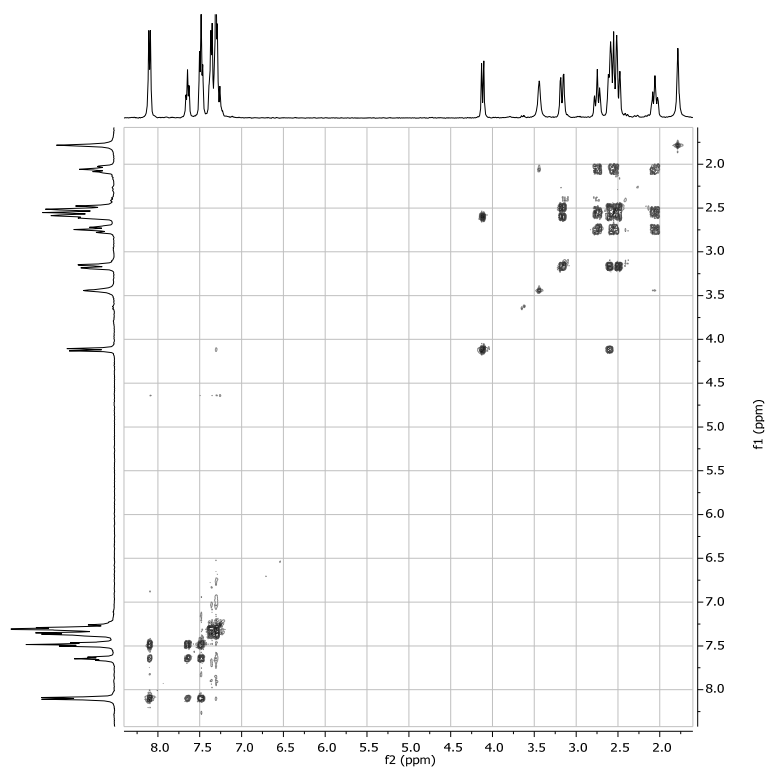
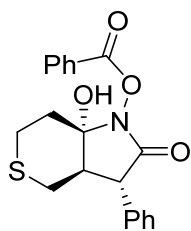
COSY (CDCl<sub>3</sub>)

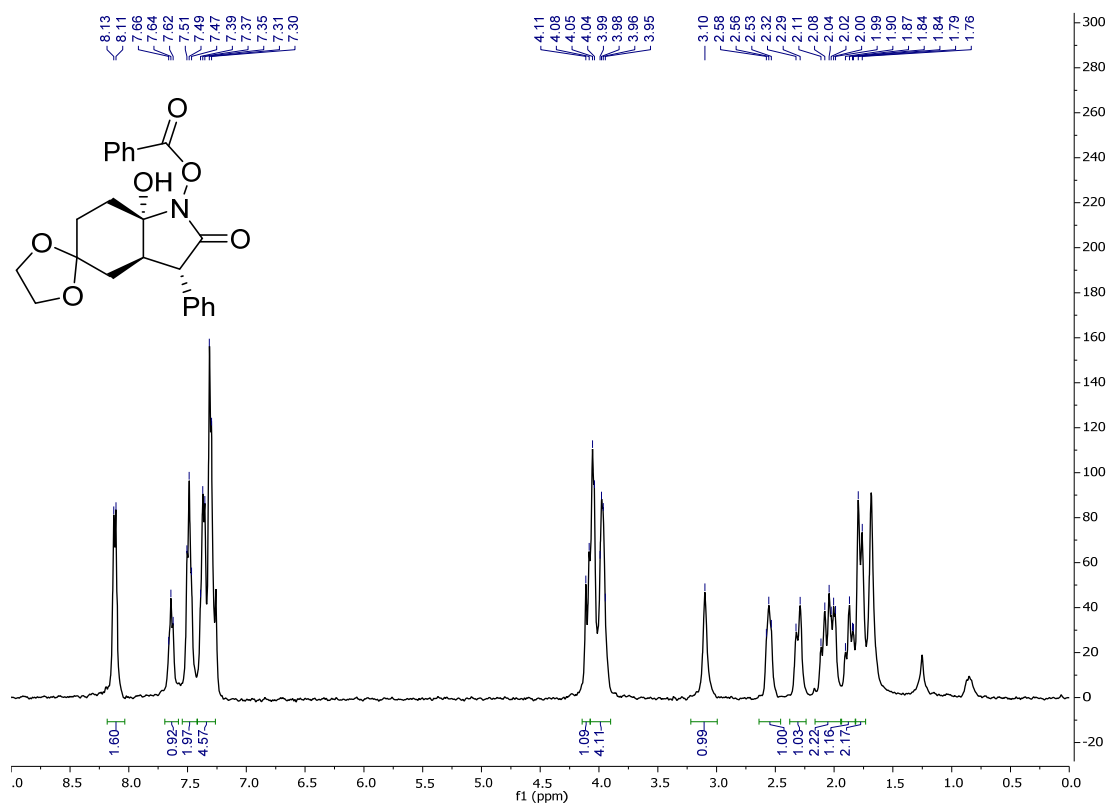
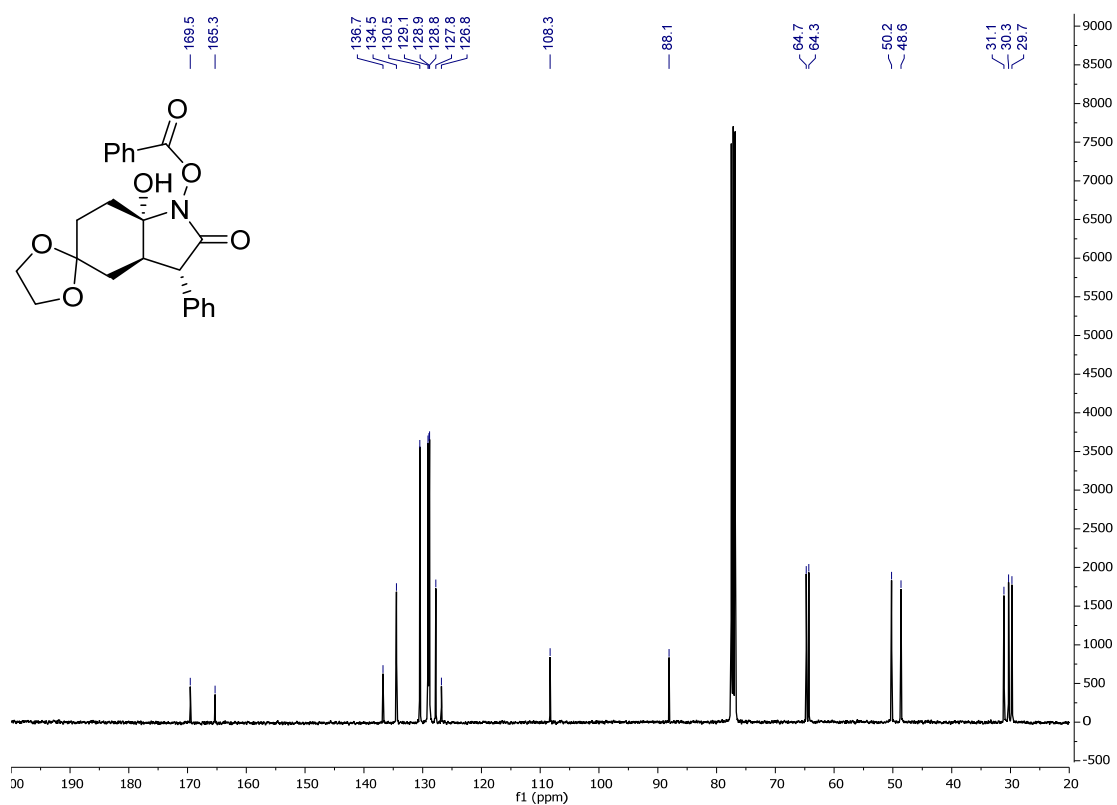


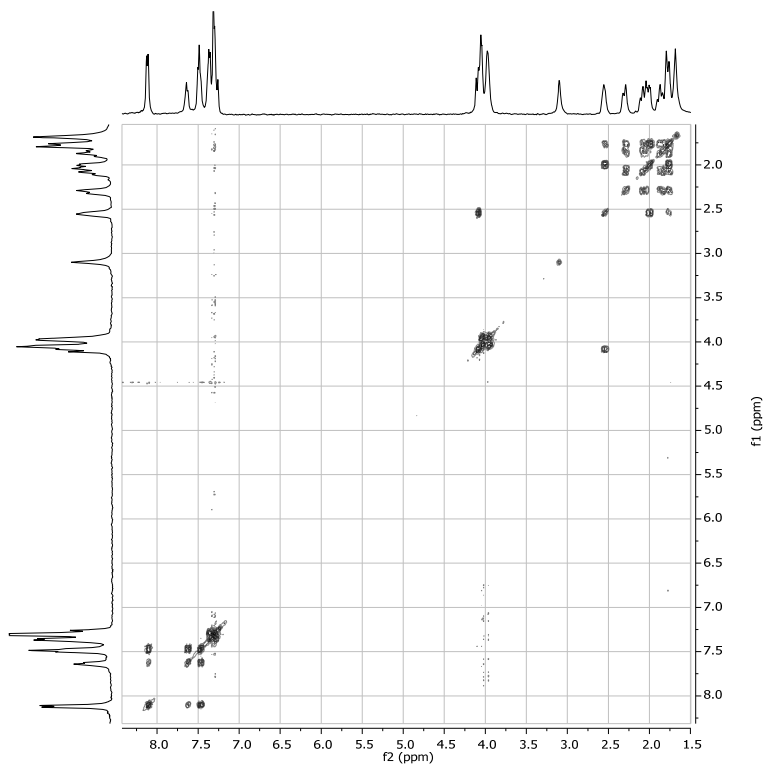
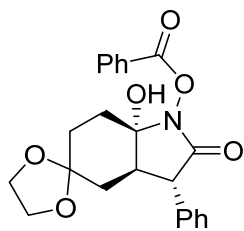
Compound **24aea** $^1\text{H}$  NMR ( $\text{CDCl}_3$ ) $^{13}\text{C}$  NMR ( $\text{CDCl}_3$ )

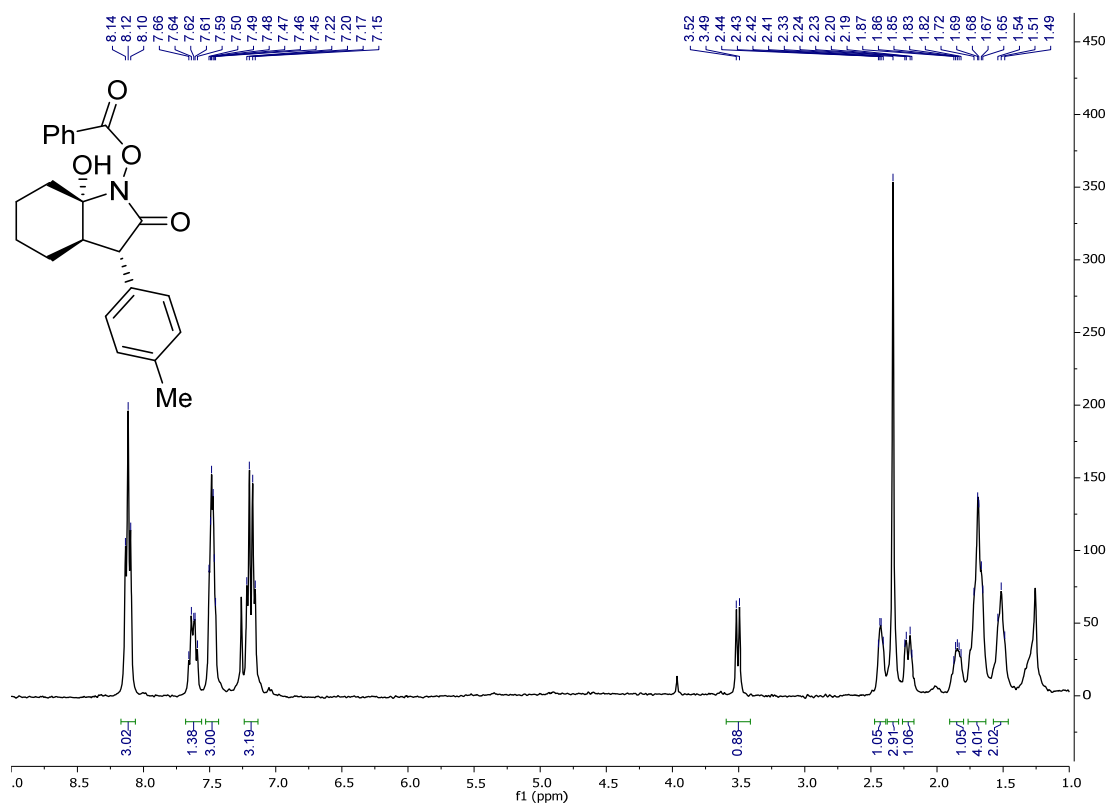
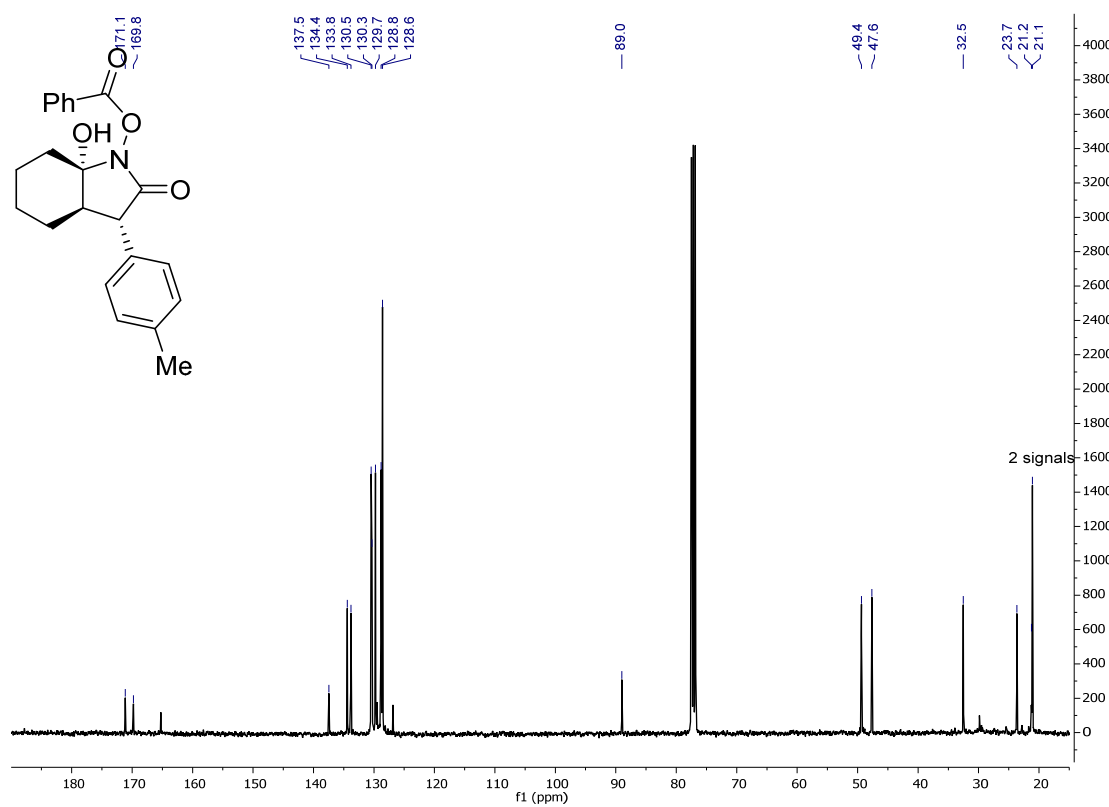
COSY (CDCl<sub>3</sub>)

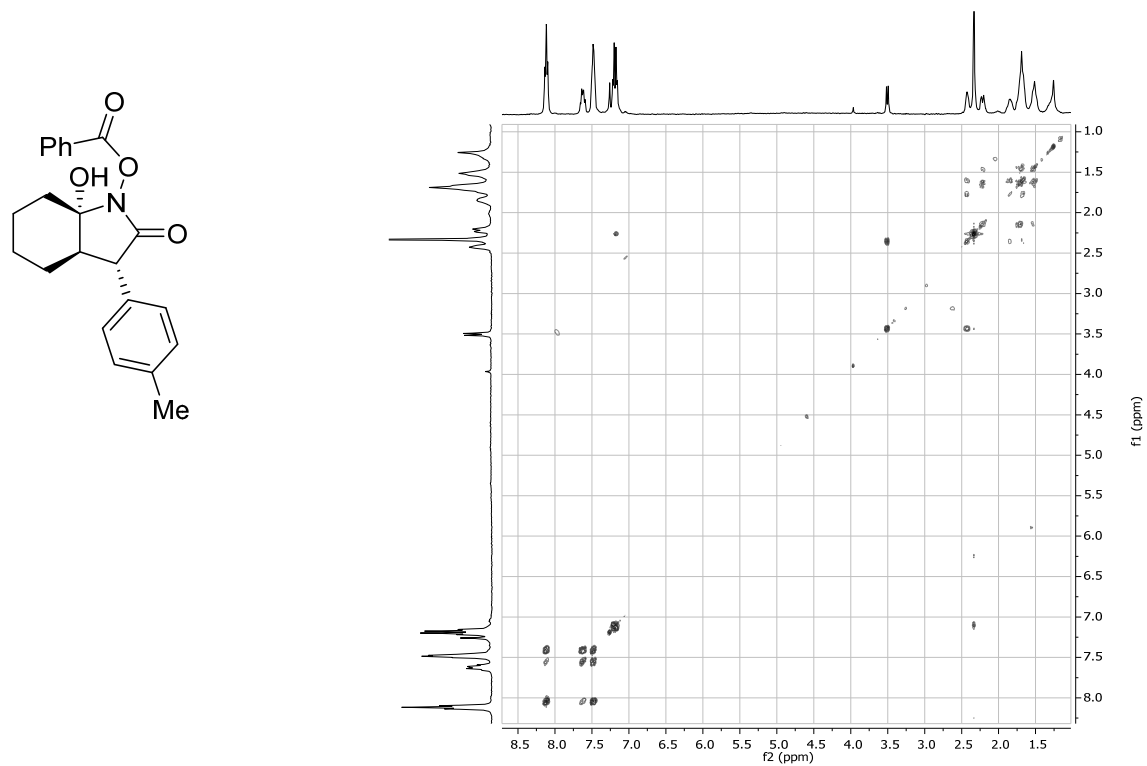
Compound **24afa** $^1\text{H}$  NMR ( $\text{CDCl}_3$ ) $^{13}\text{C}$  NMR ( $\text{CDCl}_3$ )

COSY (CDCl<sub>3</sub>)

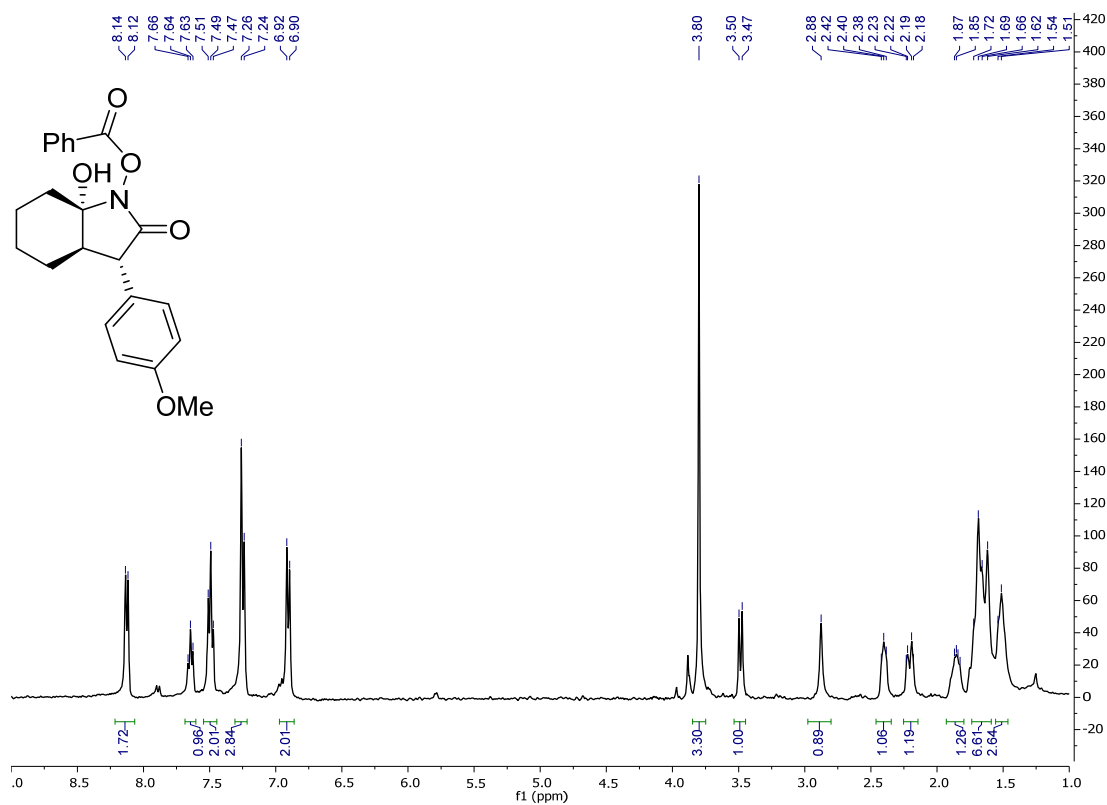
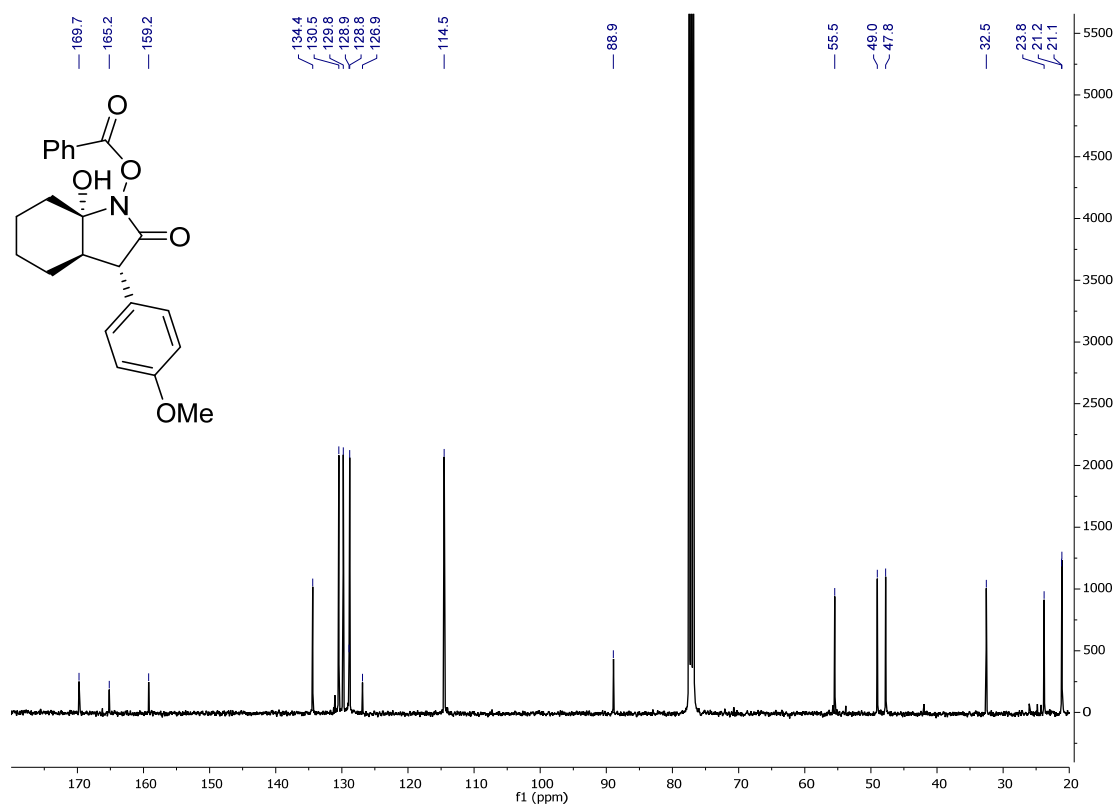
Compound **24aga** $^1\text{H}$  NMR ( $\text{CDCl}_3$ ) $^{13}\text{C}$  NMR ( $\text{CDCl}_3$ )

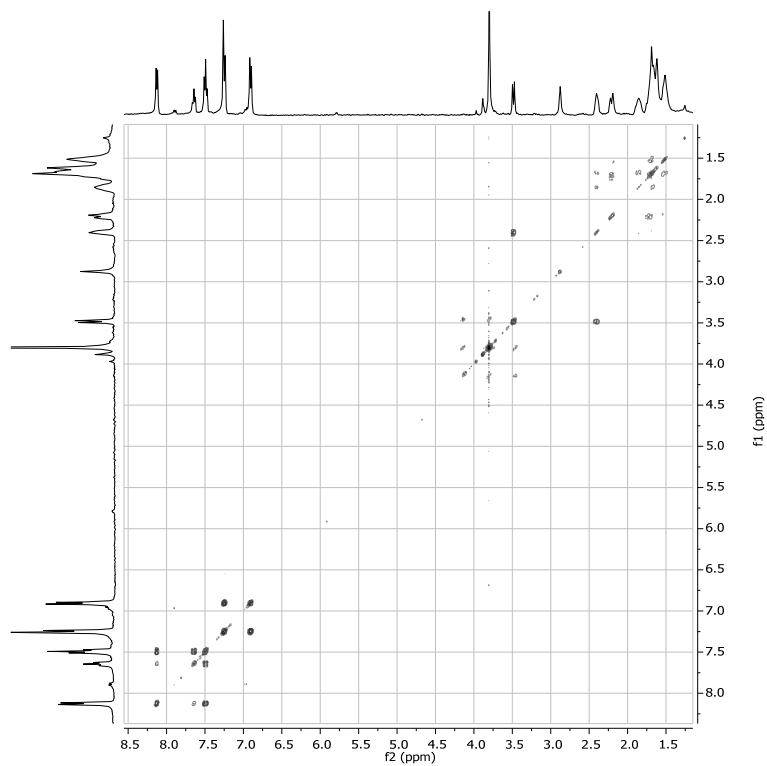
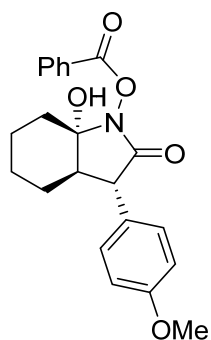
COSY (CDCl<sub>3</sub>)

Compound **24baa** $^1\text{H}$  NMR ( $\text{CDCl}_3$ ) $^{13}\text{C}$  NMR ( $\text{CDCl}_3$ )

COSY (CDCl<sub>3</sub>)

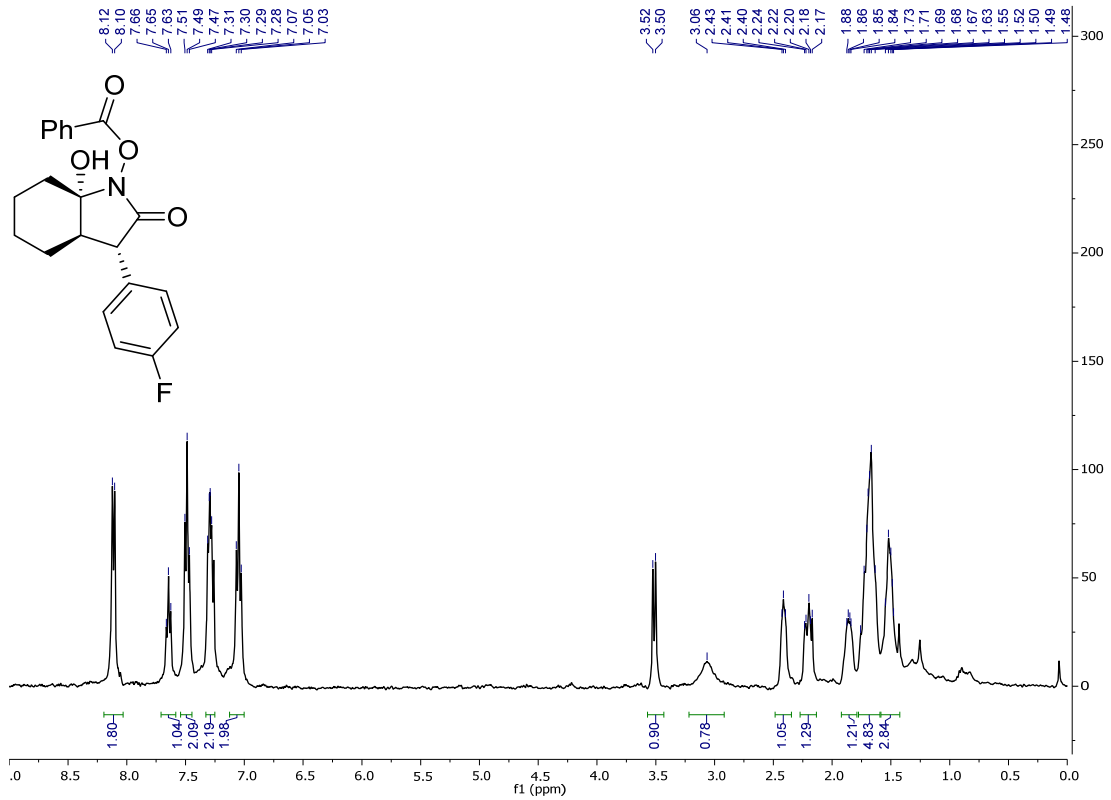


Compound **24caa** $^1\text{H}$  NMR ( $\text{CDCl}_3$ ) $^{13}\text{C}$  NMR ( $\text{CDCl}_3$ )

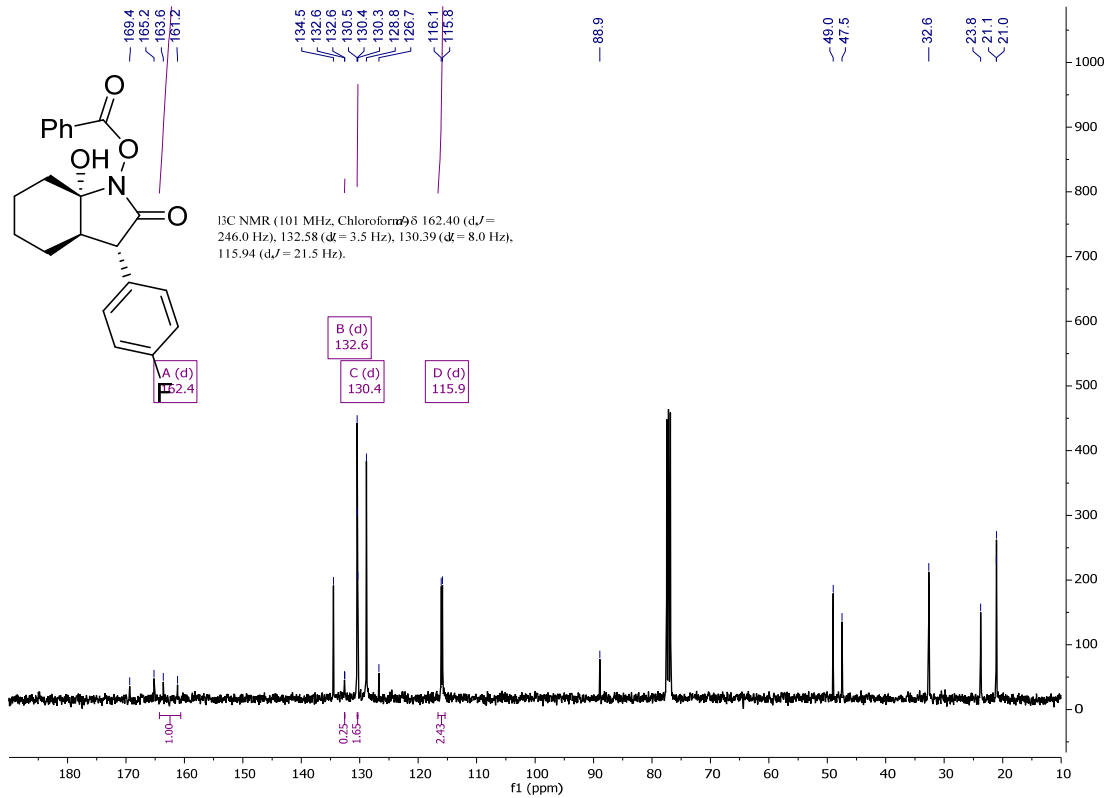
COSY (CDCl<sub>3</sub>)

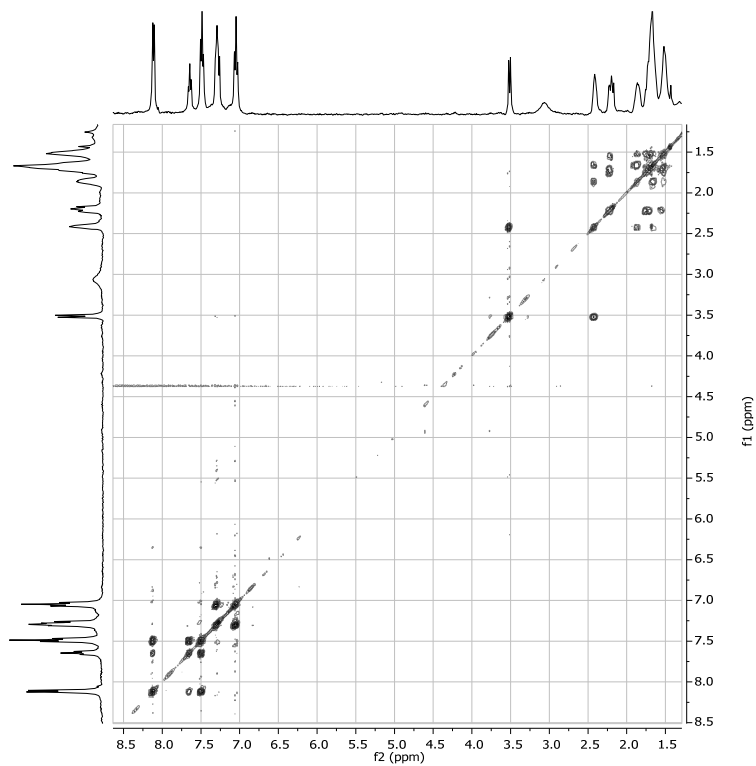
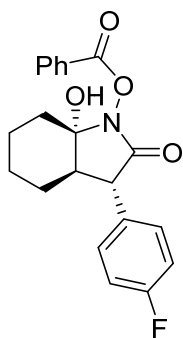
Compound **24naa**

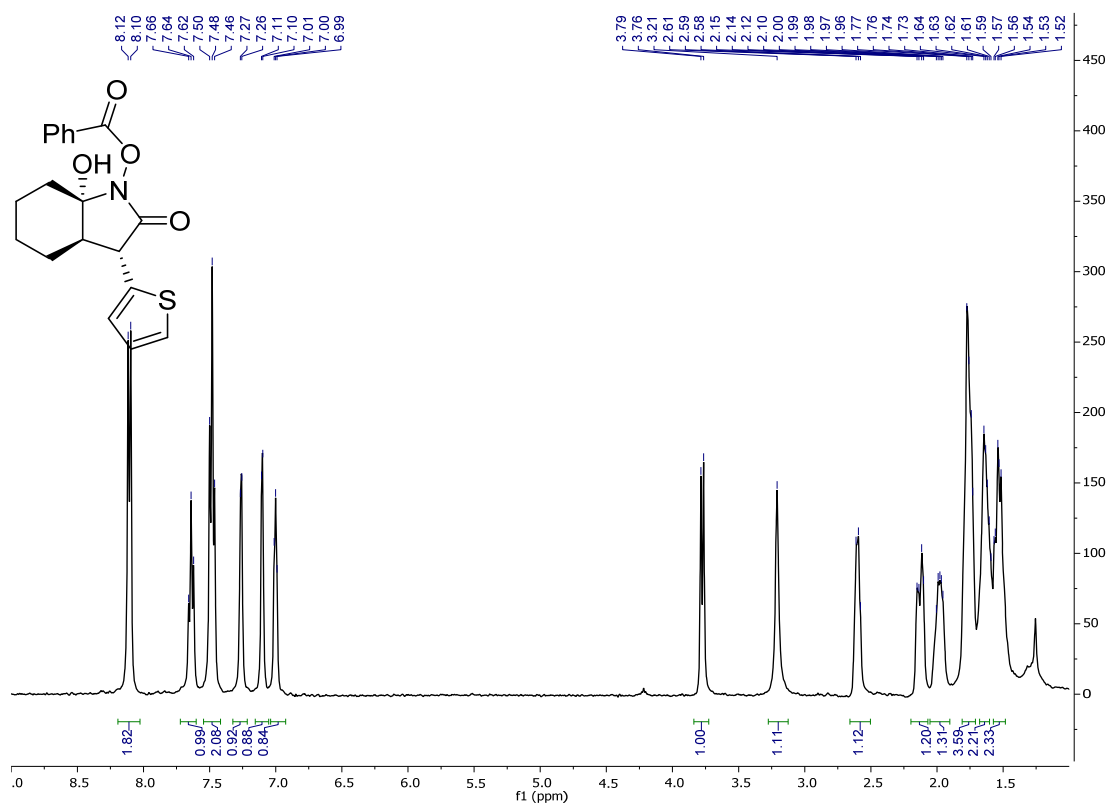
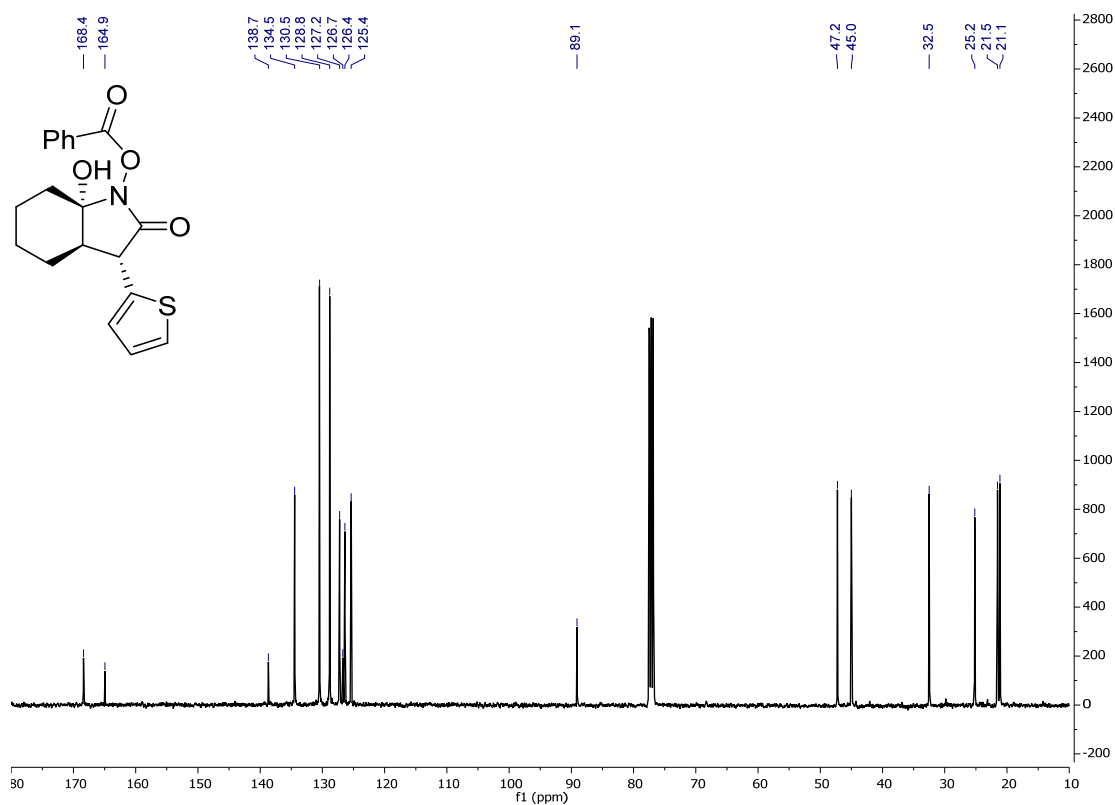
<sup>1</sup>H NMR (CDCl<sub>3</sub>)

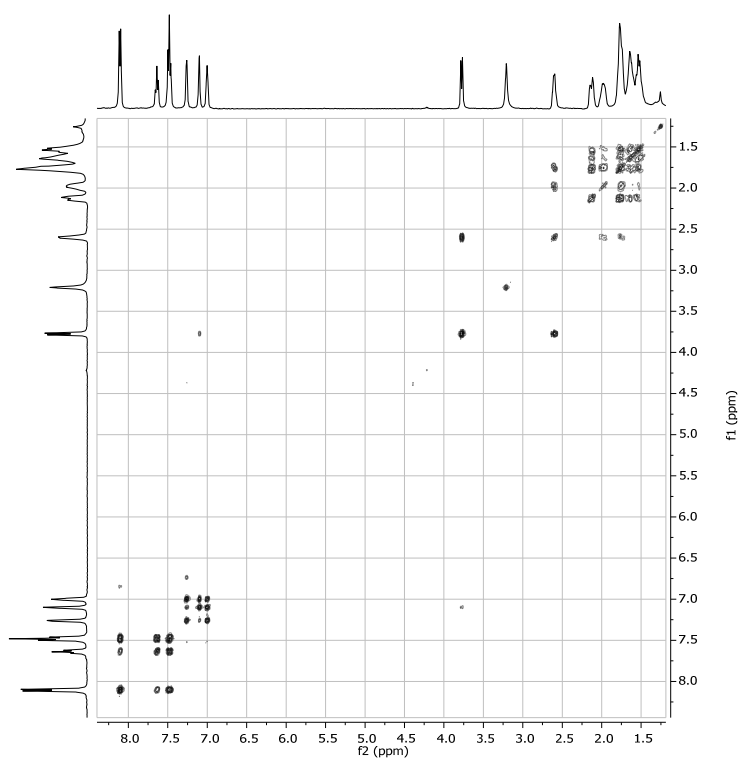
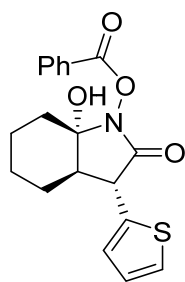


<sup>13</sup>C NMR (CDCl<sub>3</sub>)



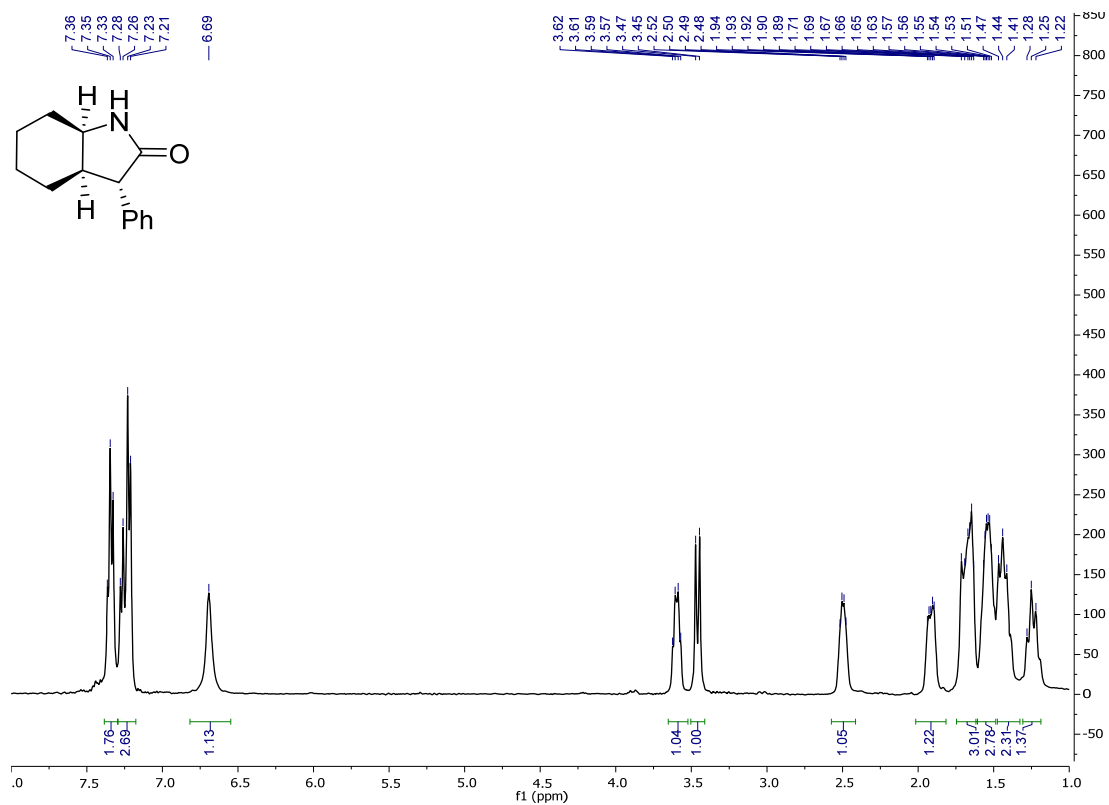
COSY (CDCl<sub>3</sub>)

Compound **24oaa** $^1\text{H}$  NMR ( $\text{CDCl}_3$ ) $^{13}\text{C}$  NMR ( $\text{CDCl}_3$ )

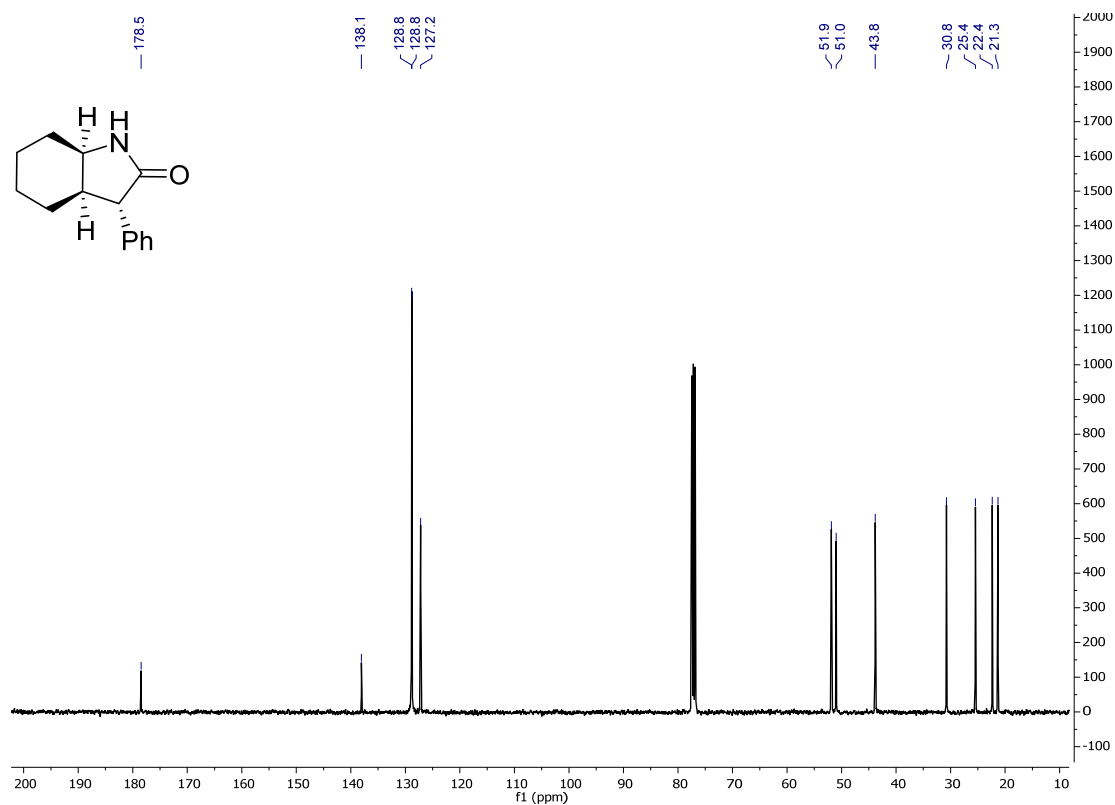
COSY (CDCl<sub>3</sub>)

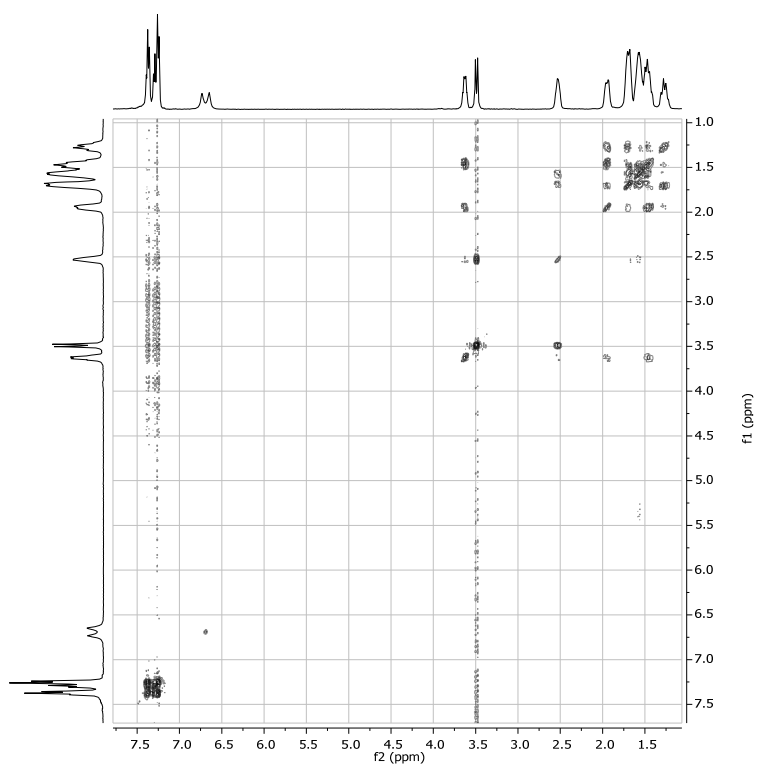
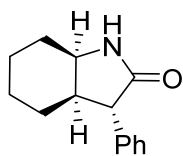
Compound **56aa**

$^1\text{H}$  NMR ( $\text{CDCl}_3$ )

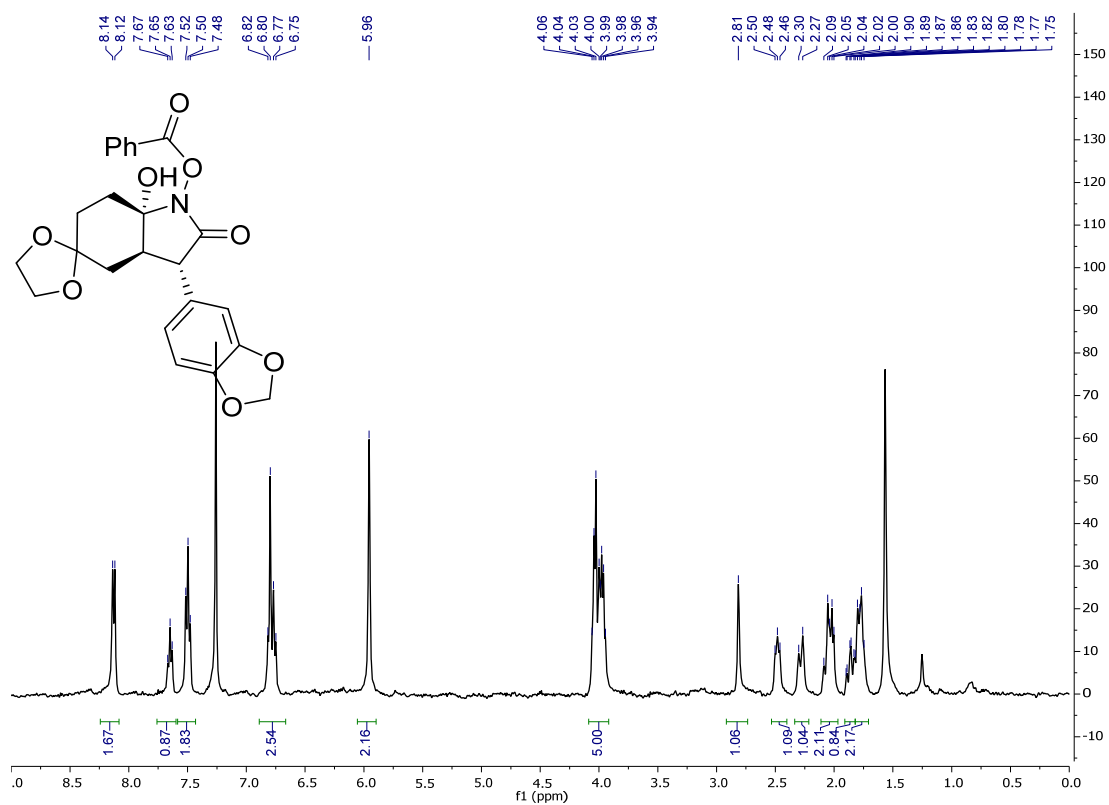
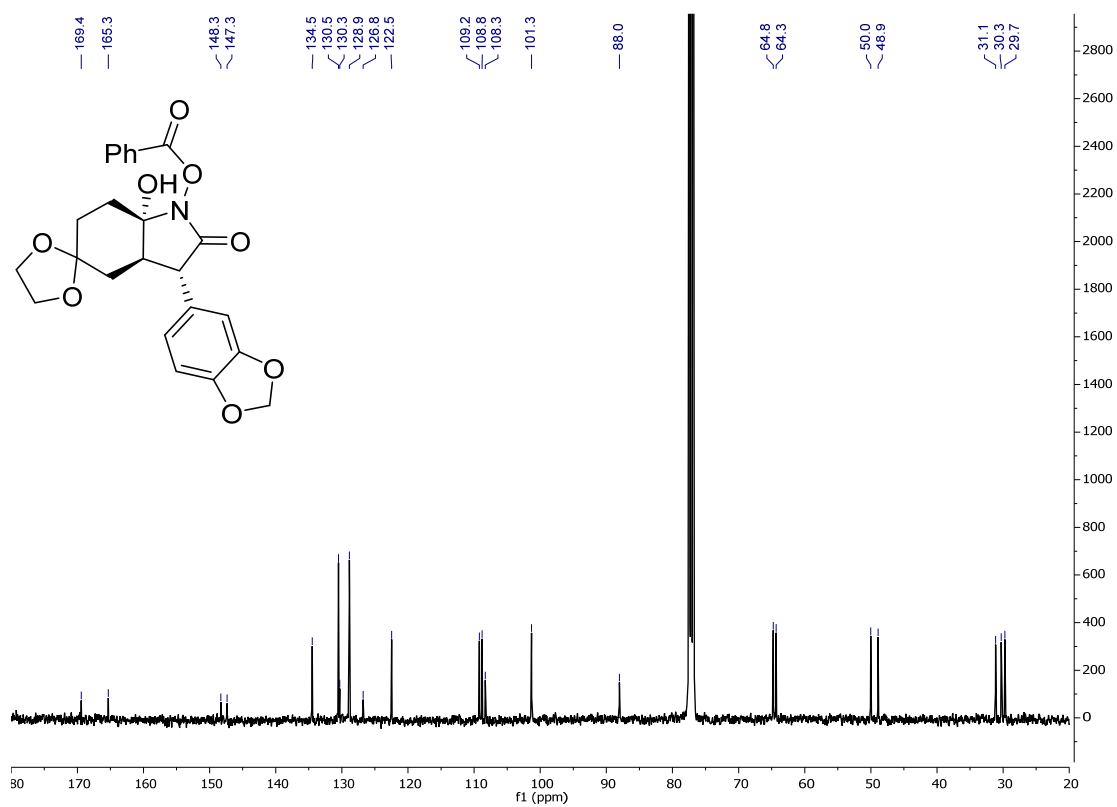


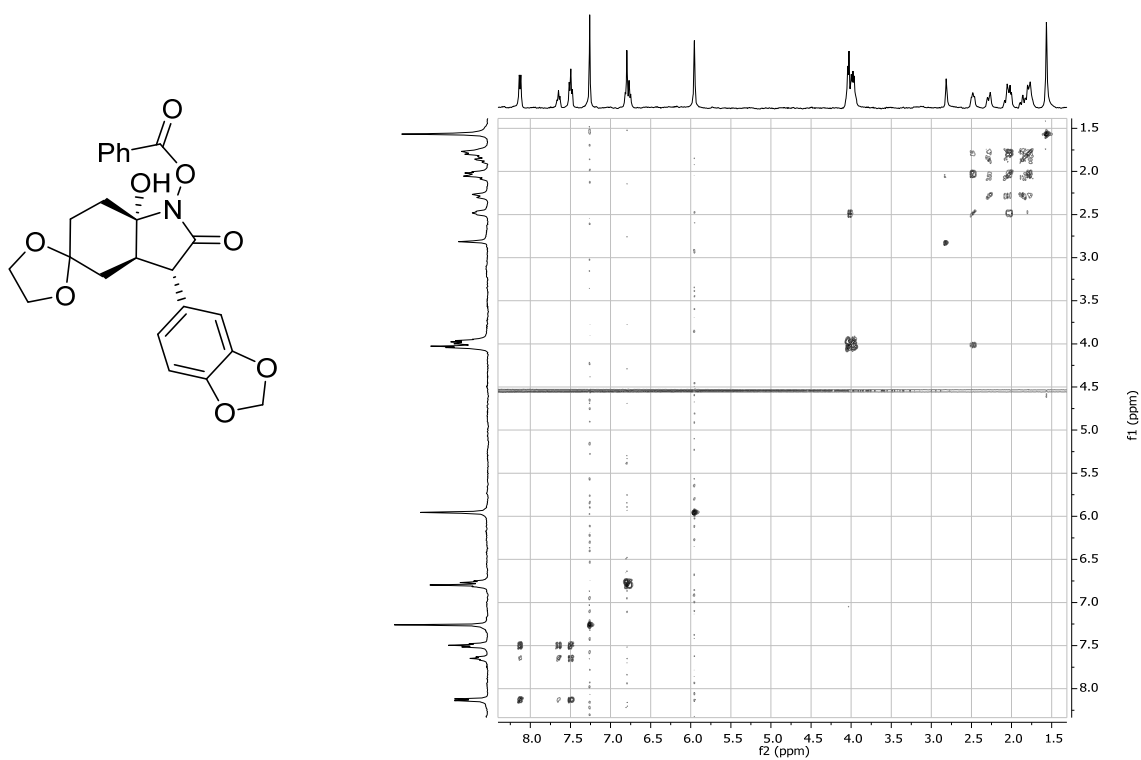
$^{13}\text{C}$  NMR ( $\text{CDCl}_3$ )

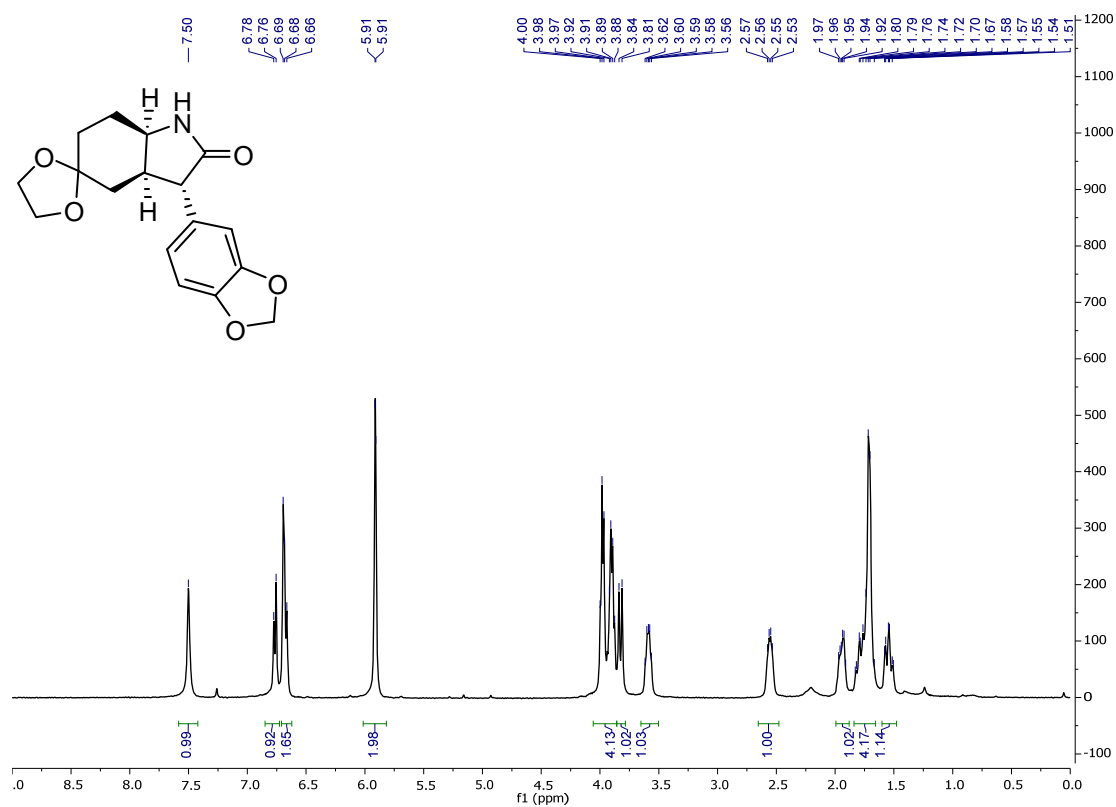
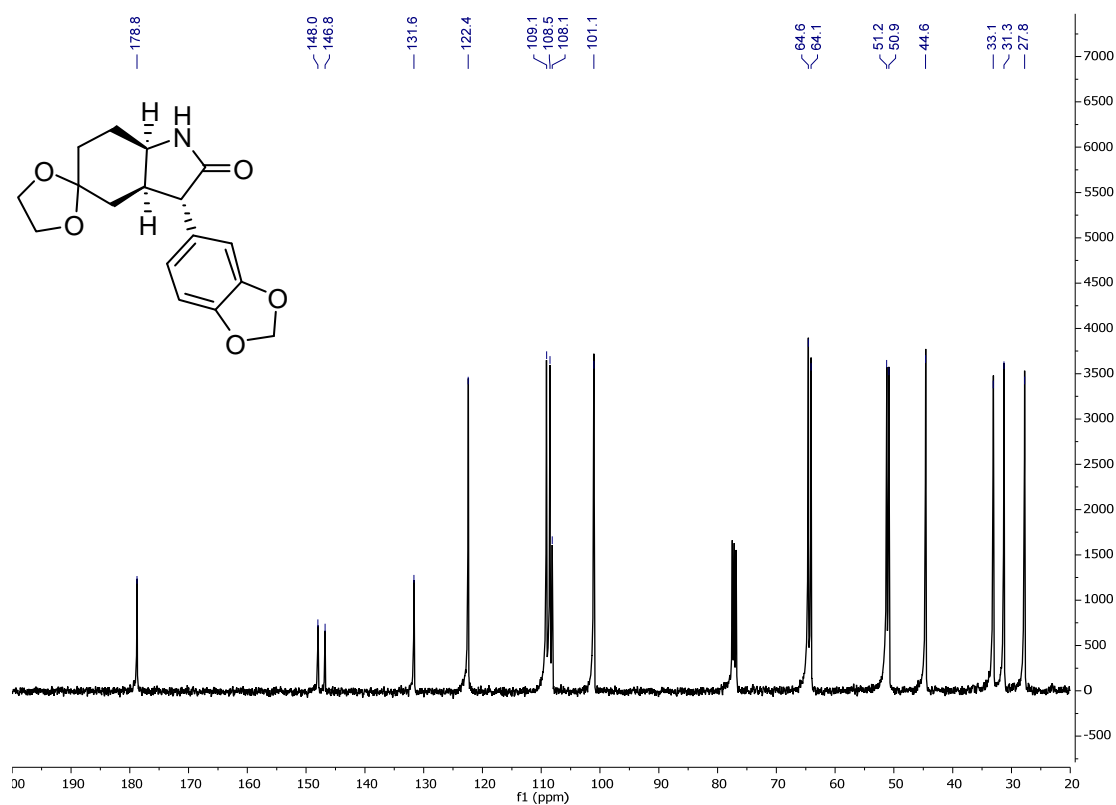


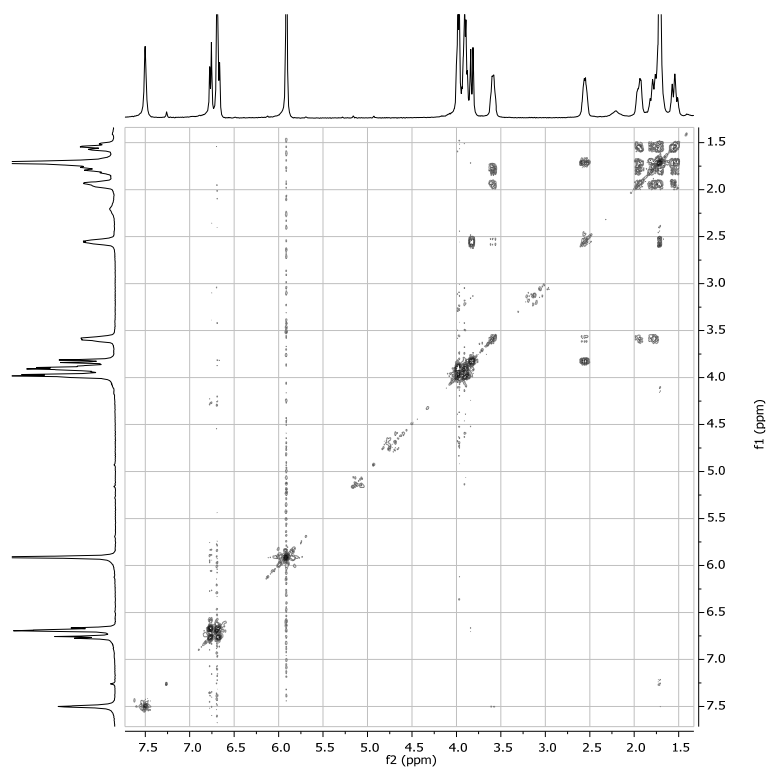
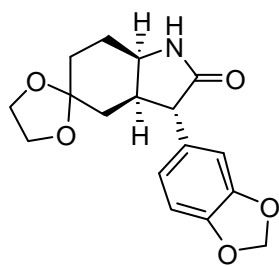
COSY (CDCl<sub>3</sub>)

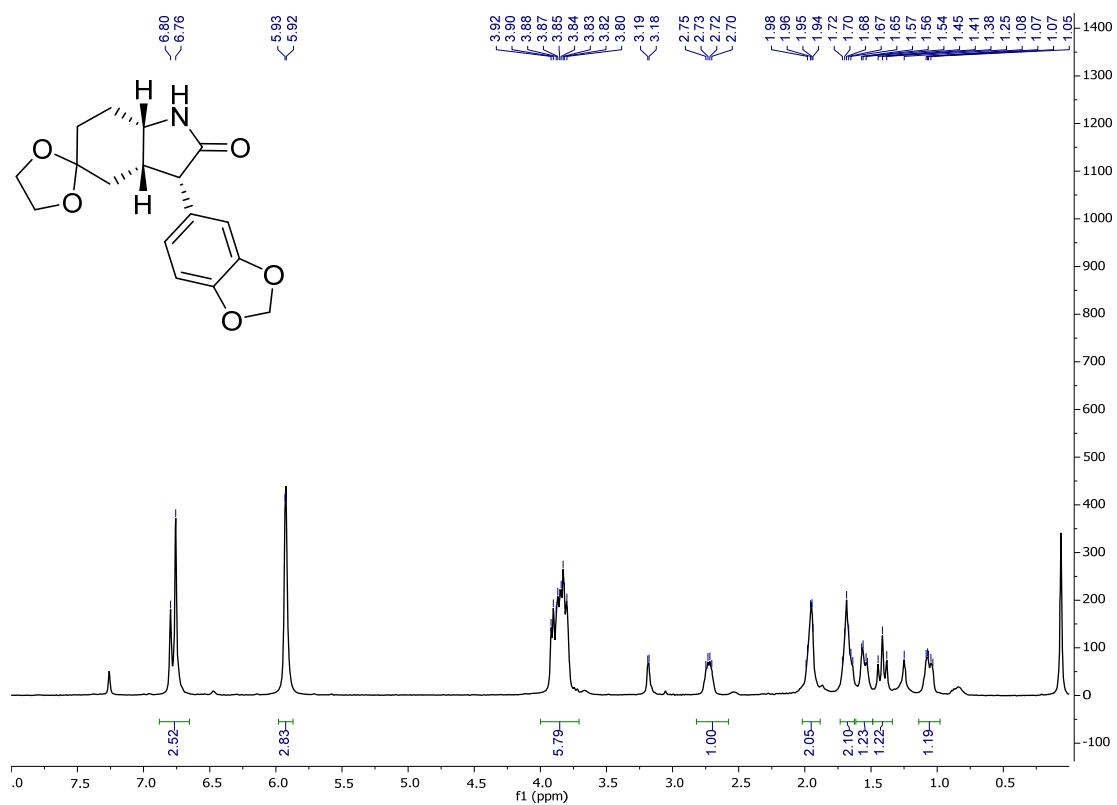
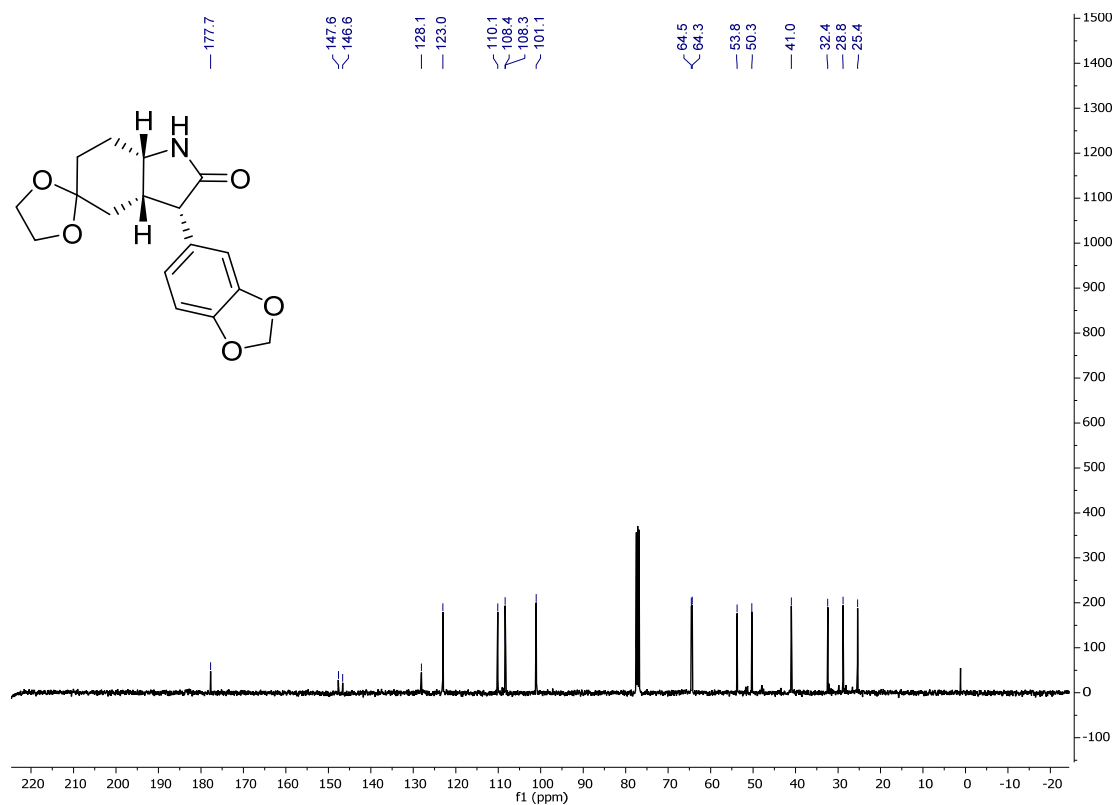


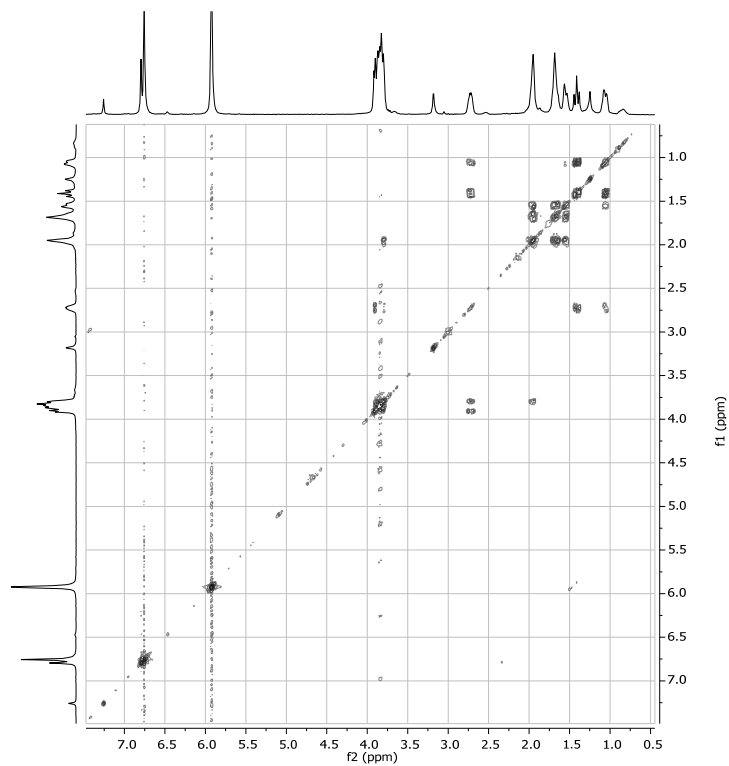
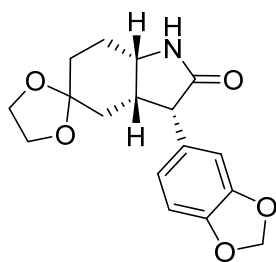
Compound **24gpa** $^1\text{H}$  NMR ( $\text{CDCl}_3$ ) $^{13}\text{C}$  NMR ( $\text{CDCl}_3$ )

COSY (CDCl<sub>3</sub>)

Compound (3*S*,3*aR*,7*aR*)-**56gp** $^1\text{H}$  NMR ( $\text{CDCl}_3$ ) $^{13}\text{C}$  NMR ( $\text{CDCl}_3$ )

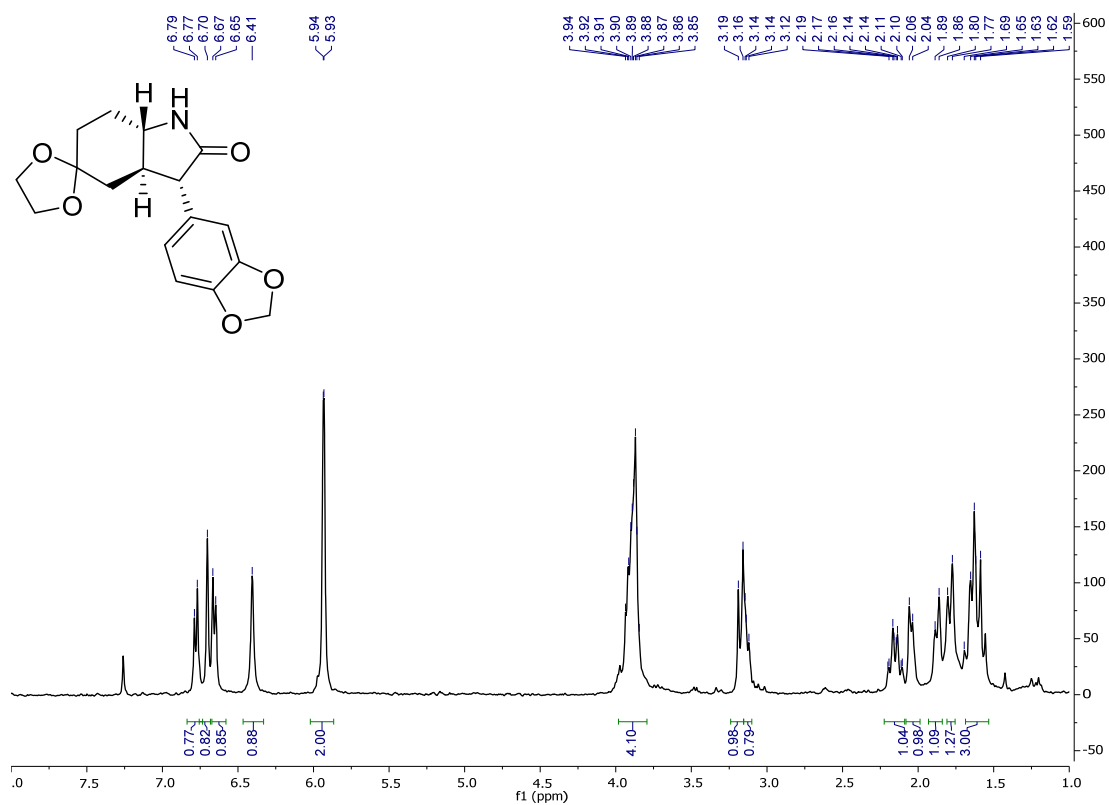
COSY (CDCl<sub>3</sub>)

Compound (3*S*,3*aS*,7*aS*)-**56gp** $^1\text{H}$  NMR ( $\text{CDCl}_3$ ) $^{13}\text{C}$  NMR ( $\text{CDCl}_3$ )

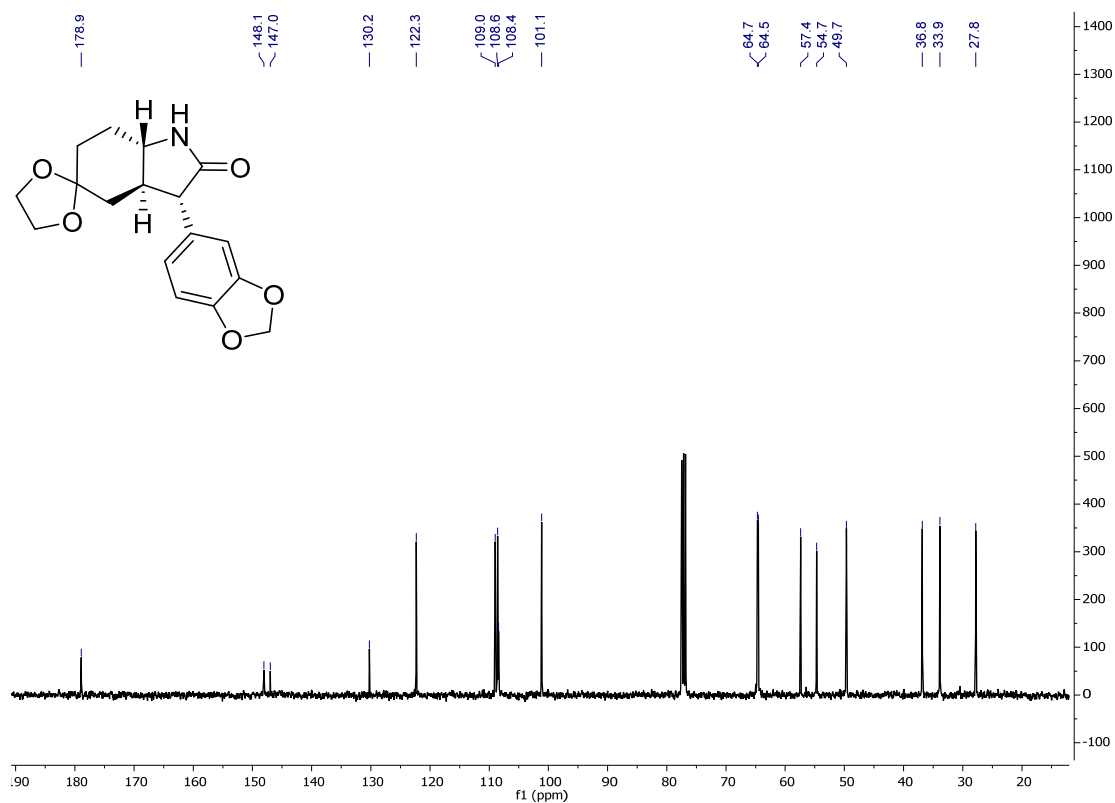
COSY (CDCl<sub>3</sub>)

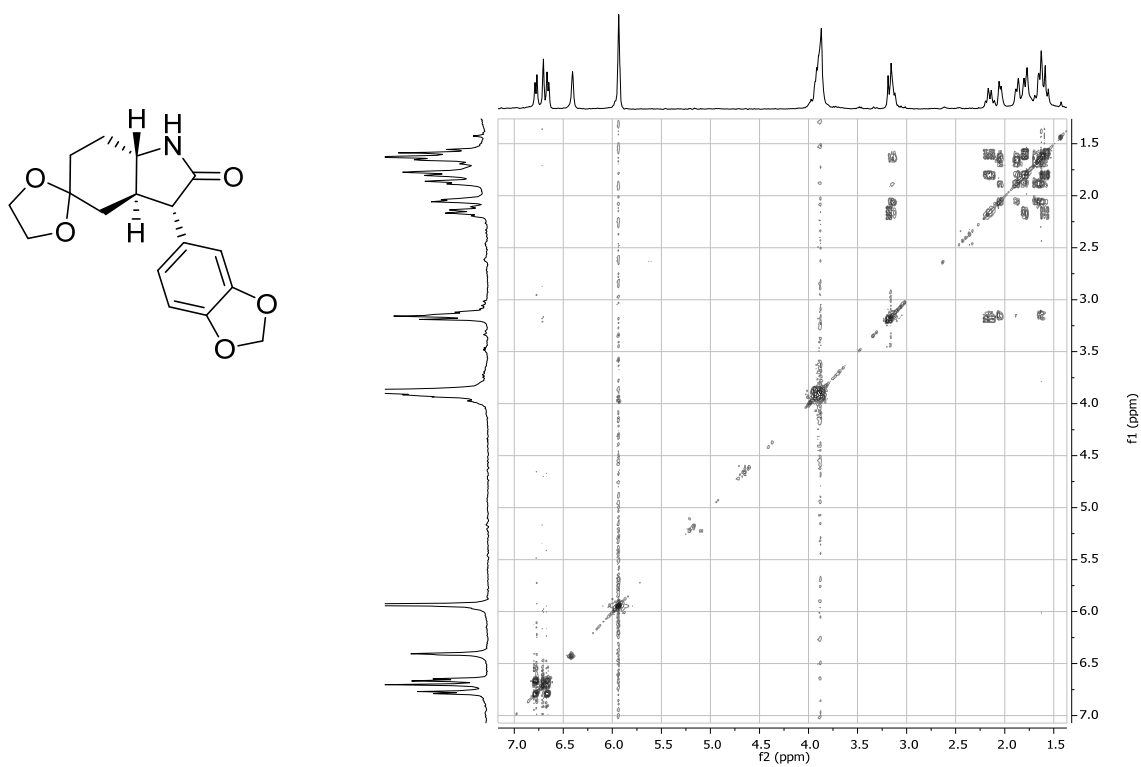
Compound (3*S*,3*aR*,7*aS*)-**56gp**

<sup>1</sup>H NMR (CDCl<sub>3</sub>)

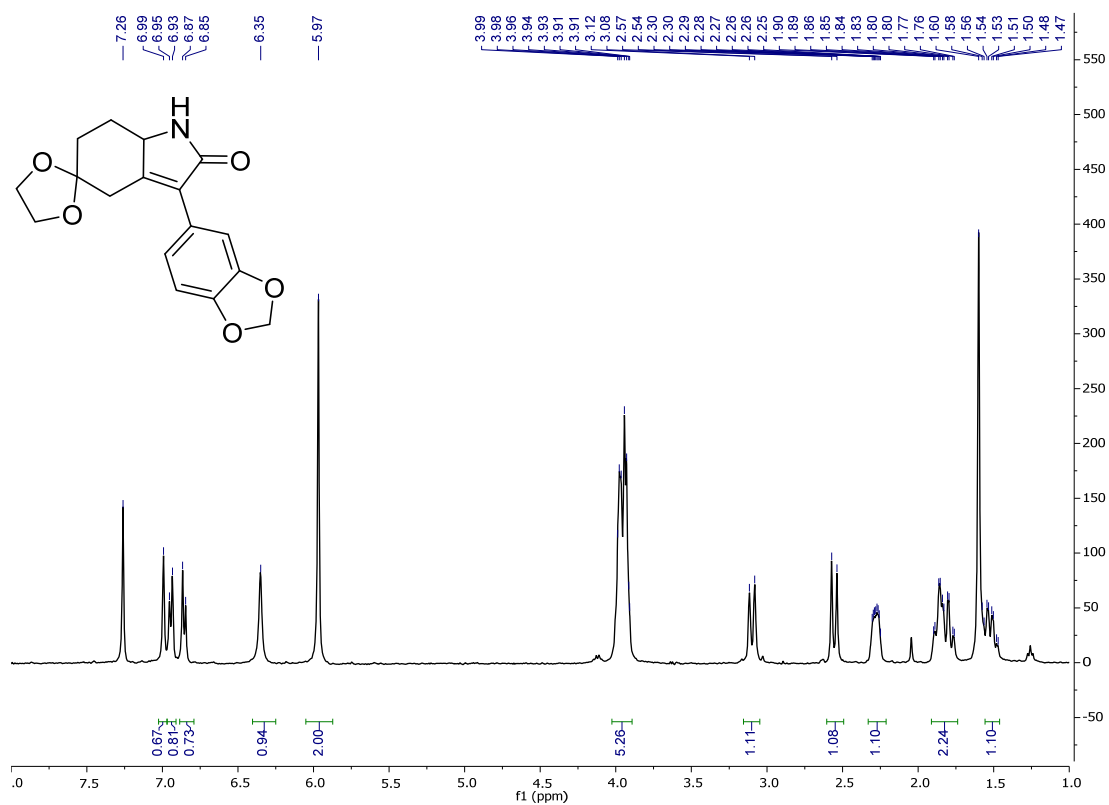
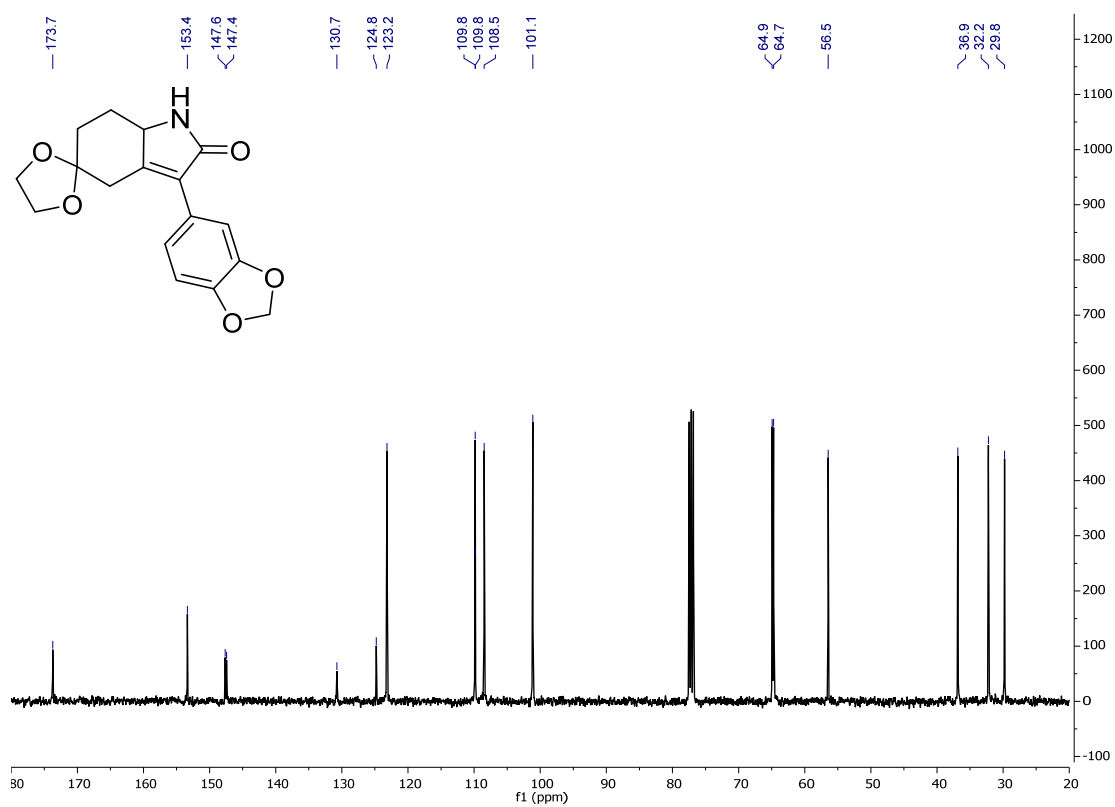


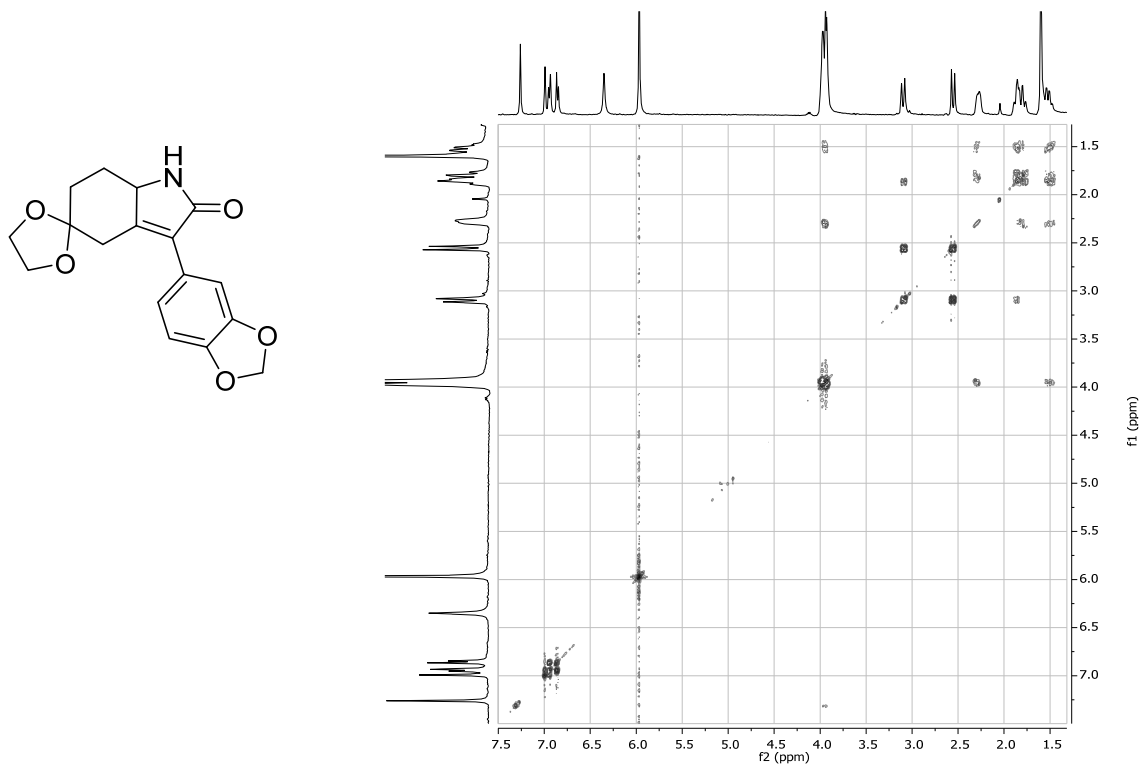
<sup>13</sup>C NMR (CDCl<sub>3</sub>)



COSY (CDCl<sub>3</sub>)

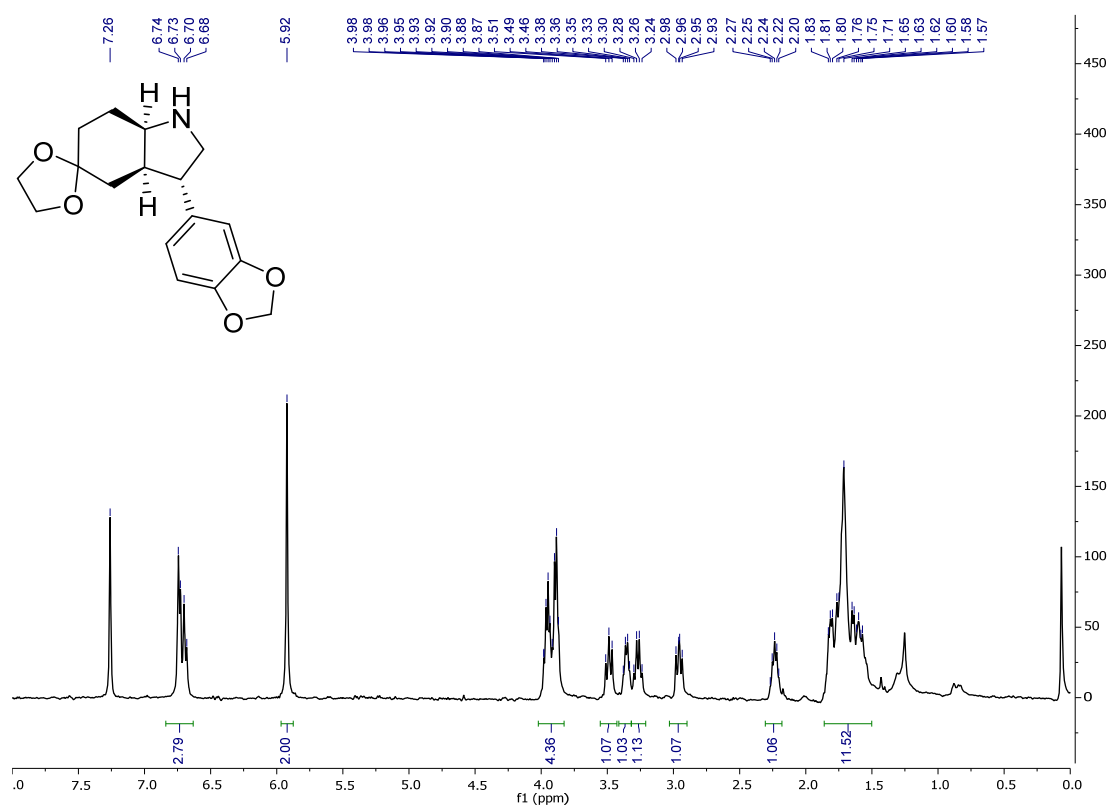


Compound **72** $^1\text{H}$  NMR ( $\text{CDCl}_3$ ) $^{13}\text{C}$  NMR ( $\text{CDCl}_3$ )

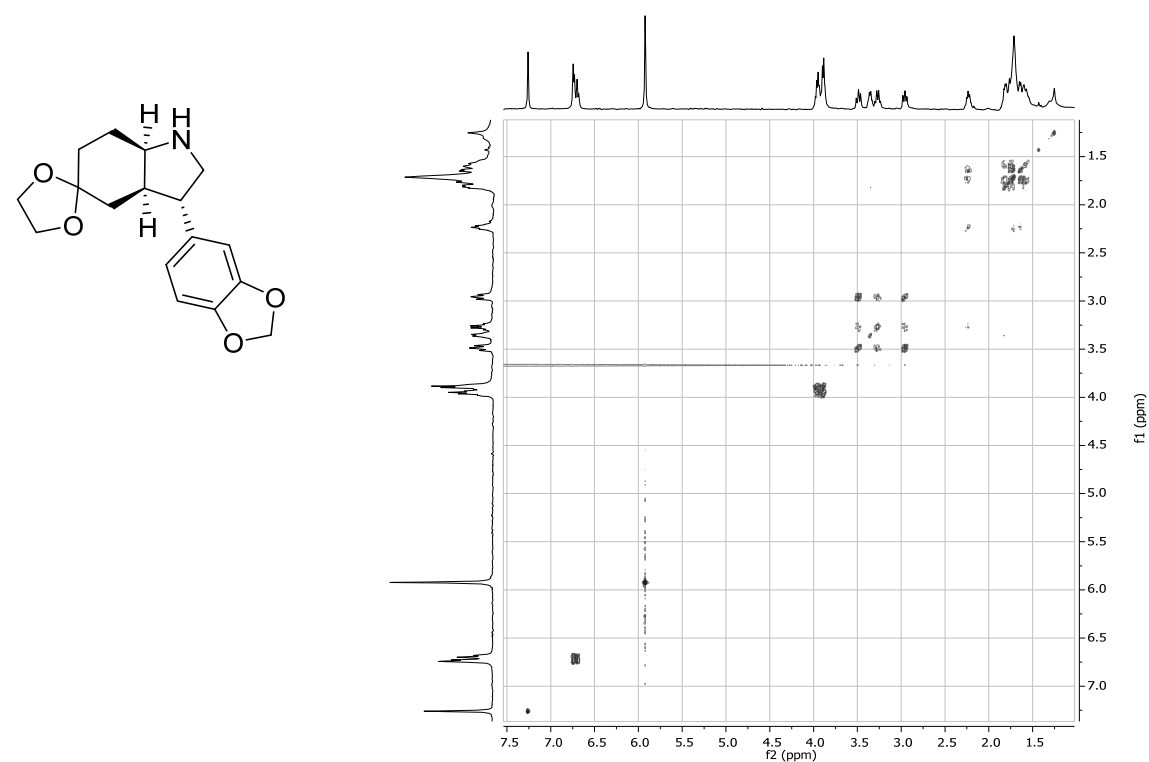
COSY (CDCl<sub>3</sub>)

Compound (3*S*,3*aR*,7*aR*)-**67**

<sup>1</sup>H NMR (CDCl<sub>3</sub>)

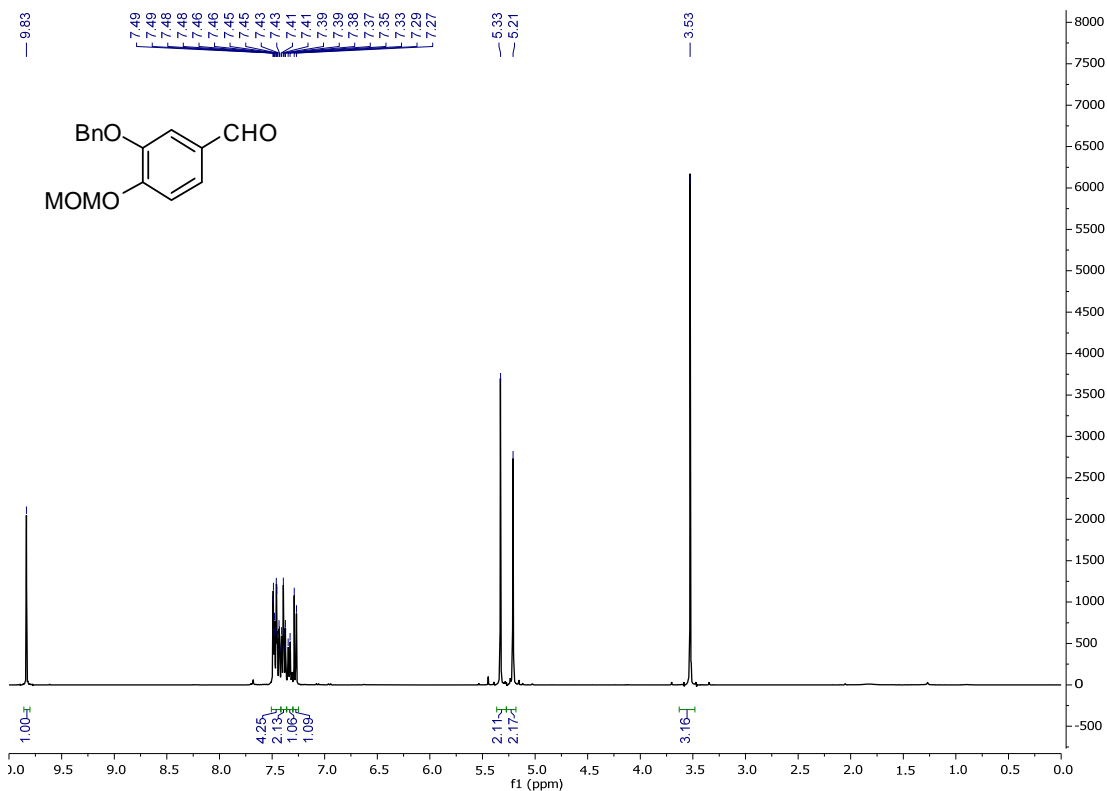
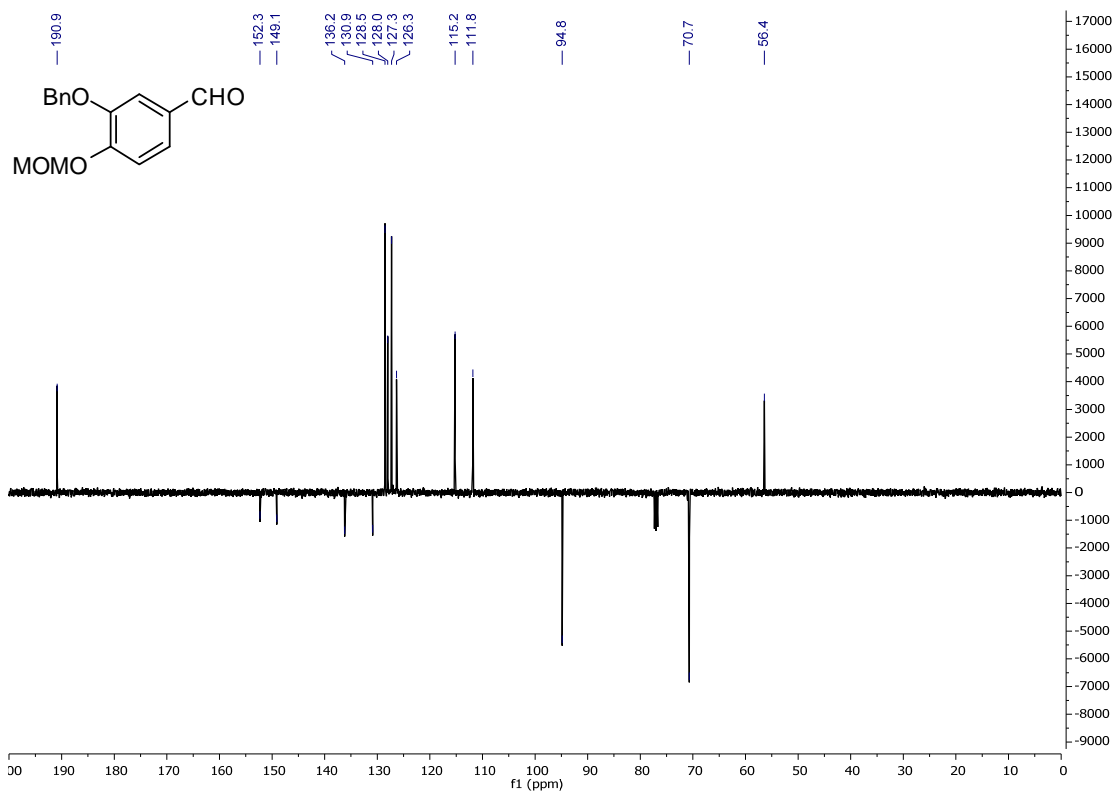


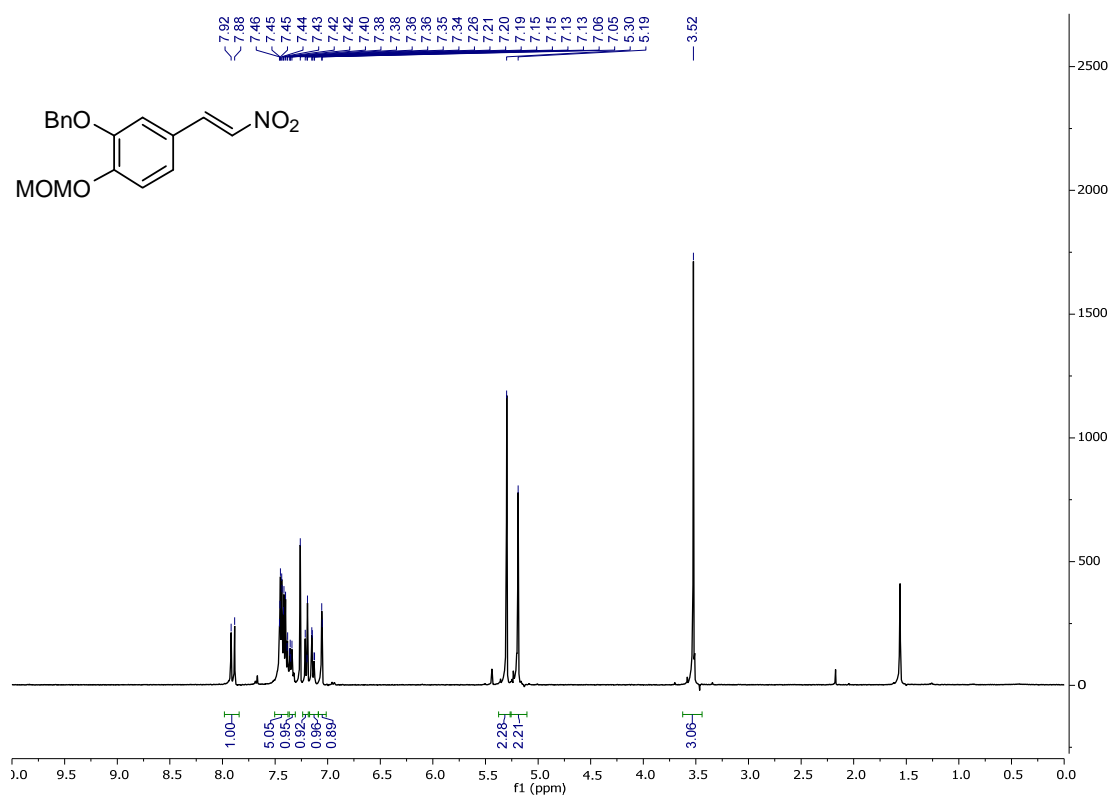
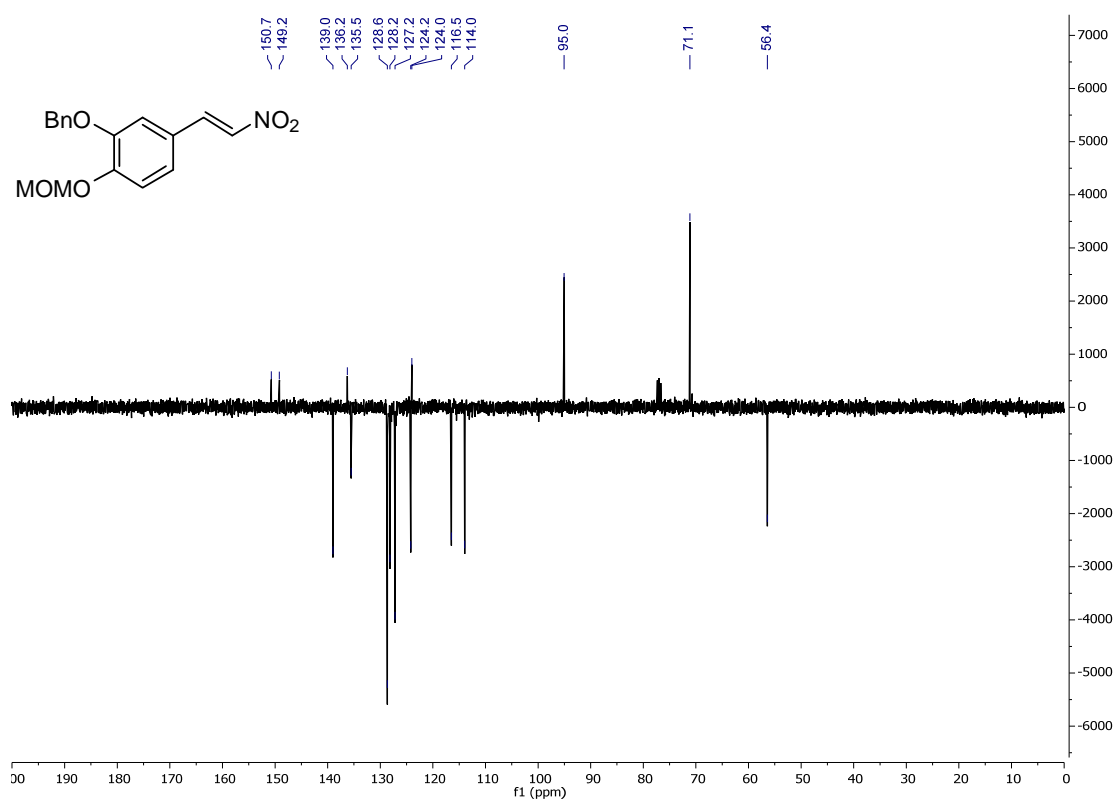
COSY (CDCl<sub>3</sub>)





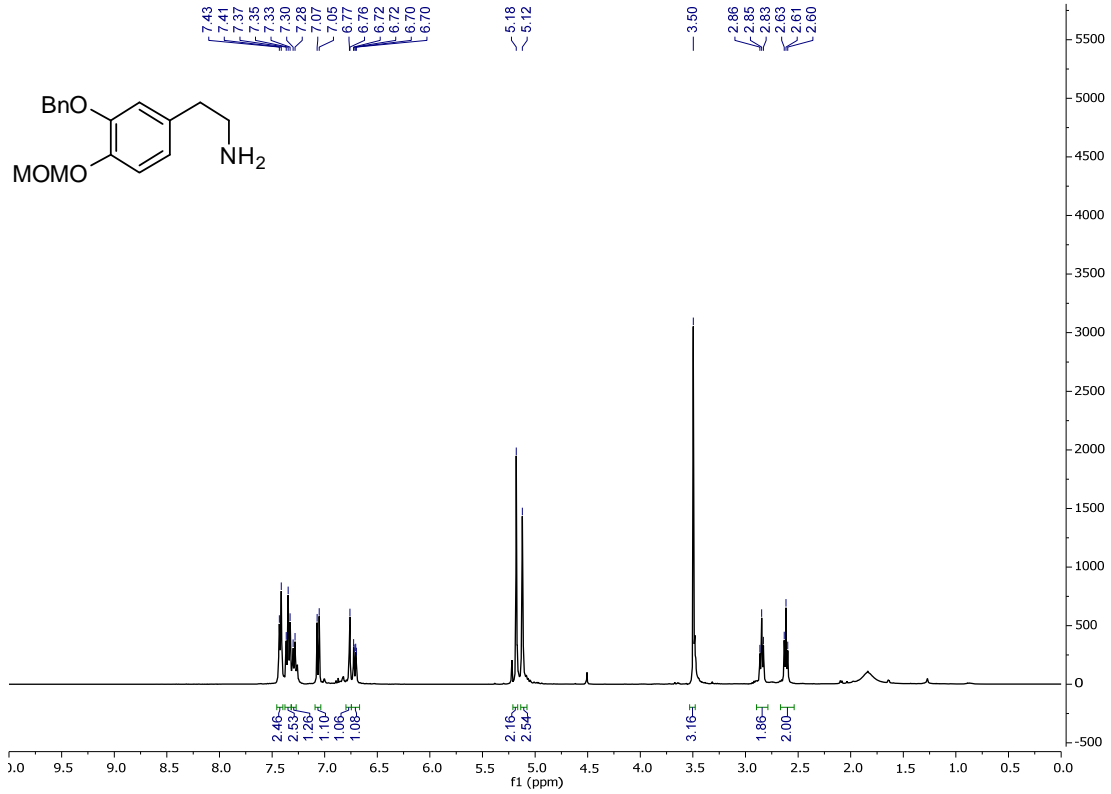
## Annex I-d. NMR spectra selection for Chapter 5

Compound **99a** $^1\text{H}$  NMR ( $\text{CDCl}_3$ ) $^{13}\text{C}$  NMR ( $\text{CDCl}_3$ )

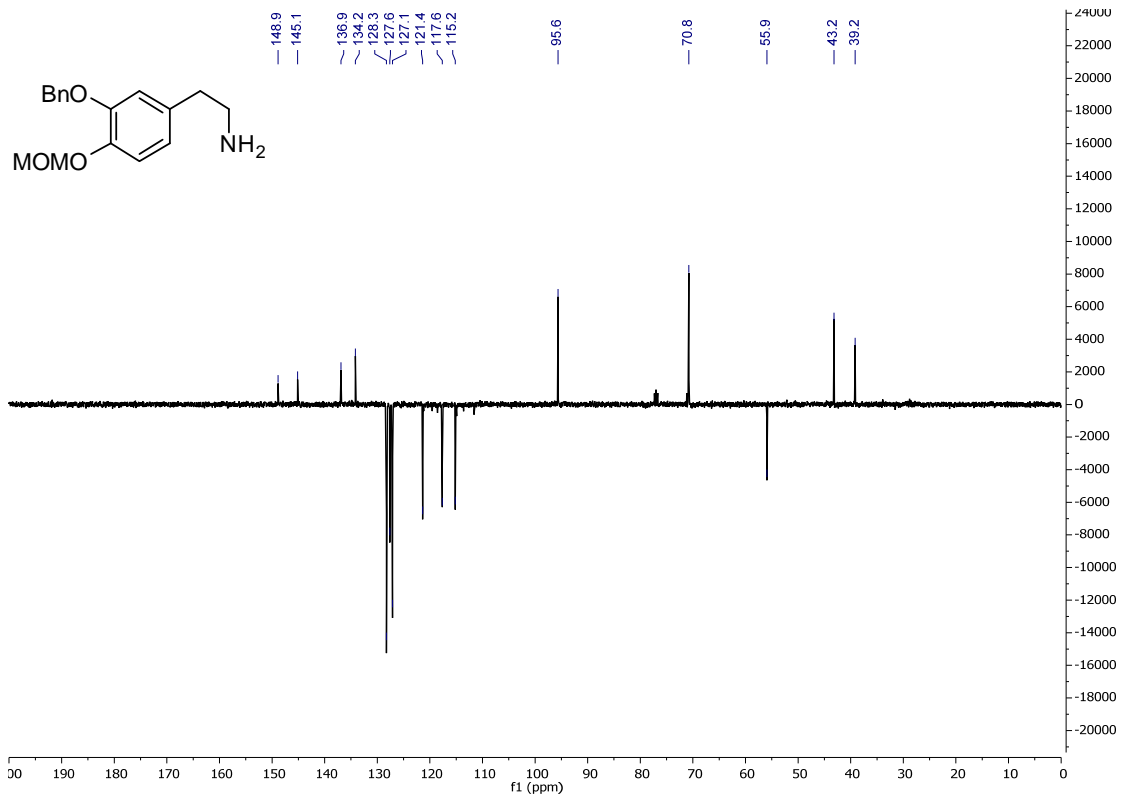
$^1\text{H}$  NMR ( $\text{CDCl}_3$ ) $^{13}\text{C}$  NMR ( $\text{CDCl}_3$ )

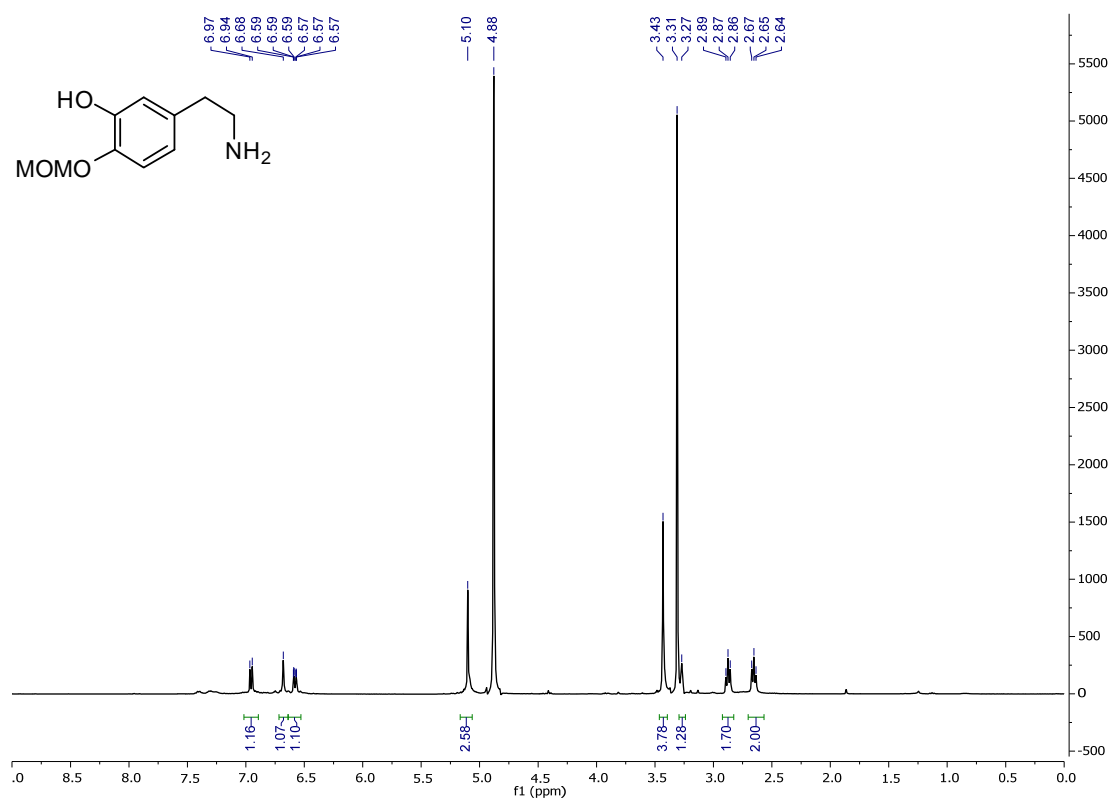
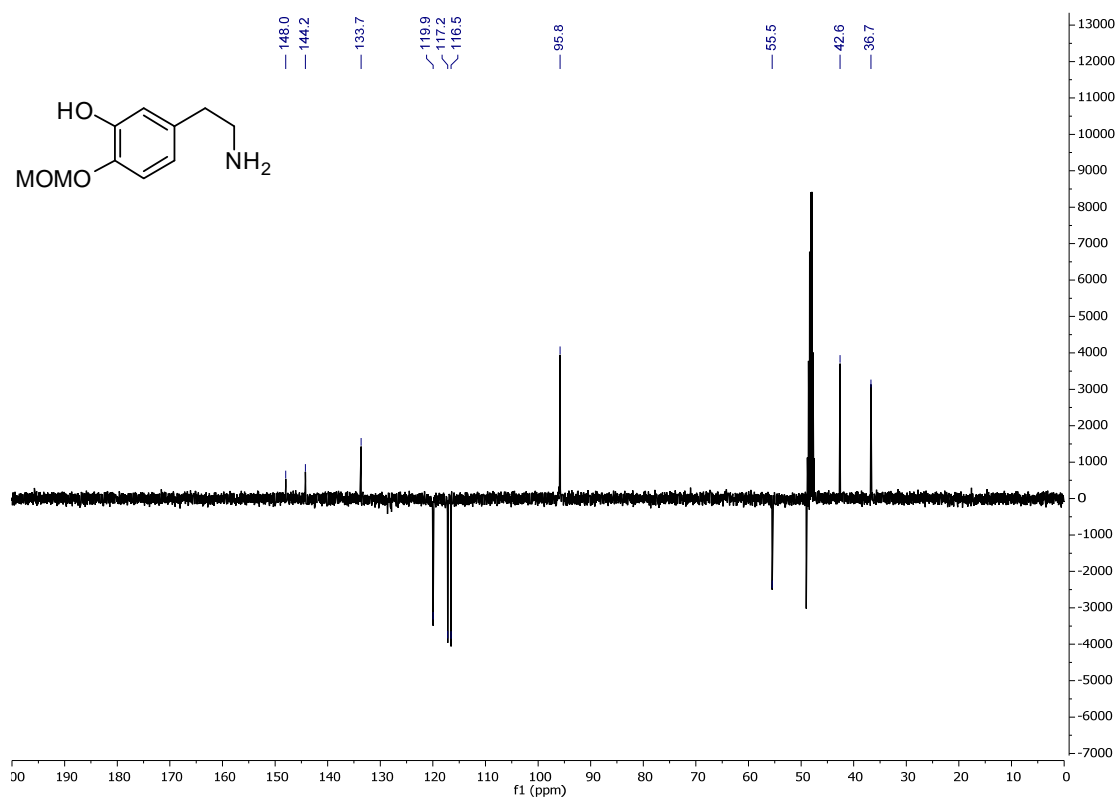
Compound **100a**

$^1\text{H}$  NMR ( $\text{CDCl}_3$ )



$^{13}\text{C}$  NMR ( $\text{CDCl}_3$ )

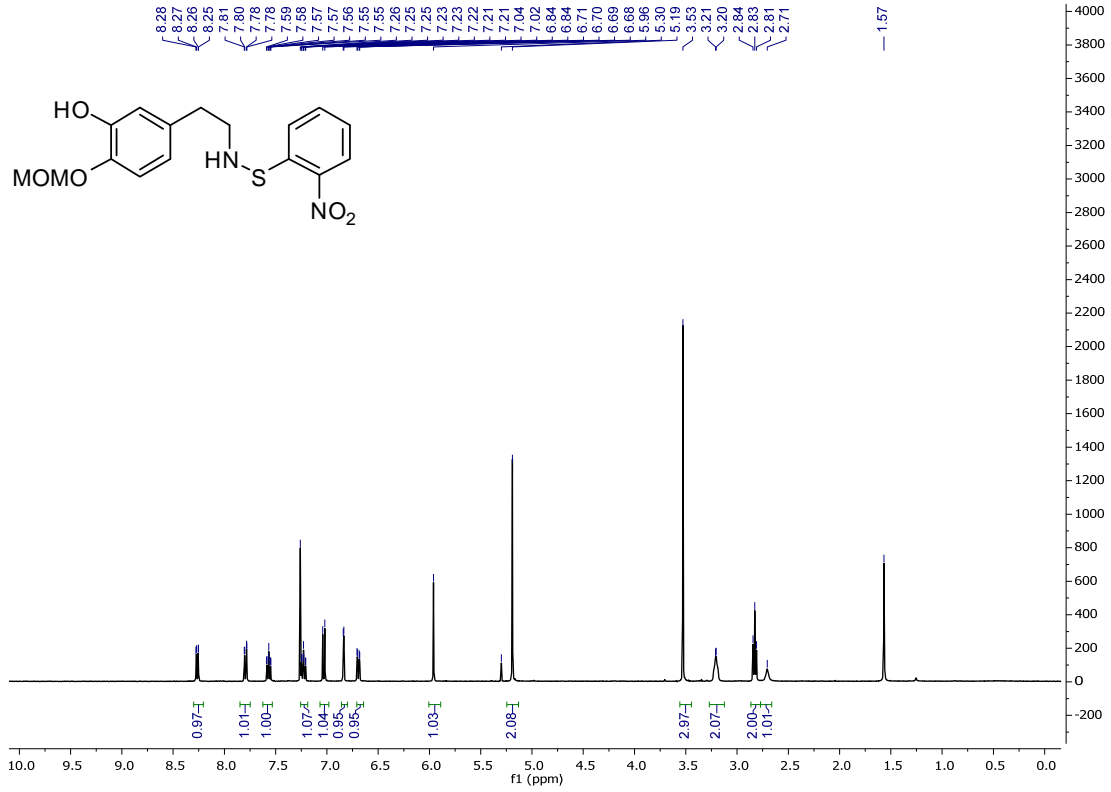


$^1\text{H}$  NMR (MeOD- $d_6$ ) $^{13}\text{C}$  NMR (MeOD- $d_6$ )

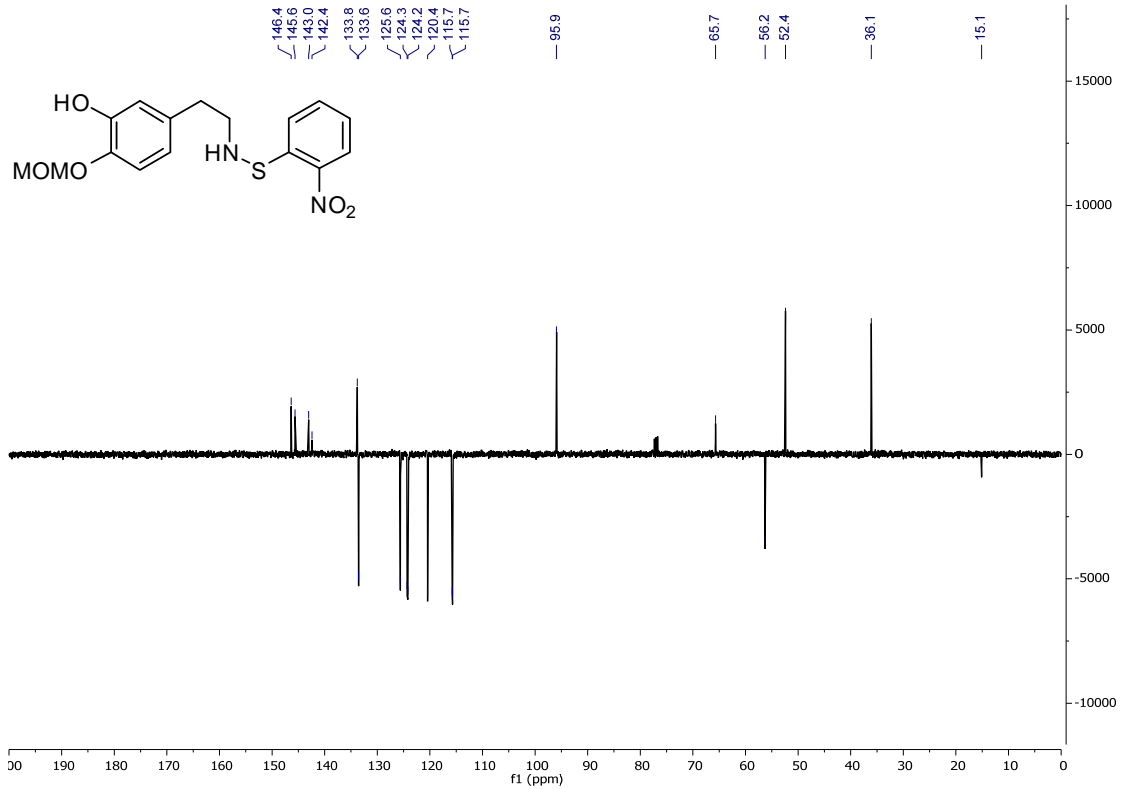


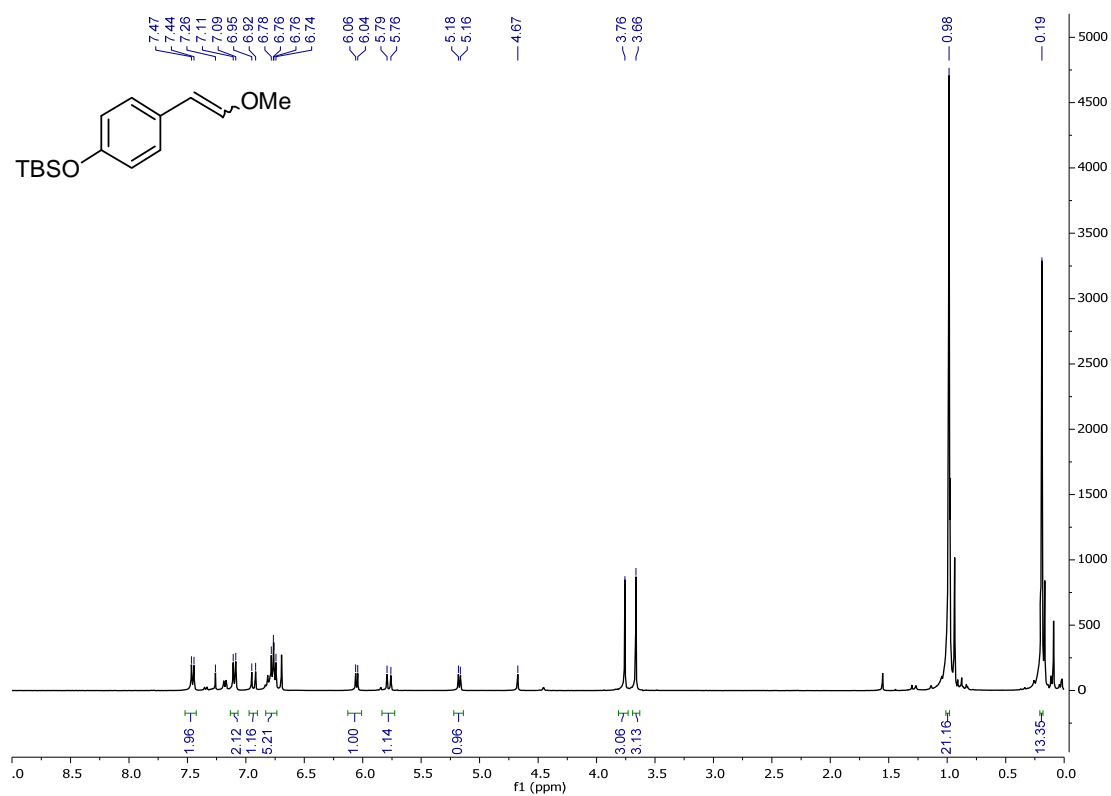
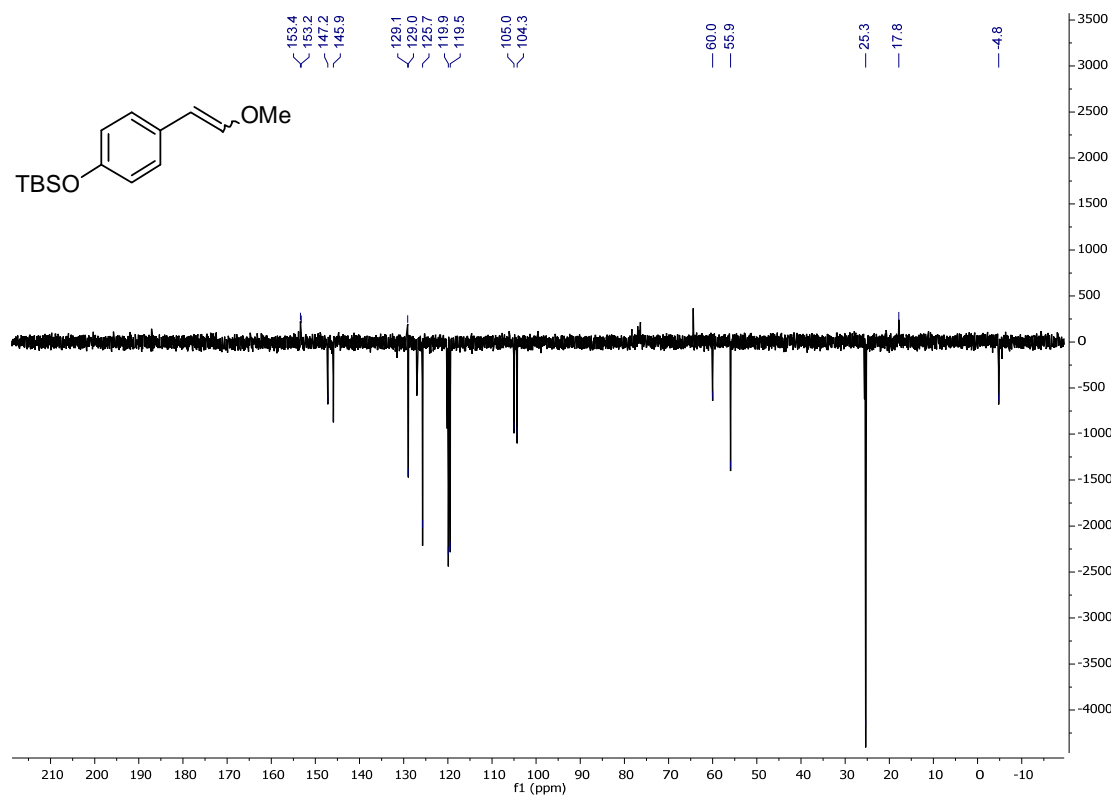
Compound **101a**

<sup>1</sup>H NMR (CDCl<sub>3</sub>)



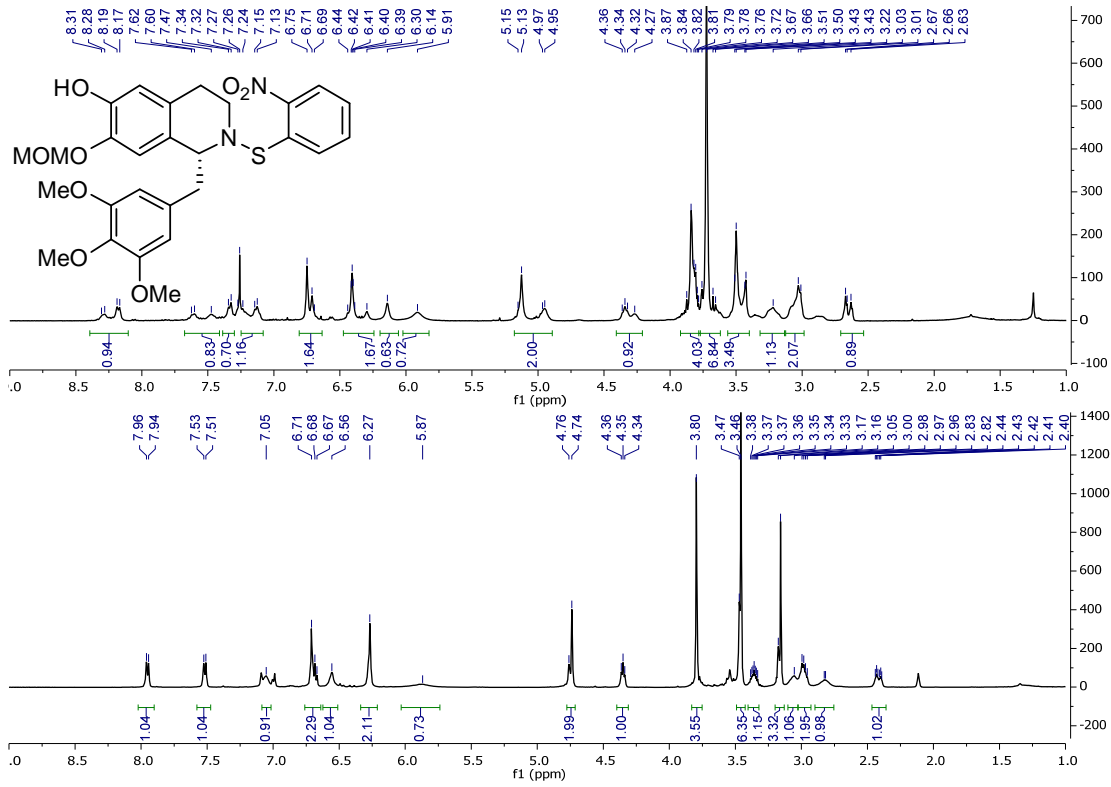
<sup>13</sup>C NMR (CDCl<sub>3</sub>)



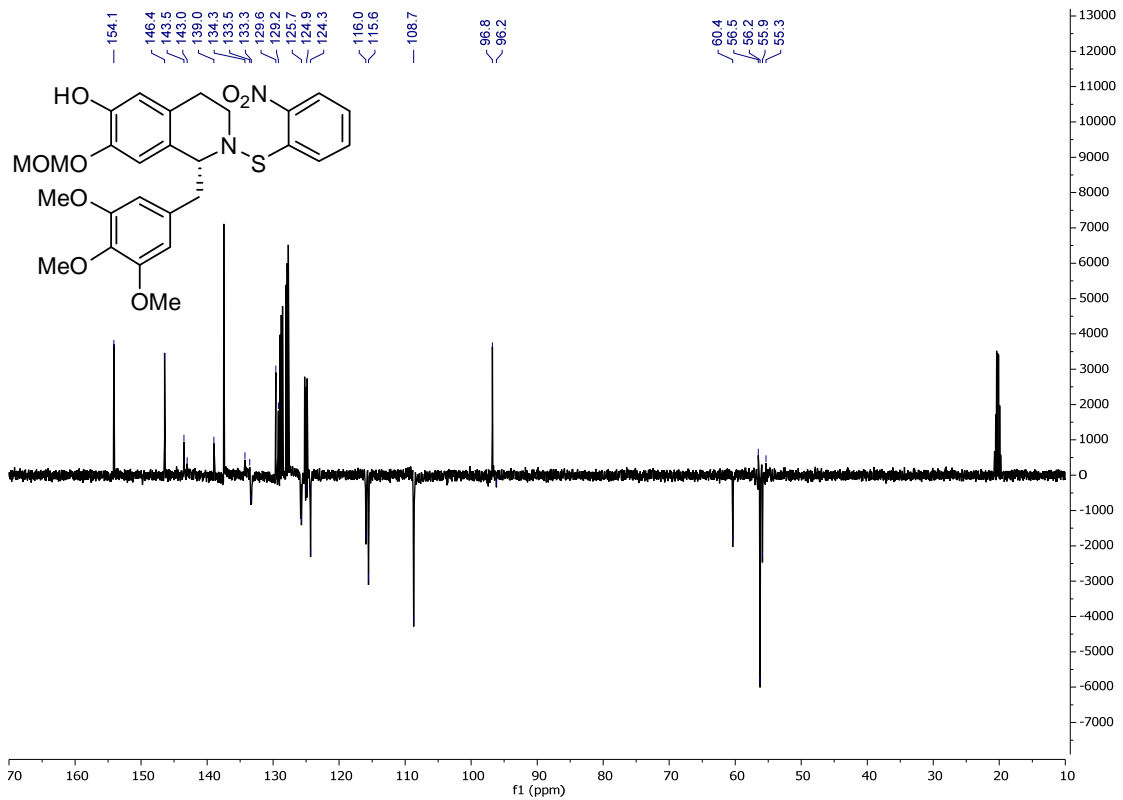
$^1\text{H}$  NMR ( $\text{CDCl}_3$ ) $^{13}\text{C}$  NMR ( $\text{CDCl}_3$ )

Compound **109a**

<sup>1</sup>H NMR (up: CDCl<sub>3</sub>, room temperature; down: toluene-d<sub>8</sub>, 90 °C)

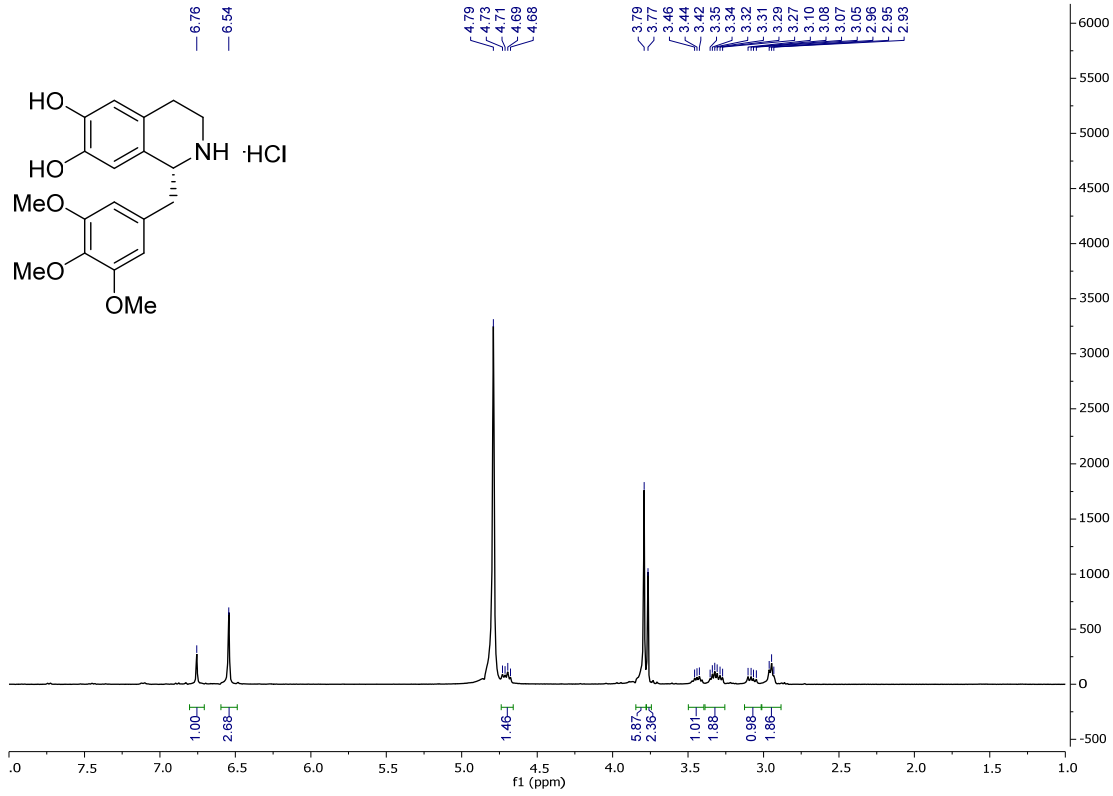


<sup>13</sup>C NMR (toluene-d<sub>8</sub>, 90 °C)

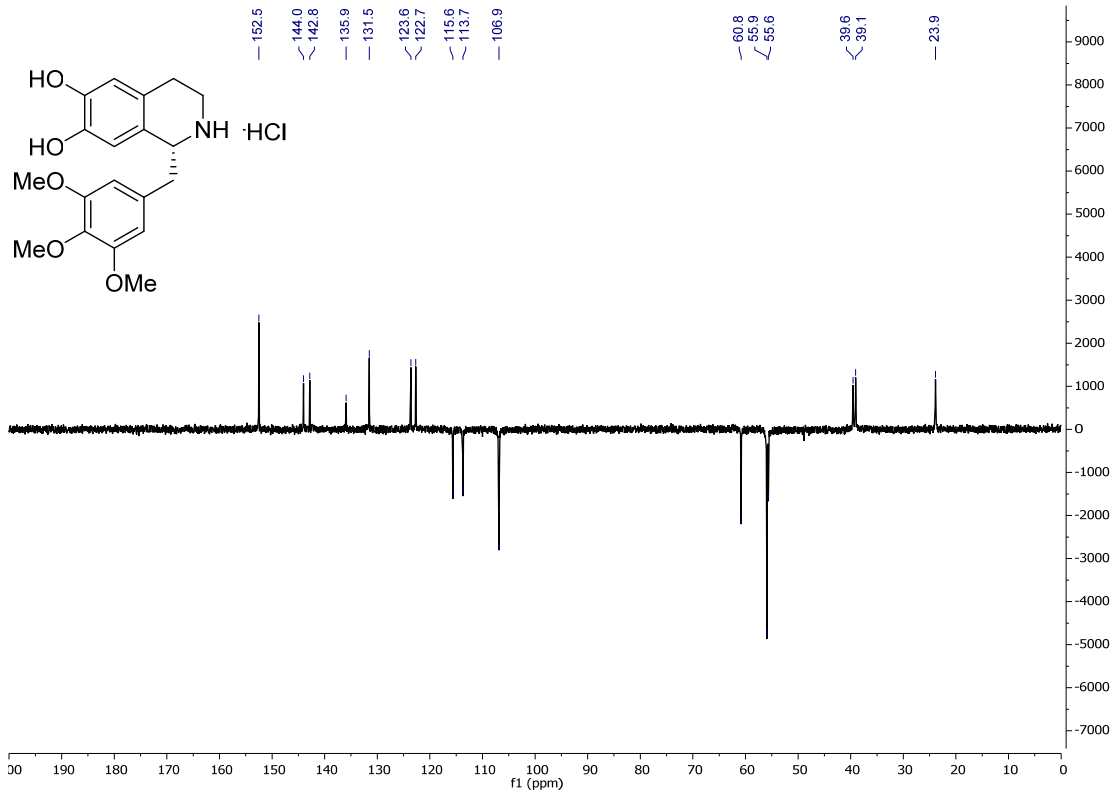


Compound **LXII**

<sup>1</sup>H NMR (D<sub>2</sub>O)



<sup>13</sup>C NMR (D<sub>2</sub>O)



## Annex II. X Ray structures for Chapters 2, 3 and 4

Intensity data were collected on an Agilent Technologies Super-Nova diffractometer, which was equipped with monochromated Cu  $\alpha$  radiation ( $\lambda = 1.54184 \text{ \AA}$ ) and Atlas CCD detector.<sup>1</sup> Measurement was carried out at 100.00 K with the help of an Oxford Cryostream 700 PLUS temperature device. Data frames were processed (unit cell determination, analytical absorption correction with face indexing, intensity data integration and correction for Lorentz and polarization effects) using the CrysAlis software package.<sup>2</sup> The structure was solved using Olex2<sup>3</sup> and refined by full-matrix least-squares with SHELXL-97.<sup>4</sup> Final geometrical calculations were carried out with Mercury<sup>5</sup> and PLATON<sup>6</sup> as integrated in WinGX.<sup>7</sup>

---

<sup>1</sup> All the presented structures were resolved by the Advanced Research Facilities (SGIker) of the University of the Basque Country, performed by Dr. San Felices at the General X-Ray Service.

<sup>2</sup> CrysAlisPro, Agilent Technologies, Version 1.171.37.31 (release 14-01-2014 CrysAlis171.NET; compiled Jan 14 2014, 18:38:05).

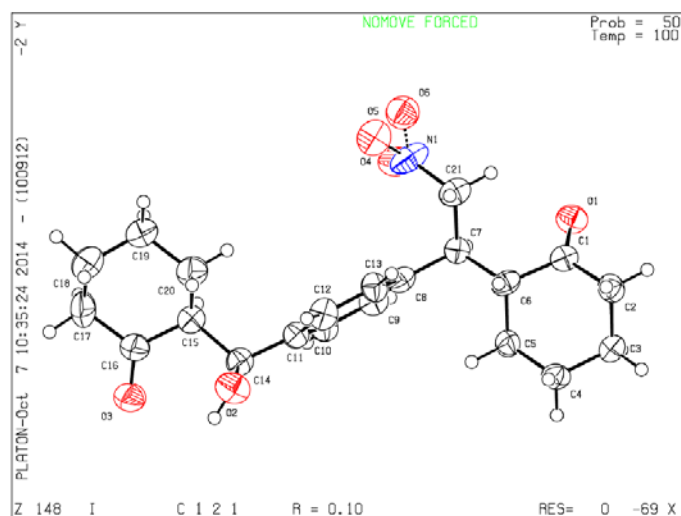
<sup>3</sup> Dolomanov, O.V.; Bourhis, L.J.; Gildea, R.J.; Howard, J.A.K.; Puschmann, H. *J. Appl. Cryst.* **2009**, *42*, 339-341.

<sup>4</sup> Sheldrick, G. M. *Acta Cryst.* **2008**, *A64*, 112-122.

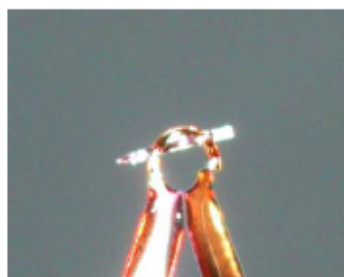
<sup>5</sup> Macrae, C. F.; Bruno, I. J.; Chisholm, J. A.; Edgington, P. R.; McCabe, P.; Pidcock, E.; Rodríguez-Monge, L.; Taylor, R.; van de Streek, J.; Wood, P. A. *J. Appl. Cryst.* **2008**, *41*, 466-740.

<sup>6</sup> Spek, A. L. *J. Appl. Cryst.* **2003**, *36*, 7-13.

<sup>7</sup> Farrugia, L. J. *J. Appl. Cryst.* **1999**, *32*, 837-838.

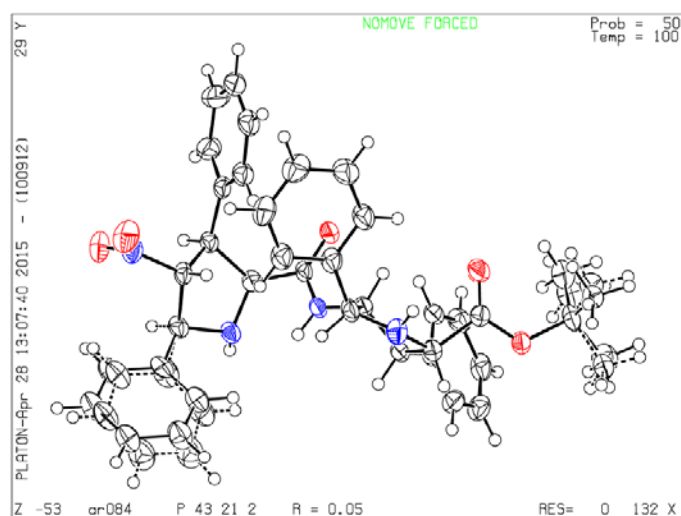
Compound *syn-21*

Datos Físicos y Cristalográficos		Condiciones de Registro y Afinamiento	
Fórmula	C <sub>21</sub> H <sub>27</sub> N O <sub>5</sub>	Difractómetro	Agilent SuperNova Cu
M <sub>r</sub> (g·mol <sup>-1</sup> )	373.44	Detector	CCD (Atlas)
Sistema cristalino	Monoclinic	Temperatura (K)	100(1)°
Grupo espacial	C2 (No. 5)	λ (CuKα) (Å)	1.54184
a (Å)	22.571(5)	Monocromador	Óptica multicapa
b (Å)	5.469(5)	Colimador (mm)	0.2
c (Å)	16.565(5)	Modo de barrido	Rotación ∞
α (°)	90	Anchura de barrido (°)	1.0
β (°)	109.897(5)	Tiempo por placa (s) (Total, h)	1;4 (6)
γ (°)	90	Intervalo de θ (°)	4.1-72.5
V (Å <sup>3</sup> )	1922.7(19)	(hkl) mínimo	(-27 -6 -20)
Z	4	(hkl) máximo	(25 6 20)
D <sub>x</sub> (g·cm <sup>-3</sup> )	1.290(1)	Reflexiones medidas	19136
μ (CuKα) (mm <sup>-1</sup> )	0.749	Reflexiones independientes (R <sub>int</sub> )	3644(0.213)
F (000)	800	Reflexiones observadas [I > 2σ(I)]	2117
Morfología	Aguja	Corrección de absorción	Análítica por caras
Color	Incoloro	Solución	OLEX2
Tamaño (mm)	0.40x0.03x0.03	Refinamiento	SHELXL97
		Número de parámetros	255
		Número de restricciones	13
		Δ/σ máximo	0.000
		Δ/σ media	0.000
		Δρ máximo (eÅ <sup>-3</sup> )	0.481
		Δρ mínimo (eÅ <sup>-3</sup> )	-0.312
		S (GOF)	987
		Coefficiente extinción secundaria <sup>[a]</sup>	0
		R(F) (I > 2σ <sub>i</sub> , todos los datos)	0.1539, 0.1049
		R <sub>w</sub> (F <sup>2</sup> ) <sup>[a]</sup> (I > 2σ <sub>i</sub> , todos los datos)	0.2422, 0.2722



[a] Esquema de pesado:  $1/[\sigma^2(F_o^2) + (0.1579P)^2]$  donde  $P = [\text{Max}(F_o^2, 0) + 2F_c^2]/3$ .

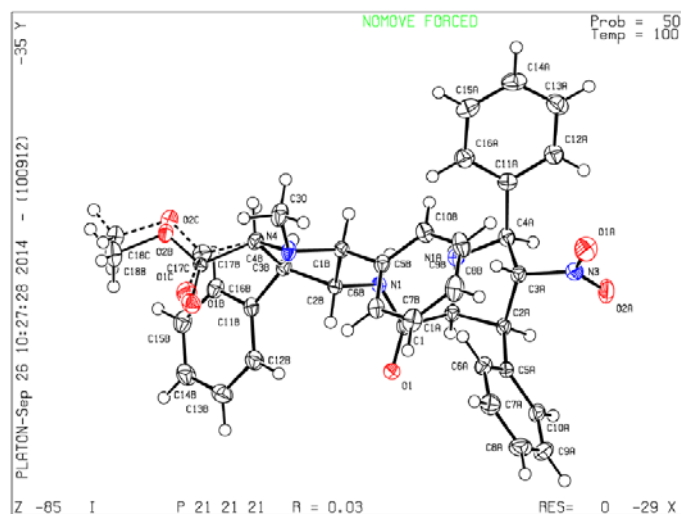
[b] Expresión de extinción secundaria tipo SHELXL:  $F_c^* = kF_c[1 + 0.001F_c^2\lambda^3/\text{sen}(2\theta)]^{-1/4}$

Compound NO<sub>2</sub>-X<sub>L</sub>X<sub>L</sub>-O<sup>t</sup>Bu-23b

Crystal Data		Data Collection and Refinement	
Formula	C <sub>38</sub> H <sub>40</sub> N <sub>4</sub> O <sub>5</sub>	Diffractometer	Agilent SuperNova Cu
Formula Weight	632.74	Detector	CCD (Atlas)
Crystal System	tetragonal	Temperature (K)	100(1) <sup>o</sup>
Space group	P 4 <sub>3</sub> 2 <sub>1</sub> 2 (No.96)	λ (CuKα) (Å)	1.54184
a (Å)	11.36753(9)	Monochromator	Óptica multicapa
b (Å)	11.36753(9)	Collimator (mm)	0.2
c (Å)	54.7978(9)	Scan mode	Rotación ω
α (°)	90	Scan width (°)	1.0
β (°)	90	Time per frame (s) (Total, h)	4;16 (10)
γ (°)	90	Interval of θ (°)	3.23, 71.96
V (Å <sup>3</sup> )	7081.02(14)	(hkl) minimum	(-13 -14 -67)
Z	8	(hkl) maximum	(14 10 67)
D <sub>x</sub> (g·cm <sup>-3</sup> )	1.187	Reflections measures	54809
μ (CuKα) (mm <sup>-1</sup> )	0.487	Reflections independent (R <sub>int</sub> )	6906(0.036)
F (000)	2688	Reflections observed [I>2σ(I)]	6454
Morphology	Plate	Absorption correction	Analytical
Colour	colourless	Solution	OLEX2
Size (mm)	0.02x 0.18x 0.27	Refinement	SHELXL97(14/7)
Friedel coverage	99%	Number of parameters	506
Flack x	0.14(9)	Number of restrictions	135
Hoof t y	0.09(6)	Δ/σ maximum	0.001
P2(wrong)	<10 <sup>-47</sup>	Δ/σ medium	0.000
		Δρ maximum (eÅ <sup>-3</sup> )	0.308
		Δρ minimum (eÅ <sup>-3</sup> )	-0.235
		S (GOF)	1.055
		Secondary extinction coefficient <sup>[a]</sup>	0
		R(F) (I>2σ <sub>i</sub> , all)	0.0468, 0.0499
		R <sub>w</sub> (F <sup>2</sup> ) <sup>[a]</sup> (I>2σ <sub>i</sub> , all)	0.1096, 0.1115

[a] Esquema de pesado:  $1/[\sigma^2(F_o^2) + (0.0402P)^2 + 3.8210P]$  donde  $P = [\text{Max}(F_o^2, 0) + 2F_c^2]/3$ .

[b] Expresión de extinción secundaria tipo SHELXL:  $F_c^* = kF_c[1 + 0.001F_c^2\lambda^3/\text{sen}(2\theta)]^{-1/4}$

Compound NO<sub>2</sub>-X<sub>L</sub>X<sub>L</sub>-OMe-25a

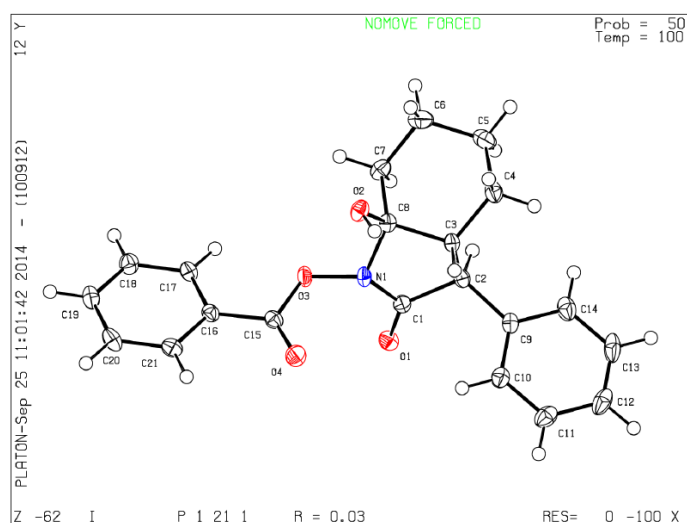
Datos Físicos y Cristalográficos		Condiciones de Registro y Afinamiento	
Fórmula	C <sub>38</sub> H <sub>38</sub> N <sub>4</sub> O <sub>5</sub>	Difractómetro	Agilent SuperNova Cu
M <sub>r</sub> (g·mol <sup>-1</sup> )	604.69	Detector	CCD (Atlas)
Sistema cristalino	Orthorhombic	Temperatura (K)	100(1) <sup>o</sup>
Grupo espacial	P2 <sub>1</sub> 2 <sub>1</sub> 2 <sub>1</sub> (No. 19)	λ (CuKα) (Å)	1.54184
a (Å)	10.9162(1)	Monocromador	Óptica multicapa
b (Å)	12.3547(1)	Colimador (mm)	0.2
c (Å)	23.4547(2)	Modo de barrido	Rotación ω
α (°)	90	Anchura de barrido (°)	1.0
β (°)	90	Tiempo por placa (s) (Total, h)	1.5;6 (8)
γ (°)	90	Intervalo de θ (°)	4.0-72.5
V (Å <sup>3</sup> )	3163.25(5)	(hkl) mínimo	(-13 -15 -29)
Z	4 (Z'=1)	(hkl) máximo	(13 14 28)
F (000)	1280	Reflexiones medidas	35748
μ (CuKα) (mm <sup>-1</sup> )	0.692	Reflexiones independientes (R <sub>int</sub> )	6256(0.029)
D <sub>x</sub> (g·cm <sup>-3</sup> )	1.270(1)	Reflexiones observadas [I>2σ(I)]	6090
Morfología	Prisma	Corrección de absorción	Análítica por caras
Color	Incoloro	Solución	OLEX2
Tamaño (mm)	0.07x 0.20x 0.26	Refinamiento	SHELXL97
		Número de parámetros	453
		Número de restricciones	54
		Δ/σ máximo	0.003
		Δ/σ media	0.000
		Δρ máximo (eÅ <sup>-3</sup> )	0.160
		Δρ mínimo (eÅ <sup>-3</sup> )	-0.168
		S (GOF)	1.040
		Coefficiente extinción secundaria <sup>[b]</sup>	0
Friedel coverage	100%	R(F) (I>2σ <sub>i</sub> , todos los datos)	0.0288, 0.0296
Flack x	-0.02(12)	R <sub>w</sub> (F <sup>2</sup> ) <sup>[a]</sup> (I>2σ <sub>i</sub> , todos los datos)	0.0727, 0.0733
Hoofit y	0.01(5)		
P2(wrong)	<10 <sup>-41</sup>		



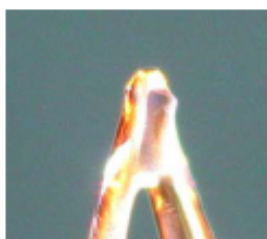
[a] Esquema de pesado:  $1/[\sigma^2(F_o^2) + (0.04560P)^2 + 1.5838P]$  donde  $P = [\text{Max}(F_o^2, 0) + 2F_c^2]/3$ .

[b] Expresión de extinción secundaria tipo SHELXL:  $F_c^* = kF_c[1 + 0.001F_c^2\lambda^3/\text{sen}(2\theta)]^{-1/4}$



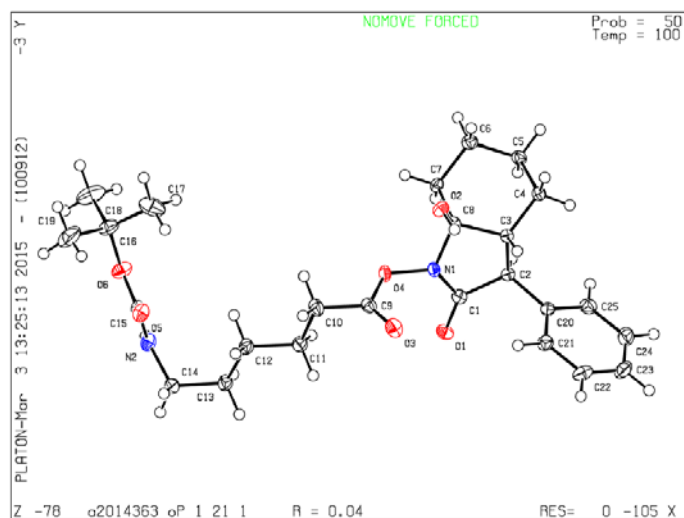
Compound (3*S*,3*aR*,7*aS*)-**24aaa**

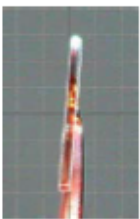
Datos Físicos y Cristalográficos		Condiciones de Registro y Afinamiento	
Fórmula	C <sub>21</sub> H <sub>21</sub> N O <sub>4</sub>	Difractómetro	Agilent SuperNova Cu
M <sub>r</sub> (g·mol <sup>-1</sup> )	351.39	Detector	CCD (Atlas)
Sistema cristalino	Monoclinic	Temperatura (K)	100(1)°
Grupo espacial	P2 <sub>1</sub> (No. 4)	λ (CuKα) (Å)	1.54184
a (Å)	8.8731(1)	Monocromador	Óptica multicapa
b (Å)	9.8039(2)	Colimador (mm)	0.2
c (Å)	10.3325(2)	Modo de barrido	Rotación ω
α (°)	90	Anchura de barrido (°)	1.0
β (°)	90 92.823(1)	Tiempo por placa (s) (Total, h)	1;4 (4)
γ (°)	90	Intervalo de θ (°)	4.3-71.0
V (Å <sup>3</sup> )	897.74(3)	(hkl) mínimo	(-9 -11 -11)
Z	2 (Z'=1)	(hkl) máximo	(10 10 12)
F (000)	372	Reflexiones medidas	9869
μ (CuKα) (mm <sup>-1</sup> )	0.733	Reflexiones independientes (R <sub>int</sub> )	3353(0.027)
D <sub>x</sub> (g·cm <sup>-3</sup> )	1.300(1)	Reflexiones observadas [I>2σ(I)]	3279
Morfología	Prisma	Corrección de absorción	Análítica por caras
Color	Incoloro	Solución	OLEX2
Tamaño (mm)	0.11x 0.15x 0.34	Refinamiento	SHELXL97
		Número de parámetros	236
		Número de restricciones	1
		Δ/σ máximo	0.000
		Δ/σ media	0.000
		Δρ máximo (eÅ <sup>-3</sup> )	0.172
		Δρ mínimo (eÅ <sup>-3</sup> )	-0.164
		S (GOF)	1.060
Friedel coverage	94%	Coefficiente extinción secundaria <sup>[a]</sup>	0
Flack x	-0.06(12)	R(F) (I>2σ <sub>i</sub> , todos los datos)	0.0262, 0.0270
Hoofit y	-0.03(7)	R <sub>w</sub> (F <sup>2</sup> ) <sup>[a]</sup> (I>2σ <sub>i</sub> , todos los datos)	0.0641, 0.0650
P2(wrong)	<10 <sup>-47</sup>		



[a] Esquema de pesado:  $1/[\sigma^2(F_o^2)+(0.0320P)^2]$  donde  $P = [\text{Max}(F_o^2,0)+2F_c^2]/3$ .

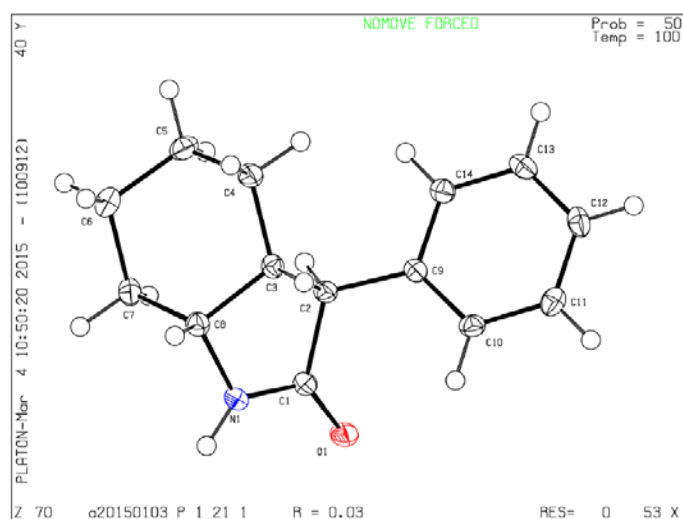
[b] Expresión de extinción secundaria tipo SHELXL:  $F_c^* = kF_c[1+0.001F_c^2\lambda^3/\text{sen}(2\theta)]^{-1/4}$

Compound (3*S*,3*aR*,7*aS*)-**24aae**

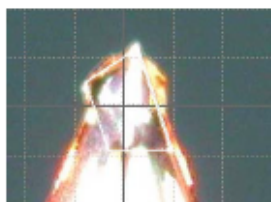
Crystal Data		Data Collection and Refinement	
Formula	C <sub>25</sub> H <sub>36</sub> N <sub>2</sub> O <sub>6</sub>	Diffractometer	Agilent SuperNova Cu
Formula Weight	460.56	Detector	CCD (Atlas)
Crystal System	Monoclinic	Temperature (K)	100(1) <sup>o</sup>
Space group	P21 (No. 4)	$\lambda$ (CuK $\alpha$ ) (Å)	1.54184
a (Å)	8.4435(3)	Monochromator	Óptica multicapa
b (Å)	9.6435(2)	Collimator (mm)	0.2
c (Å)	15.6705(6)	Scan mode	Rotación $\omega$
$\alpha$ (°)	90	Scan width (°)	1.0
$\beta$ (°)	103.422(4)	Time per frame (s) (Total, h)	1.5;6 (4)
$\gamma$ (°)	90	Interval of $\theta$ (°)	2.9, 72.5
V (Å <sup>3</sup> )	1241.12(7)	(hkl) minimum	(-10 -11 -19)
Z	2	(hkl) maximum	(10 11 18)
D <sub>x</sub> (g·cm <sup>-3</sup> )	1.232	Reflections measures	14475
$\mu$ (CuK $\alpha$ ) (mm <sup>-1</sup> )	0.716	Reflections independent (R <sub>int</sub> )	4891(0.065)
F (000)	496	Reflections observed [I>2 $\sigma$ (I)]	4408
Morphology	Needle	Absorption correction	Analytical
Colour	colourless	Solution	OLEX2
Size (mm)	0.04x 0.04x 0.69	Refinement	SHELXL97
		Number of parameters	307
		Number of restrictions	1
		$\Delta/\sigma$ maximum	0.000
		$\Delta/\sigma$ medium	0.000
		$\Delta\rho$ maximum (eÅ <sup>-3</sup> )	0.203
		$\Delta\rho$ minimum (eÅ <sup>-3</sup> )	-0.255
Friedel coverage	99%	S (GOF)	1.025
Flack x	0.06(18)	Secondary extinction coefficient [b]	0
Hooft y	-0.06(14)	R(F) (I>2 $\sigma$ <sub>i</sub> , all)	0.0442, 0.0505
P2(wrong)	<10 <sup>-13</sup>	R <sub>w</sub> (F <sup>2</sup> ) <sup>[a]</sup> (I>2 $\sigma$ <sub>i</sub> , all)	0.1083, 0.1132

[a] Esquema de pesado:  $1/[\sigma^2(F_o^2) + (0.0587P)^2]$  donde  $P = [\text{Max}(F_o^2, 0) + 2F_c^2]/3$ .

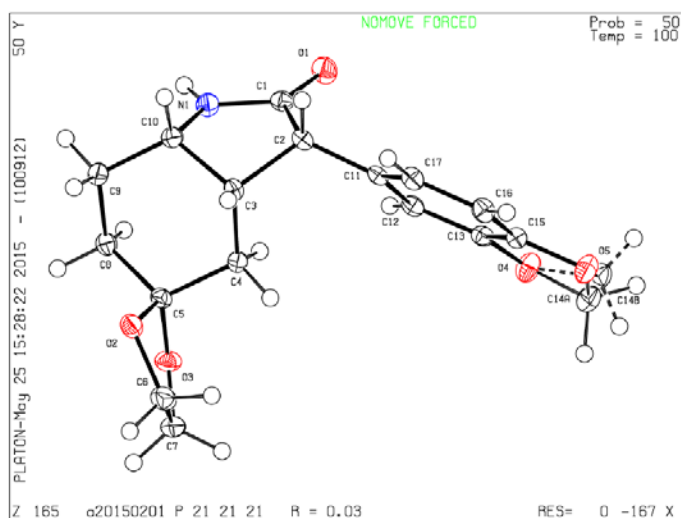
[b] Expresión de extinción secundaria tipo SHELXL:  $F_c^* = kF_c[1 + 0.001F_c^2\lambda^3/\text{sen}(2\theta)]^{-1/4}$


Compound **56aa**

Crystal Data		Data Collection and Refinement	
Formula	C14 H17 N1 O1	Diffractometer	Agilent SuperNova Cu
Formula Weight	215.29	Detector	CCD (Atlas)
Crystal System	Monoclinic	Temperature (K)	100(1) <sup>o</sup>
Space group	P21 (No. 4)	$\lambda$ (CuK $\alpha$ ) (Å)	1.54184
a (Å)	6.01020(10)	Monochromator	Óptica multicapa
b (Å)	6.9308(2)	Collimator (mm)	0.2
c (Å)	13.6422(3)	Scan mode	Rotación $\omega$
$\alpha$ (°)	90	Scan width (°)	1.0
$\beta$ (°)	95.653(2)	Time per frame (s) (Total, h)	1.5;6 (4)
$\gamma$ (°)	90	Interval of $\theta$ (°)	3.26, 71.85
V (Å <sup>3</sup> )	565.51(2)	(hkl) minimum	(-7 -8 -16)
Z	2	(hkl) maximum	(7 8 16)
D <sub>x</sub> (g·cm <sup>-3</sup> )	1.264	Reflections measures	11034
$\mu$ (CuK $\alpha$ ) (mm <sup>-1</sup> )	0.618	Reflections independent (R <sub>int</sub> )	2194 (0.034)
F (000)	232	Reflections observed [I > 2 $\sigma$ (I)]	2140
Morphology	Needle	Absorption correction	Analytical
Colour	colourless	Solution	OLEX2
Size (mm)	0.02x 0.13x 0.23	Refinement	SHELXL97
		Number of parameters	149
		Number of restrictions	1
		$\Delta/\sigma$ maximum	0.003
		$\Delta/\sigma$ medium	0.001
		$\Delta\rho$ maximum (eÅ <sup>-3</sup> )	0.162
		$\Delta\rho$ minimum (eÅ <sup>-3</sup> )	-0.182
Friedel coverage	97%	S (GOF)	1.058
Flack x	0.03(12)	Secondary extinction coefficient [a]	0
Hoofit y	-0.06(14)	R(F) (I > 2 $\sigma$ <sub>i</sub> , all)	0.0288, 0.0298
P2(wrong)	<10 <sup>-16</sup>	R <sub>w</sub> (F <sup>2</sup> ) [a] (I > 2 $\sigma$ <sub>i</sub> , all)	0.0722, 0.0728



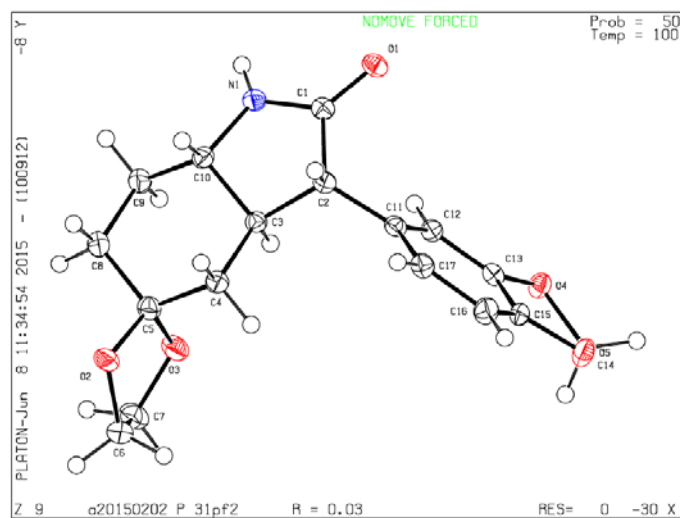
[a] Esquema de pesado:  $1/[\sigma^2(F_o^2) + (0.0420P)^2 + 0.0749P]$  donde  $P = [\text{Max}(F_o^2, 0) + 2F_c^2]/3$ .  
 [b] Expresión de extinción secundaria tipo SHELXL:  $F_c^+ = kF_c[1 + 0.001F_c^2\lambda^3/\text{sen}(2\theta)]^{-1/4}$

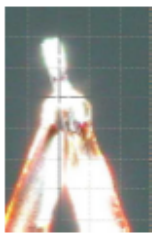
Compound (3*S*,3*aS*,7*aS*)-**56gp**

Crystal Data		Data Collection and Refinement	
Formula	C <sub>17</sub> H <sub>19</sub> N O <sub>5</sub>	Diffractometer	Agilent SuperNova Cu
Formula Weight	317.33	Detector	CCD (Atlas)
Crystal System	orthorhombic	Temperature (K)	100.01(10)
Space group	P 2 <sub>1</sub> 2 <sub>1</sub> 2 <sub>1</sub> (No.19)	λ (CuKα) (Å)	1.54184
a (Å)	6.31288(12)	Monochromator	Óptica multicapa
b (Å)	9.0074(2)	Collimator (mm)	0.2
c (Å)	28.0842(5)	Scan mode	Rotación ω
α (°)	90	Scan width (°)	1.0
β (°)	90	Time per frame (s) (Total, h)	2;8 (8)
γ (°)	90	Interval of θ (°)	3.39, 73.97
V (Å <sup>3</sup> )	1483.22(5)	(hkl) minimum	(-7 -11 -32)
Z	4	(hkl) maximum	(7 11 32)
D <sub>x</sub> (g·cm <sup>-3</sup> )	1.421	Reflections measures	11735
μ (CuKα) (mm <sup>-1</sup> )	0.875	Reflections independent (R <sub>int</sub> )	3008(0.045)
F (000)	672	Reflections observed [I>2σ(I)]	2822
Morphology	needle	Absorption correction	Analytical
Colour	colourless	Solution	OLEX2
Size (mm)	0.05x0.07x0.37	Refinement	SHELXL97(14/7)
		Number of parameters	222
		Number of restrictions	16
		Δσ maximum	0.021
		Δσ medium	0.002
		Δρ maximum (eÅ <sup>-3</sup> )	0.186
		Δρ minimum (eÅ <sup>-3</sup> )	-0.174
Friedel coverage	99%	S (GOF)	1.048
Flack x	0.07(11)	Secondary extinction coefficient <sup>[b]</sup>	0
Hoofit y	0.05(11)	R(F) (I>2σ <sub>i</sub> , all)	0.0320, 0.0352
P2(wrong)	<10 <sup>-13</sup>	R <sub>w</sub> (F <sup>2</sup> ) <sup>[a]</sup> (I>2σ <sub>i</sub> , all)	0.0755, 0.0776

[a] Esquema de pesado:  $1/[\sigma^2(F_o^2) + (0.0373P)^2 + 0.2016P]$  donde  $P = [\text{Max}(F_o^2, 0) + 2F_c^2]/3$ .

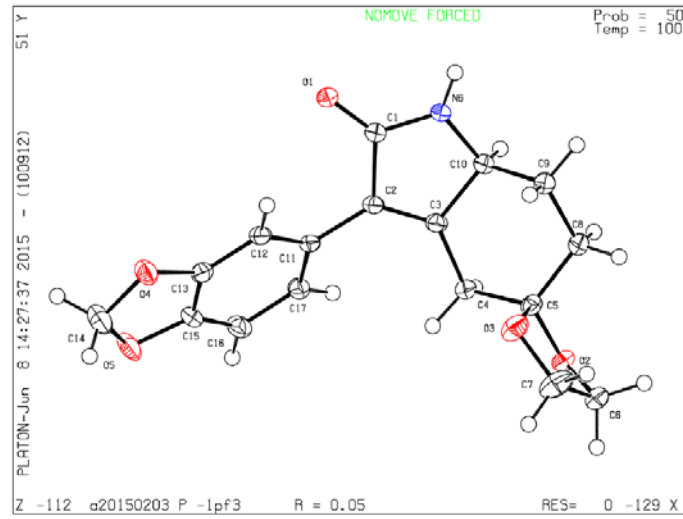
[b] Expresión de extinción secundaria tipo SHELXL:  $F_o^* = kF_c[1 + 0.001F_c^2\lambda^3/\text{sen}(2\theta)]^{-1/4}$

Compound (3*S*,3*aR*,7*aS*)-**56gp**

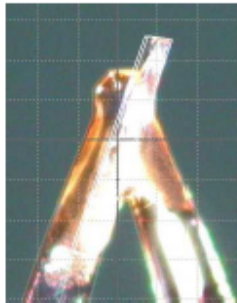
Crystal Data		Data Collection and Refinement	
Formula	C <sub>17</sub> H <sub>19</sub> N O <sub>5</sub>	Diffractometer	Agilent SuperNova Cu
Formula Weight	317.33	Detector	CCD (Atlas)
Crystal System	hexagonal	Temperature (K)	100.00(10)
Space group	P3 <sub>1</sub> (No. 144)	λ (CuKα) (Å)	1.54184
a (Å)	14.6244(2)	Monochromator	Óptica multicapa
b (Å)	14.6244(2)	Collimator (mm)	0.2
c (Å)	6.23570(10)	Scan mode	Rotación ω
α (°)	90	Scan width (°)	1.0
β (°)	90	Time per frame (s) (Total, h)	2;8 (6)
γ (°)	120	Interval of θ (°)	3.49, 73.84
V (Å <sup>3</sup> )	1154.98(3)	(hkl) minimum	(-17 -18 -7)
Z	3	(hkl) maximum	(18 15 7)
D <sub>x</sub> (g·cm <sup>-3</sup> )	1.369	Reflections measures	13799
μ (CuKα) (mm <sup>-1</sup> )	0.839	Reflections independent (R <sub>int</sub> )	3058(0.037)
F (000)	504	Reflections observed [I>2σ(I)]	2980
Morphology	needle	Absorption correction	Analytical
Colour	colourless	Solution	OLEX2
Size (mm)	0.05x0.07x0.37	Refinement	SHELXL97(14/7)
		Number of parameters	208
		Number of restraints	1
		Δ/σ maximum	0.010
		Δ/σ medium	0.001
		Δρ maximum (eÅ <sup>-3</sup> )	0.170
		Δρ minimum (eÅ <sup>-3</sup> )	-0.200
Friedel coverage	99%	S (GOF)	1.039
Flack x	0.07(11)	Secondary extinction coefficient [b]	0
Hoofit y	0.05(11)	R(F) (I>2σ <sub>I</sub> , all)	0.0268, 0.0278
P2(wrong)	<10 <sup>-13</sup>	R <sub>w</sub> (F <sup>2</sup> ) <sup>[a]</sup> (I>2σ <sub>I</sub> , all)	0.0677, 0.0690

[a] Esquema de pesado:  $1/[\sigma^2(F_o^2) + (0.0389P)^2 + 0.1742P]$  donde  $P = [\text{Max}(F_o^2, 0) + 2F_c^2]/3$ .

[b] Expresión de extinción secundaria tipo SHELXL:  $F_c^* = kF_c[1 + 0.001F_c^2\lambda^3/\text{sen}(2\theta)]^{-1/4}$

Compound *rac*-72

Crystal Data		Data Collection and Refinement	
Formula	C <sub>17</sub> H <sub>17</sub> N O <sub>5</sub>	Diffractometer	Agilent SuperNova Cu
Formula Weight	315.31	Detector	CCD (Atlas)
Crystal System	triclinic	Temperature (K)	100.00(10)
Space group	P-1 (No. 144)	$\lambda$ (CuK $\alpha$ ) (Å)	1.54184
a (Å)	6.4434(3)	Monochromator	Óptica multicapa
b (Å)	9.5718(5)	Collimator (mm)	0.2
c (Å)	12.6451(5)	Scan mode	Rotación $\omega$
$\alpha$ (°)	86.078(4)	Scan width (°)	1.0
$\beta$ (°)	76.852(4)	Time per frame (s) (Total, h)	2;8 (6)
$\gamma$ (°)	74.079(5)	Interval of $\theta$ (°)	3.49, 73.84
V (Å <sup>3</sup> )	730.29(6)	(hkl) minimum	(-7 -11 -15)
Z	2	(hkl) maximum	(8 11 15)
D <sub>x</sub> (g·cm <sup>-3</sup> )	1.434	Reflections measures	14150
$\mu$ (CuK $\alpha$ ) (mm <sup>-1</sup> )	0.887	Reflections independent (R <sub>int</sub> )	2878(0.059)
F (000)	332	Reflections observed [ $I > 2\sigma(I)$ ]	2426
Morphology	needle	Absorption correction	Analytical
Colour	colourless	Solution	OLEX2
Size (mm)	0.04x0.06x 0.60	Refinement	SHELXL97(14/7)
		Number of parameters	208
		Number of restrictions	0
		$\Delta/\sigma$ maximum	0.000
		$\Delta/\sigma$ medium	0.000
		$\Delta\rho$ maximum (eÅ <sup>-3</sup> )	0.458
		$\Delta\rho$ minimum (eÅ <sup>-3</sup> )	-0.281
		S (GOF)	1.049
		Secondary extinction coefficient <sup>[a]</sup>	0
		R(F) ( $I > 2\sigma_I$ , all)	0.0523, 0.0605
		R <sub>w</sub> (F <sup>2</sup> ) <sup>[a]</sup> ( $I > 2\sigma_I$ , all)	0.1421, 0.1520

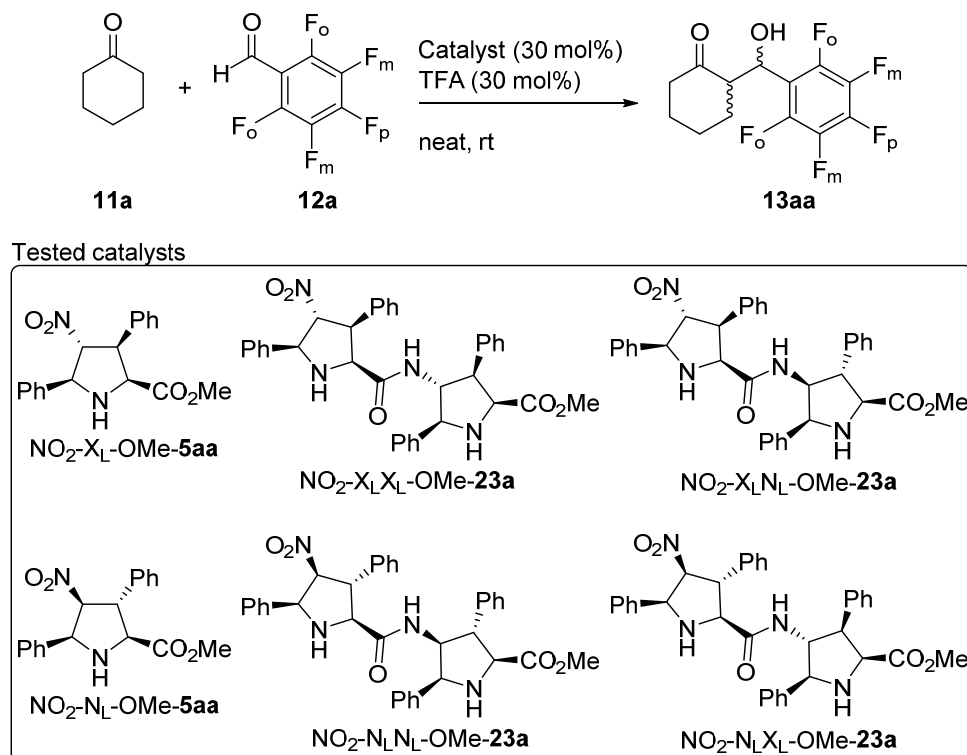


[a] Esquema de pesado:  $1/[\sigma^2(F_o^2) + (0.0971P)^2 + 0.2166P]$  donde  $P = [\text{Max}(F_o^2, 0) + 2F_c^2]/3$ .

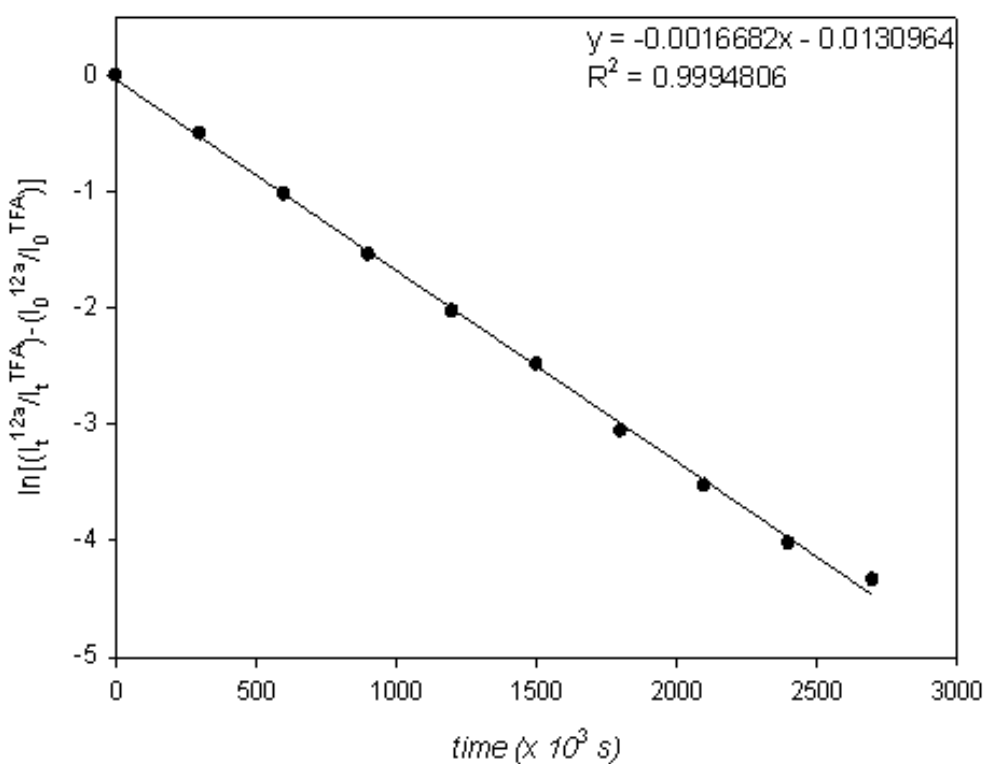
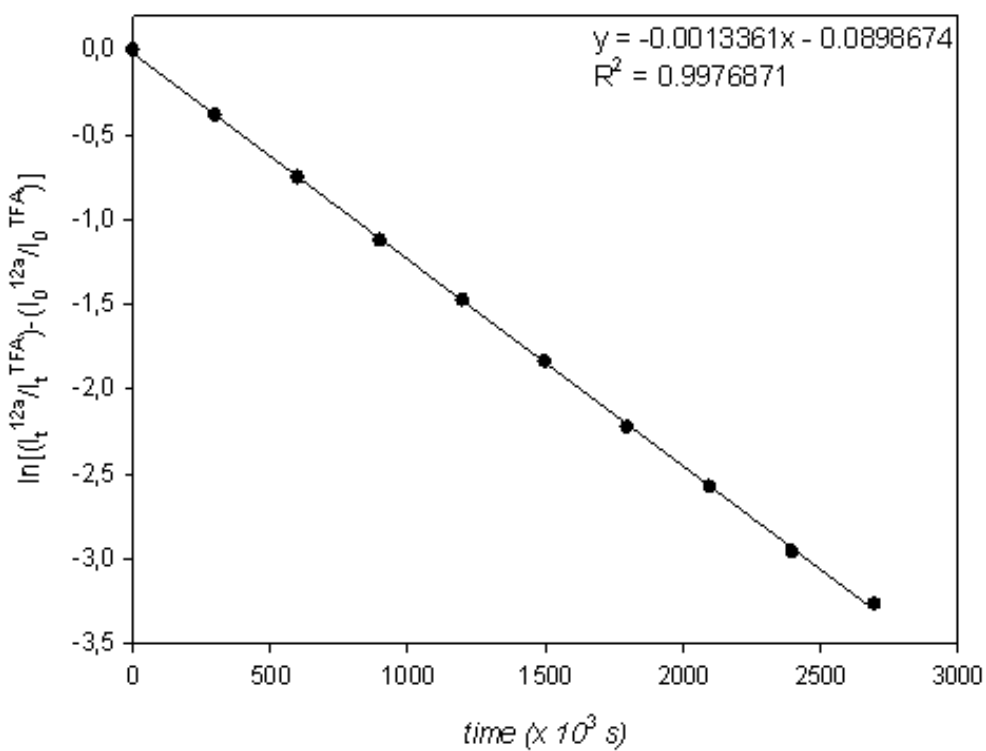
[b] Expresión de extinción secundaria tipo SHELXL:  $F_c^* = kF_c[1 + 0.001F_c^2\lambda^3/\text{sen}(2\theta)]^{-1/4}$

## Annex III. Pseudo-first order linear plots, standard deviations and error calculation

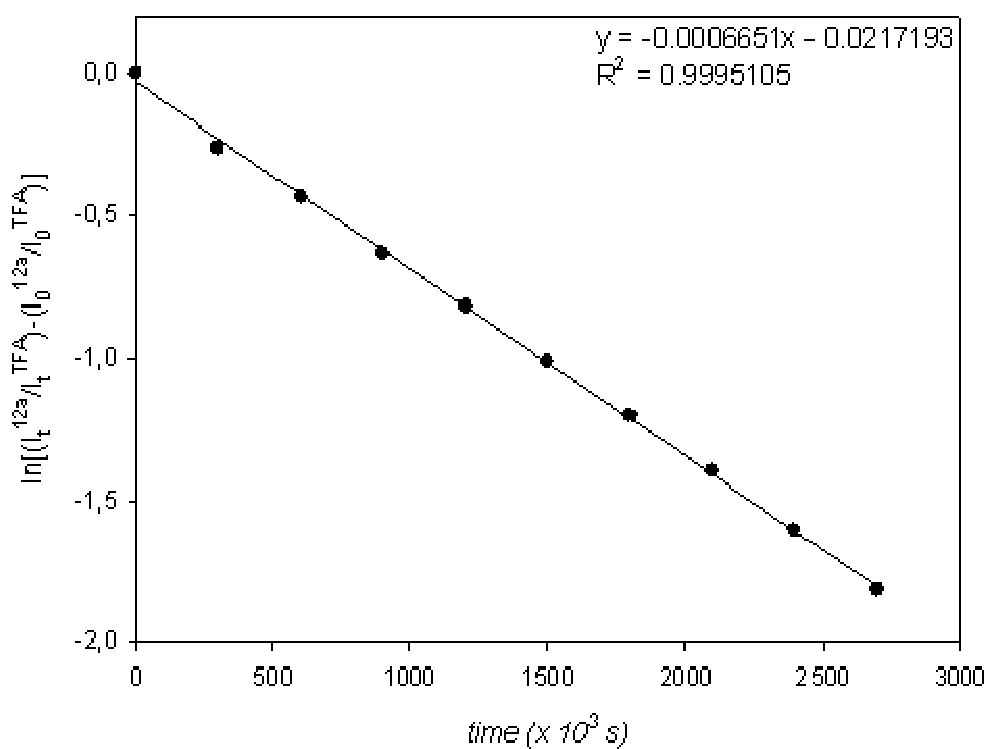
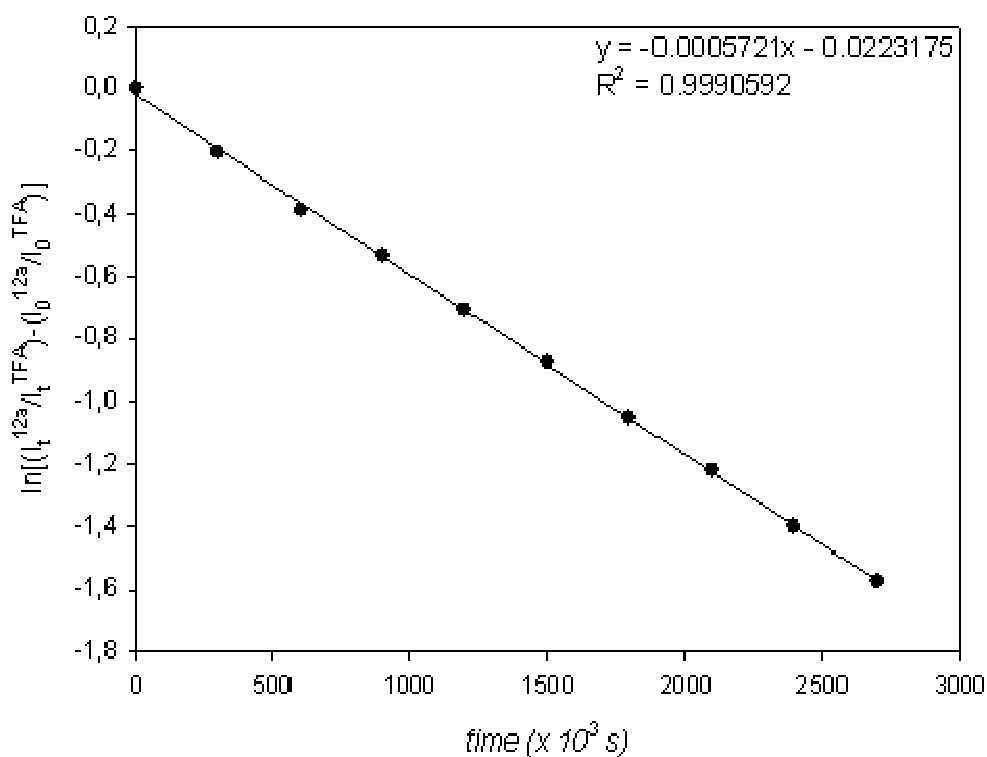
**Pseudo-first order linear plots.** Analysis of different monomeric and dimeric catalysts.



**Figure 1.** Aldol reaction between cyclohexanone **11a** and pentafluorobenzaldehyde **12a** employing organocatalysts **NO<sub>2</sub>-X<sub>L</sub>-OMe-5aa**, **NO<sub>2</sub>-N<sub>L</sub>-OMe-5aa**, **NO<sub>2</sub>-X<sub>L</sub>X<sub>L</sub>-OMe-23a**, **NO<sub>2</sub>-X<sub>L</sub>N<sub>L</sub>-OMe-23a**, **NO<sub>2</sub>-N<sub>L</sub>N<sub>L</sub>-OMe-23a**, and **NO<sub>2</sub>-N<sub>L</sub>X<sub>L</sub>-OMe-23a**.

NO<sub>2</sub>-X<sub>L</sub>X<sub>L</sub>-OMe-23aNO<sub>2</sub>-X<sub>L</sub>N<sub>L</sub>-OMe-23a



NO<sub>2</sub>-N<sub>L</sub>N<sub>L</sub>-OMe-23aNO<sub>2</sub>-N<sub>L</sub>X<sub>L</sub>-OMe-23a

**Standard deviations and error calculations.** Errors for  $k_{\text{obs}}$  were calculated<sup>i</sup> employing the standard deviation ( $s$ ) in equation 1:

$$s = \sqrt{\frac{1}{n-1} \sum_{i=1}^n (X_i - \bar{X})^2} \quad (1)$$

where

$X$  stands for the different  $k_{\text{obs}}$  values calculated by  $^{19}\text{F}$  NMR.

$\bar{X}$  is the average  $k_{\text{obs}}$ .

$n$  is the number of values ( $k_{\text{obs}}$ ) in the final calculations

---

<sup>i</sup> See reference 31 in Chapter 3.